SYNTHESIS OF ENANTIOENRICHED (POLY)FLUORINATED BUILDING BLOCKS, 2,2-DISUBSTITUTED PYRROLIDINES AND [7,7]PARACYCLOPHANES

Thesis by

Elizabeth Lee Goldstein

In Partial Fulfillment of the Requirements

for the Degree of

Doctor of Philosophy

CALIFORNIA INSTITUTE OF TECHNOLOGY

Pasadena, California

2020

(Defended March 4, 2020)

Elizabeth L. Goldstein
ORCID: 0000-0002-2208-6090

To my family,

with love and gratitude

ACKNOWLEDGEMENTS

Reflecting back on the almost 6 years I spent at Caltech, I realize how lucky I am to have so many people in my life who have made this time so amazing. Grad school is a major challenge, and I'm glad I had so many people to support me through this time, both within the school and outside of it. I will always look with fondness upon my time at Caltech, and all of the people who make it an amazing place to be.

I must start with thanking Professor Brian Stoltz, an amazing mentor, teacher, and friend to everyone in his lab. Brian gives all of his students a lot of leeway in how they approach their research, but is always there when you need his advice. I don't think I took advantage of his help enough, but I will always be thankful for his support, and his constructive criticism when I really needed it. Brian's love of baseball was probably one of the reasons I got so interested in baseball myself, though I'm not sure I'll get over the Red Sox beating the Dodgers in the 2018 World Series. I've always enjoyed getting to spend time with him outside of lab, especially with softball (Ru-Tang!). I can only hope that in the future, I'm as great of a mentor to others as Brian was to me.

In that vein, I want to acknowledge some of the other people in the chemistry department at Caltech who had a hand in my scientific development. First, Sarah Reisman, for being like a second advisor to all of those on 3rd floor Schlinger and giving me such good advice at all of my group meetings and committee meetings. I've always really appreciated how close our lab has been to the Reisman lab, and I know that wouldn't be possible without Sarah and Brian fostering that relationship. I also want to thank my other committee members, Harry Gray and Max Robb. Both of them are amazing scientists, and I am deeply thankful for their advice throughout the years.

In addition to all of the professors who have had an impact on my time at Caltech, my coworkers in the Stoltz lab have been a huge help to me. For the most part, I have not been very involved socially in the lab culture and have never been great at asking for help, but I've always known that everyone I've worked with would be willing to help if I would ask. In terms of those in the Stoltz lab, the first I'd have to thank is Beau Pritchett. Beau and I worked next to each other for my first few years, and he was somewhat of an unofficial mentor to me. I was always glad that he was the one working next to me, and knew I could count on him to help me. Even when it seemed he was being critical, I knew it was always with the best intentions, and he made me a better chemist. I also want to thank all of the others who worked in my bay throughout the years, especially Gerit Potoschnig, Fa Ngamnithiporn, Carina Jette, Zach Sercel, Trevor Lohrey and Katerina Korch. In addition, Benzi Estipona, an undergraduate who I knew from when he was in high school, was an inspiration for me, even when his brilliance sometimes made me feel less intelligent. All of the bays have different relationships, and I've always liked how well our bay got along. I am also thankful for all of the time I spent with empty fume hoods in my bay, all of the undergraduates who worked there, and the short amount of time Brian spent working in lab in my bay. It was always entertaining.

Along with those who worked in my bay, there are a number of others working in lab who had an impact on me. First, the undergratuates that I mentored, Netgie Laguerre, Dat Le and Elizabeth Park, who all taught me about chemistry through teaching. Second, I want to thank all of the collaborators I had, both those before my time (Yuji Sumii, Katsuaki Baba and Hirokazu Takada) and during my time (Yanhui Lu and Austin Wright). I also want to thank every other member of the Stoltz group I interacted with

throughout my time here. I am so very thankful for everyone I got to know during my time here, and though I never had any really close friends in the lab, I always enjoyed any time spent with my lab mates, both in lab and out of lab.

Besides those who influenced me at Caltech, I was lucky enough the get the opportunity to be a part of the NSF center for C-H functionalization (CCHF). This group contains a number of researchers across the country, and allowed me to meet a number of influential professors and industrial scientists. This opportunity allowed me to learn more about what I wanted in the future, and everyone was so supportive. In particular, I need to thank Dan Morton for being a good friend and keeping the CCHF running. Additionally, the center set up a collaboration project that was really inspiring for me. This collaboration was with the group of Professor Huw Davies at Emory University. Huw has also been extremely supportive of me and allowed me to spend time in his lab, which taught me a lot about chemistry and collaboration. My original collaborator, Kuangbiao Liao, really helped get this project started, but Aaron Bosse is the one who made the project his own and made it more than just an idea. I can't thank him enough for taking charge of the project and making something out of it when I had mostly given up. I look forward to seeing this synthesis coming to fruition soon.

My time at Caltech would not have been possible without all of those who helped me to get here. I should start by thanking Bob Thompson for giving me my first research experience while I was in high school. Mark Banaszak Holl was my main research mentor before graduate school, and his endless support and help in graduate school applications is what made me believe I could even think about applying to Caltech, let alone getting in. Not only was he a great support, but also a good friend to me. Without

him, I don't think I would have ended up where I did. My graduate student mentor, Flora Fang, was also instrumental in my development, allowing me to learn what academic research was. She really inspired me to pursue graduate school and be a better scientist. Professor Lutz Gade at Heidelberg University in Germany also played a role in my development as a researcher, allowing me to better understand what I wanted to study moving forward. My mentor there, Lena Hahn, taught me a lot about synthetic research at an advanced level, and I will forever be grateful to her.

My professors at Coe College also had a big influence on my development as a scientist. The school was very small, and the department smaller, and so I feel the professors and students developed a much closer relationship than at larger schools. Professors Marty St. Clair, Maria Dean, Scott Stoudt, and Steve Singleton were all amazing professors, and all made an impact on my development as a scientist and helped me believe I could really accomplish something in my future in chemistry. All of them are responsible for inspiring not only me but also a lot of other chemists through the years, and I will be forever grateful for my time there.

Now, with the more scientific acknowledgements completed, I will move on to the more personal ones. I was lucky enough to make a lot of friends in the area outside of the lab, mostly through church and skating. Everyone in my church choir, Canterbury, has been extremely supportive of me. Additionally, the 20/30s group at Caltech was a great source of friendship outside of chemistry, giving me people to go to when I didn't want to think about chemistry. In particular, I feel the need to thank Sarah Phillips, Alex DiBona, Will Gatlin, Justin Song and Hannah Earnshaw for being great friends and people I could go to when I wanted to get away from the stresses of graduate school. In

addition to my church friends, figure skating has been a great source of stress relief, and all of the friends I have made through skating have been very supportive. I can't thank all of them enough for being people I could always turn to when I needed to vent or be distracted from the challenges of graduate school.

Next, I need to thank Rachel Ford, one of my roommates during my time here. She was always a great friend, and I'm thankful for the times we spent watching TV together, and going to the opera (and ARIA after parties) together. We may not have always been the best roommates together, but I've always appreciated her as a friend.

Scott and Silva Virgil are next on my list of people to thank. Scott has long been regarded as crucial for the scientific perspective for the synthetic chemistry labs at Caltech. He is always there to answer questions for us, or fix an instrument if needed. However, for me, I am much more thankful for his friendship and support, along with his wife, Silva. Their Christmas parties have always been a highlight of my year, and the times we've gone to the opera, often with others from Caltech, have been really special for me. They have both always been almost too nice to me, and I will always appreciate their kindness and support.

One of the most important people to me throughout graduate school was definitely Julie Hofstra. We became close friends working together on problem sets during our first year, and then became roommates. Julie was definitely my best friend at Caltech, and her friendship has always meant a lot to me. I always knew that she was just across the hall when I needed her in lab and in life. Our dinners together, whether we cooked or went out, were always important to me, and I always enjoyed talking with her about anything, whether chemistry related or not. We had a lot of amazing adventures

together, hiking, camping, shopping etc. Our trip up north to NOS and then down through the Sierras will always be a highlight of my time in California. I will also always appreciate her family taking me under their wing and inviting me to holiday dinners when I couldn't go home. I hope that we always remain friends.

Last, but certainly not least, I must thank my family. My brother, Daniel, has always been a supporter of me, and I must thank him for being a good friend throughout my life, even if I am somewhat jealous of his job and life. Most importantly, my parents have always been a great support to me, and I don't know how I could ever put in to words how much they mean to me. Even though they are most of the way across the country, I know they are always there when I need them. Even though we haven't been able to see each other much due to distance, I've appreciated all of the times they visited and spent time with me when I visited. I love them so much, and I know they return the sentiment, and their endless support my whole life is something I can never repay. Finally, I want to thank the rest of my extended family, who have also supported me and loved me throughout my whole life. I will always be thankful for all of the love my family has given to me.

My time at Caltech has had its ups and downs, but all of the support I've received from my friends and family have made it an amazing period in my life. I know that I will look back on this time with fondness, mostly due to the people I've spent it with. Without their support, I don't think I would have made it through grad school, and I can't thank them enough for that.

ABSTRACT

The Stoltz group, and moreover the synthetic community at large, has long been interested in the synthesis of enantioenriched compounds with interesting biological activities. This thesis presents three projects unified in an attempt to access compounds with relevance to the medicinal chemistry and natural products communities, encompassing reaction development, synthetic strategy and natural product synthesis.

A general method for the enantioselective synthesis of carbo- and heterocyclic carbonyl compounds bearing fluorinated α-tetrasubstituted stereocenters using palladium-catalyzed allylic alkylation is described. These fluorinated, stereochemically rich building blocks hold potential value in medicinal chemistry and are prepared using an orthogonal and enantioselective approach into such chiral moieties compared to traditional approaches, often without the use of electrophilic fluorinating reagents.

The synthesis of a variety of enantioenriched 2,2-disubstituted pyrrolidines is described. A stereogenic quaternary center is first formed utilizing an asymmetric allylic alkylation reaction of a benzyloxy imide, which can then be reduced to a chiral hydroxamic acid. This compound can then undergo a thermal "Spino" ring contraction to afford a carbamate protected 2,2-disubstituted pyrrolidine stereospecifically, allowing access to new molecules that could be useful in the medicinal chemistry community.

Finally, we have developed a synthesis of an enantioenriched [7,7]paracyclophane compound using sequential C-H functionalization reactions, including selective Rh-catalyzed C-H insertion reactions developed by the Davies group at Emory University. Investigations are currently ongoing into potential antimicrobial activity of different [7,7]paracyclophanes and the total synthesis of naturally occurring [7,7]paracyclophanes.

PUBLISHED CONTENT AND CONTRIBUTIONS

1. Lu, Y.; Goldstein, E. L.; Stoltz, B. M. "Palladium-Catalyzed Enantioselective Csp3–Csp3 Cross-Coupling for the Synthesis of (Poly)fluorinated Chiral Building Blocks" *Org. Lett.* **2018**, *20*, 5657–5660. DOI: 10.1021/acs.orglett.8b02369

   E.L.G. participated in project design, experimental work, and manuscript preparation.

2. Liu, W.; Ren, Z.; Bosse, A. T.; Liao, K.; Goldstein, E. L.; Bacsa, J.; Musaev, D.G.; Stoltz, B. M; Davies, H. M. L. "Catalyst-Controlled Selective Functionalization of Unactivated C–H Bonds in the Presence of Electronically Activated C–H Bonds" *J. Am. Chem. Soc.* **2018**, *140*, 12247–12255.
   DOI: 10.1021/jacs.8b07534

   E.L.G. participated in project design and manuscript preparation.

TABLE OF CONTENTS

Dedication iii
Acknowledgements iv
Abstract x
Published Content and Contributions xi
Table of Contents xii
List of Figures xv
List of Schemes xxii
List of Tables xxiv
List of Abbreviations xxvi

CHAPTER 1 ***1***
Palladium-Catalyzed Enantioselective Csp^3–Csp^3 Cross Coupling for the Synthesis of (Poly)fluorinated Chiral Building Blocks

1.1 Introduction 1
1.2 Synthesis of Fluorinated Allylic Alkylation Substrates 4
1.3 Initial Reaction Optimization 5
1.4 Exploration of Reaction Scope 6
1.5 Conclusions 9
1.6 Experimental Methods and Analytical Data 10
1.6.1 Materials and Methods 10
1.6.2 Experimental Procedures 12
1.6.3 Methods for the Determination of Enantiomeric Excess 39
1.7 Notes & References 41

APPENDIX 1 ***46***
Spectra Relevant to Chapter 1

CHAPTER 2 ***144***
Synthesis of enantioenriched 2,2-disubstitutedpyrrolidines via sequential asymmetric allylic alkylation and ring contraction

2.1 Introduction 144
2.2 Synthesis of Chiral Benzyloxyimides 146
2.3 Reduction of Benzyloxyimide to Hydroxamic Acid 152
2.4 Thermal Ring Contraction of Hydroxamic Acid 152
2.5 Reactions of Hydroxamic Acid Products 157

2.6 Conclusions 159
2.7 Experimental Methods and Analytical Data 160
2.7.1 Materials and Methods 160
2.7.2 Experimental Procedures 162
2.8 Notes & References 188

APPENDIX 2-1 ***190***
Spectra Relevant to Chapter 2

APPENDIX 2-2 ***239***
Progress Toward the Total Synthesis of Tylohirsuticine

A2-2.1 Introduction 239
A2-2.2 Original Retrosynthetic Analysis 242
A2-2.3 Substituted Allylic Alkylation Substrates 247
A2-2.4 Further Retrosynthetic Strategies 251
A2-2.5 Conclusions 253
A2-2.6 Notes & References 254

CHAPTER 3 ***256***
Synthesis of [7,7]paracyclophanes

3.1 Introduction 256
3.2 Retrosynthetic Analysis of Cylindrocyclophane A 259
3.3 Synthesis of [7,7]paracyclophane core 260
3.4 Conclusions 263
3.5 Experimental Section 264
3.5.1 Materials and Methods 264
3.5.2 Experimental Procedures 265
3.6 Notes & References 270

APPENDIX 3-1 ***273***
Spectra Relevant to Chapter 3

APPENDIX 3-2 ***282***
X-Ray Crystallography Reports Relevant to Chapter 3

A3-2.1 X-Ray Crystal Structure Analysis of Cyclophane **111** 283

APPENDIX 3-3 ***301***
Progress Toward the Synthesis of Cylindrocyclophane A

A3-3.1 Model Studies Toward Cylindrocyclophane A 301
A3-3.2 Progress Toward Cylindrocyclophane A 303
A3-3.3 Conclusions 307
A3-3.4 Notes & References 307

APPENDIX 4 ***309***
Notebook Cross-Reference for New Compounds

A4.1 Contents 309
A4.2 Notebook Cross Reference Tables 309

Comprehensive Bibliography 313
Index 323
About the Author 328

LIST OF FIGURES

CHAPTER 1

Palladium-Catalyzed Enantioselective Csp^3–Csp^3 Cross Coupling for the Synthesis of (Poly)fluorinated Chiral Building Blocks

Figure 1.1.1 Marketed Active Pharmaceutical Ingredients Bearing Fluorinated Tetrasubstitued Stereocenters 2

APPENDIX 1

Spectra Relevant to Chapter 1

Figure A1.1 ^{1}H NMR (500 MHz, $CDCl_3$) of compound **4a** 47
Figure A1.2 Infrared spectrum (Thin Film, NaCl) of compound **4a** 48
Figure A1.3 ^{13}C NMR (101 MHz, $CDCl_3$) of compound **4a** 48
Figure A1.4 ^{19}F NMR (282 MHz, $CDCl_3$) of compound **4a**. 49
Figure A1.5 ^{1}H NMR (500 MHz, $CDCl_3$) of compound **4b** 50
Figure A1.6 Infrared spectrum (Thin Film, NaCl) of compound **4b** 51
Figure A1.7 ^{13}C NMR (101 MHz, $CDCl_3$) of compound **4b** 51
Figure A1.8 ^{19}F NMR (282 MHz, $CDCl_3$) of compound **4b**. 52
Figure A1.9 ^{1}H NMR (500 MHz, $CDCl_3$) of compound **4c** 53
Figure A1.10 Infrared spectrum (Thin Film, NaCl) of compound **4c** 54
Figure A1.11 ^{13}C NMR (101 MHz, $CDCl_3$) of compound **4c** 54
Figure A1.12 ^{19}F NMR (282 MHz, $CDCl_3$) of compound **4c**. 55
Figure A1.13 ^{1}H NMR (500 MHz, $CDCl_3$) of compound **9** 56
Figure A1.14 Infrared spectrum (Thin Film, NaCl) of compound **9** 57
Figure A1.15 ^{13}C NMR (101 MHz, $CDCl_3$) of compound **9** 57
Figure A1.16 ^{1}H NMR (500 MHz, $CDCl_3$) of compound **10** 58
Figure A1.17 Infrared spectrum (Thin Film, NaCl) of compound **10** 59
Figure A1.18 ^{13}C NMR (101 MHz, $CDCl_3$) of compound **10** 59
Figure A1.19 ^{1}H NMR (500 MHz, $CDCl_3$) of compound **4d** 60
Figure A1.20 Infrared spectrum (Thin Film, NaCl) of compound **4d** 61
Figure A1.21 ^{13}C NMR (101 MHz, $CDCl_3$) of compound **4d** 61
Figure A1.22 ^{19}F NMR (282 MHz, $CDCl_3$) of compound **4d**. 62
Figure A1.23 ^{1}H NMR (500 MHz, $CDCl_3$) of compound **11** 63
Figure A1.24 Infrared spectrum (Thin Film, NaCl) of compound **11** 64
Figure A1.25 ^{13}C NMR (101 MHz, $CDCl_3$) of compound **11** 64
Figure A1.26 ^{19}F NMR (282 MHz, $CDCl_3$) of compound **11**. 65
Figure A1.27 ^{1}H NMR (500 MHz, $CDCl_3$) of compound **12** 66

Figure A1.28 Infrared spectrum (Thin Film, NaCl) of compound **12** 67
Figure A1.29 ^{13}C NMR (101 MHz, $CDCl_3$) of compound **12** 67
Figure A1.30 ^{19}F NMR (282 MHz, $CDCl_3$) of compound **12**. 68
Figure A1.31 ^{1}H NMR (500 MHz, $CDCl_3$) of compound **4e** 69
Figure A1.32 Infrared spectrum (Thin Film, NaCl) of compound **4e** 70
Figure A1.33 ^{13}C NMR (101 MHz, $CDCl_3$) of compound **4e** 70
Figure A1.34 ^{19}F NMR (282 MHz, $CDCl_3$) of compound **4e**. 71
Figure A1.35 ^{1}H NMR (500 MHz, $CDCl_3$) of compound **4g** 72
Figure A1.36 Infrared spectrum (Thin Film, NaCl) of compound **4g** 73
Figure A1.37 ^{13}C NMR (101 MHz, $CDCl_3$) of compound **4g** 73
Figure A1.38 ^{19}F NMR (282 MHz, $CDCl_3$) of compound **4g**. 74
Figure A1.39 ^{1}H NMR (500 MHz, $CDCl_3$) of compound **4h** 75
Figure A1.40 Infrared spectrum (Thin Film, NaCl) of compound **4h** 76
Figure A1.41 ^{13}C NMR (101 MHz, $CDCl_3$) of compound **4h** 76
Figure A1.42 ^{19}F NMR (282 MHz, $CDCl_3$) of compound **4h**. 77
Figure A1.43 ^{1}H NMR (500 MHz, $CDCl_3$) of compound **15** 78
Figure A1.44 Infrared spectrum (Thin Film, NaCl) of compound **15** 79
Figure A1.45 ^{13}C NMR (101 MHz, $CDCl_3$) of compound **15** 79
Figure A1.46 ^{19}F NMR (282 MHz, $CDCl_3$) of compound **15**. 80
Figure A1.47 ^{1}H NMR (500 MHz, $CDCl_3$) of compound **4i** 81
Figure A1.48 Infrared spectrum (Thin Film, NaCl) of compound **4i** 82
Figure A1.49 ^{13}C NMR (101 MHz, $CDCl_3$) of compound **4i** 82
Figure A1.50 ^{19}F NMR (282 MHz, $CDCl_3$) of compound **4i**. 83
Figure A1.51 ^{1}H NMR (500 MHz, $CDCl_3$) of compound **4j** 84
Figure A1.52 Infrared spectrum (Thin Film, NaCl) of compound **4j** 85
Figure A1.53 ^{13}C NMR (101 MHz, $CDCl_3$) of compound **4j** 85
Figure A1.54 ^{19}F NMR (282 MHz, $CDCl_3$) of compound **4j**. 86
Figure A1.55 ^{1}H NMR (500 MHz, $CDCl_3$) of compound **4k** 87
Figure A1.56 Infrared spectrum (Thin Film, NaCl) of compound **4k** 88
Figure A1.57 ^{13}C NMR (101 MHz, $CDCl_3$) of compound **4k** 88
Figure A1.58 ^{19}F NMR (282 MHz, $CDCl_3$) of compound **4k**. 89
Figure A1.59 ^{1}H NMR (500 MHz, $CDCl_3$) of compound **17** 90
Figure A1.60 Infrared spectrum (Thin Film, NaCl) of compound **17** 91
Figure A1.61 ^{13}C NMR (101 MHz, $CDCl_3$) of compound **17** 91
Figure A1.62 ^{19}F NMR (282 MHz, $CDCl_3$) of compound **17**. 92
Figure A1.63 ^{1}H NMR (500 MHz, $CDCl_3$) of compound **4l** 93
Figure A1.64 Infrared spectrum (Thin Film, NaCl) of compound **4l** 94
Figure A1.65 ^{13}C NMR (101 MHz, $CDCl_3$) of compound **4l** 94

Figure A1.66 ^{19}F NMR (282 MHz, $CDCl_3$) of compound **4l**. 95
Figure A1.67 ^{1}H NMR (500 MHz, $CDCl_3$) of compound **4m** 96
Figure A1.68 Infrared spectrum (Thin Film, NaCl) of compound **4m** 97
Figure A1.69 ^{13}C NMR (101 MHz, $CDCl_3$) of compound **4m**..... 97
Figure A1.70 ^{19}F NMR (282 MHz, $CDCl_3$) of compound **4m**. 68
Figure A1.71 ^{1}H NMR (500 MHz, $CDCl_3$) of compound **4n** 99
Figure A1.72 Infrared spectrum (Thin Film, NaCl) of compound **4n** 100
Figure A1.73 ^{13}C NMR (101 MHz, $CDCl_3$) of compound **4n**..... 100
Figure A1.74 ^{19}F NMR (282 MHz, $CDCl_3$) of compound **4n**. 101
Figure A1.75 ^{1}H NMR (500 MHz, $CDCl_3$) of compound **5a**..... 102
Figure A1.76 Infrared spectrum (Thin Film, NaCl) of compound **5a** 103
Figure A1.77 ^{13}C NMR (101 MHz, $CDCl_3$) of compound **5a**..... 103
Figure A1.78 ^{19}F NMR (282 MHz, $CDCl_3$) of compound **5a**. 104
Figure A1.79 ^{1}H NMR (500 MHz, $CDCl_3$) of compound **5b** 105
Figure A1.80 Infrared spectrum (Thin Film, NaCl) of compound **5b** 106
Figure A1.81 ^{13}C NMR (101 MHz, $CDCl_3$) of compound **5b**..... 106
Figure A1.82 ^{19}F NMR (282 MHz, $CDCl_3$) of compound **5b**. 107
Figure A1.83 ^{1}H NMR (500 MHz, $CDCl_3$) of compound **5c**..... 108
Figure A1.84 Infrared spectrum (Thin Film, NaCl) of compound **5c** 109
Figure A1.85 ^{13}C NMR (101 MHz, $CDCl_3$) of compound **5c**..... 109
Figure A1.86 ^{19}F NMR (282 MHz, $CDCl_3$) of compound **5c**. 110
Figure A1.87 ^{1}H NMR (500 MHz, $CDCl_3$) of compound **5d** 111
Figure A1.88 Infrared spectrum (Thin Film, NaCl) of compound **5d** 112
Figure A1.89 ^{13}C NMR (101 MHz, $CDCl_3$) of compound **5d**..... 112
Figure A1.90 ^{19}F NMR (282 MHz, $CDCl_3$) of compound **5d**. 113
Figure A1.91 ^{1}H NMR (500 MHz, $CDCl_3$) of compound **5e**..... 114
Figure A1.92 Infrared spectrum (Thin Film, NaCl) of compound **5e** 115
Figure A1.93 ^{13}C NMR (101 MHz, $CDCl_3$) of compound **5e**..... 115
Figure A1.94 ^{19}F NMR (282 MHz, $CDCl_3$) of compound **5e**. 116
Figure A1.95 ^{1}H NMR (500 MHz, $CDCl_3$) of compound **5f** 117
Figure A1.96 Infrared spectrum (Thin Film, NaCl) of compound **5f**..... 118
Figure A1.97 ^{13}C NMR (101 MHz, $CDCl_3$) of compound **5f**..... 118
Figure A1.98 ^{19}F NMR (282 MHz, $CDCl_3$) of compound **5f**. 119
Figure A1.99 ^{1}H NMR (500 MHz, $CDCl_3$) of compound **5g**..... 120
Figure A1.100 Infrared spectrum (Thin Film, NaCl) of compound **5g** 121
Figure A1.101 ^{13}C NMR (101 MHz, $CDCl_3$) of compound **5g**..... 121
Figure A1.102 ^{19}F NMR (282 MHz, $CDCl_3$) of compound **5g**. 122
Figure A1.103 ^{1}H NMR (500 MHz, $CDCl_3$) of compound **5h** 123

Figure A1.104 Infrared spectrum (Thin Film, NaCl) of compound **5h** 124
Figure A1.105 ^{13}C NMR (101 MHz, $CDCl_3$) of compound **5h**..... 124
Figure A1.106 ^{19}F NMR (282 MHz, $CDCl_3$) of compound **5h**. 125
Figure A1.107 ^{1}H NMR (500 MHz, $CDCl_3$) of compound **5i** 126
Figure A1.108 Infrared spectrum (Thin Film, NaCl) of compound **5i** 127
Figure A1.109 ^{13}C NMR (101 MHz, $CDCl_3$) of compound **5i**..... 127
Figure A1.110 ^{19}F NMR (282 MHz, $CDCl_3$) of compound **5i**. 128
Figure A1.111 ^{1}H NMR (500 MHz, $CDCl_3$) of compound **5j** 129
Figure A1.112 Infrared spectrum (Thin Film, NaCl) of compound **5j** 130
Figure A1.113 ^{13}C NMR (101 MHz, $CDCl_3$) of compound **5j**..... 130
Figure A1.114 ^{19}F NMR (282 MHz, $CDCl_3$) of compound **5j**. 131
Figure A1.115 ^{1}H NMR (500 MHz, $CDCl_3$) of compound **5k**..... 132
Figure A1.116 Infrared spectrum (Thin Film, NaCl) of compound **5k** 133
Figure A1.117 ^{13}C NMR (101 MHz, $CDCl_3$) of compound **5k**..... 133
Figure A1.118 ^{19}F NMR (282 MHz, $CDCl_3$) of compound **5k**. 134
Figure A1.119 ^{1}H NMR (500 MHz, $CDCl_3$) of compound **5l** 135
Figure A1.120 Infrared spectrum (Thin Film, NaCl) of compound **5l** 136
Figure A1.121 ^{13}C NMR (101 MHz, $CDCl_3$) of compound **5l**..... 136
Figure A1.122 ^{19}F NMR (282 MHz, $CDCl_3$) of compound **5l**. 137
Figure A1.123 ^{1}H NMR (500 MHz, $CDCl_3$) of compound **5m** 138
Figure A1.124 Infrared spectrum (Thin Film, NaCl) of compound **5m** 139
Figure A1.125 ^{13}C NMR (101 MHz, $CDCl_3$) of compound **5m**..... 139
Figure A1.126 ^{19}F NMR (282 MHz, $CDCl_3$) of compound **5m**. 140
Figure A1.127 ^{1}H NMR (500 MHz, $CDCl_3$) of compound **5n** 141
Figure A1.128 Infrared spectrum (Thin Film, NaCl) of compound **5n** 142
Figure A1.129 ^{13}C NMR (101 MHz, $CDCl_3$) of compound **5n**..... 142
Figure A1.130 ^{19}F NMR (282 MHz, $CDCl_3$) of compound **5n**. 143

CHAPTER 2
Synthesis of enantioenriched 2,2-disubstitutedpyrrolidines via sequential asymmetric allylic alkylation and ring contraction

Figure 2.1.1 Pharmaceutical compounds containing chiral pyrrolidines 145

APPENDIX 2
Spectra Relevant to Chapter 2

Figure A2-1.1 ^{1}H NMR (400 MHz, $CDCl_3$) of compound **28c**..... 191
Figure A2-1.2 Infrared spectrum (Thin Film, NaCl) of compound **28c** 192

Figure A2-1.3 ^{13}C NMR (101 MHz, $CDCl_3$) of compound **28c** 192
Figure A2-1.4 ^{1}H NMR (400 MHz, $CDCl_3$) of compound **29c** 193
Figure A2-1.5 Infrared spectrum (Thin Film, NaCl) of compound **29c** 194
Figure A2-1.6 ^{13}C NMR (101 MHz, $CDCl_3$) of compound **29c** 194
Figure A2-1.7 ^{1}H NMR (400 MHz, $CDCl_3$) of compound **34a** 195
Figure A2-1.8 Infrared spectrum (Thin Film, NaCl) of compound **34a** 196
Figure A2-1.9 ^{13}C NMR (101 MHz, $CDCl_3$) of compound **34a** 196
Figure A2-1.10 ^{1}H NMR (400 MHz, $CDCl_3$) of compound **34b** 197
Figure A2-1.11 Infrared spectrum (Thin Film, NaCl) of compound **34b** 198
Figure A2-1.12 ^{13}C NMR (101 MHz, $CDCl_3$) of compound **34b** 198
Figure A2-1.13 ^{1}H NMR (400 MHz, $CDCl_3$) of compound **34c** 199
Figure A2-1.14 Infrared spectrum (Thin Film, NaCl) of compound **34c** 200
Figure A2-1.15 ^{13}C NMR (101 MHz, $CDCl_3$) of compound **34c** 200
Figure A2-1.16 ^{1}H NMR (400 MHz, $CDCl_3$) of compound **34d** 201
Figure A2-1.17 Infrared spectrum (Thin Film, NaCl) of compound **34d** 202
Figure A2-1.18 ^{13}C NMR (101 MHz, $CDCl_3$) of compound **34d** 202
Figure A2-1.19 ^{19}F NMR (282 MHz, $CDCl_3$) of compound **34d**. 203
Figure A2-1.20 ^{1}H NMR (400 MHz, $CDCl_3$) of compound **35a** 204
Figure A2-1.21 Infrared spectrum (Thin Film, NaCl) of compound **35a** 205
Figure A2-1.22 ^{13}C NMR (101 MHz, $CDCl_3$) of compound **35a** 205
Figure A2-1.23 ^{1}H NMR (400 MHz, $CDCl_3$) of compound **35b** 206
Figure A2-1.24 Infrared spectrum (Thin Film, NaCl) of compound **35b** 207
Figure A2-1.25 ^{13}C NMR (101 MHz, $CDCl_3$) of compound **35b** 207
Figure A2-1.26 ^{1}H NMR (400 MHz, $CDCl_3$) of compound **35c** 208
Figure A2-1.27 Infrared spectrum (Thin Film, NaCl) of compound **35c** 209
Figure A2-1.28 ^{13}C NMR (101 MHz, $CDCl_3$) of compound **35c** 209
Figure A2-1.29 ^{1}H NMR (400 MHz, $CDCl_3$) of compound **35d** 210
Figure A2-1.30 Infrared spectrum (Thin Film, NaCl) of compound **35d** 211
Figure A2-1.31 ^{13}C NMR (101 MHz, $CDCl_3$) of compound **35d** 211
Figure A2-1.32 ^{19}F NMR (282 MHz, $CDCl_3$) of compound **35d**. 212
Figure A2-1.33 ^{1}H NMR (400 MHz, $CDCl_3$) of compound **30a** 213
Figure A2-1.34 Infrared spectrum (Thin Film, NaCl) of compound **30a** 214
Figure A2-1.35 ^{13}C NMR (101 MHz, $CDCl_3$) of compound **30a** 214
Figure A2-1.36 ^{1}H NMR (400 MHz, $CDCl_3$) of compound **30b** 215
Figure A2-1.37 Infrared spectrum (Thin Film, NaCl) of compound **30b** 216
Figure A2-1.38 ^{13}C NMR (101 MHz, $CDCl_3$) of compound **30b** 216
Figure A2-1.39 ^{1}H NMR (400 MHz, $CDCl_3$) of compound **30c** 217
Figure A2-1.40 Infrared spectrum (Thin Film, NaCl) of compound **30c** 218

Figure A2-1.41 ^{13}C NMR (101 MHz, $CDCl_3$) of compound **30c** 218
Figure A2-1.42 ^{1}H NMR (400 MHz, $CDCl_3$) of compound **30d** 219
Figure A2-1.43 Infrared spectrum (Thin Film, NaCl) of compound **30d** 220
Figure A2-1.44 ^{13}C NMR (101 MHz, $CDCl_3$) of compound **30d** 220
Figure A2-1.45 ^{19}F NMR (282 MHz, $CDCl_3$) of compound **30d**. 221
Figure A2-1.46 ^{1}H NMR (400 MHz, $CDCl_3$) of compound **31a** 222
Figure A2-1.47 Infrared spectrum (Thin Film, NaCl) of compound **31a** 223
Figure A2-1.48 ^{13}C NMR (101 MHz, $CDCl_3$) of compound **31a** 223
Figure A2-1.49 ^{1}H NMR (400 MHz, $CDCl_3$) of compound **31b** 224
Figure A2-1.50 Infrared spectrum (Thin Film, NaCl) of compound **31b** 225
Figure A2-1.51 ^{13}C NMR (101 MHz, $CDCl_3$) of compound **31b** 225
Figure A2-1.52 ^{1}H NMR (400 MHz, $CDCl_3$) of compound **31c** 226
Figure A2-1.53 Infrared spectrum (Thin Film, NaCl) of compound **31c** 227
Figure A2-1.54 ^{13}C NMR (101 MHz, $CDCl_3$) of compound **31c** 227
Figure A2-1.55 ^{1}H NMR (400 MHz, $CDCl_3$) of compound **31d** 228
Figure A2-1.56 Infrared spectrum (Thin Film, NaCl) of compound **31d** 229
Figure A2-1.57 ^{13}C NMR (101 MHz, $CDCl_3$) of compound **31d** 229
Figure A2-1.58 ^{1}H NMR (400 MHz, $CDCl_3$) of compound **31e** 230
Figure A2-1.59 Infrared spectrum (Thin Film, NaCl) of compound **31e** 231
Figure A2-1.60 ^{13}C NMR (101 MHz, $CDCl_3$) of compound **31e** 231
Figure A2-1.61 ^{1}H NMR (400 MHz, $CDCl_3$) of compound **31f** 232
Figure A2-1.62 Infrared spectrum (Thin Film, NaCl) of compound **31f** 233
Figure A2-1.63 ^{13}C NMR (101 MHz, $CDCl_3$) of compound **31f** 233
Figure A2-1.64 ^{19}F NMR (282 MHz, $CDCl_3$) of compound **31f**. 234
Figure A2-1.65 ^{1}H NMR (400 MHz, $CDCl_3$) of compound **41** 235
Figure A2-1.66 Infrared spectrum (Thin Film, NaCl) of compound **41** 236
Figure A2-1.67 ^{13}C NMR (101 MHz, $CDCl_3$) of compound **41** 236
Figure A2-1.68 ^{1}H NMR (400 MHz, $CDCl_3$) of compound **40** 237
Figure A2-1.69 Infrared spectrum (Thin Film, NaCl) of compound **40** 238
Figure A2-1.70 ^{13}C NMR (101 MHz, $CDCl_3$) of compound **40** 238

APPENDIX 2-2

Progress Toward the Total Synthesis of Tylohirsuticine

Figure A2-2.1.1 Phenanthroindolizidine alkaloids 240

CHAPTER 3
Synthesis of [7,7]paracyclophanes

Figure 3.1.1 Structure of Cyclophanes 256
Figure 3.1.2 Structures of [7,7]paracyclophanes 257

APPENDIX 3-1
Spectra Relevant to Chapter 3

Figure A3-1.1 ^{1}H NMR (600 MHz, $CDCl_3$) of compound **108** 370
Figure A3-1.2 ^{13}C NMR (125 MHz, $CDCl_3$) of compound **108**..... 371
Figure A3-1.3 ^{19}F NMR (282 MHz, $CDCl_3$) of compound **108**. 234
Figure A3-1.4 ^{1}H NMR (600 MHz, $CDCl_3$) of compound **109** 370
Figure A3-1.5 ^{13}C NMR (125 MHz, $CDCl_3$) of compound **109**..... 371
Figure A3-1.6 ^{19}F NMR (282 MHz, $CDCl_3$) of compound **109**. 234
Figure A3-1.7 ^{1}H NMR (600 MHz, $CDCl_3$) of compound **110** 370
Figure A3-1.8 ^{13}C NMR (125 MHz, $CDCl_3$) of compound **110**..... 371
Figure A3-1.9 ^{19}F NMR (282 MHz, $CDCl_3$) of compound **110**. 234
Figure A3-1.10 ^{1}H NMR (600 MHz, $CDCl_3$) of compound **111** 370
Figure A3-1.11 ^{13}C NMR (125 MHz, $CDCl_3$) of compound **111**..... 371
Figure A3-1.12 ^{19}F NMR (282 MHz, $CDCl_3$) of compound **111** 234

APPENDIX 3-2
X-Ray Crystallography Reports Relevant to Chapter 3

Figure A5.1 X-ray crystal structure of cyclophane **111** 285

LIST OF SCHEMES

CHAPTER 1

Palladium-Catalyzed Enantioselective Csp^3–Csp^3 Cross Coupling for the Synthesis of (Poly)fluorinated Chiral Building Blocks

Scheme 1.1.1 Asymmetric Construction of Fluorine-Containing α-Tetrasubstitued Ketones ... 3

Scheme 1.2.1 Synthesis of Fluorinated β-Ketoesters ... 5

CHAPTER 2

Synthesis of enantioenriched 2,2-disubstitutedpyrrolidines via sequential asymmetric allylic alkylation and ring contraction

Scheme 2.1.1 Synthesis of tetrasubstituted proline derivatives by Seebach et al. ... 146

Scheme 2.1.2 Proposed synthesis of chiral 2,2-disubstituted pyrrolidines ... 146

Scheme 2.2.1 Progression of the asymmetric allylic alkylation reaction in the Stoltz laboratory ... 148

Scheme 2.2.2 Synthesis of β-amidoesters ... 149

Scheme 2.3.1 Synthesis of chiral hydroxamic acids ... 152

Scheme 2.4.1 Ring contraction reactions as reported by Spino et al. ... 153

Scheme 2.4.2 Thermal ring contraction of chiral hydroxamic acid ... 154

Scheme 2.4.3 Investigation of stereochemistry ... 157

Scheme 2.5.1 Retrosynthetic analysis of tylohirsuticine. ... 158

Scheme 2.5.2 N–alkylation of chiral pyrrolidine ... 159

APPENDIX 2-2

Progress Toward the Total Synthesis of Tylohirsuticine

Scheme A2-2.1.1 Synthesis of septicine by Reddy et al. ... 241

Scheme A2-2.1.2 Synthesis of hypoestatin 1 by Ishibashi and Wang. ... 242

Scheme A2-2.2.1 Retrosynthetic analysis of tylohirsuticine. ... 243

Scheme A2-2.2.2 Proposed epoxidation strategy. ... 244

Scheme A2-2.2.3 Dihydroxylation of the olefin. ... 245

Scheme A2-2.2.4 Plan for the installation of the final ring. ... 245

Scheme A2-2.3.1 Revised retrosynthetic analysis. ... 247

Scheme A2-2.3.2 Synthesis of 2–allyl substituted asymmetric allylic alkylation substrate. ... 248

Scheme A2-2.3.2 Selective reduction of imide ... 249

Scheme A2-2.3.4 Alternative retrosynthetic proposal ... 250

Scheme A2-2.3.5 Synthesis of 2–chloroallyl asymmetric allylic alkylation substrate.... 250

Scheme A2-2.4.1 Alternative retrosynthetic proposal 252
Scheme A2-2.4.2 Synthesis of aryl ketone compound. 252
Scheme A2-2.4.3 Synthesis of aldehyde compounds 253
Scheme A2-2.4.4 Synthesis of 2–allyl substituted pyrrolidine compound 253

CHAPTER 3
Synthesis of [7,7]paracyclophanes

Scheme 3.1.1 Previous synthetic strategies toward cylindrocyclophanes 259
Scheme 3.2.1 Retrosynthetic proposal for cylindrocyclophane A 260
Scheme 3.3.1 Development of C-H insertion reaction 261
Scheme 3.3.2 Synthesis of [7,7]paracyclophane 263

APPENDIX 3-3
Progress Toward the Synthesis of Cylindrocyclophane A

Scheme A3-3.1.1 Investigation of acetoxylation reaction 302
Scheme A3-3.1.2 Oxidative Decarboxylation Reaction 303
Scheme A3-3.2.1 Retrosynthetic proposal for cylindrocyclophane A 304
Scheme A3-3.2.2 Synthesis of a [7,7]paracyclophane enroute toward cylindrocyclophane A 305
Scheme A3-3.2.3 Investigation of acetoxylation toward cylindrocyclophane A 306
Scheme A3-3.2.4 Optimization of tetraacetoxylation reaction 307

LIST OF TABLES

CHAPTER 1

Palladium-Catalyzed Enantioselective Csp^3–Csp^3 Cross Coupling for the Synthesis of (Poly)fluorinated Chiral Building Blocks

Table 1.3.1 Optimization of Conditions for Enantioselective Palladium-Catalyzed Allyllic Alkylation 6

Table 1.4.1 Substrate Scope of Fluorine-Containing compounds in Enantioselective Allylic Alkylation 9

Table 1.6.3 Methods for the Determination of Enantiomeric Excess 39

CHAPTER 2

Synthesis of enantioenriched 2,2-disubstitutedpyrrolidines via sequential asymmetric allylic alkylation and ring contraction

Table 2.2.1 Asymmetric allylic alkylation optimization 150

Table 2.2.2 Scope of the asymmetric allylic alkylation reaction 151

Table 2.4.1 Removal of methyl carbamate group 155

Table 2.4.2 Synthesis of chiral 2,2-disubstituted pyrrolidines 156

Table 2.5.1 Optimization of ring-closing metathesis 159

APPENDIX 2-2

Progress Toward the Total Synthesis of Tylohirsuticine

Table A2-2.2.1 Investigation of Heck conditions 243

Table A2-2.2.2 Bromination of the olefin 244

Table A2-2.2.3 Epoxidation of the olefin 245

Table A2-2.2.4 Hydroxylation of the olefin 246

Table A2-2.2.5 Oxidation of the alcohol 247

Table A2-2.3.1 Asymmetric allylic alkylation reaction of 2–allyl substituted substrate 249

Table A2-2.3.2 Asymmetric allylic alkylation reaction of 2–chloroallyl substrate 251

APPENDIX 3-2

X-Ray Crystallography Reports Relevant to Chapter 4

Table A3-2.1.1 Fractional Atomic Coordinates ($x10^4$) and Equivalent Isotropic Displacement Parameters ($Å^2x10^3$) for Aaron-macrocycle_P2. U_{eq} is defined as 1/3 of the trace of the orthogonalised U_{ij}. 288

Table A3-2.1.2 Fractional Atomic Coordinates ($x10^4$) Aaron-macrocycle_P2. The anisotropic displacement factor exponent takes the form: $-2\ ^2[h^2a^{*2} \times U_{11}+\ldots 2hka^* \times b^* \times U_{12}]$ 290

Table A3-2.1.3 Bond Lengths in Å for Aaron-macrocycle_P2 291

Table A3-2.1.4 Bond Angles in ° for Aaron-macrocycle_P2 292

Table A3-2.1.5 Torsion Angles in ° for Aaron-macrocycle_P2 293

Table A3-2.1.6 Hydrogen Fractional Atomic Coordinates ($x10^4$) and Equivalent Isotropic Displacement Parameters ($Å^2x10^3$) for Aaron-macrocycle_P2. U_{eq} is defined as 1/3 of the trace of the orthogonalised U_{ij}. 297

APPENDIX 4

Notebook Cross-Reference for New Compounds

Table A4.2.1 Notebook cross-reference for compounds in Chapter 1 309

Table A4.2.2 Notebook cross-reference for compounds in Chapter 2 311

LIST OF ABBREVIATIONS

$[\alpha]_D$	specific rotation at wavelength of sodium D line
°C	degrees Celsius
Å	Ångstrom
Ac	acetyl
AcOH	acetic acid
APCI	atmospheric pressure chemical ionization
app	apparent
aq	aqueous
Ar	aryl
9-BBN	9-Borabicyclo[3.3.1]nonane
Bn	benzyl
Boc	*tert*-butyloxycarbonyl
bp	boiling point
br	broad
Bu	butyl
Bz	benzoyl
c	concentration for specific rotation measurements (g/100 mL)
calc'd	calculated
cat	catalytic
Cbz	benzyloxycarbonyl
CDI	1,1'-carbonyldiimidazole
cm^{-1}	wavenumber(s)
d	doublet
dba	dibenzylideneacetone
DBU	1,8-diazabicyclo[5.4.0]undec-7-ene
DIBAL	diisobutylaluminum hydride

DIPEA	*N,N*-diisopropylethylamine
DMF	*N*,*N*-dimethylformamide
DMP	Dess–Martin periodinane
dmphen	2,9-dimethyl-1,10-phenanthroline
DMS	dimethyl sulfide
DMSO	dimethyl sulfoxide
dr	diastereomeric ratio
e.g.	for example (Latin exempli gratia)
ee	enantiomeric excess
EI+	electron impact
equiv	equivalent(s)
ESI	electrospray ionization
Et	ethyl
et al.	and others (Latin et alia)
EtOAc	ethyl acetate
FAB	fast atom bombardment
FDA	food and drug administration
g	gram(s)
Gly	glycine
h	hour(s)
HATU	hexafluorophosphate azabenzotriazole tetramethyl uronium
HFIP	hexafluoroisopropanol
HMDS	1,1,1,3,3,3-hexamethyldisilazane
HPLC	high-performance liquid chromatography
HRMS	high-resolution mass spectroscopy
Hz	hertz
$h\nu$	light
i-Pr	isopropyl

i.e.	that is (Latin id est)
IPA	isopropanol, 2-propanol
IR	infrared (spectroscopy)
IUPAC	International union of pure and applied chemistry
J	coupling constant
kcal	kilocalorie
L	liter; ligand
LCMS	Liquid chromatography/mass spectrometry
LDA	lithium diisopropylamide
LiHMDS	lithium hexamethyldisilazide
m	multiplet; milli
m	meta
M	metal; molar; molecular ion
m-CPBA	*meta*-chloroperoxybenzoic acid
m/z	mass to charge ratio
Me	methyl
mg	milligram(s)
MHz	megahertz
MIC	minimum inhibitory concentration
min	minute(s)
mol	mole(s)
mp	melting point
MRSA	Methicillin-resistant Staphylococcus aureus
Ms	methanesulfonyl (mesyl)
MS	molecular sieves
n	nano
N	normal
n-Bu	butyl
NBS	*N*-bromosuccinimide

NMM	N-methylmorpholine
NMO	*N*-methylmorpholine *N*-oxide
NMR	nuclear magnetic resonance
o	ortho
p	para; pentet
PCC	pyridimiun chlorochromate
Ph	phenyl
pH	hydrogen ion concentration in aqueous solution
PHOX	phosphinooxazoline ligand
pin	2,3-dimethylbutane-2,3-diol (pinacol)
pmdba	bis(4-methoxybenzylidene)acetone
ppm	parts per million
Py	pyridine
q	quartet
R	generic for any atom or functional group
RCM	ring-closing metathesis
Ref.	reference
R_f	retention factor
r.r.	regiomeric ratio
s	singlet or strong or selectivity factor
SAR	structure activity relationship
sat.	saturated
SFC	supercritical fluid chromatography
t	triplet
t-Bu	*tert*-butyl
TBAT	tetrabutylammonium difluorotriphenylsilicate
TBHP	*tert*-butyl hydroperoxide
TBME	*tert*-butyl methyl ether
TBS	*tert*-butyldimethylsilyl

Tf	trifluoromethanesulfonyl (triflyl)
TFA	trifluoroacetic acid
TFAA	trifluoroacetic anhydride
THF	tetrahydrofuran
TLC	thin-layer chromatography
TOF	time-of-flight
Tol	tolyl
TPCP	1,2,2-triphenylcyclopropane carboxylate
UHP	urea hydrogen peroxide
UV	ultraviolet
λ	wavelength
μ	micro

CHAPTER 1

Palladium-Catalyzed Enantioselective Csp^3–Csp^3 Cross-Coupling for the Synthesis of (Poly)fluorinated Chiral Building Blocks[*]

1.1 INTRODUCTION:

Organofluorine compounds often play a critical role in the lead optimization phase of drug discovery, due to their impact on various physico-chemical properties such as absorption, distribution, metabolitic stability, and excretion. Consequently, more than 20% of marketed pharmaceuticals contain C–F motifs, despite the fact that organofluorinated compounds are exceedingly rare in nature.[1] Recently, molecules with tetrasubstituted stereocenters have attracted the interest of medicinal chemists aiming to incorporate three-dimensionality and added novelty.[2] Importantly, there are many successful marketed pharmaceuticals bearing fluorinated tetrasubstituted stereocenters (**1–3**, Figure 1.1.1). For these reasons, there has been renewed interest in the synthesis of fluorinated tetrasubstituted stereocenters for use in drug discovery, and in particular, access to new classes of fluorinated analogs. Therefore, we believe that a general method

[*] This research was performed in collaboration with Yanhui Lu, an alumni of the Stoltz group. Additionally, this research has been published and adapted with permission Lu, Y.; Goldstein, E. L.; Stoltz, B. M. *Org. Lett.* **2018**, *20*, 5657–5660.

for the construction of fluorine-containing tetrasubstituted stereocenters will be of particular interest to chemists in the area of drug discovery and development.

Figure 1.1.1. Marketed Active Pharmaceutical Ingredients Bearing Fluorinated Tetrasubstitued Stereocenters.

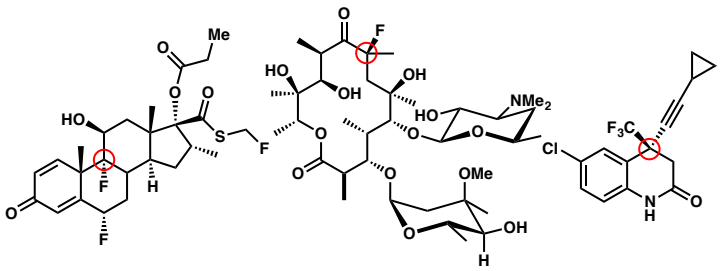

Fluticasone propionate (1) ***Flurithromycin (2)*** ***Efavirenz (3)***

Methods to construct fluorine-containing α-tetrasubstituted ketones have been the subject of intense investigation over the past decade. The most prevalent strategy for fluorine incorporation is intermolecular catalytic asymmetric electrophilic fluorination (or trifluoromethylation) of enolates (Scheme 1.1.1A).[3] Despite their potential utility in organic synthesis, the relatively low abundance of cheap, commercially available electrophilic fluorinating and trifluoromethylating reagents prohibit their widespread usage. As far back as 2005, the Stoltz and Nakamura groups independently reported the intramolecular asymmetric allylic alkylation of prochiral enolates derived from the decarboxylation of 1,3-dicarbonyl substrates (Scheme 1.1.1B).[4,5] Using this strategy, several optically active α-fluoro α-tetrasubstitued cyclic carbonyl derivatives have been synthesized in high yield and enantioselectivity.

While stereogenic C–F moieties have been previously investigated, the compatibility of fluoroalkyl groups in palladium-catalyzed asymmetric allylic alkylation has remained unknown until recently. In 2011, Shibata and coworkers reported the first

example of the construction of trifluoromethyl-bearing quaternary centers by intramolecular decarboxylative allylic alkylation of α-trifluoromethyl β−ketoesters (Scheme 1.1.1C).[6] Unfortunately, attempts to render their reaction enantioselective were unsuccessful. Due to our interest in the field of asymmetric allylic alkylation, we endeavored to build on these previous reports and investigate a number of fluoroalkyl and fluoroallyl derivatives in asymmetric allylic alkylation reactions. Herein, we report the first general method for the construction of carbo- and heterocyclic carbonyl derivatives bearing α-fluoro-, α-fluoroalkyl-, or α-(2-fluoro)allyl substituents using palladium-catalyzed enantioselective decarboxylative allylic alkylation (Scheme 1.1.1D).

Scheme 1.1.1. Asymmetric Construction of Fluorine-Containing α-Tetrasubstitued Ketones

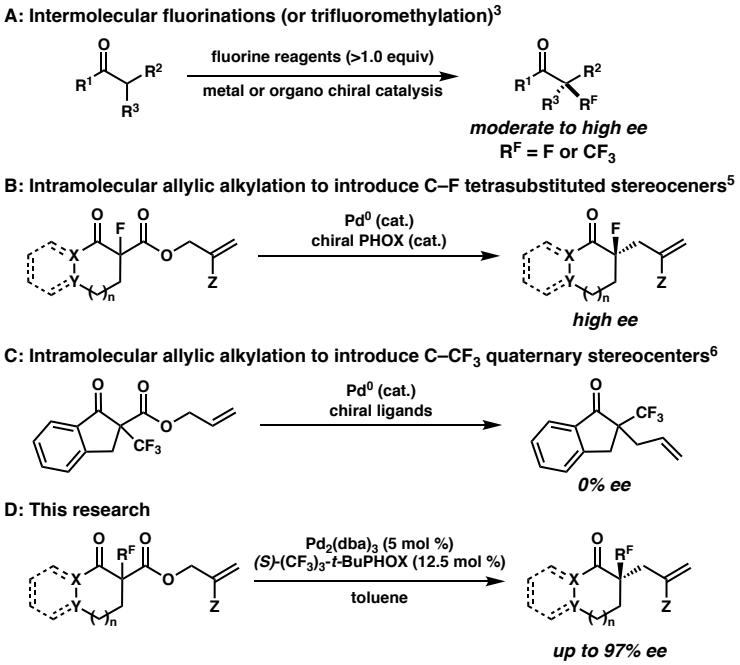

1.2. SYNTHESIS OF FLUORINATED ALLYLIC ALKYLATION SUBSTRATES

Importantly, with this strategy, a number of fluorinated alkyl and allyl groups are introduced into the substrate via standard 1,3-dicarbonyl chemistry (thermal, acidic or basic conditions) to produce racemic mixtures of compounds that serve as substrates for the mild and neutral asymmetric allylic alkylation reaction. In some cases, these fluorinated substrates are synthesized without the use of electrophilic fluorinating reagents. Furthermore, this allows for the non-asymmetric formation of the C–F or C–CF_3 bonds, which are significantly more developed than their asymmetric equivalents. For example, 1,1,1,-trifluoropropyl groups can be installed using standard β−keto ester alkylation conditions utilizing 1,1,1-trifluoropropyl iodide and base in moderate yields (Scheme 1.2.1A). The synthesis of 1,1,1-trifluoroethyl substituted β−keto esters proceeded smoothly with the use of 2,2,2-Trifluoroethyl (mesityl)iodonium trifluoromethanesulfonate[7] (available in 2 steps from commercial materials) in the presence of LiHMDS. (Scheme 1.2.1B) During the preparation of this manuscript, a report using 2,2,2-Trifluoroethyl(mesityl) iodonium trifluoromethanesulfonate for the alkylation of 1,3-dicarbonyls was disclosed using similar conditions.[8]

In addition to α-fluoroalkyl groups, a number of 2-fluoro allyl substrates were prepared without the use of electrophilic fluorinating reagents. Starting from commercially available Methyl 2-fluoroacrylate, reduction of the ester to the alcohol, followed by treatment with 1,1'-carbonyldiimidazole (CDI) resulting in the formation of an acylating reagent (Scheme 1.2.1C). This reagent could then be used as previously reported[9] to form a β−keto ester (Scheme 1.2.1D), which can be subsequently alkylated

or fluorinated.[4,5] Additionally, using known chemistry, α-fluoro β−keto esters can be synthesized using Selectfluor[5d] and α-trifluoromethyl β−keto esters can be synthesized using Umemoto's Reagent[10], both of which are commercially available.

Scheme 1.2.1. Synthesis of Fluorinated β-Ketoesters

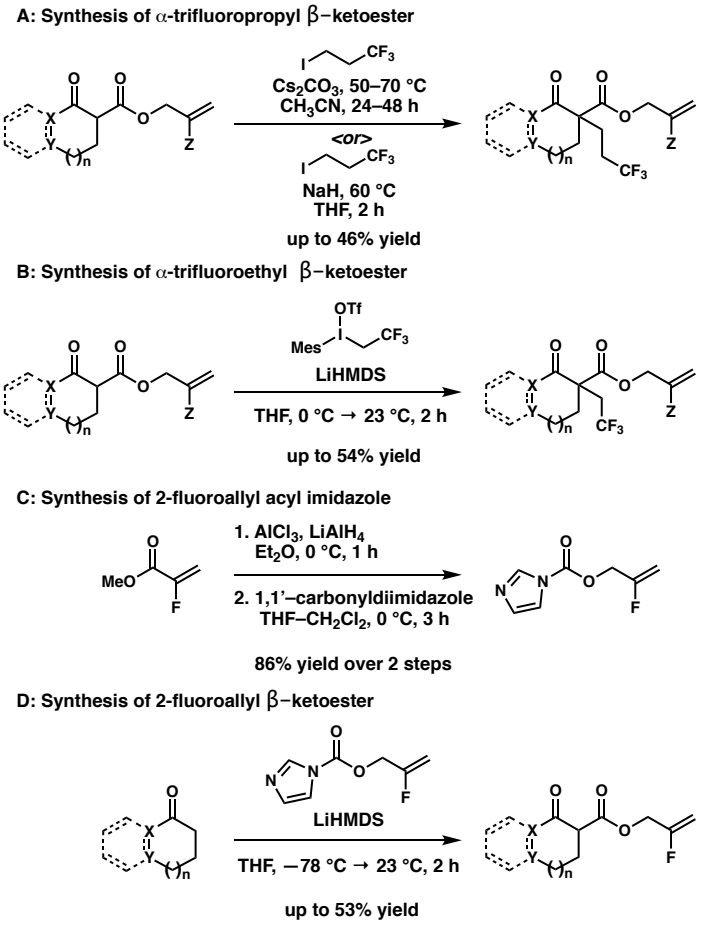

1.3 INITIAL REACTION OPTIMIZATION

Initial reaction optimization started with trifluoroethyl substituted β-ketoester **4a** using catalytic $Pd_2(dba)_3$ at 23 °C in diethylether in the presence of a chiral PHOX ligand toward the synthesis of ketone **5a**. (Table 1.3.1).[11] Employing the classic (*S*)-*t*-BuPHOX

ligand **6**, the desired product was formed in 88% yield and 85% ee (entry 1). Switching to the electron deficient (*S*)-$(CF_3)_3$-*t*-BuPHOX ligand **7**, the desired product was furnished in an improved 99% yield and 90% ee (entry 2). Solvent effects were not very significant (entries 3–5), however THF gave a decreased ee of 86% (entry 3), while the less polar TBME and non-polar toluene performed similarly to diethyl ether. Based on these results, we determined that using $Pd_2(dba)_3$ (5.0 mol %) with (*S*)-$(CF_3)_3$-*t*-BuPHOX in toluene (0.033 M) at room temperature proved optimal.[12]

Table 1.3.1. Optimization of Conditions for Enantioselective Palladium-Catalyzed Allyllic Alkylation[a]

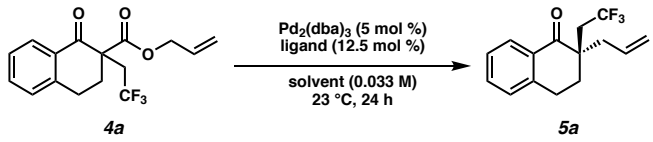

4a *5a*

entry	ligand	solvent	yield (%)	ee (%)[b]
1	(*S*)-*t*-BuPHOX	Et_2O	88	85
2	(*S*)-$(CF_3)_3$-*t*-BuPHOX	Et_2O	99	90
3	(*S*)-$(CF_3)_3$-*t*-BuPHOX	THF	93	86
4	(*S*)-$(CF_3)_3$-*t*-BuPHOX	TBME	95	90
5	(*S*)-$(CF_3)_3$-*t*-BuPHOX	toluene	99	90

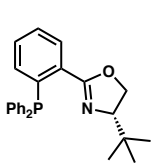

(*S*)-*t*-BuPHOX, *6*

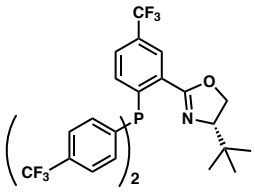

(*S*)-$(CF_3)_3$-*t*-BuPHOX, *7*

[a] Conditions: β-ketoester **4a** (0.1 mmol), $Pd_2(dba)_3$ (5.0 mol %), ligand (12.5 mol %), toluene (3 mL). [b] Determined by analytical chiral SFC.

1.4 EXPLORATION OF REACTION SCOPE

Subsequently, we explored the substrate scope of the enantioselective allylic alkylation of fluorine-containing 1,3-dicarbonyl compounds (Table 1.4.1). We found that our reaction was tolerant of a variety of α-fluoro-, α-fluoroalkyl-, and α-fluoroallyl

substituents to deliver five- and six-membered ketone and lactam products bearing fluorinated tetrasubstituted stereocenters in high yields and enantioselectivities. Trifluoropropyl substituted **4b** exhibited similar enantio-induction as **4a** to furnish **5b** in 92% ee and an extremely high yield. α-Fluoro tetrasubstituted compounds, which are usually introduced by direct fluorination with fluorine reagents and chiral catalysts,[3] were prepared in a very efficient manner with high enantioselectivity (**5c**, **5d**), even in the presence of a chloroallyl substituent (**5d**). Surprisingly, 2-fluoroallyl groups survived the palladium-catalyzed allylic alkylation even at elevated temperatures (40 °C),[13] albeit in a slightly decreased enantioselectivity (**5e**). Recently, Shibata and coworkers described that enantioenriched indanone α-trifluoromethyl β-ketoesters lost their optical activity under the palladium-catalyzed allylic alkylation reaction conditions in the presence of achiral ligands to deliver a racemic α-quaternary ketone, and when they tried to render the transformation enantioselective, they were unsuccessful.[6] However, we were pleased to see that α-trifluoromethyl substituted tetralone substrate **4f** reacted to furnish **5f** with a moderate level of enantioselectivity. Generally, five membered cyclic β-ketoesters have performed worse than the corresponding 6-membered ring substrates, often providing the α-tetrasubstituted ketone products in comparatively low ee.[4k] Under these conditions, alkylation of the five membered indanone substrates **4g** and **4h** occurred with levels of enantioinduction similar to those observed for the tetralone substrates, with only a slightly diminished 87% ee for trifluoropropyl-substituted indanone **5h**. Indanone substrates bearing a 2-fluoroallyl substituent proceeded in high yield, but only moderate enantioselectivity, to form products **5i** and **5j**, following the trend of the 2-fluoroallyl tetralone substrates. Gratifyingly, lactam substrates were also well tolerated in the

reaction. Trifluoropropyl-substituted *N*-benzoyl δ-valero-lactam (**5k**) was obtained in 94% yield, and 89% ee. Surprisingly, in contrast to the negative influence of the 2-fluoroallyl substituent on substrates **5e**, **5i**, and **5j**, the fluorine on the allyl group of *N*-benzoyl δ-valerolactam **4l** enhanced the enantioselectivity, providing **5l** in 97% ee. Additionally, trifluoropropyl-substituted *N*-benzyloxy glutarimide was furnished in 89% ee with high yield. Finally, *N*-benzoyl pyrrolidinone **5n** was obtained in diminished yield and ee.

Table 1.4.1. Substrate Scope of Fluorine-Containing compounds in Enantioselective Allylic Alkylation

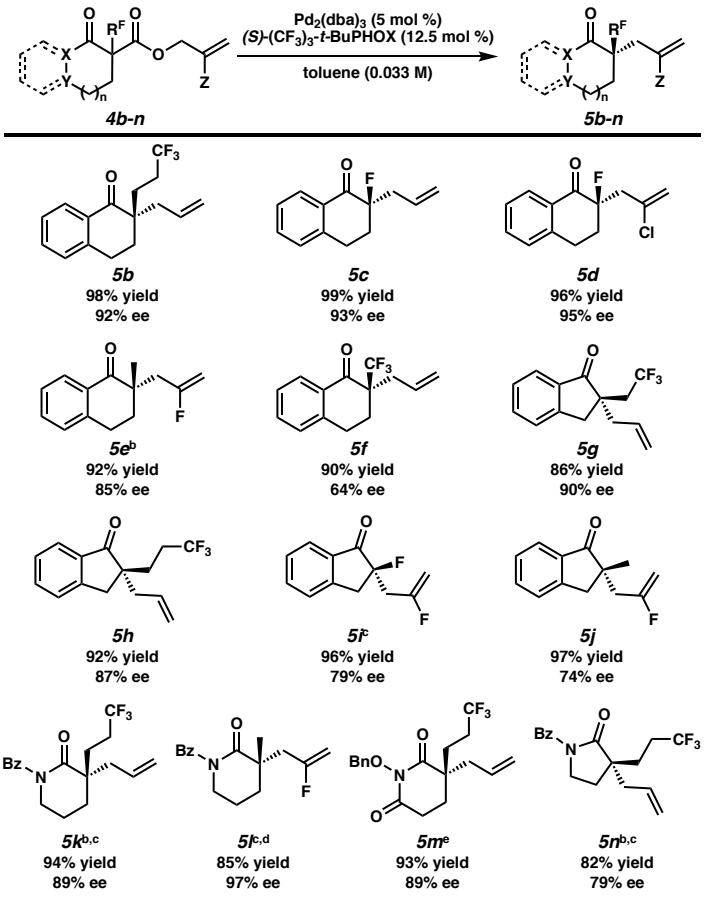

[a] Unless otherwise noted, all reported yields are isolated yields. Enantiomeric excess (ee) was determined by chiral SFC. Standard conditions: β-ketoester **5** (0.1 mmol), $Pd_2(dba)_3$ (5 mol %), (*S*)-$(CF_3)_3$-*t*-BuPHOX (12.5 mol %), toluene (3 mL), 23 °C, 24 h. [b]Reaction performed at 40 °C. [c]Reaction performed in the presence of $Pd_2(pmdba)_3$ instead of $Pd_2(dba)_3$. [d]Reaction performed at 60 °C. [e] Reaction performed at 23 °C for 70 h.

1.5 CONCLUSIONS

In conclusion, we have developed a general method to construct fluorine-containing tetrasubstitued stereocenters by enantioselective palladium-catalyzed decarboxylative allylic alkylation. A strategy was adopted with the pre-introduction of fluorine on racemic substrates, which could be used as an orthogonal approach to the traditional fluorination and trifluoromethylation strategies. The reaction manifold

demonstrated significant substitution tolerance to furnish a wide range of five- and six-membered ketone and lactam products bearing fluorinated tetrasubstituted stereocenters in high yields and enantioselectivities. Furthermore, we provide the first examples demonstrating that 2-fluoroallyl substituents can survive in the presence of certain palladium sources, and deliver related fluoroalkylated products in elevated enantiopurity.

1.6 EXPERIMENTAL METHODS AND ANALYTICAL DATA

1.6.1 MATERIALS AND METHODS

Unless stated otherwise, reactions were performed in flame-dried or oven-dried glassware under an argon or nitrogen atmosphere using dry, deoxygenated solvents (distilled or passed over a column of activated alumina).[14] Commercially obtained reagents were used as received with the exception of dipalladium tris(dibenzylideneacetone) ($Pd_2(dba)_3$), tetrakis(triphenylphosphine)palladium(0), which were stored in a nitrogen-filled glovebox. Dipalladium tris(para-methoxydibenzylideneacetone) ($Pd_2(pmdba)_3$),[15] (*S*)-*t*-BuPHOX,[16] (*S*)-$(CF_3)_3$-*t*BuPHOX,[17] were prepared by known methods. Reactions requiring external heat were modulated to the specified temperatures using an IKAmag temperature controller. Reaction progress was monitored by thin-layer chromatography (TLC), which was performed using E. Merck silica gel 60 F254 precoated glass plates (0.25 mm) and visualized by UV fluorescence quenching, potassium permanganate, or *p*-anisaldehyde staining. Silicycle SiliaFlash® P60 Academic Silica gel (particle size 40-63 nm) was used for column chromatography. ^1H and ^{13}C NMR spectra were recorded on a Varian Inova 500 (500 MHz and 126 MHz, respectively), and a Bruker AV III HD spectrometer equipped with a Prodigy liquid nitrogen temperature cryoprobe (400 MHz and 101 MHz, respectively) and are reported in terms of chemical shift relative to $CHCl_3$

(δ 7.26 and δ 77.16, respectively). ^{19}F NMR spectra were recorded on a Varian Inova 300 spectrometer (282 MHz) and are reported in terms of absolute chemical shift according to IUPAC standard recommendations from $CFCl_3$. Data for ^1H NMR are reported as follows: chemical shift (δ ppm) (multiplicity, coupling constant (Hz), integration). Multiplicities are reported as follows: s = singlet, d = doublet, t = triplet, m = multiplet, br s = broad singlet, app t = apparently triplet. Infrared (IR) spectra were recorded on a Perkin Elmer Paragon 1000 spectrometer using thin films deposited on NaCl plates and are reported in frequency of absorption (cm^{-1}). Optical rotations were measured with a Jasco P-2000 polarimeter operating on the sodium D-line (589 nm), using a 100 mm path-length cell and are reported as: $[\alpha]^D_T$ (concentration in g/100 mL, solvent). Analytical SFC was performed with a Mettler SFC supercritical CO_2 analytical chromatography system utilizing Chiralpak (AD-H, AS-H, IC) or Chiralcel (OD-H, OJ-H) columns (4.6 mm x 25 cm) obtained from Daicel Chemical Industries, Ltd. High resolution mass spectra were obtained from the Caltech Mass Spectral Facility using a JEOL JMS-600H. High Resolution Mass Spectrometer in fast atom bombardment (FAB+) ionization mode or a Agilent 6200 Series TOF with an Agilent G1978A Multimode source in electrospray ionization (ESI+), atmospheric pressure chemical ionization (APCI+), or mixed (ESI/APCI) ionization mode. Julabo Presto LH45 was used to control reaction temperatures inside the nitrogen-filled glovebox.

1.6.2 EXPERIMENTAL PROCEDURES

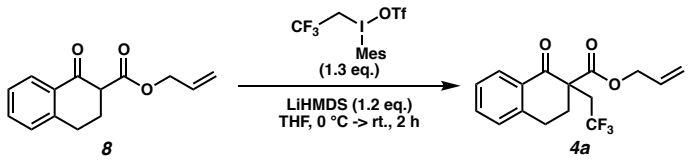

Allyl 1-oxo-2-(2,2,2-trifluoroethyl)-1,2,3,4-tetrahydronaphthalene-2-carboxylate (4a): To a solution of **8**[18] (780 mg, 3.39 mmol, 1.0 equiv) in THF (10 mL) was added LiHMDS (2M solution in THF, 4.0 mmol, 1.2 equiv) at 0 °C, the resulting solution was allowed to stir at room temperature for 15 min. Then the mixture was cooled again to 0 °C, followed an addition of a THF solution (7 mL) of mesityl(2,2,2-trifluoroethyl)-λ^3-iodanyl trifluoromethanesulfonate[19] (2.1 g, 4.4 mmol, 1.3 equiv). After 2 hours stirring at room temperature, the mixture was quenched with aqueous solution of NH_4Cl, extracted with Et_2O, dried over Na_2SO_4, filtered, and concentrated in vacuo. The crude oil was purified by column chromatography (SiO_2, 5% EtOAc in hexane) to afford ketoester **4a** (570 mg, 54% yield) as a white solid; R_f = 0.43 (10:1 Hexane:EtOAc); ^{1}H NMR (500 MHz, $CDCl_3$) δ 8.06 (dd, *J* = 7.9, 1.4 Hz, 1H), 7.50 (app td, *J* = 7.5, 1.5 Hz, 1H), 7.33 (app t, *J* = 7.7 Hz, 1H), 7.24 (d, *J* = 7.7 Hz, 1H), 5.82 – 5.74 (m, 1H), 5.20 – 5.13 (m, 2H), 4.66 – 4.54 (m, 2H), 3.26 – 3.16 (m, 1H), 3.10 – 3.00 (m, 1H), 2.98 – 2.91 (m, 2H), 2.74 (dt, *J* = 14.0, 4.3 Hz, 1H), 2.35 – 2.30 (m, 1H). ^{13}C NMR (101 MHz, $CDCl_3$) δ 192.29, 169.54, 143.06, 134.14, 131.25, 131.05, 128.94, 128.54, 127.08, 126.02 (q, $J_{C\text{-}F}$ = 278.5 Hz, 1C), 118.94, 66.58, 54.70 (q, $J_{C\text{-}F}$ = 1.8 Hz, 1C), 37.35 (q, $J_{C\text{-}F}$ = 29.3 Hz, 1C), 29.74 (q, $J_{C\text{-}F}$ = 1.7 Hz, 1C), 25.83. ^{19}F NMR (282 MHz, $CDCl_3$) δ -59.46 (t, *J* = 11.1 Hz, 3F). IR (thin film, NaCl) 1737, 1693, 1601, 1260, 1134 cm $^{-1}$. HRMS (APCI/ESI) m/z calc'd for $C_{16}H_{16}F_3O_3$ $[M+H]^+$: 313.1046, found: 313.1044.

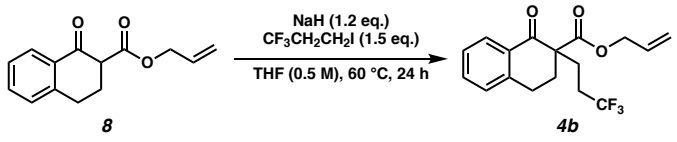

Allyl 1-oxo-2-(3,3,3-trifluoropropyl)-1,2,3,4-tetrahydronaphthalene-2-carboxylate (4b): To a suspension of NaH (60% in oil, 72 mg, 1.8 mmol, 1.2 equiv) in THF (2 mL) was added a THF solution of **8** (345 mg, 1.5 mmol, 1.0 equiv), the mixture was allowed to stir at room temperature for 15 minutes followed the addition of 1,1,1-trifluoro-3-iodopropane. The resulting mixture was allowed to heat at 60 °C for 24 hours. After cooling to room temperature, quenched with aqueous solution of NH_4Cl, extracted with Et_2O, dried over Na_2SO_4, filtered, and concentrated in vacuo. The crude oil was purified by column chromatography (SiO_2, 10% Et_2O in hexane) to afford ester **4b** (148 mg, 30% yield) as a colorless oil; R_f = 0.43 (10:1 Hexane:EtOAc); ^{1}H NMR (500 MHz, $CDCl_3$) δ 8.05 (dd, *J* = 7.9, 1.4 Hz, 1H), 7.49 (app td, *J* = 7.5, 1.5 Hz, 1H), 7.33 (dd, *J* = 7.9 Hz, 1H), 7.23 (d, *J* = 7.6 Hz, 1H), 5.79 (ddt, *J* = 17.6, 10.1, 5.6 Hz, 1H), 5.26 – 5.09 (m, 2H), 4.70 – 4.51 (m, 2H), 3.14 – 3.05 (m, 1H), 2.96 (dt, *J* = 17.4, 5.0 Hz, 1H), 2.59 (dt, *J* = 13.6, 4.9 Hz, 1H), 2.47 – 2.30 (m, 1H), 2.28 – 2.06 (m, 4H). ^{13}C NMR (101 MHz, $CDCl_3$) δ 194.82, 171.10, 142.74, 133.93, 131.89, 131.25, 128.89, 128.17, 127.13, 127.09 (q, $J_{C\text{-}F}$ = 277.4 Hz, 1C), 118.87, 66.08, 56.26, 31.62, 29.80 (q, $J_{C\text{-}F}$ = 29.1 Hz, 1C), 26.67 (q, $J_{C\text{-}F}$ = 3.2 Hz, 1C), 25.90. ^{19}F NMR (282 MHz, $CDCl_3$) δ -66.78 (t, *J* = 11.1 Hz, 3F). IR (thin film, NaCl) 1735, 1670, 1602, 1258, 1228 cm^{-1}. HRMS (APCI/ESI) m/z calc'd for $C_{17}H_{18}F_3O_3$ $[M+H]^+$: 327.1203, found: 327.1204.

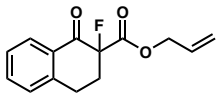

4c

Allyl 2-fluoro-1-oxo-1,2,3,4-tetrahydronaphthalene-2-carboxylate (4c): The title compound **4c** was synthesized according to the known method as describe. All spectroscopic data were in agreement with the literature.[20] ^{1}H NMR (500 MHz, $CDCl_3$) δ 8.07 (d, *J* = 7.9 Hz, 1H), 7.55 (app td, *J* = 7.5, 1.4 Hz, 1H), 7.36 (m, 1H), 7.28 (d, *J* = 7.8 Hz, 1H), 5.91 – 5.82 (m, 1H), 5.30 – 5.22 (m, 2H), 4.76 – 4.68 (m, 2H), 3.19 (dt, *J* = 17.2, 5.2 Hz, 1H), 3.08 (ddd, *J* = 17.1, 7.8, 5.0 Hz, 1H), 2.79 – 2.70 (m, 1H), 2.60 – 2.52 (m, 1H). ^{13}C NMR (101 MHz, $CDCl_3$) δ 188.51 (d, $J_{C\text{-}F}$ = 19.0 Hz, 1C), 167.05 (d, $J_{C\text{-}F}$ = 25.9 Hz, 1C), 143.17, 134.66, 130.81, 130.47, 128.84, 128.37 (d, $J_{C\text{-}F}$ = 0.94 Hz, 1C), 127.29, 119.12, 93.25 (d, $J_{C\text{-}F}$ = 194.2 Hz, 1C), 66.56, 31.87 (d, $J_{C\text{-}F}$ = 22.6 Hz, 1C), 24.83 (d, $J_{C\text{-}F}$ = 7.24 Hz, 1C). ^{19}F NMR (282 MHz, $CDCl_3$) δ -164.16 (ddd, *J* = 22.8, 11.0, 1.2 Hz, 1F).

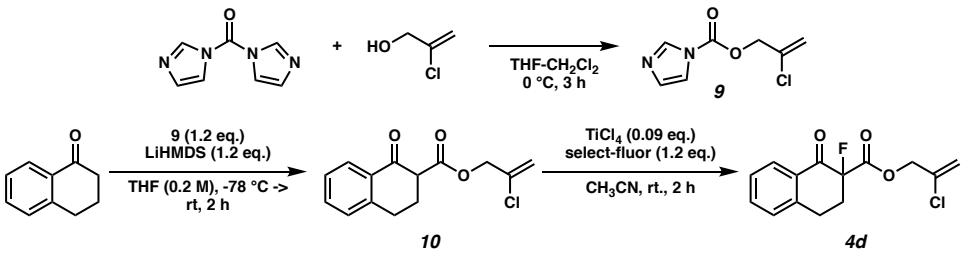

2-chloroallyl 2-fluoro-1-oxo-1,2,3,4-tetrahydronaphthalene-2-carboxylate (4d):

To the mixture of 1,1-carbonyldiimidazole (CDI) (4.86 g, 30 mmol) and THF (15 mL) was added a solution of 2-chloro allyl alcohol (20 mmol) in 15 mL of CH_2Cl_2 at 0 °C slowly, the resulting mixture was allowed to stir for 3 h at the same temperature. Most

solvent was removed in vacuo and the crude product was purified by column chromatography (SiO_2, 35% EtOAc in hexane) to afford 2-chloroallyloxycarbonyl imidazole (**9**) (3.2 g, 86% yield) as a white solid; R_f = 0.15 (3:1 Hexane:EtOAC); ^{1}H NMR (500 MHz, $CDCl_3$) δ 8.18 (m, 1H), 7.46 (m, 1H), 7.10 (dd, *J* = 1.6, 0.8 Hz, 1H), 5.61 (dt, *J* = 2.1, 1.0 Hz, 1H), 5.55 (d, *J* = 2.0 Hz, 1H), 4.97 (dd, *J* = 1.1, 0.4 Hz, 2H). ^{13}C NMR (101 MHz, $CDCl_3$) δ 148.11, 137.27, 134.40, 131.05, 117.35, 117.24, 69.30. IR (thin film, NaCl) 3137, 3122, 1755, 1650, 892, 758 cm^{-1}. HRMS (APCI/ESI) m/z calc'd for $C_7H_8ClN_2O_2$ $[M+H]^+$: 187.0269, found: 187.0265.

To a solution of Tetralone (585 mg, 4 mmol, 1.0 equiv) in THF (8 mL) was added LiHMDS (2M solution in THF, 4.4 mmol, 1.1 equiv) at -78 °C, the resulting solution was allowed to stir at the same temperature for 15 min. Then a THF solution (7 mL) of 2-chloroallyloxycarbonyl imidazole (**9**) (896 mg, 4.8 mmol, 1.2 equiv) was added. After 2 hours stirring at room temperature, the mixture was quenched with aqueous solution of NH_4Cl, extracted with Et_2O, dried over Na_2SO_4, filtered, and concentrated in vacuo. The crude oil was purified by column chromatography (SiO_2, 5% EtOAc in hexane) to afford **10** (718 mg, 67% yield) as a light yellow oil; R_f = 0.41 (10:1 Hexane:EtOAc); Mixture of enol ketone form (3/2). ^{1}H NMR (500 MHz, $CDCl_3$): for enol form: δ 12.22 (s, 0.6H), 7.81 (dd, *J* = 7.6, 1.4 Hz, 0.6H), 7.36 – 7.25 (m, 1.2H), 7.20 – 7.18 (m, 0.6H), 5.70 – 5.37 (m, 1.2H), 4.77 – 4.72 (m, 1.2H), 2.85 (dd, *J* = 8.8, 6.7 Hz, 1.2H), 2.64 (dd, *J* = 8.8, 6.6 Hz, 1.2H); for ketone form δ 8.05 (dd, *J* = 7.9, 1.4 Hz, 0.4H), 7.51 (app td, *J* = 7.5, 1.5 Hz, 0.4H), 7.36 – 7.25 (m, 0.4H), 5.67 – 5.37 (m, 0.8H), 4.80 (s, 0.8H), 3.70 (dd, *J* = 10.8, 4.7 Hz, 0.4H), 3.29 – 2.93 (m, 0.8H), 2.55 (dddd, *J* = 13.4, 10.9, 9.6, 5.0 Hz, 0.4H), 2.48 – 2.36 (m, 0.4H). ^{13}C NMR (101 MHz, $CDCl_3$): for enol form: δ 169.44, 166.16,

139.61, 135.95, 130.94, 129.81, 128.95, 127.59, 126.73, 114.82, 96.44, 65.84, 27.78, 26.47; for ketone form: ^{13}C NMR (101 MHz, $CDCl_3$) δ 192.86, 171.65, 143.67, 135.29, 134.13, 131.71, 127.84, 127.07, 124.57, 115.07, 66.40, 54.60, 27.75, 20.50. IR (thin film, NaCl) 1750, 1686, 1651, 1617, 1597, 1569, 1266, 1212, 1132, 1085 cm^{-1}. HRMS (APCI/ESI) m/z calc'd for $C_{14}H_{14}ClO_2$ $[M+H]^+$: 265.0626, found: 265.0627.

Neat $TiCl_4$ (10 μL, 0.09 mmol, 0.09 equiv) was added to a solution of **10** (265 mg, 1.0 mmol, 1.0 equiv) in CH_3CN (5 mL), resulting in an immediate color change from pale yellow to dark orange-brown. After 5 min, Selectfluor (425 mg, 1.2 mmol, 1.2 equiv) was added in one portion. The mixture was stirred vigorously at room temperature for 2 h, during which time the dark orange-brown color faded to yellow. The reaction was quenched by addition of H_2O, extracted with Et_2O, dried over Na_2SO_4, filtered, and concentrated in vacuo. The crude oil was purified by column chromatography (SiO_2, 10% EtOAc in hexane) to afford ester 4d (217 mg, 77% yield) as a colorless oil;[7] R_f = 0.12 (10:1 Hexane:EtOAc); ^{1}H NMR (500 MHz, $CDCl_3$) δ 8.08 (dd, J = 7.9, 1.4 Hz, 1H), 7.56 (app td, J = 7.5, 1.4 Hz, 1H), 7.38 (app t, J = 7.8 Hz, 1H), 7.29 (d, J = 7.7 Hz, 1H), 5.49 – 5.34 (m, 2H), 4.79 (dd, J = 13.7, 41.56 Hz, 2H), 3.22 (ddd, J = 17.2, 7.7, 5.7 Hz, 1H), 3.11 (ddd, J = 17.2, 7.4, 5.0 Hz, 1H), 2.86 – 2.69 (m, 1H), 2.67 – 2.53 (m, 1H). ^{13}C NMR (101 MHz, $CDCl_3$) δ 188.16 (d, $J_{C\text{-}F}$ = 18.5 Hz), 166.56 (d, $J_{C\text{-}F}$ = 26.8 Hz, 1C), 143.18, 134.78, 134.35, 130.30, 128.88, 128.37 (d, $J_{C\text{-}F}$ = 1.2 Hz, 1C), 127.32, 115.82, 93.22 (d, $J_{C\text{-}F}$ = 194.0 Hz, 1C), 66.96, 31.79 (d, $J_{C\text{-}F}$ = 22.2 Hz, 1C), 24.67 (d, $J_{C\text{-}F}$ = 7.1 Hz, 1C). ^{19}F NMR (282 MHz, $CDCl_3$) δ -164.46 (dd, J = 23.7, 11.3 Hz, 1F). IR (thin film, NaCl) 1764, 1701, 1600,1272, 1184, 1084 cm^{-1}. HRMS (APCI/ESI) m/z calc'd for $C_{14}H_{13}ClFO_3$ $[M+H]^+$: 283.0532, found: 283.0530.

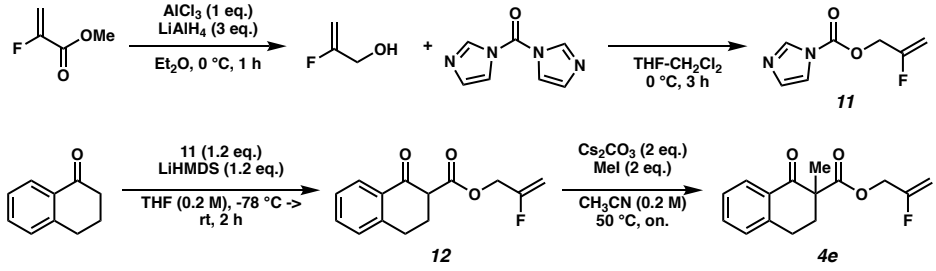

2-fluoroallyl 2-methyl-1-oxo-1,2,3,4-tetrahydronaphthalene-2-carboxylate (4e):

The procedure for preparation of 2-fluoroprop-2-en-1-ol was adapted from the work of Herzon and coworkers.[21]

Solid aluminum chloride (1.0 g, 8.78 mmol, 1.0 equiv) was added portion-wise over 10 min to a solution of lithium aluminum hydride (1.17 g, 26.3 mmol, 3.0 equiv) in Et_2O (20 mL) at 0 °C. The resulting mixture was stirred for 30 min at 0 °C. Methyl 2-fluoroacrylate (820 μL, 8.78 mmol, 1.0 equiv) was then added dropwise via syringe to the mixture. The reaction mixture was stirred for 1 h at 0 °C at atmosphere of nitrogen. Distilled water (1.0 mL) and 15% aqueous sodium hydroxide solution (1.0 mL) were then added in sequence dropwise via syringe over 20 min (10 min addition of each reagent). A second portion of distilled water (3.0 mL) was then added dropwise via syringe over 5 min. The resulting mixture was stirred for 10 min at 0 °C. The heterogeneous mixture was filtered through a Buchner funnel, and the filter cake was rinsed with Et_2O (100 mL). The filtrates were combined and and dried over anhydrous $MgSO_4$. The dried solution was filtered and the filtrate was concentrated (150 torr, 0 °C). The product is very volatile; therefore Et_2O was not completely removed. The solution of 2- fluoroallyl alcohol in Et_2O was used directly and immediately in the following step.

To the mixture of 1,1-carbonyldiimidazole (CDI)(1.3 g, 8 mmol) and CH_2Cl_2 (5 mL) was added a solution of 2- fluoroallyl alcohol from last step in Et_2O at 0 °C slowly, the

resulting mixture was allowed to stir for 3 h at the same temperature. Most solvent was removed in vacuo and the crude product was purified by column chromatography (SiO_2, 50% EtOAc in hexane) to afford 2-flouroallyloxycarbonyl imidazole (**11**) (1.3 g, 86% yield over two steps) as a white solid; R_f = 0.43 (1:1 Hexane:EtOAC); ^{1}H NMR (500 MHz, $CDCl_3$) δ 8.16 (m, 1H), 7.44 (dd, *J* = 2.8, 1.4 Hz, 1H), 7.09 (m, 1H), 4.96 (ddd, *J* = 15.1, 3.5, 1.2 Hz, 1H), 4.92 (d, *J* = 15.5 Hz, 2H), 4.79 (dd, *J* = 46.2, 3.5 Hz, 1H). ^{13}C NMR (101 MHz, $CDCl_3$) δ 158.55 (d, $J_{C\text{-}F}$ = 258.7 Hz, 1C), 148.26, 137.29, 131.05, 117.26, 96.83 (d, $J_{C\text{-}F}$ = 16.9 Hz, 1C), 64.73 (d, $J_{C\text{-}F}$ = 32.7 Hz, 1C). ^{19}F NMR (282 MHz, $CDCl_3$) δ -105.69 – -106.02 (m, 1F). IR (thin film, NaCl) 1766, 1682, 1408, 1384, 1316, 1295, 1242, 1168, 997 cm^{-1}. HRMS (APCI/ESI) m/z calc'd for $C_7H_7FN_2O_2$ $[M+H]^+$: 171.0564, found: 171.0564.

To a solution of Tetralone (585 mg, 4 mmol, 1.0 equiv) in THF (8 mL) was added LiHMDS (2M solution in THF, 4.8 mmol, 1.2 equiv) at -78 °C, the resulting solution was allowed to stir at the same temperature for 15 min. Then a THF solution (7 mL) of 2-fluoroallyloxycarbonyl imidazole (**11**) (817 mg, 4.8 mmol, 1.2 equiv) was added. After 2 hours stirring at room temperature, the mixture was quenched with aqueous solution of NH_4Cl, extracted with Et_2O, dried over Na_2SO_4, filtered, and concentrated in vacuo. The crude oil was purified by column chromatography (SiO_2, 10% Et_2O in hexane) to afford **12** (417 mg, 42% yield) as a light yellow oil; R_f = 0.43 (10:1 Hexane:EtOAc); Mixture of enol ketone form (3/2). ^{1}H NMR (500 MHz, $CDCl_3$): for enol form: δ 12.22 (s, 0.6H), 7.86 – 7.76 (m, 0.6H), 7.42 – 7.27 (m, 1.2H), 7.22 – 7.15 (m, 0.6H), 4.86 (dd, *J* = 16.0, 3.2 Hz, 0.6H), 4.79 – 4.69 (m, 1.8H), 2.90 – 2.78 (m, 1.2H), 2.69 – 2.57 (m, 1.2H); for ketone form: δ 8.09 – 8.00 (m, 0.4H), 7.51 (dd, *J* = 7.5, 1.5 Hz, 0.4H), 7.38 – 7.28 (m,

0.8H), 4.83 (dd, *J* = 16.3, 3.3 Hz, 0.4H), 4.74 – 4.64 (m, 1.2H), 3.69 (dd, *J* = 11.0, 4.7 Hz, 0.4H), 3.13 – 2.99 (m, 0.8H), 2.57 – 2.49 (m, 0.4H), 2.44 – 2.36 (m, 0.4H). ^{13}C NMR (101 MHz, $CDCl_3$): for enol form δ 169.69, 166.15, 160.39 (d, $J_{C\text{-}F}$ = 257.9 Hz, 0.6C), 139.69, 130.97, 129.87, 128.97, 127.63, 124.62, 96.51, 94.56 (d, $J_{C\text{-}F}$ = 17.1 Hz, 0.6C), 61.31 (d, $J_{C\text{-}F}$ = 34.4 Hz, 0.6C), 27.84, 26.48; for ketone form: δ 192.88, 171.88, 159.94 (d, $J_{C\text{-}F}$ = 257.9 Hz, 0.4C), 143.70, 134.17, 131.75, 127.93, 127.13, 126.77, 94.63 (d, $J_{C\text{-}F}$ = 16.8 Hz, 0.4C), 61.89 (d, *J* = 34.8 Hz, 0.4C), 54.66, 27.84, 20.55. ^{19}F NMR (282 MHz, $CDCl_3$) δ -105.33 – -105.98 (m, 1F). IR (thin film, NaCl) 1749, 1686, 1651, 1617, 1598, 1569, 1263, 1210, 1198, 1132, 1085 cm^{-1}. HRMS (APCI/ESI) m/z calc'd for $C_{14}H_{14}FO_3$ $[M+H]^+$: 249.0921, found: 249.0923.

The mixture of **12** (451 mg, 1.81 mmol, 1.0 equiv), cesium carbonate (1.29 g, 3.92 mmol, 2.0 equiv) and MeI (244 mL, 3.92 mmol, 2.0 equiv) in CH_3CN was heated at 50 °C for 12 hours. After cooling, the solution was filtered and concentrated in vacuo. The crude product was purified by column chromatography (SiO_2, 10% Et_2O in hexane) to furnish β-ketoester **4e** (370 mg, 78% yield) as a colorless oil; R_f = 0.28 (10:1 Hexane:EtOAC); ^{1}H NMR (500 MHz, $CDCl_3$) δ 8.06 (dd, *J* = 7.8, 1.4 Hz, 1H), 7.48 (app td, *J* = 7.5, 1.5 Hz, 1H), 7.32 (app t, *J* = 7.8 Hz, 1H), 7.23 (d, *J* = 7.8 Hz, 1H), 4.72 (dd, *J* = 16.1, 3.3 Hz, 1H), 4.69 – 4.54 (m, 2H), 4.48 (dd, *J* = 3.3, 47.7 Hz, 1H), 3.06 (ddd, *J* = 17.4, 9.3, 4.9 Hz, 1H), 2.97 (dt, *J* = 17.3, 5.5 Hz, 1H), 2.70 (ddd, *J* = 13.6, 6.2, 4.8 Hz, 1H), 2.15 (ddd, *J* = 13.9, 9.2, 4.9 Hz, 1H), 1.54 (s, 3H). ^{13}C NMR (101 MHz, $CDCl_3$) δ 195.79, 172.35, 159.79 (d, $J_{C\text{-}F}$ = 258.7 Hz, 1C), 143.16, 133.76, 131.59, 128.90, 128.22, 127.02, 94.15 (d, $J_{C\text{-}F}$ = 16.5 Hz, 1C), 61.72 (d, $J_{C\text{-}F}$ = 35.2 Hz, 1C), 54.07, 33.81, 25.95, 20.47. ^{19}F NMR (282 MHz, $CDCl_3$) δ -106.01 – -106.32 (m, 1F). IR (thin film, NaCl) 1738, 1682,

1601, 1227, 1164 cm^{-1}. HRMS (APCI/ESI) m/z calc'd for $C_{15}H_{16}FO_3$ $[M+H]^+$: 263.1078, found: 263.1078.

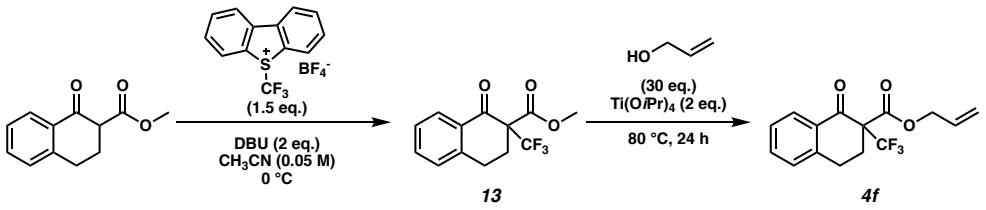

allyl 1-oxo-2-(trifluoromethyl)-1,2,3,4-tetrahydronaphthalene-2-carboxylate (4f):

The procedure for preparation of **4f** was adapted from the work of Shibata and coworkers.[22]

To a stirred solution of methyl 1-oxo-1,2,3,4-tetrahydronaphthalene-2-carboxylate[23] (224 mg, 1.1 mmol, 1.0 equiv) in CH_3CN (11 mL) was added DBU (328 mL, 2.2 mmol, 2.0 equiv) at room temperature. After stirring at room temperature for 15 min, the mixture was cooled down to 0 °C and a solution of the trifluoromethylating reagent (561 mg, 1.65 mmol, 1.5 equiv.) in acetonitrile (11 mL) was added dropwise at the same temperature. Reaction mixture was stirred 10 min, and then warmed up to room temperature, the solvent was evaporated, after which the crude product was purified by column chromatography (SiO_2, 10% EtOAc in pentane) to furnish α-trifluoromethyl-β-ketoester **13** (281mg, 94% yield) as a colorless oil; $R_f = 0.18$ (10:1 Hexane:EtOAc).

To a stirred solution of **13** (281mg, 1.03 mmol, 1.0 equiv) in allyl alcohol (30.0 equiv.) was added $Ti(OiPr)_4$ (2.0 equiv) at 80 °C under nitrogen atmosphere. After reaction mixture was stirred at the same temperature for 24 h, it was cooled down to room temperature and quenched with aqueous solution of NH_4Cl. Aqueous layer was extracted with CH_2Cl_2 (20 mL x 4), and the combined organic layers was washed with brine, dried

over Na_2SO_4, filtered, and concentrated in vacuo. The crude oil was purified by column chromatography (SiO_2, 10% EtOAc in hexane) to afford **4f** (242 mg, 74% yield) as a light yellow oil; R_f = 0.50 (5:1 Hexane:EtOAc); All spectroscopic data were in agreement with the literature.[9] ^{1}H NMR (500 MHz, $CDCl_3$) δ 8.12 (dd, *J* = 7.8, 1.4 Hz, 1H), 7.53 (app td, *J* = 7.5, 1.4 Hz, 1H), 7.38 –7.32 (m, 1H), 7.24 (d, *J* = 7.8 Hz, 1H), 5.92 – 5.67 (m, 1H), 5.32 – 5.07 (m, 2H), 4.84 – 4.56 (m, 2H), 3.22 – 2.97 (m, 2H), 2.85 (dt, *J* = 13.6, 4.2 Hz, 1H), 2.50 (ddd, *J* = 13.6, 10.3, 6.7 Hz, 1H). ^{13}C NMR (101 MHz, $CDCl_3$) δ 187.09, 165.11 (q, $J_{C\text{-}F}$ = 1.9 Hz, 1C), 142.14, 134.44, 131.62 (q, $J_{C\text{-}F}$ = 1.5 Hz, 1C), 130.53, 128.82, 128.54, 127.44, 123.95 (q, $J_{C\text{-}F}$ = 284.0 Hz, 1C), 119.28, 67.09, 62.15 (q, $J_{C\text{-}F}$ = 24.1 Hz, 1C), 27.83 (q, $J_{C\text{-}F}$ = 2.3 Hz, 1C), 25.19. ^{19}F NMR (282 MHz, $CDCl_3$) δ -68.73 (s, 3F).

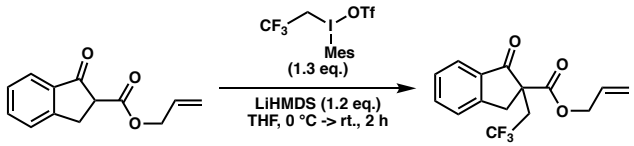

14 *4g*

Allyl 1-oxo-2-(2,2,2-trifluoroethyl)-2,3-dihydro-1*H*-indene-2-carboxylate (4g): was synthesized using the same method with 4a from allyl 1-oxo-2,3-dihydro-1*H*-indene-2-carboxylate (**14**).[24] The crude oil was purified by column chromatography (SiO_2, 50% CH_2Cl_2 in hexane) to afford **4g** (110 mg, 37% yield) as a light yellow oil; R_f = 0.38 (1:1 Hexane:CH_2Cl_2); ^{1}H NMR (500 MHz, $CDCl_3$) δ 7.78 (dd, *J* = 7.7, 0.9 Hz, 1H), 7.66 (app td, *J* = 7.5, 1.2 Hz, 1H), 7.53 (app dt, *J* = 7.7, 1.0 Hz, 1H), 7.42 (app td, *J* = 7.9, 0.9 Hz, 1H), 5.81 (ddt, *J* = 17.2, 10.5, 5.6 Hz, 1H), 5.39 – 5.15 (m, 2H), 4.64 – 4.53 (m, 2H), 3.88 (d, *J* = 17.3 Hz, 1H), 3.52 – 3.15 (m, 2H), 2.66 (dq, *J* = 15.5, 10.5 Hz, 1H). ^{13}C NMR

(101 MHz, $CDCl_3$) δ 199.24, 168.43, 153.15, 136.10, 133.83, 131.18, 128.20, 126.50, 126.10 (q, $J_{C\text{-}F}$ = 277.7 Hz, 1C), 125.32, 118.86, 66.91, 57.37 (q, $J_{C\text{-}F}$ = 1.9 Hz, 1C), 37.62 (q, $J_{C\text{-}F}$ = 29.1 Hz, 1C), 35.34 (q, $J_{C\text{-}F}$ = 1.7 Hz 1C). ^{19}F NMR (282 MHz, $CDCl_3$) -60.61 (t, J = 10.5 Hz, 3F). IR (thin film, NaCl) 1745, 1719, 1608, 1257, 1169 cm^{-1}. HRMS (APCI/ESI) m/z calc'd for $C_{15}H_{14}F_3O_3$ $[M+H]^+$: 299.0890, found: 299.0898.

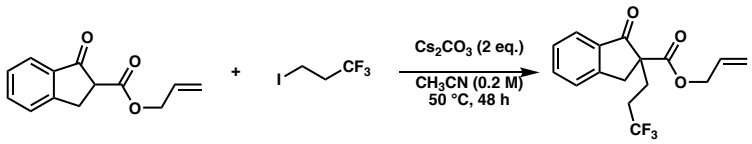

14 *4h*

Allyl 1-oxo-2-(3,3,3-trifluoropropyl)-2,3-dihydro-1*H*-indene-2-carboxylate (4h): The mixture of allyl 1-oxo-2,3-dihydro-1*H*-indene-2-carboxylate (**14**) (216 mg, 1.0 mmol, 1.0 equiv), Cesium carbonate (652 mg, 2.0 mmol, 2.0 equiv) and 1,1,1-trifluoro-3-iodopropane (447 mL, 2.0 mmol, 2.0 equiv) in CH_3CN (5 mL) was heated at 50 °C for 48 hours. After cooling, the solution was filtered and concentrated in vacuo. The crude product was purified by column chromatography (SiO_2, 50% CH_2Cl_2 in hexane) to furnish β-ketoester **4h** (98 mg, 31% yield) as a colorless oil; R_f = 0.37 (1:1 Hexane:CH_2Cl_2); ^{1}H NMR (500 MHz, $CDCl_3$) δ 7.80 (ddd, J = 7.7, 1.3, 0.8 Hz, 1H), 7.66 (app td, J = 7.5, 1.2 Hz, 1H), 7.50 (app dt, J = 7.7, 0.9 Hz, 1H), 7.44 (ddd, J = 7.9, 7.2, 0.9 Hz, 1H), 5.83 (ddt, J = 17.1, 10.4, 5.6 Hz, 1H), 5.34 – 5.14 (m, 2H), 4.69 – 4.54 (m, 2H), 3.73 (d, J = 17.2 Hz, 1H), 3.06 (d, J = 17.2 Hz, 1H), 2.39 – 2.24 (m, 2H), 2.22 – 2.06 (m, 2H). ^{13}C NMR (101 MHz, $CDCl_3$) δ 201.52, 170.28, 152.45, 135.93, 134.96, 131.37, 128.34, 126.89 (q, $J_{C\text{-}F}$ = 275.9 Hz, 1C), 126.58, 125.20, 118.83, 66.36, 58.81, 37.62, 29.70 (q, $J_{C\text{-}F}$ = 29.2 Hz, 1C), 27.16 (q, $J_{C\text{-}F}$ = 3.3 Hz, 1C). ^{19}F NMR (282 MHz, $CDCl_3$) δ -66.70 (t, J = 10.1

Hz, 3F). IR (thin film, NaCl) 1741, 1711, 1255, 1141 cm^{-1}. HRMS (APCI/ESI) m/z calc'd for $C_{16}H_{16}F_3O_3$ $[M+H]^+$: 313.1046, found: 313.1040.

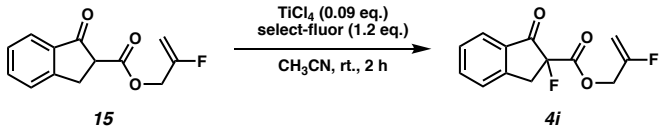

2-Fluoroallyl 1-oxo-2,3-dihydro-1*H*-indene-2-carboxylate (15): was synthesized using the same method with **11** from 1-Indanone and **14**. The crude oil was purified by column chromatography (SiO_2, 20% Et_2O in hexane) to afford **15** (515 mg, 73% yield) as a colorless oil; R_f = 0.28 (10:1 Hexane: EtOAc); Mixture of enol ketone form (1/4). ^1H NMR (300 MHz, $CDCl_3$): ketone form δ 7.82 – 7.74 (m, 0.8H), 7.69 – 7.59 (m, 0.8H), 7.56 – 7.47 (m, 0.8H), 7.47 – 7.36 (m, 0.8H), 4.95 – 4.57 (m, 3.2H), 3.79 (dd, *J* = 8.3, 4.2 Hz, 0.8H), 3.70 – 3.51 (m, 0.8H), 3.49 – 3.30 (m, 0.8H). ^{13}C NMR (101 MHz, $CDCl_3$): ketone form δ 199.00, 168.60, 159.81 (d, $J_{C\text{-}F}$ = 257.5 Hz, 0.8C), 153.54, 135.70, 135.23, 128.06, 126.70, 124.92, 94.69 (d, $J_{C\text{-}F}$ = 16.6 Hz, 0.8C), 62.20 (d, $J_{C\text{-}F}$ = 35.1 Hz, 0.8C), 53.16, 30.38. ^{19}F NMR (282 MHz, $CDCl_3$) δ -105.40 – -105.71 (m, 0.2F), -105.72 – -106.08 (m, 0.8F). IR (thin film, NaCl) 1745, 1713, 1685, 1204, 1150, 761 cm^{-1}; HRMS (APCI/ESI) m/z calc'd for $C_{13}H_{10}FO_3$ $[M-H]^-$: 233.0619, found: 233.0618.

2-Fluoroallyl 2-fluoro-1-oxo-2,3-dihydro-1*H*-indene-2-carboxylate (4i): was synthesized using the same method with **4d** from **15**. The crude oil was purified by column chromatography (SiO_2, 10% EtOAc in hexane) to afford **4i** (176 mg, 70% yield) as a pale solid; R_f = 0.28 (10:1 Hexane:EtOAc); ^1H NMR (500 MHz, $CDCl_3$) δ 7.85 (dd, *J* = 7.7, 0.7 Hz, 1H), 7.72 (app td, *J* = 7.5, 1.2 Hz, 1H), 7.55 – 7.43 (m, 2H), 4.85 – 4.64 (m, 3H), 4.60 (dd, *J* = 47.0, 3.5 Hz, 1H), 3.82 (dd, *J* = 17.7, 11.7 Hz, 1H), 3.48 (dd, *J* =

23.3, 17.6 Hz, 1H). ^{13}C NMR (101 MHz, $CDCl_3$) δ 194.81 (d, $J_{C\text{-}F}$ = 18.2 Hz, 1C), 166.79 (d, $J_{C\text{-}F}$ = 28.5 Hz, 1C), 158.91 (d, $J_{C\text{-}F}$ = 257.6 Hz, 1C), 150.85 (d, $J_{C\text{-}F}$ = 3.4 Hz, 1C), 137.02, 133.20, 128.88, 126.76 (d, $J_{C\text{-}F}$ = 1.3 Hz, 1C), 125.87 (d, $J_{C\text{-}F}$ = 1.1 Hz, 1C), 95.41 (d, J = 16.6 Hz, 1C), 94.57 (d, $J_{C\text{-}F}$ = 202.0 Hz, 1C), 62.67 (d, $J_{C\text{-}F}$ = 34.7 Hz, 1C), 38.33 (d, $J_{C\text{-}F}$ = 23.8 Hz, 1C). ^{19}F NMR (282 MHz, $CDCl_3$) δ -106.19 – -106.51 (m, 1F), -164.54 (dd, J = 23.3, 11.9 H, 1F). IR (thin film, NaCl) 1771, 1724, 1600, 1282, 1184, 1071 cm^{-1}. HRMS (APCI/ESI) m/z calc'd for $C_{13}H_{11}F_2O_2$ $[M+H]^+$: 253.0671, found: 253.0672.

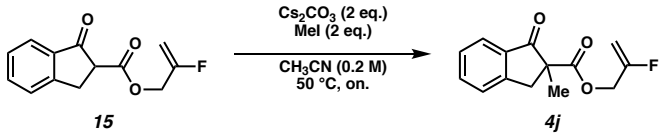

15 *4j*

2-Fluoroallyl 2-methyl-1-oxo-2,3-dihydro-1*H*-indene-2-carboxylate (4j): was synthesized using the same method with **4e** from **15**. The crude oil was purified by column chromatography (SiO_2, 100% CH_2Cl_2) to afford **4j** (170 mg, 69% yield) as a colorless oil; R_f = 0.34 (10:1 Hexane:EtOAc); ^{1}H NMR (500 MHz, $CDCl_3$) δ 7.80 (dd, J = 7.7, 0.5 Hz, 1H), 7.64 (app td, J = 7.5, 1.2 Hz, 1H), 7.49 (app dt, J = 7.7, 1.0 Hz, 1H), 7.45 – 7.40 (m, 1H), 4.75 (dd, J = 16.1, 3.3 Hz, 1H), 4.70 – 4.47 (m, 3H), 3.74 (dd, J = 17.1, 0.9 Hz, 1H), 3.04 (dq, J = 17.0, 0.7 Hz, 1H), 1.55 (s, 3H). ^{13}C NMR (101 MHz, $CDCl_3$) δ 203.01, 171.38, 159.77 (d, $J_{C\text{-}F}$ = 257.4 Hz, 1C), 152.58, 135.62, 134.61, 128.07, 126.63, 125.18, 94.21 (d, $J_{C\text{-}F}$ = 16.6 Hz, 1C), 61.90 (d, $J_{C\text{-}F}$ = 35.4 Hz, 1C), 56.08, 40.04, 21.13. ^{19}F NMR (282 MHz, $CDCl_3$) δ -106.09 – -106.41 (m, 1F). IR (thin film, NaCl) 1748, 1712, 1606, 1280, 1156, 1091 cm^{-1}; HRMS (APCI/ESI) m/z calc'd for $C_{14}H_{14}FO_3$ $[M+H]^+$: 249.0921, found: 249.0919.

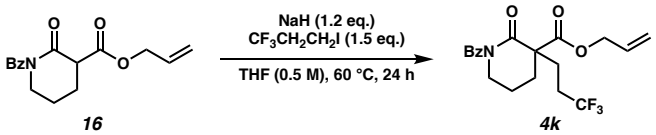

16 *4k*

Allyl 1-benzoyl-2-oxo-3-(3,3,3-trifluoropropyl)piperidine-3-carboxylate (4k): was synthesized using the same method as **4b** from allyl 1-benzoyl-2-oxopiperidine-3-carboxylate (**16**)[12]. The crude oil was purified by column chromatography (SiO_2, 100% CH_2Cl_2) to afford **4k** (142 mg, 37% yield) as a colorless oil; R_f = 0.54 (3:1 Hexane:EtOAc); ^{1}H NMR (500 MHz, $CDCl_3$) δ 7.75 – 7.70 (m, 2H), 7.52 – 7.48 (m, 1H), 7.41 – 7.38 (m, 2H), 5.99 (ddt, *J* = 17.2, 10.4, 6.1 Hz, 1H), 5.43 (dq, *J* = 17.1, 1.4 Hz, 1H), 5.37 (dq, *J* = 10.4, 1.1 Hz, 1H), 4.76 (dq, *J* = 6.1, 1.1 Hz, 2H), 3.87 – 3.25 (m, 2H), 2.52 – 2.40 (m, 1H), 2.42 – 2.28 (m, 1H), 2.18 – 1.99 (m, 5H), 1.87 (ddd, *J* = 13.7, 9.6, 5.9 Hz, 1H). ^{13}C NMR (101 MHz, $CDCl_3$) δ 174.99, 171.51, 171.21, 135.65, 132.12, 131.09, 128.31 (2C), 128.22 (2C), 126.89 (q, $J_{C\text{-}F}$ = 276.4 Hz, 1C), 120.47, 67.02, 55.42, 46.71, 31.71, 29.97 (q, $J_{C\text{-}F}$ = 29.0 Hz), 28.41 (q, $J_{C\text{-}F}$ = 3.3 Hz, 1C), 20.24. ^{19}F NMR (282 MHz, $CDCl_3$) δ -66.79 (t, *J* = 10.1 Hz, 3F). IR (thin film, NaCl) 1735, 1685, 1451, 1393, 1276, 1256, 1147 cm^{-1}. HRMS (APCI/ESI) m/z calc'd for $C_{19}H_{21}F_3NO_4$ $[M+H]^+$: 384.1417, found: 384.1414.

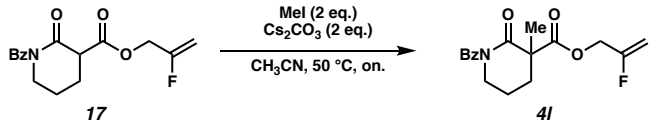

17 *4l*

2-Fluoroallyl 1-benzoyl-2-oxopiperidine-3-carboxylate (17): was synthesized using the same method as **10** from 1-benzoylpiperidin-2-one and **9**. The crude oil was purified by column chromatography (SiO_2, 100% CH_2Cl_2) to afford **17** (482 mg, 53% yield) as a

colorless oil; R_f = 0.37 (3:1 Hexane: EtOAc); 93% purity, ketone form. ^{1}H NMR (500 MHz, $CDCl_3$) δ 7.73 – 7.64 (m, 2H), 7.52 – 7.46 (m, 1H), 7.42 – 7.36 (m, 2H), 4.87 (ddd, *J* = 15.6, 3.4, 0.6 Hz, 1H), 4.78 – 4.64 (m, 3H), 3.95 – 3.78 (m, 2H), 3.64 (t, *J* = 6.6 Hz, 1H), 2.39 – 2.32 (m, 1H), 2.26 – 2.18 (m, 1H), 2.14 – 2.06 (m, 1H), 2.03 – 1.93 (m, 1H). ^{13}C NMR (101 MHz, $CDCl_3$) δ 174.60, 169.34, 169.05, 159.56 (d, $J_{C\text{-}F}$ = 258.1 Hz, 1C), 135.46, 132.06, 128.33 (2C), 128.29 (2C), 95.53 (d, $J_{C\text{-}F}$ = 16.9 Hz, 1C), 62.51 (d, $J_{C\text{-}F}$ = 33.1 Hz, 1C), 51.03, 46.40, 25.59, 20.75. ^{19}F NMR (282 MHz, $CDCl_3$) δ -105.57 (dq, *J* = 46.2, 15.1 Hz, 1F). IR (thin film, NaCl) 1744, 1682, 1449, 1394, 1283, 1257, 1151, 1114 cm^{-1}. HRMS (APCI/ESI) m/z calc'd for $C_{16}H_{17}FNO_4$ $[M+H]^+$: 306.1136, found: 306.1131.

2-Fluoroallyl 1-benzoyl-3-methyl-2-oxopiperidine-3-carboxylate (4l): was synthesized using the same method as **4e** from **17**. The crude oil was purified by column chromatography (SiO_2, 100% CH_2Cl_2) to afford **4l** (186 mg, 56% yield) as light yellow oil; R_f = 0.30 (3:1 Hexane:EtOAc); ^{1}H NMR (500 MHz, $CDCl_3$) δ 7.73 – 7.66 (m, 2H), 7.52 – 7.45 (m, 1H), 7.41 – 7.35 (m, 2H), 4.90 (dd, *J* = 15.5, 3.4 Hz, 1H), 4.82 – 4.63 (m, 3H), 3.89 (dt, *J* = 12.8, 7.1 Hz, 1H), 3.83 – 3.76 (m, 1H), 2.68 – 2.43 (m, 1H), 2.12 – 1.96 (m, 2H), 1.91 – 1.80 (m, 1H), 1.52 (s, 3H). ^{13}C NMR (101 MHz, $CDCl_3$) δ 175.06, 172.57, 172.32, 159.58 (d, $J_{C\text{-}F}$ = 258.4 Hz, 1C), 135.91, 131.84, 128.22 (2C), 128.06 (2C), 95.76 (d, $J_{C\text{-}F}$ = 17.0 Hz, 1C), 62.63 (d, $J_{C\text{-}F}$ = 32.5 Hz, 1C), 52.99, 46.91, 33.87, 22.58, 20.25. ^{19}F NMR (282 MHz, $CDCl_3$) δ-105.20 – -105.53 (m, 1F). IR (thin film, NaCl) 1718, 1684, 1458, 1390, 1276, 1189, 1127 cm^{-1}; HRMS (APCI/ESI) m/z calc'd for $C_{17}H_{19}FNO_4$ $[M+H]^+$: 320.1293, found: 320.1298.

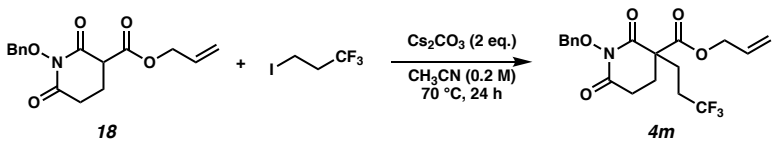

Allyl 1-(benzyloxy)-2,6-dioxo-3-(3,3,3-trifluoropropyl)piperidine-3-carboxylate (4m): was synthesized using the same method with 4h from allyl 1-(benzyloxy)-2,6-dioxopiperidine-3-carboxylate (**18**)[25] except that the temperature was 70 °C and reaction time was 24 hours. The crude oil was purified by column chromatography (SiO_2, 50% EtOAc in hexane) to afford **4m** (120 mg, 30% yield) as a colorless oil; R_f= 0.28 (3:1 Hexane: EtOAc); (99.7% purity determined by ^{19}F NMR). ^1H NMR (500 MHz, $CDCl_3$) δ 7.53 – 7.49 (m, 2H), 7.40 – 7.34 (m, 3H), 5.87 (ddt, *J* = 16.5, 10.3, 6.0 Hz, 1H), 5.36 (dq, *J* = 17.2, 1.4 Hz, 1H), 5.32 (dq, *J* = 10.4, 1.1 Hz, 1H), 5.02 (s, 2H), 4.69 (d, *J* = 6.1 Hz, 2H), 2.81 (ddd, *J* = 18.1, 5.0, 3.3 Hz, 1H), 2.69 (ddd, *J* = 18.0, 12.6, 5.3 Hz, 1H), 2.49 – 2.30 (m, 1H), 2.29 – 1.98 (m, 4H), 1.90 (td, *J* = 13.2, 5.0 Hz, 1H). ^{13}C NMR (101 MHz, $CDCl_3$) δ 169.37, 166.85, 166.65, 133.69, 130.52, 130.24 (2C), 129.44, 128.60 (2C), 126.64 (q, $J_{C\text{-}F}$ = 276.4 Hz, 1C), 120.74, 77.98, 67.29, 54.56, 30.21, 29.58 (q, $J_{C\text{-}F}$ = 29.5 Hz, 1C), 27.82 (q, $J_{C\text{-}F}$ = 3.3 Hz, 1C), 26.30. ^{19}F NMR (282 MHz, $CDCl_3$) δ -66.78 (t, *J* = 10.1 Hz, 3F). IR (thin film, NaCl) 1738, 1710, 1454, 1258, 1189, 1160, 1000, 977 cm^{-1}. HRMS (APCI/ESI) m/z calc'd for $C_{19}H_{21}F_3NO_5$ $[M+H]^+$: 400.1366, found: 400.1379.

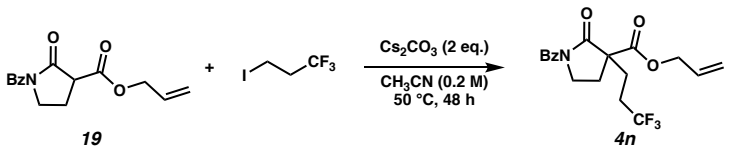

Allyl 1-benzoyl-2-oxo-3-(3,3,3-trifluoropropyl)pyrrolidine-3-carboxylate (4n): was synthesized using the same method with 4h from allyl 1-benzoyl-2-oxopyrrolidine-3-carboxylate (**19**).[26] The crude oil was purified by column chromatography (SiO_2, 25% EtOAc in hexane) to afford **4n** (170 mg, 46% yield) as a colorless oil; R_f = 0.50 (3:1 Hexane: EtOAc); ^{1}H NMR (500 MHz, $CDCl_3$) δ 7.62 – 7.59 (m, 2H), 7.57 – 7.52 (m, 1H), 7.44 – 7.39 (m, 2H), 5.92 (ddt, *J* = 17.1, 10.3, 5.8 Hz, 1H), 5.37 (dq, *J* = 17.1, 1.4 Hz, 1H), 5.32 (dq, *J* = 10.4, 1.2 Hz, 1H), 4.71 (dt, *J* = 5.8, 1.3 Hz, 2H), 4.08 (ddd, *J* = 11.4, 8.7, 3.6 Hz, 1H), 3.96 (ddd, *J* = 11.4, 8.2, 7.7 Hz, 1H), 2.63 (ddd, *J* = 13.3, 7.7, 3.7 Hz, 1H), 2.54 – 2.36 (m, 1H), 2.28 – 1.97 (m, 3H). ^{13}C NMR (101 MHz, $CDCl_3$) δ 171.49, 170.34, 169.63, 133.73, 132.44, 130.95, 128.94 (2C), 128.05 (2C), 126.74 (q, $J_{C\text{-}F}$ = 276.0 Hz, 1C), 119.86, 66.89, 56.37, 43.49, 29.41 (q, $J_{C\text{-}F}$ = 29.4 Hz, 1C), 28.62, 26.64 (q, $J_{C\text{-}F}$ = 3.4 Hz, 1C). ^{19}F NMR (282 MHz, $CDCl_3$) δ -66.79 (t, *J* = 9.9 Hz, 3F). IR (thin film, NaCl) 1748, 1731, 1682, 1449, 1293, 1253, 1218, 1131 cm^{-1}. HRMS (APCI/ESI) m/z calc'd for $C_{18}H_{19}F_3NO_4$ $[M+H]^+$: 370.1261, found: 370.1254.

Representative Procedure 1: Enantioselective Allylic Alkylation.

Oven-dried half-dram vials were charged with the palladium source (Pd_2dba_3 or Pd_2pmdba_3, 0.005 mmol, 0.05 equiv) and (*S*)-$(CF_3)_3$-*t*Bu-PHOX (7.4 mg, 0.0125 mmol, 0.125 equiv) and toluene (2 mL) in a nitrogen-filled glovebox. After stirring at ambient glovebox temperature (~28 °C) for 30 min, solutions of the substrates (0.1 mmol, 1.0

equiv) in 1 mL of toluene were added. The reaction vials were tightly capped and removed from the glovebox. After 24 hours at ambient temperature or heating at the desired temperatures, the solvent was removed by vacuo. The crude mixture were separated on the preparative thin layer plate, filtered, washed with Et_2O, removed solvent and analyzed for enantiomeric excess and optical rotations (see Methods for the Determination of Enantiomeric Excess).

Representative Procedure 2: Racemic Allylic Alkylation.

Oven-dried half-dram vials were charged with the $Pd(PPh_3)_4$ (0.1 equiv) and substrate (1.0 equiv) and toluene (0.1 M) in a nitrogen-filled glovebox. The reaction vials were tightly capped and removed from the glovebox. After 24 hours at ambient temperature or heating at the desired temperatures, the solvent was removed by vacuo. The crude mixture were separated on the preparative thin layer plate, filtered, washed with Et_2O, removed solvent to give the desired racemic products.

Representative Procedure 3: Racemic Allylic Alkylation.

Oven-dried half-dram vials were charged with the palladium source (Pd_2dba_3 or Pd_2pmdba_3, 0.05 equiv) and Gly-PHOX (0.125 equiv) and toluene (0.1 M) in nitrogen-filled glovebox. After stirring at ambient glovebox temperature (~28 °C) for 30 min, solutions of the substrates (1.0 equiv) in toluene were added. The reaction vials were tightly capped and removed from the glovebox. After 24 hours at ambient temperature or heating at the desired temperatures, the solvent was removed by vacuo. The crude mixture was separated on the preparative thin layer plate, filtered, and washed with Et_2O, and the solvent removed to give desired racemic products.

Representative Procedure 4: Preparatory Scale Reaction.

An oven-dried 250 mL Schlenck flask was charged with Pd_2dba_3 (94 mg, 0.103 mmol, 0.05 equiv) and (*S*)-$(CF_3)_3$-*t*-Bu-PHOX (152 mg, 0.26 mmol, 0.125 equiv) and toluene (12 mL) in a nitrogen-filled glovebox. After stirring at ambient glovebox temperature (~28 °C) for 30 min, a solution of **4c** (512 mg, 2.06 mmol, 1.0 equiv) in 50 mL of toluene was added. The reaction vessel was sealed and removed from the glovebox. After 24 hours at ambient temperature the solvent was removed in vacuo. The product was purified by column chromatography (SiO_2, 5% EtOAc in hexanes) to afford **5c** (419 mg, 99% yield, 92% ee).

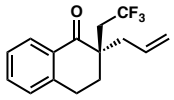

(*S*)-2-allyl-2-(2,2,2-trifluoroethyl)-3,4-dihydronaphthalen-1(2*H*)-one (5a): 26.5 mg, 99% yield; colorless oil; R_f = 0.47 (10:1 Hexane:EtOAc); ^{1}H NMR (500 MHz, $CDCl_3$) δ 8.07 (dd, *J* = 7.9, 1.4 Hz, 1H), 7.50 (app td, *J* = 7.5, 1.5 Hz, 1H), 7.33 (app t, *J* = 7.6 Hz, 1H), 7.24 (d, *J* = 7.8 Hz, 1H), 5.72 (ddt, *J* = 17.4, 10.1, 7.4 Hz, 1H), 5.19 (d, *J* = 10.1 Hz, 1H), 5.12 (dd, *J* = 16.9, 1.6 Hz, 1H), 3.14 (ddd, *J* = 16.9, 11.6, 4.9 Hz, 1H), 3.00 – 2.82 (m, 2H), 2.49 (dd, *J* = 14.3, 7.4 Hz, 1H), 2.41 – 2.24 (m, 3H), 2.17 (dt, *J* = 14.0, 4.4 Hz, 1H). ^{13}C NMR (101 MHz, $CDCl_3$) δ 198.27, 142.73, 133.72, 132.15, 130.92, 128.88, 128.58, 127.08, 126.79 (q, $J_{C\text{-}F}$ = 277.8 Hz, 1C), 120.17, 45.95, 38.58, 37.54 (d, $J_{C\text{-}F}$ = 28.8 Hz, 1C), 29.60 (q, $J_{C\text{-}F}$ = 1.7 Hz, 1C), 24.88. ^{19}F NMR (282 MHz, $CDCl_3$) δ -58.69 (t, *J* = 11.7 Hz, 3F). IR (thin film, NaCl) 1683, 1600, 1256, 1130, 740 cm^{-1}. HRMS (FAB) m/z calc'd for $C_{15}H_{16}F_3O$ $[M+H]^+$: 269.1148, found: 269.1159.

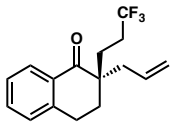

(*R*)-2-allyl-2-(3,3,3-trifluoropropyl)-3,4-dihydronaphthalen-1(2*H*)-one (5b): 27.4 mg, 97% yield; colorless oil; R_f = 0.50 (10:1 Hexane:EtOAc); ^{1}H NMR (500 MHz, $CDCl_3$) δ 8.04 (ddd, *J* = 7.9, 1.4, 0.5 Hz, 1H), 7.49 (app td, *J* = 7.5, 1.5 Hz, 1H), 7.32 (app t, *J* = 7.6 Hz, 1H), 7.24 (d, *J* = 7.5 Hz, 1H), 5.75 (ddt, *J* = 16.8, 10.2, 7.4 Hz, 1H), 5.23 – 5.04 (m, 2H), 3.07 (ddd, *J* = 17.5, 7.9, 5.6 Hz, 1H), 2.99 (dt, *J* = 17.5, 6.0 Hz, 1H), 2.45 (ddt, *J* = 14.2, 7.3, 1.2 Hz, 1H), 2.33 (ddt, *J* = 14.1, 7.4, 1.2 Hz, 1H), 2.24 – 2.01 (m, 4H), 1.97 (td, *J* = 13.7, 4.4 Hz, 1H), 1.79 (td, *J* = 13.5, 4.2 Hz, 1H). ^{13}C NMR (101 MHz, $CDCl_3$) δ 200.39, 142.94, 133.64, 132.82, 131.53, 128.91, 128.23, 127.42 (q, $J_{C\text{-}F}$ = 276.9 Hz, 1C), 127.02, 119.27, 46.63, 38.72, 31.04, 28.93 (q, $J_{C\text{-}F}$ = 28.8 Hz, 1C), 26.54 (q, $J_{C\text{-}F}$ = 3.3 Hz, 1C), 24.99. ^{19}F NMR (282 MHz, $CDCl_3$) δ -66.62 (t, *J* = 10.4 Hz, 3F). IR (thin film, NaCl) 1682, 1601, 1259, 1136, 743 cm^{-1}. HRMS (APCI/ESI) m/z calc'd for $C_{16}H_{18}F_3O$ $[M+H]^+$: 283.1304, found: 283.1305.

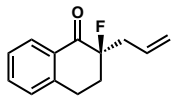

(*R*)-2-allyl-2-fluoro-3,4-dihydronaphthalen-1(2*H*)-one (5c)[27, 28]: 20.3 mg, 99% yield; colorless oil; R_f = 0.28 (10:1 Hexane:EtOAc); ^{1}H NMR (500 MHz, $CDCl_3$) δ 8.06 (dd, *J* = 7.8, 1.4 Hz, 1H), 7.52 (app td, *J* = 7.5, 1.5 Hz, 1H), 7.35 (app td, *J* = 7.5, 1.1 Hz, 1H), 7.28 – 7.24 (m, 1H), 5.95 – 5.84 (m, 1H), 5.25 – 5.07 (m, 2H), 3.19 – 3.07 (m, 1H), 3.02

(ddd, J = 17.3, 9.6, 5.3 Hz, 1H), 2.77 – 2.66 (m, 1H), 2.64 – 2.49 (m, 1H), 2.48 – 2.26 (m, 2H). ^{13}C NMR (101 MHz, $CDCl_3$) δ 194.12 (d, $J_{C\text{-}F}$ = 17.6 Hz, 1C), 142.82, 134.20, 130.97 (d, $J_{C\text{-}F}$ = 4.1 Hz, 1C), 128.87, 128.40, 128.39, 127.23, 120.01, 95.11 (d, $J_{C\text{-}F}$ = 185.0 Hz, 1C), 38.09 (d, $J_{C\text{-}F}$ = 23.5 Hz, 1C), 32.01 (d, $J_{C\text{-}F}$ = 22.6 Hz, 1C), 26.01 (d, $J_{C\text{-}F}$ = 10.1 Hz, 1C). ^{19}F NMR (282 MHz, $CDCl_3$) δ -159.85 – -160.09 (m, 1F). IR (thin film, NaCl) 1678, 1602, 1221, 930, 741 cm^{-1}. HRMS (APCI/ESI) m/z calc'd for $C_{13}H_{14}FO$ $[M+H]^+$: 205.1023, found: 205.1023.

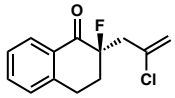

(*R*)-2-(2-chloroallyl)-2-fluoro-3,4-dihydronaphthalen-1(2*H*)-one (5d): 22.9 mg, 96% yield; colorless oil; R_f = 0.43 (10:1 Hexane:EtOAc); ^{1}H NMR (500 MHz, $CDCl_3$) δ 8.06 (dd, J = 7.8, 1.3 Hz, 1H), 7.54 (app td, J = 7.5, 1.5 Hz, 1H), 7.36 (app t, J = 7.8 Hz, 1H), 7.28 (d, J = 7.8 Hz, 1H), 5.45 (d, J = 1.2 Hz, 1H), 5.39 (d, J = 0.7 Hz, 1H), 3.24 – 3.01 (m, 3H), 2.90 (dd, J = 27.4, 15.3 Hz, 1H), 2.60 – 2.42 (m, 2H). ^{13}C NMR (101 MHz, $CDCl_3$) δ 192.92 (d, $J_{C\text{-}F}$ = 18.5 Hz, 1C), 142.94, 134.78 (d, $J_{C\text{-}F}$ = 2.6 Hz, 1C), 134.41, 130.74, 128.88, 128.60 (d, $J_{C\text{-}F}$ = 1.2 Hz, 1C), 127.31, 118.62 (d, $J_{C\text{-}F}$ = 1.1 Hz, 1C), 94.03 (d, $J_{C\text{-}F}$ = 185.8 Hz, 1C), 42.67 (d, $J_{C\text{-}F}$ = 24.4 Hz, 1C), 31.69 (d, $J_{C\text{-}F}$ = 22.3 Hz, 1C), 26.00 (d, $J_{C\text{-}F}$ = 9.9 Hz, 1C). ^{19}F NMR (282 MHz, $CDCl_3$) δ -158.17 – -158.43 (m, 1F). IR (thin film, NaCl) 1680, 1631, 1602, 1223, 743 cm^{-1}. HRMS (APCI/ESI) m/z calc'd for $C_{13}H_{13}ClFO$ $[M+H]^+$: 239.0633, found: 239.0633.

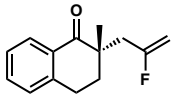

(*S*)-2-(2-fluoroallyl)-2-methyl-3,4-dihydronaphthalen-1(2*H*)-one (5e): 20.0 mg, 92% yield; colorless oil; R_f = 0.53 (10:1 Hexane:EtOAc); ^{1}H NMR (500 MHz, $CDCl_3$) δ 8.04 (dd, *J* = 7.9, 1.4 Hz, 1H), 7.47 (app td, *J* = 7.4, 1.5 Hz, 1H), 7.31 (app t, *J* = 7.5 Hz, 1H), 7.23 (d, *J* = 7.7 Hz, 1H), 4.64 (dd, *J* = 17.2, 2.6 Hz, 1H), 4.32 (dd, *J* = 49.5, 2.6 Hz, 1H), 3.09 – 2.94 (m, 2H), 2.66 (dd, *J* = 20.5, 14.6 Hz, 1H), 2.50 (dd, *J* = 25.1, 14.6 Hz, 1H), 2.17 (dddd, *J* = 14.4, 9.1, 5.2, 1.3 Hz, 1H), 2.04 (dddd, *J* = 13.8, 6.0, 5.0, 1.1 Hz, 1H), 1.26 (d, *J* = 0.9 Hz, 3H). ^{13}C NMR (101 MHz, $CDCl_3$) δ 201.14, 164.07 (d, $J_{C\text{-}F}$ = 157.8 Hz, 1C), 143.28, 133.41, 131.34, 128.81, 128.28, 126.86, 93.85 (d, $J_{C\text{-}F}$ = 20.2 Hz, 1C), 44.26 (d, $J_{C\text{-}F}$ = 3.3 Hz, 1C), 39.39 (d, $J_{C\text{-}F}$ = 25.7 Hz, 1C), 33.30 (d, $J_{C\text{-}F}$ = 1.8 Hz, 1C), 25.48, 21.94 (d, $J_{C\text{-}F}$ = 1.5 Hz, 1C). ^{19}F NMR (282 MHz, $CDCl_3$) δ -88.59 – -88.99 (m, 1F). IR (thin film, NaCl) 1680, 1601, 1222, 741 cm^{-1}. HRMS (APCI/ESI) m/z calc'd for $C_{14}H_{16}FO$ $[M+H]^+$: 219.1180, found: 219.1185.

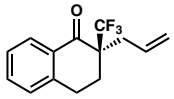

(*R*)-2-allyl-2-(trifluoromethyl)-3,4-dihydronaphthalen-1(2*H*)-one (5f)[29]: 22.8 mg, 90% yield; colorless oil; R_f = 0.36 (10:1 Hexane:EtOAc); ^{1}H NMR (500 MHz, $CDCl_3$) δ 8.07 (dd, *J* = 7.9, 1.4 Hz, 1H), 7.51 (app td, *J* = 7.5, 1.5 Hz, 1H), 7.34 (app t, *J* = 7.6 Hz, 1H), 7.25 (d, *J* = 7.9 Hz, 1H), 5.87 – 5.65 (m, 1H), 5.21 – 5.11 (m, 2H), 3.10 (dt, *J* = 17.5, 6.7 Hz, 1H), 3.02 (dt, *J* = 17.3, 6.1 Hz, 1H), 2.76 (dd, *J* = 14.3, 7.3 Hz, 1H), 2.59 (dd, *J* = 14.3, 2.6 Hz, 1H), 2.43 – 2.25 (m, 2H). ^{13}C NMR (101 MHz, $CDCl_3$) δ 192.89, 143.09,

134.20, 131.84, 131.57 (d, J = 1.5 Hz), 128.88, 128.50, 127.18, 126.57 (q, $J_{C\text{-}F}$ = 285.3 Hz, 1C), 120.08, 53.58 (q, $J_{C\text{-}F}$ = 22.3 Hz, 1C), 35.56 (q, $J_{C\text{-}F}$ = 2.2 Hz, 1C), 26.47 (q, $J_{C\text{-}F}$ = 2.0 Hz, 1C), 24.71. ^{19}F NMR (282 MHz, $CDCl_3$) δ -69.26 (s, 3F). IR (thin film, NaCl) 1688, 1601, 1161, 741cm^{-1}.

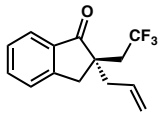

(*R*)-2-allyl-2-(2,2,2-trifluoroethyl)-2,3-dihydro-1*H*-inden-1-one (5g): 21.8 mg, 86% yield; colorless oil; R_f = 0.40 (10:1 Hexane:EtOAc); ^{1}H NMR (500 MHz, $CDCl_3$) δ 7.77 (d, J = 7.7 Hz, 1H), 7.62 (app td, J = 7.5, 1.2 Hz, 1H), 7.45 (d, J = 7.7 Hz, 1H), 7.40 (app t, J = 7.4 Hz, 1H), 5.58 – 5.47 (m, 1H), 5.19 – 4.96 (m, 2H), 3.36 (d, J = 17.6 Hz, 1H), 3.14 (d, J = 17.6 Hz, 1H), 2.64 – 2.48 (m, 2H), 2.45 (dd, J = 13.7, 6.7 Hz, 1H), 2.34 (dd, J = 13.7, 8.0 Hz, 1H). ^{13}C NMR (101 MHz, $CDCl_3$) δ 207.28, 152.43, 135.55, 135.38, 131.99, 127.87, 126.60 (q, $J_{C\text{-}F}$ = 278.7 Hz, 1C), 126.59, 124.51, 119.93, 49.03 (d, $J_{C\text{-}F}$ = 1.7 Hz, 1C), 42.44, 39.20 (q, $J_{C\text{-}F}$ = 27.7 Hz, 1C), 36.24 (q, $J_{C\text{-}F}$ = 1.9 Hz, 1C). ^{19}F NMR (282 MHz, $CDCl_3$) δ -59.71 (t, J = 11.3 Hz, 3F). IR (thin film, NaCl) 1715, 1608, 1258, 1122 cm^{-1}. HRMS (FAB$^+$) m/z calc'd for $C_{14}H_{14}F_3O$ [M+H]$^+$: 255.0991, found: 255.0995.

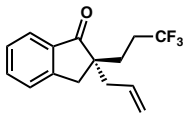

(*R*)-2-allyl-2-(3,3,3-trifluoropropyl)-2,3-dihydro-1*H*-inden-1-one (5h): 24.8 mg, 92% yield; colorless oil; R_f = 0.41 (10:1 Hexane:EtOAc); ^{1}H NMR (500 MHz, $CDCl_3$) δ 7.75

(app dt, *J* = 7.6, 0.9 Hz, 1H), 7.62 (app td, *J* = 7.5, 1.2 Hz, 1H), 7.45 (app dt, *J* = 7.7, 0.9 Hz, 1H), 7.39 (app t, *J* = 7.6 Hz, 1H), 5.53 (dddd, *J* = 16.8, 10.1, 8.0, 6.7 Hz, 1H), 5.12 (dq, *J* = 16.9, 1.5 Hz, 1H), 5.03 (dd, *J* = 10.1, 1.0 Hz, 1H), 3.17 (dd, *J* = 17.4, 0.9 Hz, 1H), 2.91 (d, *J* = 17.4 Hz, 1H), 2.42 (ddt, *J* = 13.7, 6.6, 1.3 Hz, 1H), 2.34 (ddt, *J* = 13.7, 8.1, 1.0 Hz, 1H), 2.16 – 1.90 (m, 3H), 1.86 – 1.74 (m, 1H). ^{13}C NMR (101 MHz, $CDCl_3$) δ 209.23, 152.52, 136.37, 135.51, 132.76, 127.92, 127.09 (q, $J_{C\text{-}F}$ = 276.0 Hz, 1C), 126.67, 124.31, 119.33, 50.95, 41.37, 37.27, 31.54 – 27.19 (m, 2C). ^{19}F NMR (282 MHz, $CDCl_3$) δ -66.65 (t, *J* = 10.3 Hz, 3F). IR (thin film, NaCl) 1709, 1608, 1256, 1150 cm^{-1}. HRMS (APCI/ESI) m/z calc'd for $C_{15}H_{16}F_3O$ $[M+H]^+$: 269.1148, found: 269.1158.

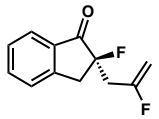

(*R*)-2-fluoro-2-(2-fluoroallyl)-2,3-dihydro-1*H*-inden-1-one (5i): 20.0 mg, 96% yield; colorless oil; R_f = 0.30 (5:1 Hexane:EtOAc); ^{1}H NMR (500 MHz, $CDCl_3$) δ 7.82 (ddd, *J* = 7.7, 1.3, 0.7 Hz, 1H), 7.67 (App td, *J* = 7.5, 1.3 Hz, 1H), 7.50 – 7.40 (m, 2H), 4.71 (dd, *J* = 17.0, 3.0 Hz, 1H), 4.48 (dd, *J* = 49.1, 3.0 Hz, 1H), 3.61 (ddt, *J* = 17.8, 13.7, 0.7 Hz, 1H), 3.40 (dd, *J* = 23.7, 17.8 Hz, 1H), 3.00 (ddd, *J* = 22.5, 15.1, 10.7 Hz, 1H), 2.77 – 2.63 (m, 1H). ^{13}C NMR (101 MHz, $CDCl_3$) δ 199.64 (d, $J_{C\text{-}F}$ = 17.6 Hz, 1C), 160.59 (dd, $J_{C\text{-}F}$ = 257.4, 7.6 Hz, 1C), 150.61 (d, $J_{C\text{-}F}$ = 3.4 Hz, 1C), 136.67, 133.63 (d, $J_{C\text{-}F}$ = 1.2 Hz, 1C), 128.49, 126.85 (d, $J_{C\text{-}F}$ = 1.2 Hz, 1C), 125.33, 95.17 (dd, $J_{C\text{-}F}$ = 18.7, 1.3 Hz, 1C), 94.75 (dd, $J_{C\text{-}F}$ = 188.4, 2.4 Hz, 1C), 37.73 (dd, $J_{C\text{-}F}$ = 24.6, 2.3 Hz, 1C), 37.28 (t, $J_{C\text{-}F}$ = 27.1 Hz, 1C). ^{19}F NMR (282 MHz, $CDCl_3$) δ -92.01 – -92.40 (m, 1F), -154.37 – -154.65 (m, 1F).

IR (thin film, NaCl) 1732, 1608, 1227, 730 cm^{-1}. HRMS (APCI/ESI) m/z calc'd for $C_{12}H_{11}F_2O$ $[M+H]^+$: 209.0772, found: 209.0770.

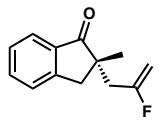

(*S*)-2-(2-fluoroallyl)-2-methyl-2,3-dihydro-1*H*-inden-1-one (5j): 21.8 mg, 97% yield; colorless oil; R_f = 0.33 (10:1 Hexane:EtOAc); ^{1}H NMR (500 MHz, $CDCl_3$) δ 7.76 (dt, *J* = 7.6, 1.0 Hz, 1H), 7.60 (app td, *J* = 7.4, 1.2 Hz, 1H), 7.44 (dt, *J* = 7.7, 1.0 Hz, 1H), 7.38 (app td, *J* = 7.4, 0.9 Hz, 1H), 4.58 (ddd, *J* = 17.3, 2.8, 0.7 Hz, 1H), 4.30 (ddd, *J* = 49.6, 2.8, 0.7 Hz, 1H), 3.36 (d, *J* = 17.3 Hz, 1H), 2.93 (d, *J* = 17.3 Hz, 1H), 2.58 – 2.45 (m, 2H), 1.25 (s, 3H). ^{13}C NMR (101 MHz, $CDCl_3$) δ 209.74, 164.02 (d, $J_{C\text{-}F}$ = 258.2 Hz, 1C), 152.63, 135.20, 127.66, 126.76, 124.62, 93.46 (d, $J_{C\text{-}F}$ = 19.9 Hz, 1C), 47.85 (d, $J_{C\text{-}F}$ = 2.8 Hz, 1C), 43.62 – 34.74 (m, 2C), 24.19. ^{19}F NMR (282 MHz, $CDCl_3$) δ -91.35 – -91.74 (m, 1F). IR (thin film, NaCl) 1732, 1608, 1227, 730 cm^{-1}. HRMS (APCI/ESI) m/z calc'd for $C_{13}H_{14}FO$ $[M+H]^+$: 205.1023, found: 205.1022.

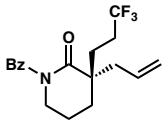

(*R*)-3-allyl-1-benzoyl-3-(3,3,3-trifluoropropyl)piperidin-2-one (5k): 27.4 mg, 94% yield; colorless oil; R_f = 0.37 (3:1 Hexane:EtOAc); ^{1}H NMR (500 MHz, $CDCl_3$) δ 7.55 – 7.47 (m, 3H), 7.40 – 7.38 (m, 2H), 5.72 (ddt, *J* = 17.4, 10.2, 7.3 Hz, 1H), 5.22 – 5.15 (m, 2H), 3.84 – 3.71 (m, 2H), 2.55 (ddt, *J* = 13.9, 7.2, 1.2 Hz, 1H), 2.38 (ddt, *J* = 13.9, 7.5,

1.2 Hz, 1H), 2.21 – 1.93 (m, 5H), 1.93 – 1.86 (m, 2H), 1.84 – 1.77 (m, 1H). ^{13}C NMR (101 MHz, $CDCl_3$) δ 177.21, 175.61, 136.46, 132.11, 131.79, 128.44 (2C), 127.47 (2C), 127.23 (q, $J_{C\text{-}F}$ = 276.9 Hz, 1C), 120.09, 47.20, 46.09, 41.13, 31.62, 29.32, 29.13 (q, $J_{C\text{-}F}$ = 28.8 Hz, 1C), 19.41. ^{19}F NMR (282 MHz, $CDCl_3$) δ -66.53 (t, J = 10.5 Hz, 3F). IR (thin film, NaCl) 2950, 1682, 1258, 1149 cm^{-1}; HRMS (APCI/ESI) m/z calc'd for $C_{18}H_{21}F_3NO_2$ $[M+H]^+$: 340.1519, found: 340.1519.

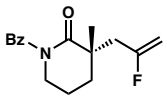

(*S*)-1-benzoyl-3-(2-fluoroallyl)-3-methylpiperidin-2-one (5l): 23.5 mg, 85% yield; colorless oil; R_f = 0.52 (3:1 Hexane:EtOAc); ^{1}H NMR (500 MHz, $CDCl_3$) δ 7.55 – 7.50 (m, 2H), 7.49 – 7.44 (m, 1H), 7.41 – 7.35 (m, 2H), 4.67 (ddd, J = 17.3, 2.7, 0.7 Hz, 1H), 4.32 (ddd, J = 49.7, 2.7, 0.5 Hz, 1H), 4.00 – 3.84 (m, 1H), 3.79 – 3.62 (m, 1H), 2.76 (dd, J = 19.4, 14.6 Hz, 1H), 2.41 (ddd, J = 24.8, 14.6, 0.8 Hz, 1H), 2.19 – 1.95 (m, 3H), 1.93 – 1.75 (m, 1H), 1.42 (s, 3H). ^{13}C NMR (101 MHz, $CDCl_3$) δ 176.80 (d, $J_{C\text{-}F}$ = 289.8 Hz, 1C), 163.47 (d, $J_{C\text{-}F}$ = 258.1 Hz, 1C), 136.47, 131.55, 128.28 (2C), 127.52 (2C), 94.42 (d, $J_{C\text{-}F}$ = 20.0 Hz, 1C), 47.16, 43.60 (d, $J_{C\text{-}F}$ = 3.1 Hz, 1C), 41.10 (d, $J_{C\text{-}F}$ = 25.5 Hz, 1C), 33.28 (d, $J_{C\text{-}F}$ = 1.9 Hz, 1C), 25.83 (d, $J_{C\text{-}F}$ = 1.5 Hz, 1C), 19.72. ^{19}F NMR (282 MHz, $CDCl_3$) δ -89.31 – 89.70 (m, 1F). IR (thin film, NaCl) 2942, 1697, 1672, 1277, 1144 cm^{-1}. HRMS (APCI/ESI) m/z calc'd for $C_{16}H_{19}FNO_2$ $[M+H]^+$: 276.1394, found: 276.1397.

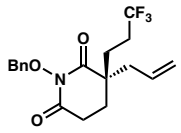

(*R*)-3-allyl-1-(benzyloxy)-3-(3,3,3-trifluoropropyl)piperidine-2,6-dione (5m): 33.0 mg, 93% yield; colorless oil; R_f = 0.24 (3:1 Hexane:EtOAc); ^{1}H NMR (500 MHz, $CDCl_3$) δ 7.51 – 7.46 (m, 2H), 7.40 – 7.34 (m, 3H), 5.61 (ddt, *J* = 17.4, 10.1, 7.4 Hz, 1H), 5.25 – 5.06 (m, 2H), 5.02 (s, 2H), 2.83 – 2.70 (m, 2H), 2.39 (ddt, *J* = 14.2, 7.3, 1.2 Hz, 1H), 2.30 (ddt, *J* = 14.2, 7.4, 1.1 Hz, 1H), 2.09 – 1.94 (m, 2H), 1.90 – 1.80 (m, 2H), 1.78 – 1.66 (m, 2H). ^{13}C NMR (101 MHz, $CDCl_3$) δ 171.63, 167.45, 133.67, 131.03, 130.38 (2C), 129.45, 128.54 (2C), 126.88 (q, $J_{C\text{-}F}$ = 275.9 Hz, 1C), 120.75, 78.04, 45.18, 39.76, 29.22, 28.75 (q, $J_{C\text{-}F}$ = 29.2Hz, 1C), 27.76 (q, *J* = 3.0 Hz, 1C), 25.35. ^{19}F NMR (282 MHz, $CDCl_3$) δ -66.56 (t, *J* = 10.1 Hz, 3F). IR (thin film, NaCl) 1741, 1702, 1258, 1184 cm^{-1}. HRMS (APCI/ESI) m/z calc'd for $C_{18}H_{21}F_3NO_3$ $[M+H]^+$: 356.1468, found: 356.1470.

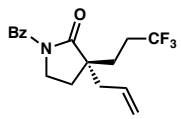

(*R*)-3-allyl-1-benzoyl-3-(3,3,3-trifluoropropyl)pyrrolidin-2-one (5n): 26.7 mg, 82% yield; colorless oil; R_f = 0.35 (5:1 Hexane:EtOAc); ^{1}H NMR (500 MHz, $CDCl_3$) δ 7.58 – 7.51 (m, 3H), 7.45 – 7.39 (m, 2H), 5.76 (dddd, *J* = 17.1, 10.2, 7.8, 7.0 Hz, 1H), 5.29 – 5.16 (m, 2H), 3.96 – 3.85 (m, 2H), 2.38 (ddt, *J* = 13.8, 7.0, 1.3 Hz, 1H), 2.34 – 2.28 (m, 1H), 2.28 – 2.06 (m, 3H), 1.95 (ddd, *J* = 13.3, 8.3, 6.4 Hz, 1H), 1.86 – 1.81 (m, 2H). ^{13}C NMR (101 MHz, $CDCl_3$) δ 176.93, 170.74, 134.18, 132.23, 131.91, 128.90 (2C), 128.00 (2C), 127.0 (q, $J_{C\text{-}F}$ = 276.9 Hz, 1C), 120.39, 48.44, 42.96, 39.93, 28.94 (q, $J_{C\text{-}F}$ = 29.2 Hz,

1C), 28.02 (q, $J_{C\text{-}F}$ = 3.0 Hz, 1C), 27.60. ^{19}F NMR (282 MHz, $CDCl_3$) δ -66.60 (t, *J* = 10.4 Hz, 3F). IR (thin film, NaCl) 1738, 1678, 1305, 1258, 1138 cm^{-1}. HRMS (APCI/ESI) m/z calc'd for $C_{17}H_{19}F_3NO_2$ $[M+H]^+$: 326.1362, found: 326.1352.

1.6.3 METHODS FOR THE DETERMINATION OF ENANTIOMERIC EXCESS

	products	assigned as	assay conditions	ee (%)	$[\alpha]_D^{25}$ (c = 1, $CHCl_3$)
5a	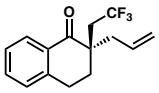	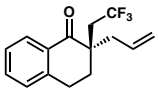	SFC, Chiralcel OD-H 0% IPA isocratic, 2.5 mL/min t (major) = 9.21 t (minor) = 8.65	90	-21.307
5b	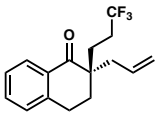	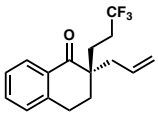	SFC, Chiralcel OD-H 1% IPA isocratic, 2.5 mL/min t (major) = 5.71 t (minor) = 8.86	92	+0.267
5c	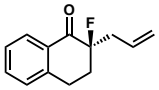	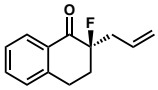	SFC, Chiralcel OJ-H 0% IPA isocratic, 2.5 mL/min t (major) = 6.38 t (minor) = 5.98	93	-28.692
5d	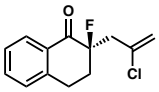	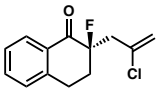	SFC, Chiralpak AD-H 3% IPA isocratic, 2.5 mL/min t (major) = 9.73 t (minor) = 11.11	95	-32.885
5e	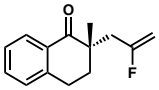	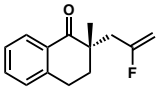	SFC, Chiralpak IC 5% IPA isocratic, 2.5 mL/min t (major) = 4.78 t (minor) = 4.21	85	-9.688
5f	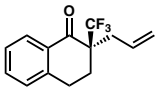	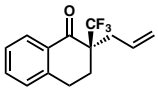	SFC, Chiralpak AD-H 5% IPA isocratic, 2.5 mL/min t (major) = 2.72 t (minor) = 3.04	64	-31.191
5g	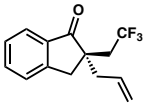	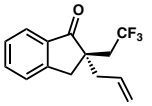	SFC, Chiralpak AS-H 0% IPA isocratic, 2.5 mL/min t (major) = 2.81 t (minor) = 2.55	90	-25.986
5h	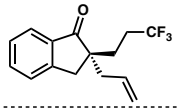	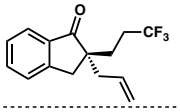	SFC, Chiralpak AD-H 3% IPA isocratic, 2.5 mL/min t (major) = 3.85 t (minor) = 3.16	87	-28.049
5i	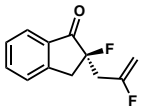	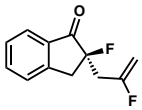	SFC, Chiralpak AD-H 5% IPA isocratic, 2.5 mL/min t (major) = 2.98 t (minor) = 3.54	79	-85.633
5j	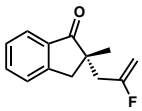	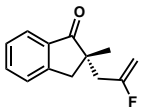	SFC, Chiralpak IC 3% IPA isocratic, 2.5 mL/min t (major) = 8.09 t (minor) = 7.23	74	-58.663
5k	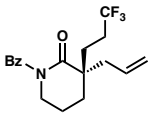	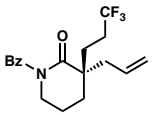	SFC, Chiralpak AD-H 5% IPA isocratic, 2.5 mL/min t (major) = 6.15 t (minor) = 4.63	89	-5.691
5l	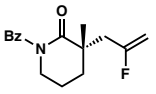	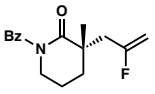	SFC, Chiralpak AD-H 5% IPA isocratic, 2.5 mL/min t (major) = 9.04 t (minor) = 11.38	97	-65.009
5m	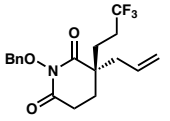	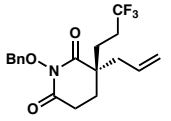	SFC, Chiralcel OJ-H 3% IPA isocratic, 2.5 mL/min t (major) = 10.67 t (minor) = 9.86	89	+3.302
5n	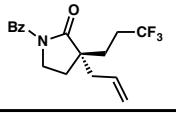	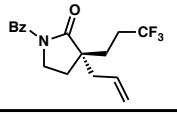	SFC, Chiralpak AD-H 10% IPA isocratic, 2.5 mL/min t (major) = 2.28 t (minor) = 3.25	79	-14.268

1.7 NOTES & REFERENCES

[1] For reviews on fluorine in medicinal chemistry, see: (a) Böhm, H.-J.; Banner, D.; Bendels, S.; Kansy, M.; Kuhn, B.; Müller, K.; ObstSander, U.; Stahl, M. *ChemBioChem* **2004**, *5*, 637–643. (b) Isanbor, C.; O'Hagan, D. *J. Fluorine Chem.* **2006**, *127*, 303–319. (c) Kirk, K. L. *J. Fluorine Chem.* **2006**, *127*, 1013–1029. (d) Müller, K.; Faeh, C.; Diederich, F. *Science* **2007**, *317*, 1881–1886. (e) Kirk, K. L. *Org. Process Res. Dev.* **2008**, *12*, 305–321. (f) O'Hagan, D. *Chem. Soc. Rev.* **2008**, *37*, 308–319. (g) Purser, S.; Moore, P. R.; Swallow, S.; Gouverneur, V. *Chem. Soc. Rev.* **2008**, *37*, 320–330. (h) Hagmann, W. K. *J. Med. Chem.* **2008**, *51*, 4359–4369. (i) Qiu, X.-L.; Xu, X.-H.; Qing, F.-L. *Tetrahedron* **2010**, *66*, 789–843. (j) Hunter, L. *Beilstein J. Org. Chem.* **2010**, *6*, 38. (k) Vulpettil, A.; Dalvit, C. *Drug Discovery Today* **2012**, *17*, 890–897. (l) Wang, J.; Sánchez-Roselló, M.; Aceña, J. L.; del Pozo, C.; Sorochinsky, A. E.; Fustero, S.; Soloshonok, V. A.; Liu, H. *Chem. Rev.* **2013**, *114*, 2432–2506. (m) Gillis, E. P.; Eastman, K. J.; Hill, M. D.; Donnelly, D. J.; Meanwell, N. A. *J. Med. Chem.* **2015**, *58*, 8315–8359.

[2] Lovering, F.; Bikker, J.; Humblet, C. *J. Med. Chem.* **2009**, *52*, 6752–6756.

[3] For reviews on fluorination and trifluoromethylation to construct α-tetrasubstituted stereocenters on ketones, see: (a) Babbio, C.; Gouverneur, V. *Org. Biomol. Chem.* **2006**, *4*, 2065–2075. (b) Prakash, G. K. S.; Beier, P. *Angew. Chem., Int. Ed.* **2006**, *45*, 2172–2174. (c) Pihko, P. M. *Angew. Chem., Int. Ed.* **2006**, *45*, 544–547. (d) Hamashima, Y.; Sodeoka, M. *Synlett* **2006**, 1467–1478. (e) Shibata, N.; Ishimaru, T.; Nakamura, S.; Toru, T. *J. Fluorine Chem.* **2007**, *128*, 469–483. (f) Ma, J.-A.; Cahard, D. *Chem. Rev.* **2008**, *108*, PR1–PR43. (g) Shibata, N.; Mizuta, S.; Kawai, H. *Tetrahedron: Asymmetry* **2008**,

19, 2633–2752. (h) Brunet, V. A.; O'Hagan, D. *Angew. Chem. Int. Ed.* **2008**, *47*, 1179–1182. (i) Ueda, M.; Kano, T.; Maruoka, K. *Org. Biomol. Chem.* **2009**, *7*, 2005–2012. (j) Lectard, S.; Hamashima, Y.; Sodeoka, M. *Adv. Synth. Catal.* **2010**, *352*, 2708–2732. (k) Cahard, D.; Xu, X.; Couve-Bonnaire, C.; Pannecoucke, X. *Chem. Soc. Rev.* **2010**, *39*, 558–568. (l) Zheng, Y.; Ma, J.-A. *Adv. Synth. Catal.* **2010**, *352*, 2745–2750. (m) Shibata, N.; Matsnev, A.; Cahard, D. *Beilstein J. Org. Chem.* **2010**, *6*, 65. (n) Furuya, T.; Kamlet, A. S.; Ritter, T. *Nature* **2011**, *473*, 470–477. (o) Valero, G.; Companyó, X.; Rios, R. *Chem. Eur. J.* **2011**, *17*, 2018–2037. (p) Hollingworth, C.; Gouverneur, V. *Chem. Commun.* **2012**, *48*, 2929–2942. (q) Macé, Y.; Magnier, E. *Eur. J. Org. Chem.* **2012**, 2479–2492. (r) Liang, T.; Neumann, C. N.; Ritter, T. *Angew. Chem. Int. Ed.* **2013**, *52*, 8214–8264. (s) Yang, X.; Wu, T.; Phipps, R. J.; Toste, D. F. *Chem. Rev.* **2015**, *115*, 826–870.

[4] For accounts and reviews on palladium-catalyzed allylic alkylation chemistry, see: (a) Trost, B. M.; Vranken, Van D. L. *Chem. Rev.* **1996**, *96*, 395–422. (b) Trost, B. M. *Acc. Chem. Res.* **1996**, *29*, 355–364. (c) Pfaltz, A.; Lautens, M. *"Comprehensive Asymmetric Catalysis" III, Vol. 2* (Eds.: Jacobsen, E. N.; Pfaltz, A.; Yamamoto, H.), Springer: New York, 1999, pp. 833–884. (d) Helmchen, G. *J. Organomet. Chem.* **1999**, *576*, 203–214. (e) Trost, B. M.; Lee, C. *"Catalytic Asymmetric Synthesis"*, *2nd ed.* (Ed.: Ojima, I.), Wiley: New York, 2000, pp. 593–649. (f) Trost, B. M. *Chem. Pharm. Bull.* **2002**, *50*, 1–14. (g) Graening, T.; Schmalz, H.-G. *Angew. Chem.* **2003**, *115*, 2684–2688; *Angew. Chem. Int. Ed.* **2003**, *42*, 2580–2584. (h) Trost, B. M. *J. Org. Chem.* **2004**, *69*, 5813–5837. (i) Lu, Z.; Ma, S. *Angew. Chem.* **2008**, 120, 264–303.; *Angew. Chem. Int. Ed.* **2008**, 47, 258–297. (j) Behenna, D. C.; Mohr, J. T.; Sherden, N. H.; Marinescu, S. C.; Harned,

A. W.; Tani, K.; Seto, M.; Ma, S.; Novák, Z.; Krout, M. R.; McFadden, R. M.; Roizen, J. L.; Enquist, Jr. J. A.; White, D. E.; Levine, S. R.; Petrova, K. V.; Iwashita, A.; Virgil, S. C.; Stoltz, B. M. *Chem. Eur. J.* **2011**, *17*, 14199–14223. (k) Liu, Y.; Han, S.; Liu, W.; Stoltz, B. M. *Acc. Chem. Res.* **2015**, *48*, 740–751.

[5] (a) Mohr, J. T.; Behenna, D. C.; Harned, A. M.; Stoltz, B. M. *Angew. Chem., Int. Ed.* **2005**, *44*, 6924–6927. (b) Nakamura, M.; Hajra, A.; Endo, K.; Nakamura, E. *Angew. Chem.* **2005**, *117*, 7414–7417.; *Angew. Chem. Int. Ed.* **2005**, *44*, 7248–7251. (c) Behenna, D. C.; Liu, Y.; Yurino, T.; Kim, J.; White, D. E.; Virgil, S. C.; Stoltz, B. M. *Nat. Chem.* **2012**, *4*, 130–133. (d) Mohr, J. T.; Nishimata, T.; Behenna, D. C.; Stoltz, B. M. *J. Am. Chem. Soc.* **2006**, *128*, 11348–11349.

[6] Shibata, N.; Suzuki, S.; Furukawa,T.; Kawai, H.; K. *Adv. Synth. Catal.* **2011**, *353*, 2037–2041.

[7] Tolnai, G.L.; Szekely, A.; Mako, Z.; Gati, T.; Daru, J.; Bihari, T.; Stirling, A.; Novak, Z. *Chem. Commun.,* **2015**, *51*, 4488–4491.

[8] Zhao, C.-L.; Yang, J.; Han, Z.-Z.; Zheng, C.-P. *J. Fluor. Chem.,* **2017**, *204*, 23–30.

[9] Trost, B.M.; Xu, J. *J. Org. Chem.* **2007**, *72*, 9372–9375.

[10] Shibata, N.; Suzuki, S.; Furukawa, T.; Kawai, H.; Tokunaga, E.; Yuan, Z.; Cahardb, D. *Adv. Synth. Catal.* **2011**, *353*, 2037–2041.

[11] Absolute configuration of **5c** was determined by comparison of the optical rotation of the same compound to the known literature value, see: Nakamura, M.; Hajra, A.; Endo, K.; Nakamura, E. *Angew. Chem.* **2005**, 117, 7414–7417.; *Angew. Chem. Int. Ed.* **2005**, *44*, 7248–7251. The absolute configuration of all other products generated herein was

assigned by analogy to the absolute configuration of **5c**. For full details, see the Supporting Information.

[12] With the consideration of heating requirements for some less reactive substrates, toluene was assigned as the best solvent.

[13] A de-fluorinated side product was obtained in the presence of $Pd(PPh_3)_4$ for preparing racemic standards. Therefore, racemic samples were prepared in the presence of $Pd_2(dba)_3$ (or $Pd_2(pmdba)_3$) and achiral Gly-PHOX for fluoro-allyl products. For full details, see the Supporting Information.

[14] Pangborn, A. M.; Giardello, M. A.; Grubbs, R. H.; Rosen, R. K.; Timmers, F. *J. Organometallics* **1996**, *15*, 1518–1520.

[15] Firmansjah, L.; Fu, G. C. *J. Am. Chem. Soc.*, **2007**, *129*, 11340–11341.

[16] Krout, M. R.; Mohr, J. T.; Stoltz, B. M. *Org. Synth.* **2009**, *86*, 181–205.

[17] McDougal, N. T.; Streuff, J.; Mukherjee, H.; Virgil, S. C.; Stoltz, B. M. *Tetrahedron Lett.* **2010**, *51*, 5550–5554.

[18] Rambla, M.; Duroure, L.; Chabaud, L.; Guillou, C. *Eur. J. Org. Chem.* **2014,** 7716–7720.

[19] Tolnai, G. L.; Szekely, S.; Mako, Z.; Gati, T.; Daru, J.; Bihari,T.; Stirling, A; Novak, Z. *Chem. Commun.*, **2015**, *51*, 4488–4491.

[20] Mohr, J. T.; Nishimata, T.; Behenna, D. C.; Stoltz, B. M. *J. Am. Chem. Soc.* **2006**, *128*, 11348–11349.

[21] King, S.; Ma, X.; Herzon, S. B. *J. Am. Chem. Soc.* **2014**, *136*, 6884–6887.

[22] Shibata, N.; Suzuki, S.; Furukawa, T.; Kawai, H.; Tokunaga, E.; Yuan, Z.; Cahardb, D. *Adv. Synth. Catal.* **2011**, *353*, 2037–2041.

[23] Smith, A. M. R.; Rzepa, H. S.; White, A. J. P.; Billen, D.; Hii, K. K. *J. Org. Chem.* **2010**, *75*, 3085–3096.

[24] Craig, R. A.; Loskot, S. A.; Mohr, J. T.; Behenna, D. C.; Harned, A. M.; Stoltz, B. M. *Org. Lett.* **2015**, *17*, 5160–5163.

[25] Bennett, N. B.; Duquette, D. C.; Kim, J.; Liu, W.; Marziale, A. N.; Behenna, D. C.; Virgil, S. C.; Stoltz, B. M. *Chem. Eur. J.* **2013**, *19*, 4414–4418.

[26] Behenna, D. C.; Liu, Y.; Yurino, T.; Kim, J.; White, D. E.; Virgil, S. C.; Stoltz, B. M. *Nature Chem.* **2012**, *4*, 130–133.

[27] Bélanger, É.; Cantin, K.; Messe, O.; Tremblay, M.; Paquin, J.-F. *J. Am. Chem. Soc.* **2007**, *129*, 1034–1035.

[28] Nakamura, M.; Hajra, A.; Endo, K.; Nakamura, E. *Angew. Chem. Int. Ed.* **2005**, *44*, 7248–7251.

[29] Shibata, N.; Suzuki, S.; Furukawa, T.; Kawai, H.; Tokunaga, E.; Yuan, Z.; Cahardb, D. *Adv. Synth. Catal.* **2011**, *353*, 2037–2041.

APPENDIX 1

Spectra Relevant to Chapter 1:

Palladium-Catalyzed Enantioselective

Csp^3–Csp^3 Cross-Coupling for the Synthesis

of (Poly)fluorinated Chiral Building Blocks

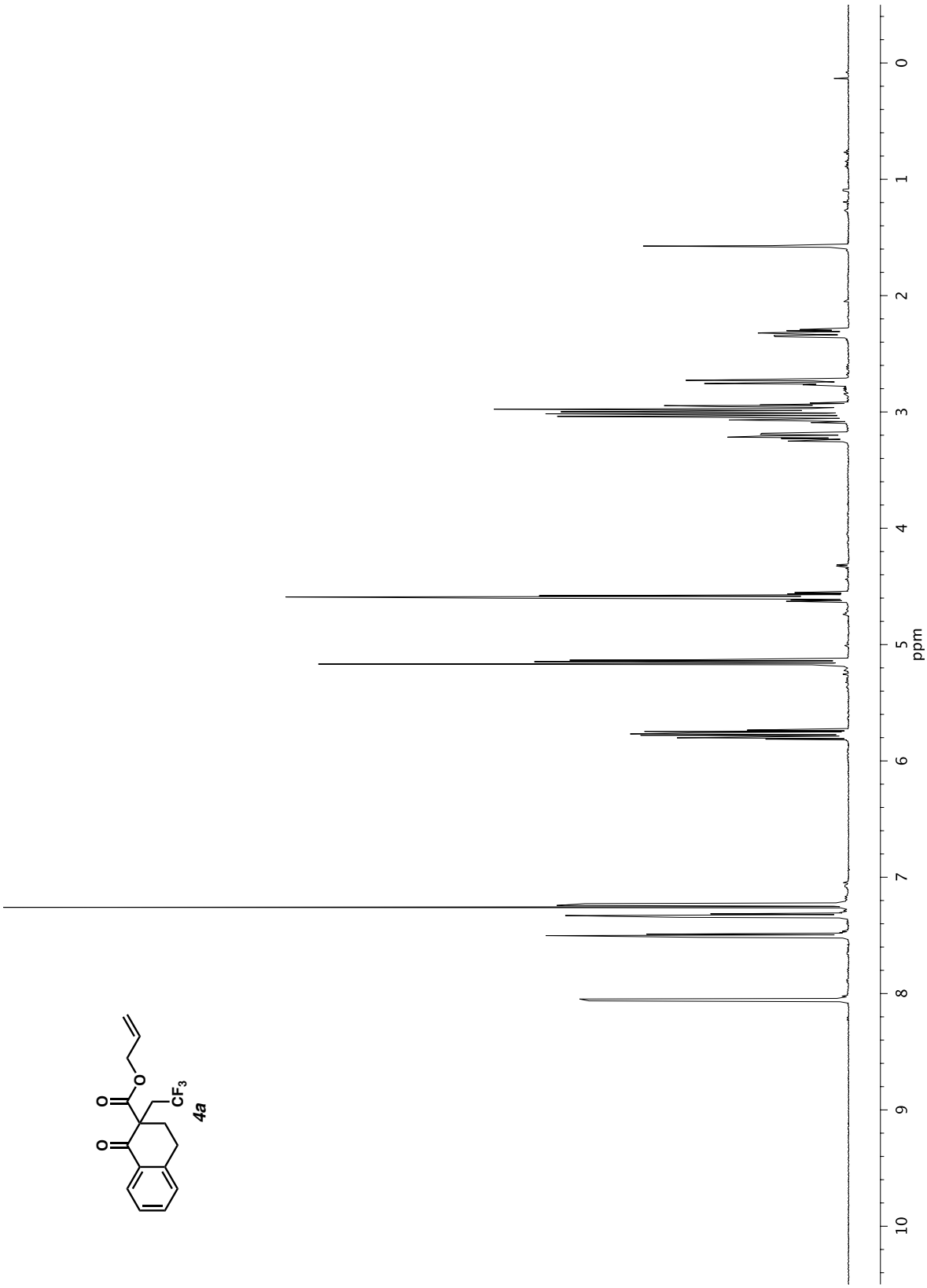

Figure A1.1. ^{1}H NMR (500 MHz, $CDCl_3$) of compound **4a**.

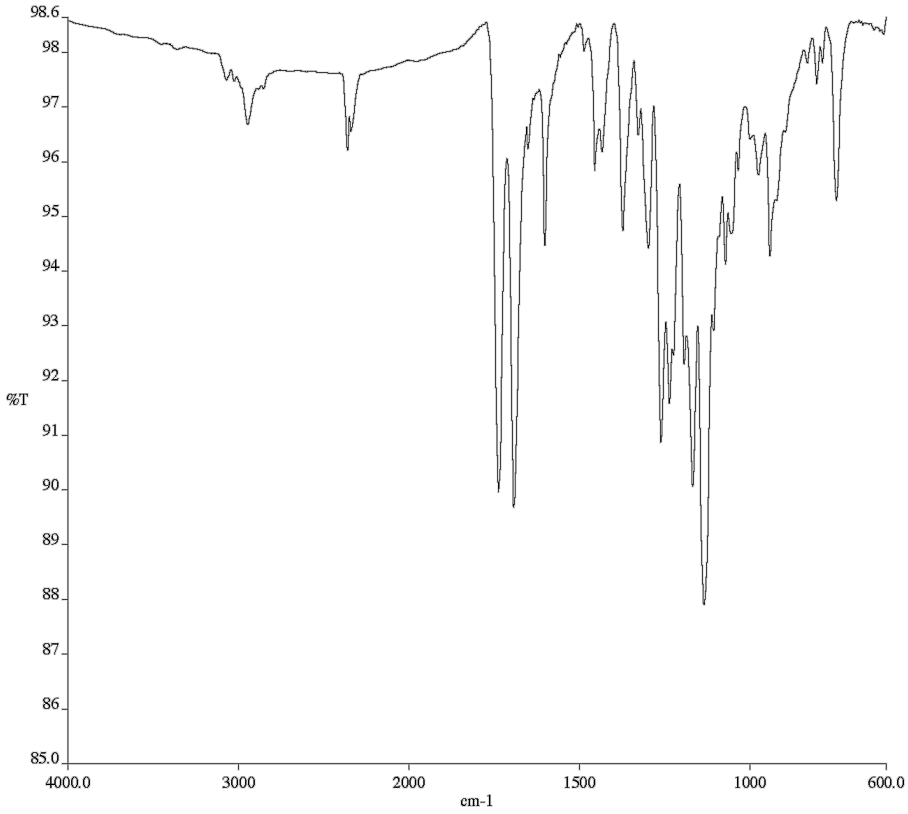

Figure A1.2. Infrared spectrum (Thin Film, NaCl) of compound **4a**.

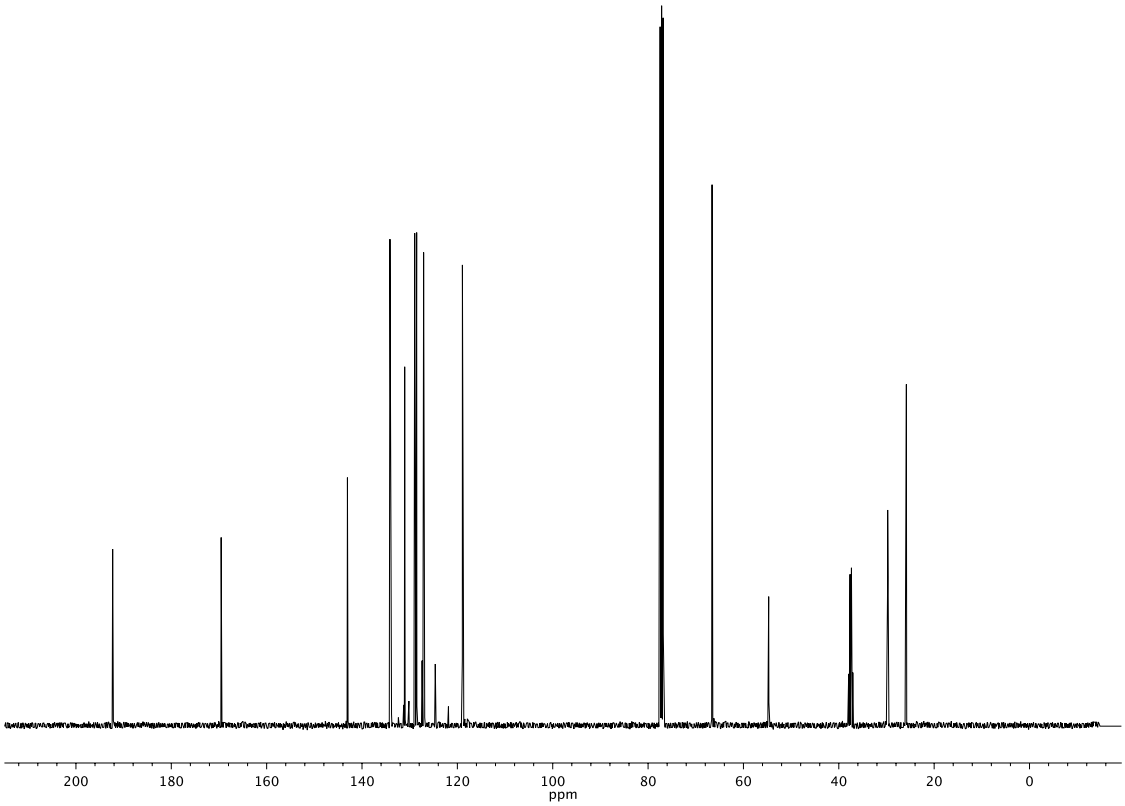

Figure A1.3. ^{13}C NMR (101 MHz, $CDCl_3$) of compound **4a**.

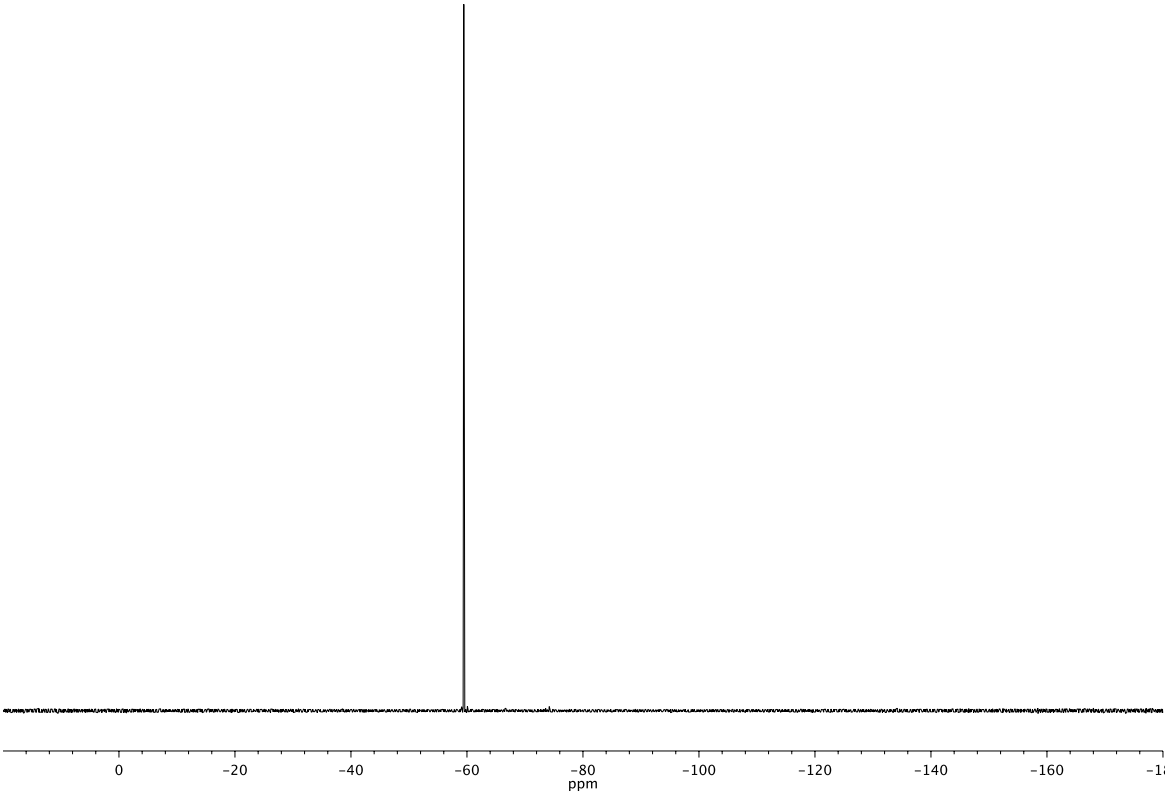

Figure A1.4. ^{19}F NMR (282 MHz, $CDCl_3$) of compound **4a**.

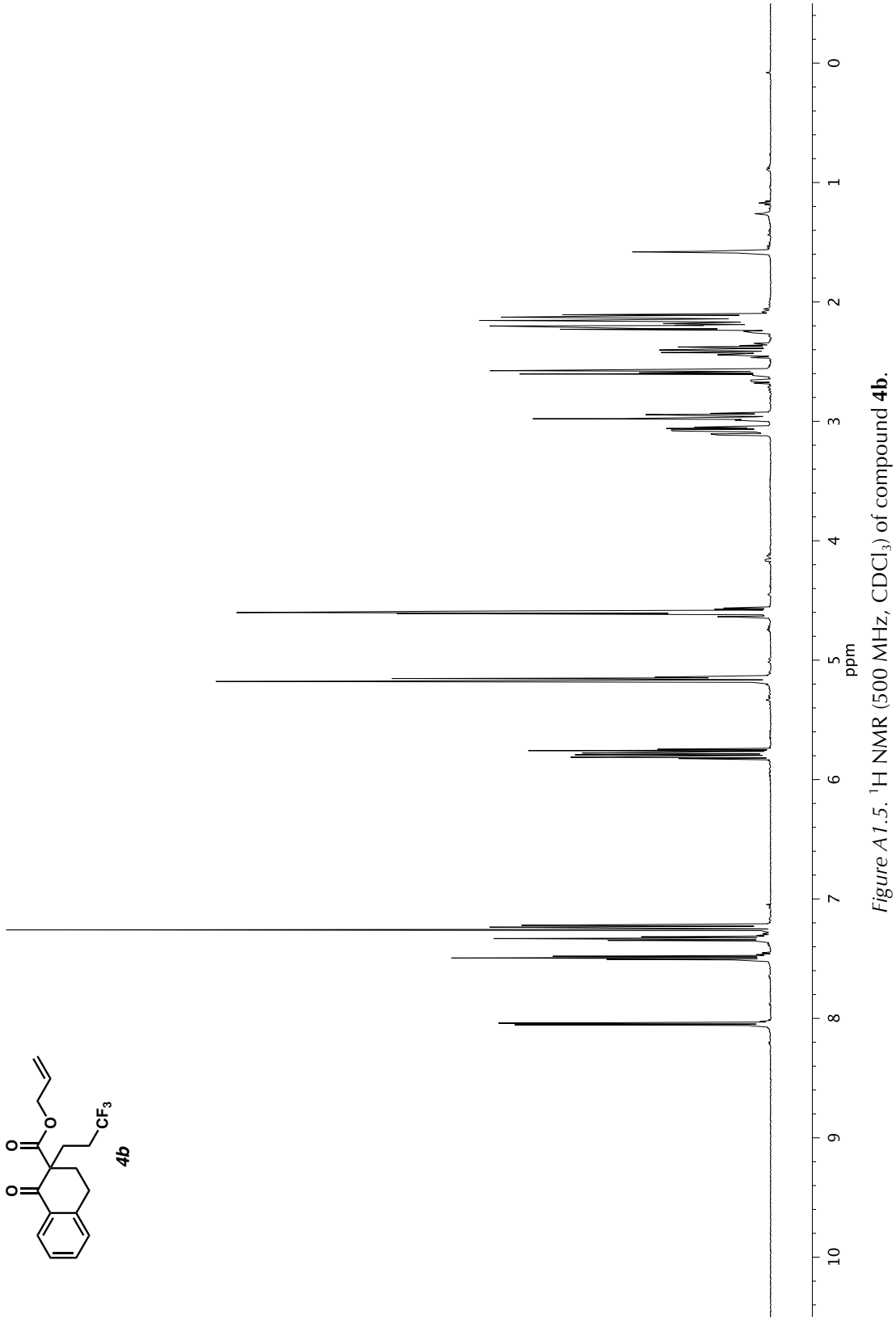

Figure A1.5. ^{1}H NMR (500 MHz, $CDCl_3$) of compound **4b**.

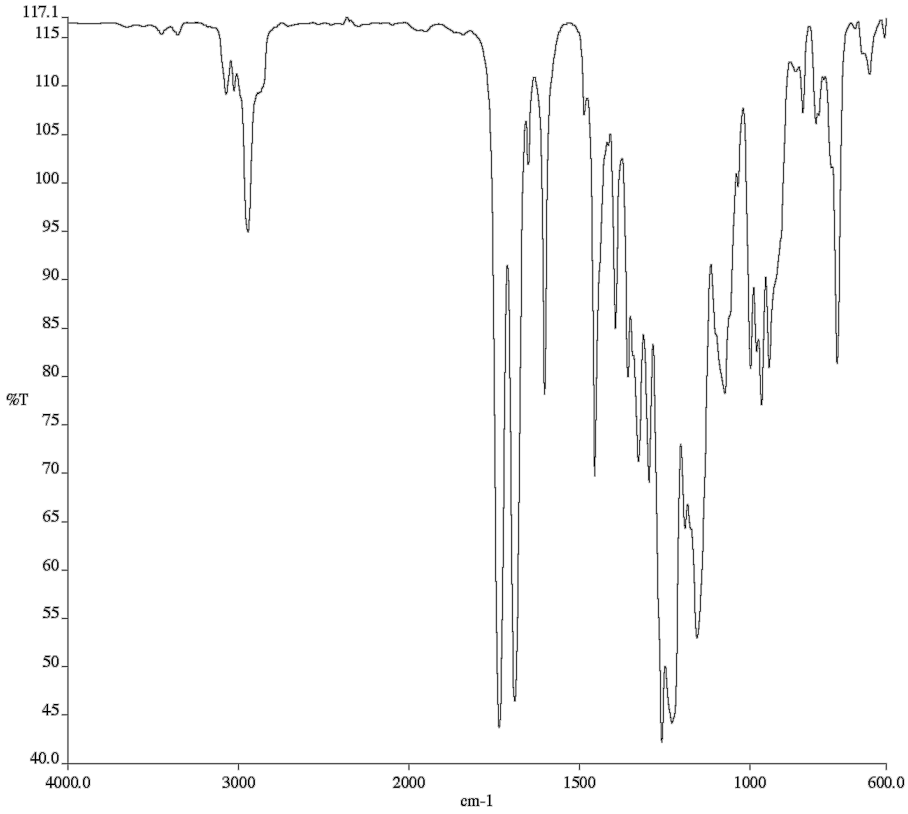

Figure A1.6. Infrared spectrum (Thin Film, NaCl) of compound **4b**.

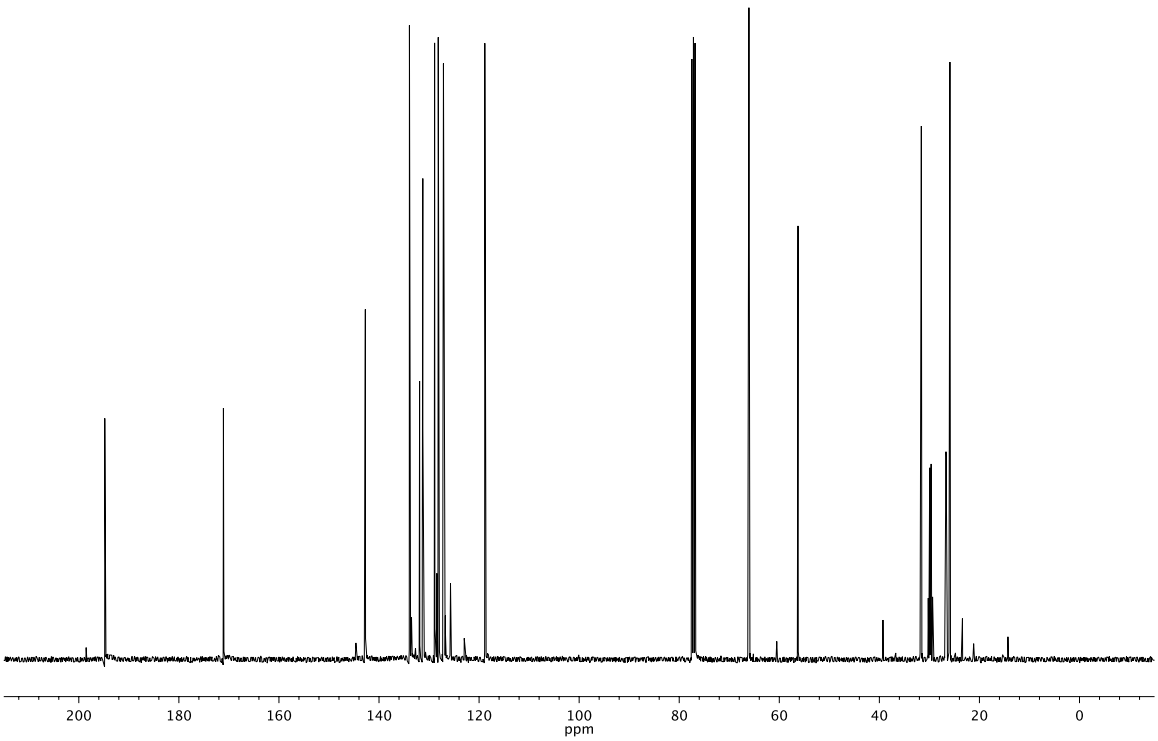

Figure A1.7. ^{13}C NMR (101 MHz, $CDCl_3$) of compound **4b**.

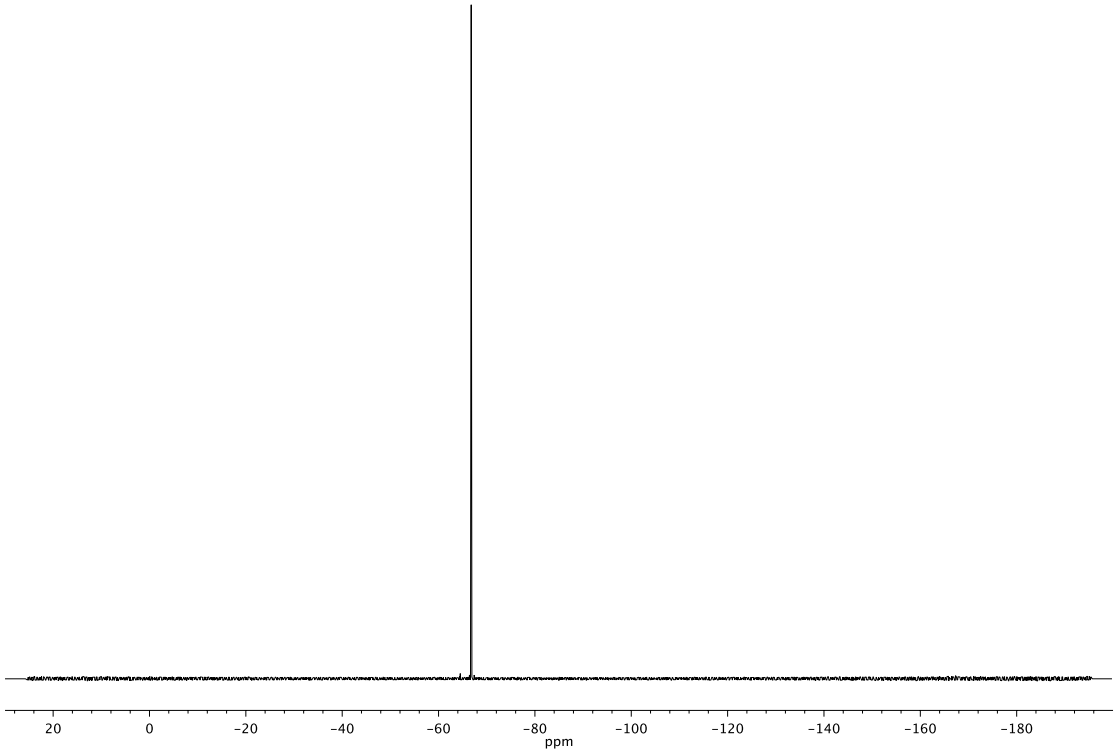

Figure A1.8. ^{19}F NMR (282 MHz, $CDCl_3$) of compound **4b**.

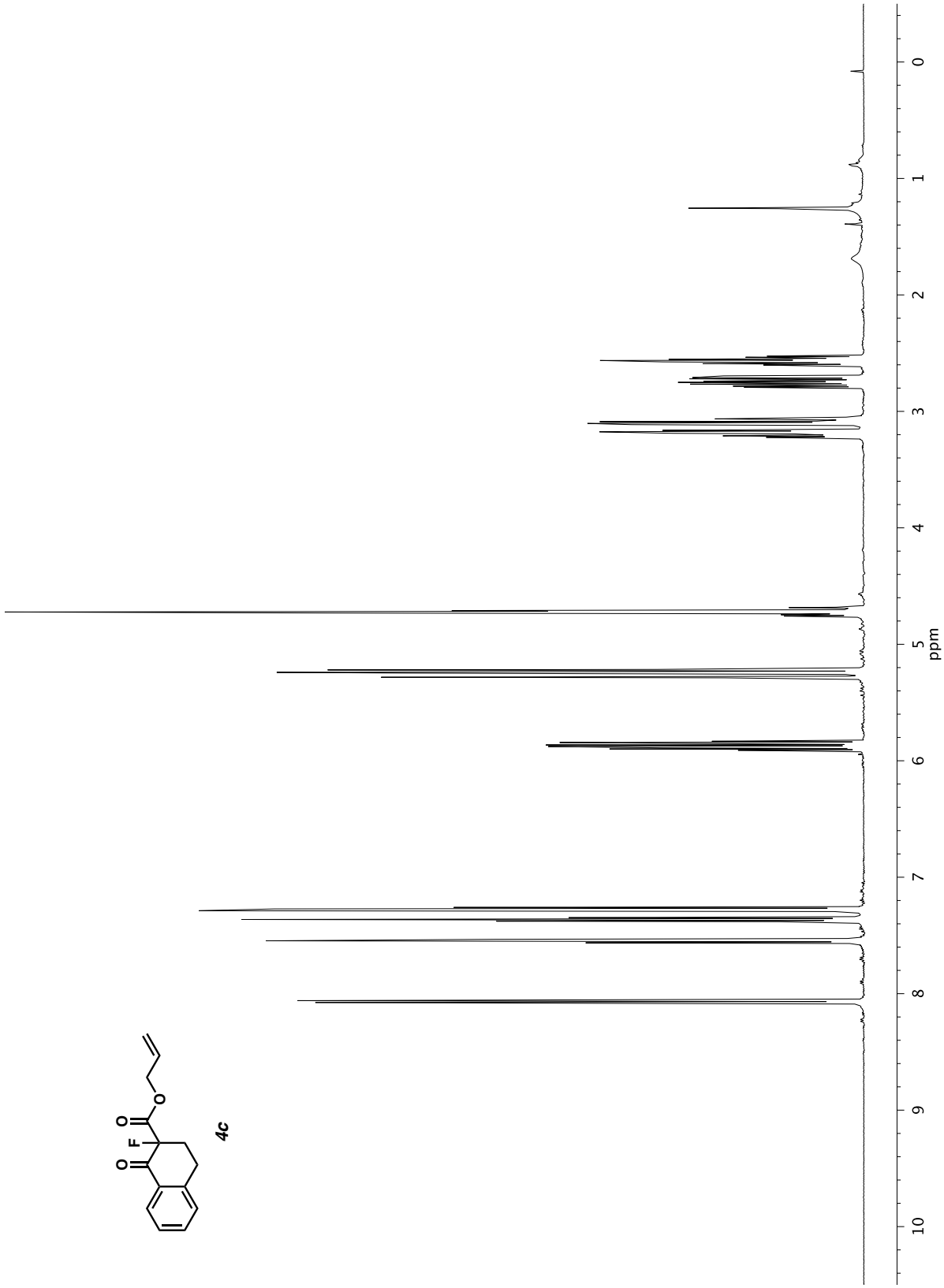

Figure A1.9. ^{1}H NMR (500 MHz, $CDCl_3$) of compound **4c**.

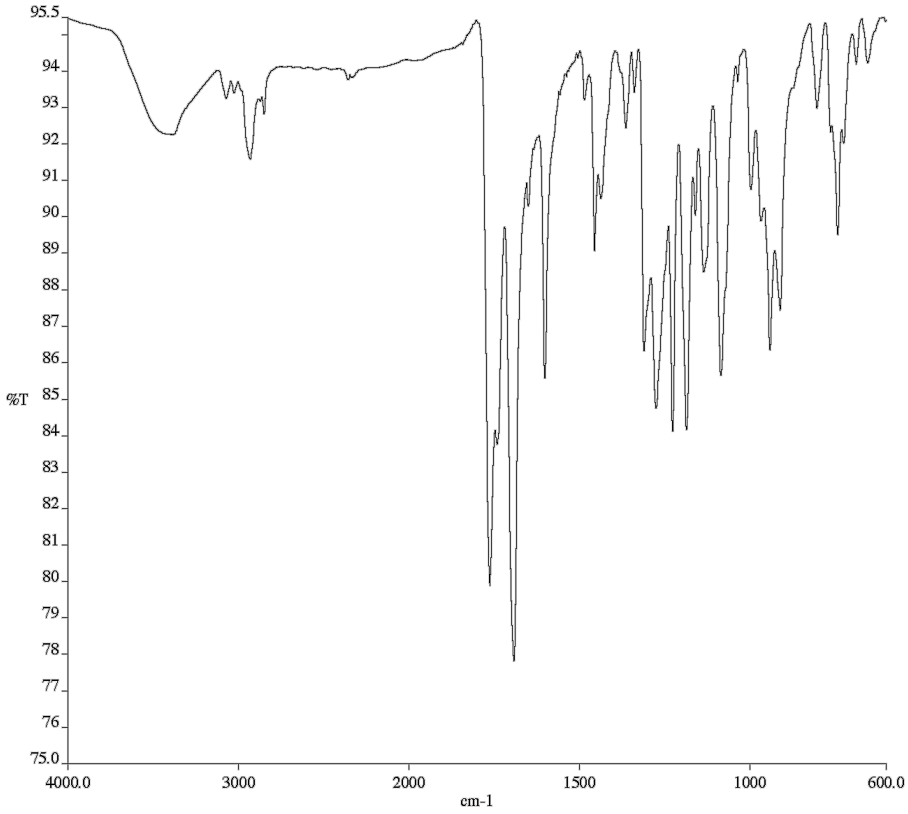

Figure A1.10. Infrared spectrum (Thin Film, NaCl) of compound **4c**.

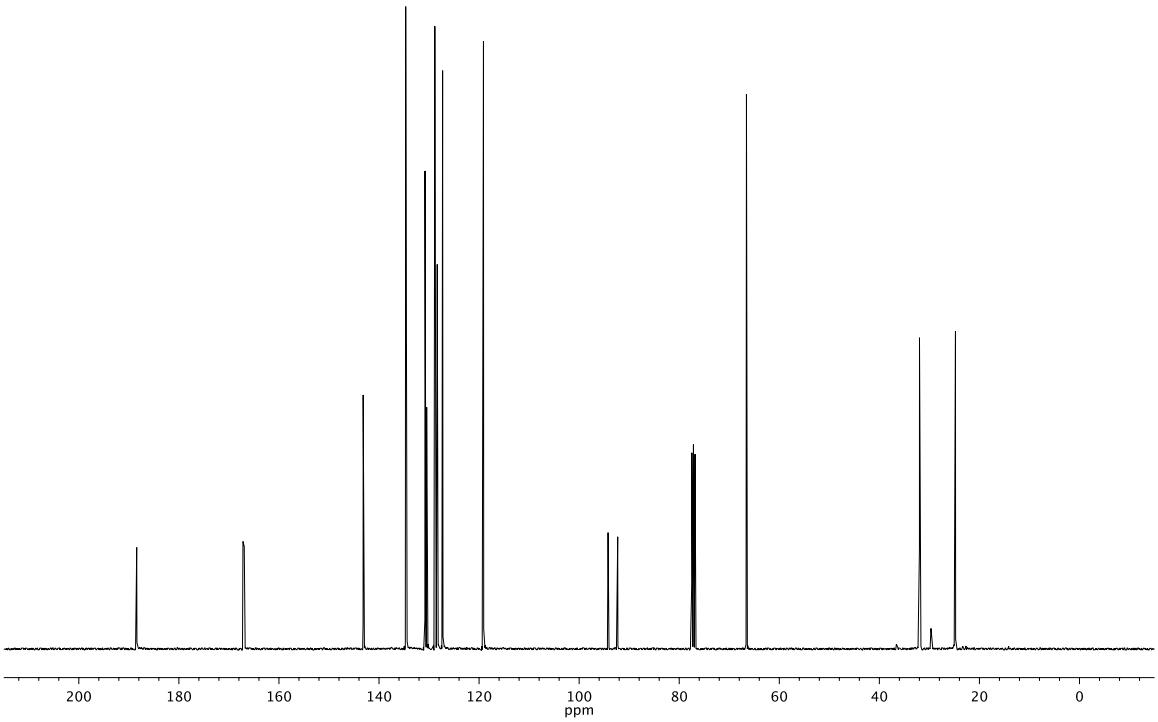

Figure A1.11. ^{13}C NMR (101 MHz, $CDCl_3$) of compound **4c**.

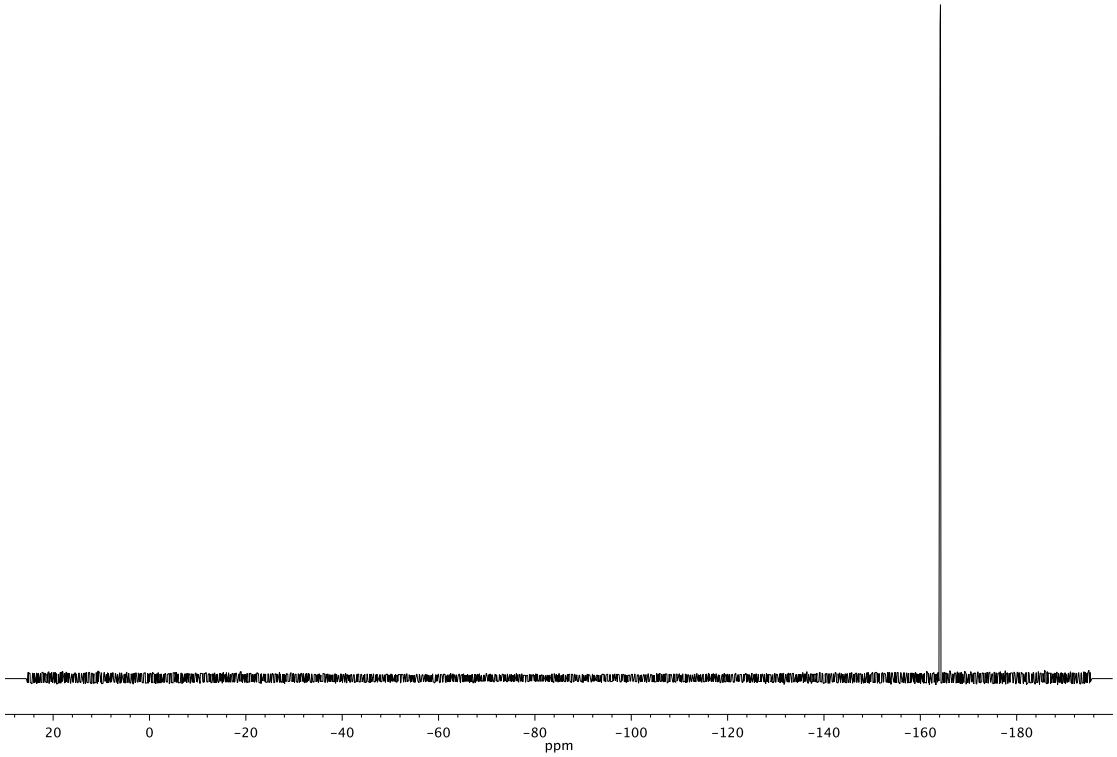

Figure A1.12. ^{19}F NMR (282 MHz, $CDCl_3$) of compound **4c**.

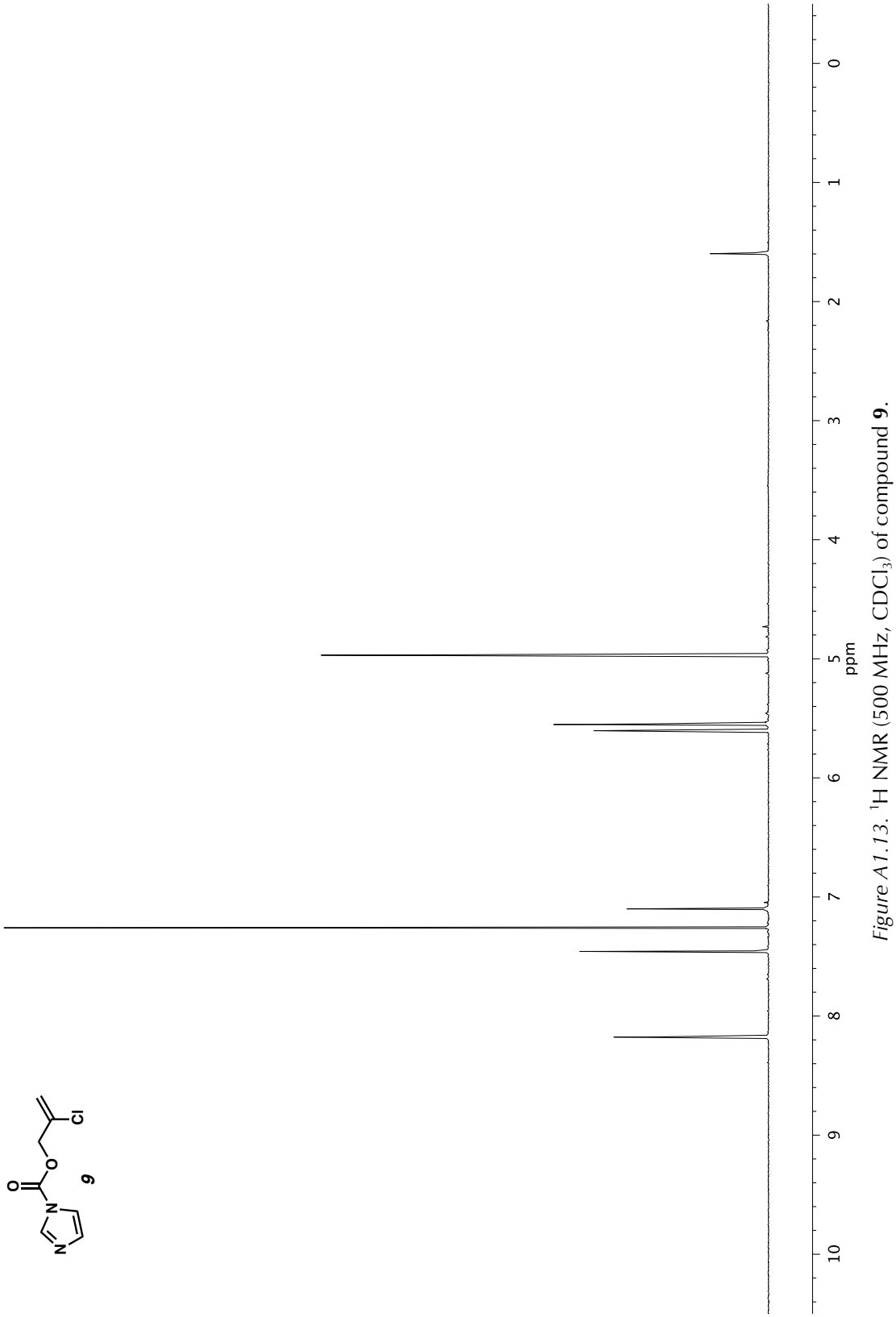

Figure A1.13. ^{1}H NMR (500 MHz, $CDCl_3$) of compound **9**.

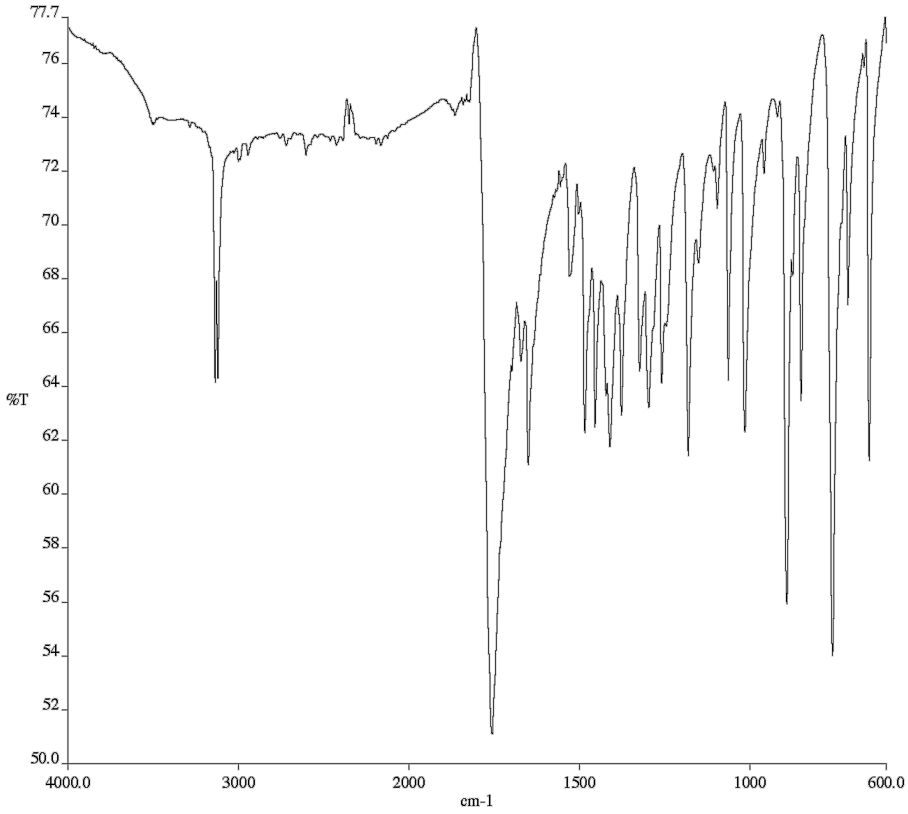

Figure A1.14. Infrared spectrum (Thin Film, NaCl) of compound **9**.

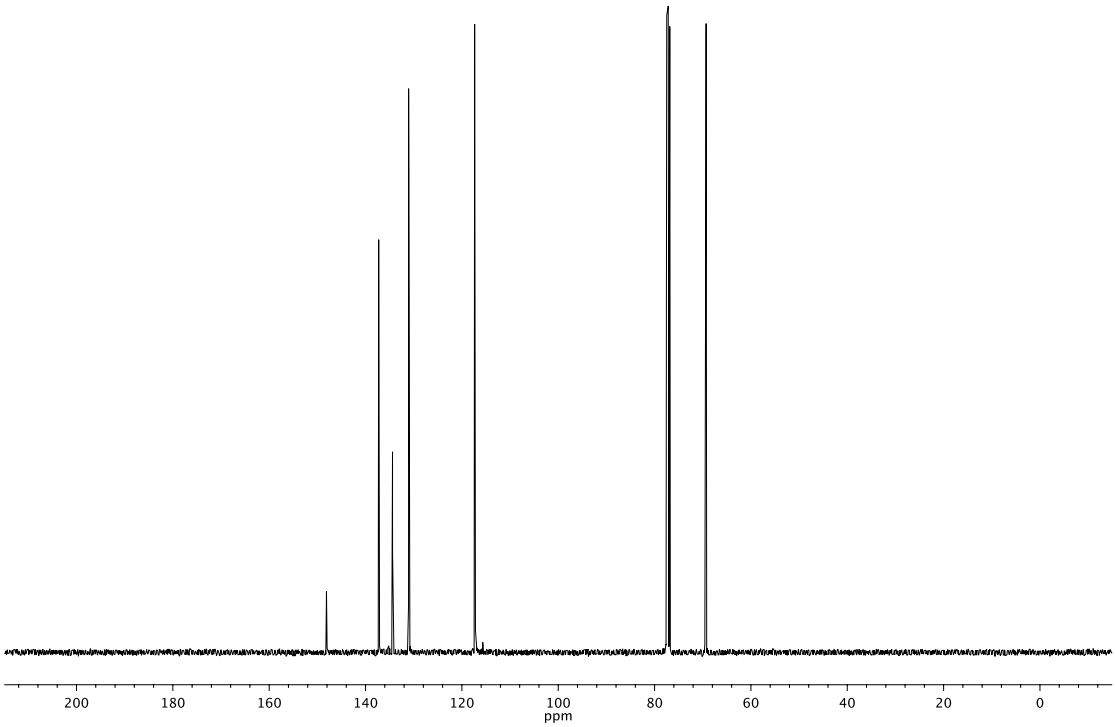

Figure A1.14. ^{13}C NMR (101 MHz, $CDCl_3$) of compound **9**.

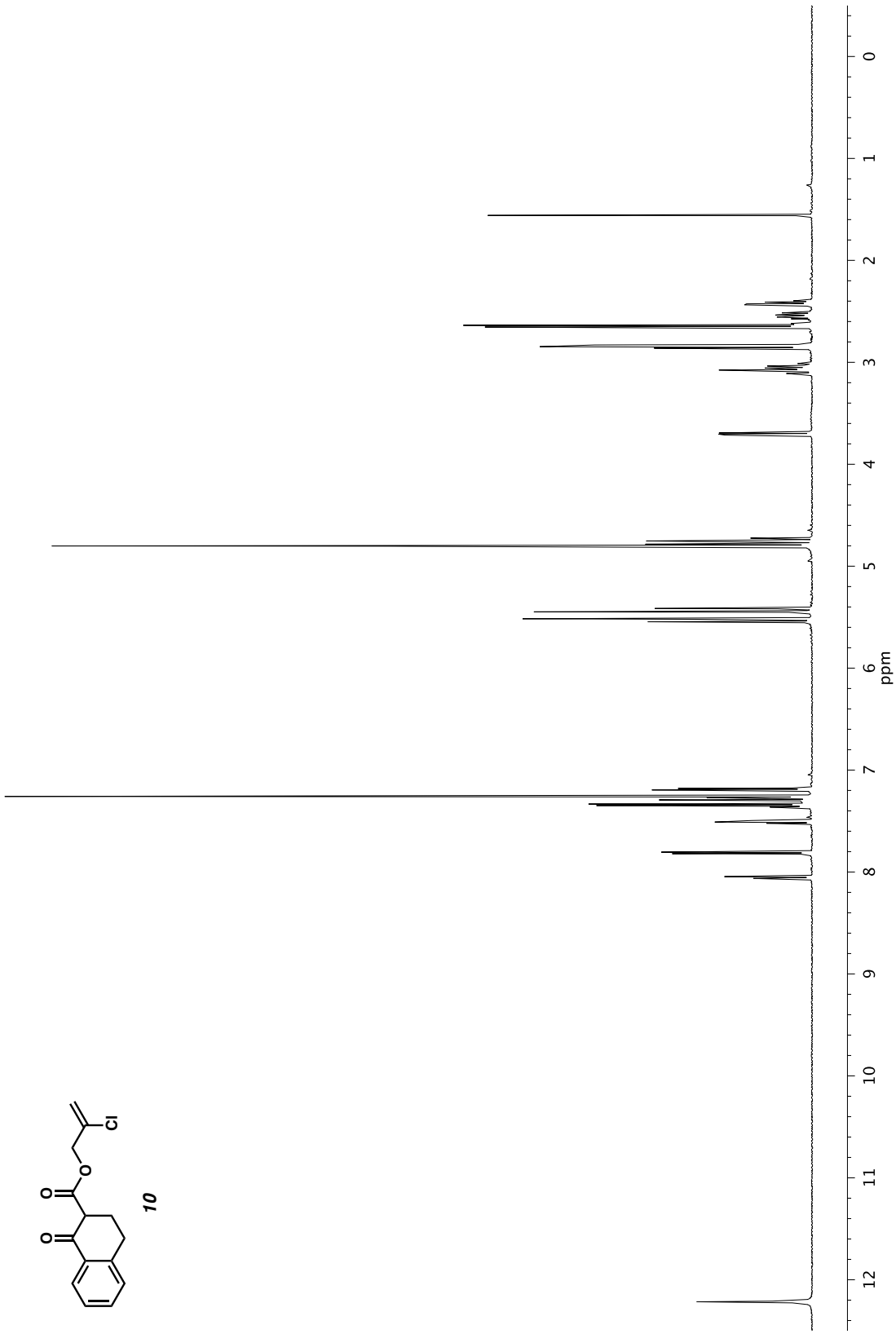

Figure A1.16. ^{1}H NMR (500 MHz, $CDCl_3$) of compound **10**.

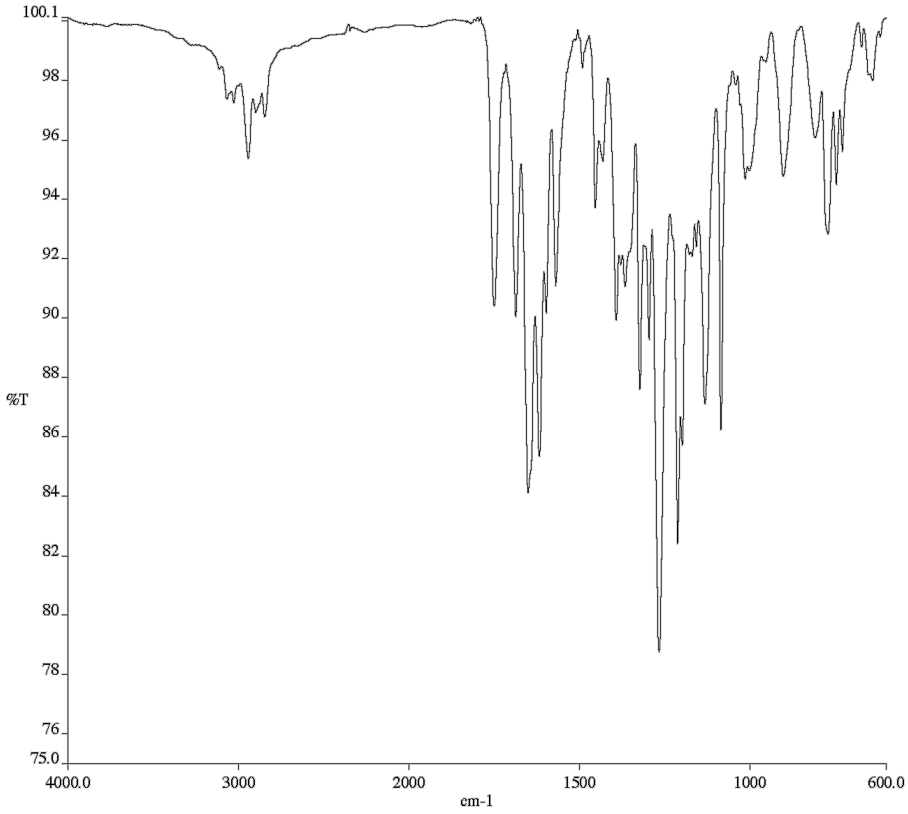

Figure A1.17. Infrared spectrum (Thin Film, NaCl) of compound **10**.

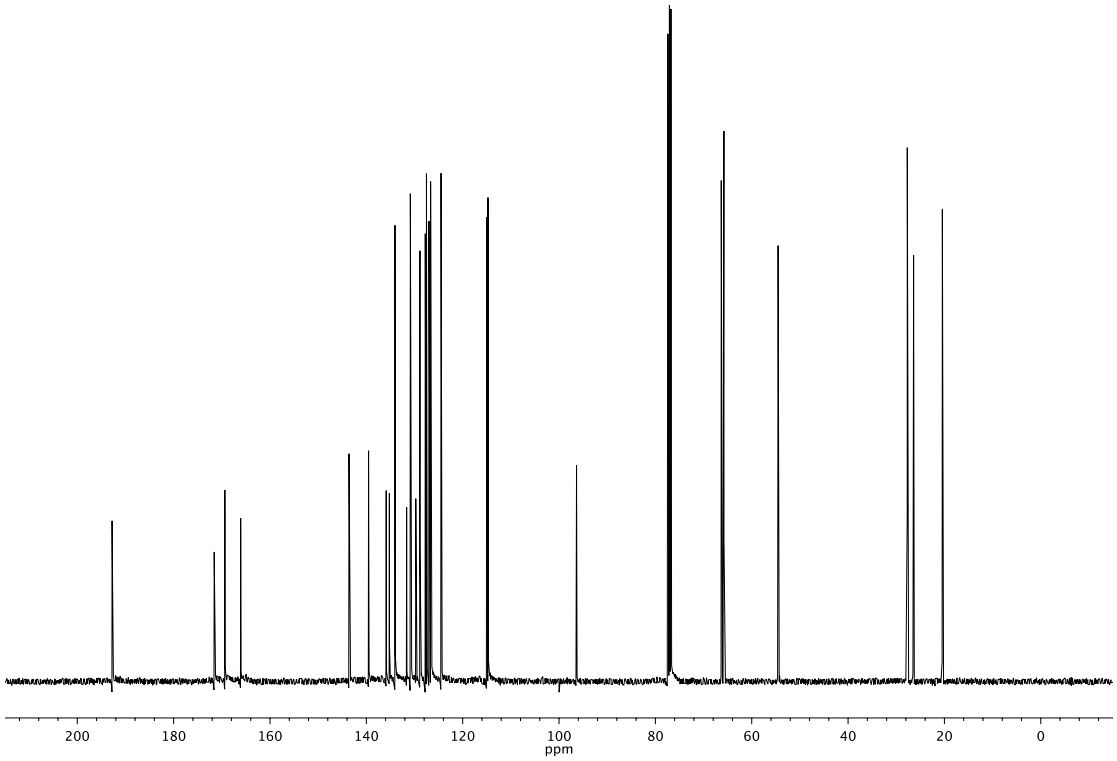

Figure A1.18. ^{13}C NMR (101 MHz, $CDCl_3$) of compound **10**.

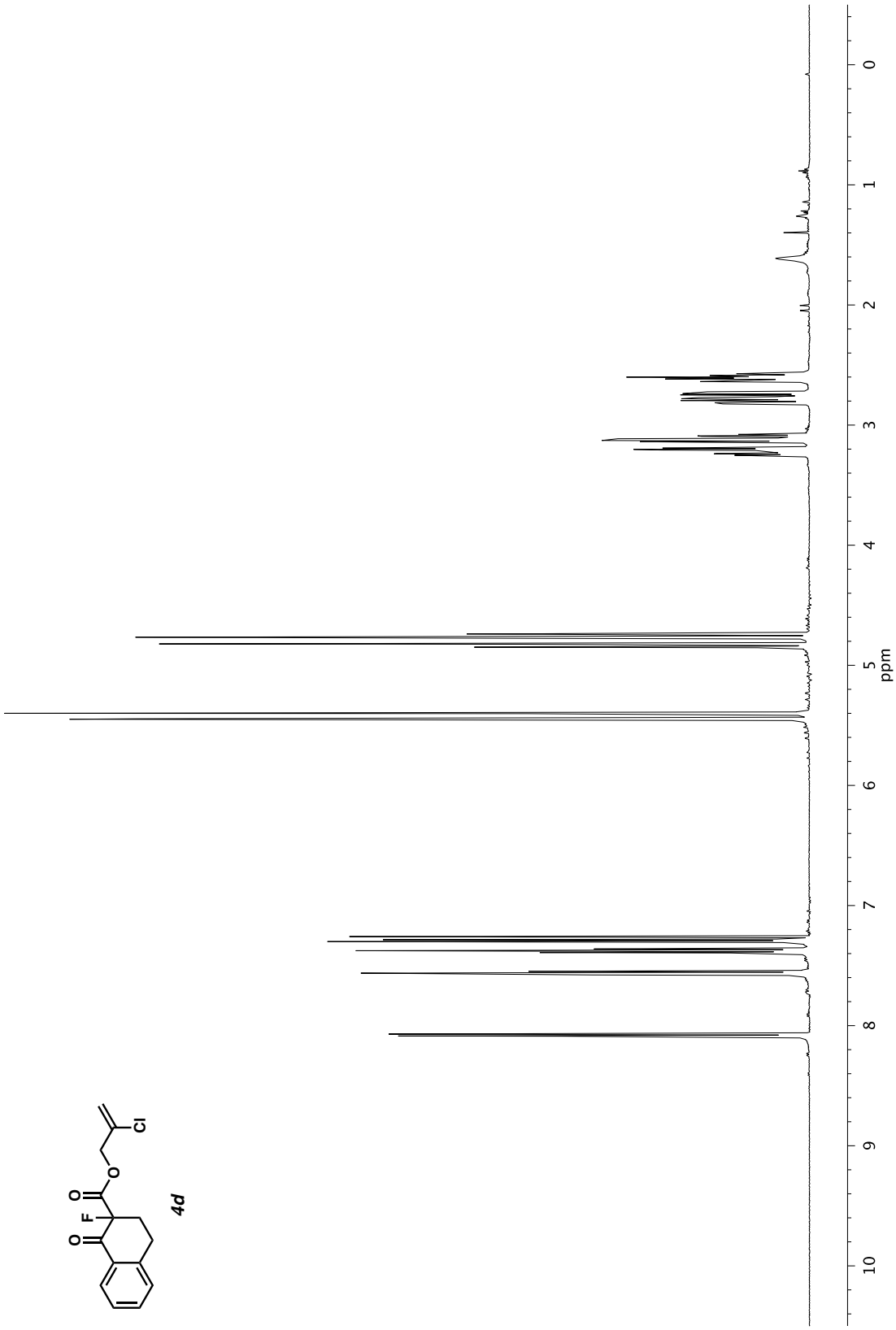

Figure A1.19. ^{1}H NMR (500 MHz, $CDCl_3$) of compound **4d**.

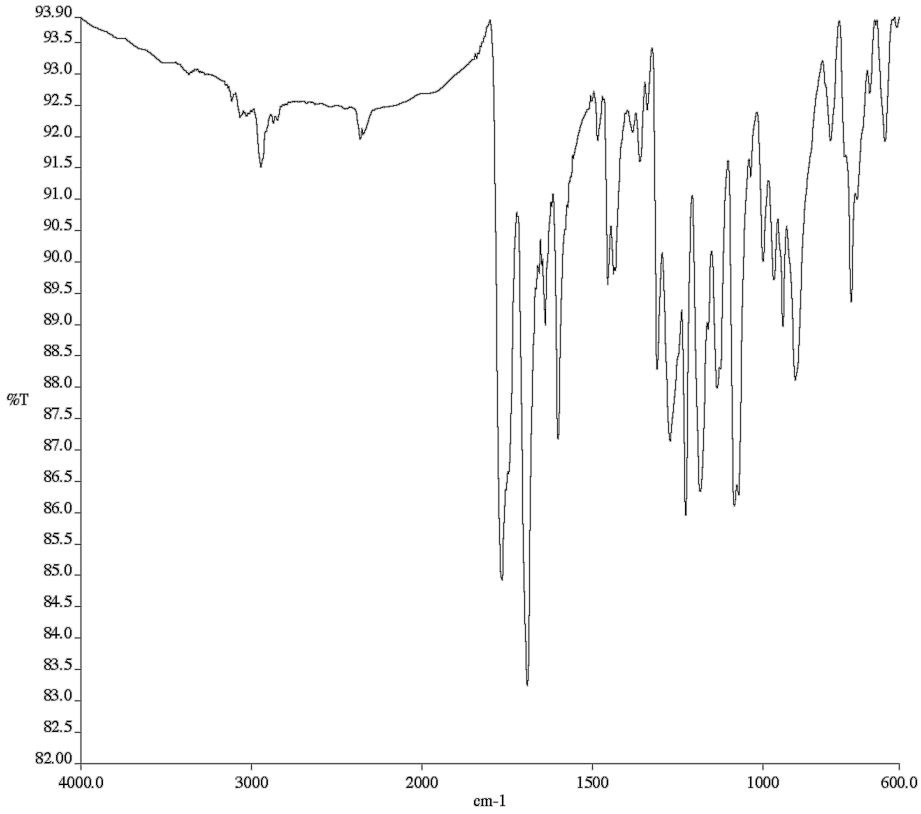

Figure A1.20. Infrared spectrum (Thin Film, NaCl) of compound **4d**.

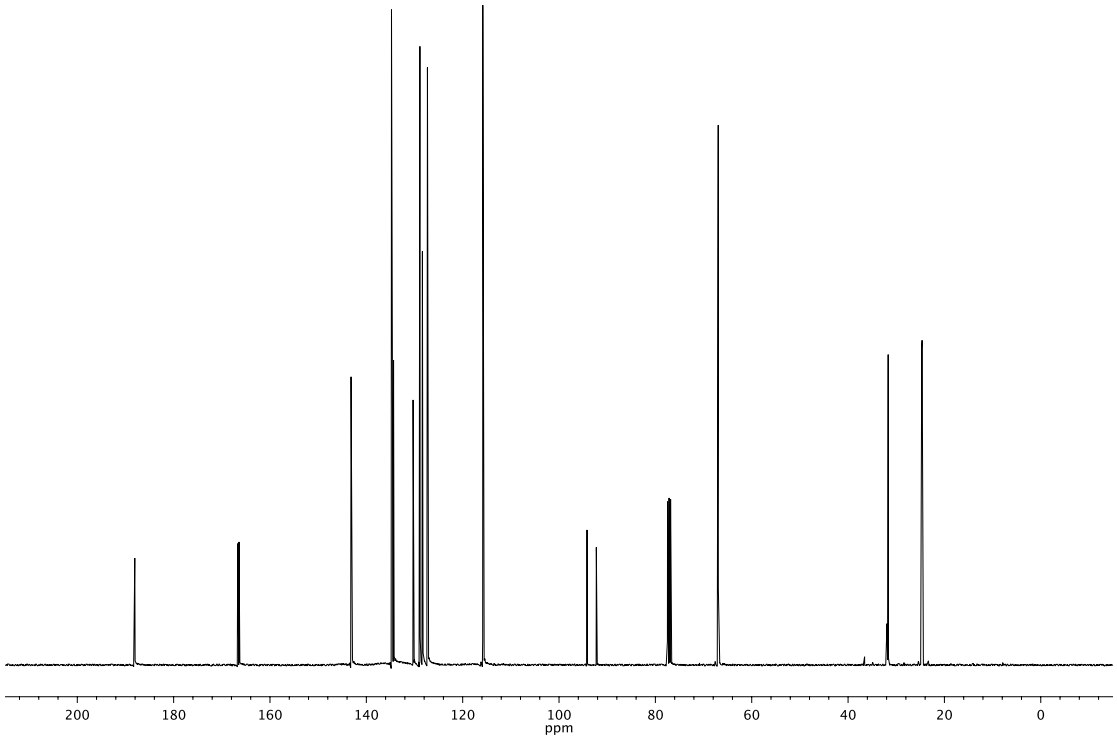

Figure A1.21. ^{13}C NMR (101 MHz, $CDCl_3$) of compound **4d**.

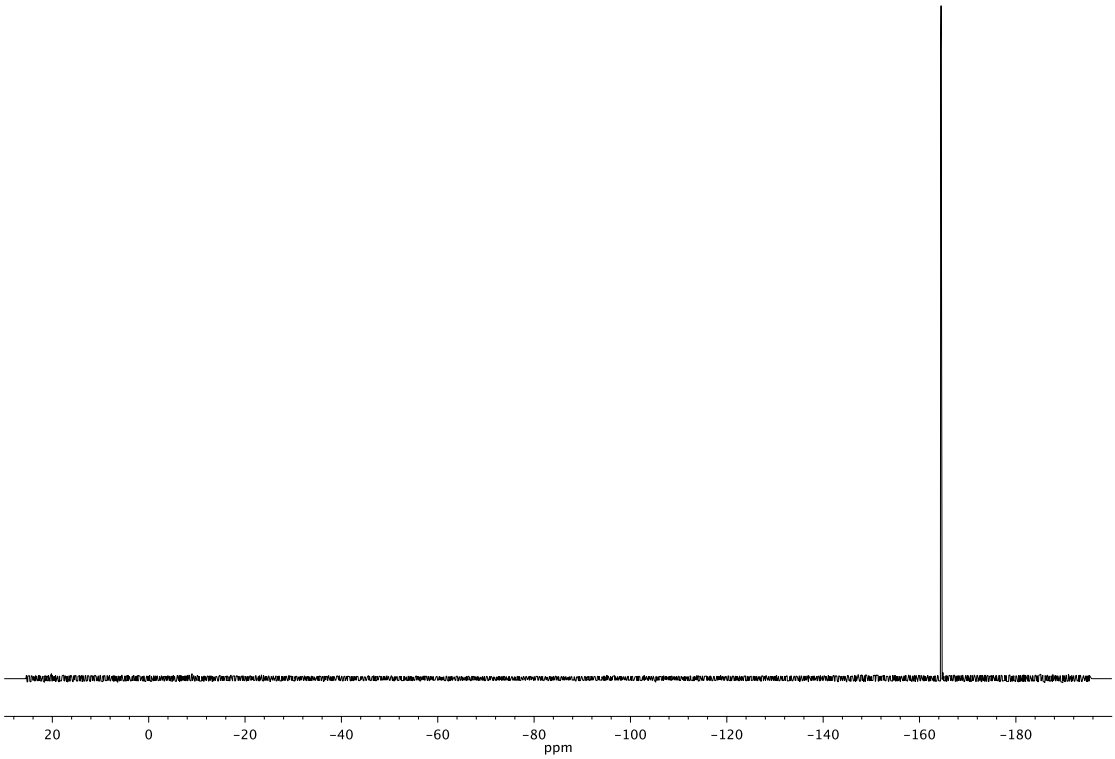

Figure A1.22. ^{19}F NMR (282 MHz, $CDCl_3$) of compound **4d**.

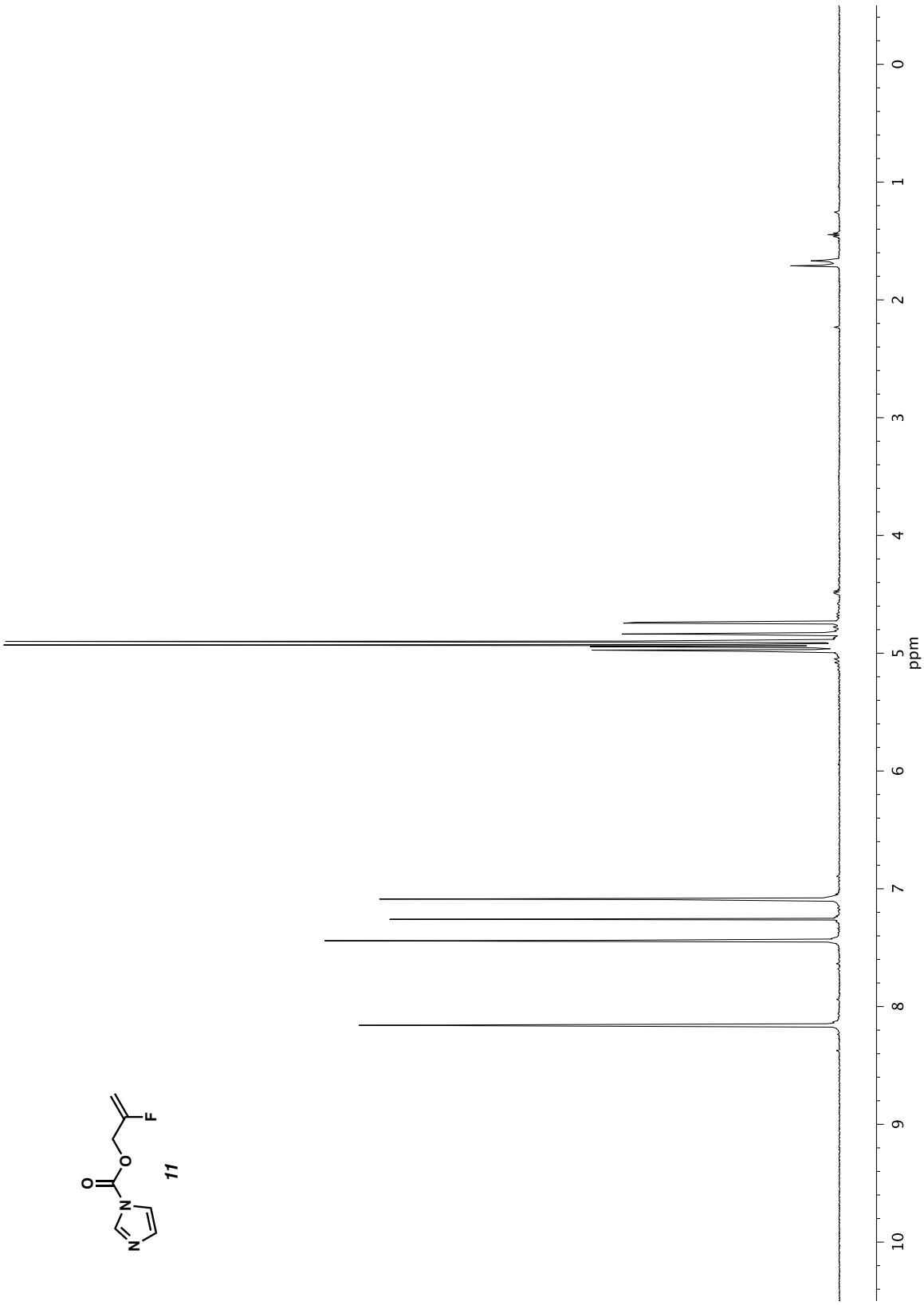

Figure A1.23. ^{1}H NMR (500 MHz, $CDCl_3$) of compound **11**.

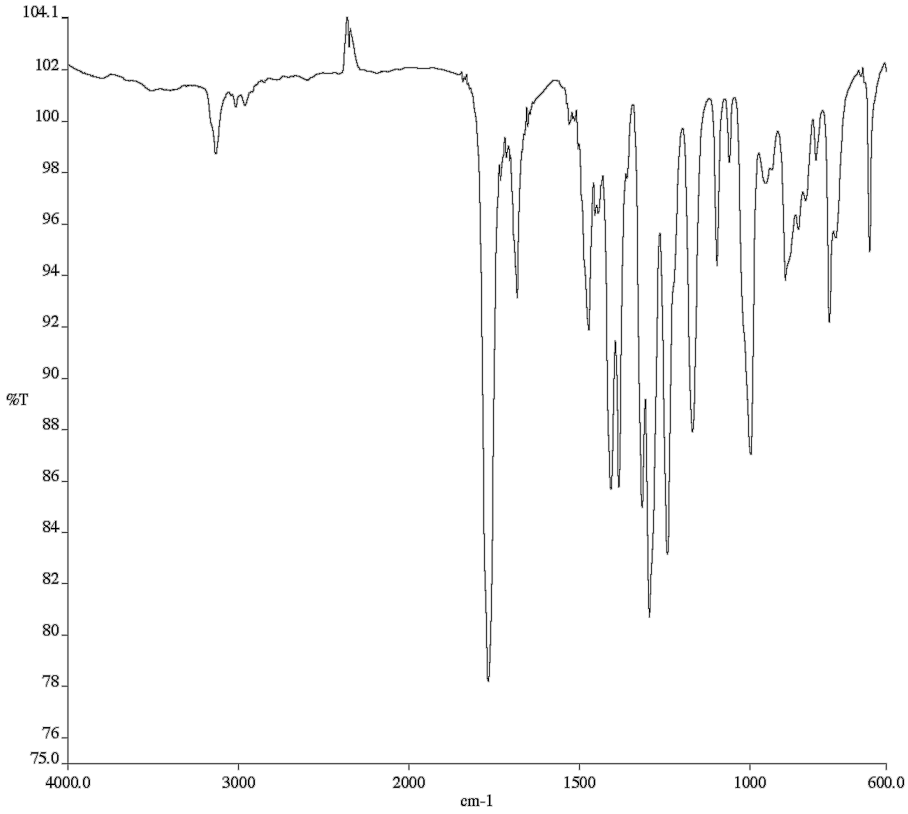

Figure A1.24. Infrared spectrum (Thin Film, NaCl) of compound **11**.

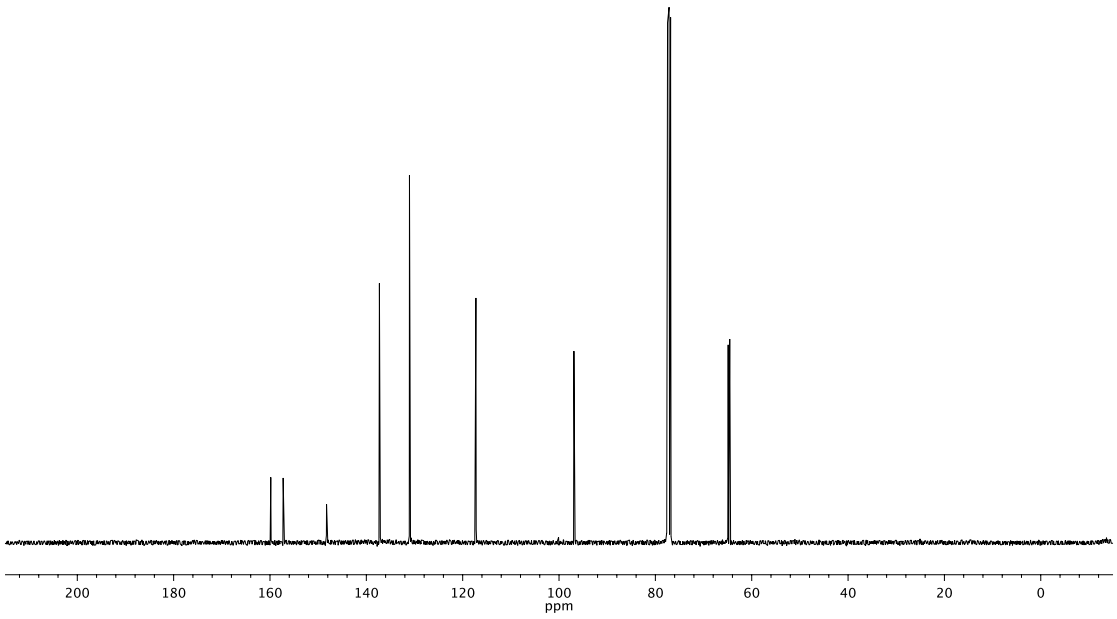

Figure A1.25. ^{13}C NMR (101 MHz, $CDCl_3$) of compound **11**.

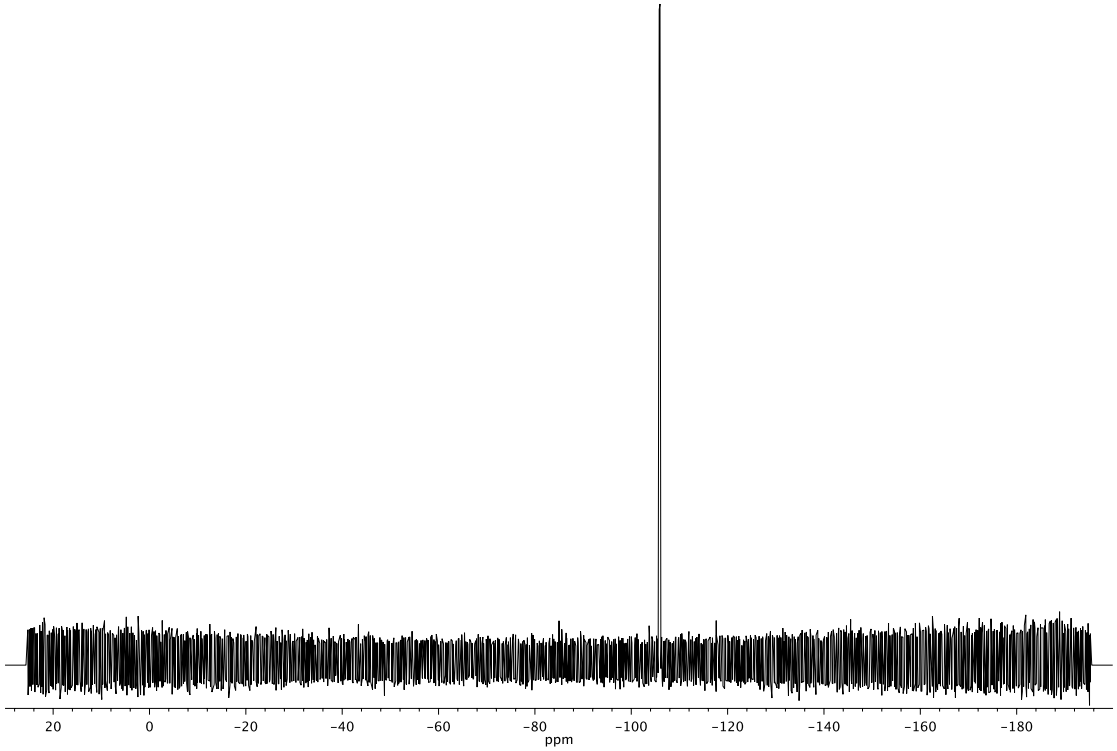

Figure A1.26. ^{19}F NMR (282 MHz, $CDCl_3$) of compound **11**.

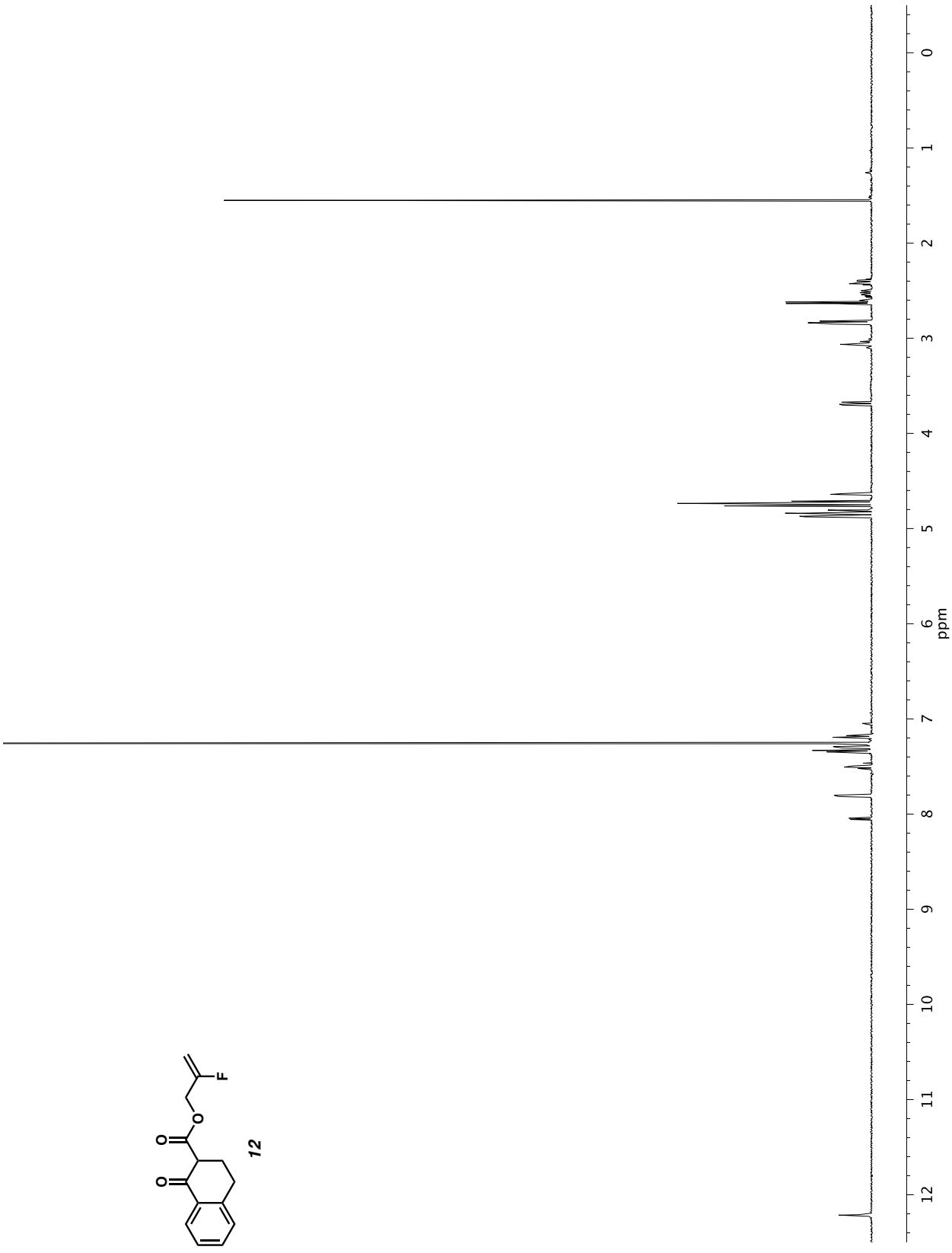

Figure A1.27. ^{1}H NMR (500 MHz, $CDCl_3$) of compound **12**.

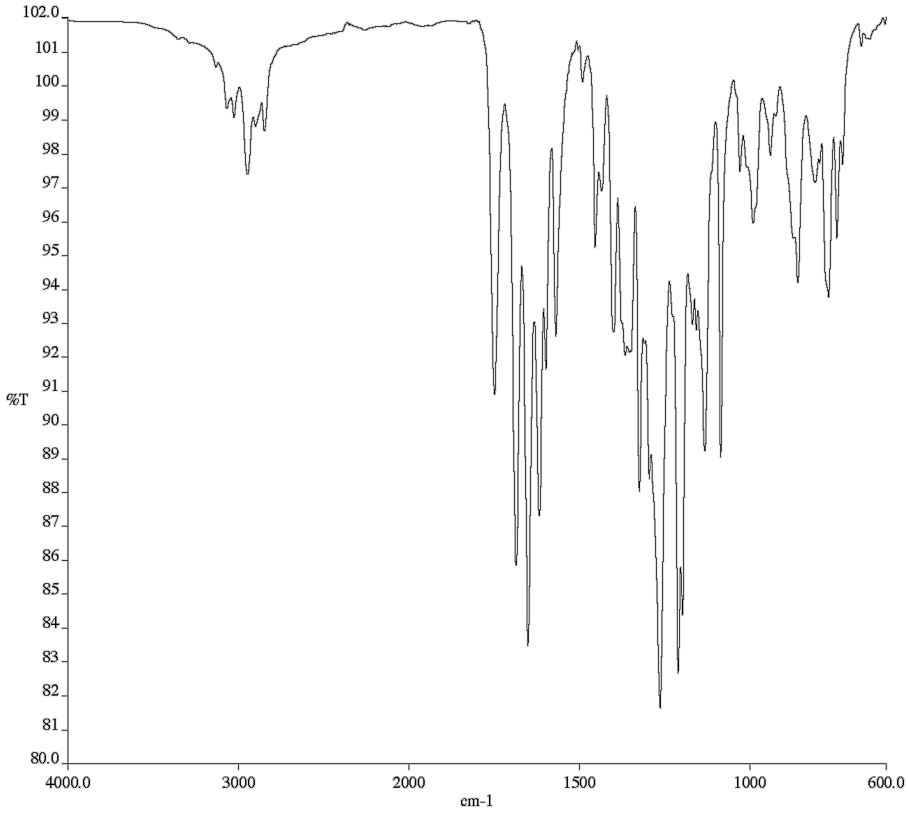

Figure A1.28. Infrared spectrum (Thin Film, NaCl) of compound **12**.

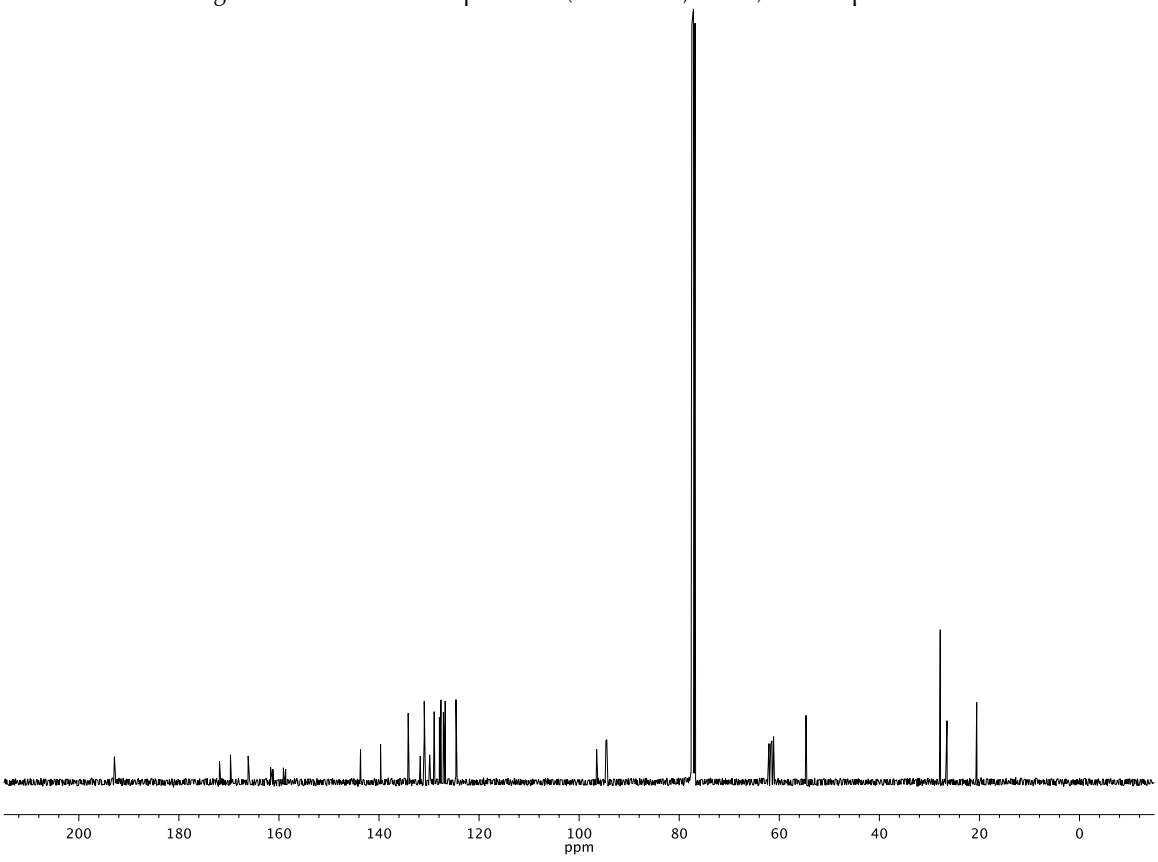

Figure A1.29. ^{13}C NMR (101 MHz, $CDCl_3$) of compound **12**.

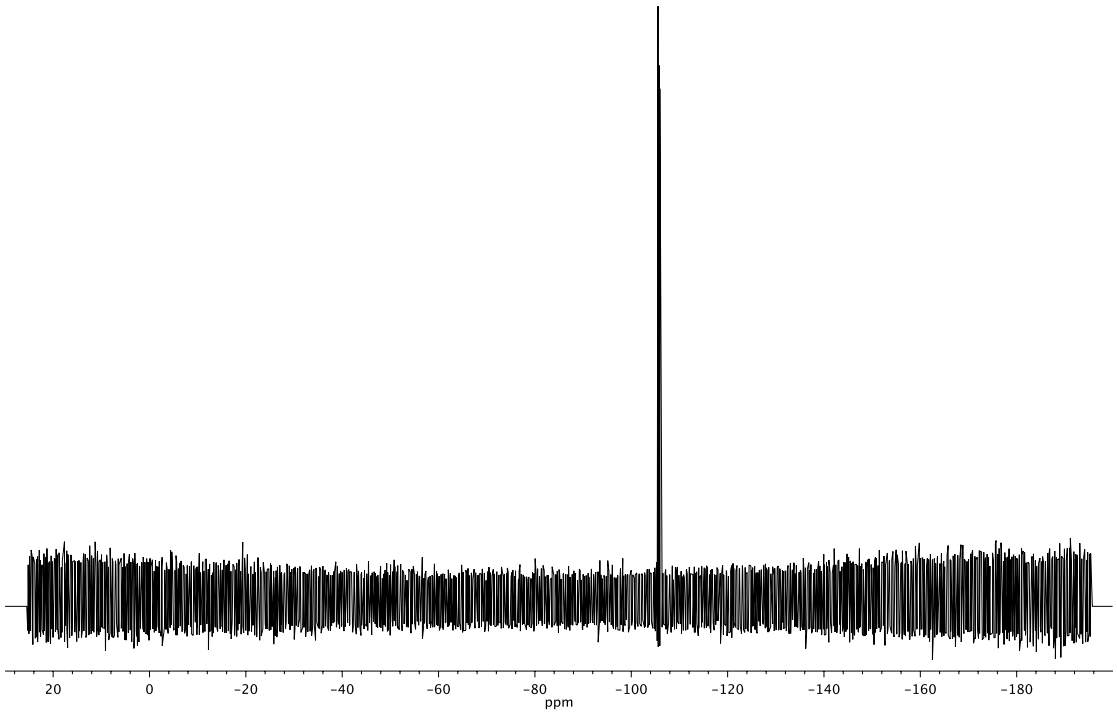

Figure A1.30. ^{19}F NMR (282 MHz, $CDCl_3$) of compound **12**.

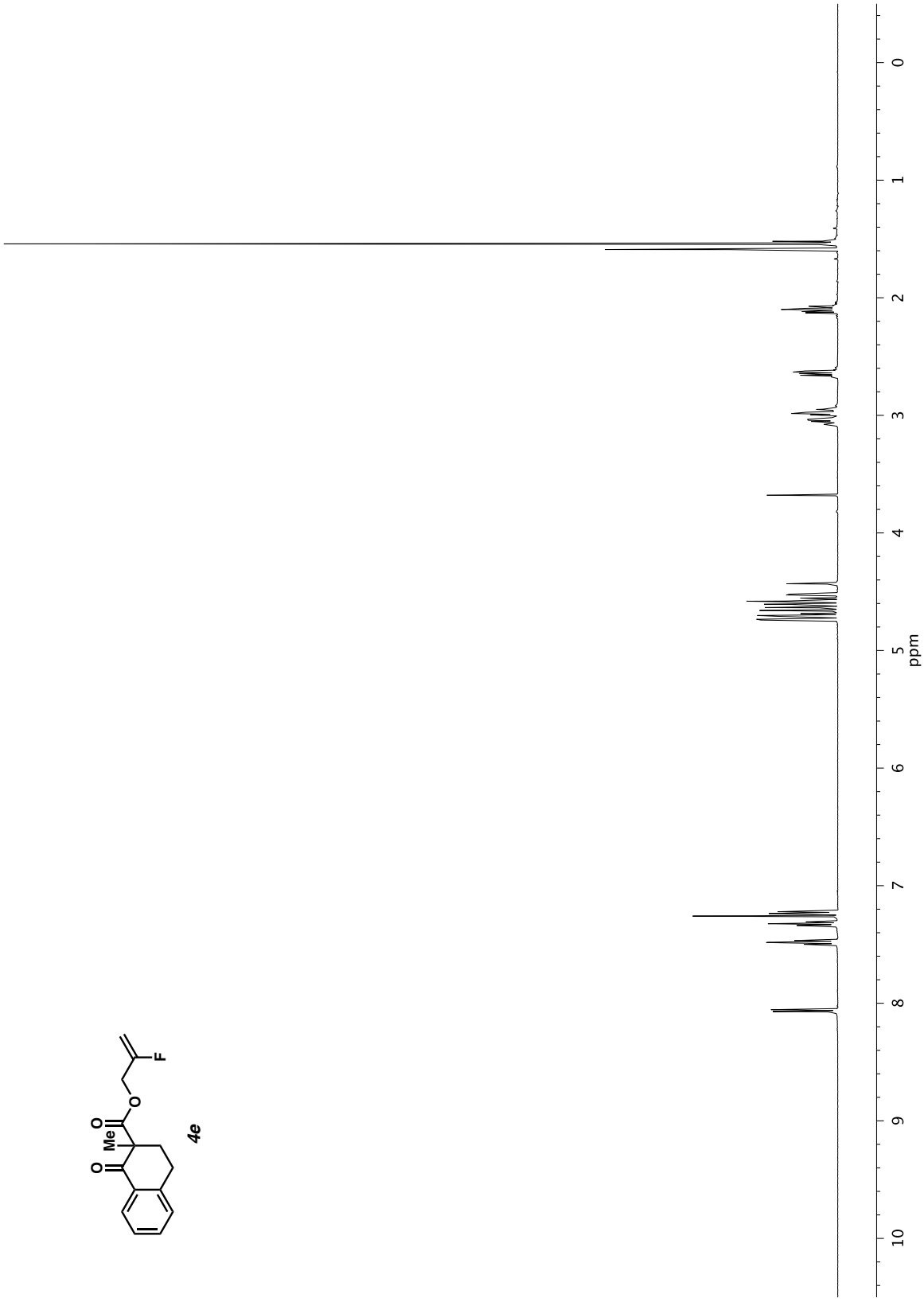

Figure A1.31. ^{1}H NMR (500 MHz, $CDCl_3$) of compound **4e**.

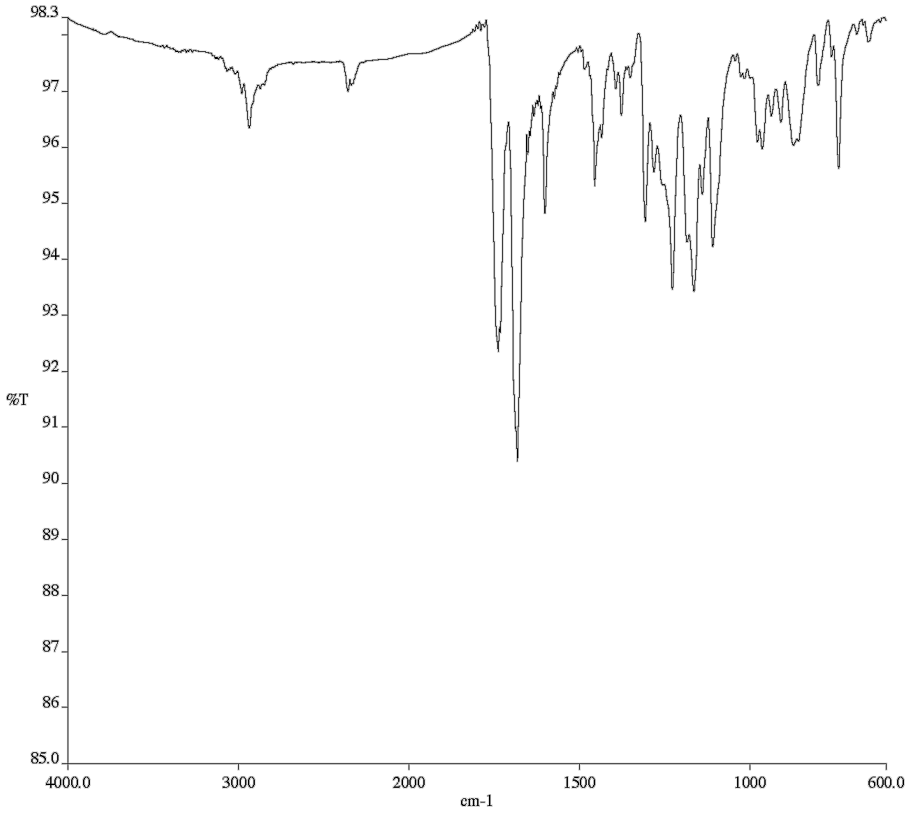

Figure A1.32. Infrared spectrum (Thin Film, NaCl) of compound **4e**.

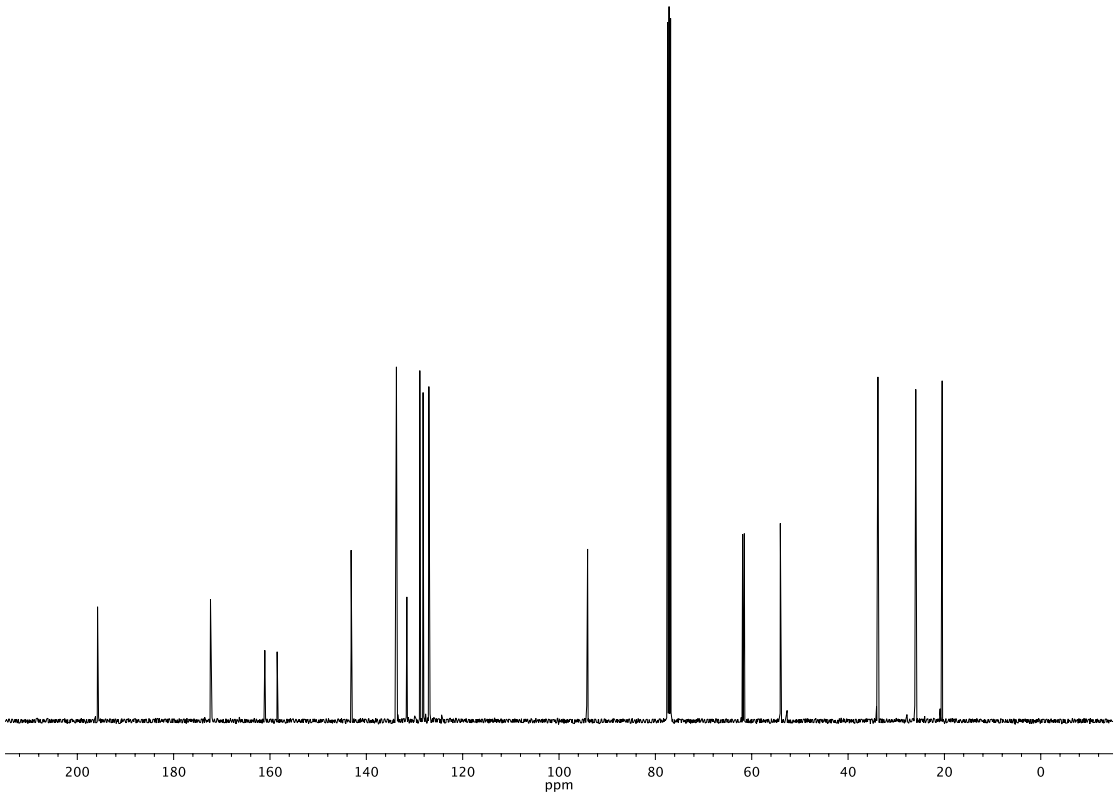

Figure A1.33. ^{13}C NMR (101 MHz, $CDCl_3$) of compound **4e**.

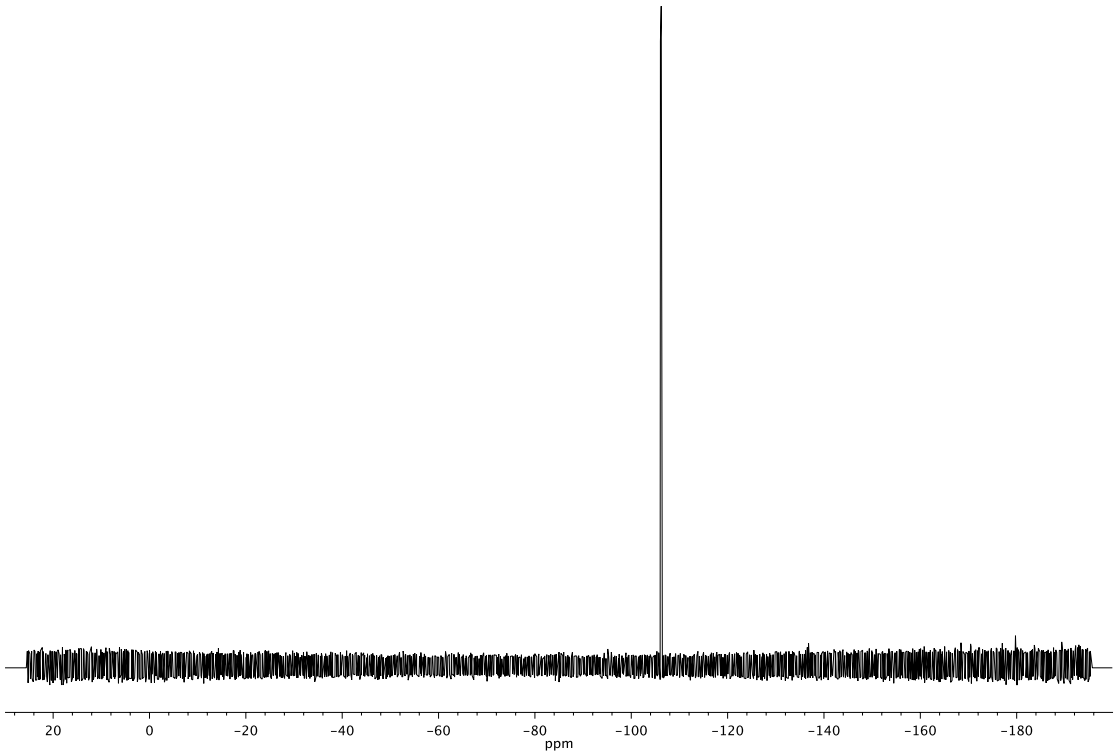

Figure A1.34. ^{19}F NMR (282 MHz, $CDCl_3$) of compound **4e**.

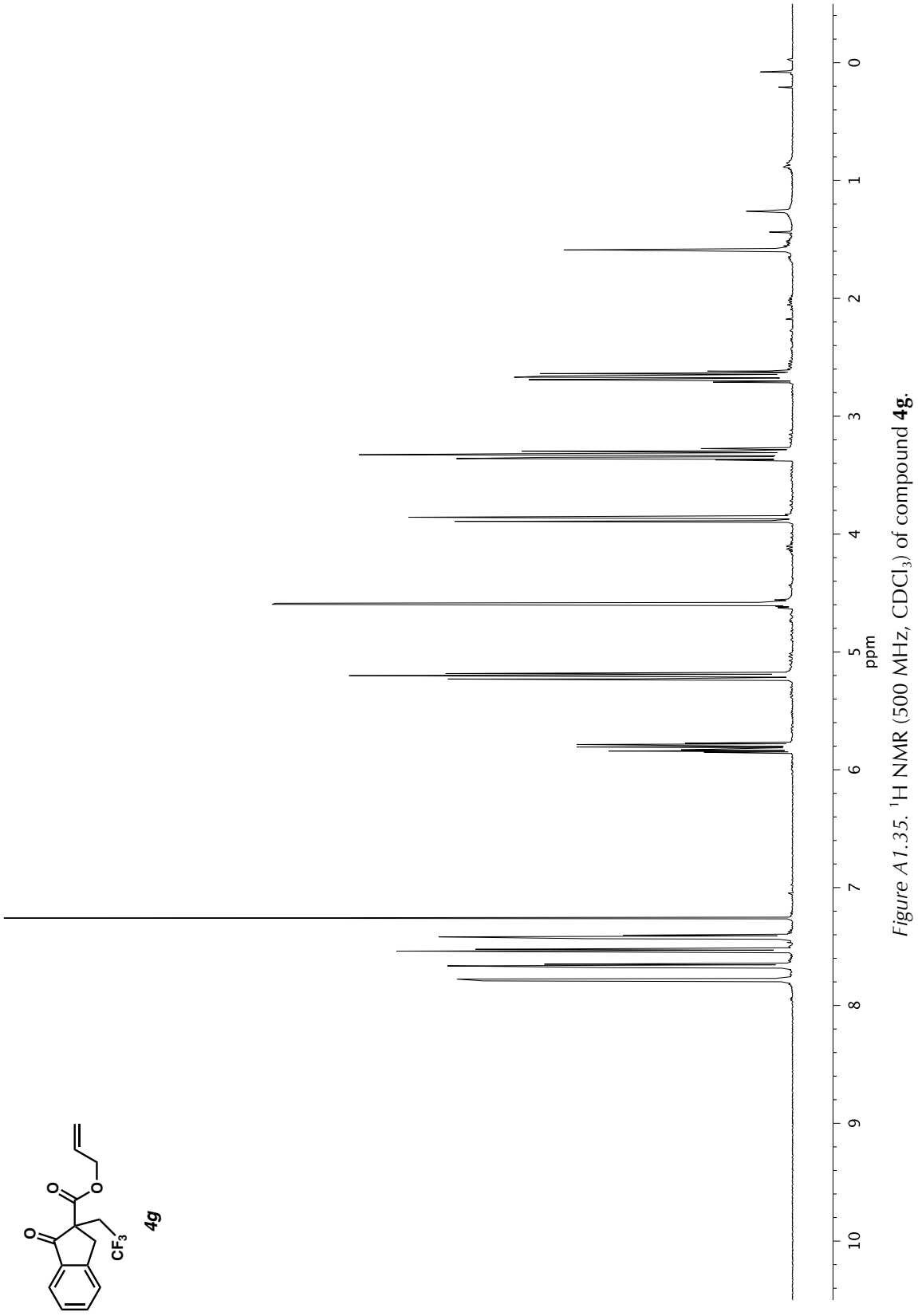

Figure A1.35. ^{1}H NMR (500 MHz, $CDCl_3$) of compound **4g**.

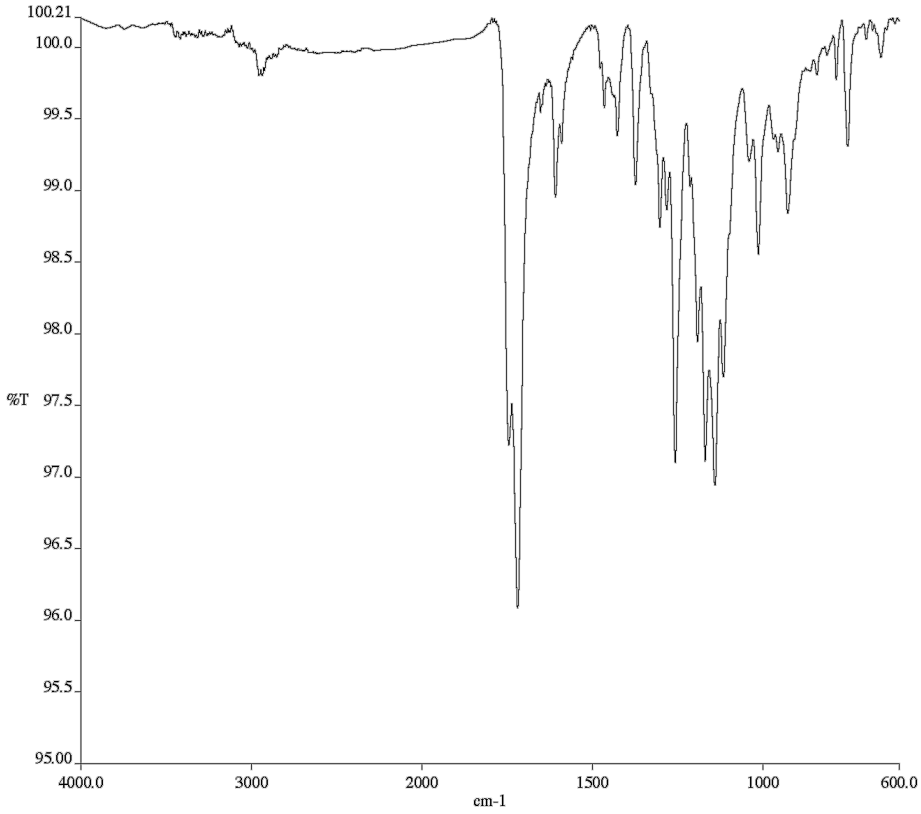

Figure A1.35. Infrared spectrum (Thin Film, NaCl) of compound **4g**.

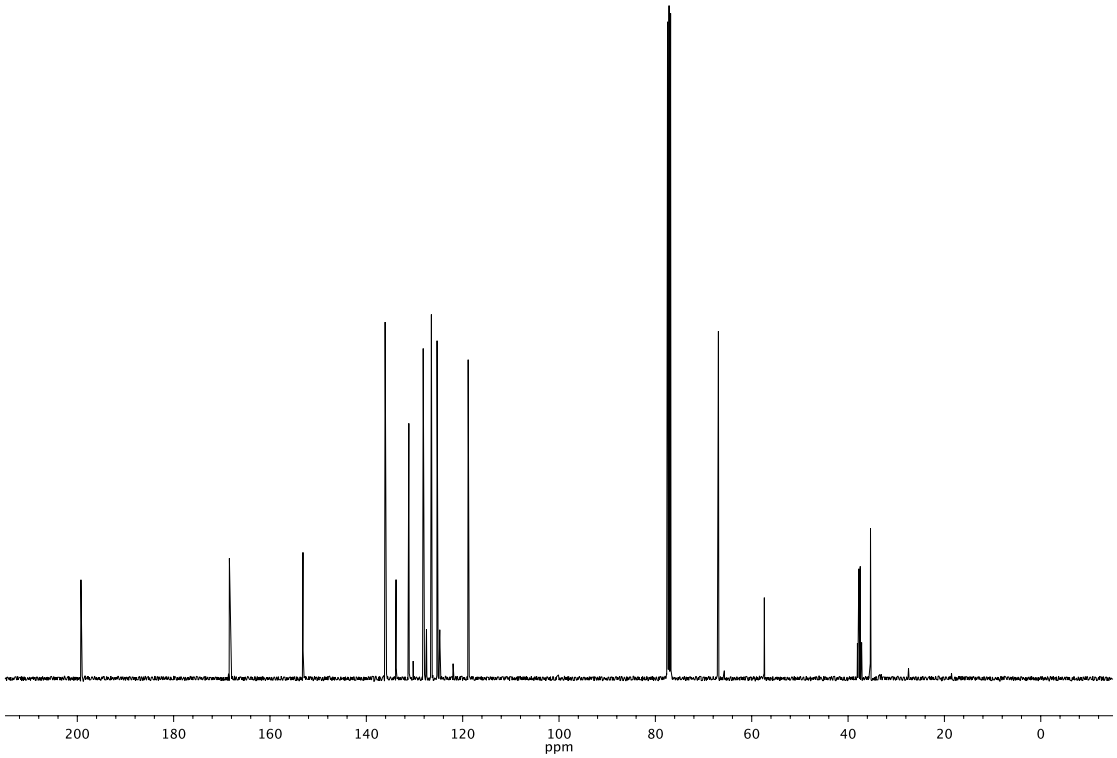

Figure A1.36. ^{13}C NMR (101 MHz, $CDCl_3$) of compound **4g**.

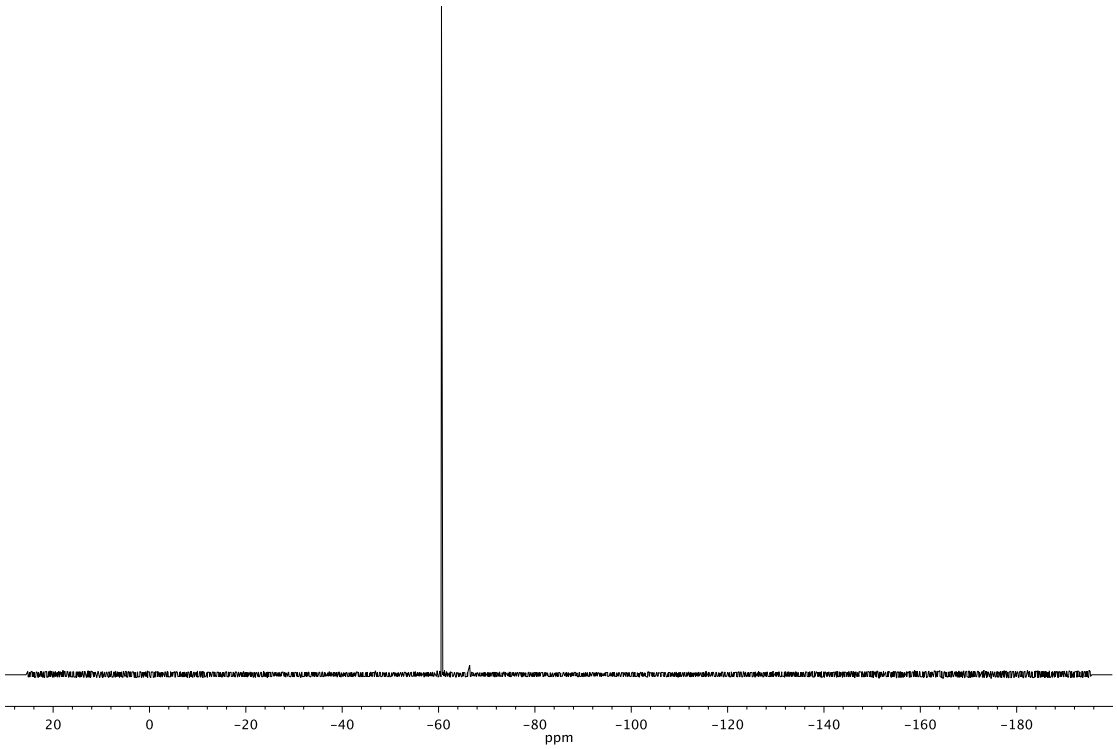

Figure A1.36. ^{19}F NMR (282 MHz, $CDCl_3$) of compound **4g**.

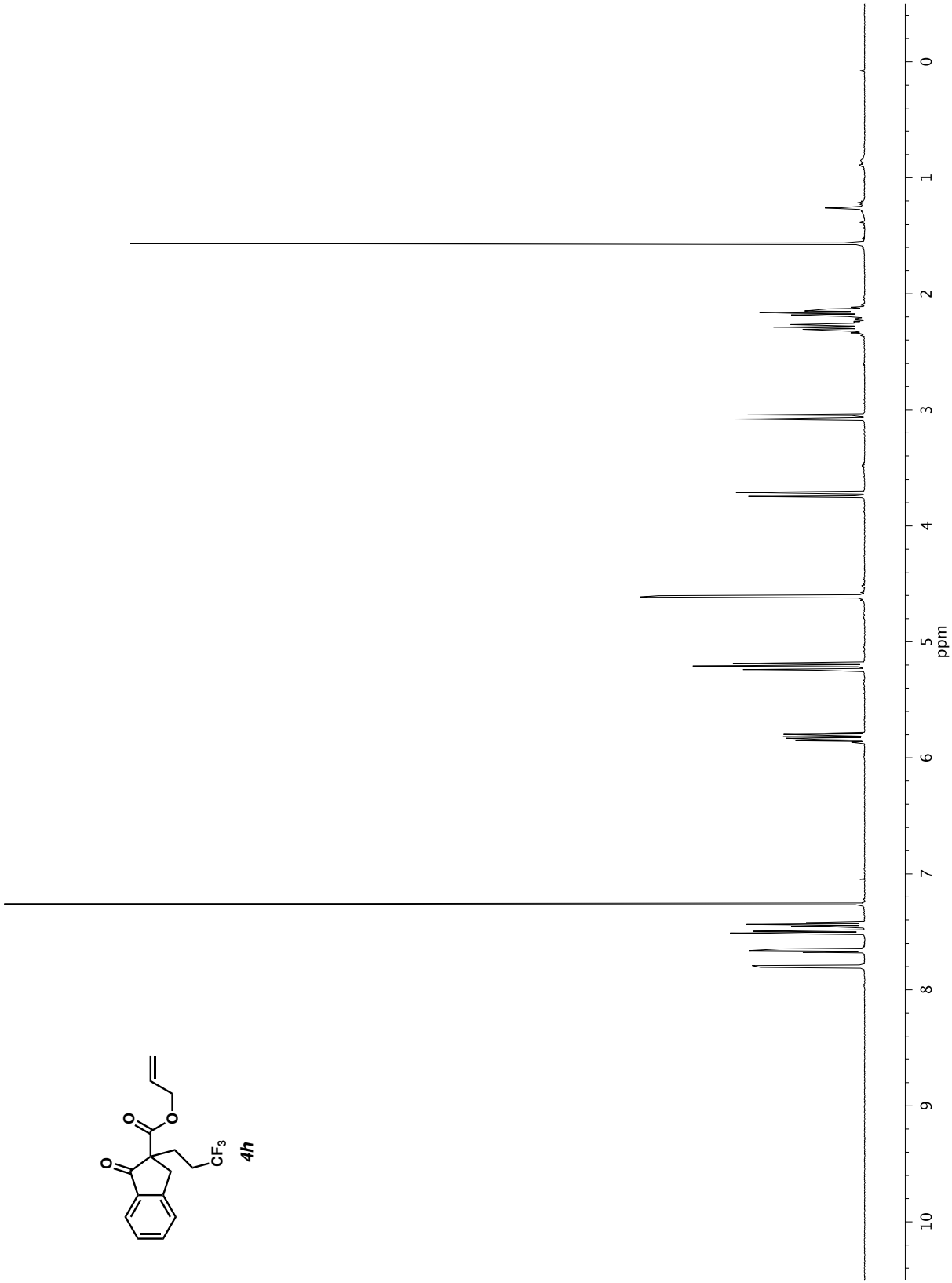

Figure A1.39. ^{1}H NMR (500 MHz, $CDCl_3$) of compound **4h**.

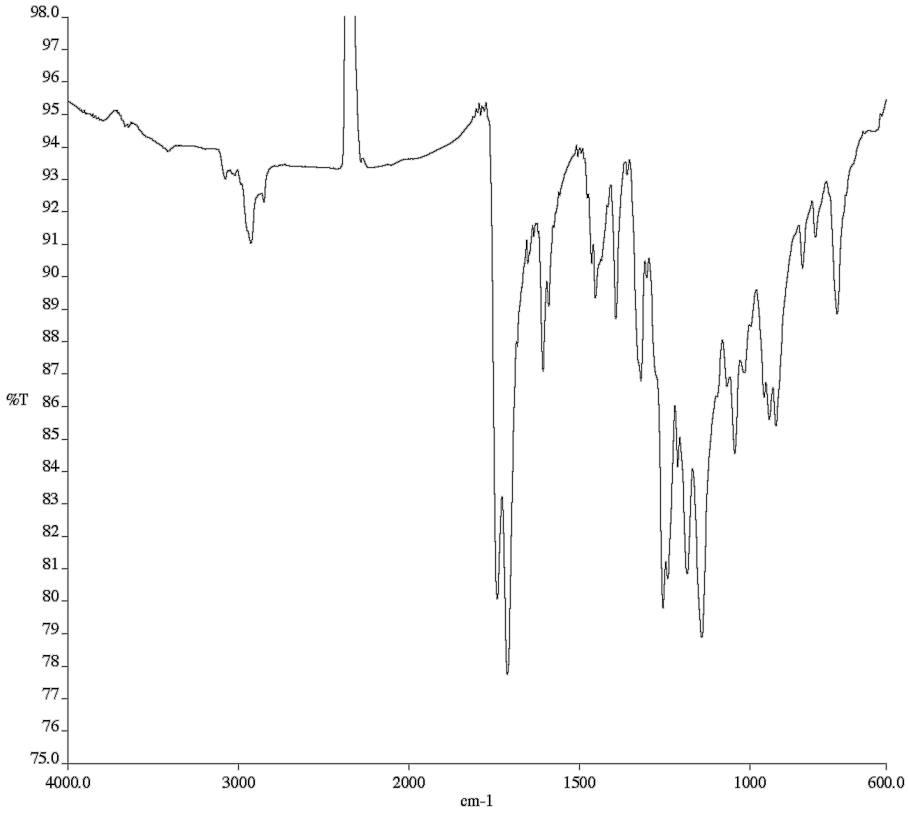

Figure A1.40. Infrared spectrum (Thin Film, NaCl) of compound **4h**.

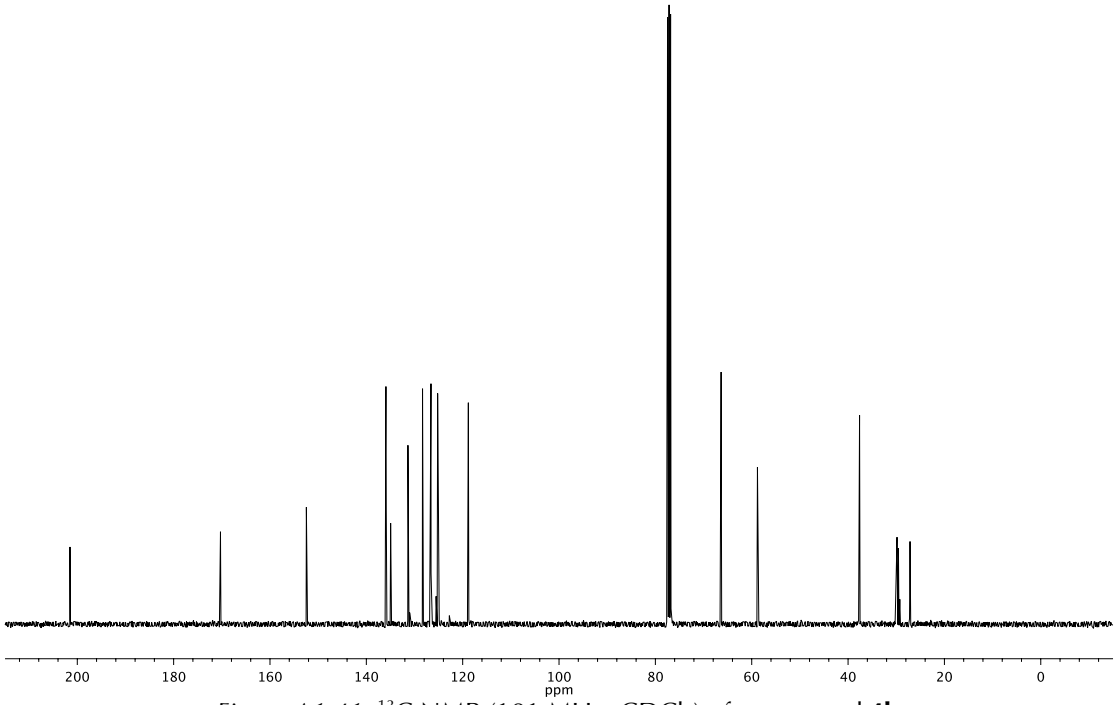

Figure A1.41. ^{13}C NMR (101 MHz, $CDCl_3$) of compound **4h**.

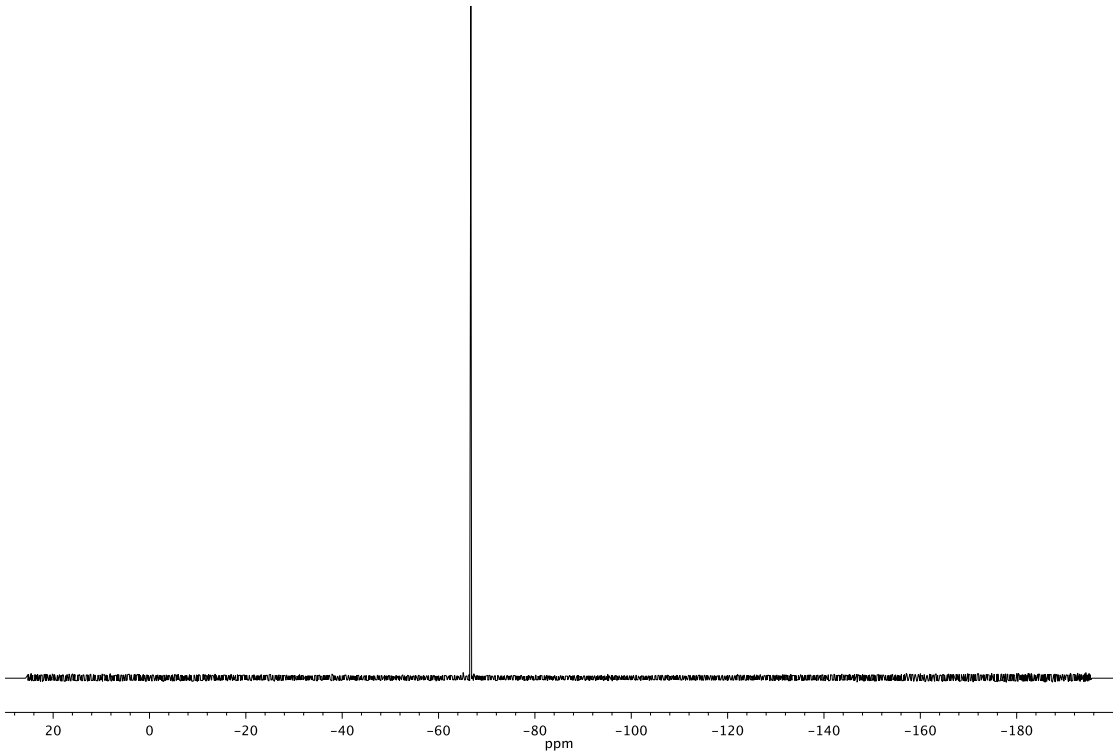

Figure A1.42. ^{19}F NMR (282 MHz, $CDCl_3$) of compound **4h**.

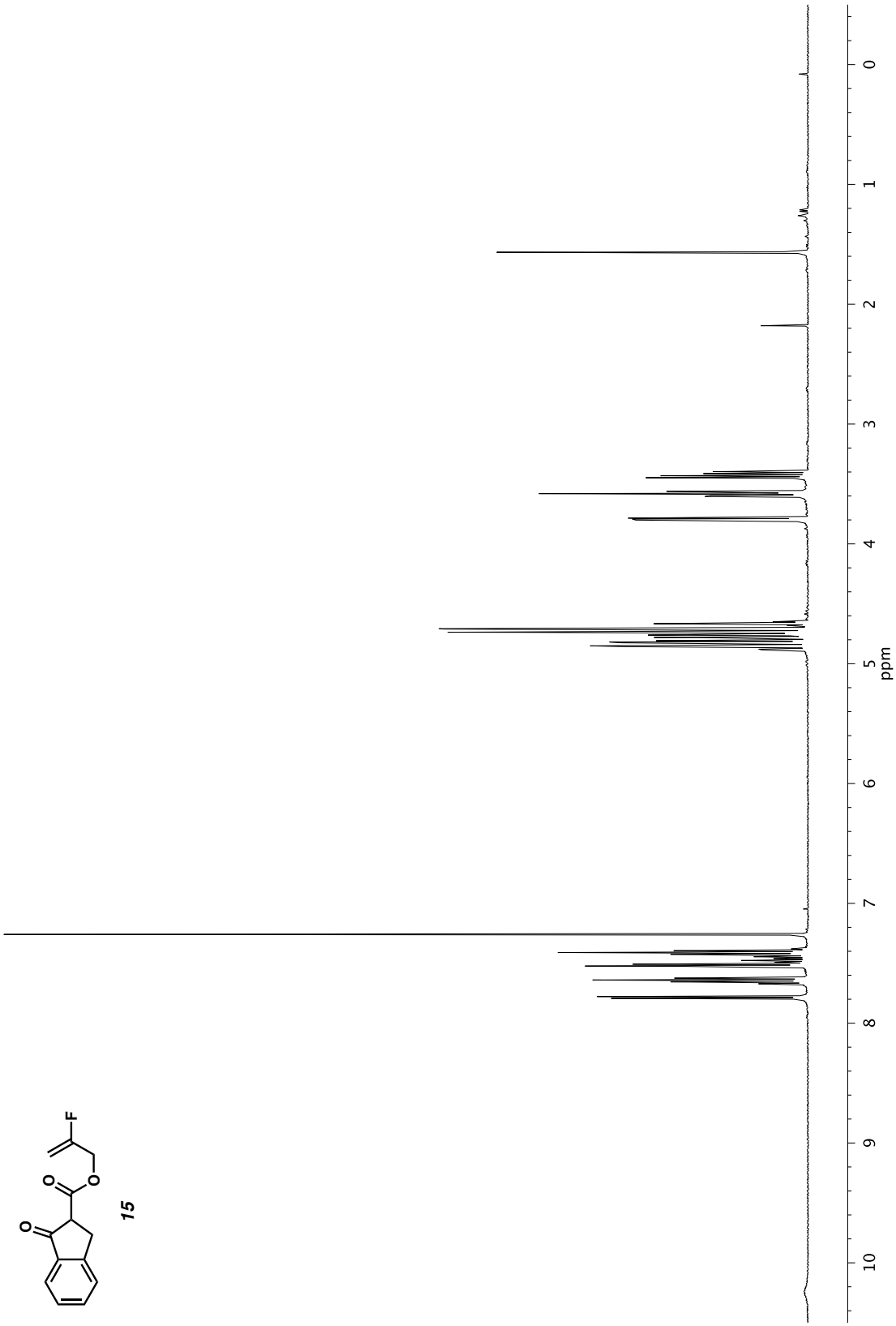

Figure A1.43. ^{1}H NMR (500 MHz, $CDCl_3$) of compound **15**.

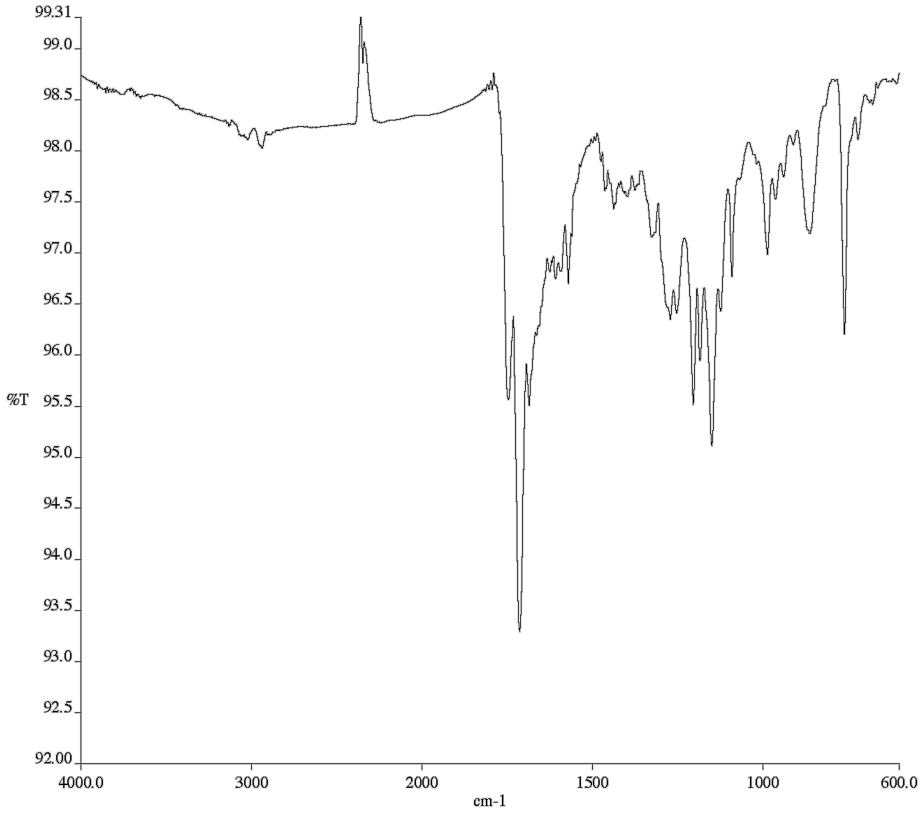

Figure A1.44. Infrared spectrum (Thin Film, NaCl) of compound **15**.

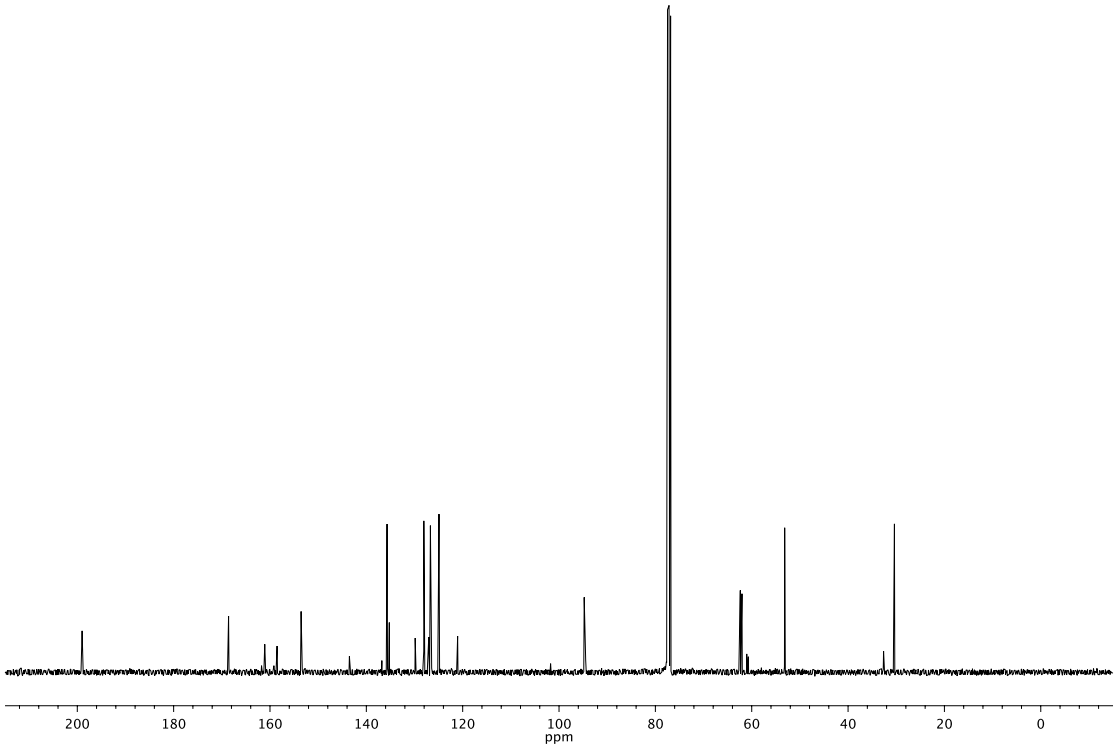

Figure A1.45. ^{13}C NMR (101 MHz, $CDCl_3$) of compound **15**.

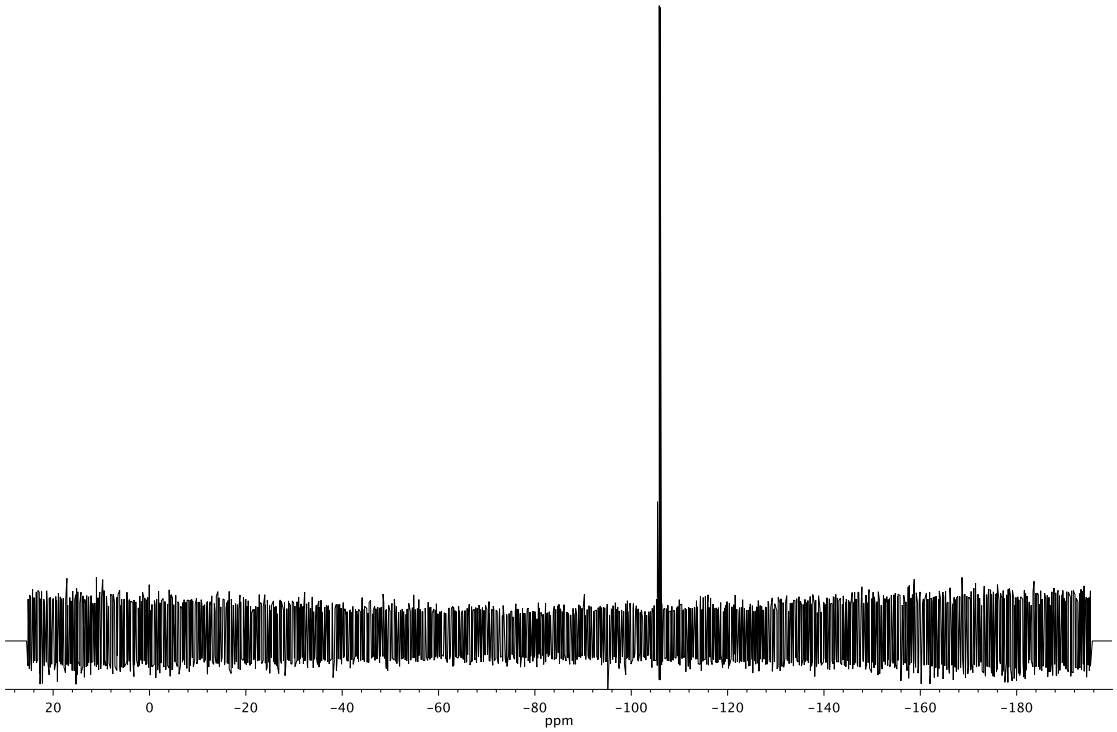

Figure A1.46. ^{19}F NMR (282 MHz, $CDCl_3$) of compound **15**.

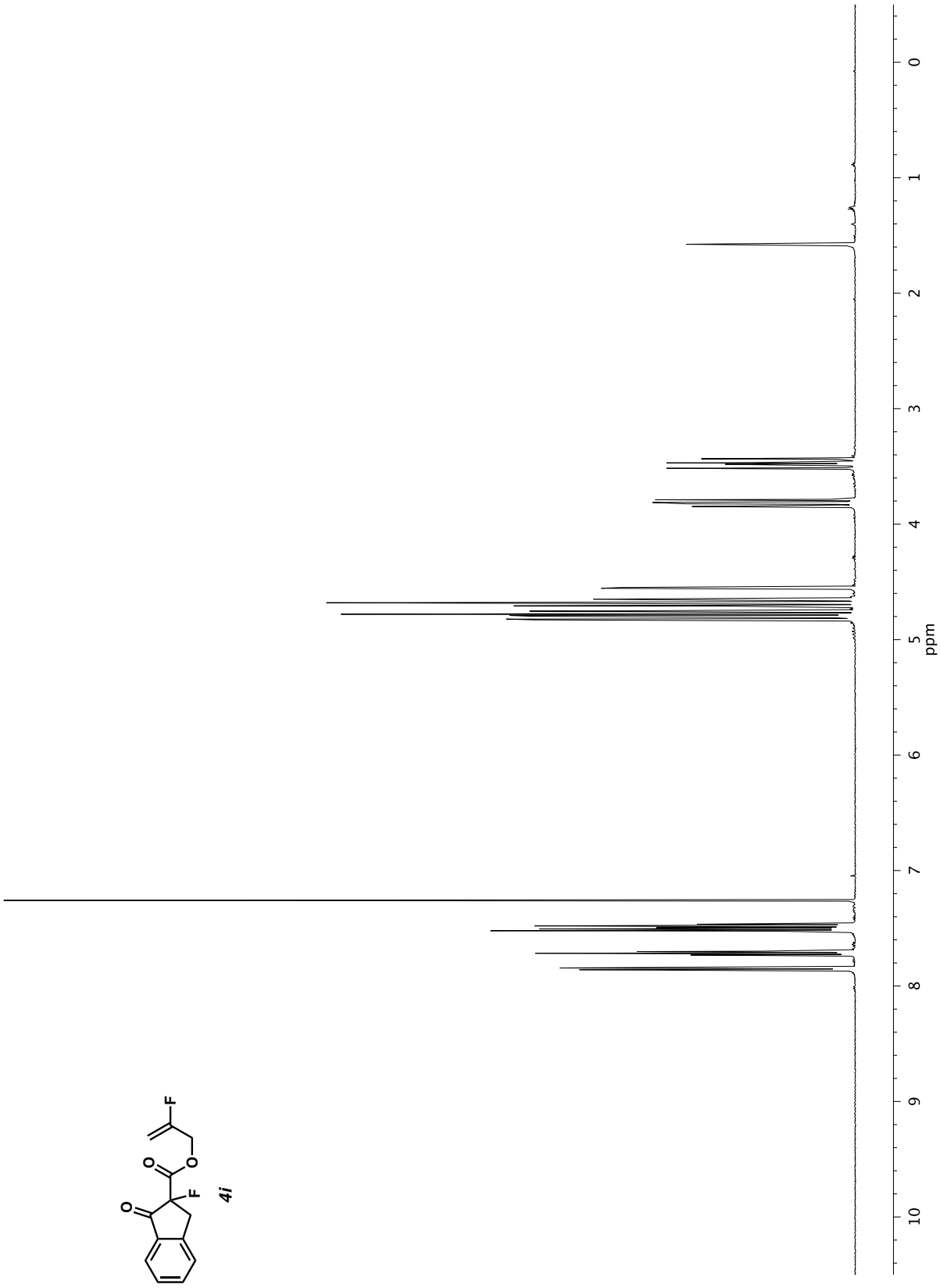

Figure A1.47. ^{1}H NMR (500 MHz, $CDCl_3$) of compound **4i**.

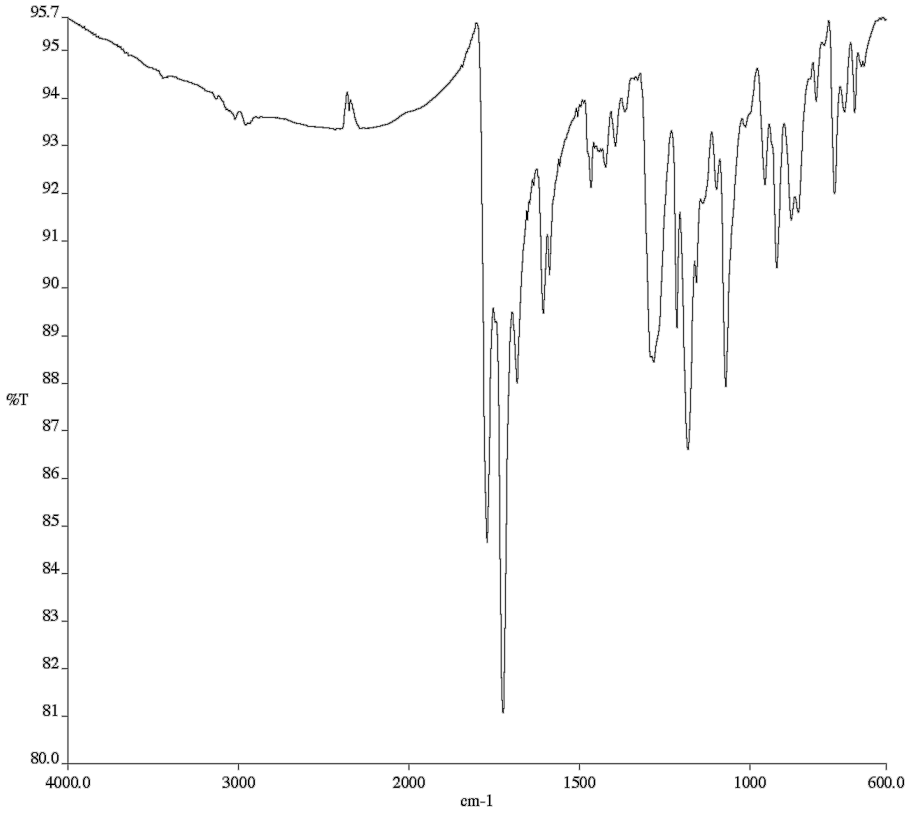

Figure A1.48. Infrared spectrum (Thin Film, NaCl) of compound **4i**.

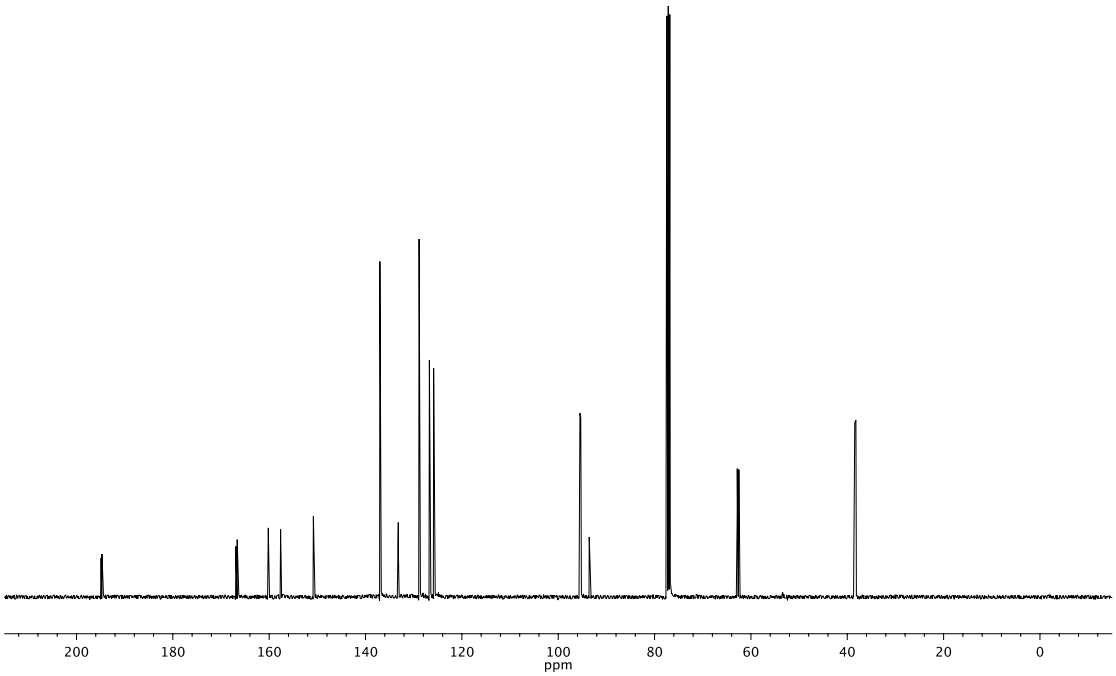

Figure A1.49. ^{13}C NMR (101 MHz, $CDCl_3$) of compound **4i**.

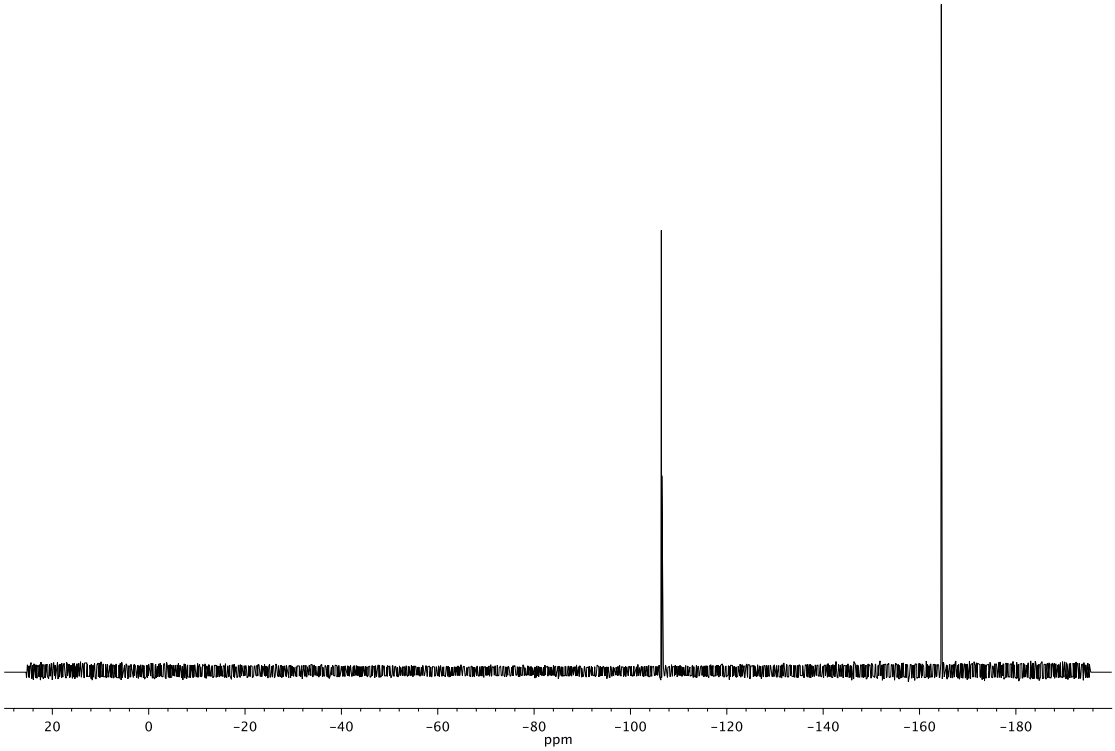

Figure A1.50. ^{19}F NMR (282 MHz, $CDCl_3$) of compound **4i**.

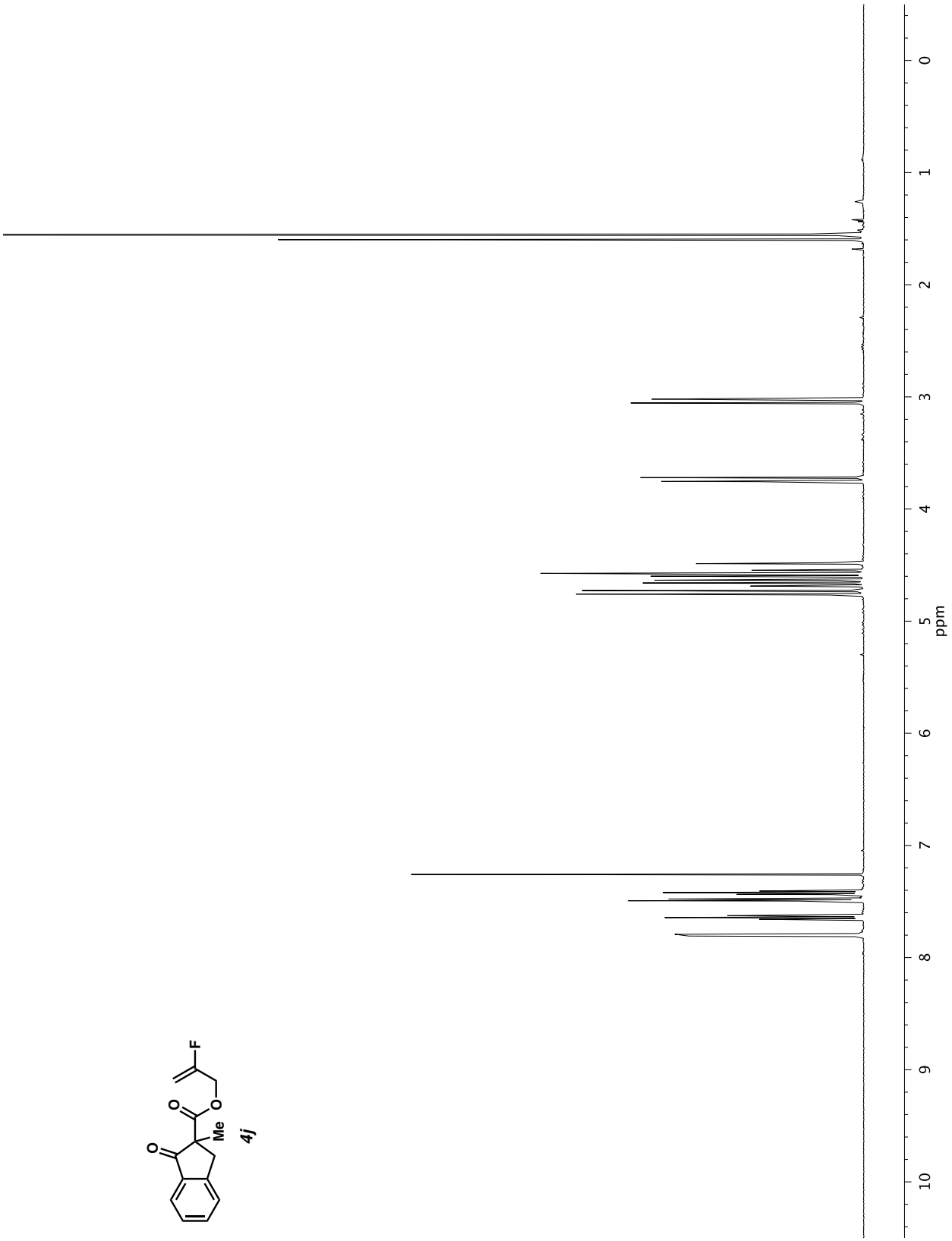

Figure A1.51. ^{1}H NMR (500 MHz, $CDCl_3$) of compound **4j**.

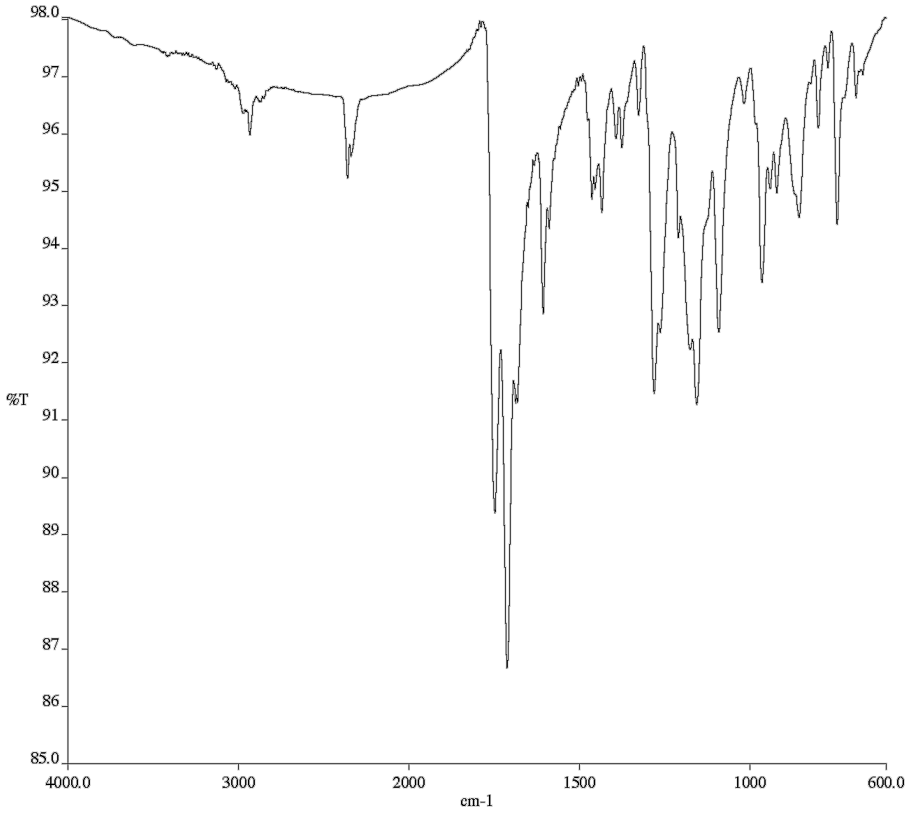

Figure A1.52. Infrared spectrum (Thin Film, NaCl) of compound **4j**.

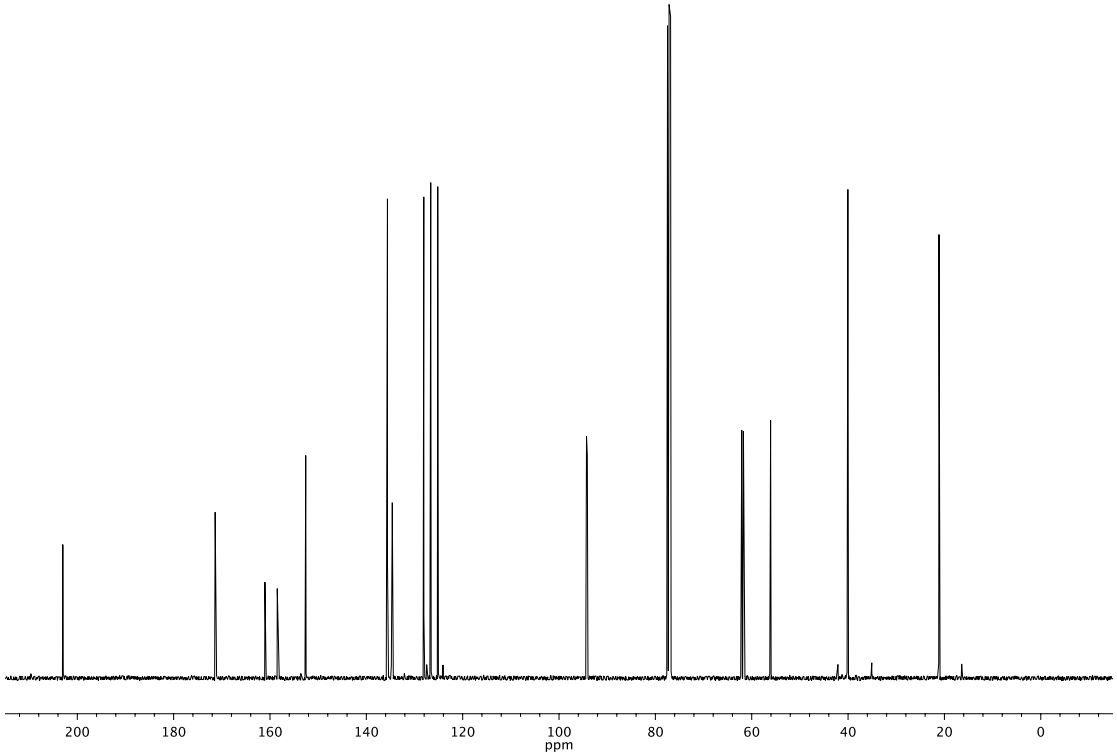

Figure A1.53. ^{13}C NMR (101 MHz, $CDCl_3$) of compound **4j**.

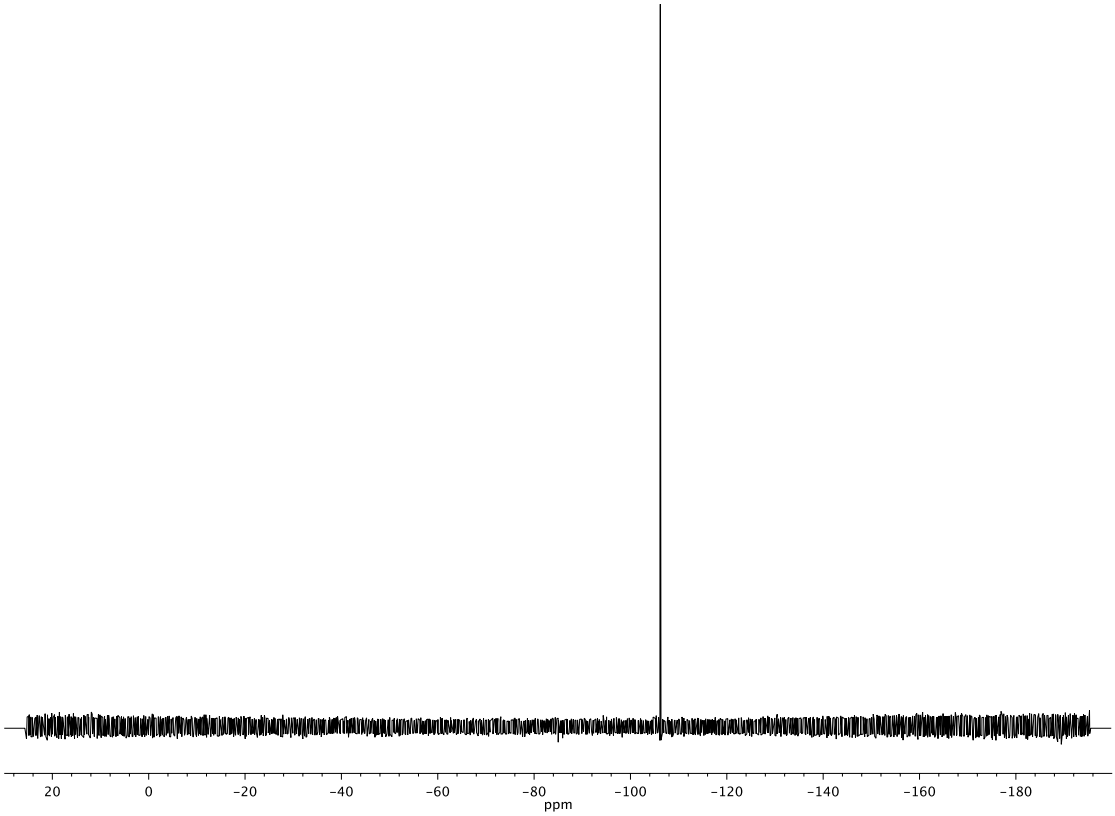

Figure A1.54. ^{19}F NMR (282 MHz, $CDCl_3$) of compound **4j**.

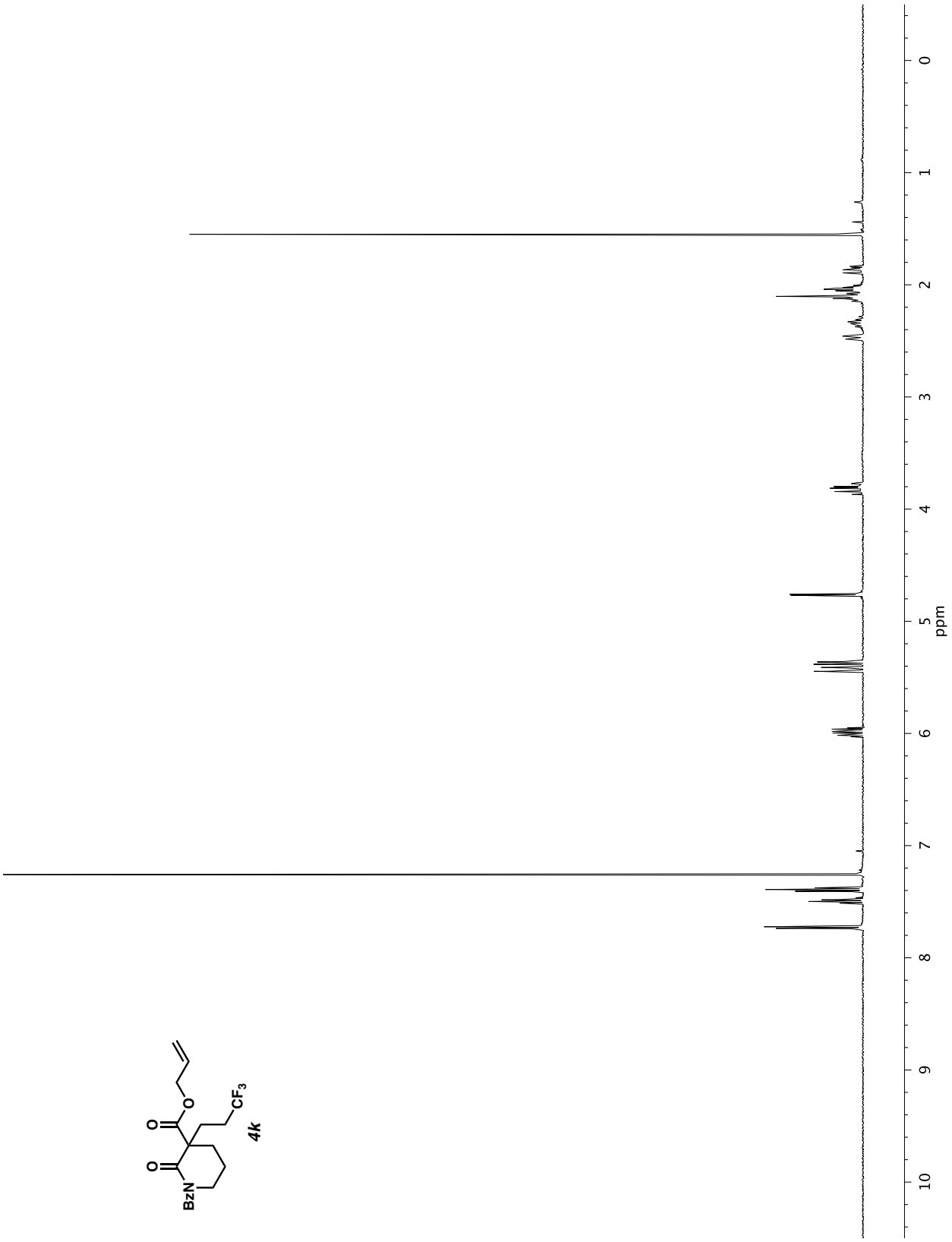

Figure A1.55. ^{1}H NMR (500 MHz, $CDCl_3$) of compound **4k**.

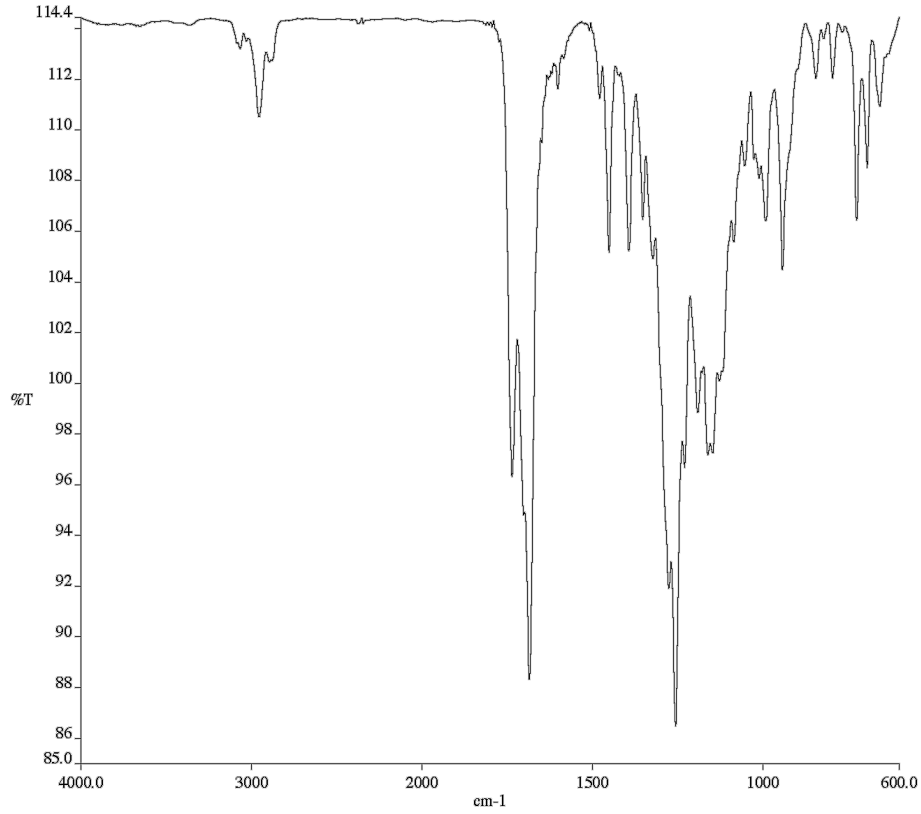

Figure A1.56. Infrared spectrum (Thin Film, NaCl) of compound **4k**.

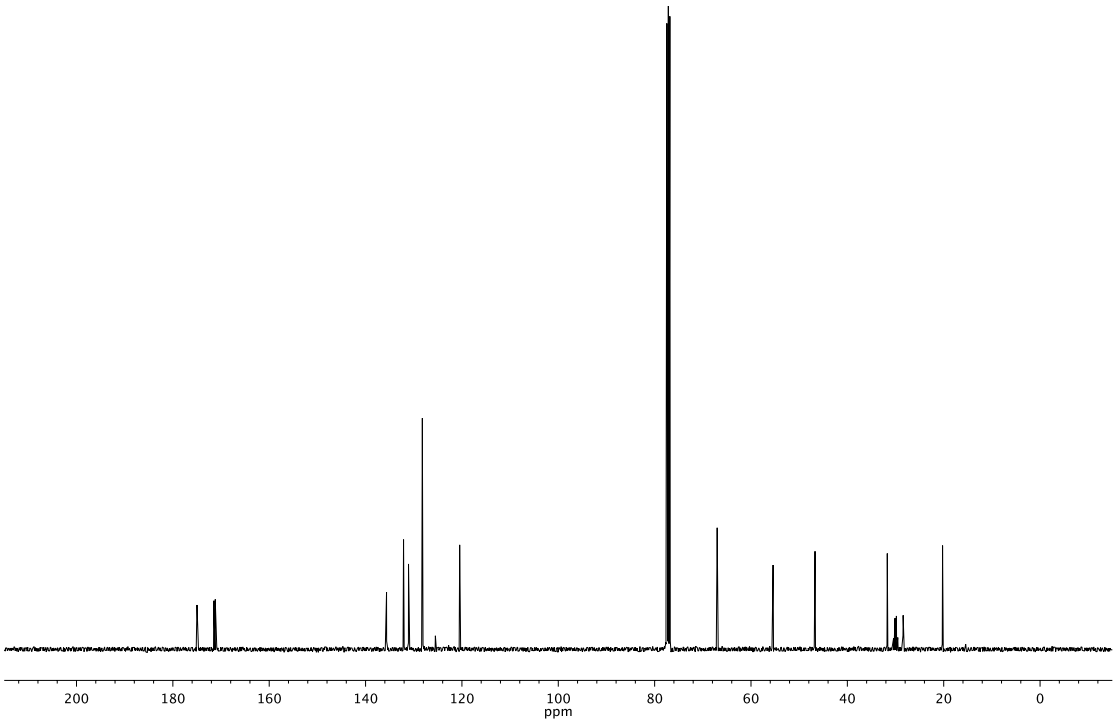

Figure A1.57. ^{13}C NMR (101 MHz, $CDCl_3$) of compound **4k**.

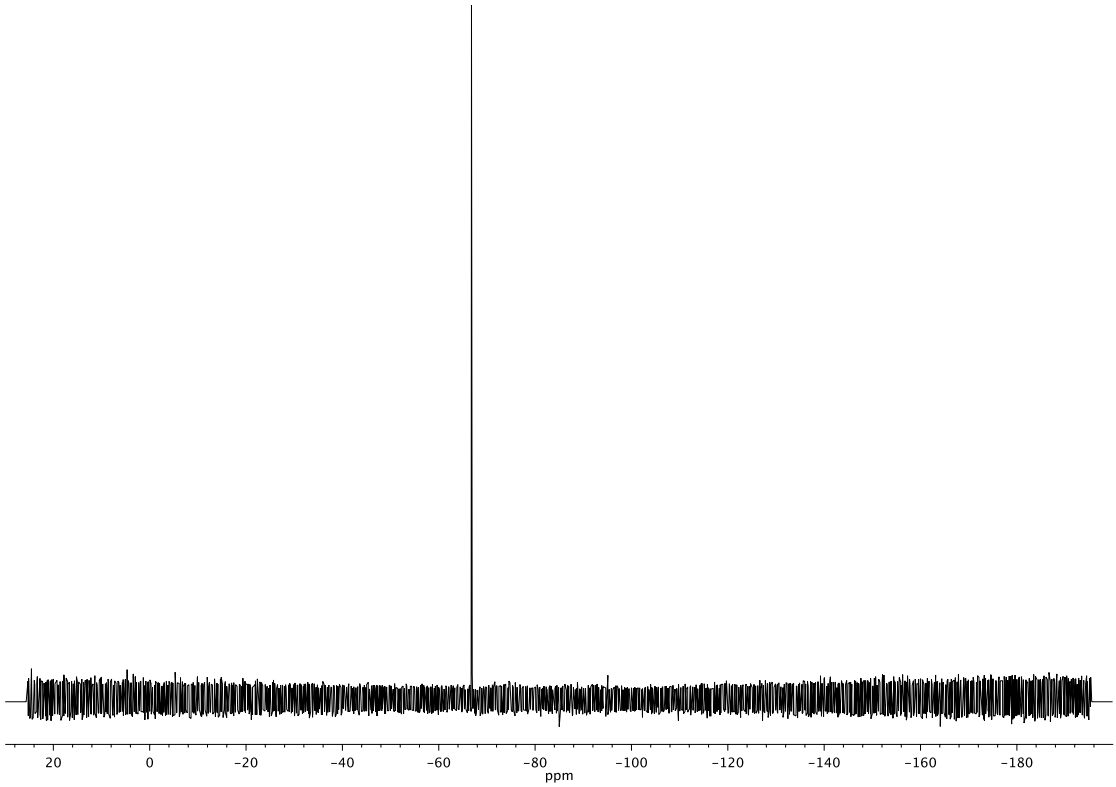

Figure A1.58. ^{19}F NMR (282 MHz, $CDCl_3$) of compound **4k**.

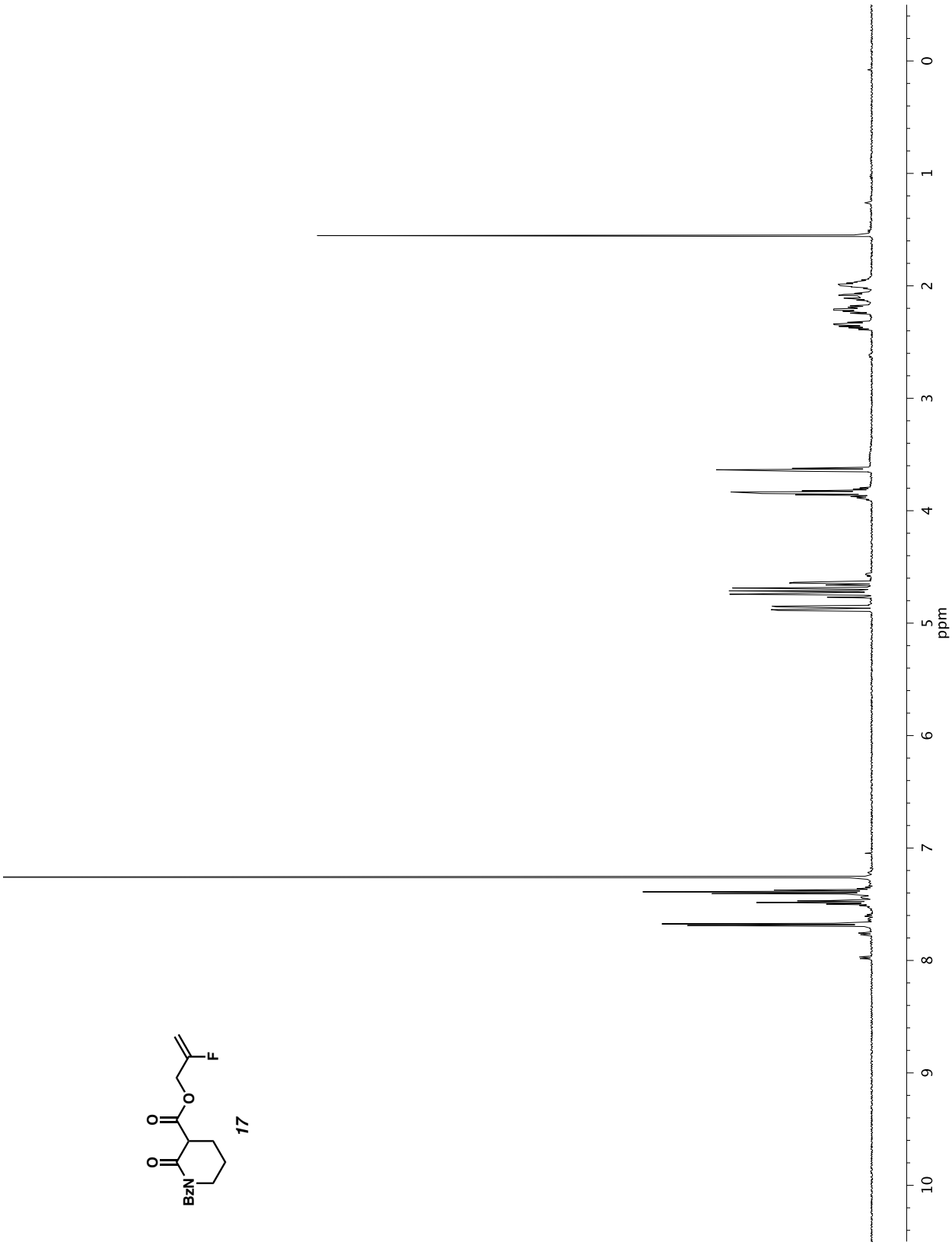

Figure A1.59. ^{1}H NMR (500 MHz, $CDCl_3$) of compound **17**.

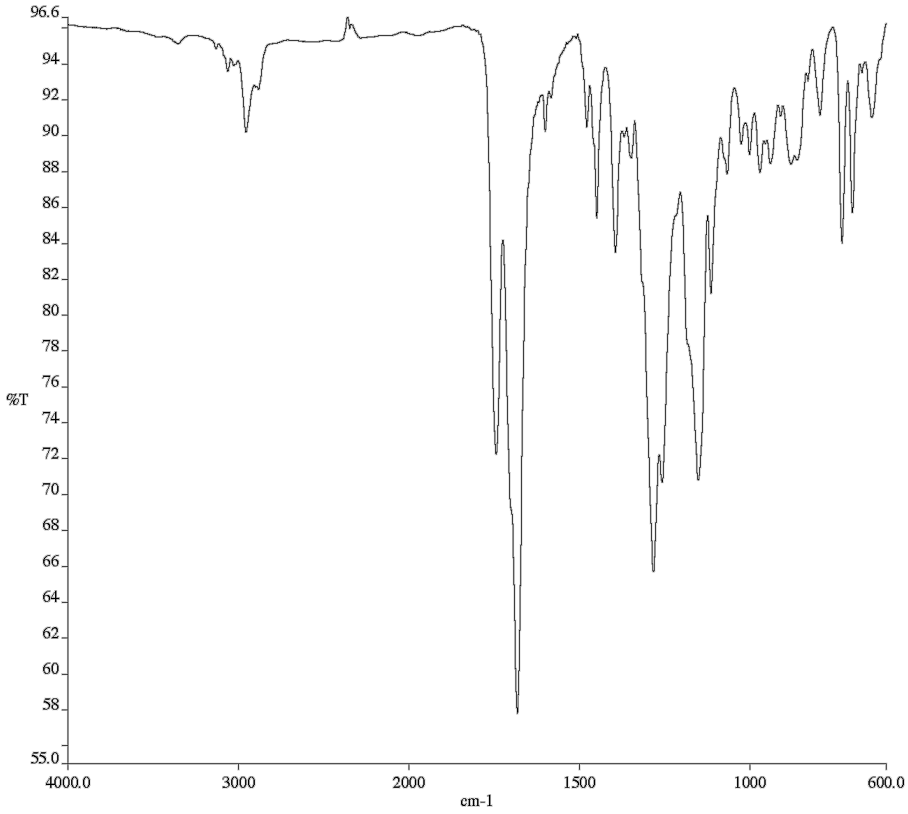

Figure A1.60. Infrared spectrum (Thin Film, NaCl) of compound **17**.

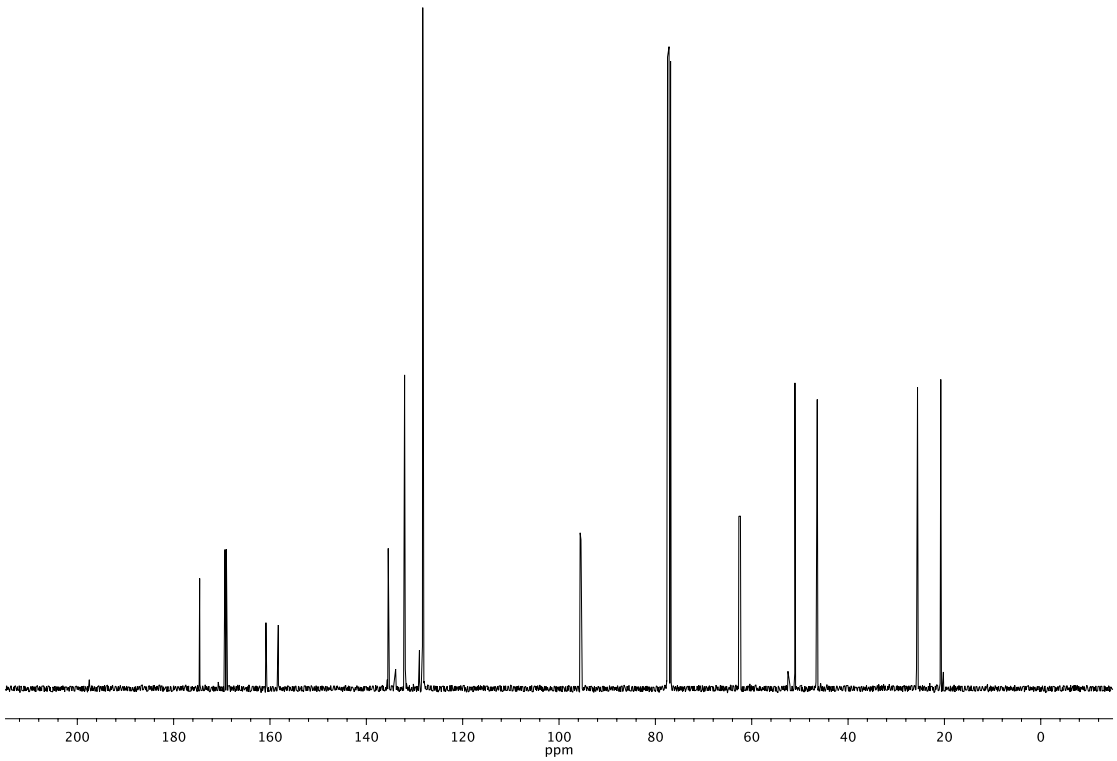

Figure A1.61. ^{13}C NMR (101 MHz, $CDCl_3$) of compound **17**.

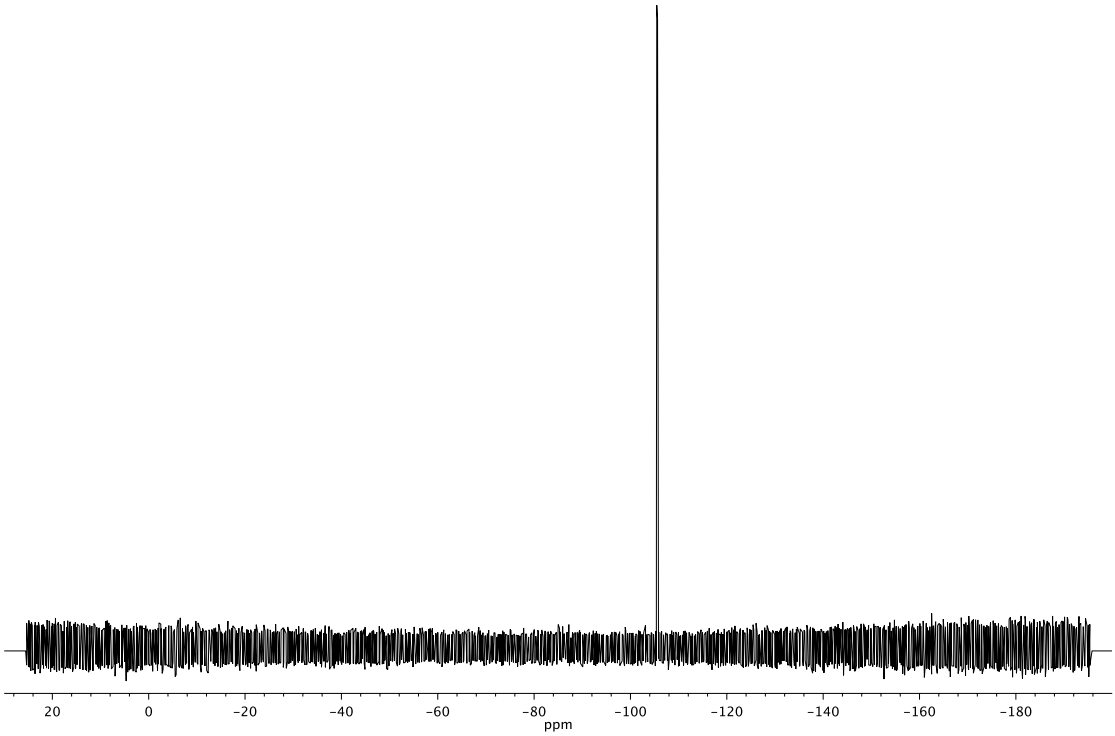

Figure A1.62. ^{19}F NMR (282 MHz, $CDCl_3$) of compound **17**.

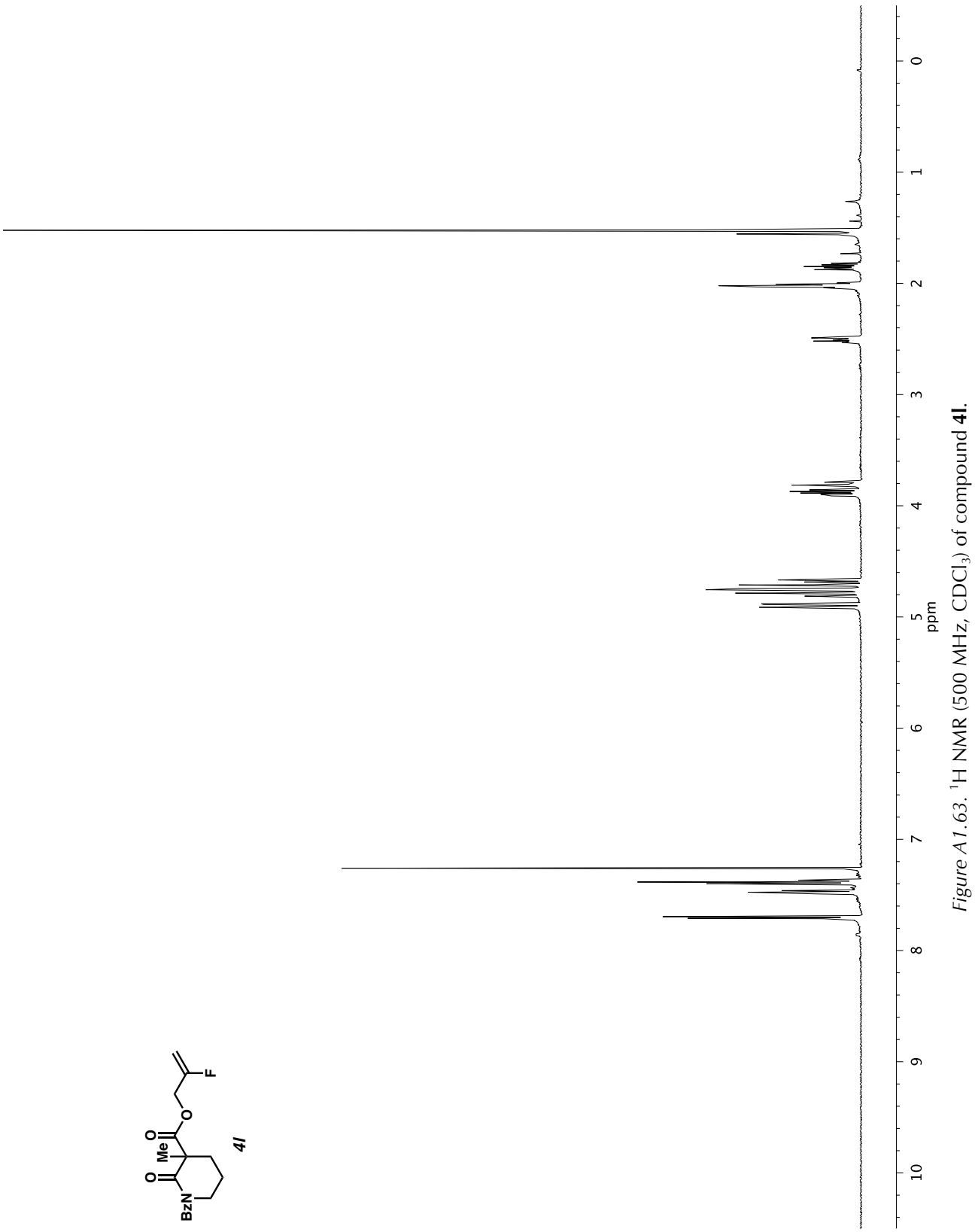

Figure A1.63. ^{1}H NMR (500 MHz, $CDCl_3$) of compound **4l**.

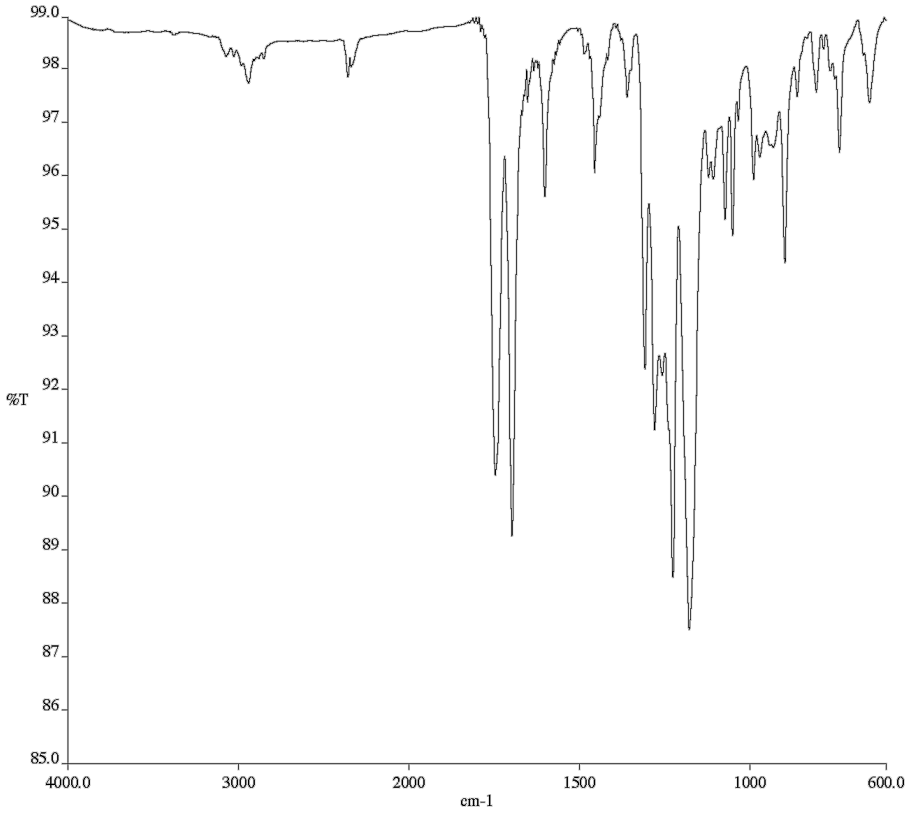

Figure A1.64. Infrared spectrum (Thin Film, NaCl) of compound **4l**.

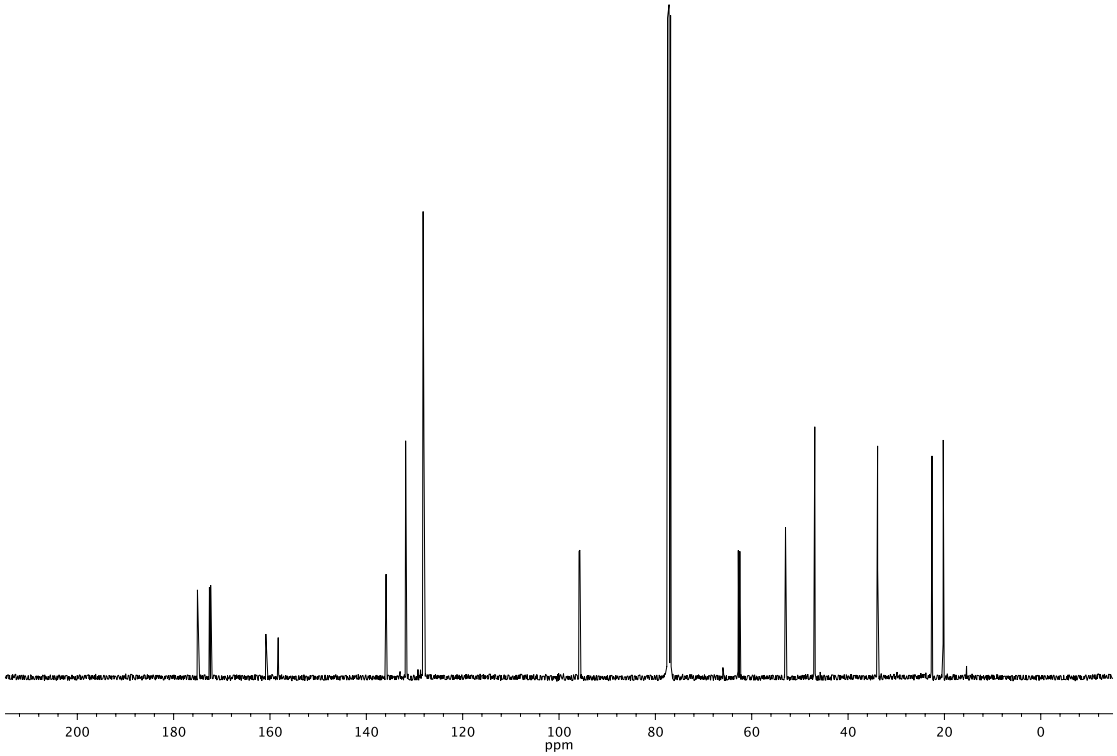

Figure A1.65. ^{13}C NMR (101 MHz, $CDCl_3$) of compound **4l**.

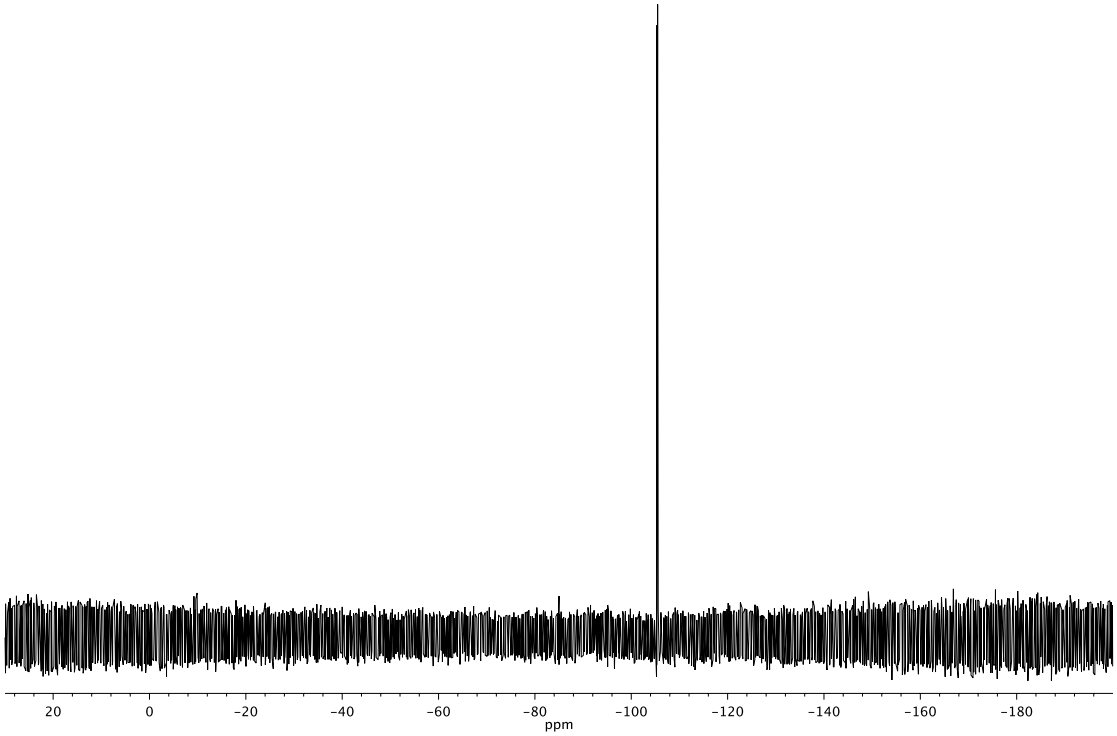

Figure A1.66. ^{19}F NMR (282 MHz, $CDCl_3$) of compound **4l**.

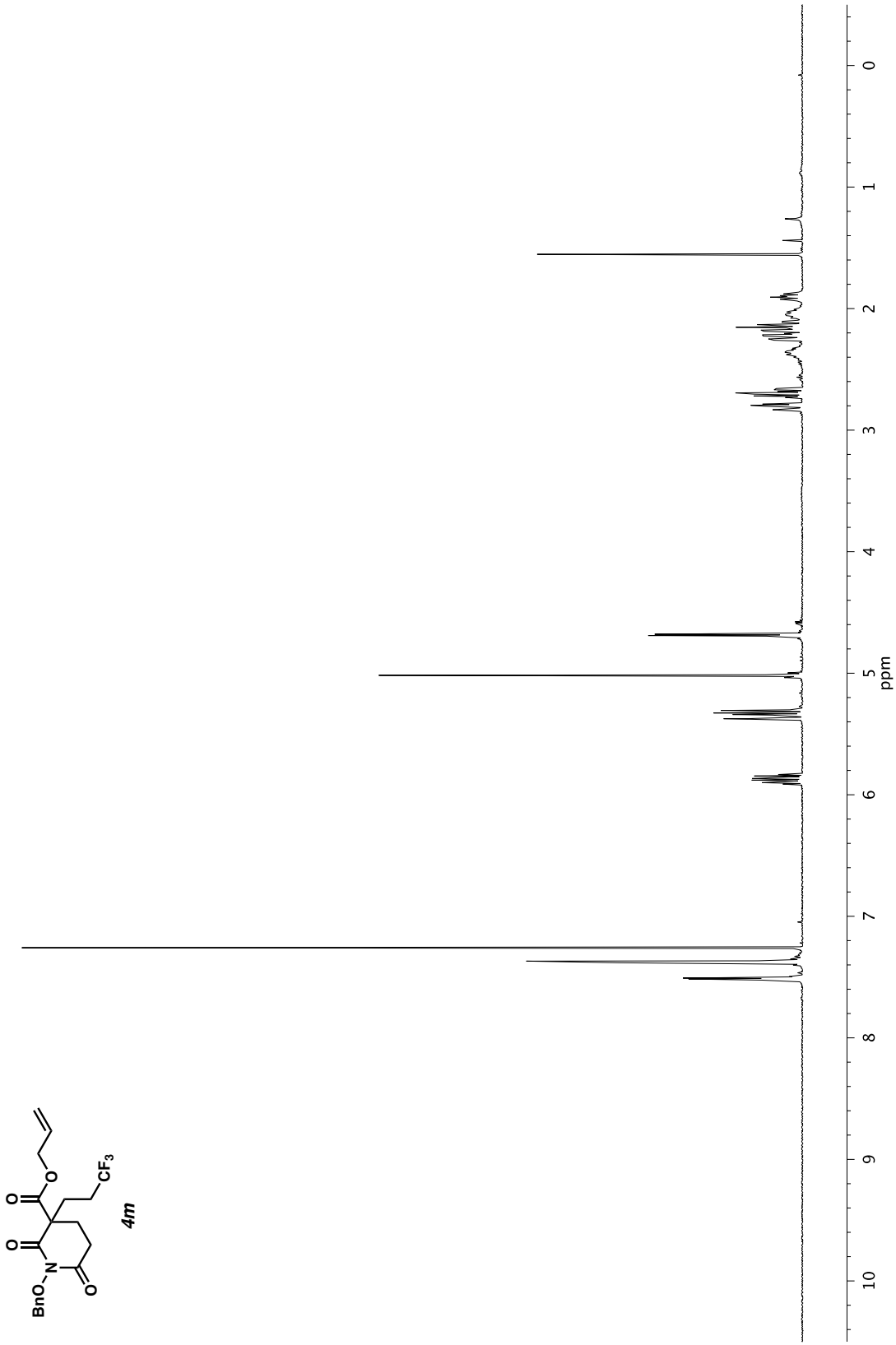

Figure A1.67. ^{1}H NMR (500 MHz, $CDCl_3$) of compound **4m**.

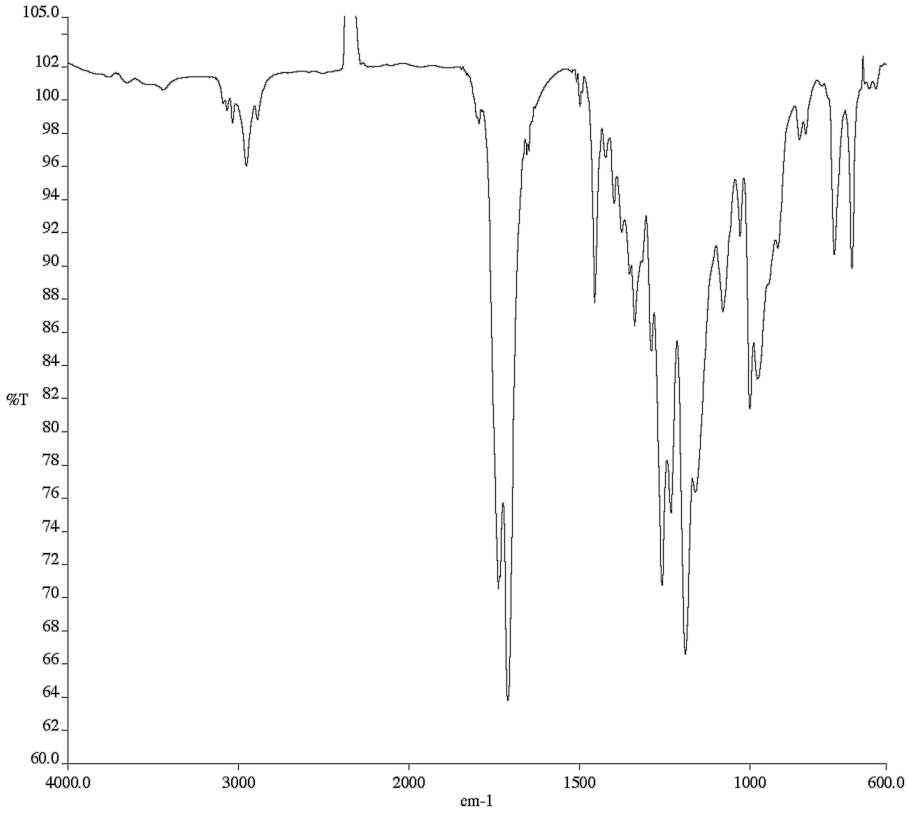

Figure A1.68. Infrared spectrum (Thin Film, NaCl) of compound **4m**.

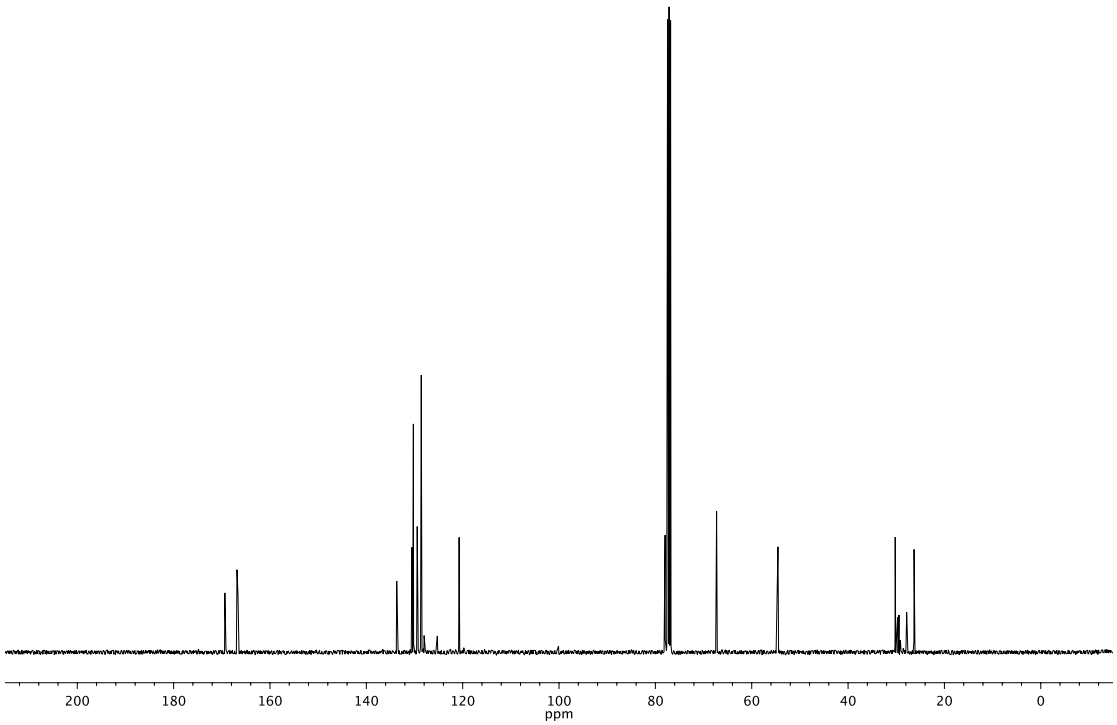

Figure A1.69. ^{13}C NMR (101 MHz, $CDCl_3$) of compound **4m**.

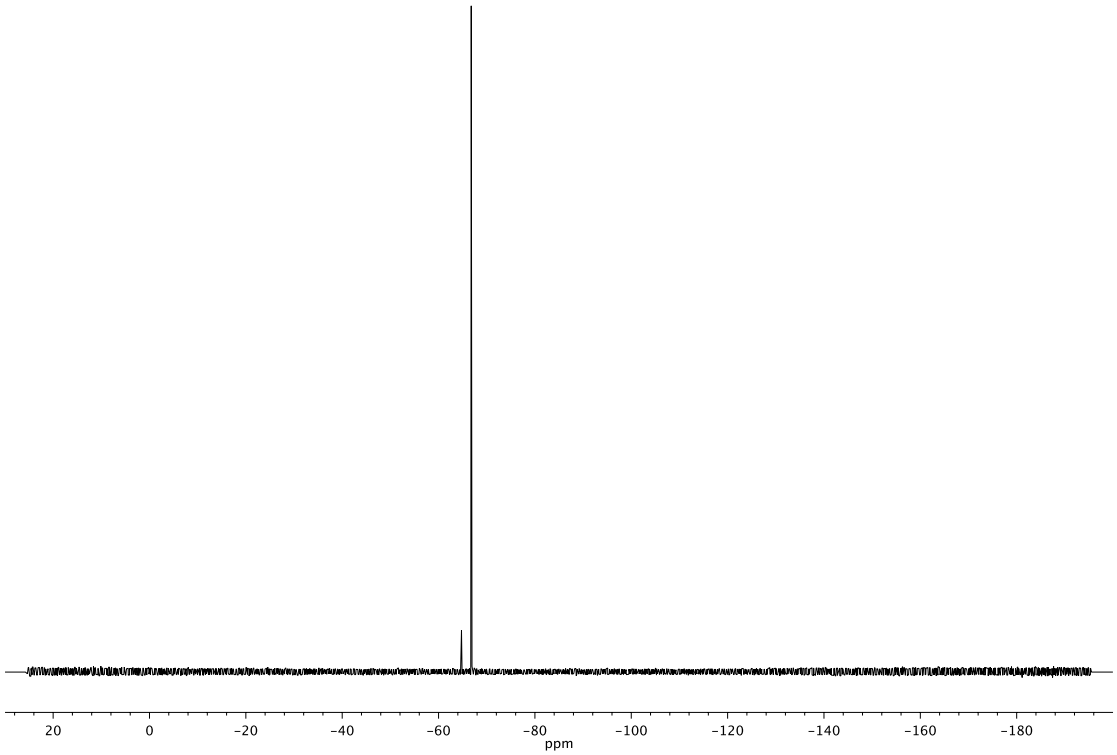

Figure A1.70. ^{19}F NMR (282 MHz, $CDCl_3$) of compound **4m**.

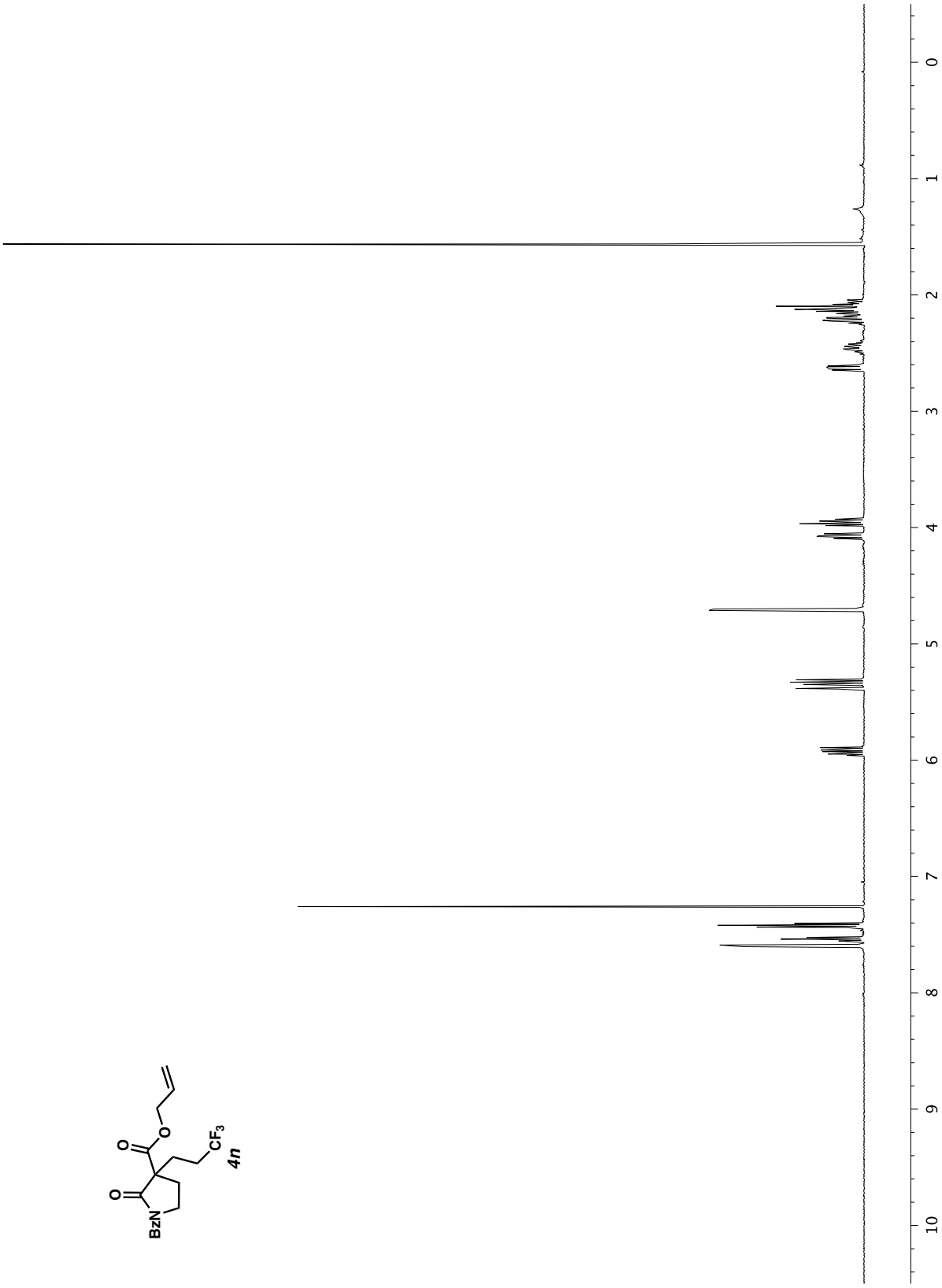

Figure A1.71. ^{1}H NMR (500 MHz, $CDCl_3$) of compound **4n**.

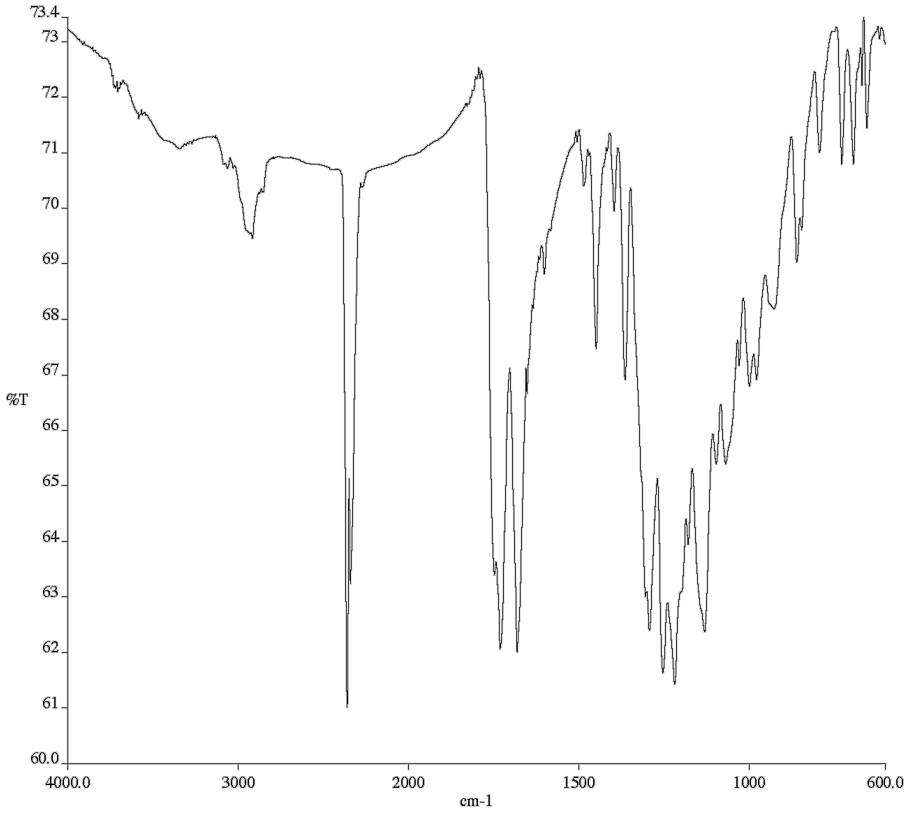

Figure A1.72. Infrared spectrum (Thin Film, NaCl) of compound **4n**.

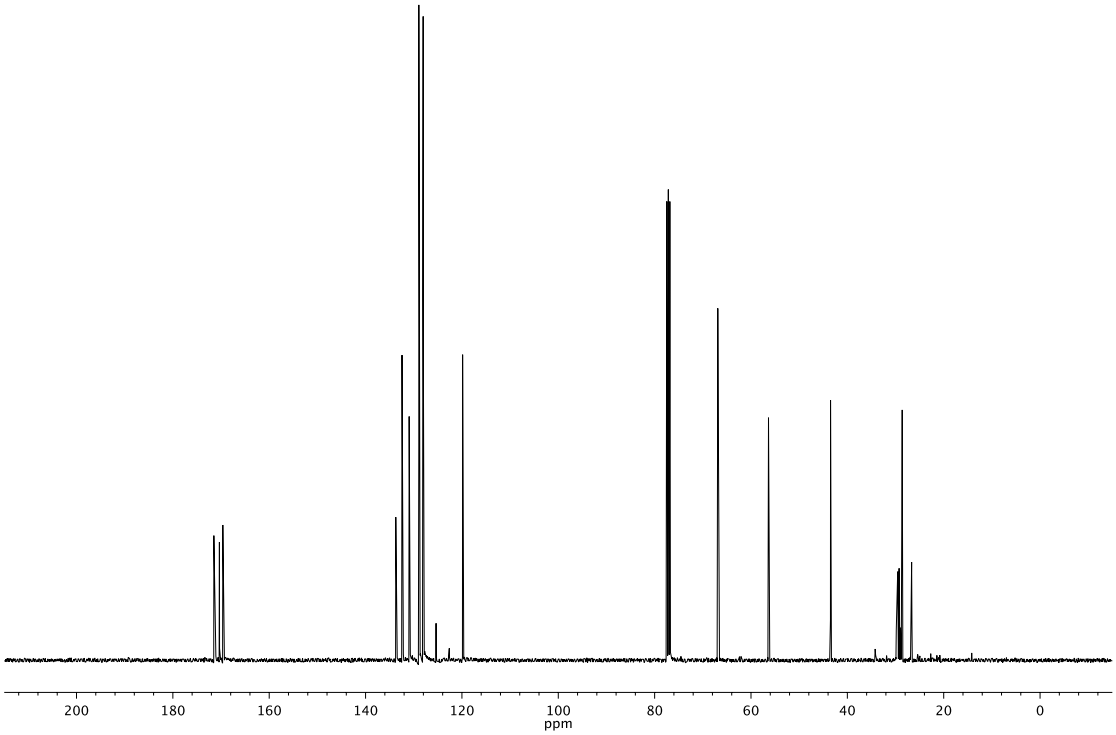

Figure A1.73. ^{13}C NMR (101 MHz, $CDCl_3$) of compound **4n**.

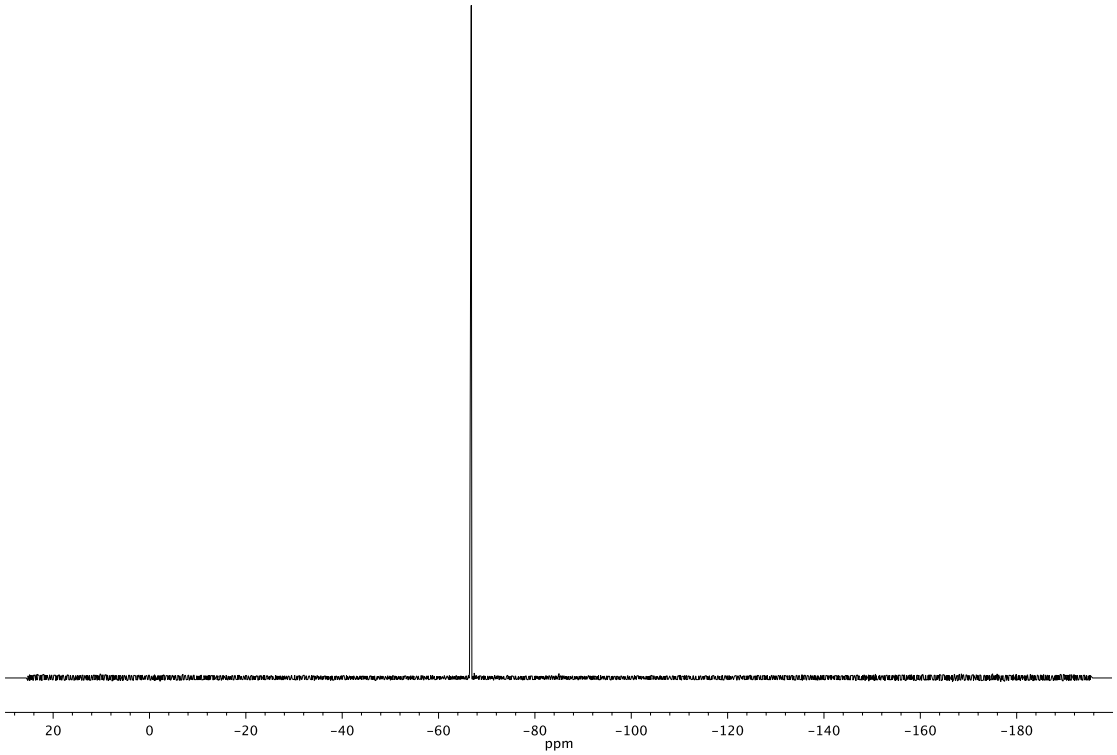

Figure A1.74. ^{19}F NMR (282 MHz, $CDCl_3$) of compound **4n**.

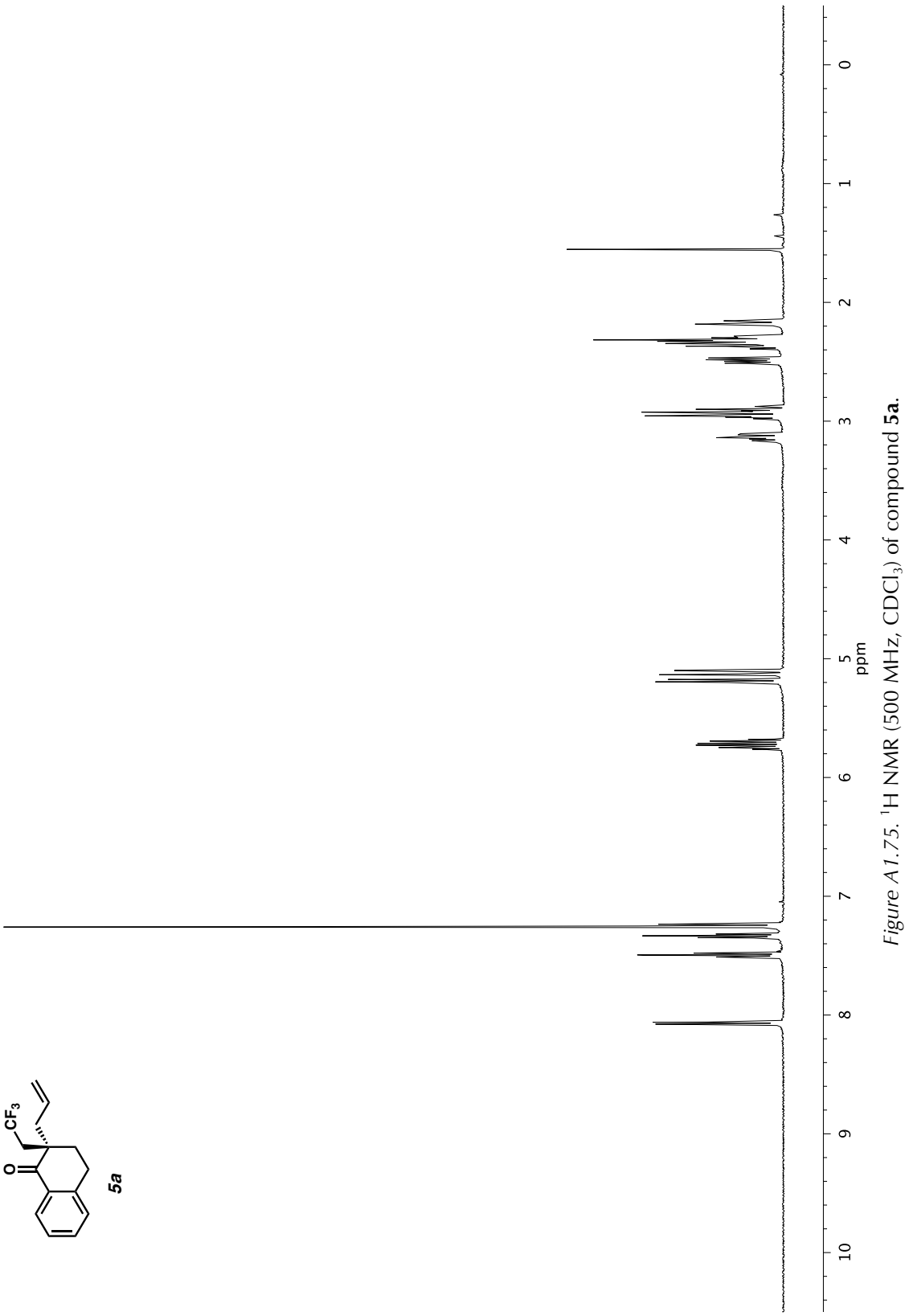

Figure A1.75. ^{1}H NMR (500 MHz, $CDCl_3$) of compound **5a**.

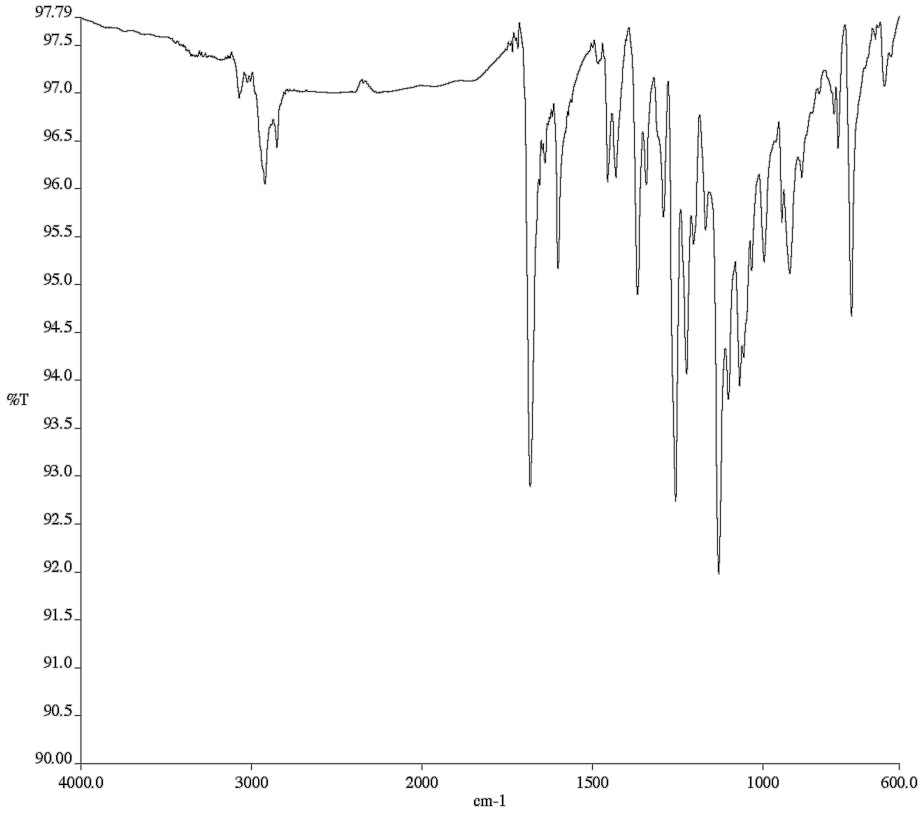

Figure A1.76. Infrared spectrum (Thin Film, NaCl) of compound **5a**.

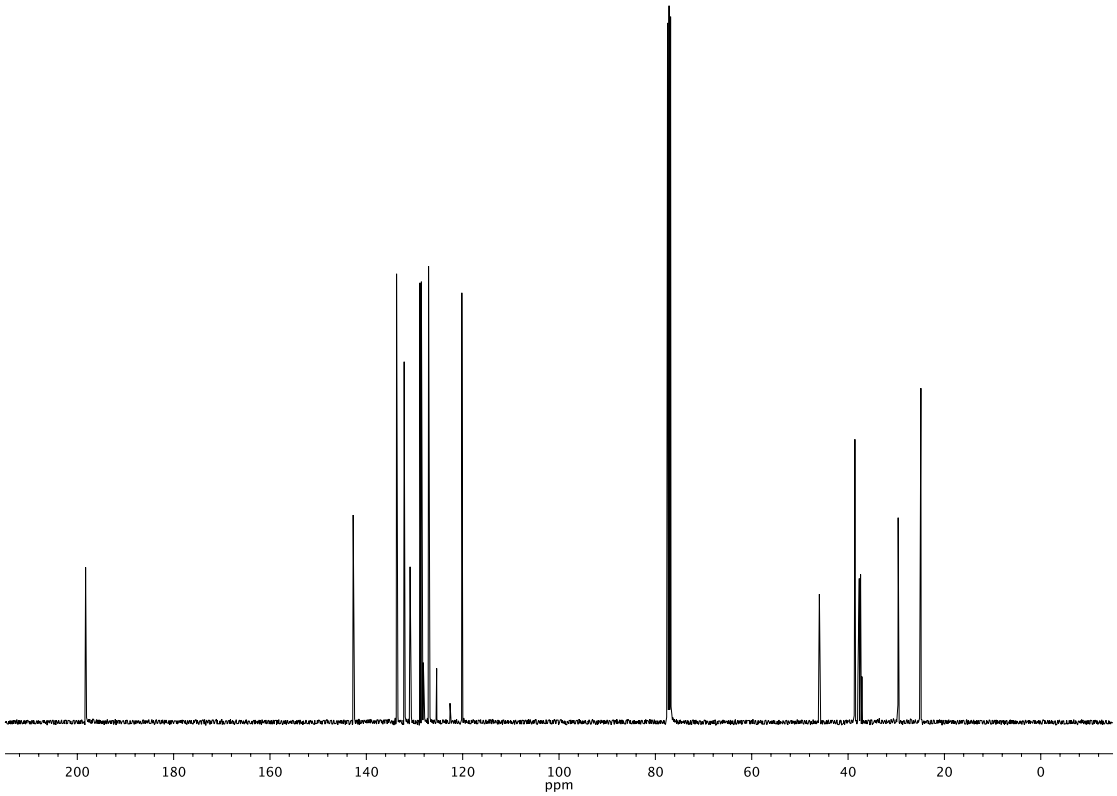

Figure A1.77. ^{13}C NMR (101 MHz, $CDCl_3$) of compound **5a**.

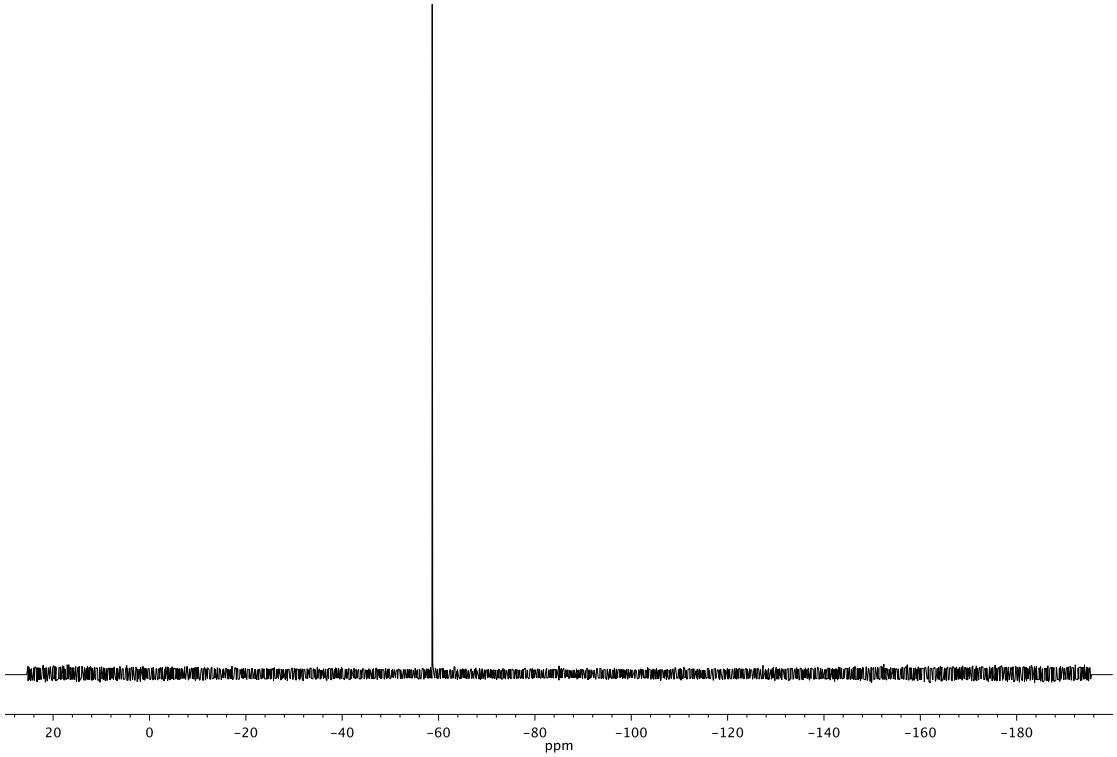

Figure A1.78. ^{19}F NMR (282 MHz, $CDCl_3$) of compound **5a**.

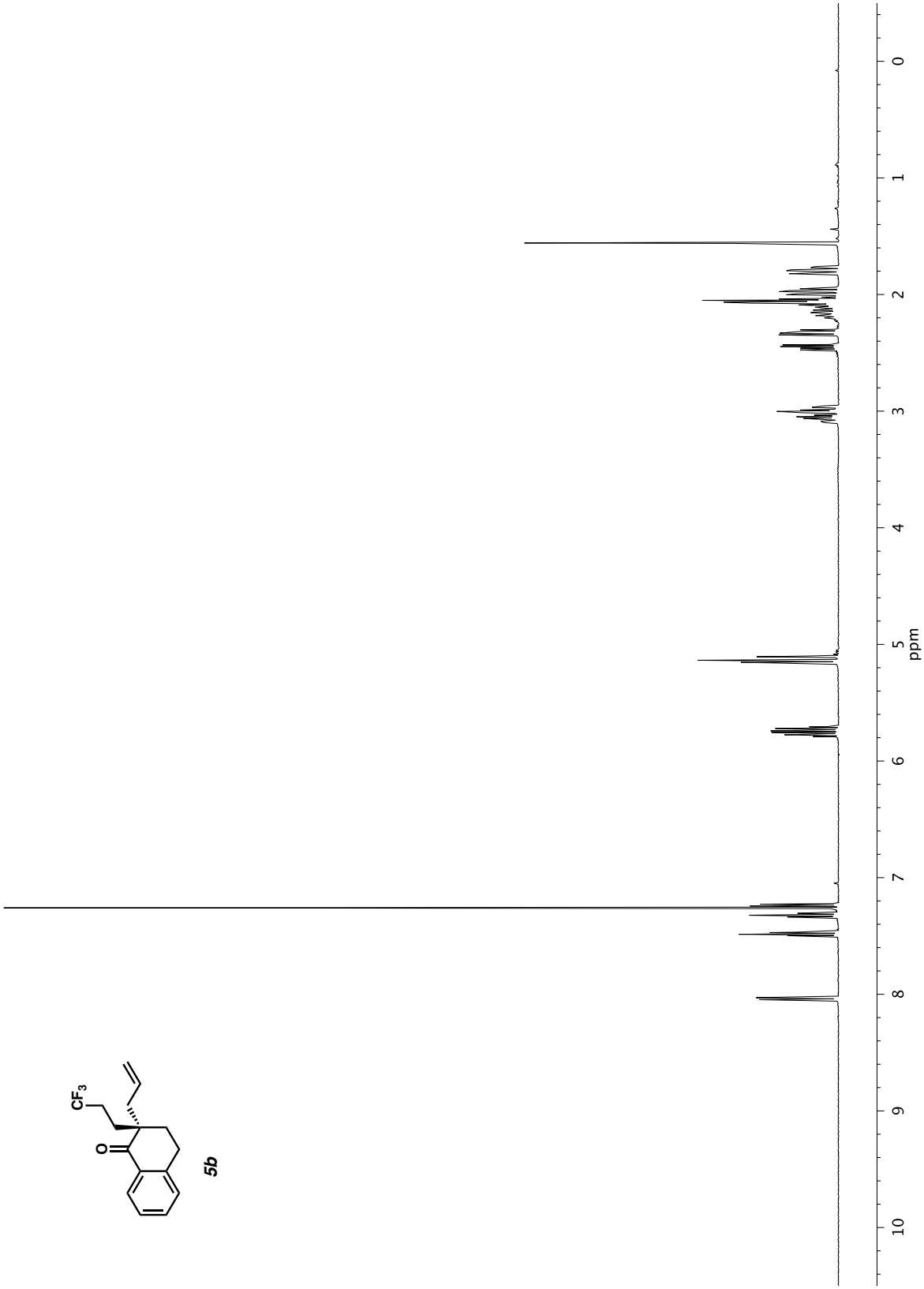

Figure A1.79. ^{1}H NMR (500 MHz, $CDCl_3$) of compound **5b**.

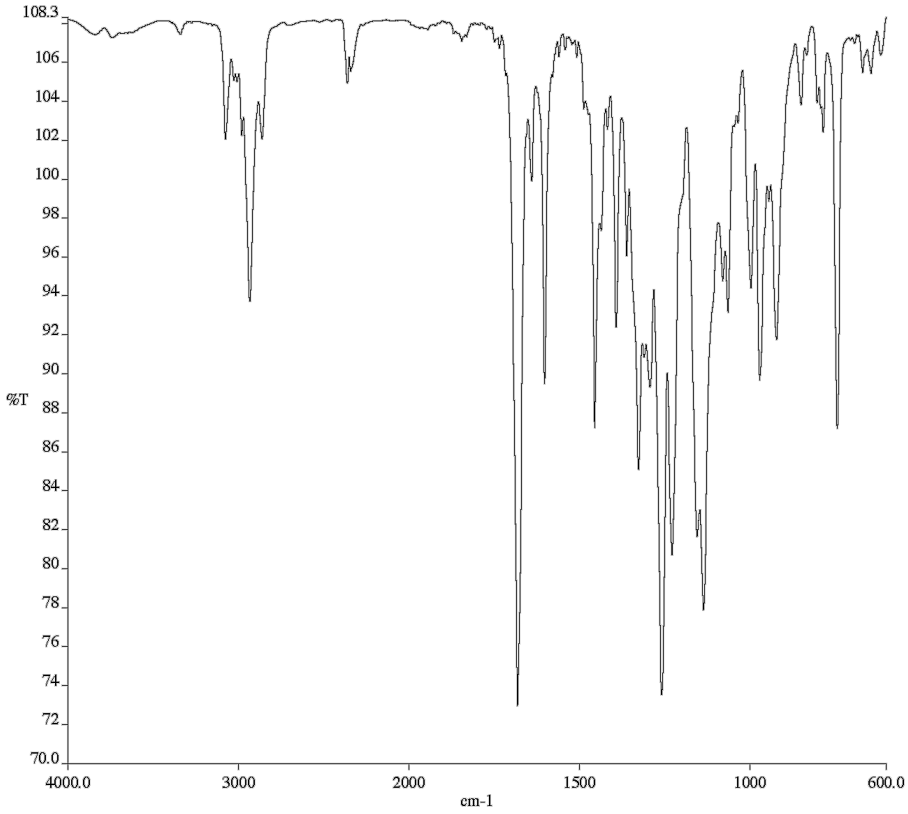

Figure A1.80. Infrared spectrum (Thin Film, NaCl) of compound **5b**.

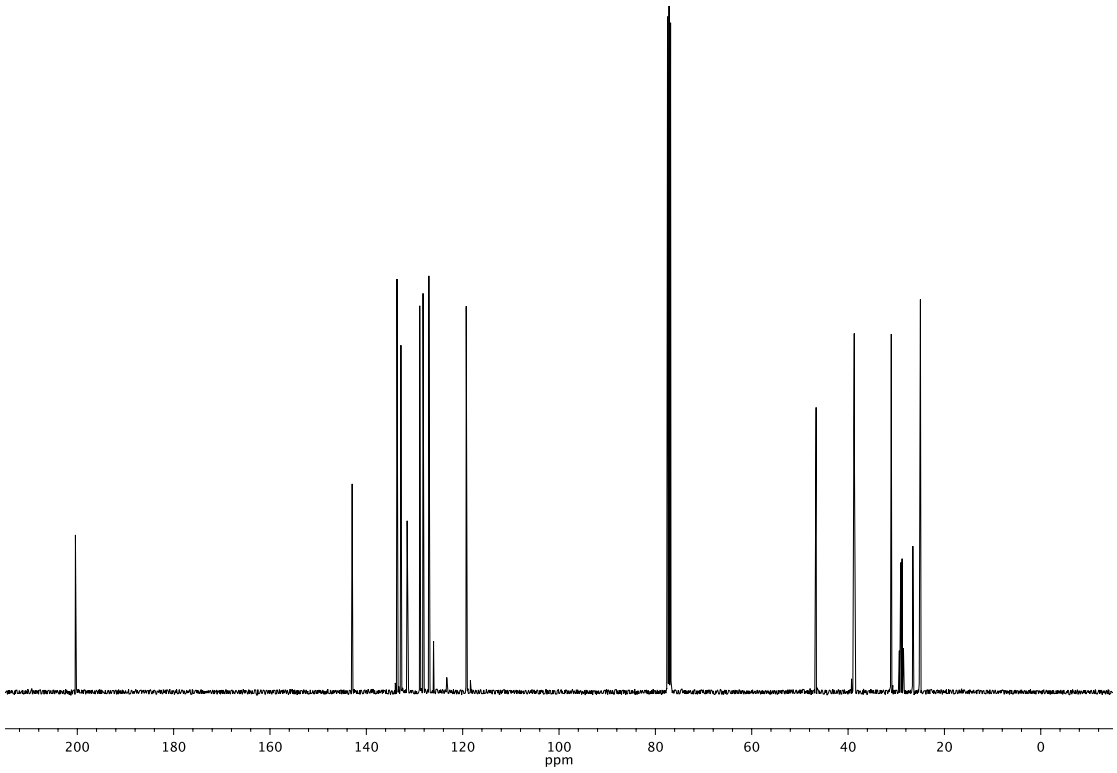

Figure A1.81. ^{13}C NMR (101 MHz, $CDCl_3$) of compound **5b**.

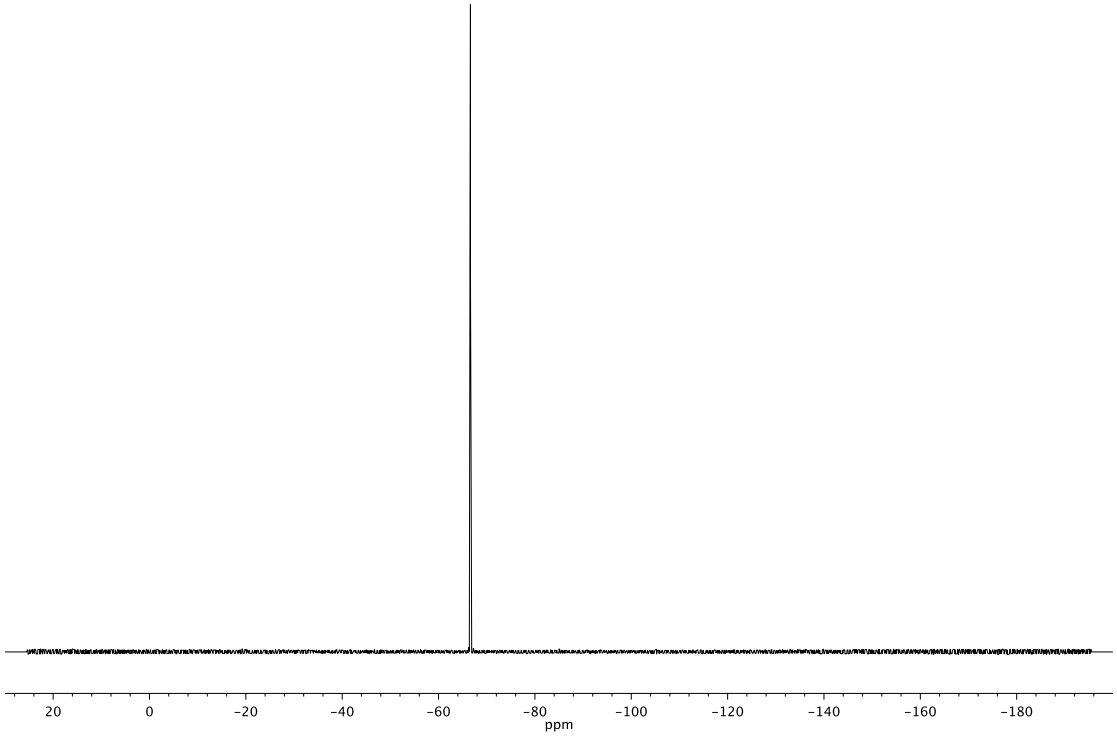

Figure A1.82. ^{19}F NMR (282 MHz, $CDCl_3$) of compound **5b**.

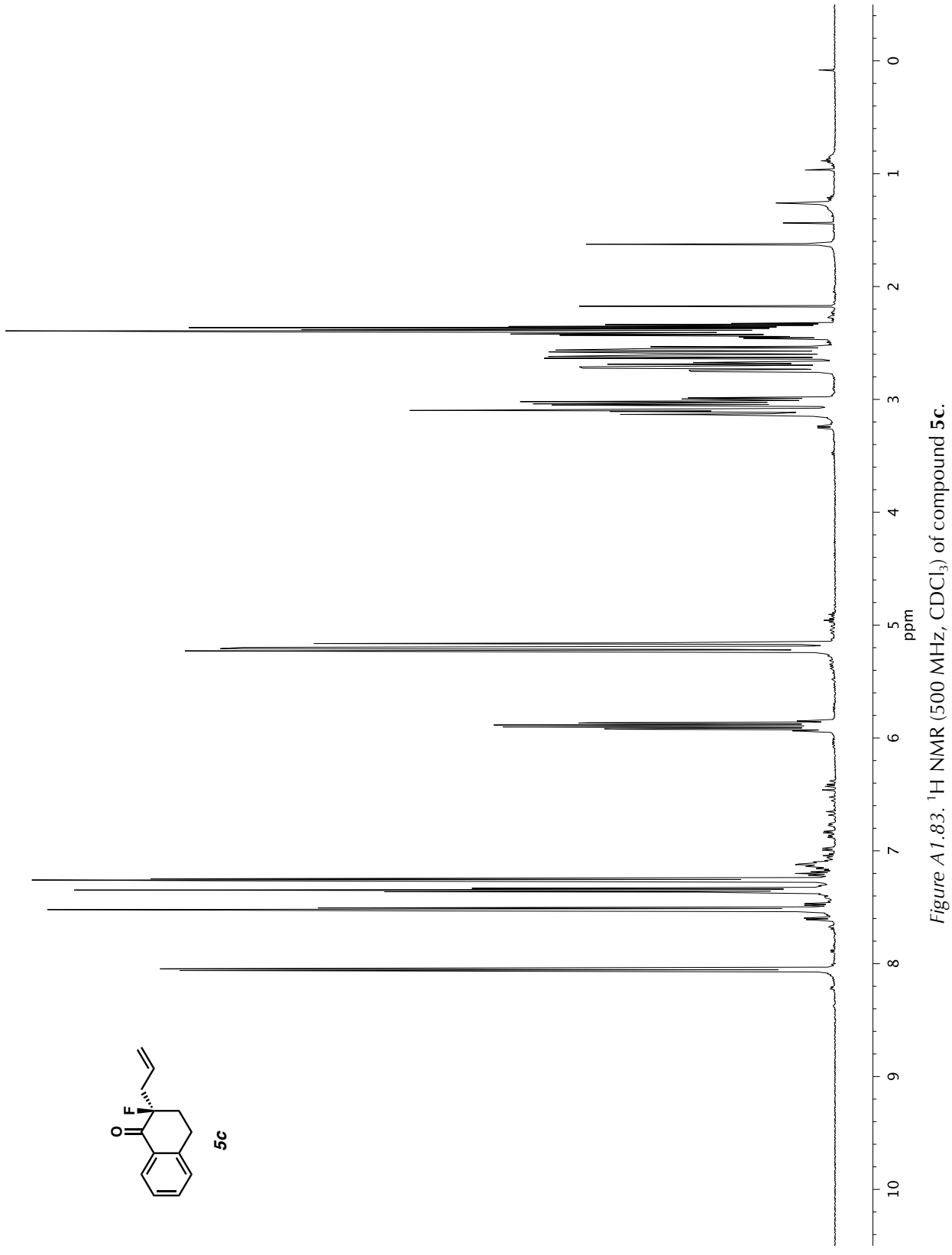

Figure A1.83. ^{1}H NMR (500 MHz, $CDCl_3$) of compound **5c**.

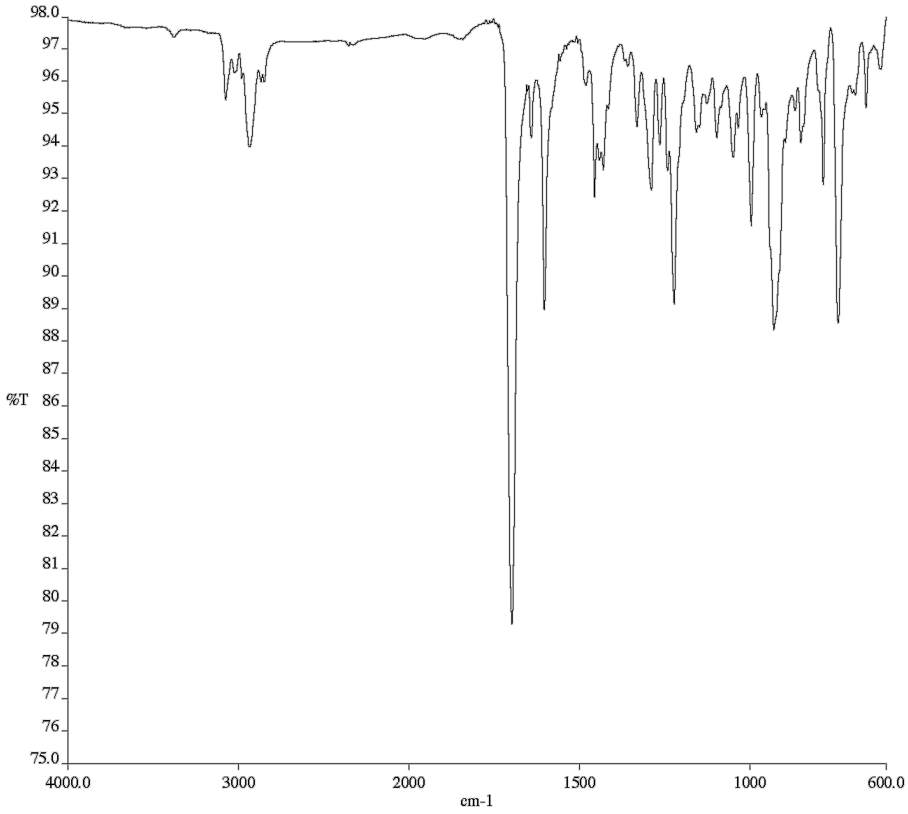

Figure A1.84. Infrared spectrum (Thin Film, NaCl) of compound **5c**.

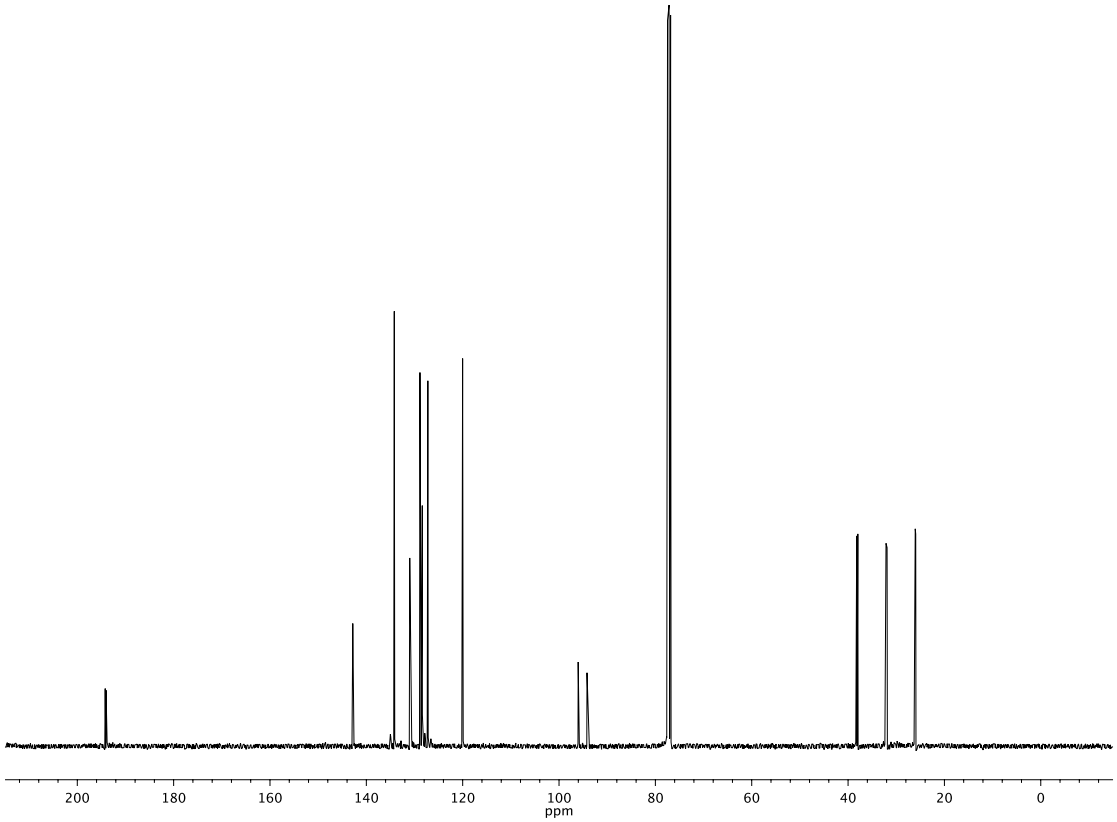

Figure A1.85. ^{13}C NMR (101 MHz, $CDCl_3$) of compound **5c**.

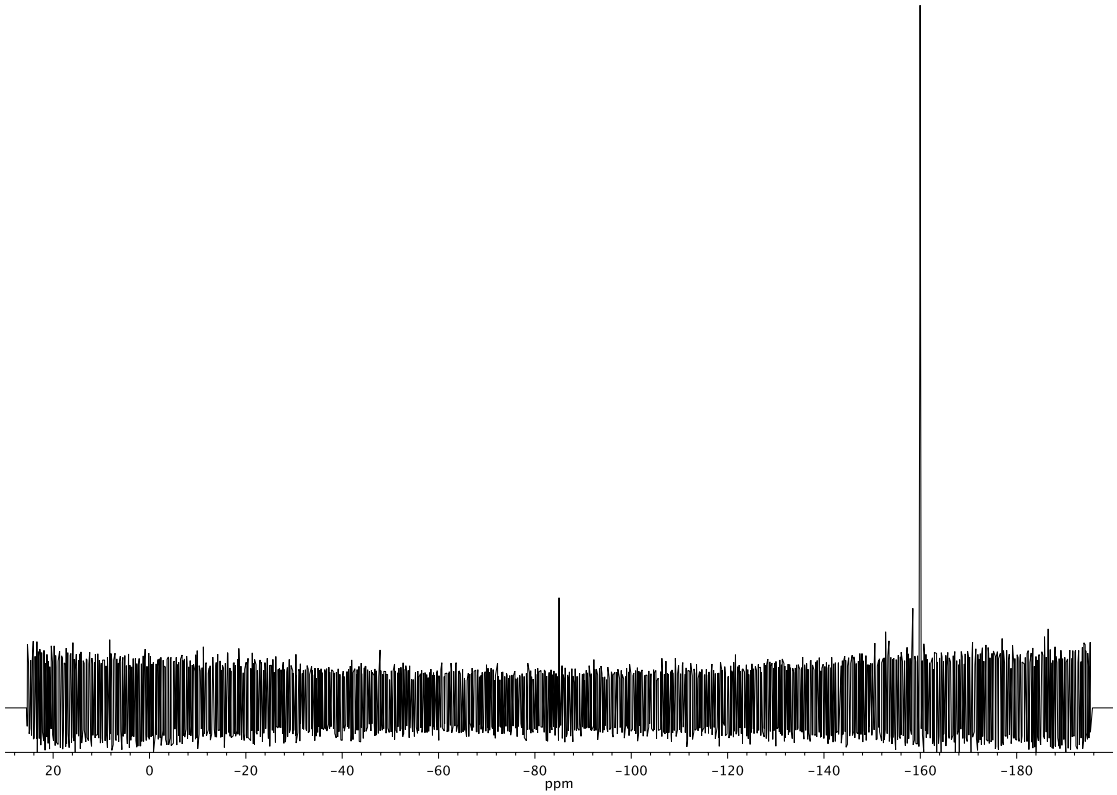

Figure A1.86. ^{19}F NMR (282 MHz, $CDCl_3$) of compound **5c**.

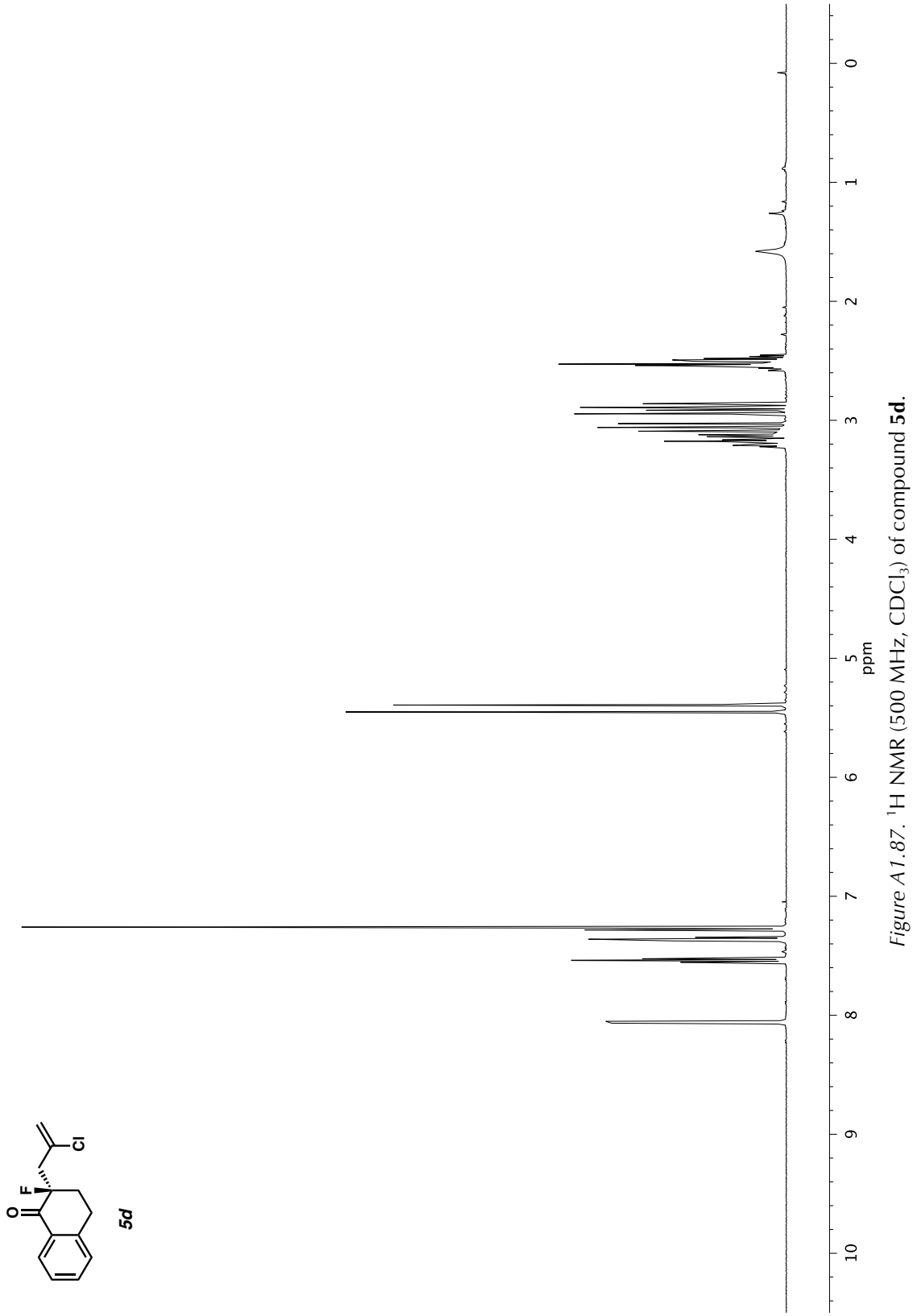

Figure A1.87. ^{1}H NMR (500 MHz, $CDCl_3$) of compound **5d**.

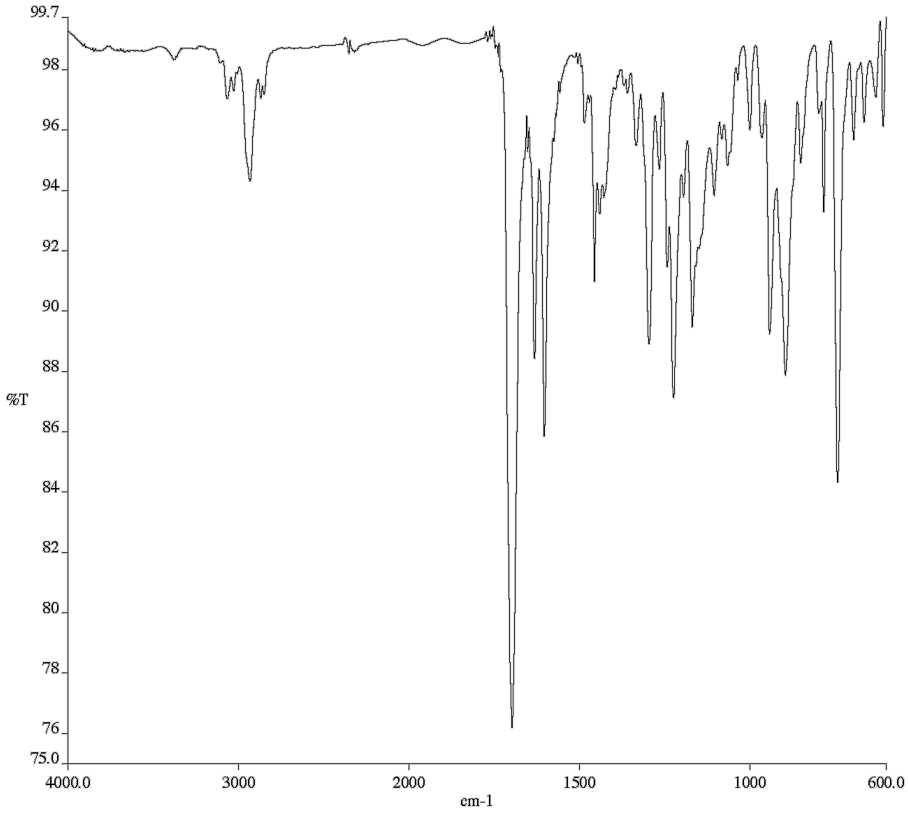

Figure A1.88. Infrared spectrum (Thin Film, NaCl) of compound **5d**.

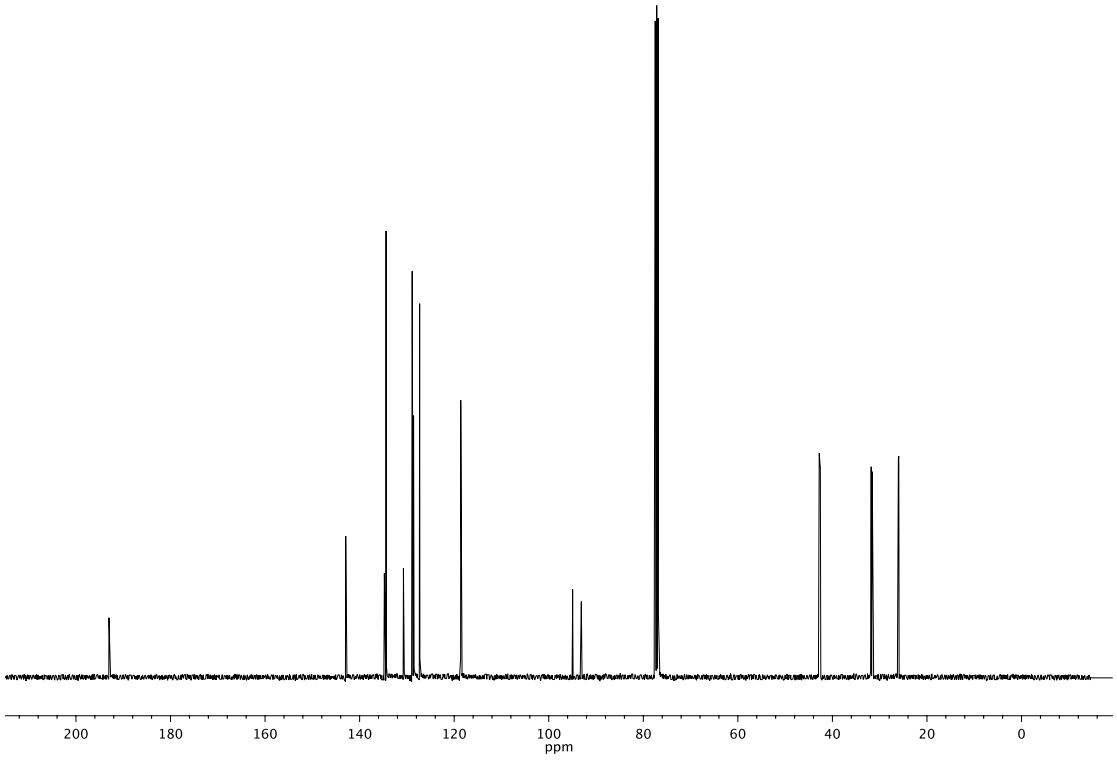

Figure A1.89. ^{13}C NMR (101 MHz, $CDCl_3$) of compound **5d**.

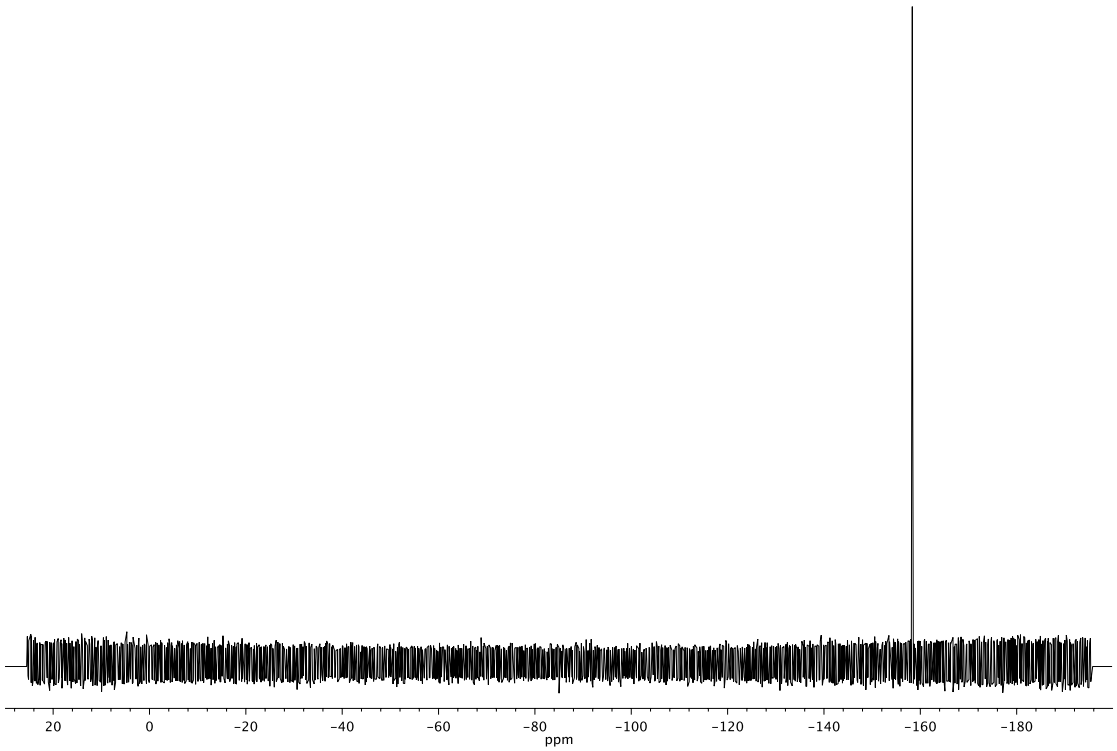

Figure A1.90. ^{19}F NMR (282 MHz, $CDCl_3$) of compound **5d**.

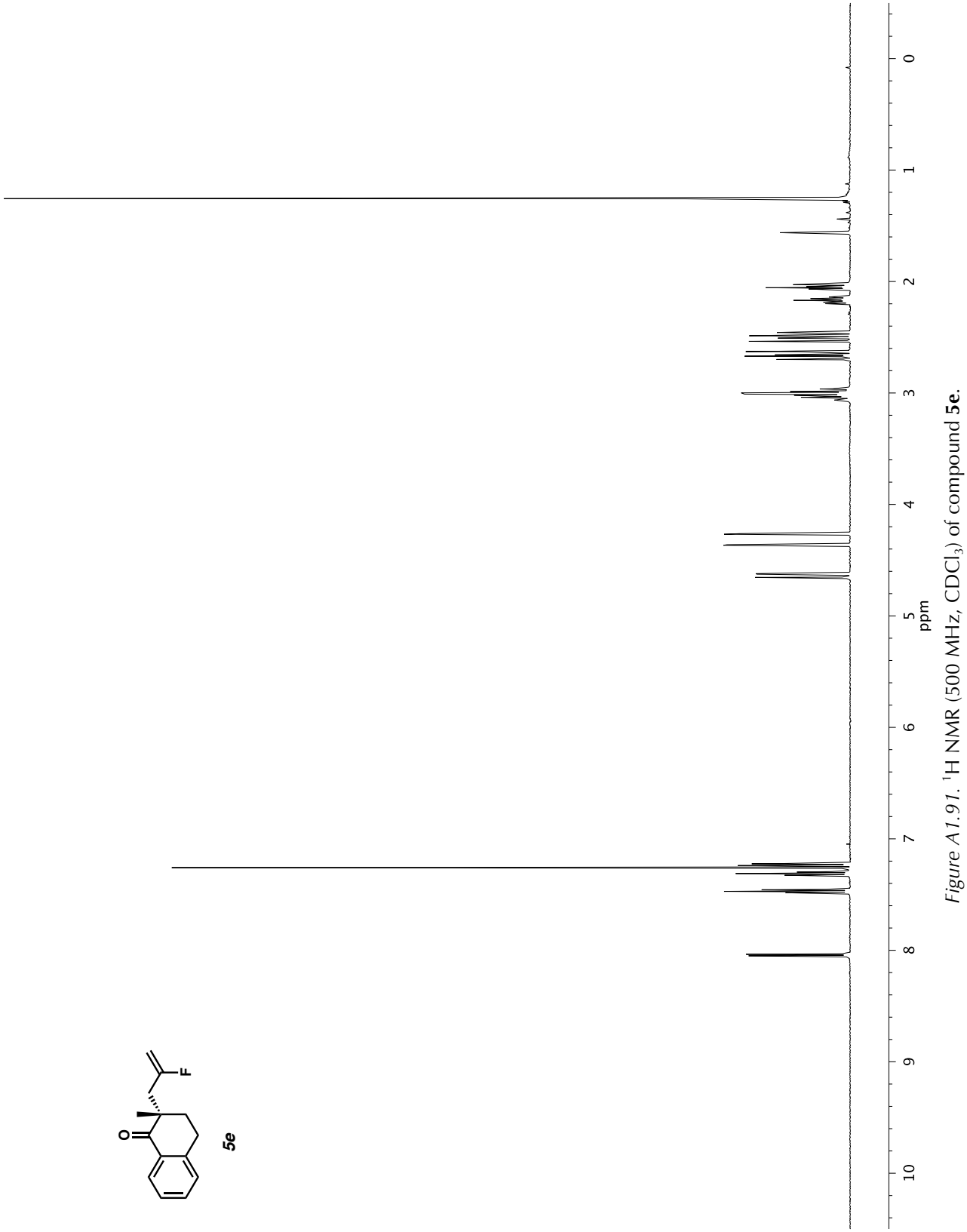

Figure A1.91. ^{1}H NMR (500 MHz, $CDCl_3$) of compound **5e**.

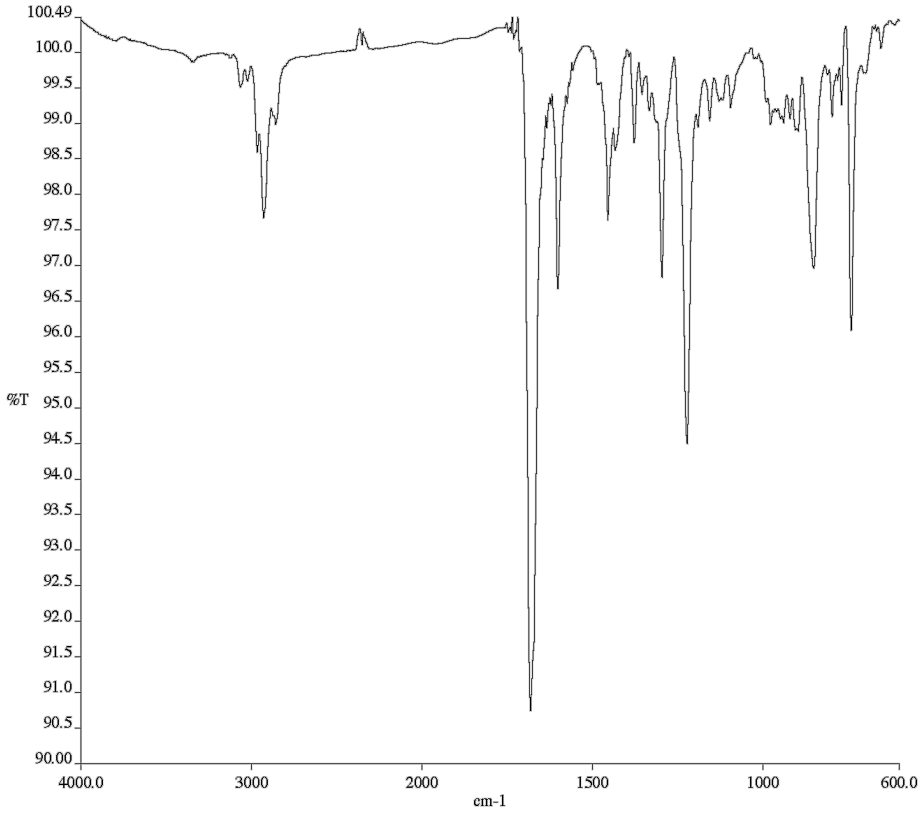

Figure A1.92. Infrared spectrum (Thin Film, NaCl) of compound **5e**.

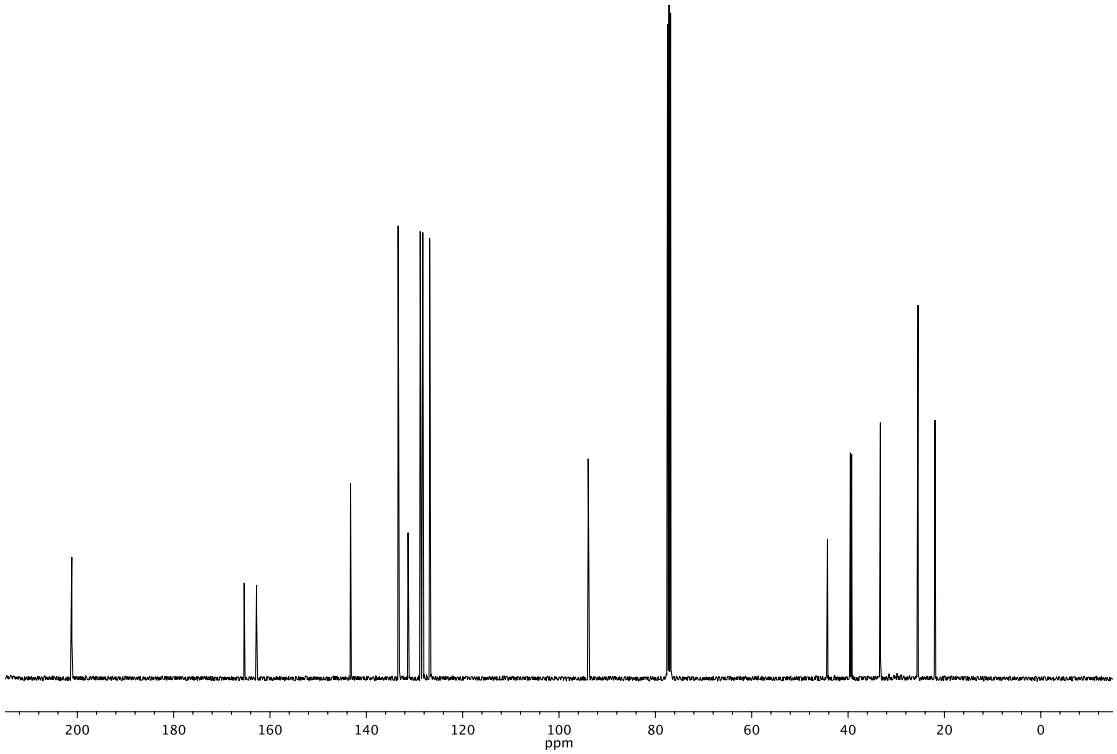

Figure A1.93. ^{13}C NMR (101 MHz, $CDCl_3$) of compound **5e**.

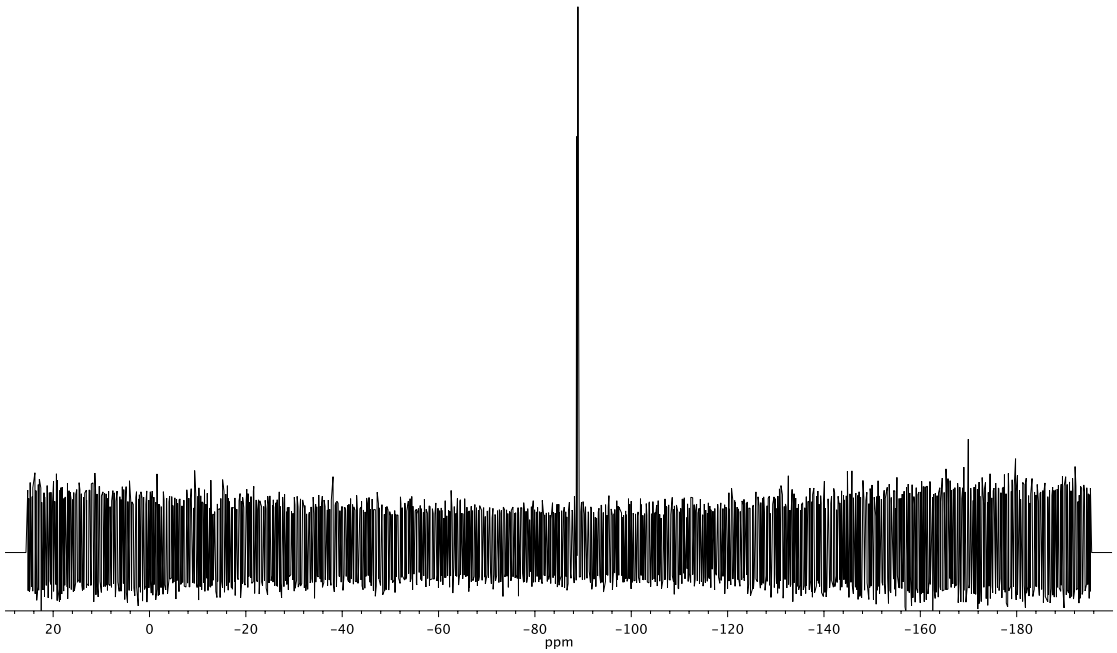

Figure A1.94. ^{19}F NMR (282 MHz, $CDCl_3$) of compound **5e**.

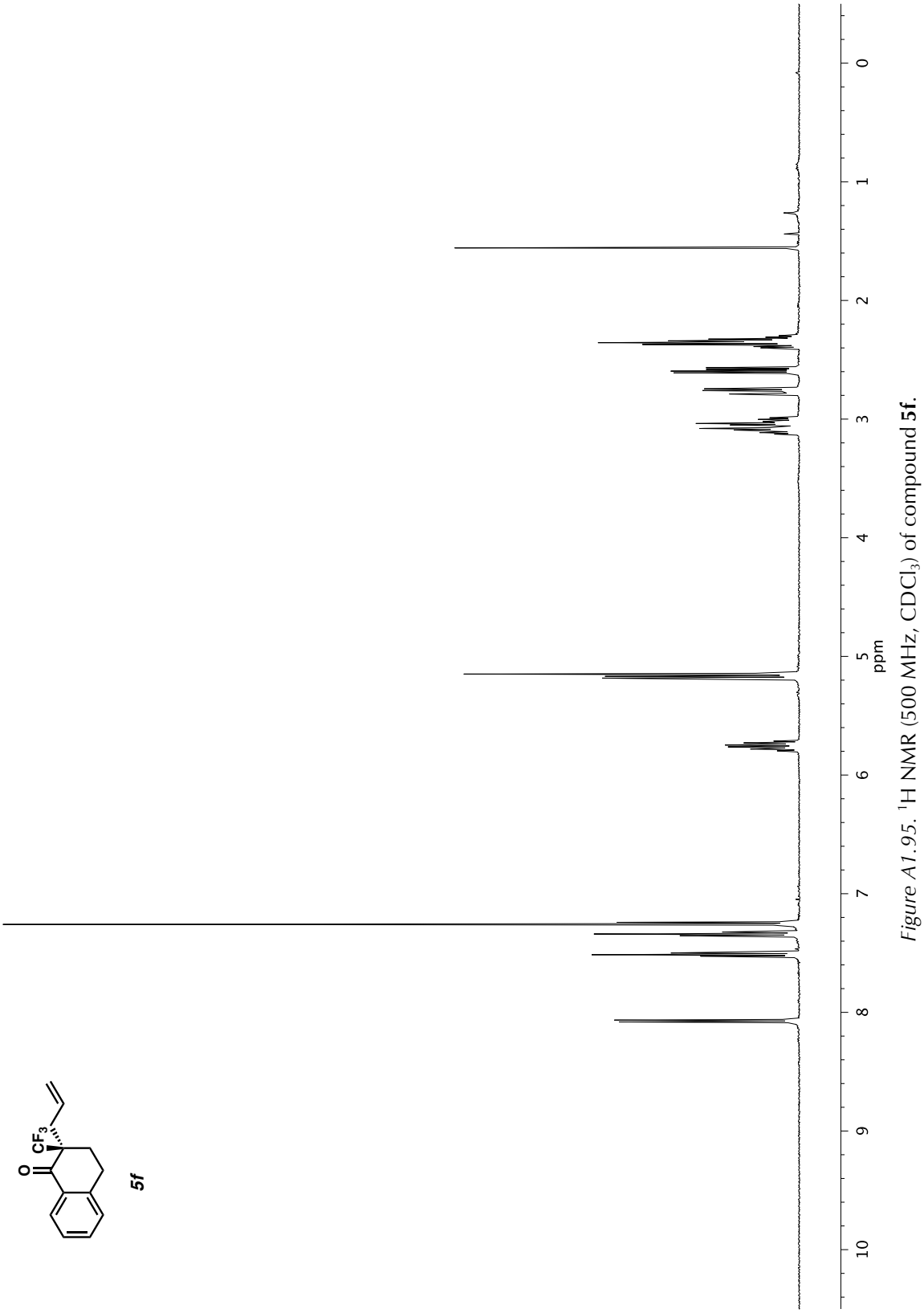

Figure A1.95. ^{1}H NMR (500 MHz, $CDCl_3$) of compound **5f**.

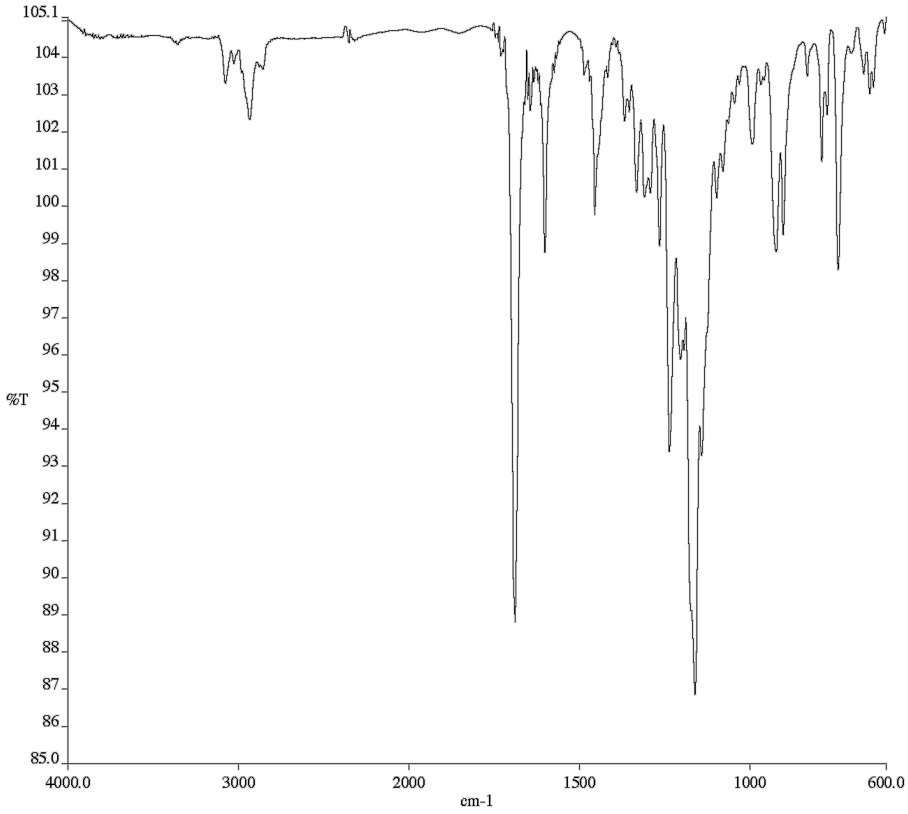

Figure A1.96. Infrared spectrum (Thin Film, NaCl) of compound **5f**.

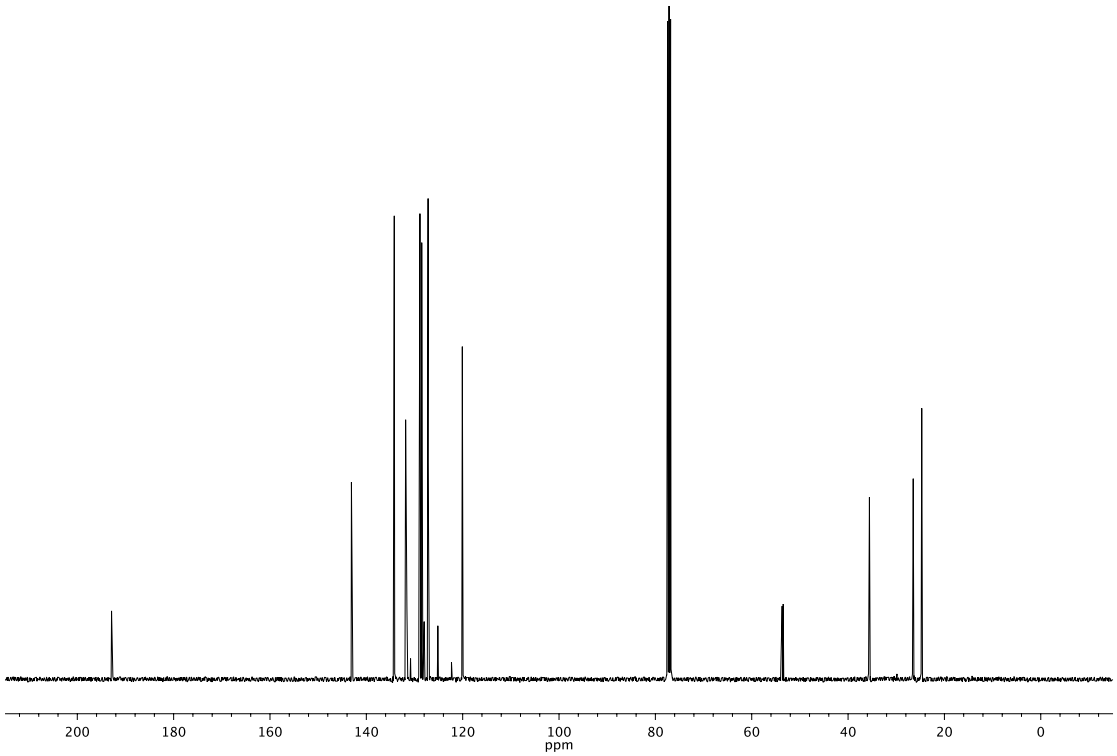

Figure A1.97. ^{13}C NMR (101 MHz, $CDCl_3$) of compound **5f**.

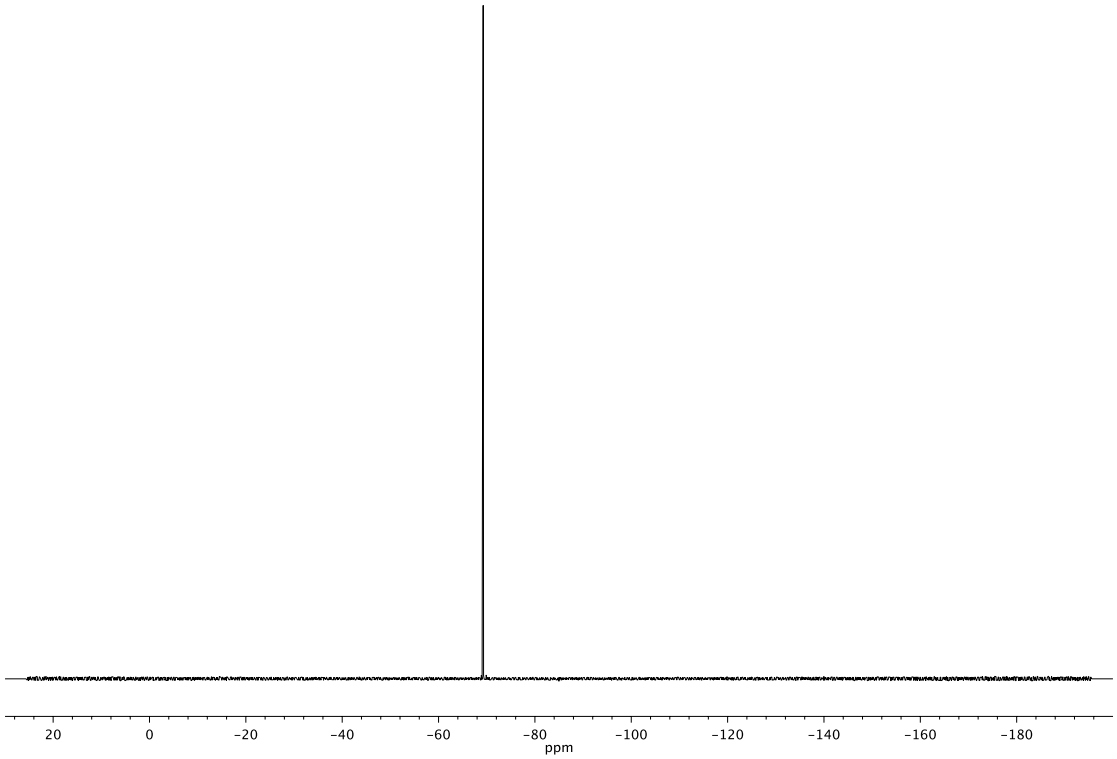

Figure A1.98. ^{19}F NMR (282 MHz, $CDCl_3$) of compound **5f**.

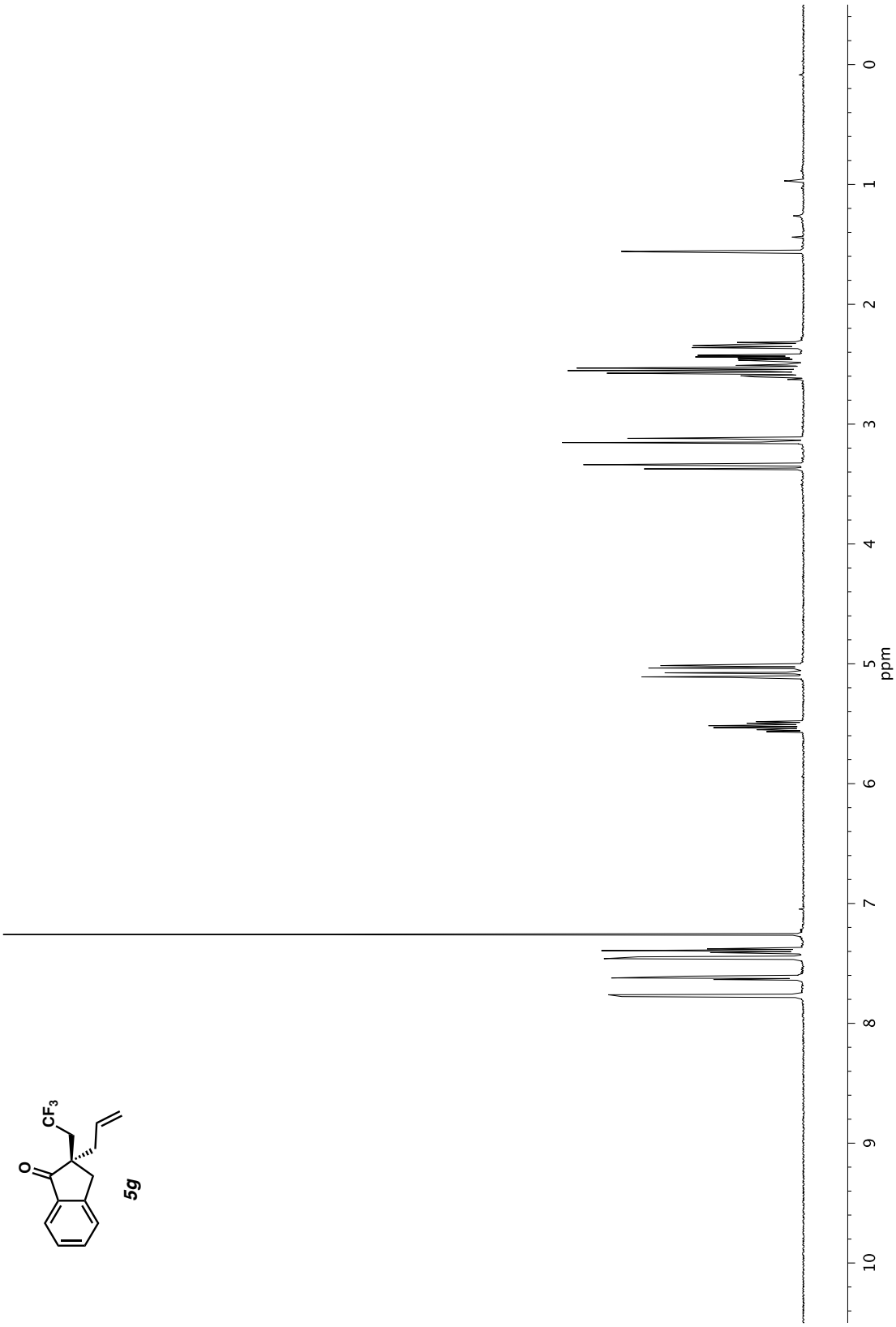

Figure A1.99. ^{1}H NMR (500 MHz, $CDCl_3$) of compound **5g**.

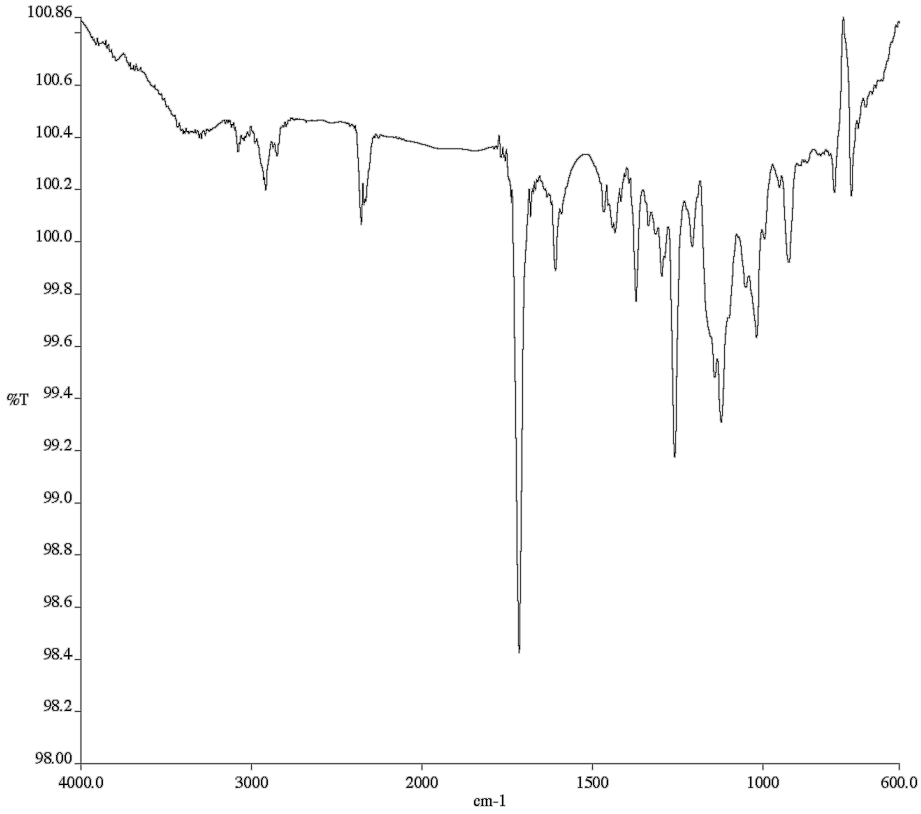

Figure A1.100. Infrared spectrum (Thin Film, NaCl) of compound **5g**.

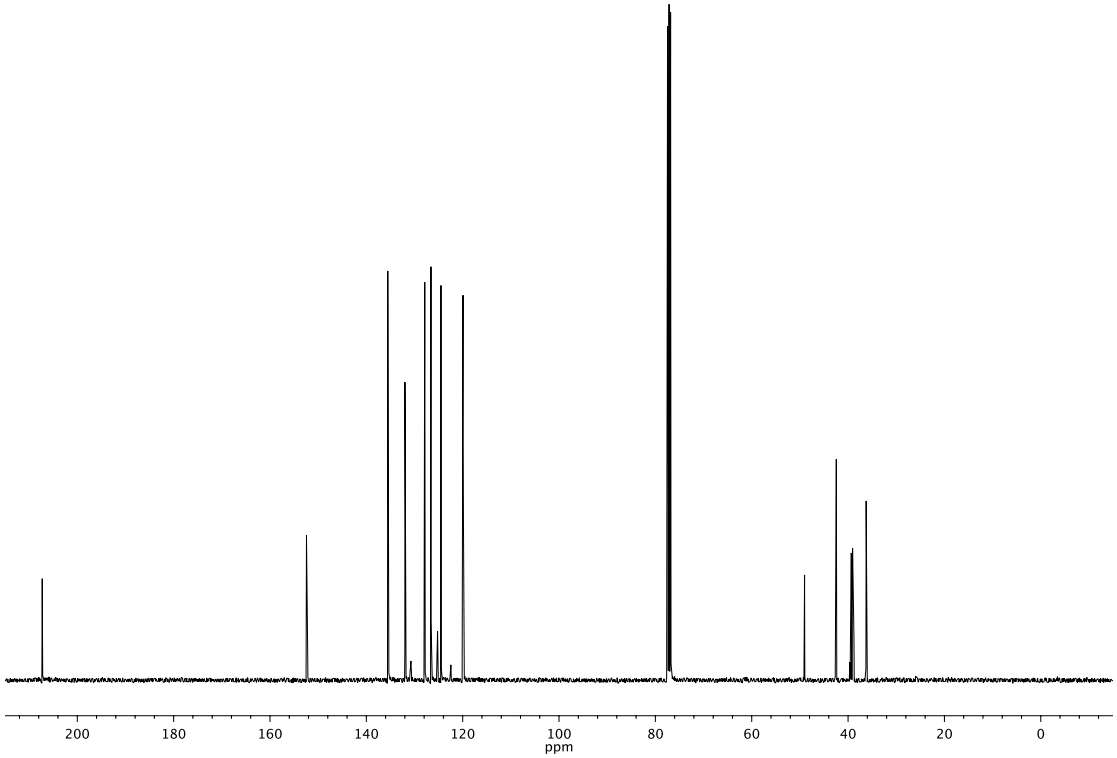

Figure A1.101. ^{13}C NMR (101 MHz, $CDCl_3$) of compound **5g**.

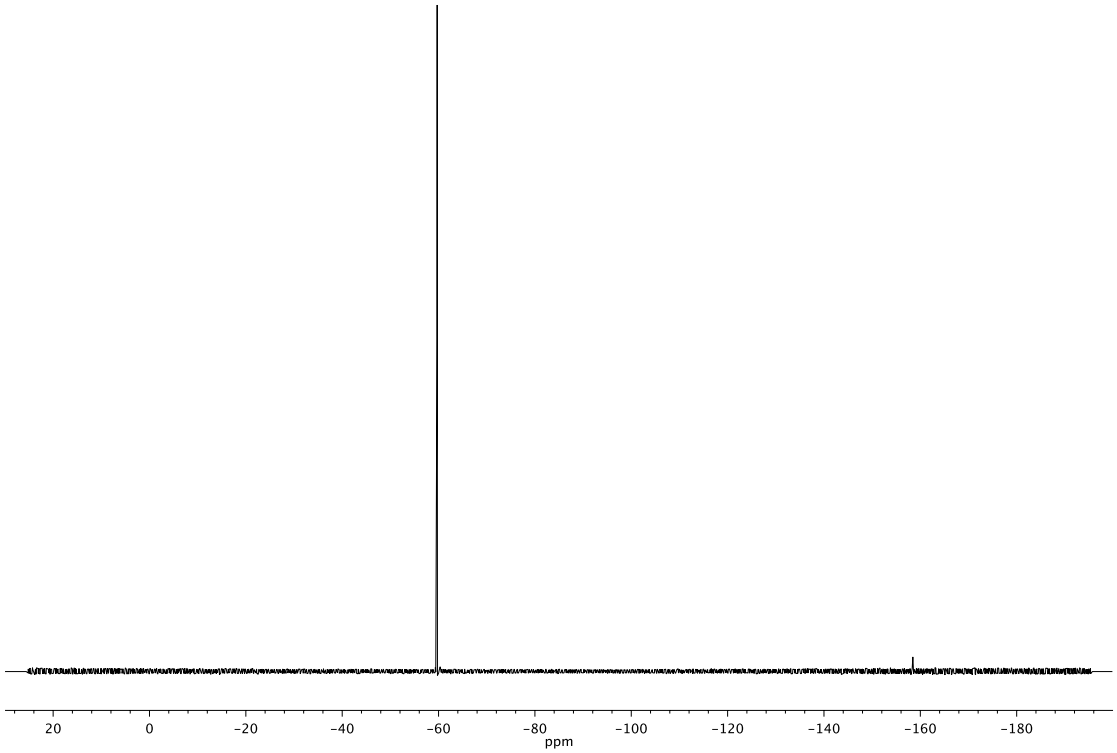

Figure A1.102. ^{19}F NMR (282 MHz, $CDCl_3$) of compound **5g**.

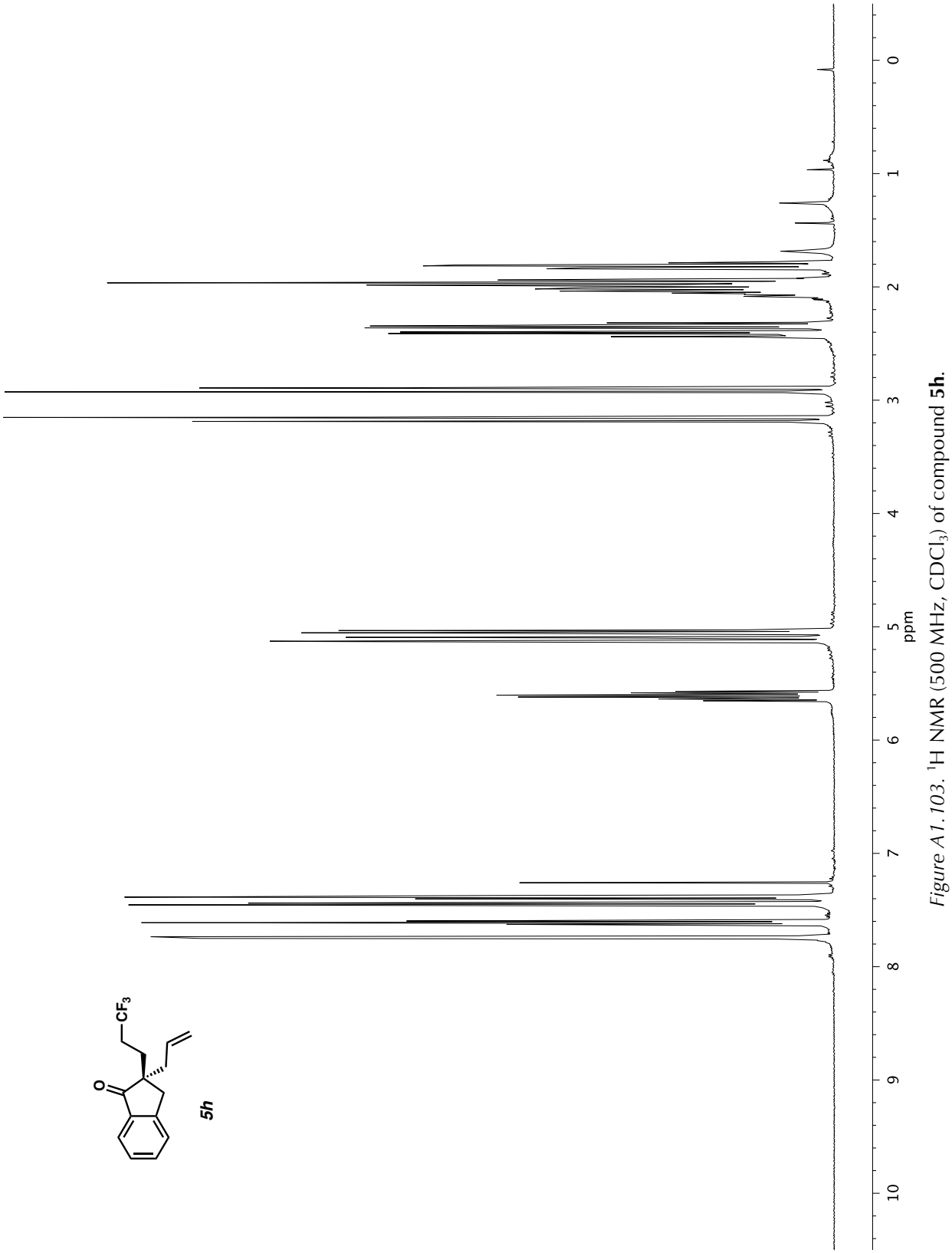

Figure A1.103. ^{1}H NMR (500 MHz, $CDCl_3$) of compound **5h**.

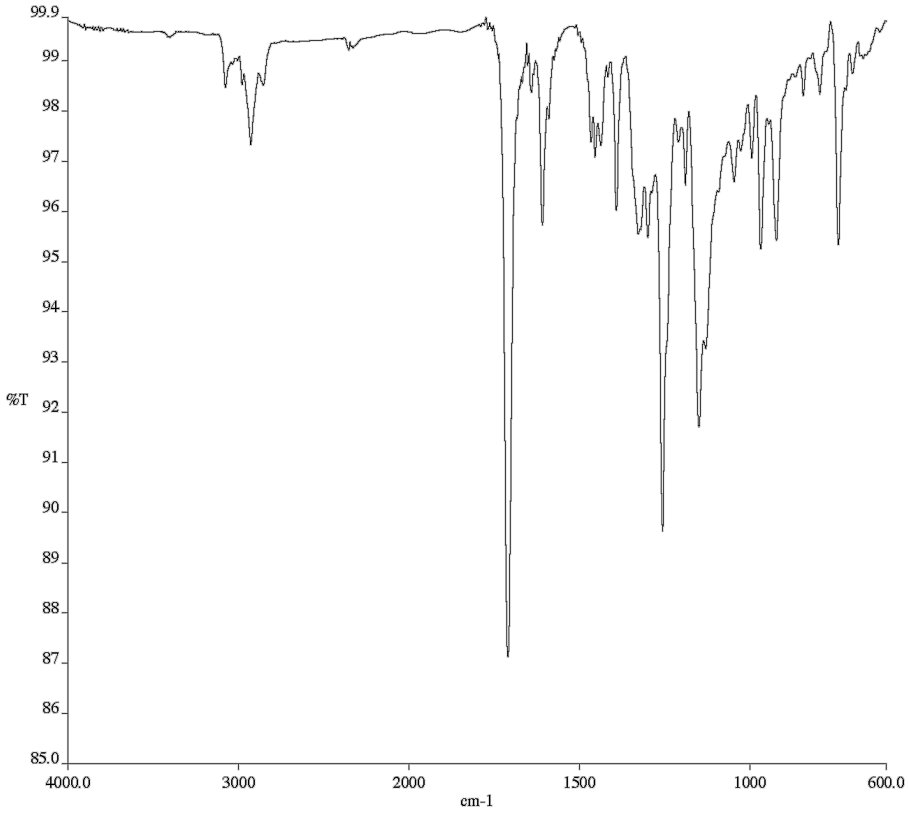

Figure A1.104. Infrared spectrum (Thin Film, NaCl) of compound **5h**.

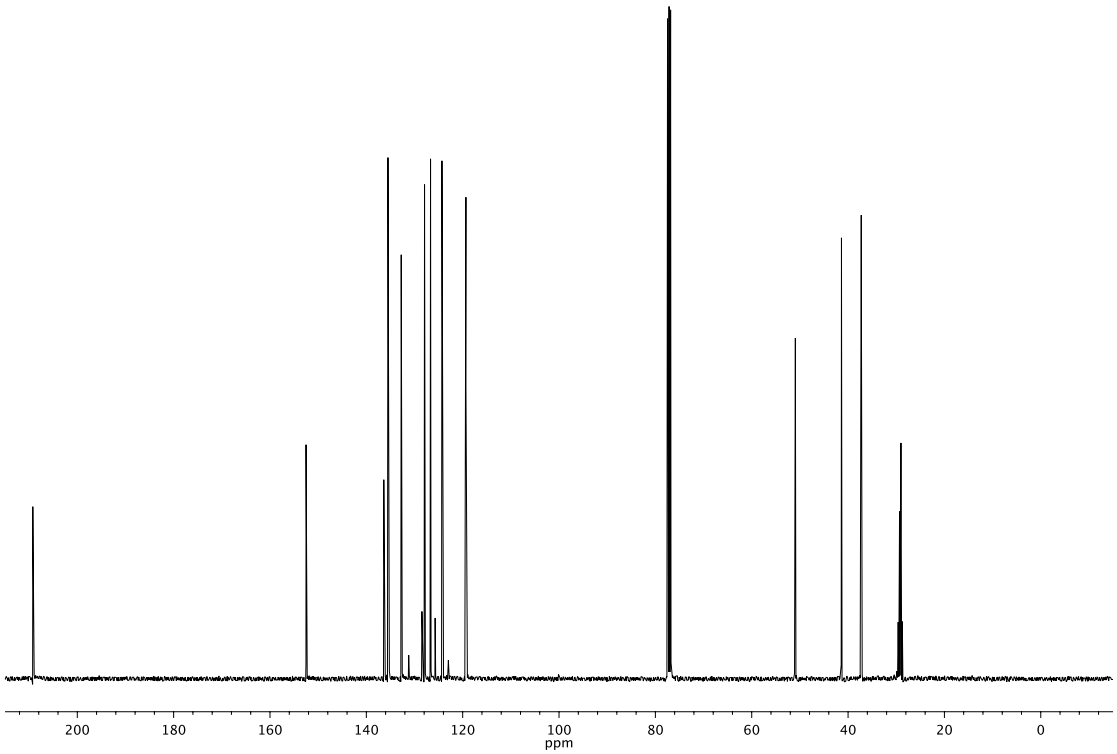

Figure A1.105. ^{13}C NMR (101 MHz, $CDCl_3$) of compound **5h**.

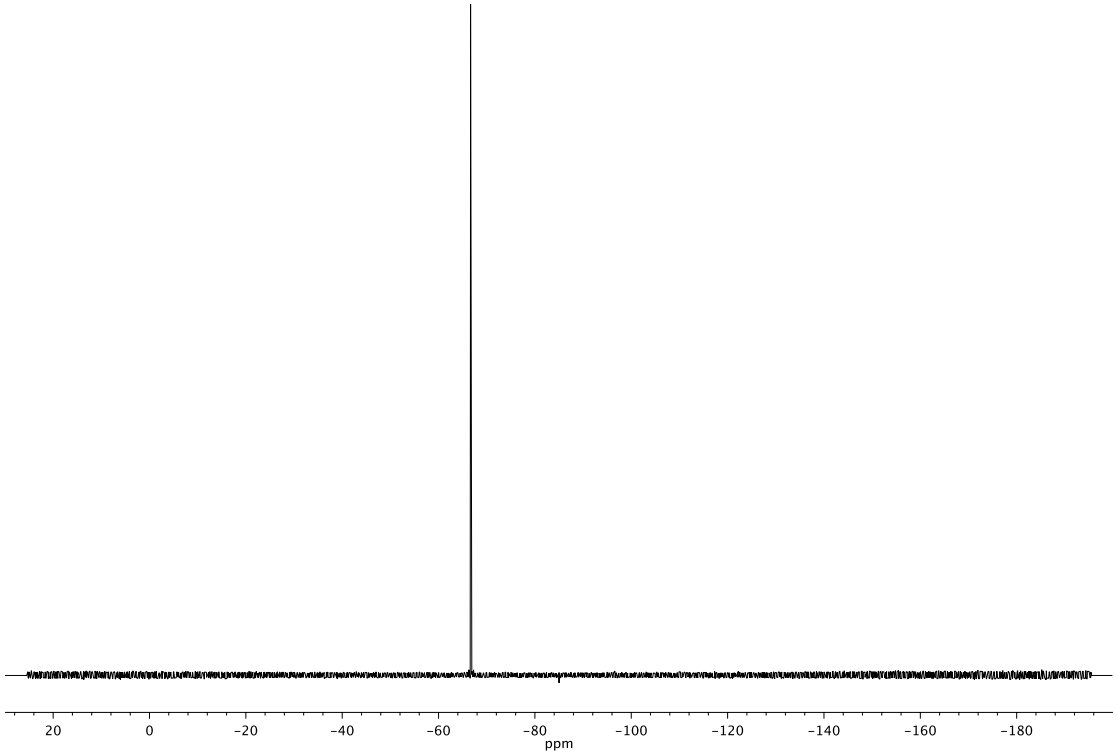

Figure A1.106. ^{19}F NMR (282 MHz, $CDCl_3$) of compound **5h**.

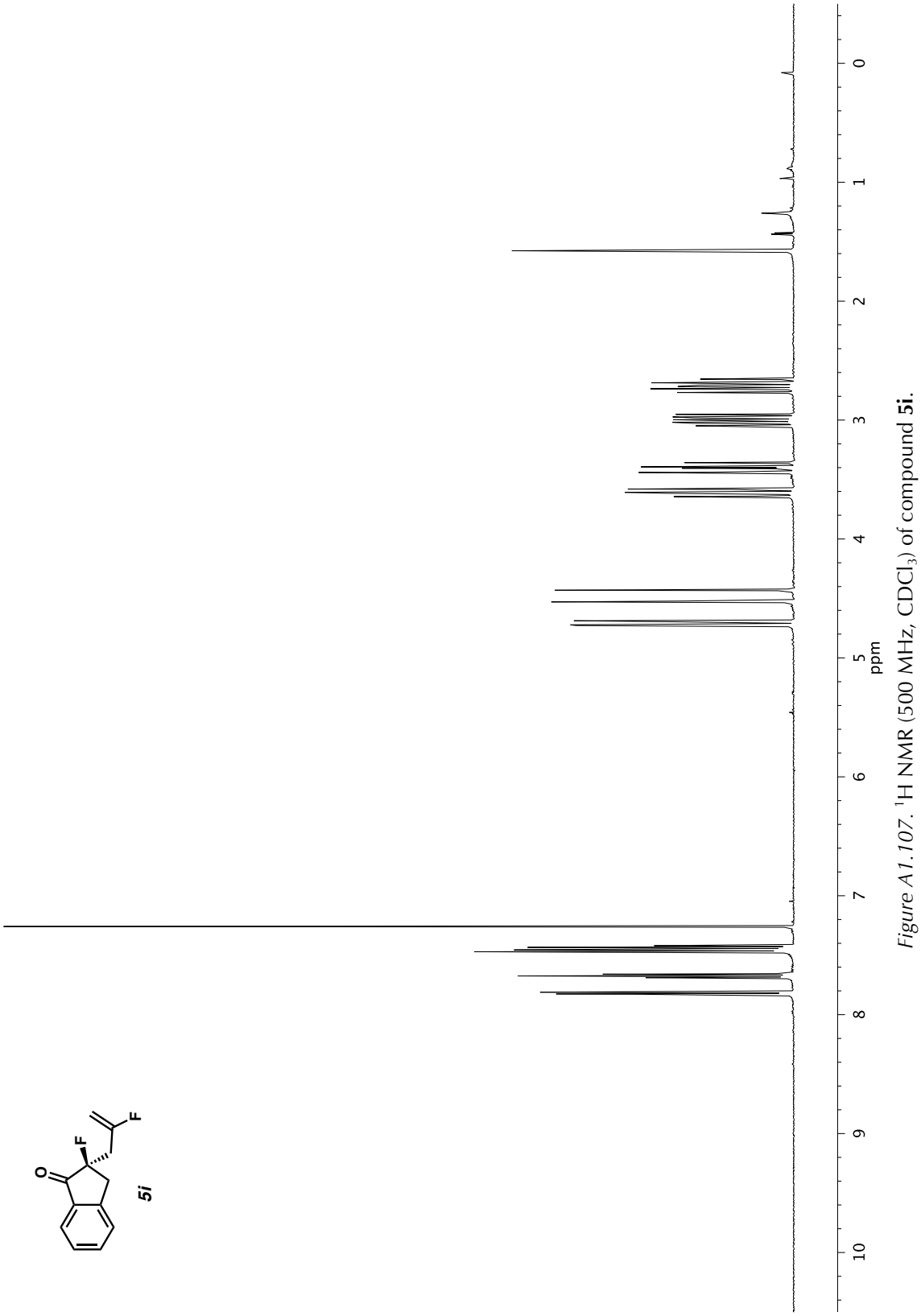

Figure A1.107. ^{1}H NMR (500 MHz, $CDCl_3$) of compound **5i**.

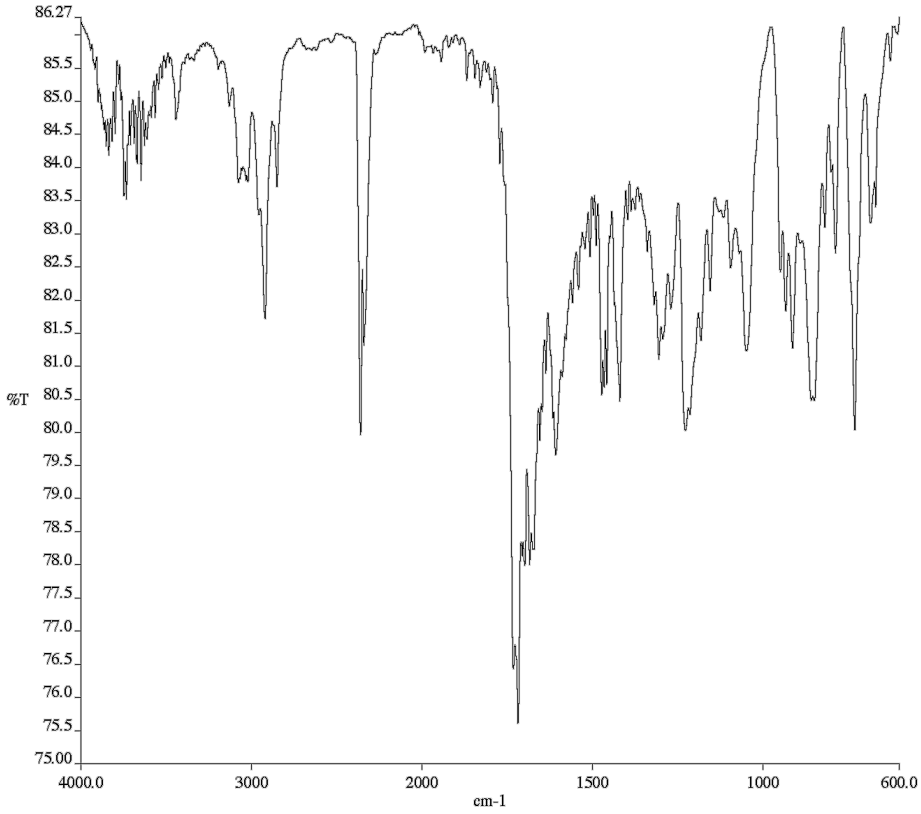

Figure A1.108. Infrared spectrum (Thin Film, NaCl) of compound **5i**.

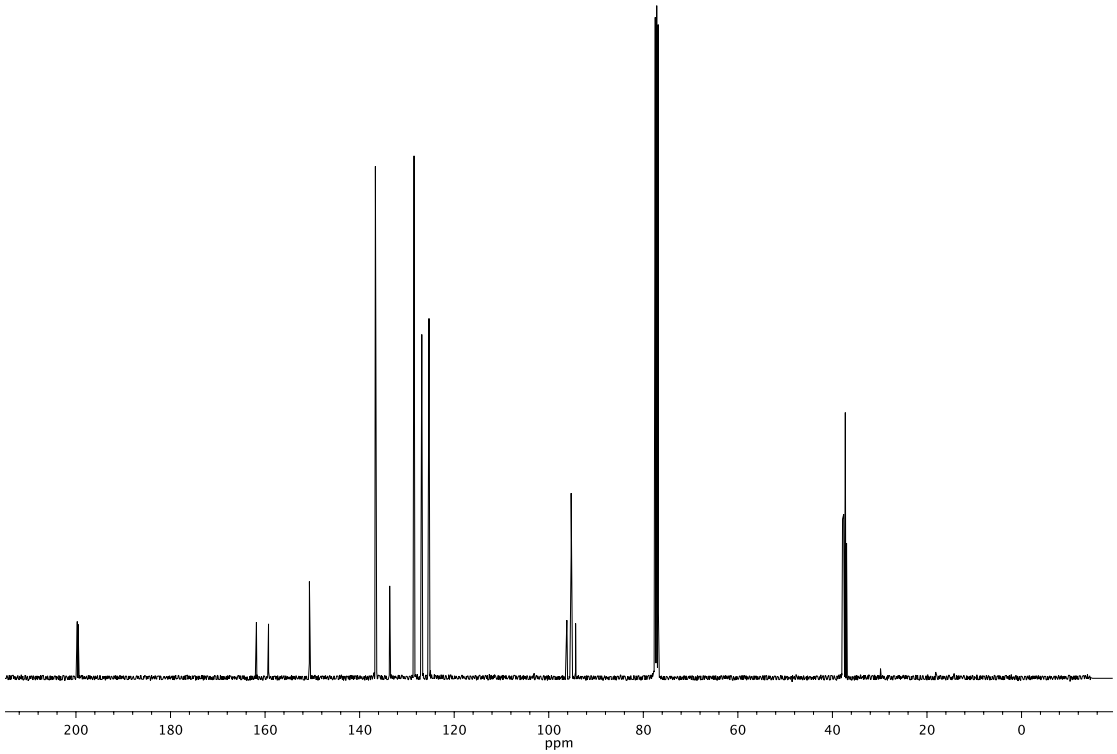

Figure A1.109. ^{13}C NMR (101 MHz, $CDCl_3$) of compound **5i**.

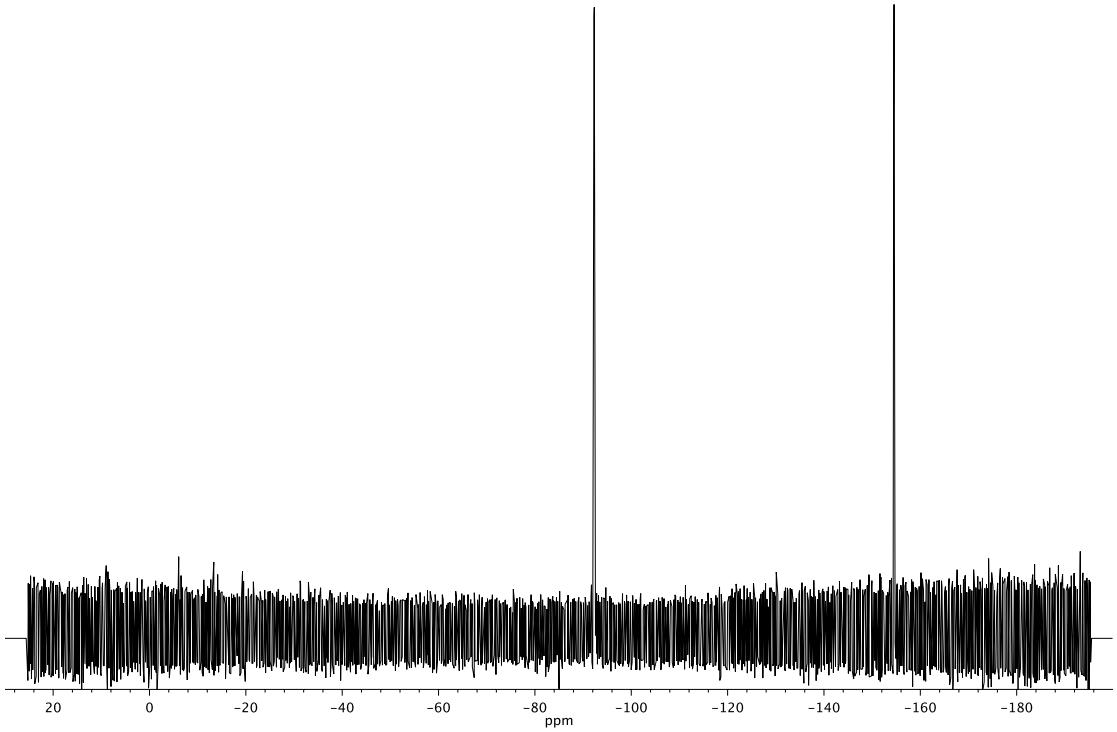

Figure A1.110. ^{19}F NMR (282 MHz, $CDCl_3$) of compound **5i**.

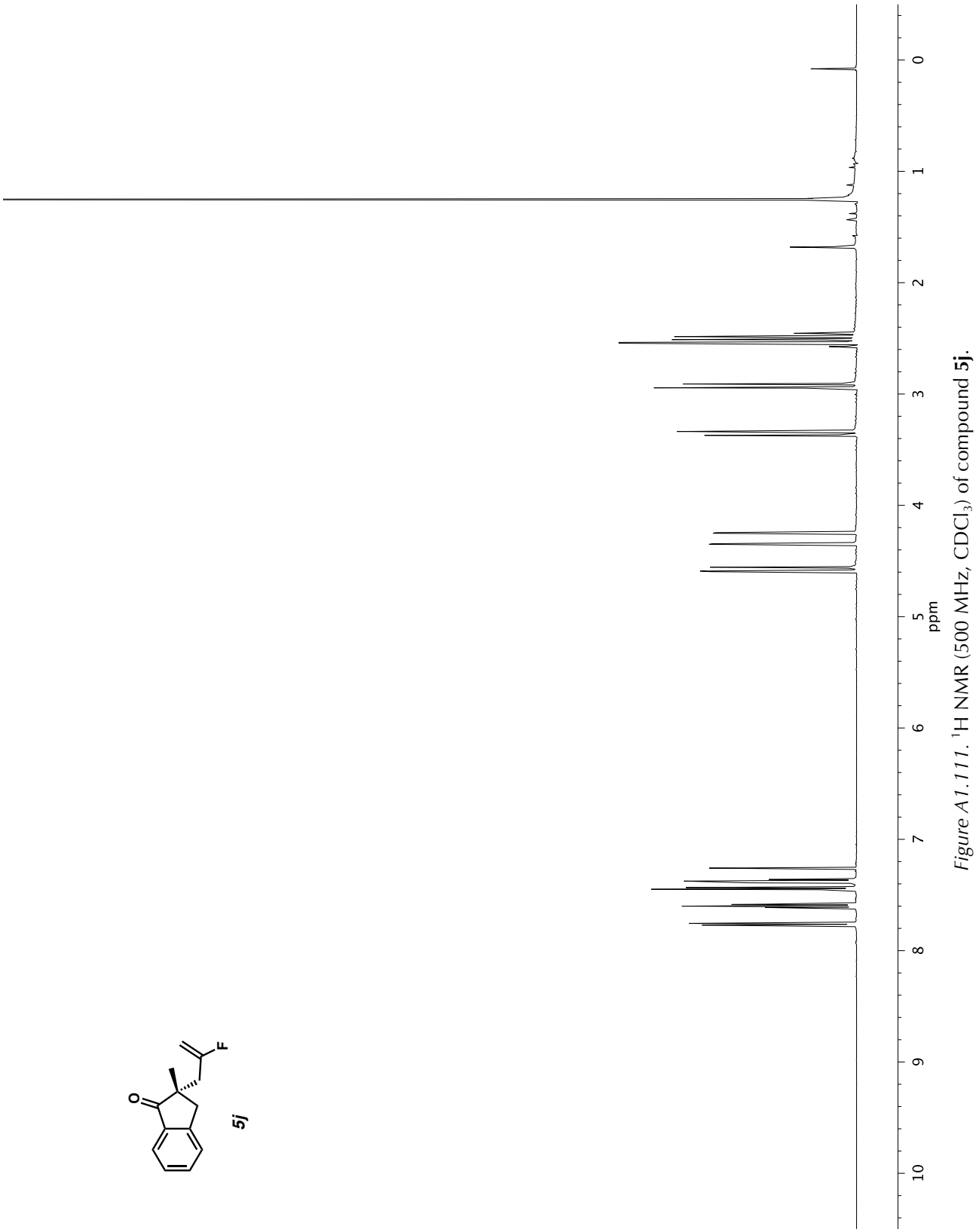

Figure A1.111. ^{1}H NMR (500 MHz, $CDCl_3$) of compound **5j**.

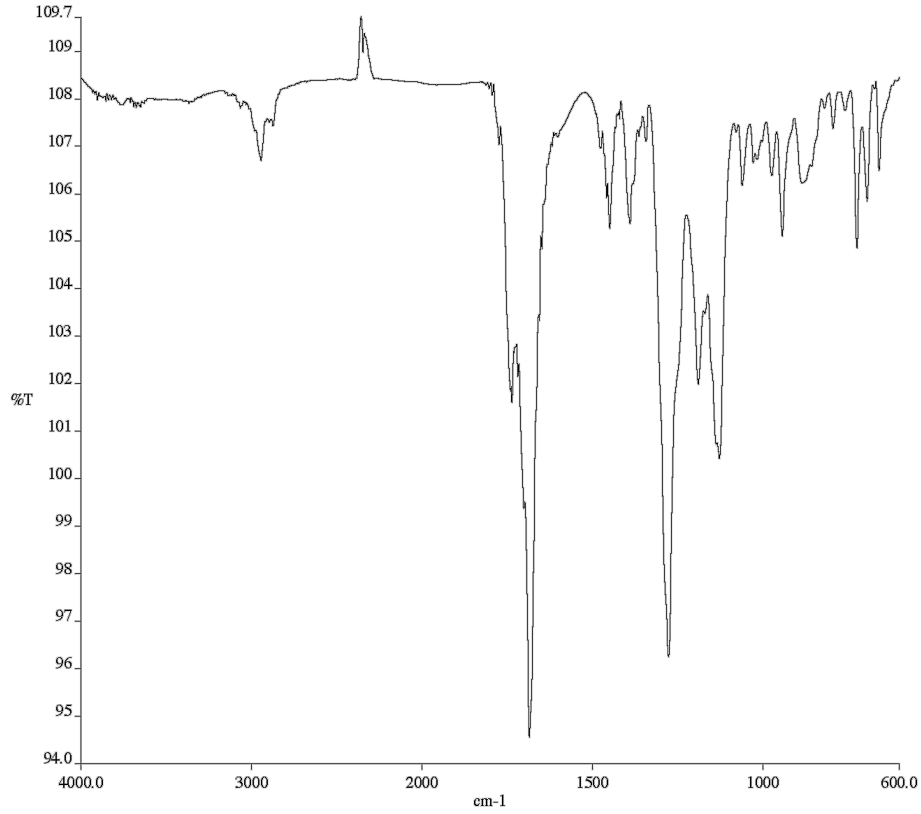

Figure A1.112. Infrared spectrum (Thin Film, NaCl) of compound **5j**.

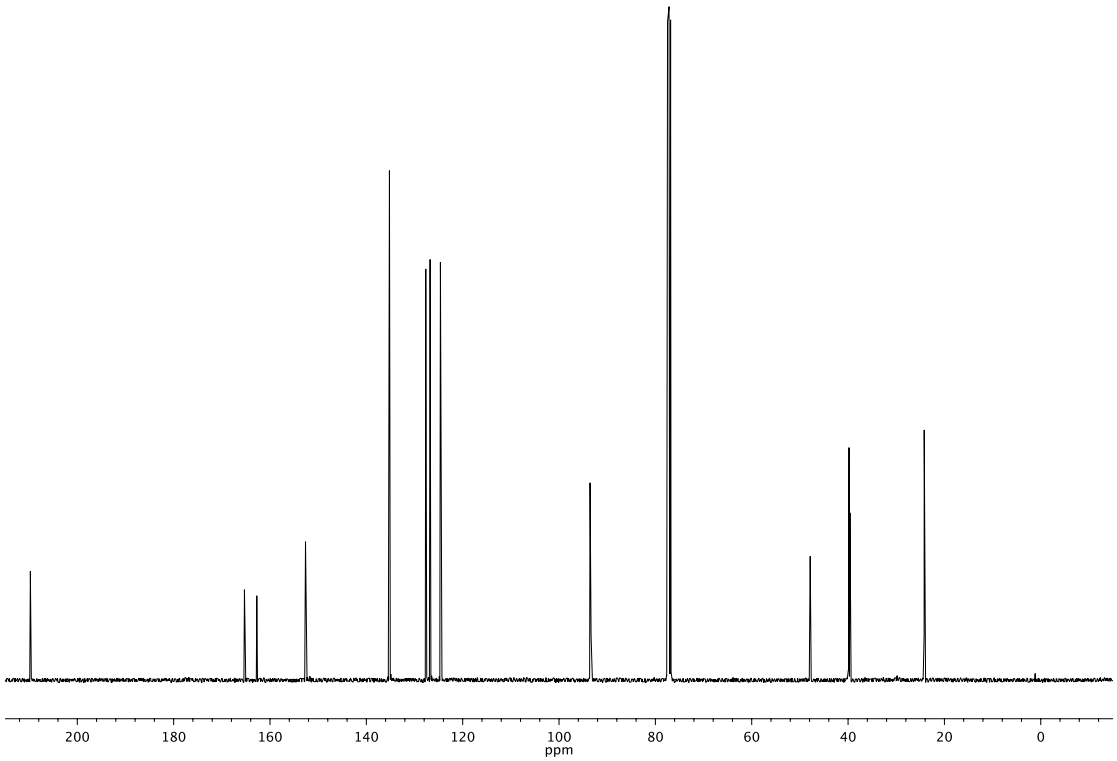

Figure A1.113. ^{13}C NMR (101 MHz, $CDCl_3$) of compound **5j**.

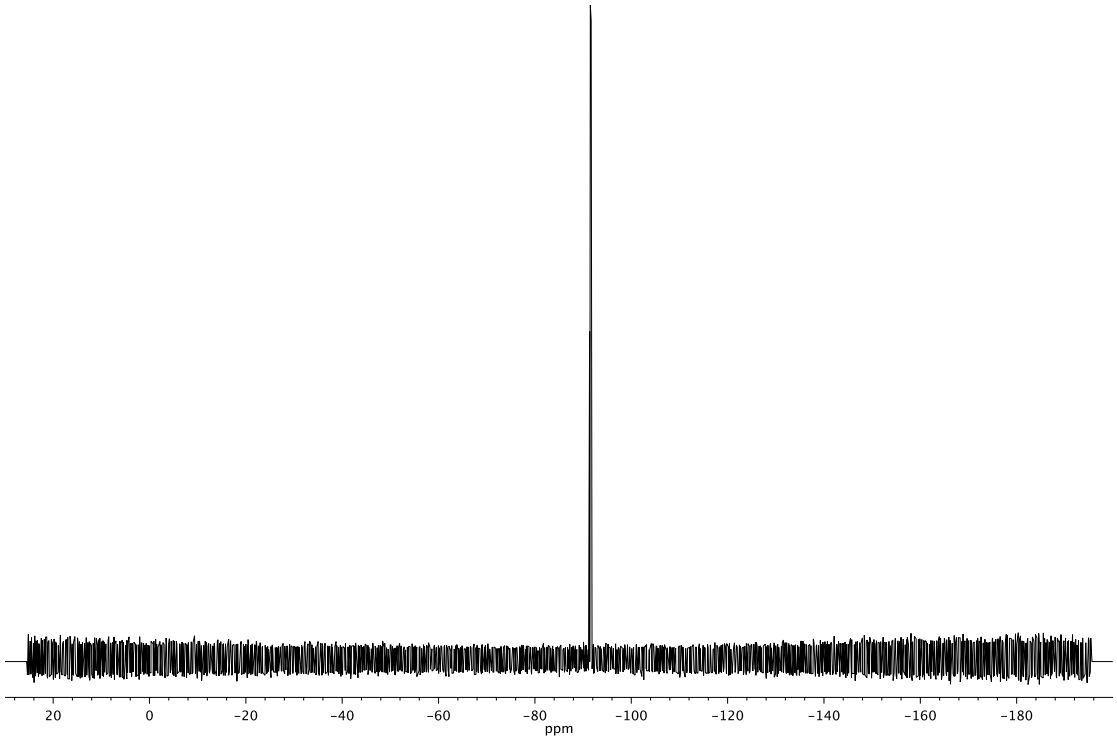

Figure A1.114. ^{19}F NMR (282 MHz, $CDCl_3$) of compound **5j**.

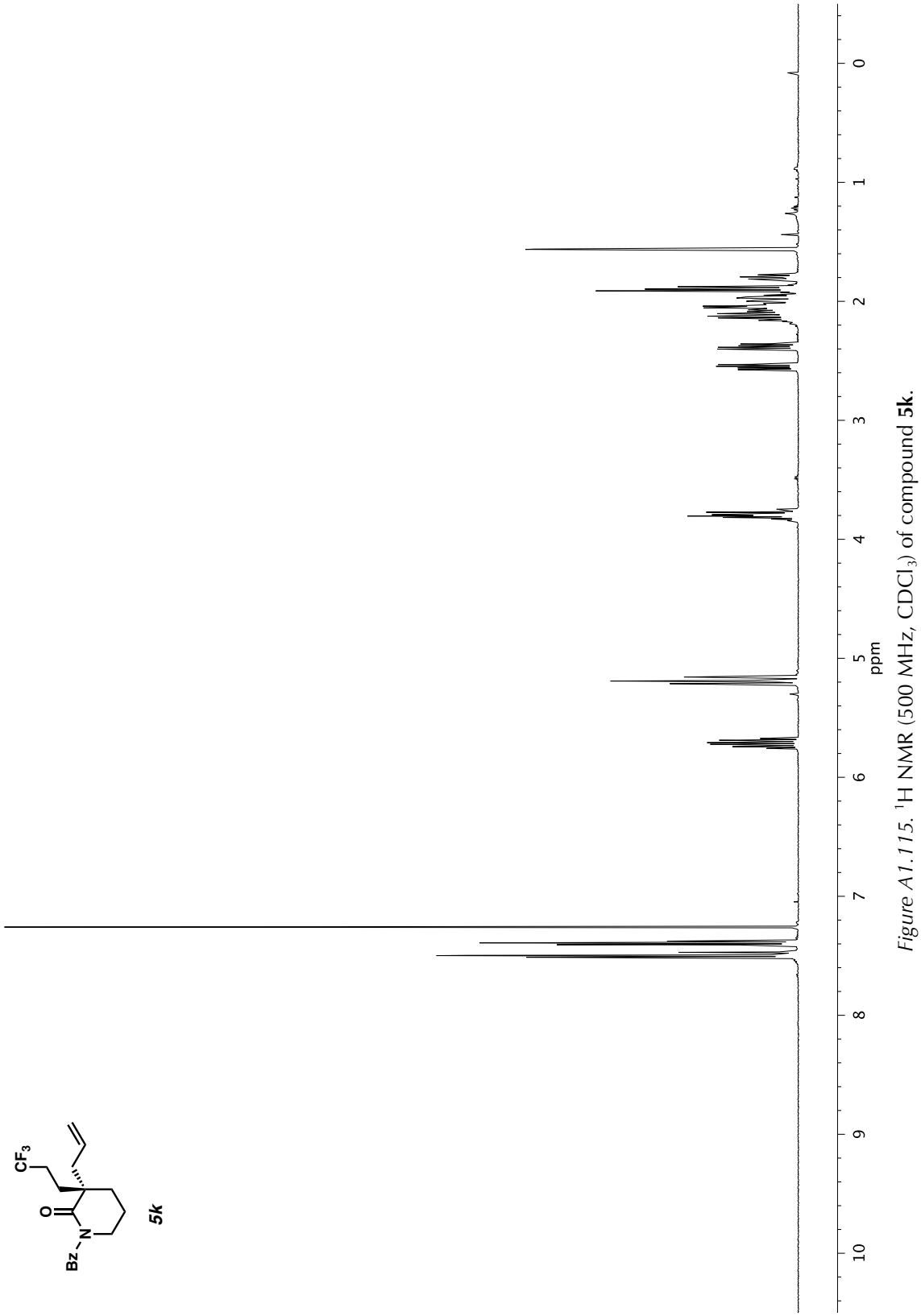

Figure A1.115. ^{1}H NMR (500 MHz, $CDCl_3$) of compound **5k**.

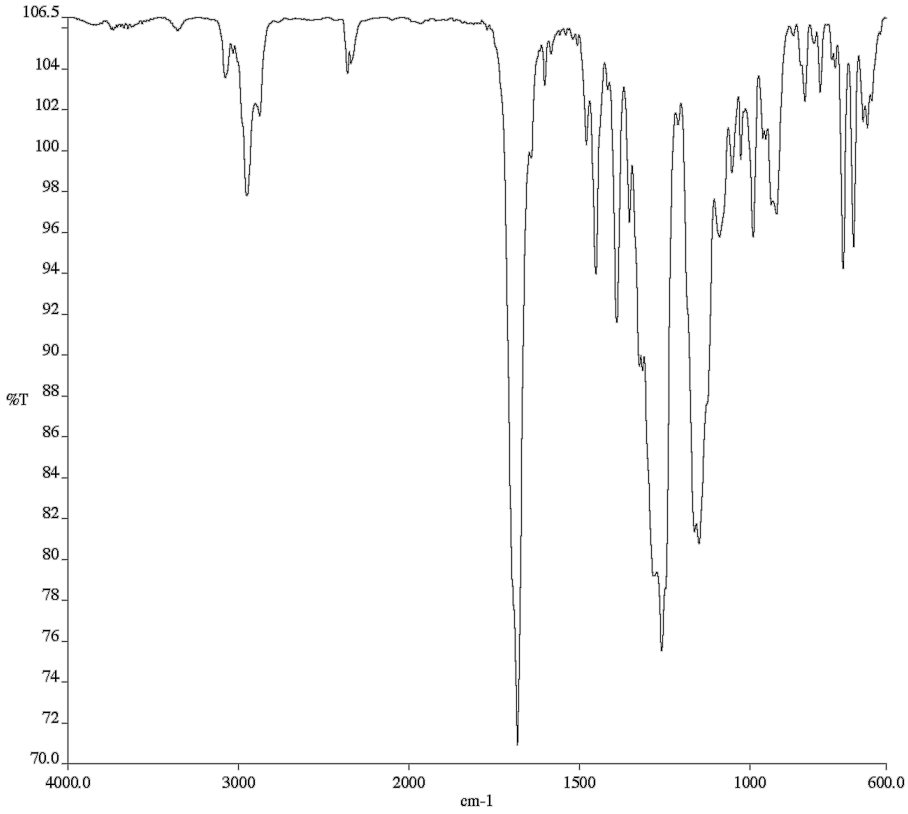

Figure A1.116. Infrared spectrum (Thin Film, NaCl) of compound **5k**.

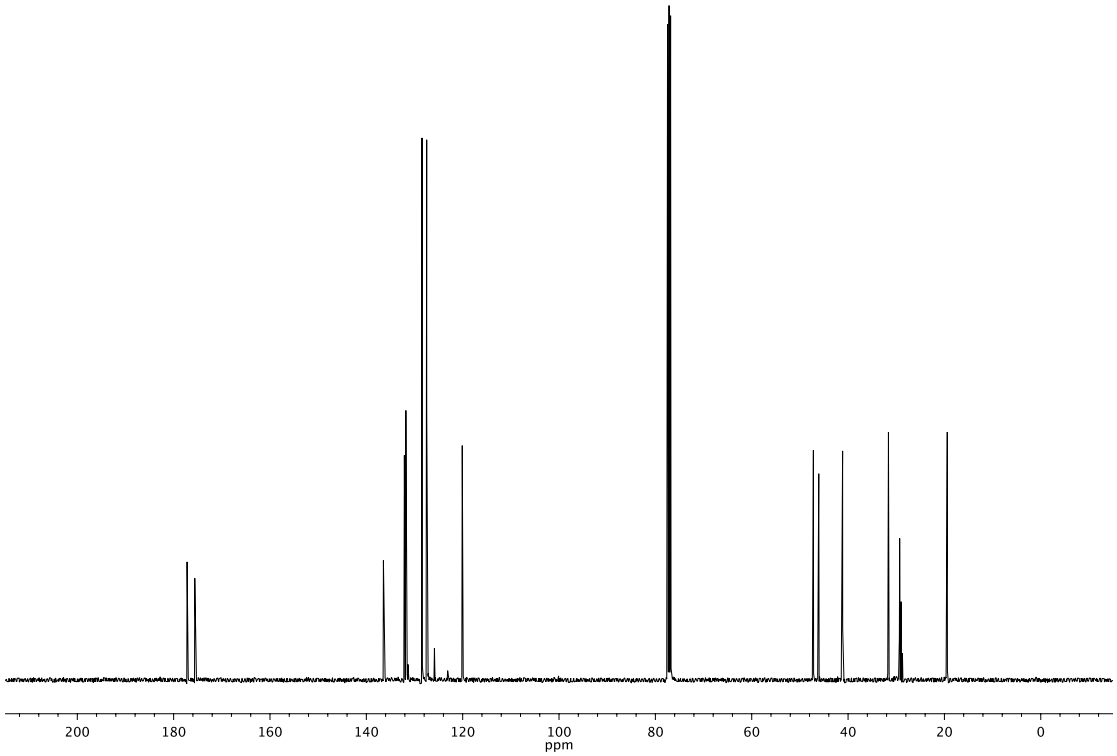

Figure A1.117. ^{13}C NMR (101 MHz, $CDCl_3$) of compound **5k**.

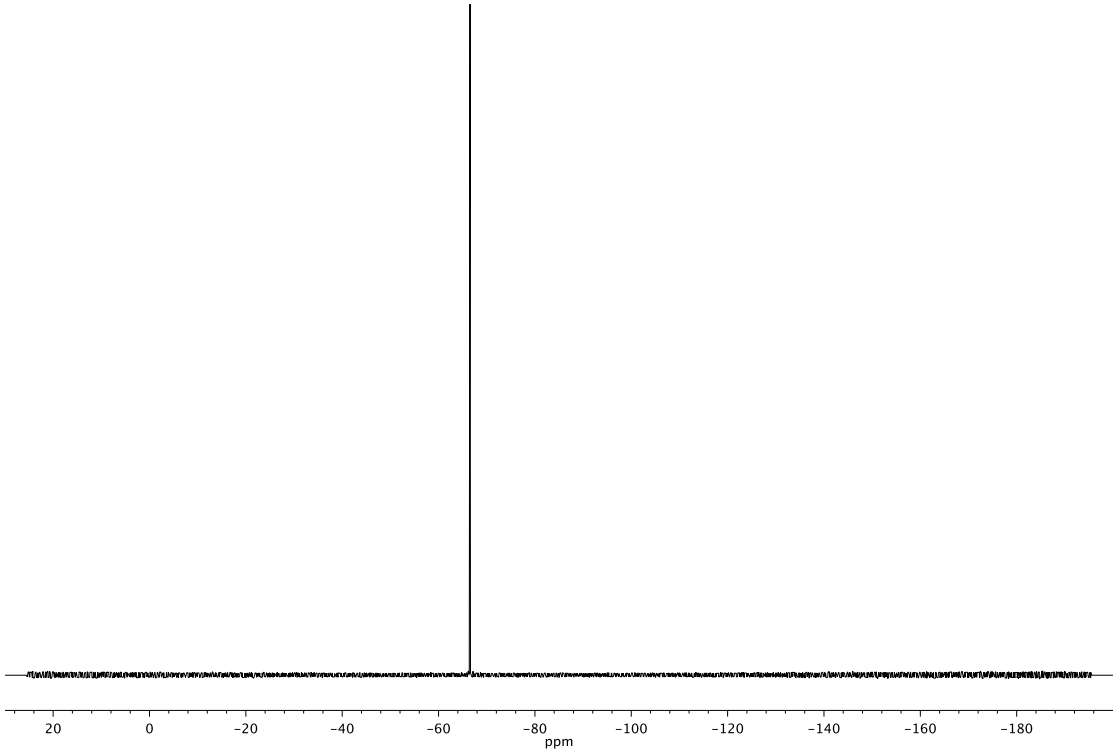

Figure A1.118. ^{19}F NMR (282 MHz, $CDCl_3$) of compound **5k**.

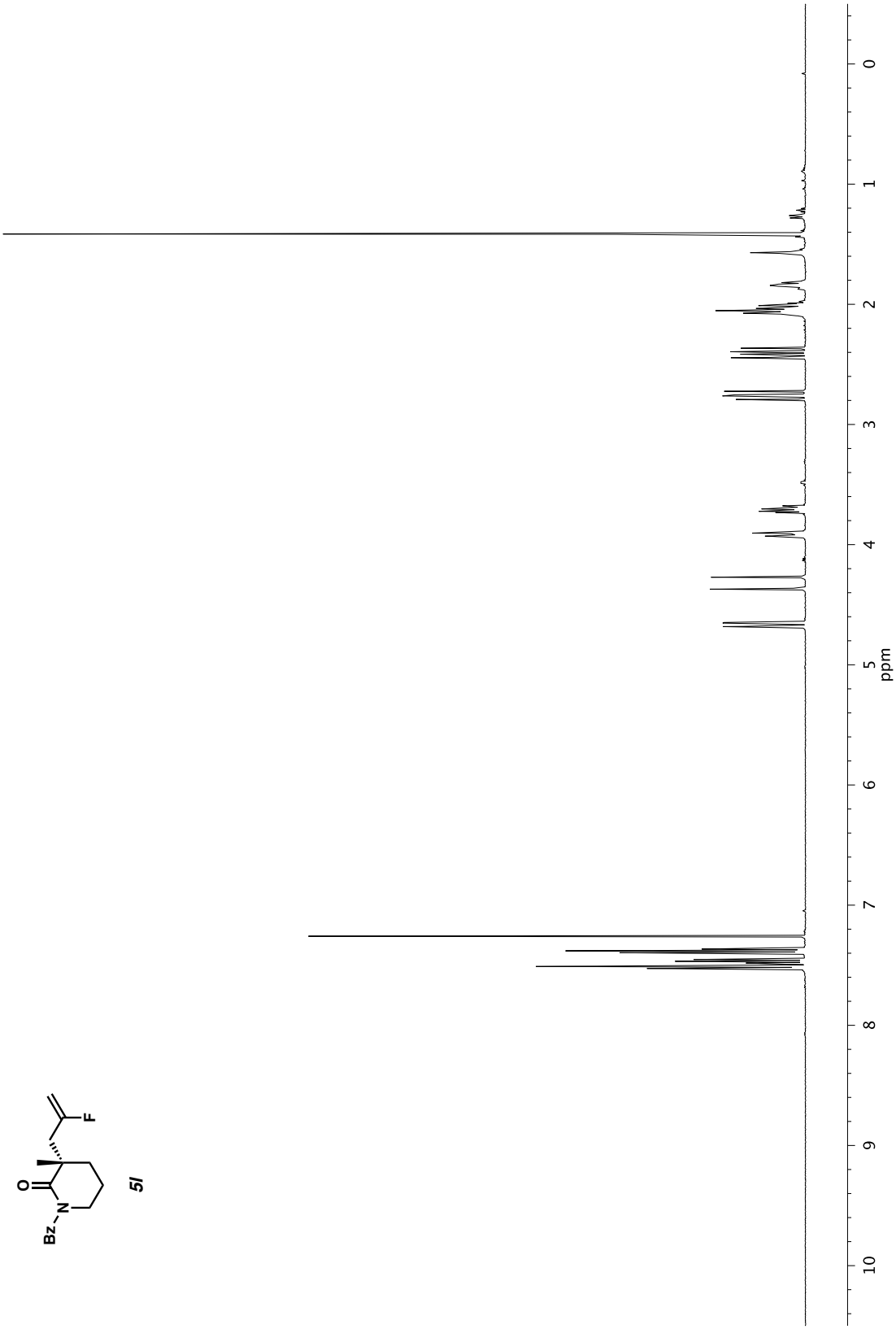

Figure A1.119. ^{1}H NMR (500 MHz, $CDCl_3$) of compound **5l**.

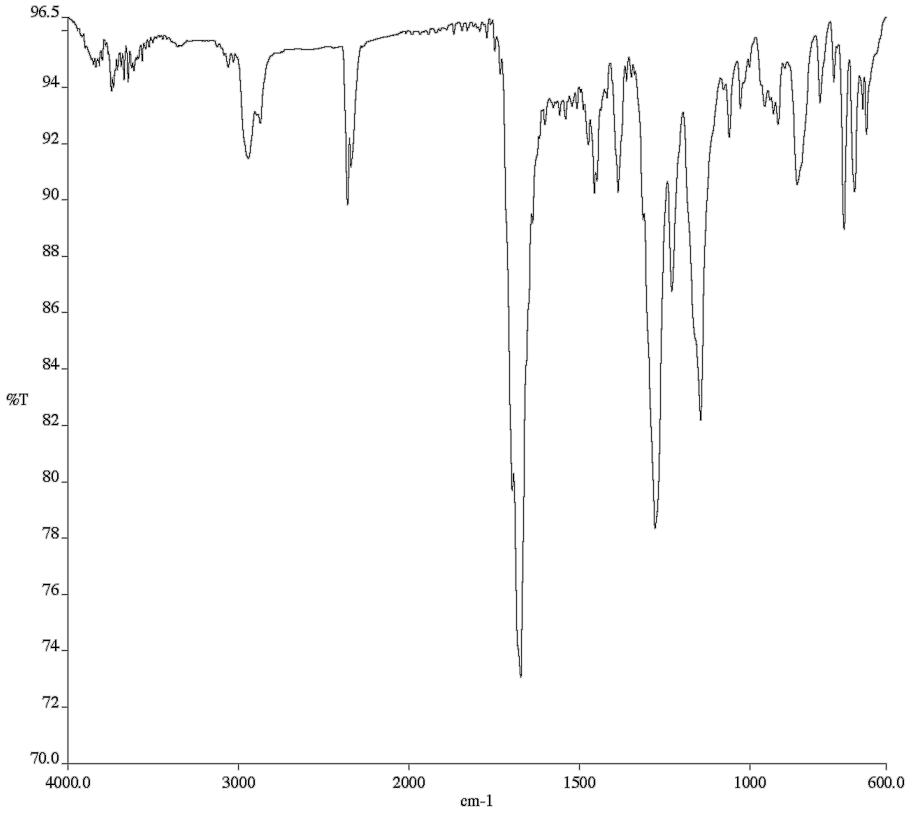

Figure A1.120. Infrared spectrum (Thin Film, NaCl) of compound **5l**.

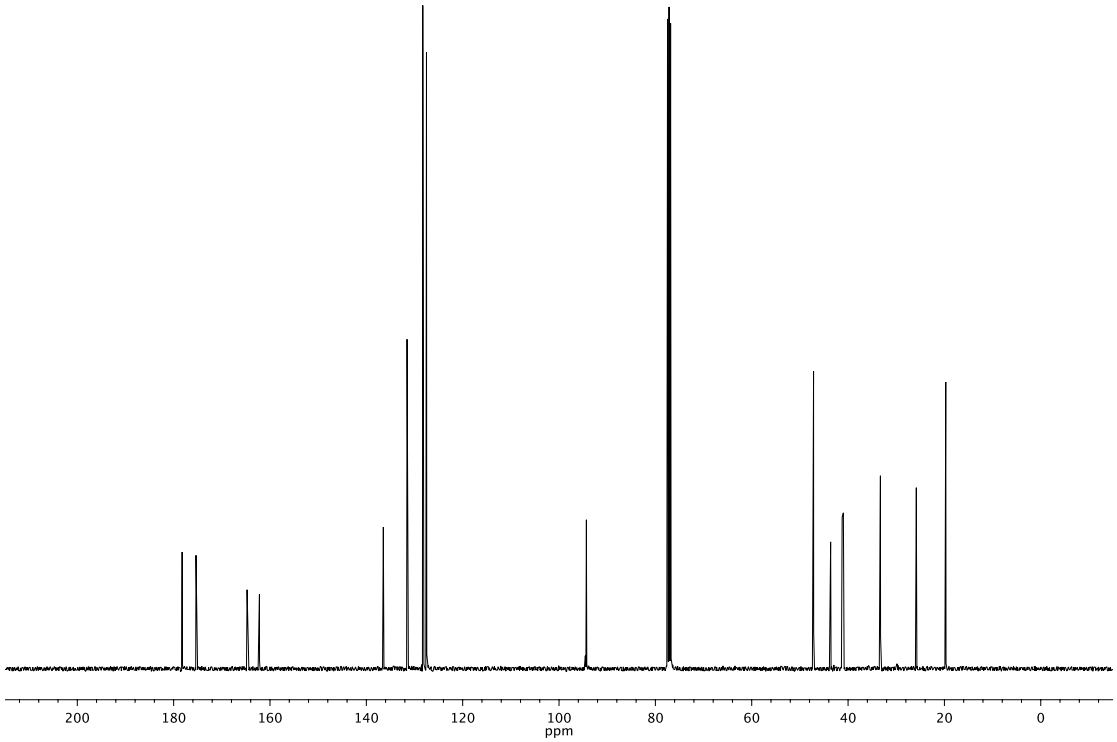

Figure A1.121. ^{13}C NMR (101 MHz, $CDCl_3$) of compound **5l**.

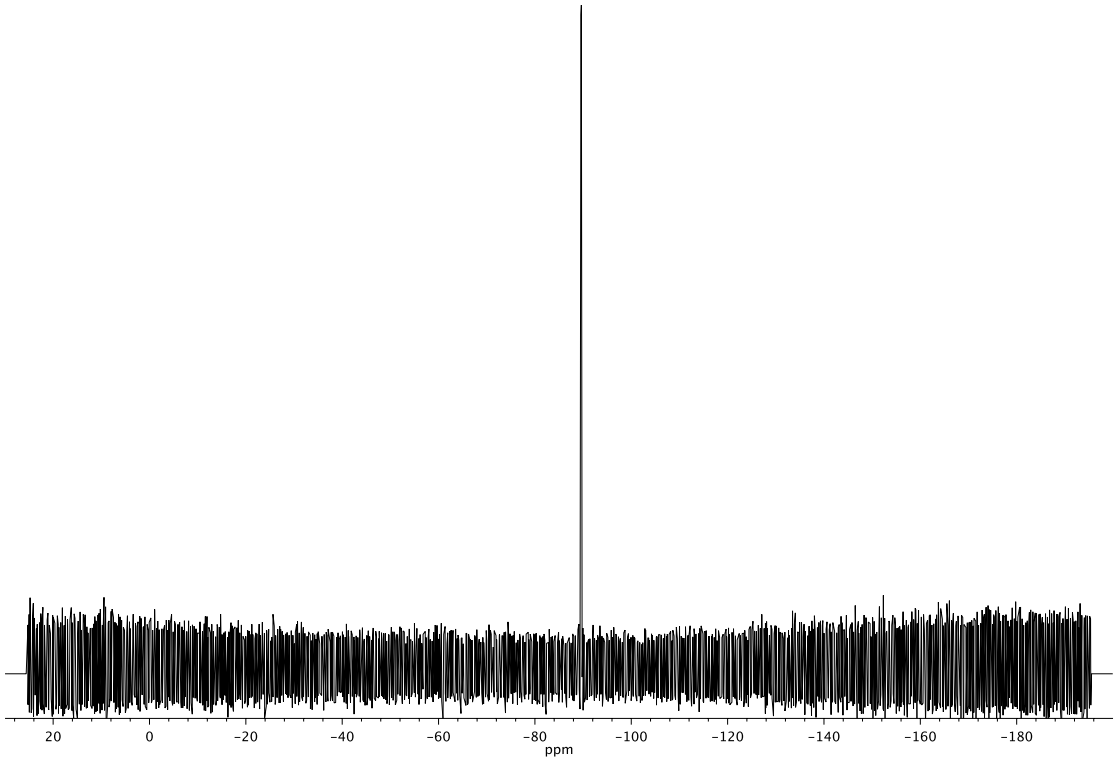

Figure A1.122. ^{19}F NMR (282 MHz, $CDCl_3$) of compound **5l**.

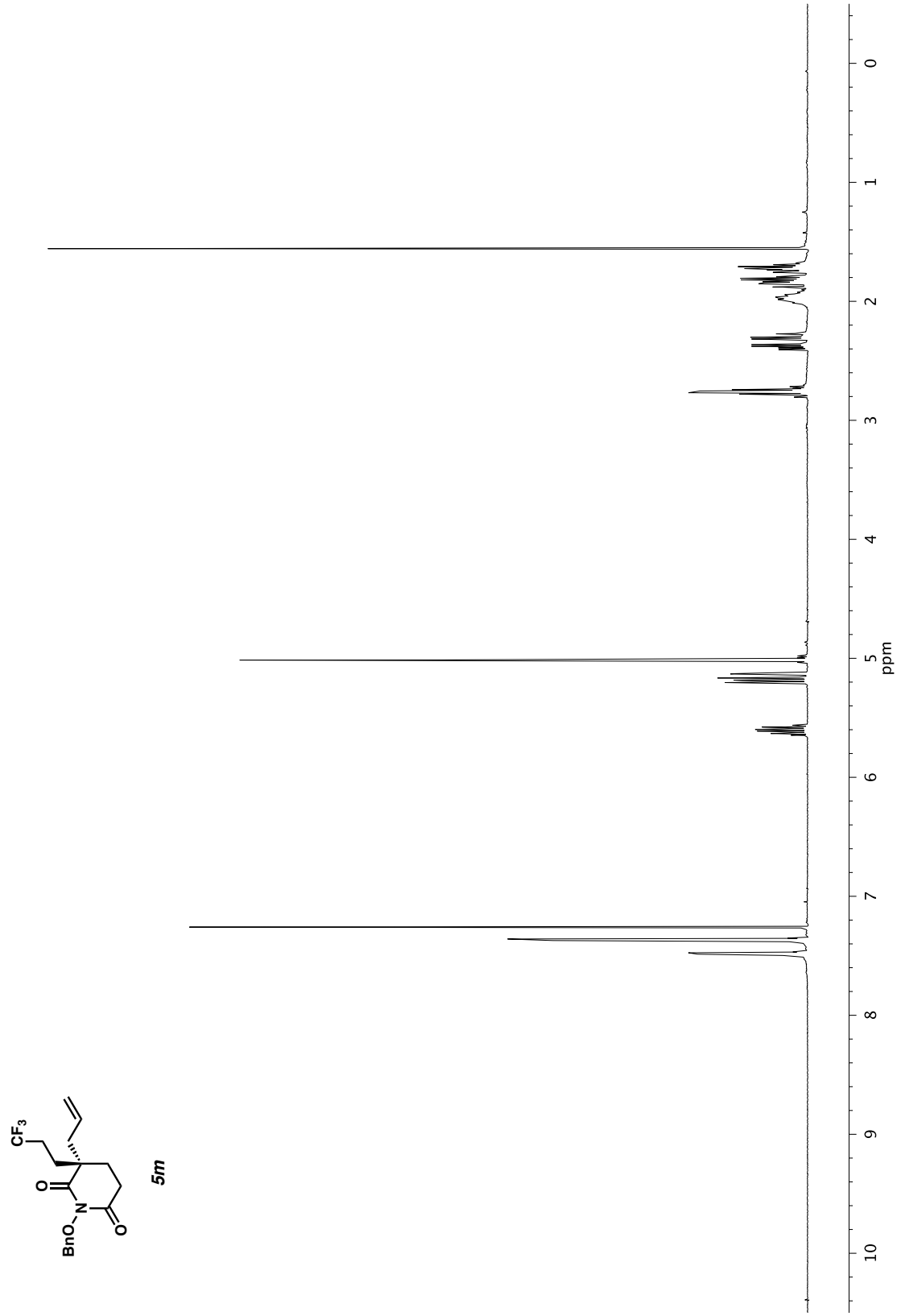

Figure A1.123. ^{1}H NMR (500 MHz, $CDCl_3$) of compound **5m**.

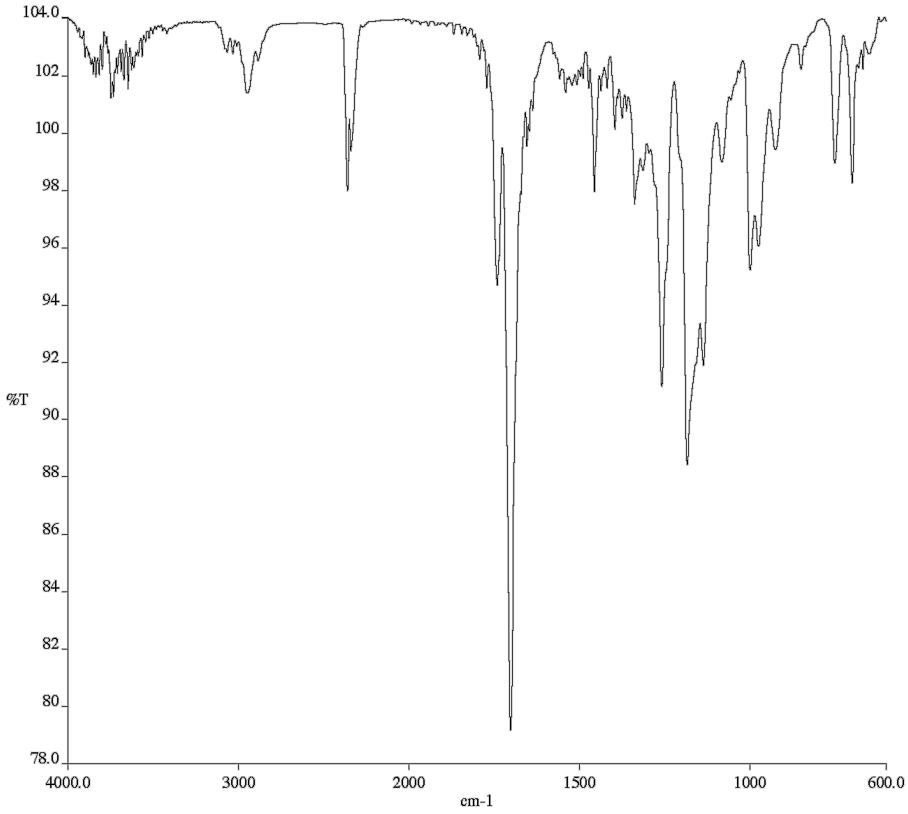

Figure A1.124. Infrared spectrum (Thin Film, NaCl) of compound **5m**.

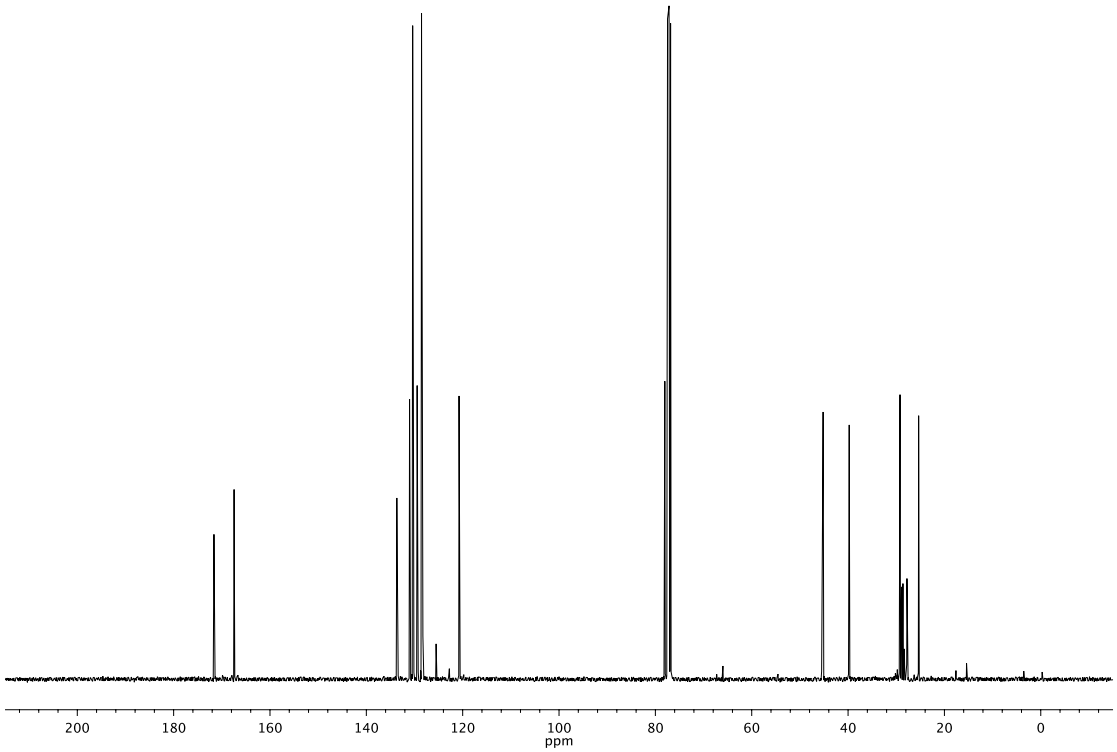

Figure A1.125. ^{13}C NMR (101 MHz, $CDCl_3$) of compound **5m**.

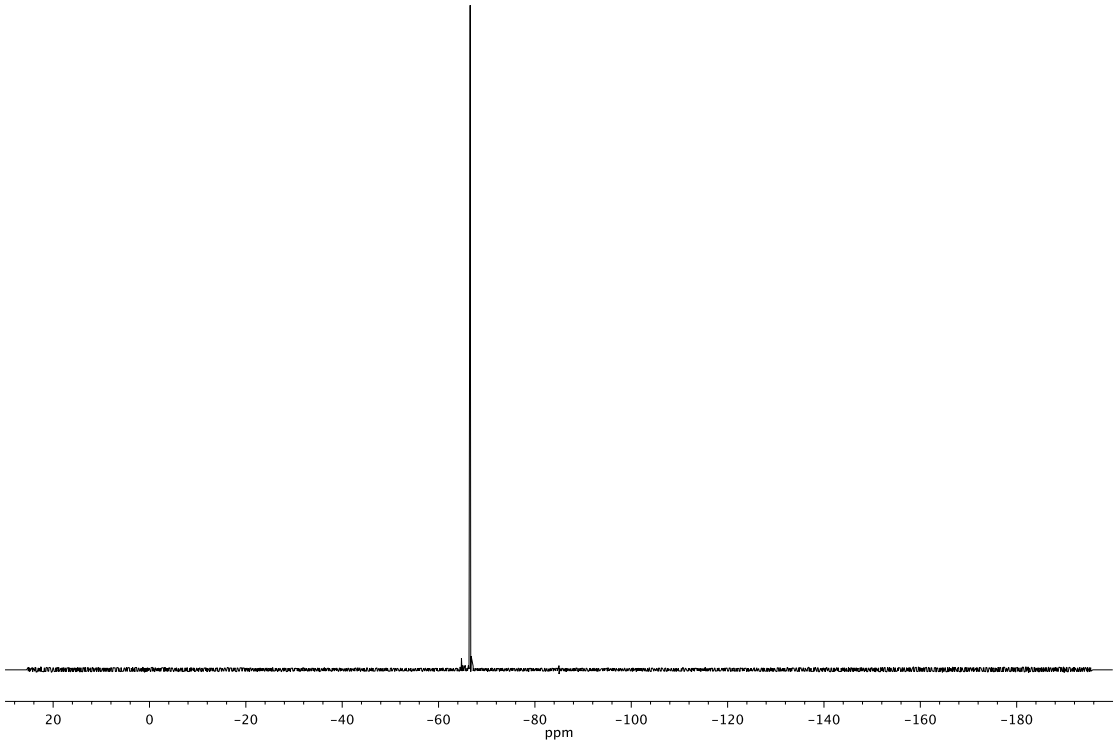

Figure A1.126. ^{19}F NMR (282 MHz, $CDCl_3$) of compound **5m**.

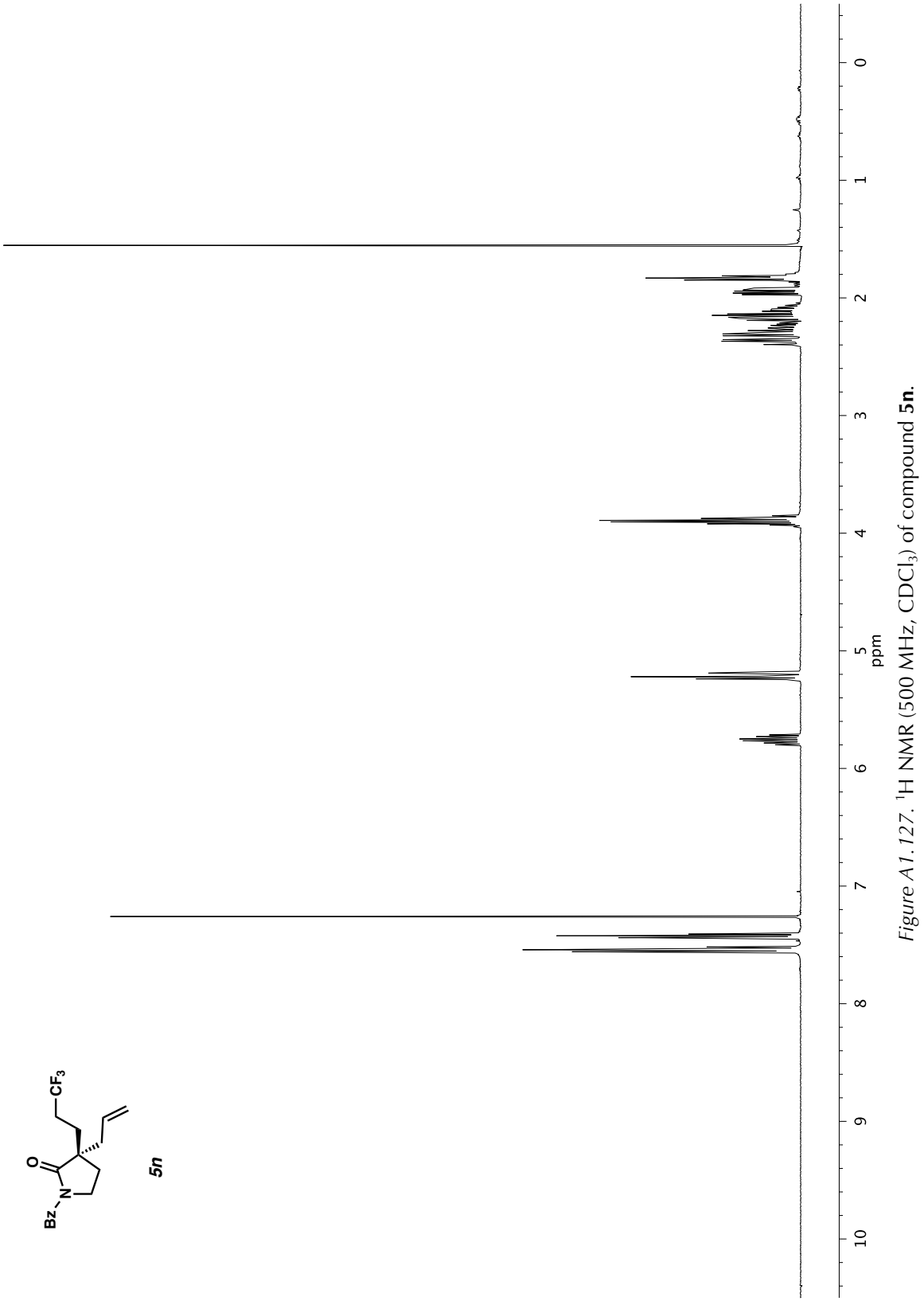

Figure A1.127. ^{1}H NMR (500 MHz, $CDCl_3$) of compound **5n**.

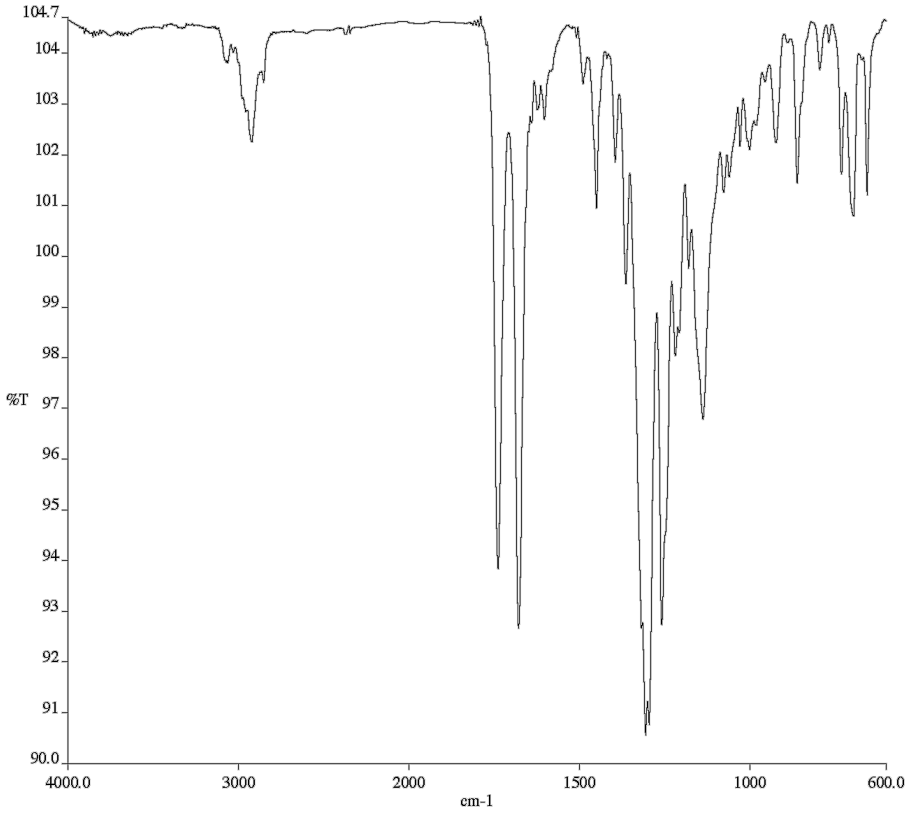

Figure A1.128. Infrared spectrum (Thin Film, NaCl) of compound **5n**.

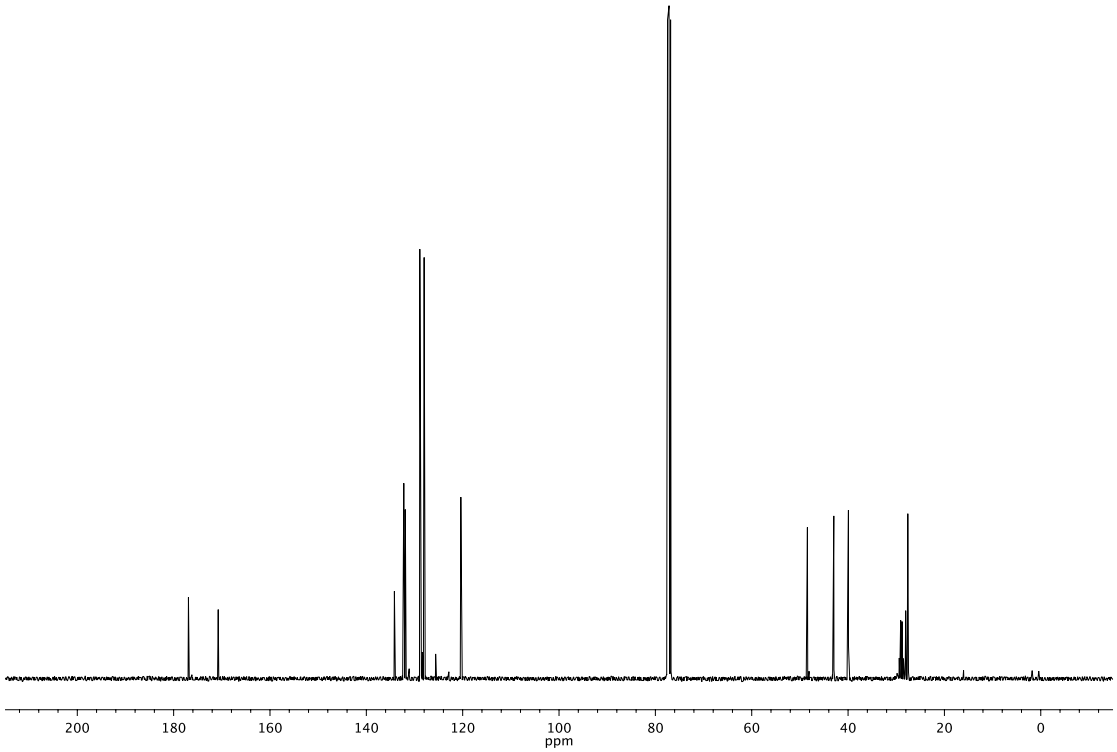

Figure A1.129. ^{13}C NMR (101 MHz, $CDCl_3$) of compound **5n**.

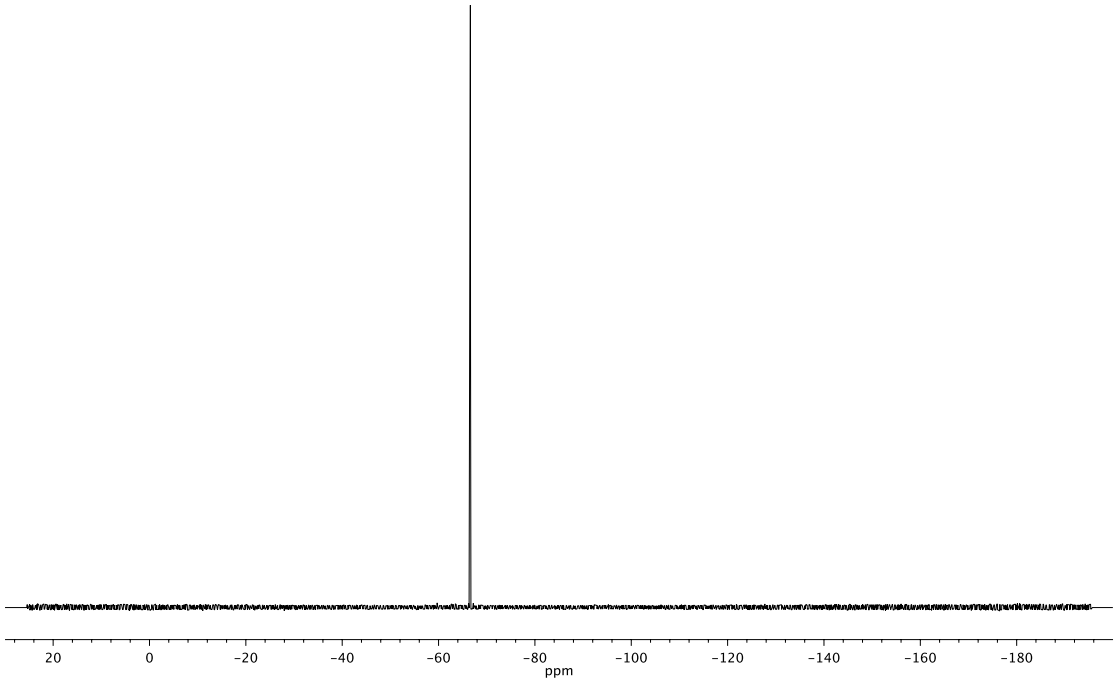

Figure A1.130. ^{19}F NMR (282 MHz, $CDCl_3$) of compound **5n**.

CHAPTER 2

Synthesis of enantioenriched 2,2-disubstituted pyrrolidines via sequential asymmetric allylic alkylation and ring contraction[*]

2.1 INTRODUCTION

More than half of current FDA approved drug molecules contain at least one nitrogen containing heterocycle, with the most common motifs (in order) being piperidine, pyridine, piperazine, cephem and pyrrolidine.[1] Additionally, it has been demonstrated that three-dimensionality, particularly in the form of stereogenic centers, is of great interest to the medicinal chemistry community.[2] For these reasons, unsaturated nitrogen heterocycles containing tetrasubstituted chiral centers have proven desirable. Looking more closely at the pyrrolidine containing drug molecules, it is quickly apparent that none contain tetrasubstituted centers (e.g. Figure 2.1.1, **20**–**24**), and many are derived from the amino acid proline **20**, such as **21**, **22**, and **23**.[1] We envisioned an opportunity to

[*] This research was performed in collaboration with Hirokazu Takada, Yuji Sumii and Katsuaki Baba, all alumni of the Stoltz group.

bring novelty to this motif in pharmaceutical compounds by developing a divergent approach to related molecules containing tetrasubstituted stereocenters.

Figure 2.1.1 Pharmaceutical compounds containing chiral pyrrolidines

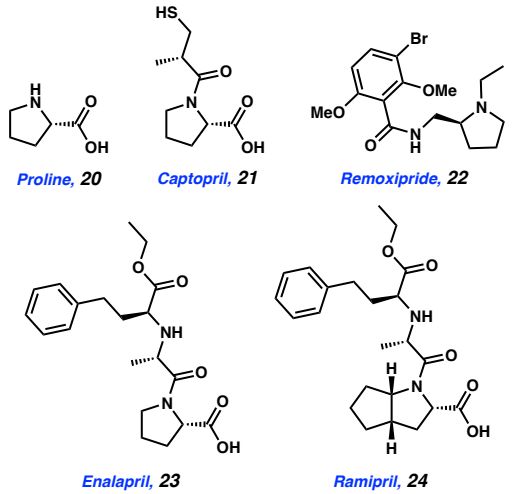

Much progress has been made in the synthesis of proline derivatives as demonstrated by the prevalence of that motif in pharmaceutical compounds. In fact, the synthesis of chiral proline derivatives was described in a review by Cativiela,[3] of which an example is highlighted in Scheme 2.1.1 from the pioneering work of Seebach et al.[4] Starting from proline **20**, condensation affords oxazolidinone **25**, which can undergo enolate formation followed by alkylation resulting in **26**. Hydrolysis of the resulting oxazolidinone then affords the proline derivative **27** in good yield and high ee. While this method is successful for the synthesis of a number of interesting molecules, it is limited to the synthesis of proline derivatives. Additionally, deprotection of the oxazolidinone can require harsh conditions, which may not be amenable to all substrates. We believed that a catalytic, enantioselective method toward the synthesis of 2,2-disubstituted chiral

pyrrolidines would allow for the synthesis of previously unknown compounds that would be of interest to the medicinal chemistry and natural products communities.

Scheme 2.1.1 Synthesis of tetrasubstituted proline derivatives by Seebach et al.[4]

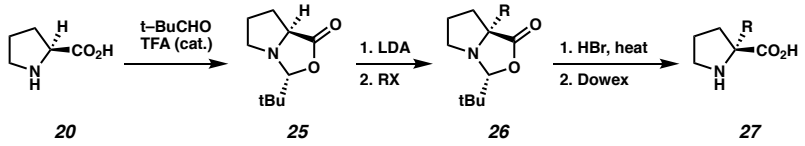

Our overall strategy toward the synthesis of chiral 2,2-disubstituted pyrrolidines is summarized in Scheme 2.1.2. The imides **28** can be synthesized in a known procedure from glutaric anhydride, followed by a decarboxylative asymmetric allylic alkylation as described previously to afford **29**. These imides can then undergo a series of functional group manipulations to afford hydroxamic acids **30**, which we propose would undergo a stereospecifc ring contraction to afford chiral 2,2-disubstituted pyrrolidines **31**. The final ring contraction, pioneered by Spino,[5] has previously not been investigated with respect to stereochemical fidelity, although we hypothesized that it would be stereospecific.

Scheme 2.1.2 Proposed synthesis of chiral 2,2-disubstituted pyrrolidines

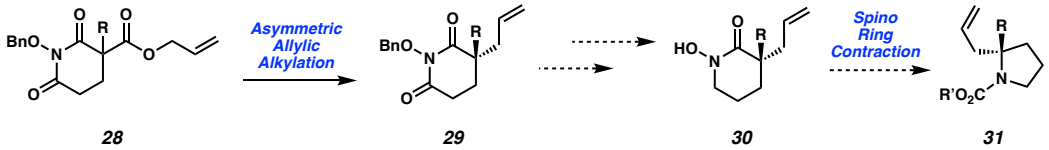

2.2 SYNTHESIS OF CHIRAL BENZYLOXYIMIDES

Our lab has a long-standing interest in allylic alkylation reactions for the synthesis of quaternary centers, having reported the first asymmetric variant of the classic Tsuji

reaction in 2004 using cyclic enol carbonates or enol silanes to afford α-quaternary ketone products under palladium catalysis utilizing chiral phosphinooxazaline (PHOX) ligand **6** (Scheme 2.2.1A–B)[6]. A year later, we demonstrated the decarboxylative asymmetric allylic alkylation reaction of cyclic β-keto esters, affording the same α-quaternary ketone products (Scheme 2.2.1C).[7] Since those initial reports, we have significantly expanded the scope of this reaction to include various ring sizes and heterocycles, particularly following our development of an electron deficient PHOX ligand (**7**).[8] Of particular note is the advancement in the realm of nitrogen heterocyles, including both lactams and imides, in the decarboxylative allylic alkylation reaction.[9] We were pleased to note that a variety of β-amidoesters were tolerated in this reaction with only small changes to the reaction conditions (Scheme 2.2.1D). We believed that we could use some of these products as intermediates for the synthesis of chiral 2,2-disubstituted pyrrolidines in a catalytic asymmetric manner.

Scheme 2.2.1 Progression of the asymmetric allylic alkylation reaction in the Stoltz laboratory

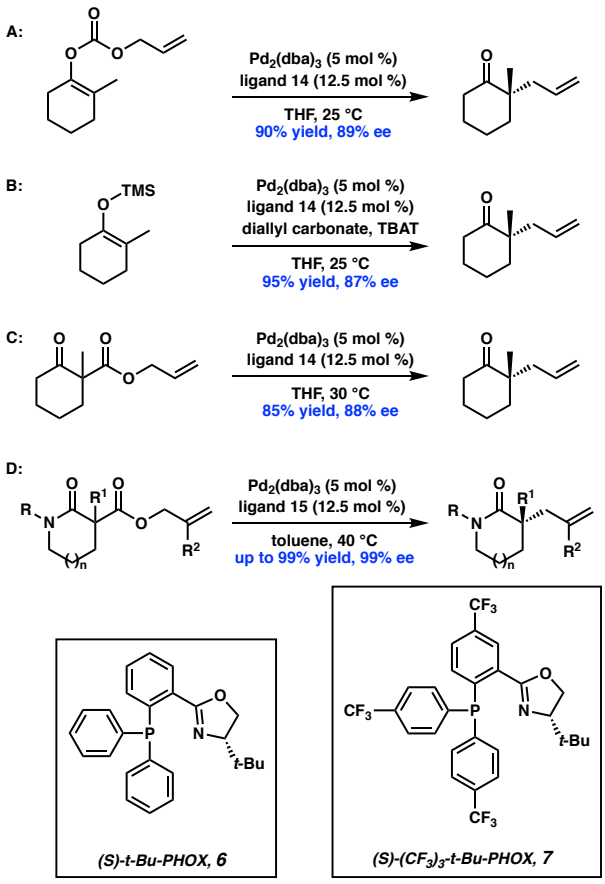

The substrates for this reaction, as mentioned above, can be synthesized from glutaric anhydride **32** in a previously reported four-step procedure, involving condensation of *O*-benzylhydroxylamine with glutaric anhydride followed by enolate α–acylation and alkylation events (Scheme 2.2.2A).[10] During the course of our investigations, we discovered a number of small changes to this procedure that improved material throughput (Scheme 2.2.2B). First, we determined that *O*-benzyloxyimide **33** could be isolated by recrystallization, affording the product in an improved yield over column chromatography. Second, we noted that use of allylchloroformate in the acylation

reaction instead of allylcyanoformate afforded a better yield of the desired α–carboxy lactams **28**. In addition to the higher material throughput, use of commercially available allylchloroformate is preferable to the use of allylcyanoformate. The latter must be prepared from allylchloroformate and involves the use of cyanide, which necessitates more complicated workup and waste disposal procedures. We were able to use conditions optimized for the synthesis of **28a** to access a number of β-amidoesters for the asymmetric allylic alkylation reaction, as shown in Scheme 2.2.2C.

Scheme 2.2.2 Synthesis of β-amidoesters

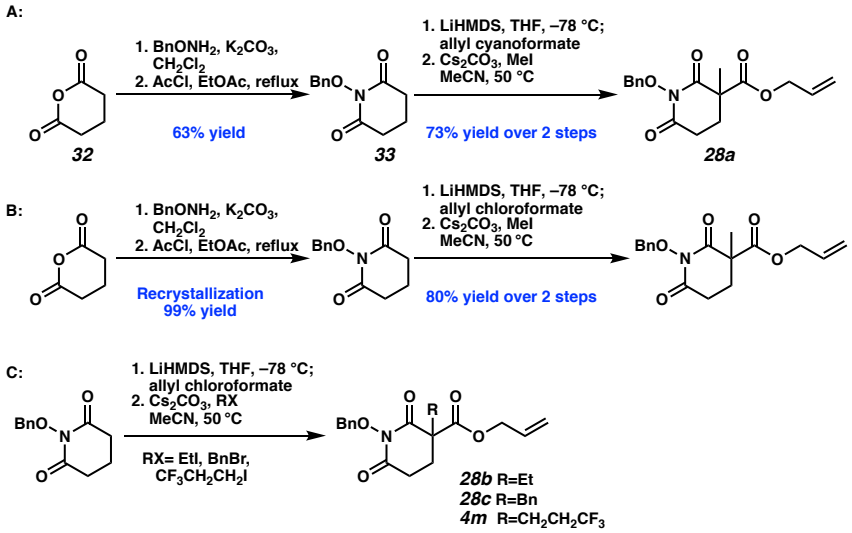

With a reliable synthesis of substrates in hand, we turned our attention to the asymmetric allylic alkylation reaction. While we had previously reported similar chemistry on this class of substrates,[9] we aimed to improve a couple of aspects, particularly with regard to larger scale reactions. Specifically, we pursued a lower catalyst loading and an increased concentration of the reaction. We first started by reproducing the previously reported results to afford **29a** (Entry 1, Table 2.2.1). We were

very pleased to note that reducing the catalyst loading in half did not adversely effect the enantioselectivity of the reaction (Entry 2). We previously reported conditions with low catalyst loadings that utilize $Pd(OAc)_2$, instead of $Pd_2(dba)_3$ or $Pd_2(pmdba)_3$, and TBME (*tert*-butyl methyl ether) instead of toluene. So, we continued our investigations with these two changes (Entry 3),[11] and were pleased to note that the yield and selectivity remained the same. Increasing the concentration to 0.1 M resulted in a slightly accelerated reaction with similar selectivity and yield (Entry 4), but increasing the concentration further resulted in lower yields and selectivities (Entry 5–6). Lowering the catalyst loading even further (Entry 7-9) resulted in similar selectivity and reactivity, although extended reaction times and elevated temperatures were required. Thus, we decided that the best overall combination of reactivity and catalyst loading is achieved in Entry 7.

Table 2.2.1 Asymmetric allylic alkylation optimization

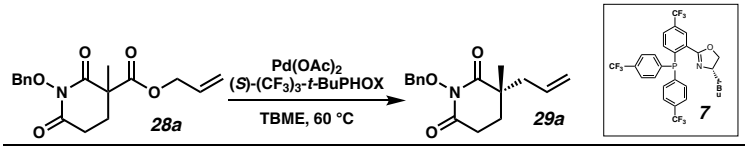

Entry	mol % Pd	mol % ligand	concentration	time	ee	yield
1[a]	5.0	12.5	0.033 M	72 h	93%	78%
2[b]	2.0	6.0	0.033 M	19 h	93%	nr
3	2.0	6.0	0.033 M	60 h	94%	80%
4	2.0	6.0	0.1 M	48 h	90%	83%
5	2.0	6.0	0.25 M	36 h	88%	74%
6	2.0	6.0	0.5 M	36 h	75%	74%
7[c]	1.0	3.0	0.1 M	66 h	92%	97%
8[c]	0.5	1.5	0.1 M	90 h	91%	90%
9[c,d]	0.1	1.0	0.1M	9 days	91%	58%

(a) $Pd_2(pmdba)_3$, toluene, 50 °C, (b) $Pd_2(pmdba)_3$ (c) 60 °C, 51 hr then 70 °C (d) Based on recovered starting material: 84%

With these optimized conditions in hand, we turned our attention to investigating the reactivity of the other substrates, one of which had never been investigated in an asymmetric allylic alkylation reaction. We were pleased again to observe good reactivity and selectivity for the parent substrate **29a** on a larger scale, up to 11 g of substrate (Table 2.2.2). Additionally, compound **29b** also performed well under these conditions. Unfortunately, the enantioselectivity was diminished when slightly more complex substrates (**29c**, **5m**) were investigated, though the reactivity remained good. While this was somewhat disappointing, we were able to demonstrate that both of those substrates could be synthesized in good enantiomeric excess when the previously reported conditions for **5m** were applied to both substrates (Entry B).[12] With all four of our desired compounds in hand, we turned our attention to advancing the compounds toward chiral pyrrolidines.

Table 2.2.2 Scope of the asymmetric allylic alkylation reaction

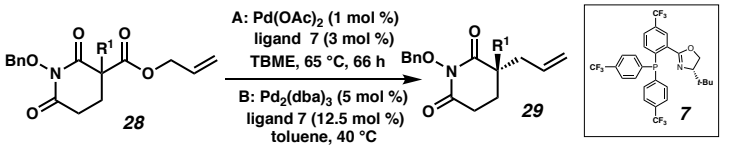

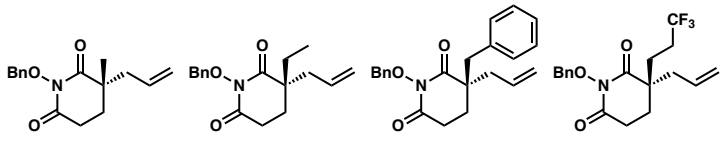

	29a	29b	29c	5m
A:	88% yield 92% ee	88% yield 94% ee	86% yield 78% ee	87% yield 71% ee
B:	99% yield 96% ee[a]	80% yield 98% ee[a]	89% yield 86% ee	80% yield 84% ee

a) previously reported in Reference 10.

2.3 REDUCTION OF BENZYLOXY IMIDE TO HYDROXAMIC ACID

In order to test the ring contraction reaction, a number of functional group manipulations were required. We were pleased to discover that a three-step sequence of reactions afforded the desired hydroxamic acids **30a–d** (Scheme 2.3.1). First, a selective carbonyl reduction proceeded with good yield in the presence of DIBAL-H to afford alcohols **34a–d** as a mixture of diastereomers. A subsequent dehydroxylation afforded lactams **35a–d** in nearly quantitative yield upon treatment with a mixture of triethylsilane and trifluoroacetic acid (TFA). Finally, the protected hydroxamic acids underwent debenzylation with boron trichloride to afford the free hydroxamic acids **30a–d**. This sequence of reactions was highly scalable and has been performed on up to 6 g scale on substrate **29a** (R=Me).

Scheme 2.3.1 Synthesis of chiral hydroxamic acids

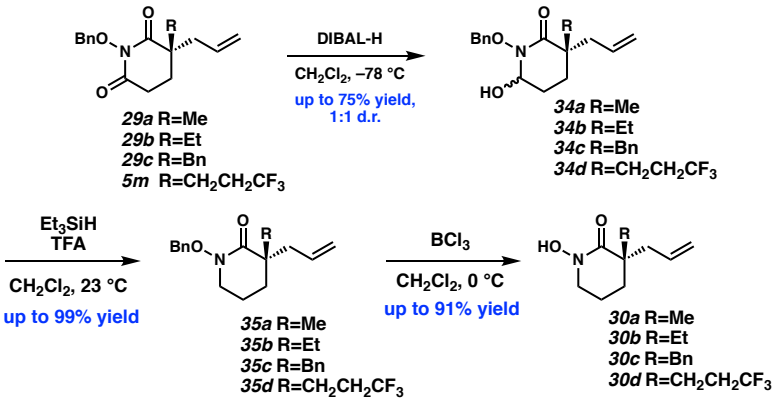

2.4 THERMAL RING CONTRACTION OF HYDROXAMIC ACID

Spino and coworkers have previously reported the ring contraction of lactams to pyrrolidines in either a photochemical process from *N*–chloro[5a] (Scheme 2.4.1a) or *N*–

mesyloxy[5b] (Scheme 2.4.1b) lactams, or a thermal process from hydroxamic acids through a *N*–trifloxy lactam[5c] (Figure 2.4.1c). These reactions are proposed to occur via an isocyanate-like intermediate in a manner similar to that proposed for the Hofmann rearrangement (Scheme 2.4.1d).[5] As the Hofmann rearrangement is known to proceed in a stereospecific fashion, we envisioned that the Spino reaction would also display the same specificity, and we were poised to address this fundamental question. With our enatioenriched lactams **30a–d** in hand and Spino's effort on the ring contraction of lactams in mind, we proceeded to investigate the stereospecificity of that ring contraction for the synthesis of asymmetric 2,2-disubstituted pyrrolidines.

Scheme 2.4.1 Ring contraction reactions as reported by Spino et al.[5]

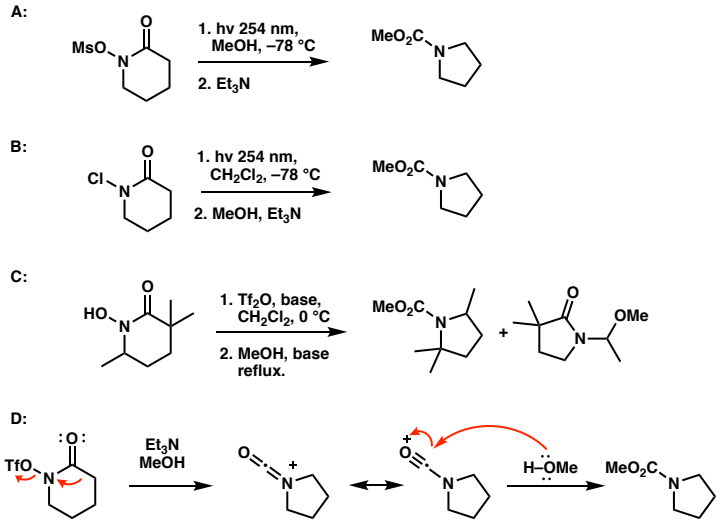

With a number of substrates in hand, we first began investigating the thermal ring contraction of parent substrate **30a** (Scheme 2.4.2). We were very pleased to discover that using the conditions developed by Spino and coworkers, we observed an 83% yield of the desired pyrrolidine product **31a** over the two steps. Additionally, we found that column

chromatography of the *N*-trifloxylactam **36a** was unnecessary to obtain good yields, allowing for a more streamlined synthesis.

Scheme 2.4.2 Thermal ring contraction of chiral hydroxamic acid

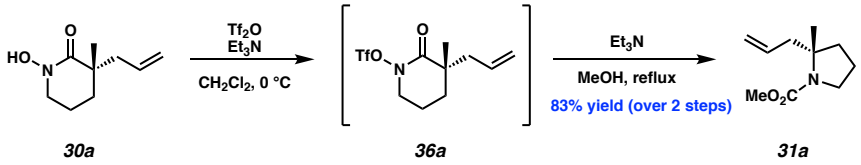

At this stage, owing to our interest in further functionalizing these pyrrolidines, we investigated the removal of the methyl carbamate group to afford free pyrrolidine **37**. In our hands, this proved to be a challenge, as described in Table 2.4.1. A variety of basic conditions (Entries 1-3), acidic conditions (Entries 5-6), and other previously reported conditions (Entries 7-9) mostly displayed low conversion to product, and when significant reactivity was detected, decomposition or undesired byproduct **38** were observed. In fact, only when subjecting the substrate to concentrated KOH in a mixture of water and 1,2-propanediol under microwave irradiation at 200 °C for an hour were we able to finally detect our desired product, which upon exposure to anhydrous HCl could be isolated as an HCl salt.[13]

Table 2.4.1 Removal of methyl carbamate group

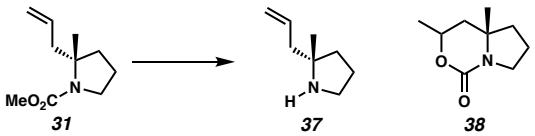

31 ***37*** ***38***

Entry	Conditions	Time	Temperature	Result
1	NaOH, MeOH	26 h	reflux	no reaction
2	KOH, $N_2H_4 \cdot H_2O$, ethylene glycol	18 h	110 °C	low conversion
3	KOH, H_2O, 1,2-propanediol	15 h	reflux	low conversion
4	KOH, H_2O, 1,2-propanediol	1 h	200 °C (μ wave)	***37***: 95%*
5	4N HCl aq.	18 h	reflux	no reaction
6	6N HCl-dioxane	2.5 h	reflux	***38***: 87%
7	NaI, TMSCl, CH_3CN	18 h	23 °C to reflux	low conversion
8	*n*-BuLi, DIBAL-H, toluene	15 h	23 °C	low conversion
9	LiI, DMF	28 h	80 °C	no reaction

*Desired compound **37** was isolated as an HCl salt.

While we were in fact able to isolate the pyrrolidine **37** as an HCl salt, we believed the harsh conditions required were not ideal for more functionalized substrates, and the necessity of microwave irradiation proved to be a bottleneck when applied to larger scales. With these thoughts in mind, we wondered whether it would be possible to synthesize other carbamates through a similar procedure, such as benzyl or *tert*-butyl (Cbz and Boc, respectively), which have more well known reactivity and are often used as protecting groups. Returning our attention to the proposed mechanism for the reaction, we were reminded that the methyl carbamate arose due to the methanol solvent, and decided to investigate the use of benzyl or *tert*-butyl alcohol as a solvent. We were pleased to discover that using a 3:1 mixture of toluene and the desired alcohol, we could synthesize both the Cbz and Boc protected pyrrolidines (Table 2.4.2, **31b** and **31c**, respectively) in good yield when slightly longer reactions times were applied. Additionally, we were able to use these conditions to access Cbz protected pyrrolidines **31d–f** in good to moderate yield from the corresponding hydroxamic acid precursors.

Table 2.4.2 Synthesis of chiral 2,2-disubstituted pyrrolidines

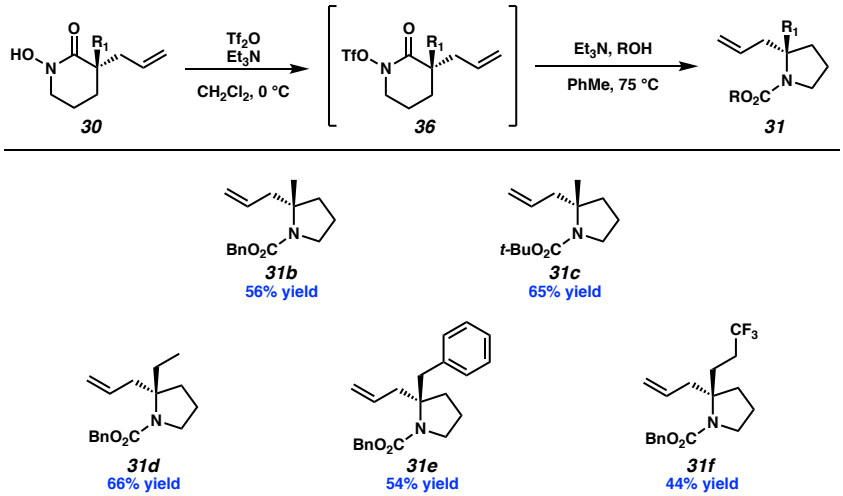

With the synthesis of these compounds completed, we proceeded to investigate our hypothesis that this reaction proceeds with stereoretention. Our development of the synthesis of Cbz protected pyrrolidines proved to expedite this process significantly, as we could use super-critical fluid chromatography (SFC) to determine the enantiomeric excess of pyrrolidine **31b**. We began by synthesizing racemic allylic alkylation product **29a** and advancing it toward pyrrolidine **31b** via the synthetic sequence described in this paper (Scheme 2.4.3A). Upon SFC analysis, we were able to determine that both compounds had 0% ee. We then proceeded to follow the same sequence again, except utilizing enantioenriched allylic alkylation product **29a** (92% ee, Scheme 2.4.3B). We were pleased to observe that pyrrolidine product **31b** derived from enantioenriched **29a** also retained the same enantiomeric excess (92% ee). Therefore, we could conclude that this reaction does indeed proceed with retention of stereochemistry.

Scheme 2.4.3 Investigation of stereochemistry

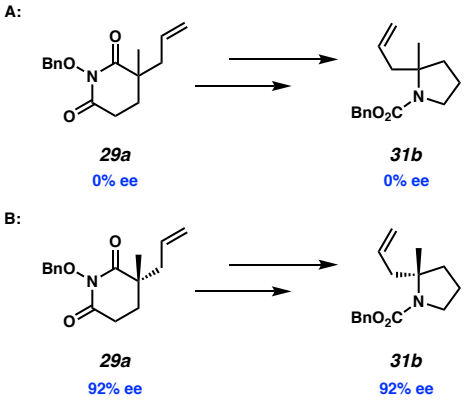

2.5 REACTIONS OF HYDROXAMIC ACID PRODUCTS

With this new method for synthesizing chiral pyrrolidines in hand, we sought to apply our new strategy toward the synthesis of a natural product. We believed that tylohirsuticine **39**, a *seco*-phenanthroindolizidine alkaloid, would serve as a good target for synthesis (Scheme 2.5.1).[14] Retrosynthetically, we believed that a cross-coupling reaction of indolizidine **40** with an arene would result in the natural product. That mono-arylated indolizidine **40** could arise from a ring closing metathesis (RCM) of **41**, which could itself arise from an *N*-alkylation of **37** (which we have previously demonstrated the synthesis of) and known allyl bromide **42**.[15]

Scheme 2.5.1 Retrosynthetic analysis of tylohirsuticine

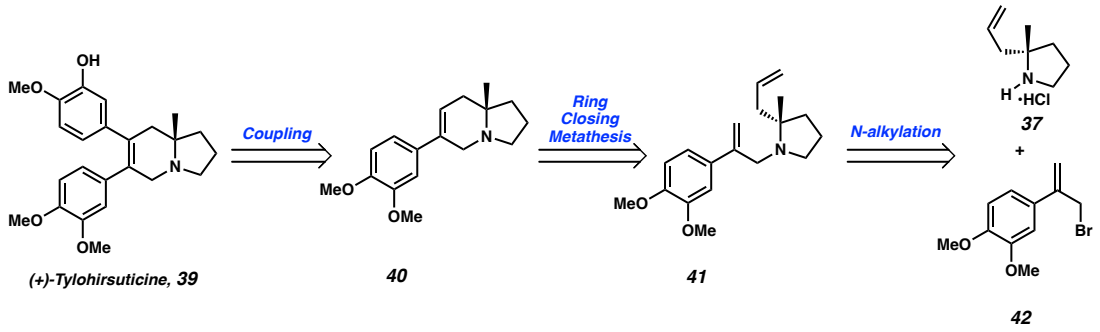

In the forward sense, starting from the HCl salt of pyrrolidine **37** and allyl bromide **42**, *N*-alkylation proceeded smoothly to afford **41** in good yield in the presence of potassium carbonate in refluxing acetonitrile (Scheme 2.5.2). With diallyl **41** in hand, we were pleased to observe promising reactivity under standard RCM conditions using Grubbs II catalyst **44** to afford desired product **40** (Table 5), though incomplete conversion and the presence of undesired isomerization byproduct **43** resulted in the need for some optimization (Entry 1). Switching to the Hoveyda-Grubbs II catalyst **45** provided higher reactivity, but the undesired isomerization product was still observed (Entry 2), and the addition of 1,4-benzoquinone proved only to favor isomerization (Entry 3). However, when we applied conditions disclosed by Lindsley and coworkers (Entry 4) we were delighted to observe an 85% yield of our desired product **40**, and no observed isomerization product.[16] As they believed that this difference in reactivity was due to the formation of a TFA salt, we also performed the reaction using the same conditions with the exception of TFA (Entry 5). In this case, we again saw significant amounts of isomerization, which supports their hypothesis that the TFA is integral to the

selectivity in this reaction. With this indolizidine compound **40** in hand, we began our investigation into the total synthesis of tylohirsuticine, which is currently ongoing.

Scheme 2.5.2 N–alkylation of chiral pyrrolidine

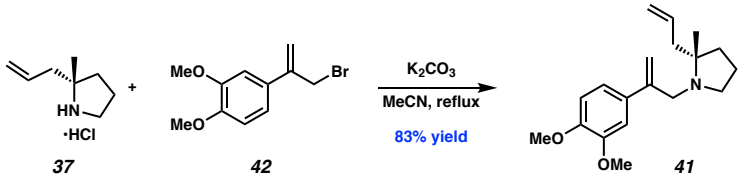

Table 2.5.1 Optimization of ring-closing metathesis

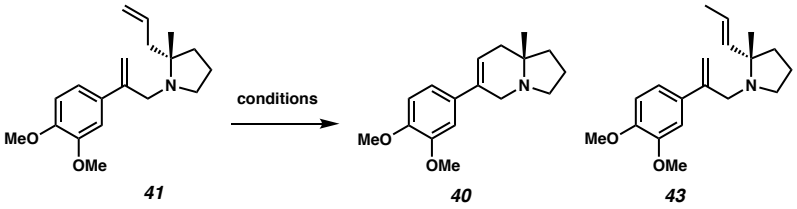

Entry	Conditions	Time	Temperature	Result
1	Grubbs II, CH_2Cl_2	24 h	reflux	SM + 40 + 43
2	Hoveyda–Grubbs II,toluene	1 h	reflux	40:43 = 1:1
3	Hoveyda–Grubbs II,1,4-benzoquinone,toluene	2 h	reflux	40:43 = 1:2
4	Grubbs II, TFA, toluene, μwave	1 h	100 °C	40: 85%
5	Grubbs II, toluene, μwave	1 h	100 °C	40:43 = 1:2

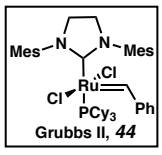

Grubbs II, *44*

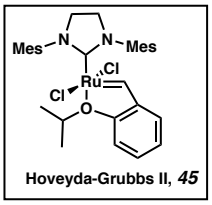

Hoveyda-Grubbs II, *45*

2.6 CONCLUSIONS

The first catalytic enantioselective method for the synthesis of chiral 2,2-disubstituted pyrrolidines is reported, consisting of an asymmetric allylic alkylation reaction to set the stereochemistry, followed by a stereoretentive ring contraction reaction

to afford the desired products. A number of compounds were synthesized using this method to afford products with three different carbamate protecting groups on pyrrolidine, which could prove useful for further derivitization of these compounds. Furthermore, we demonstrated that one of these substrates can be further elaborated to form a new indolizidine compound, which we hope to further advance to the natural product tylohirsuticine in the future.

2.7 EXPERIMENTAL METHODS AND ANALYTICAL DATA

2.7.1 MATERIALS AND METHODS

Unless stated otherwise, reactions were performed in flame-dried or oven-dried glassware under an argon or nitrogen atmosphere using dry, deoxygenated solvents (distilled or passed over a column of activated alumina).[17] Commercially obtained reagents were used as received with the exception of dipalladium tris(dibenzylideneacetone) ($Pd_2(dba)_3$), tetrakis(triphenylphosphine)palladium(0), which were stored in a nitrogen-filled glovebox. Dipalladium tris(para-methoxydibenzylideneacetone) ($Pd_2(pmdba)_3$),[18] (*S*)-*t*-BuPHOX,[19] (*S*)-$(CF_3)_3$-*t*BuPHOX,[20] were prepared by known methods. Reactions requiring external heat were modulated to the specified temperatures using an IKAmag temperature controller. Reaction progress was monitored by thin-layer chromatography (TLC), which was performed using E. Merck silica gel 60 F254 precoated glass plates (0.25 mm) and visualized by UV fluorescence quenching, potassium permanganate, or *p*-anisaldehyde staining. Silicycle SiliaFlash® P60 Academic Silica gel (particle size 40-63 nm) was used for column chromatography. ^1H and ^{13}C NMR spectra were recorded on a Varian Inova 500 (500

MHz and 126 MHz, respectively), and a Bruker AV III HD spectrometer equipped with a Prodigy liquid nitrogen temperature cryoprobe (400 MHz and 101 MHz, respectively) and are reported in terms of chemical shift relative to $CHCl_3$ (δ 7.26 and δ 77.16, respectively). ^{19}F NMR spectra were recorded on a Varian Inova 300 spectrometer (282 MHz) and are reported in terms of absolute chemical shift according to IUPAC standard recommendations from $CFCl_3$. Data for ^1H NMR are reported as follows: chemical shift (δ ppm) (multiplicity, coupling constant (Hz), integration). Multiplicities are reported as follows: s = singlet, d = doublet, t = triplet, m = multiplet, br s = broad singlet, app t = apparently triplet. Infrared (IR) spectra were recorded on a Perkin Elmer Paragon 1000 spectrometer using thin films deposited on NaCl plates and are reported in frequency of absorption (cm^{-1}). Optical rotations were measured with a Jasco P-2000 polarimeter operating on the sodium D-line (589 nm), using a 100 mm path-length cell and are reported as: $[\alpha]^D_T$ (concentration in g/100 mL, solvent). Analytical SFC was performed with a Mettler SFC supercritical CO_2 analytical chromatography system utilizing Chiralpak (AD-H, AS-H, IC) or Chiralcel (OD-H, OJ-H) columns (4.6 mm x 25 cm) obtained from Daicel Chemical Industries, Ltd. High resolution mass spectra were obtained from the Caltech Mass Spectral Facility using a JEOL JMS-600H. High Resolution Mass Spectrometer in fast atom bombardment (FAB+) ionization mode or a Agilent 6200 Series TOF with an Agilent G1978A Multimode source in electrospray ionization (ESI+), atmospheric pressure chemical ionization (APCI+), or mixed (ESI/APCI) ionization mode. Julabo Presto LH45 was used to control reaction temperatures inside the nitrogen-filled glovebox.

2.7.2 EXPERIMENTAL PROCEDURES

1-(benzyloxy)piperidine-2,6-dione (33)

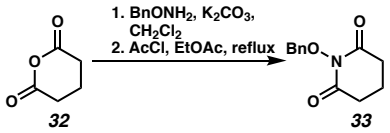

O-Benzyloxyamine hydrochloride (10.30 g, 64.57 mmol, 1.1 equiv) in a 500 mL round-bottom flask was taken up in CH_2Cl_2 (117 mL) and saturated aqueous K_2CO_3 (117 mL) and stirred for 1 hour. The mixture was transferred to a separatory funnel and the phases were separated. The aqueous phase was extracted twice with dichloromethane (120 mL), the combined organic phases were washed with brine (120 mL), dried over Na_2SO_4, filtered, and concentrated under reduced pressure. The resulting crude colorless oil was diluted with dichloromethane (58.7 mL, 1.0 M) in a 250 mL round-bottom flask and glutaric anhydride **32** (6.70 g, 58.7 mmol, 1.00 equiv) was added. An exotherm was observed, and the mixture was immediately concentrated under reduced pressure. The resulting residue was taken up in EtOAc (78.3 mL, 0.75 M) and acetyl chloride (11.6 mL, 164.36 mmol, 2.81 equiv) was added. A water condenser was affixed and the reaction was heated to a gentle reflux (oil bath, 85 °C) for 12 h. The reaction was diluted with EtOAc (30 mL), dried over Na_2SO_4, filtered, and concentrated under reduced pressure. The residue was purified by recrystallization in a 1:1 mixture of CH_2Cl_2/hexanes to afford *N*-benzyloxyimide **33** (12.77 g, 99% yield) as a white solid. Spectral data were in agreement with the literature.[10]

allyl 1-(benzyloxy)-3-methyl-2,6-dioxopiperidine-3-carboxylate (28a)

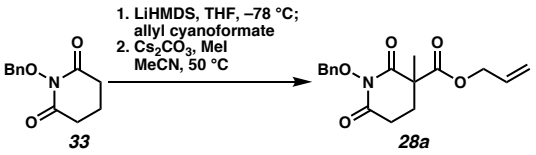

A flame-dried flask charged with a magnetic stir-bar, imide **33** (12.5 g, 57.0 mmol, 1.0 equiv), and THF (570 mL) was lowered into a –78 °C bath. A flame-dried 250 mL round-bottom flask was cycled into a glove box and loaded with LiHMDS (16.21 g, 96.9 mmol, 1.7 equiv). The flask was removed from the glove box, reconnected to a manifold, and charged with THF (96.9 mL, 1 M). This 1 M solution of LiHMDS was added to the flask containing imide **17** dropwise. After 1 h at –78 °C, allylchloroformate (6.08 mL, 57.0 mmol, 1 equiv) was added dropwise and the reaction was stirred for 5 min before being quenched with saturated aqueous ammonium chloride and transferred to a separatory funnel, where the aqueous layer was extracted with ether (500 mL). The combined organics were washed with brine, dried over Na_2SO_4, filtered, and concentrated under reduced pressure. The resulting crude oil was purified by flash column chromatography (SiO_2, CH_2Cl_2 to 10% Et_2O in CH_2Cl_2) to afford **18** as a yellow oil (14.26 g, 83% yield). Spectral data were in agreement with the literature.[10]

The resulting yellow oil was taken up in acetonitrile (156 mL, 0.3 M) in a flame-dried 250 mL Schlenck flask equipped with a magnetic stir bar. Cs_2CO_3 (19.8 g, 60.84 mmol, 1.30 equiv) and methyl iodide (8.74 mL, 140.4 mmol, 3.00 equiv) were added and the reaction was heated to 50 °C and stirred for 10 h. The reaction was diluted with 50 mL EtOAc, filtered over Celite, and concentrated under reduced pressure. The resulting crude

oil was purified by flash column chromatography (SiO_2, 20% to 33% EtOAc in hexanes) to afford imide **28a** (14.25 g, 96% yield) as a pale yellow oil. Spectral data were in agreement with the literature.[10]

allyl 1-(benzyloxy)-3-ethyl-2,6-dioxopiperidine-3-carboxylate (28b)

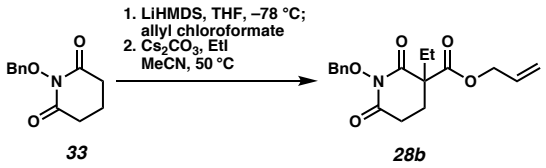

Compound **28b** was prepared according to the procedure for **28a** using Ethyl iodide. The crude product was purified by column chromatography (SiO_2, 20% EtOAc in hexanes) to furnish **28b** (888 mg, 81% yield). Spectral data were in agreement with the literature.[10]

allyl 3-benzyl-1-(benzyloxy)-2,6-dioxopiperidine-3-carboxylate (28c)

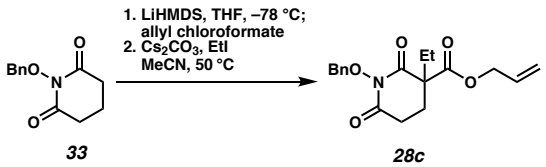

Compound **28c** was prepared according to the procedure for **28a** using benzyl bromide. The crude product was purified by column chromatography (SiO_2, 15% EtOAc in hexanes) to furnish **28c** (367 mg, 81% yield) as a white solid. R_f= 0.67 (hexanes/EtOAc = 2:1); IR (neat film, NaCl) 3528, 3031, 2945, 1734, 1707, 1496, 1454, 1232, 1175, 993, 972, 941, 749, 700; ^{1}H NMR (500 MHz, $CDCl_3$) δ 7.53 (dq, *J* = 8.1, 4.5, 4.0 Hz, 2H), 7.41 (ddd, *J* = 6.3, 4.7, 2.5 Hz, 4H), 7.38 – 7.31 (m, 4H), 7.29 – 7.25 (m, 2H), 5.95 (ddt, *J* = 16.4, 10.3, 5.9 Hz, 1H), 5.46 – 5.34 (m, 2H), 4.99 (s, 2H), 4.76 – 4.73 (m, 2H), 3.72 (d,

J = 13.7 Hz, 1H), 3.28 (d, *J* = 13.7 Hz, 1H), 2.75 – 2.68 (m, 2H), 2.25 – 2.18 (m, 1H), 1.89 (ddd, *J* = 13.9, 11.2, 7.0 Hz, 1H); ^{13}C NMR (126 MHz, $CDCl_3$) δ 169.90, 167.12, 166.56, 140.91, 134.72, 133.75, 130.85, 130.70, 129.98, 129.09, 128.55, 128.39, 127.61, 127.48, 126.96, 120.08, 77.84, 66.99, 65.34, 56.93, 40.22, 30.13, 24.78.; HRMS (*m*/*z*): $[M+H]^+$ calcd for $C_{23}H_{24}NO_5$, 394.1649; found, 394.1662.

allyl 1-(benzyloxy)-2,6-dioxo-3-(3,3,3-trifluoropropyl)piperidine-3-carboxylate (4m)

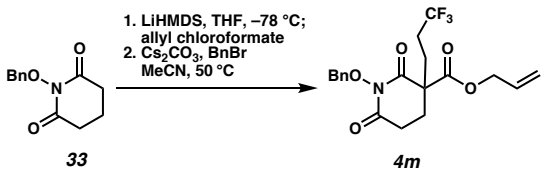

Compound **4m** was prepared according to the procedure for **10a** using trifluoropropyl iodide. The crude product was purified by column chromatography (SiO_2, 33% EtOAc in hexanes) to furnish **4m** (723 mg, 30% yield). Spectral data were in agreement with the literature.[12]

(*S*)-3-allyl-1-(benzyloxy)-3-methylpiperidine-2,6-dione (29a)

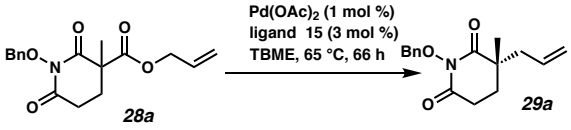

An oven-dried scintillation vial was cycled into a glove box and loaded with $Pd(OAc)_2$ (2 mg, 0.008 mmol, 0.01 equiv), (S)-$(CF_3)_3$-*t*-BuPHOX (14 mg, 0.023 mmol, 0.03 equiv), and TBME (1.6 mL). The flask was stirred for 30 min. Imide **28a** (242 mg, 0.76 mmol, 1 equiv) was taken up in TBME (6 mL), and added to the reaction mixture. The reaction

was stirred at 65 °C for 66 hours. The reaction mixture was then cooled, concentrated, and purified by flash column chromatography (SiO_2, 20% EtOAc in hexanes) to afford imide **29a** as a pale yellow oil (182 mg, 88% yield, 92% ee). Spectral data were in agreement with the literature.[10]

Gram Scale Reaction:

A flame-dried 500 mL Schlenck tube was cycled into a glove box and loaded with $Pd(OAc)_2$ (79 mg, 0.35 mmol, 0.01 equiv), (S)-$(CF_3)_3$-*t*-BuPHOX (621 mg, 1.05 mmol, 0.03 equiv), and TBME (50 mL). The flask was stirred for 30 min. Imide **28a** (11.1 g, 35 mmol, 1 equiv) was taken up in TBME (200 mL), and added to the reaction mixture. The reaction was stirred at 65 °C for 66 hours. The reaction mixture was then cooled, concentrated, and purified by flash column chromatography (SiO_2, 20% EtOAc in hexanes) to afford imide **29a** as a pale yellow oil (7.71 g, 81% yield, 92% ee). Spectral data were in agreement with the literature.

(*S*)-3-allyl-1-(benzyloxy)-3-ethylpiperidine-2,6-dione (29b)

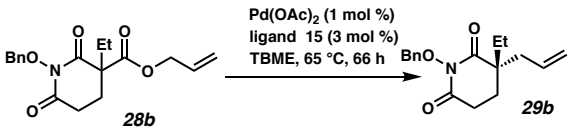

Compound **29b** was prepared from **28b** according to the procedure for **29a**. The crude product was purified by column chromatography (SiO_2, 20% EtOAc in hexanes) to furnish **29b** (216 mg, 86% yield, 94% ee). Spectral data were in agreement with the literature.[10]

(*S*)-3-allyl-3-benzyl-1-(benzyloxy)piperidine-2,6-dione (29c)

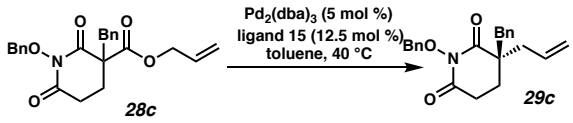

An oven-dried 100 mL Schlenck flask was cycled into a glove box and loaded with $Pd_2(dba)_3$ (46 mg, 0.051 mmol, 0.05 equiv), (S)-$(CF_3)_3$-*t*-BuPHOX (75 mg, 0.126 mmol, 0.015 equiv), and toluene (11 mL). The reaction mixture was stirred 30 min. Imide **28c** (398 mg, 1.01 mmol, 1 equiv) was taken up in 20 mL toluene, and added to the reaction mixture. The reaction was stirred at 40 °C for 66 hours. The reaction mixture was then cooled, concentrated, and purified by flash column chromatography (SiO_2, 20% EtOAc in hexanes) to afford imide **29c** as a white solid (311 mg, 89% yield, 86% ee). R_f = 0.44 (hexanes/EtOAc = 4:1); $[\alpha]^{25}_D$ +25.3° (*c* 1.00, $CHCl_3$); IR (neat film, NaCl) 3063, 3031, 2941, 1739, 1698, 1454, 1173, 991, 742, 701; ^{1}H NMR (500 MHz, $CDCl_3$) δ 7.52 – 7.45 (m, 2H), 7.36 (dp, *J* = 4.8, 1.9 Hz, 3H), 7.33 – 7.26 (m, 3H), 7.19 – 7.13 (m, 2H), 5.69 (ddt, *J* = 17.2, 10.0, 7.3 Hz, 1H), 5.21 – 5.10 (m, 2H), 4.99 – 4.91 (m, 2H), 3.29 (d, *J* = 13.6 Hz, 1H), 2.74 (d, *J* = 13.6 Hz, 1H), 2.68 (ddd, *J* = 17.8, 8.5, 5.6 Hz, 1H), 2.59 – 2.48 (m, 2H), 2.27 (dd, *J* = 13.9, 7.9 Hz, 1H), 1.83 – 1.69 (m, 2H).; ^{13}C NMR (126 MHz, $CDCl_3$) δ 172.37, 167.75, 136.05, 133.85, 132.08, 130.52 (2C), 130.14 (2C), 129.14, 128.55 (2C), 128.42 (2C), 127.22, 120.22, 78.05, 47.81, 42.42, 41.68, 29.49, 24.00.; HRMS (*m*/*z*): $[M+H]^+$ calcd for $C_{22}H_{24}NO_3$, 350.1751; found, 350.1758.

(*R*)-3-allyl-1-(benzyloxy)-3-(3,3,3-trifluoropropyl)piperidine-2,6-dione (5m)

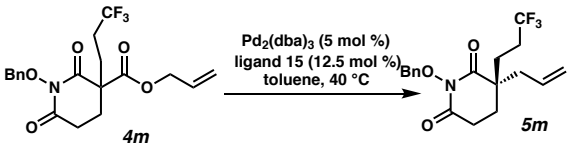

Compound **5m** was prepared from **4m** according to the procedure for **29c**. The reaction mixture was then cooled, concentrated, and purified by flash column chromatography (SiO_2, 20% EtOAc in hexanes) to afford imide **5m** (307 mg, 80% yield, 84% ee). Spectral data were in agreement with the literature.[12]

(3*S*)-3-Allyl-1-(benzyloxy)-6-hydroxy-3-methylpiperidin-2-one (34a)

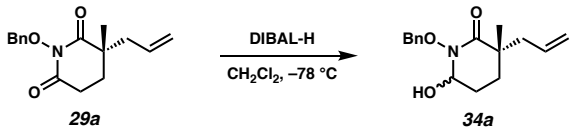

To a 10 mL round bottom flask charged with a magnetic stirring bar and a solution of **29a** (50.4 mg, 184 μmol) in CH_2Cl_2 (1.84 mL) was slowly added DIBAL-H in CH_2Cl_2 (1.0 M, 239 μL, 239 μmol) at –78 ˚C under N_2 atmosphere. After being stirred at –78 ˚C for 15 min, the reaction mixture was quenched with saturated aq. Rochelle salt (2.0 mL) and vigorously stirred at room temperature. Resultant two layers were separated and the aqueous phase was extracted with CH_2Cl_2 (3.0 mL × 1). The combined organic layers were washed with brine (5.0 mL × 1), dried over sodium sulfate, filtered, and concentrated under reduced pressure to afford the crude product. The residue was purified by silica gel flash column chromatography (SiO_2, 15% EtOAc in hexanes) to

afford inseparable mixture **34a** (d.r. = 1:1, 37.8 mg, 75%) as a colorless oil; R_f = 0.42 (hexanes/EtOAc = 1:1); $[\alpha]^{25}_D$ –174.2 (*c* 1.00, $CHCl_3$); IR (neat film, NaCl) 3367, 3069, 2942, 1638, 1455, 1286, 1081, 1006, 920, 748, 699; ^{1}H NMR (500 MHz, $CDCl_3$) δ 7.45-7.42 (complex m, 2H), 7.40-7,34 (complex m, 3H), 5.77 (m, 1H), 5.13-5.06 (complex m, 2H), 4.98-4.88 (complex m, 3H), 3.19 (br s, 1/2H), 3.03 (br s, 1/2H), 2.57 (app ddd, *J* = 13.7, 6.5, 1.4 Hz, 1/2H), 2.33 (app dd, *J* = 7.5, 1.2 Hz, 1/2H), 2.22 (app dd, *J* = 13.7, 8.3 Hz, 1/2H), 2.13 (app dt, *J* = 13.4, 3.9 Hz, 1/2H), 2.05-1.91 (complex m, 1H), 1.88-1.78 (complex m, 2H), 1.60 (m, 1/2H), 1.31 (app ddd, *J* = 13.9, 4.2, 4.2 Hz, 1/2H); 1.22 (s, 1.5H), 1.21 (s, 1.5H); ^{13}C NMR (126 MHz, $CDCl_3$) δ 174.9 (1/2C), 174.3 (1/2C), 135.5 (1/2C), 135.4 (1/2C), 133.9 (1/2C), 133.4 (1/2C), 129.8, 129.7 (1/2C), 129.7 (1/2C), 128.9 (1/2C), 128.9 (1/2C), 128.6, 128.6, 118.6 (1/2C), 118.6 (1/2C), 82.8 (1/2C), 82.5 (1/2C), 76.9, 43.6 (1/2C), 43.2 (1/2C), 43.2 (1/2C), 43.0 (1/2C), 27.6 (1/2C), 27.0 (1/2C), 26.4 (1/2C), 26.4 (1/2C), 24.9 (1/2C), 23.9 (1/2C); HRMS (*m*/*z*): [M–H_2O] calcd for $C_{16}H_{19}NO_2$, 258.1489; found, 258.1477.

(3*S*)-3-allyl-1-(benzyloxy)-6-hydroxy-3-ethylpiperidin-2-one (34b)

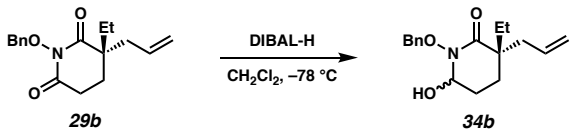

29b *34b*

Compound **34b** was prepared from **29b** according to the procedure for **34a**. The residue was purified by silica gel flash column chromatography (SiO_2, 15% EtOAc in hexanes) to afford inseparable mixture **34b** (d.r. = 1:1, 49 mg, 60% yield) as a colorless oil; R_f = 0.42 (hexanes/EtOAc = 4:1); $[\alpha]^{25}_D$ –37.7° (*c* 1.00, $CHCl_3$); IR (neat film, NaCl) 3382, 3073,

2963, 2938, 1650, 1643, 1455, 1284, 1080, 979, 916, 751, 698; ^{1}H NMR (500 MHz, $CDCl_3$) δ 7.43 (ddt, *J* = 8.0, 6.3, 1.9 Hz, 2H), 7.40 – 7.32 (m, 3H), 5.83 – 5.72 (m, 1H), 5.12 – 5.05 (m, 2H), 4.99 – 4.87 (m, 3H), 3.17 (br s, 1H), 2.55 (ddt, *J* = 13.8, 6.2, 1.4 Hz, 1/2H), 2.35 (ddt, *J* = 7.7, 6.5, 1.2 Hz, 1H), 2.24 – 2.16 (m, 1/2H), 2.12 – 1.93 (m, 1 1/2H), 1.89 – 1.79 (m, 2H), 1.74 – 1.56 (m, 1H), 1.53 – 1.41 (m, 1 1/2H) 0.91 (td, *J* = 7.5, 1.6 Hz, 3H).; ^{13}C NMR (126 MHz, $CDCl_3$) δ 174.23 (1/2C), 173.78 (1/2C), 135.44, 134.19, 133.80, 129.71, 128.93, 128.88, 128.62 (1/2C), 128.58 (1/2C), 118.40 (1/2C), 118.26 (1/2C), 82.74 (1/2C), 82.62 (1/2C), 47.00 (1/2C), 46.60 (1/2C), 42.26, 40.45, 30.24 (1/2C), 29.60 (1/2C), 26.17 (1/2C), 26.07 (1/2C), 24.45 (1/2C), 23.73 (1/2C), 8.51 (1/2C), 8.44 (1/2C).; HRMS (*m*/*z*): $[M+H]^+$ calcd for $C_{17}H_{24}NO_3$, 290.1762; found, 290.1762.

(3*S*)-3-allyl-3-benzyl-1-(benzyloxy)-6-hydroxypiperidin-2-one (34c)

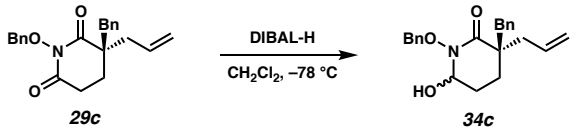

Compound **34c** was prepared from **29c** according to the procedure for **34a**. The residue was purified by silica gel flash column chromatography (SiO_2, 15% EtOAc in hexanes) to afford inseparable mixture **34c** (d.r. = 1:1, 111 mg, 37% yield) as a white solid; R_f = 0.44 (hexanes/EtOAc = 2:1); $[\alpha]^{25}_{D}$ +29.1° (*c* 1.00, $CHCl_3$); IR (neat film, NaCl) 3390, 3063, 3028, 2939, 1671, 1495, 1453, 1299, 1071, 997, 919, 750, 700; ^{1}H NMR (400 MHz, $CDCl_3$) δ 7.44 – 7.32 (m, 5H), 7.33 – 7.25 (m, 3H), 7.23 – 7.14 (m, 2H), 5.90 – 5.74 (m, 1H), 5.19 – 4.78 (m, 5H), 3.30 (d, *J* = 13.4 Hz, 1/2H), 3.18 (d, *J* = 13.3 Hz, 1/2H), 2.95

(dd, *J* = 3.3, 1.2 Hz, 1/2H), 2.77 – 2.66 (m, 1 1/2H), 2.61 (d, *J* = 3.8 Hz, 1/2H), 2.49 (ddt, *J* = 13.8, 7.1, 1.3 Hz, 1/2H), 2.35 (dd, *J* = 13.9, 7.6 Hz, 1/2H), 2.13 – 1.94 (m, 2H), 1.75 – 1.63 (m, 1 1/2H), 1.53 – 1.41 (m, 1H).; ^{13}C NMR (126 MHz, $CDCl_3$) δ 172.87 (1/2 C), 172.86 (1/2 C), 137.43 (1/2 C), 137.30 (1/2 C), 135.54 (1/2 C), 135.50 (1/2 C), 133.84 (1/2 C), 133.68 (1/2 C), 130.98, 130.69, 129.81, 129.79, 129.07 (1/2 C), 129.05 (1/2 C), 128.76, 128.73, 128.36, 128.26, 126.93 (1/2 C), 126.69 (1/2 C), 119.12 (1/2 C), 118.94 (1/2), 82.68 (1/2 C), 82.46 (1/2 C), 48.01 (1/2 C), 47.99 (1/2 C), 44.24, 42.90, 42.72 (1/2 C), 42.61 (1/2 C), 26.53 (1/2 C), 26.45 (1/2 C), 23.70 (1/2 C), 23.18 (1/2 C). HRMS (*m*/*z*): $[M+H]^+$ calcd for $C_{22}H_{26}NO_3$, 351.1907; found, 351.1915.

(3*R*)-3-allyl-1-(benzyloxy)-6-hydroxy-3-(3,3,3-trifluoropropyl)piperidin-2-one (34d)

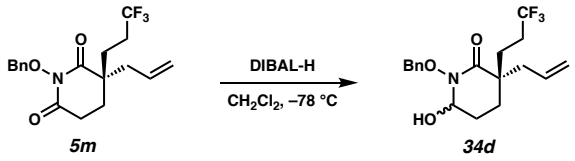

Compound **34d** was prepared from **5m** according to the procedure for **34a**. The residue was purified by silica gel flash column chromatography (SiO_2, 15% EtOAc in hexanes) to afford inseparable mixture **34d** (d.r. = 1:1, 125 mg, 41% yield) as a colorless oil;. R_f = 0.27 (hexanes/EtOAc = 3:1); $[\alpha]^{25}_D$ +15.0° (*c* 1.00, $CHCl_3$); IR (neat film, NaCl) 3390, 3063, 3028, 2939, 1671, 1495, 1453, 1299, 1071, 997, 919, 750, 700; ^{1}H NMR (500 MHz, $CDCl_3$) δ 7.47 – 7.29 (m, 5H), 5.72 (dddd, *J* = 16.7, 15.0, 10.2, 7.8 Hz, 1H), 5.21 – 5.08 (m, 2H), 4.98 – 4.84 (m, 3H), 3.21 (br s, 1H), 2.51 (ddt, *J* = 13.9, 6.3, 1.5 Hz, 1/2H), 2.44 – 2.32 (m, 1H), 2.26 (dd, *J* = 14.0, 8.4 Hz, 1/2H), 2.23 – 2.12 (m, 2H), 2.12 – 1.93 (m, 2 1/2H), 1.95 – 1.81 (m, 1 1/2H), 1.66 (td, *J* = 13.3, 4.6 Hz, 1/2H), 1.60 – 1.48 (m,

1H), 1.42 (dt, *J* = 14.1, 4.2 Hz, 1/2H).; ^{13}C NMR (126 MHz, $CDCl_3$) δ 173.49, 135.24, 132.84, 132.51, 129.84 (2C), 129.18, 128.77 (1/2C), 128.75 (1/2C), 127.29 (q, *J* = 276.5 Hz), 119.55 (1/2C), 119.52 (1/2C), 82.68, 45.95 (1/2C), 45.23 (1/2C), 42.46 (1/2C), 40.20 (1/2C), 29.24 (q, *J* = 29.1 Hz), 29.12 (q, *J* = 3.0 Hz), 26.15, 25.96 (1/2C), 25.84 (1/2C), 24.24.; ^{19}F NMR (282 MHz, $CDCl_3$) δ -66.48 – -66.68 (m, 3F); HRMS (*m*/*z*): $[M+H]^+$ calcd for $C_{18}H_{23}F_3NO_3$, 358.1625; found, 358.1641.

(*S*)-3-Allyl-1-(benzyloxy)-3-methylpiperidin-2-one (35a)

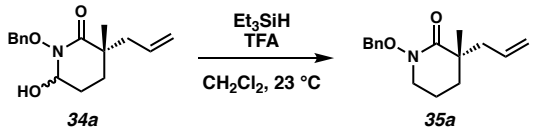

34a *35a*

To a 250 mL round bottom flask charged with a magnetic stirring bar and a solution of **34a** (1.53 g, 5.56 mmol) in CH_2Cl_2 (55.6 mL) was added Et_3SiH (1.77 mL, 11.1 mmol) and TFA (8.51 mL, 111 mmol) at room temperature under N_2 atmosphere. After being stirred at ambient temperature for 5 min, the reaction mixture was evaporated *in vacuo*. The residue was purified by flash column chromatography (SiO_2, 20% EtOAc in hexanes) to afford **35a** (1.45 g, quant.) as a colorless oil; R_f = 0.38 (hexanes/EtOAc = 2:1); $[\alpha]^{25}_D$ –36.3° (*c* 1.00, $CHCl_3$); IR (neat film, NaCl) 3069, 2944, 2873, 1774, 1654, 1456, 1324, 1207, 1171, 998, 918, 750, 700; ^{1}H NMR (500 MHz, $CDCl_3$) δ 7.46-7.41 (complex m, 2H), 7.39-7.32 (complex m, 3H), 5.74 (m, 1H), 5.12-5.05 (complex m, 2H), 4.95 (d, *J* = 10.6 Hz, 1H), 4.91 (d, *J* = 10.5 Hz, 1H), 3.41-3.30 (complex m, 2H), 2.49 (dd, *J* = 13.7, 6.8 Hz, 1H), 2.24 (dd, *J* = 13.7, 8.0 Hz, 1H), 1.82-1.69 (complex m, 3H), 1.43 (m, 1H), 1.21 (s, 3H); ^{13}C NMR (126 MHz, $CDCl_3$) δ 172.9, 135.3, 133.9, 129.7

(2C), 128.8, 128.5 (2C), 118.6, 75.6, 51.1, 43.7, 43.0, 31.9, 25.1, 19.6; HRMS (*m*/*z*): $[M+H]^+$ calcd for $C_{16}H_{22}NO_2$, 260.1645; found, 260.1630.

(*S*)-3-allyl-1-(benzyloxy)-3-ethylpiperidin-2-one (35b)

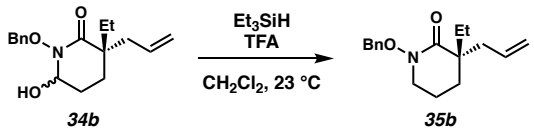

34b *35b*

Compound **35b** was prepared from **34b** according to the procedure for **35a**. The residue was purified by silica gel flash column chromatography (SiO_2, 20% EtOAc in hexanes) to afford inseparable mixture **35b** (60 mg, 94% yield) as a colorless oil; R_f = 0.42 (hexanes/EtOAc = 4:1); $[\alpha]^{25}_D$ –30.5° (*c* 1.00, $CHCl_3$); IR (neat film, NaCl) 3069, 3032, 2941, 2879, 1777, 1659, 1454, 1308, 1207, 1169, 998, 975, 918, 749, 699; ^{1}H NMR (500 MHz, $CDCl_3$) δ 7.46 – 7.39 (m, 2H), 7.39 – 7.32 (m, 3H), 5.75 (dddd, *J* = 16.9, 10.4, 8.0, 6.8 Hz, 1H), 5.10 (q, *J* = 1.4 Hz, 1H), 5.07 (dq, *J* = 10.7, 1.5 Hz, 1H), 4.92 (s, 2H), 3.42 – 3.34 (m, 2H), 2.49 (ddt, *J* = 13.7, 6.8, 1.4 Hz, 1H), 2.27 – 2.20 (m, 1H), 1.80 (dddd, *J* = 8.8, 7.4, 6.1, 4.9 Hz, 2H), 1.77 – 1.71 (m, 1H), 1.68 – 1.60 (m, 2H), 1.60 – 1.54 (m, 1H), 0.90 (t, *J* = 7.5 Hz, 3H).; ^{13}C NMR (126 MHz, $CDCl_3$) δ 172.71, 135.14, 133.99, 129.69 (2C), 128.84, 128.50 (2C), 118.50, 75.83, 51.01, 46.45, 42.02, 30.57, 28.19, 19.59, 8.53.; HRMS (*m*/*z*): $[M+H]^+$ calcd for $C_{17}H_{24}NO_2$, 274.1802; found, 274.1813.

(*S*)-3-allyl-3-benzyl-1-(benzyloxy)piperidin-2-one (35c)

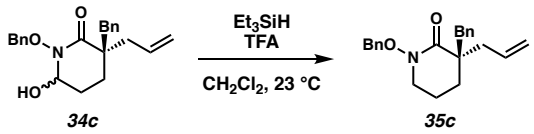

34c *35c*

Compound **35c** was prepared from **34c** according to the procedure for **35a**. The residue was purified by silica gel flash column chromatography (SiO_2, 20% EtOAc in hexanes) to afford inseparable mixture **35c** (75 mg, 79% yield) as a colorless oil; R_f = 0.36 (hexanes/EtOAc = 4:1); $[\alpha]^{25}_D$ +15.4° (*c* 1.00, $CHCl_3$); IR (neat film, NaCl) 3065, 3029, 2943, 2875, 1777, 1651, 1603, 1454, 1209, 1166, 994, 919, 751, 702; ^{1}H NMR (500 MHz, $CDCl_3$) δ 7.42 – 7.25 (m, 10H), 5.84 (dddd, *J* = 16.8, 10.1, 8.1, 6.6 Hz, 1H), 5.23 – 5.12 (m, 2H), 5.01 – 4.85 (m, 2H), 3.39 – 3.31 (m, 2H), 3.19 (ddd, *J* = 11.6, 6.7, 5.2 Hz, 1H), 2.75 – 2.66 (m, 2H), 2.27 (dd, *J* = 13.6, 8.1 Hz, 1H), 1.81 – 1.72 (m, 1H), 1.72 – 1.66 (m, 2H), 1.61 – 1.53 (m, 1H).; ^{13}C NMR (126 MHz, $CDCl_3$) δ 171.73, 137.35, 135.10, 133.48, 130.79 (2C), 129.69 (2C), 128.85, 128.51 (2C), 128.26 (2C), 126.71, 119.20, 76.01, 50.95, 47.61, 43.68, 43.30, 27.60, 19.53.; HRMS (*m/z*): $[M+H]^+$ calcd for $C_{22}H_{26}NO_2$, 336.1958; found, 336.1973.

(*R*)-3-allyl-1-(benzyloxy)-3-(3,3,3-trifluoropropyl)piperidin-2-one (35d)

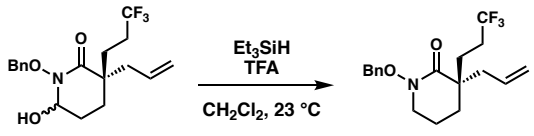

34d *35d*

Compound **35d** was prepared from **34d** according to the procedure for **35a**. The residue was purified by silica gel flash column chromatography (SiO_2, 20% EtOAc in hexanes) to

afford inseparable mixture **35d** (45 mg, 54% yield) as a colorless oil; R_f = 0.34 (hexanes/EtOAc =4:1); $[\alpha]^{25}_D$ –4.0° (*c* 0.50, $CHCl_3$); IR (neat film, NaCl) 3068, 3033, 2952, 2875, 1658, 1454, 1324, 1259, 1149, 983, 919, 750, 699; ^{1}H NMR (500 MHz, $CDCl_3$) δ 7.41 (dq, *J* = 5.4, 3.3, 2.6 Hz, 2H), 7.37 (dt, *J* = 4.4, 2.9 Hz, 3H), 5.70 (dddd, *J* = 16.9, 10.1, 7.8, 6.9 Hz, 1H), 5.18 – 5.09 (m, 2H), 4.96 – 4.88 (m, 2H), 3.40 (t, *J* = 6.1 Hz, 2H), 2.46 (ddt, *J* = 13.8, 6.8, 1.3 Hz, 1H), 2.30 (dd, *J* = 13.8, 7.8 Hz, 1H), 2.20 – 2.05 (m, 2H), 1.90 – 1.78 (m, 3H), 1.74 (ddt, *J* = 13.6, 11.1, 4.7 Hz, 2H), 1.54 (ddd, *J* = 13.8, 8.3, 3.6 Hz, 1H).; ^{13}C NMR (126 MHz, $CDCl_3$) δ 171.52, 134.79, 132.59, 129.73 (2C), 129.34 (q, $J_{C\text{-}F}$ = 276.3 Hz), 129.02, 128.54 (2C), 119.55, 75.77, 50.86, 44.92, 41.44, 29.53, 29.52 (q, $J_{C\text{-}F}$ = 3.4 Hz), 29.15 (q, $J_{C\text{-}F}$ = 28.8 Hz), 19.23.; ^{19}F NMR (282 MHz, $CDCl_3$) δ -66.54 (t, J=10.7 Hz, 3F); HRMS (*m/z*): $[M+H]^+$ calcd for $C_{18}H_{23}F_3NO_2$, 342.1675; found, 342.1692.

(*S*)-3-Allyl-1-hydroxy-3-methylpiperidin-2-one (30a)

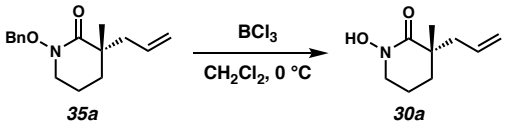

35a *30a*

To a 250 mL round bottom flask charged with a magnetic stirring bar and a solution of **35a** (1.39 g, 5.01 mmol) in CH_2Cl_2 (50.1 mL) was added BCl_3 in CH_2Cl_2 (1.0 M, 6.01 mL, 6.01 mmol) dropwise over 10 min at –78 ˚C under N_2 atmosphere. After being stirred at 0 ˚C for 10 min, the solvent was removed *in vacuo*. The residue was diluted with hexanes/Et_2O (v/v = 10/1, 30 mL) and 1N NaOH (30 mL) was carefully added to adjust the pH to >14. Resultant two layers were separated and the organic phase was washed with aqueous 1N NaOH (20 mL × 2). Concentrated HCl was added to adjust the

pH to <1, followed by addition of CH_2Cl_2 (60 mL). The two layers were separated and the aqueous phase was extracted with CH_2Cl_2 (50 mL × 1). The combined organic layers were washed with brine (120 mL × 1), dried over sodium sulfate, filtered, and concentrated under reduced pressure to afford pure hydroxamic acid **30a** (773 mg, 91%) as a pale orange crystal, which was used in the next reaction without further purification; R_f = 0.38 (CH_2Cl_2/MeOH = 8:1); mp = 41-42 °C; $[\alpha]^{25}_D$ –68.0° (*c* 1.00, $CHCl_3$); IR (neat film, NaCl) 3073, 2938, 2869, 1628, 1456, 1329, 1021, 999, 919; ^{1}H NMR (500 MHz, $CDCl_3$) δ 5.72 (m, 1H), 5.13-5.05 (complex m, 2H), 3.62 (app t, *J* = 6.2 Hz, 2H), 2.47 (app dd, *J* = 13.7, 6.8 Hz, 1H), 2.27 (dd, *J* = 13.7, 8.0 Hz, 1H), 1.99-1.92 (complex m, 2H), 1.83 (m, 1H), 1.53 (m, 1H), 1.23 (s, 3H); ^{13}C NMR (126 MHz, $CDCl_3$) δ 170.0, 133.9, 118.6, 49.6, 43.6, 41.4, 31.9, 24.7, 19.0; HRMS (*m/z*): $[M+H]^+$ calcd for $C_9H_{16}NO_2$, 170.1176; found, 170.1167.

(*S*)-3-allyl-3-ethyl-1-hydroxypiperidin-2-one (30b)

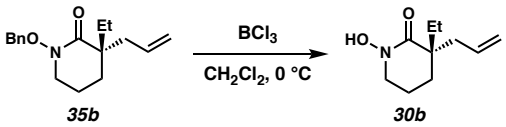

35b *30b*

Compound **30b** was prepared from **35b** according to the procedure for **30a**. The residue was concentrated under reduced pressure to afford pure hydroxamic acid **30b** (13 mg, 62%) as a pale orange solid, which was used in the next reaction without further purification; R_f = 0.45 (hexanes/EtOAc = 1:1); $[\alpha]^{25}_D$ –40.7° (*c* 1.00, $CHCl_3$); IR (neat film, NaCl) 3076, 2941, 2879, 1626, 1455, 919; ^{1}H NMR (500 MHz, $CDCl_3$) δ 7.26 (br s, 1H), 5.73 (dddd, *J* = 16.8, 10.5, 8.0, 6.7 Hz, 1H), 5.12 – 4.99 (m, 2H), 3.61 (td, *J* = 6.2,

1.8 Hz, 2H), 2.46 (ddt, *J* = 13.8, 6.7, 1.4 Hz, 1H), 2.25 (dd, *J* = 13.8, 7.9 Hz, 1H), 2.04 – 1.87 (m, 2H), 1.71 (ddd, *J* = 12.1, 9.6, 6.4 Hz, 3H), 1.58 (dq, *J* = 14.6, 7.4 Hz, 1H), 0.88 (t, *J* = 7.4 Hz, 3H).; ^{13}C NMR (126 MHz, $CDCl_3$) δ 168.86, 134.07, 118.33, 48.75, 44.67, 41.71, 30.24, 28.49, 18.88, 8.57; HRMS (*m*/*z*): $[M+H]^+$ calcd for $C_{10}H_{18}NO_2$, 184.1332; found, 184.1331.

(*S*)-3-allyl-3-benzyl-1-hydroxypiperidin-2-one (30c)

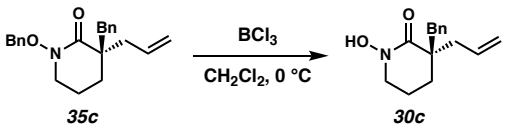

35c *30c*

Compound **30c** was prepared from **35c** according to the procedure for **30a**. The residue was concentrated under reduced pressure to afford pure hydroxamic acid **30c** (33 mg, 80%) as a pale orange solid, which was used in the next reaction without further purification; R_f = 0.55 (hexanes/EtOAc = 1:1); $[\alpha]^{25}_D$ +18.0° (*c* 1.00, $CHCl_3$); IR (neat film, NaCl) 3076, 3029, 2926, 2869, 1624, 1453, 917, 703; ^{1}H NMR (500 MHz, $CDCl_3$) δ 7.37 – 7.25 (m, 3H), 7.24 – 7.17 (m, 2H), 5.81 (dddd, *J* = 16.6, 10.1, 8.3, 6.3 Hz, 1H), 5.21 – 5.11 (m, 2H), 3.60 (ddd, *J* = 12.2, 7.3, 5.3 Hz, 1H), 3.48 (dt, *J* = 11.0, 5.4 Hz, 1H), 3.31 (d, *J* = 13.3 Hz, 1H), 2.74 (d, *J* = 13.4 Hz, 1H), 2.69 (ddt, *J* = 13.7, 6.3, 1.4 Hz, 1H), 2.24 (dd, *J* = 13.6, 8.3 Hz, 1H), 1.88 (ddtd, *J* = 13.3, 8.4, 5.5, 2.1 Hz, 1H), 1.81 – 1.63 (m, 3H).; ^{13}C NMR (126 MHz, $CDCl_3$) δ 167.69, 137.37, 133.74, 130.47 (2C), 128.24 (2C), 126.65, 118.97, 48.32, 45.78, 43.49, 43.06, 27.96, 18.82.; HRMS (*m*/*z*): $[M+H]^+$ calcd for $C_{15}H_{20}NO_2$, 246.1489; found, 246.1487.

(*R*)-3-allyl-1-hydroxy-3-(3,3,3-trifluoropropyl)piperidin-2-one (30d)

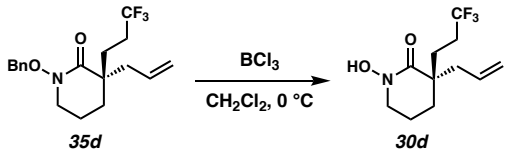

Compound **30d** was prepared from **35d** according to the procedure for **30a**. The residue was concentrated under reduced pressure to afford pure hydroxamic acid **30d** (30 mg, 81%) as a pale yellow solid, which was used in the next reaction without further purification; R_f = 0.60 (hexanes/EtOAc = 1:1); $[\alpha]^{25}_D$ –16.9° (*c* 1.00, $CHCl_3$); IR (neat film, NaCl) 3080, 2926, 2855, 1633, 1454, 1324, 1260, 1118, 981, 916; ^{1}H NMR (500 MHz, $CDCl_3$) δ 9.08 (br s, 1H), 5.70 (dddd, *J* = 16.9, 10.1, 7.8, 6.9 Hz, 1H), 5.22 – 5.00 (m, 2H), 3.64 (t, *J* = 6.2 Hz, 2H), 2.46 (ddt, *J* = 13.9, 6.8, 1.4 Hz, 1H), 2.33 (dd, *J* = 13.9, 7.8 Hz, 1H), 2.26 – 2.09 (m, 2H), 2.07 – 1.92 (m, 2H), 1.90 – 1.73 (m, 3H), 1.63 (ddd, *J* = 13.9, 8.4, 3.8 Hz, 1H).; ^{13}C NMR (126 MHz, $CDCl_3$) δ 167.54, 132.62, 127.15 (q, *J* = 276.2 Hz), 119.51, 48.69, 43.14, 41.19, 29.72, 29.29 (q, *J* = 3.0 Hz), 29.27 (q, *J* = 28.8 Hz), 18.55. ; ^{19}F NMR (282 MHz, $CDCl_3$) δ -66.56 (t, J=10.6 Hz, 3F); HRMS (*m*/*z*): $[M+H]^+$ calcd for $C_{11}H_{17}F_3NO_2$, 252.1206; found, 252.1203.

(*S*)-3-Allyl-3-methyl-2-oxopiperidin-1-yl trifluoromethanesulfonate (36a)

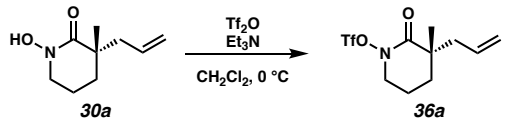

To a 100 mL round bottom flask charged with a magnetic stirring bar and a solution of **30a** (771 mg, 4.56 mmol) in CH_2Cl_2 (45.6 mL) was added Et_3N (948 μL, 6.84 mmol) and

Tf_2O (898 μL, 5.47 mmol) at 0 ˚C under N_2 atmosphere. After being stirred at 0 ˚C for 5 min, the reaction mixture was quenched with saturated aq. NH_4Cl (50 mL). Resultant two layers were separated and the aqueous phase was extracted with CH_2Cl_2 (50 mL × 1). The combined organic layers were washed with brine (100 mL × 1), dried over sodium sulfate, filtered, and concentrated under reduced pressure to afford the crude product. This resulting triflate **36a** was used in the next reaction without further purification due to it's instability; R_f = 0.48 (hexanes/EtOAc = 2:1).

Methyl (*S*)-2-allyl-2-methylpyrrolidine-1-carboxylate (31a)

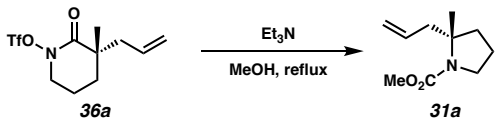

36a *31a*

To a 100 mL round bottom flask charged with a magnetic stirring bar and a solution of fleshly prepared **36a** in freshly distilled MeOH (30.4 mL) was added Et_3N (1.26 mL, 9.12 mmol) at room temperature under N_2 atmosphere and the stirred mixture was heated to reflux and stirred for 50 min. The reaction mixture was cooled to room temperature before the solvent was removed under reduced pressure. The residue was purified by flash column chromatography (SiO_2, 5% EtOAc in hexanes) to afford **31a** (695 mg, 83%) as a yellow oil; R_f = 0.48 (hexanes/EtOAc = 2:1); $[\alpha]^{25}_D$ –70.3˚ (*c* 1.00, $CHCl_3$); IR (neat film, NaCl) 2961, 2927, 2871, 1700, 1444, 1375, 1212, 1189, 1082, 912, 772, 694; ^{1}H NMR (500 MHz, $CDCl_3$) δ Rotamer A: 5.70 (m, 1H), 5.11-5.01 (m, 2H), 3.70 (s, 3H), 3.58 (m, 1H), 3.37 (m, 1H), 2.56 (dd, *J* = 13.7, 6.9 Hz, 1H), 2.37 (dd, *J* = 13.7, 7.8 Hz, 1H), 2.00 (m, 1H), 1.80-1.71 (complex m, 2H), 1.65 (m, 1H), 1.30 (s, 3H); Rotamer B:

5.70 (m, 1H), 5.11-5.01 (m, 2H), 3.64 (s, 3H), 3.47 (m, 1H), 3.31 (m, 1H), 2.68 (dd, *J* = 13.6, 6.8 Hz, 1H), 2.51 (dd, *J* = 13.6, 8.0 Hz, 1H), 1.95 (m, 1H), 1.80-1.71 (complex m, 2H), 1.60 (m, 1H), 1.37 (s, 3H); ^{13}C NMR (126 MHz, $CDCl_3$) δ Rotamer A: 155.7, 134.5, 118.0, 62.3, 51.9, 49.1, 43.6, 38.9, 25.9, 21.7; Rotamer B: 154.4, 134.8, 117.9, 63.0, 51.7, 48.1, 42.5, 37.8, 24.7, 22.2; HRMS (*m*/*z*): $[M+H]^+$ calcd for $C_{10}H_{18}NO_2$, 183.1259; found, 183.12.

benzyl (*S*)-2-allyl-2-methylpyrrolidine-1-carboxylate (31b)

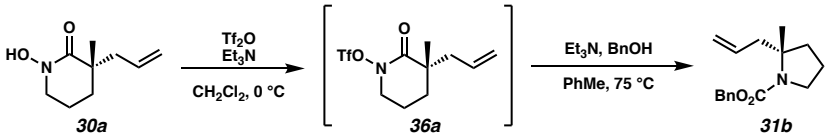

To a 5 mL round bottom flask charged with a magnetic stirring bar and a solution of fleshly prepared **36a** (0.21 mmol, 1 equiv) in a 3:1 mixture of toluene and benzyl alcohol (1.42 mL, 0.15 M) was added Et_3N (0.059 mL, 0.18 mmol, 2 equiv) at room temperature under N_2 atmosphere and the stirred mixture was heated to reflux and stirred for 3 hours. The reaction mixture was cooled to room temperature before the solvent was removed under reduced pressure. The residue was purified by flash column chromatography (SiO_2, 5% EtOAc in hexanes) to afford **31b** (31 mg, 56% yield, 92% ee) as a orange oil; R_f = 0.75 (hexanes/EtOAc = 2:1); $[\alpha]^{25}_D$ –90.9° (*c* 1.00, $CHCl_3$); IR (neat film, NaCl) 3068, 3032, 2966, 2875, 1698, 1453, 1403, 1353, 1213, 1128, 1068, 914, 769, 697; ^{1}H NMR (500 MHz, $CDCl_3$) δ 7.40 – 7.27 (m, 5H), 5.76 – 5.61 (m, 1H), 5.20 – 4.96 (m, 4H), 3.65 – 3.52 (m, 1H), 3.39 (tt, *J* = 10.8, 7.4 Hz, 1H), 2.66 (dddt, *J* = 63.2, 13.7, 6.8, 1.4 Hz, 1H), 2.52 (dd, *J* = 13.6, 7.9 Hz, 1H), 2.06 – 1.94 (m, 1H), 1.82 – 1.73 (m, 2H), 1.64 (tt, *J*

= 12.5, 6.2 Hz, 1H), 1.36 (d, *J* = 40.5 Hz, 3H).; ^{13}C NMR (126 MHz, $CDCl_3$) δ Rotamer A: 153.77, 137.45, 134.79, 128.51 (2C), 128.20, 127.74 (2C), 118.06, 66.08, 63.24, 48.30, 42.51, 37.85, 24.83, 22.25. Rotamer B: 155.05, 136.93, 134.47, 128.58 (2C), 128.01, 127.83 (2C), 118.18, 66.98, 62.58, 49.32, 43.69, 39.03, 26.15, 21.83. HRMS (*m*/*z*): $[M+H]^+$ calcd for $C_{16}H_{22}NO_2$, 260.1645; found, 260.1656.

***tert*-butyl (*S*)-2-allyl-2-methylpyrrolidine-1-carboxylate (31c)**

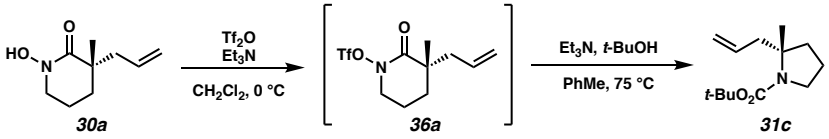

To a 50 mL round bottom flask charged with a magnetic stirring bar and a solution of fleshly prepared **36a** (1.93 mmol, 1 equiv) in a 3:1 mixture of toluene and *tert*-butyl alcohol (13 mL, 0.15 M) was added Et_3N (0.53 mL, 3.85 mmol, 2 equiv) at room temperature under N_2 atmosphere and the stirred mixture was heated to reflux and stirred for 3 hours. The reaction mixture was cooled to room temperature before the solvent was removed under reduced pressure. The residue was purified by flash column chromatography (SiO_2, 5% EtOAc in hexanes) to afford **31c** (280 mg, 65% yield) as a yellow oil;. R_f = 0.32 (hexanes/EtOAc = 19:1); $[\alpha]^{25}_D$ –55.4° (*c* 1.00, $CHCl_3$); IR (neat film, NaCl) 3078, 2970, 2928, 2870, 1697, 1457, 1387, 1170, 1066, 912, 771; ^{1}H NMR (400 MHz, $CDCl_3$) δ 5.70 (dddd, *J* = 17.6, 9.8, 8.0, 6.7 Hz, 1H), 5.06 (dt, *J* = 15.6, 3.7 Hz, 2H), 3.48 (ddt, *J* = 39.8, 12.0, 6.1 Hz, 1H), 3.28 (ddt, *J* = 25.5, 10.7, 7.4 Hz, 1H), 2.61 (dd, *J* = 13.7, 6.5 Hz, 1H), 2.33 (dd, *J* = 13.7, 8.0 Hz, 1H), 2.08 – 1.84 (m, 1H), 1.77 – 1.66 (m, 2H), 1.61 (tt, *J* = 12.0, 5.6 Hz, 1H), 1.46 (d, *J* = 17.4 Hz, 9H), 1.28 (d, *J* = 19.6

Hz, 3H).; ^{13}C NMR (101 MHz, $CDCl_3$) δ Rotamer A: 154.49, 134.90, 117.91, 79.41, 61.98, 48.73, 43.81, 39.12, 28.76 (3C), 26.11, 21.67. Rotamer B: ^{13}C NMR (101 MHz, $CDCl_3$) δ 153.57, 135.14, 117.80, 78.58, 62.65, 48.66, 42.64, 38.07, 28.76 (3C), 25.03, 22.13.

(*S*)-3-allyl-3-ethyl-1-hydroxypiperidin-2-one (31d)

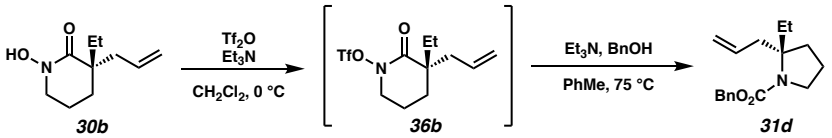

Compound **36b** was prepared from compound **30b** according to the procedure for **36a**, and was used without further purification. Compound **31d** was prepared from **36b** according to the procedure for **31b**. The residue was purified by flash column chromatography (SiO_2, 5% EtOAc in hexanes) to afford **31d** (90 mg, 66% yield) as a colorless oil;. R_f= 0.65 (hexanes/EtOAc = 4:1); $[\alpha]^{25}_D$ –69.5° (*c* 1.00, $CHCl_3$); IR (neat film, NaCl) 3069, 3032, 2968, 2877, 1702, 1455, 1403, 1356, 1338, 1214, 1123, 1071, 914, 768, 697; ^{1}H NMR (500 MHz, $CDCl_3$) δ Rotamer A: 7.39 – 7.33 (m, 4H), 7.33 – 7.27 (m, 1H), 5.77 – 5.62 (m, 1H), 5.20 – 5.12 (m, 1H), 5.11 (d, *J* = 2.5 Hz, 1H), 5.09 – 4.94 (m, 2H), 3.55 – 3.41 (m, 2H), 2.79 (ddt, *J* = 13.4, 6.8, 1.4 Hz, 1H), 2.36 (dd, *J* = 13.5, 7.9 Hz, 1H), 2.07 (dq, *J* = 13.5, 7.4 Hz, 1H), 1.94 – 1.78 (m, 2H), 1.74 (tdd, *J* = 12.4, 8.8, 5.5 Hz, 2H), 1.66 (dt, *J* = 14.7, 7.4 Hz, 1H), 0.82 (t, *J* = 7.4 Hz, 3H),; Rotamer B: 7.39 – 7.33 (m, 4H), 7.33 – 7.27 (m, 1H), 5.77 – 5.62 (m, 1H), 5.20 – 5.12 (m, 1H), 5.11 (d, *J* = 2.5 Hz, 1H), 5.09 – 4.94 (m, 2H), 3.55 – 3.41 (m, 2H), 2.61 (ddt, *J* = 13.5, 6.7, 1.4 Hz, 1H), 2.26 (dd, *J* = 13.7, 7.9 Hz, 1H), 1.94 – 1.78 (m, 3H), 1.74 (tdd, *J* = 12.4,

8.8, 5.5 Hz, 2H), 1.56 (dq, *J* = 14.6, 7.4 Hz, 1H), 0.78 (t, *J* = 7.4 Hz, 3H).; ^{13}C NMR (126 MHz, $CDCl_3$) δ Rotamer A: 153.63, 137.44, 134.73, 128.42 (2C), 128.15, 127.56 (2C), 117.89, 66.45, 65.97, 48.84, 41.69, 33.66, 29.98, 22.45, 8.60. Rotamer B: 154.99, 136.84, 134.45, 128.48 (2C), 127.93, 127.71 (2C), 117.99, 66.90, 65.77, 49.82, 43.13, 35.02, 31.21, 22.00, 8.47.; HRMS (*m/z*): $[M+H]^+$ calcd for $C_{17}H_{24}NO_2$, 274.1777; found, 274.1812.

(*S*)-3-allyl-3-benzyl-1-hydroxypiperidin-2-one (31e)

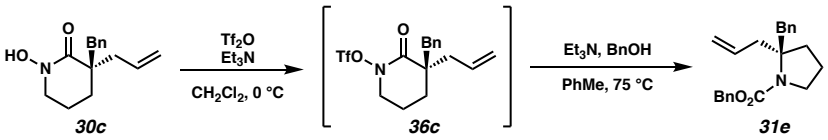

Compound **36c** was prepared from compound **30c** according to the procedure for **36a**, and was used without further purification. Compound **31e** was prepared from **36c** according to the procedure for **31b**. The residue was purified by flash column chromatography (SiO_2, 5% EtOAc in hexanes) to afford **31e** (14 mg, 54% yield) as a yellow solid;. R_f = 0.78 (hexanes/EtOAc = 2:1); $[\alpha]^{25}_D$ +88.6° (*c* 1.00, $CHCl_3$); IR (neat film, NaCl) 3063, 3029, 2954, 2927, 2876, 1697, 1454, 1402, 1357, 1336, 1210, 1103, 917, 748, 700; ^{1}H NMR (500 MHz, $CDCl_3$) δ 7.49 – 7.30 (m, 5H), 7.25 – 7.14 (m, 3H), 7.09 – 7.00 (m, 2H), 5.80 – 5.62 (m, 1H), 5.34 – 5.19 (m, 1H), 5.15 – 5.10 (m, 1H), 5.08 (tdd, *J* = 6.1, 3.9, 2.3 Hz, 1H), 3.53 (d, *J* = 13.2 Hz, 1H), 3.34 – 3.21 (m, 2H), 3.15 (ddd, *J* = 10.5, 8.0, 4.4 Hz, 1H), 3.01 (ddt, *J* = 13.5, 6.5, 1.4 Hz, 1H), 2.67 (t, *J* = 13.8 Hz, 1H), 2.44 (dd, *J* = 13.6, 8.2 Hz, 1H), 1.95 – 1.85 (m, 2H), 1.46 (dddd, *J* = 14.2, 12.1, 5.8, 4.3 Hz, 1H), 0.98 – 0.87 (m, 1H).; ^{13}C NMR (126 MHz, $CDCl_3$) δ Rotamer A: 153.81,

138.33, 137.49, 134.20, 130.45 (2C), 128.45 (2C), 128.02 (2C), 127.83, 127.80 (2C), 126.16, 118.46, 66.64, 66.09, 48.69, 42.42, 42.27, 33.82, 21.82. Rotamer B: 154.81, 138.00, 136.60, 133.78, 130.29 (2C), 128.60 (2C), 128.52 (2C), 128.20 (2C), 128.16, 126.40, 118.61, 67.24, 65.91, 49.72, 43.92, 43.57, 35.25, 21.34.; HRMS (*m*/*z*): $[M+H]^+$ calcd for $C_{22}H_{26}NO_2$, 336.1958; found, 336.1966.

(*R*)-3-allyl-1-hydroxy-3-(3,3,3-trifluoropropyl)piperidin-2-one (31f)

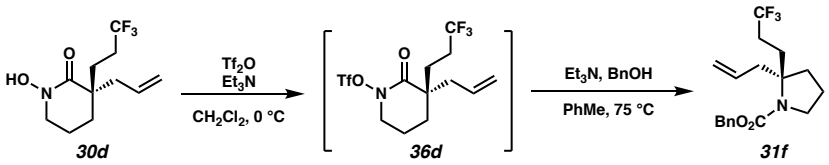

Compound **36d** was prepared from compound **30d** according to the procedure for **36a**, and was used without further purification. Compound **13f** was prepared from **36d** according to the procedure for **31b**. The residue was purified by flash column chromatography (SiO_2, 5% EtOAc in hexanes) to afford **31f** (21 mg, 44% yield) as a colorless oil;. R_f= 0.73 (hexanes/EtOAc = 2:1); $[\alpha]^{25}_D$ –21.1° (*c* 0.33, $CHCl_3$); IR (neat film, NaCl) 3074, 2925, 2852, 1698, 1455, 1403. 1341, 1261, 1142, 1019, 919, 771, 696; ^{1}H NMR (400 MHz, $CDCl_3$) δ 7.45 – 7.27 (m, 5H), 5.77 – 5.59 (m, 1H), 5.20 – 4.95 (m, 4H), 3.60 – 3.38 (m, 2H), 2.76 (ddt, *J* = 13.6, 7.0, 1.3 Hz, 1H), 2.47 – 2.24 (m, 2H), 2.10 – 1.90 (m, 3H), 1.90 – 1.66 (m, 4H).; ^{13}C NMR (101 MHz, $CDCl_3$) δ Rotamer A: 153.82, 137.19, 133.75, 128.59 (2C), 128.37, 127.84 (2C), 127.46 (q, *J* = 276.0 Hz), 118.96, 66.48, 64.99, 48.75, 41.64, 34.51, 29.76 (q, *J* = 2.7 Hz), 29.48 (q, *J* = 28.6 Hz), 22.28. Rotamer B: 154.76, 136.36, 133.44, 128.72 (2C), 128.37, 128.03 (2C), 127.46 (d, *J* =

276.0 Hz), 119.08, 67.47, 64.22, 49.76, 43.39, 35.75, 29.76 (d, J = 2.7 Hz), 29.48 (d, J = 28.6 Hz), 21.91.; ^{19}F NMR (282 MHz, $CDCl_3$) δ -66.24 (dt, J = 17.7, 10.5 Hz).;

(2*S*)-2-methyl-2-(2-propene-1-yl)-pyrrolidine hydrochloride (37)

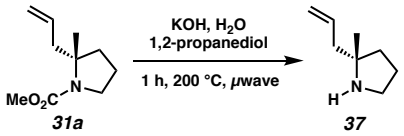

31a *37*

To a 10-20 mL microwave vial charged with a magnetic stirring bar and a solution of **31a** (299 mg, 1.63 mmol) in 1,2-propanediol (12.5 mL) was added KOH (4.12 g, 73.4 mmol) and H_2O (1.63 mL) at room temperature, after which an exotherm was observed. The reaction mixture was submitted to microwave irradiation for 1 h at 200 ˚C. The reaction mixture was diluted with H_2O (15 mL) and extracted with CH_2Cl_2 (30 mL × 2). The combined organic layers were washed with brine (100 mL × 1), dried over sodium sulfate, and filtered, followed by the addition of a solution of HCl in Et_2O (2.0 M, 2.45 mL, 4.89 mmol) to form the HCl salt. This resulting mixture was concentrated under reduced pressure to afford **37** (257 mg, 98%) as a hygroscopic pale brown solid which was carried on without further purification; R_f = 0.27 (CH_2Cl_2/MeOH/NH_4OH = 6:1:0.1);

(*S*)-2-Allyl-1-{2-(3,4-dimethoxyphenyl)allyl}-2-methylpyrrolidine (41)

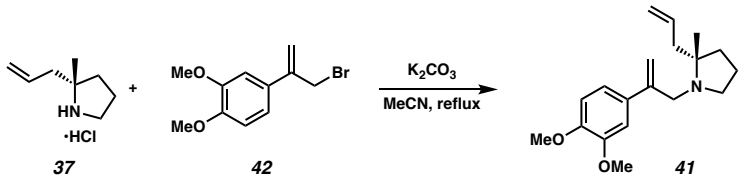

To a 100 mL round bottom flask charged with a magnetic stirring bar and a solution of **37** (606 mg, 3.75 mmol) in CH_3CN (27.5 mL) was added K_2CO_3 (2.07 g, 15.0 mmol) and a solution of freshly prepared allyl bromide **42**[15] (1.93 g, 7.50 mmol) in CH_3CN (10.0 mL) at room temperature under N_2 atmosphere. The mixture was heated to reflux and stirred for 10 hours, and then the reaction mixture was cooled to room temperature before the solvent was removed under reduced pressure. The residue was diluted with Et_2O (40 mL), washed with H_2O (40 mL × 1) and brine (40 mL × 1), dried over sodium sulfate, filtered, and concentrated under reduced pressure to afford the crude product. The residue was purified by flash column chromatography (SiO_2, CH_2Cl_2 to 10% EtOAc in CH_2Cl_2) to afford **41** (939 mg, 83%) as an orange oil; R_f= 0.50 (hexanes/EtOAc = 2:1); $[\alpha]^{25}_D$ –17.8° (*c* 1.00, $CHCl_3$); IR (neat film, NaCl) 3074, 2959, 2833, 1579, 1516, 1463, 1257, 1222, 1144, 1028, 904, 809, 766; ^{1}H NMR (500 MHz, $CDCl_3$) δ 7.12 (d, *J* = 2.1 Hz, 1H), 7.07 (dd, *J* = 8.3, 2.1 Hz, 1H), 6.82 (d, *J* = 8.3 Hz, 1H), 5.83 (m, 1H), 5.30 (app s, 1H), 5.20 (app s, 1H), 5.07-4.97 (complex m, 2H), 3.89 (s, 3H), 3.88 (s, 3H), 3.56 (d, *J* = 13.2 Hz, 1H), 3.26 (d, *J* = 13.3, 1H), 2.82 (m, 1H), 2.54 (m, 1H), 2.20 (d, *J* = 7.3 Hz, 2H), 1.79 (m, 1H), 1.65 (complex m, 2H), 1.46 (m, 1H), 1.00 (s, 3H); ^{13}C NMR (126 MHz, $CDCl_3$) δ 148.5, 148.5, 145.9, 136.2, 133.8, 118.8, 116.7, 113.0, 110.7, 110.0, 62.4, 55.9, 55.9,

53.5, 50.7, 42.6, 36.8, 20.8, 19.9; HRMS (*m*/*z*): $[M+H]^+$ calcd for $C_{19}H_{28}NO_2$, 302.2115; found, 302.2117.

(*S*)-6-(3,4-Dimethoxyphenyl)-8a-methyl-1,2,3,5,8,8a-hexahydroindolizine (40)

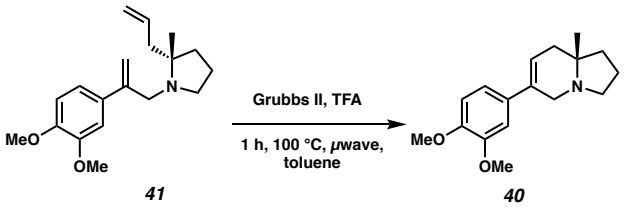

41 *40*

To two 10-20 mL microwave vial charged with a magnetic stirring bar and a solution of **41** (445 mg, 1.48 mmol) in toluene (29.5 mL) were added TFA (126 mL, 1.63 mmol) at room temperature followed by addition of Grubbs 2nd generation catalyst (126 mg, 148 μmol). The reaction mixture was submitted to microwave irradiation for 1 h at 100 ˚C. Aqueous 1N HCl (30 mL) was added to the reaction mixture to adjust the pH to <1. Resultant two layers were separated and the organic phase was washed with 1N HCl (30 mL × 1). Aqueous 6N NaOH was added to the combined aqueous layers to adjust the pH to >14, and the mixture was extracted with CH_2Cl_2 (60 mL × 1). The combined organic layers were washed with brine (150 mL × 1), dried over sodium sulfate, filtered, and concentrated under reduced pressure to afford the crude product. The residue was purified by flash column chromatography (SiO_2, 2% to 5% to 10% MeOH in CH_2Cl_2, 0.3% Et_3N) to afford **40** (411 mg, 92%) as a pale brown solid; R_f = 0.50 (hexanes/EtOAc = 2:1); mp = 51-53 ˚C; $[\alpha]^{25}_D$ +51.8˚ (*c* 1.00, $CHCl_3$); IR (neat film, NaCl) 2923, 2853, 1602, 1518, 1456, 1251, 1213, 1168, 1146, 1024, 794, 732; ^{1}H NMR (500 MHz, $CDCl_3$) δ 6.92-6.88 (complex m, 2H), 6.82 (d, *J* = 8.6 Hz, 1H), 6.02 (m, 1H), 3.90 (s, 3H), 3.88

(s, 3H), 3.66 (d, *J* = 16.8 Hz, 1H), 3.47 (d, *J* = 16.9, 1H), 3.04 (m, 1H), 2.77 (m, 1H), 2.32 (d, *J* = 17.8 Hz, 1H), 2.13 (ddd, *J* = 17.5, 5.9, 2.7 Hz, 1H), 1.93-1.83 (complex m, 2H), 1.79 (m, 1H), 1.69 (m, 1H), 1.02 (s, 3H); ^{13}C NMR (126 MHz, $CDCl_3$) δ 148.8, 148.3, 133.2, 133.1, 120.7, 117.2, 111.0, 108.5, 57.0, 55.9, 55.9, 50.4, 47.9, 38.5, 35.8, 20.0, 17.2; HRMS (*m/z*): $[M+H]^+$ calcd for $C_{17}H_{24}NO_2$, 274.1802; found, 274.1817.

2.8 NOTES & REFERENCES

[1] Vitaku, E.; Smith, D. T.; Njardarson, J. T. *J. Med. Chem.* **2014**, *57*, 10257–10274.

[2] Lovering, F.; Bikker, J.; Humblet, C. *J. Med. Chem.* **2009**, *52*, 6752–6756.

[3] Calaza, M. I.; Cativiela, C. *Eur. J. Org. Chem.* **2008**, 3427–3448.

[4] Seebach, D.; Boes, M.; Naef, R.; Schweizer, W. B. *J. Am. Chem. Soc.* **1983**, *105*, 5390–5398.

[5] a) Winter, D. K.; Drouin, A.; Lessard, J.; Spino, C. *J. Org. Chem.* **2010**, *75*, 2610–2618. b) Drouin, A.; Winter, D. K.; Pichette, S.; Aubert-Nicol, S.; Lessard, J.; Spino, C. *J. Org. Chem.* **2011**, *76*, 164–169. c) Pichette, S.; Aubert-Nicol, S.; Lessard, J.; Spino, C. *J. Org. Chem.* **2012**, *77*, 11216–11226.

[6] Behenna, D. C.; Stoltz, B. M. *J. Am. Chem. Soc.* **2004**, *126*, 15044–15045.

[7] Mohr, J. T.; Behenna, D. C.; Harned, A. M.; Stoltz, B. M. *Angew. Chem. Int. Ed.* **2005**, *44*, 6924–6927.

[8] Streuff, J.; White, D. E.; Virgil, S. C.; Stoltz, B. M. *Nat. Chem.* **2010**, *2*, 192–196.

[9] Behenna, D. C.; Liu, Y.; Yurino, T.; Kim, J.; White, D. E.; Virgil, S. C.; Stoltz, B. M. *Nat. Chem.* **2012**, *4,* 130–133.

[10] Bennett, N. B.; Duquette, D. C.; Kim, J.; Liu, W.–B.; Marziale, A. N.; Behenna, D. C.; Virgil, S. C.; Stoltz, B. M. *Chem. Eur. J.* **2013**, *19*, 4414–4418.

[11] Marziale, A. N.; Duquette, D. C.; Craig, R. A.; Kim, K. E.; Liniger, M.; Numajiri, Y. Stoltz, B. M. *Adv. Synth. Catal.* **2015**, *357*, 2238–2245.

[12] Lu, Y.; Goldstein, E. L.; Stoltz, B. M. *Org. Lett.* **2018**, *20*, 5657–5660.

[13] Roy, A.; Roberts, F. G.; Wilderman, P. R.; Zhou, K.; Peters, R. J.; Coates, R. M. *J. Am. Chem. Soc.* **2007**, *129*, 12453–12460.

[14] Ali, M.; Bhutani, K. K. *Phytochemistry* **1987**, *26*, 2089–2092.

[15] Gong, W.; Liu, Y.; Xue, J.; Xie, Z.; Li, Y. *Chem. Lett.* **2012**, *41*, 1597–1599.

[16] Senter, T. J.; Schulte, M. L.; Konkol, L. C.; Wadzinski, T. E.; Lindsley, C. W. *Tetrahedron Lett.* **2013**, *54*, 1645–1648.

[17] Pangborn, A. M.; Giardello, M. A.; Grubbs, R. H.; Rosen, R. K.; Timmers, F. *J. Organometallics* **1996**, *15*, 1518–1520.

[18] Firmansjah, L.; Fu, G. C. *J. Am. Chem. Soc.*, **2007**, *129*, 11340–11341.

[19] Krout, M. R.; Mohr, J. T.; Stoltz, B. M. *Org. Synth.* **2009**, *86*, 181–205.

[20] McDougal, N. T.; Streuff, J.; Mukherjee, H.; Virgil, S. C.; Stoltz, B. M. *Tetrahedron Lett.* **2010**, *51*, 5550–5554.

APPENDIX 2-1

Spectra Relevant to Chapter 2:

Synthesis of enantioenriched 2,2-disubstituted pyrrolidines via sequential asymmetric allylic alkylation and ring contraction

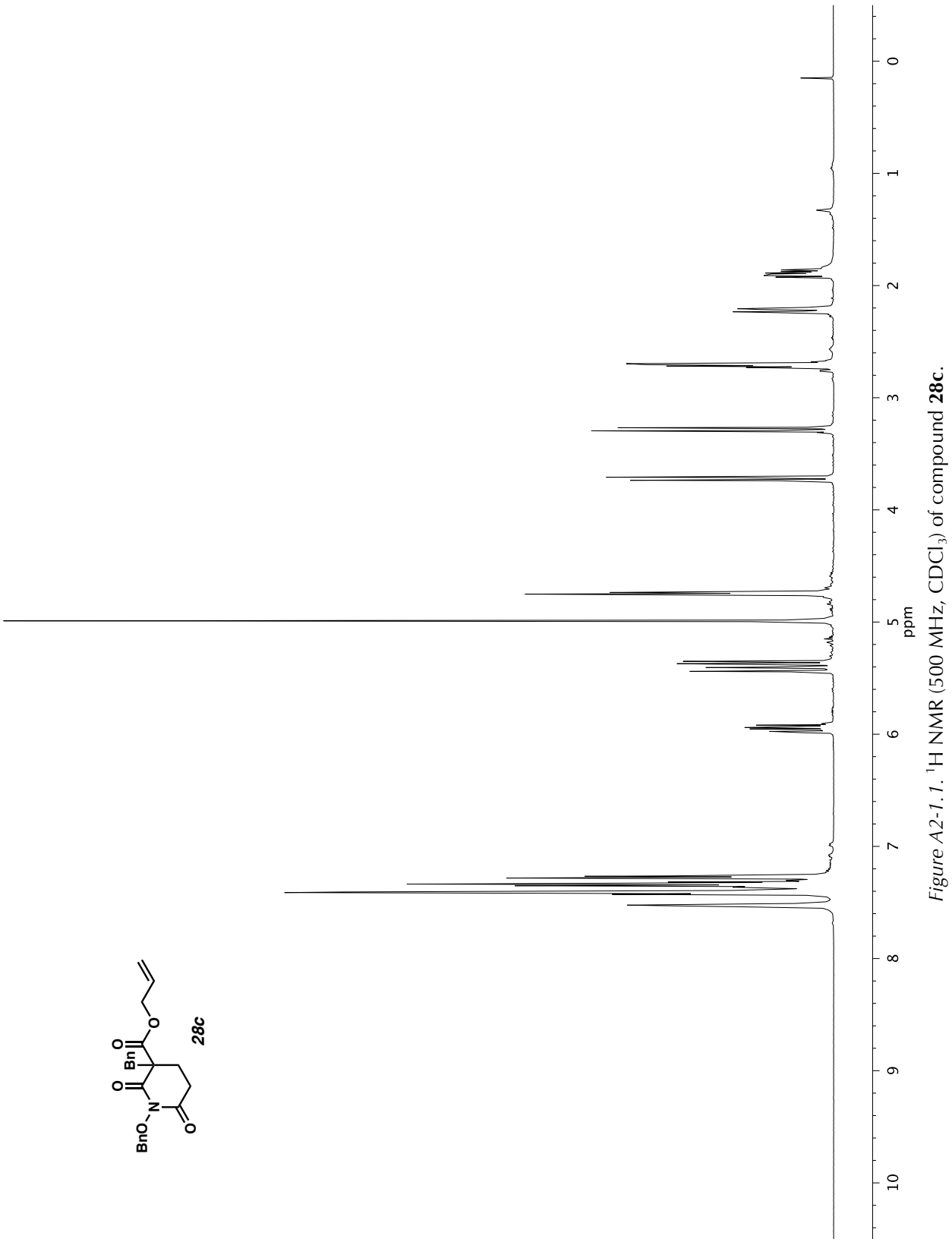

Figure A2-1.1. ^{1}H NMR (500 MHz, $CDCl_3$) of compound **28c**.

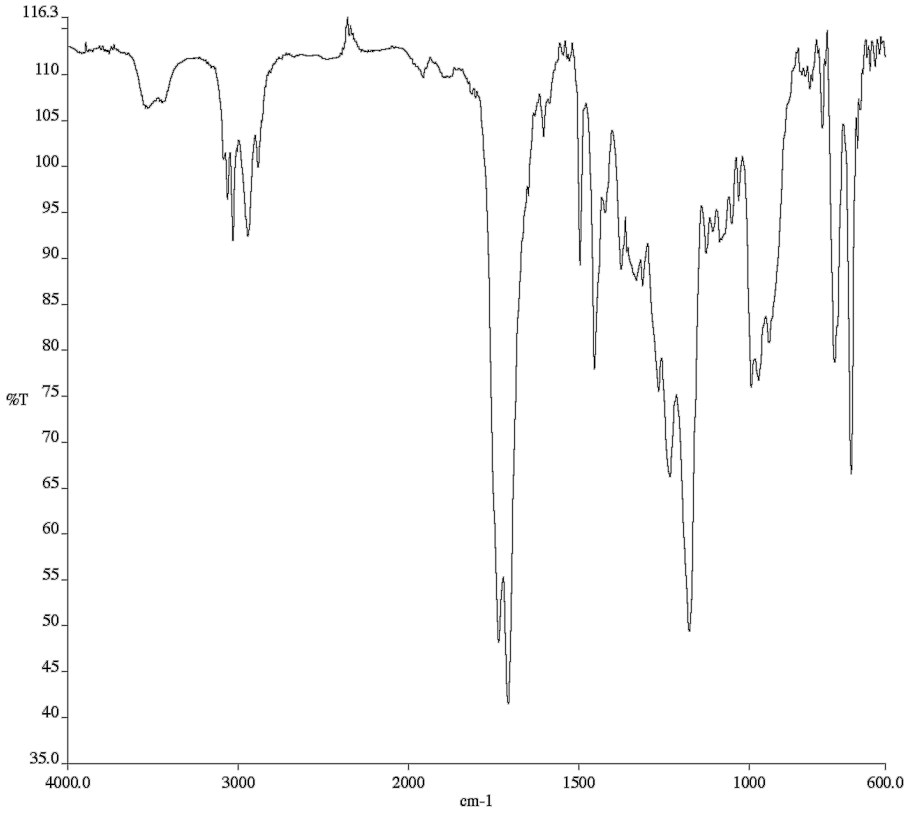

Figure A2-1.2. Infrared spectrum (Thin Film, NaCl) of compound **28c**.

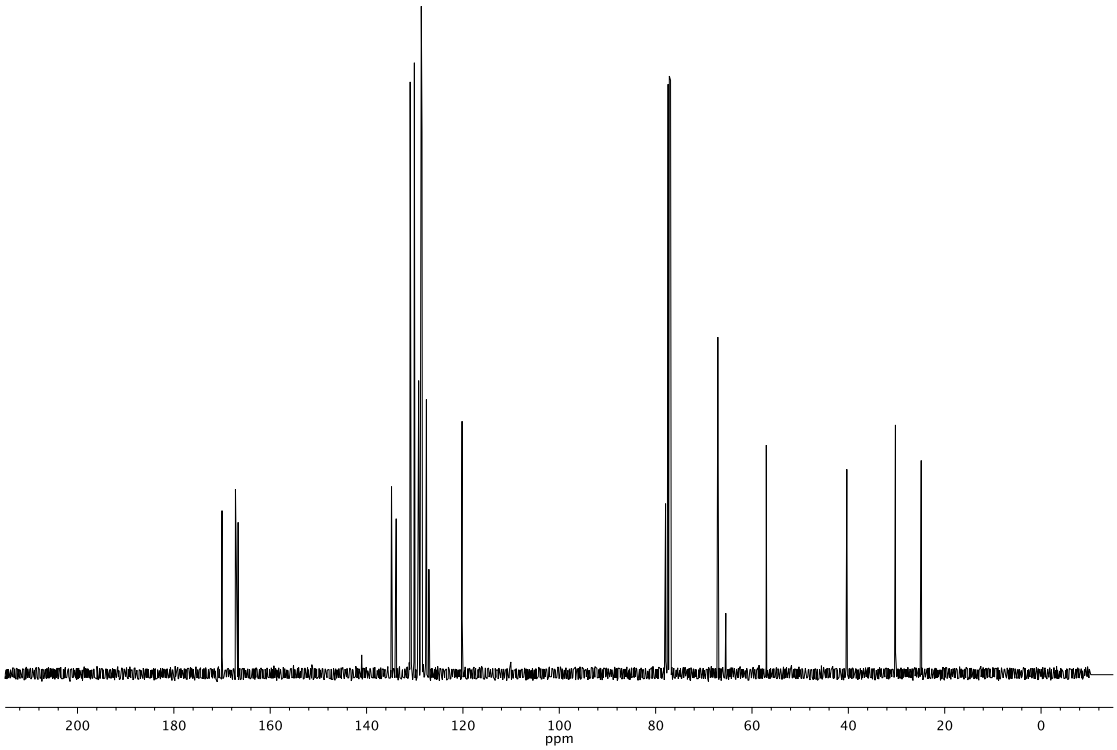

Figure A2-1.3. ^{13}C NMR (126 MHz, $CDCl_3$) of compound **28c**.

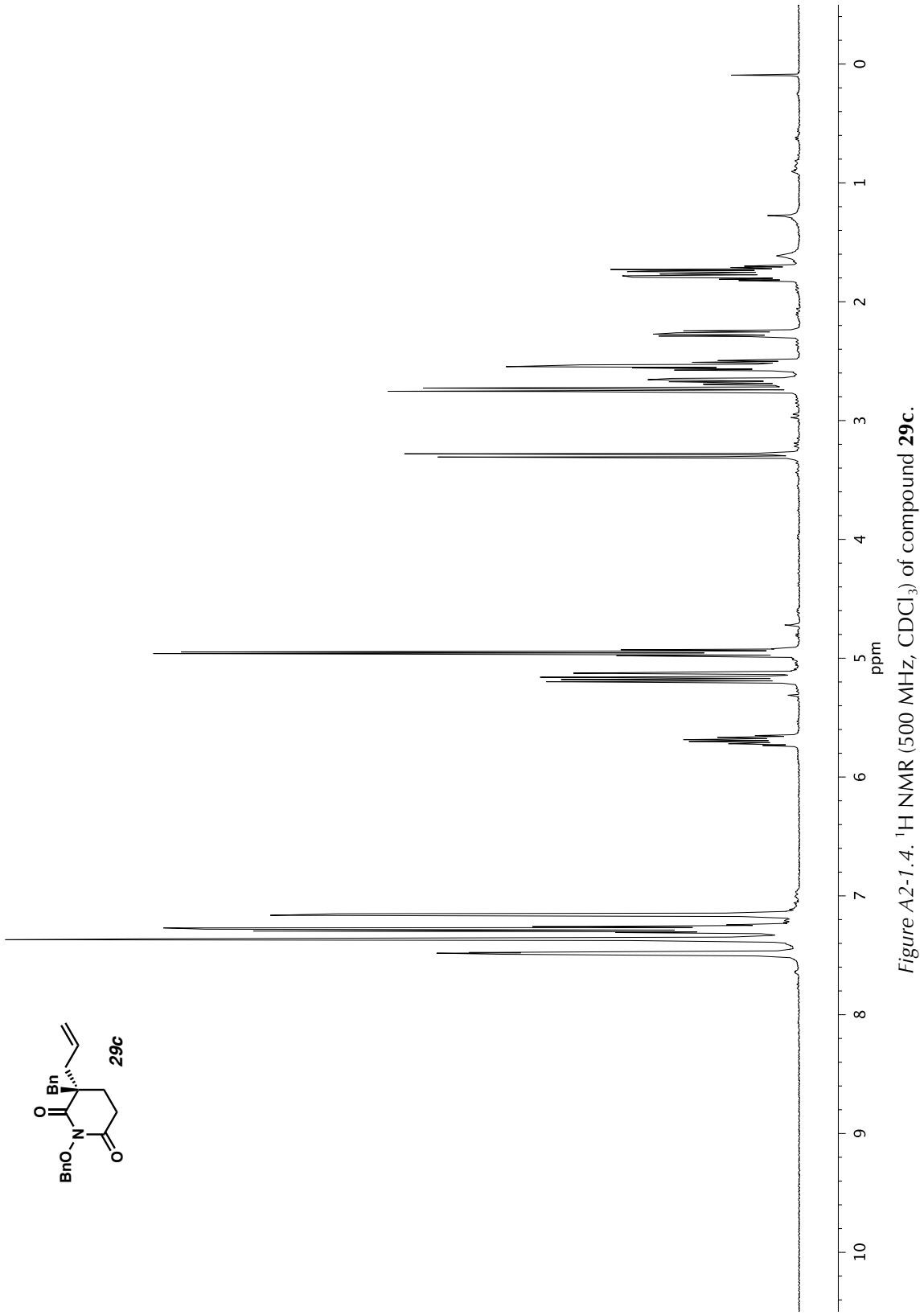

Figure A2-1.4. ^{1}H NMR (500 MHz, $CDCl_3$) of compound **29c**.

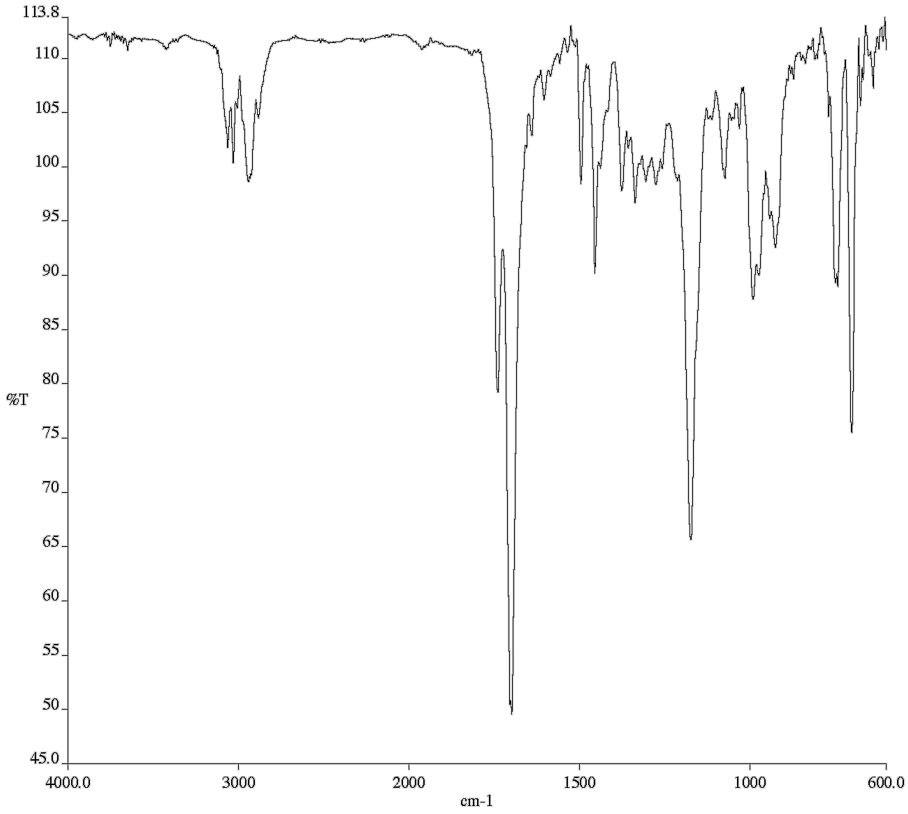

Figure A2-1.5. Infrared spectrum (Thin Film, NaCl) of compound **29c**.

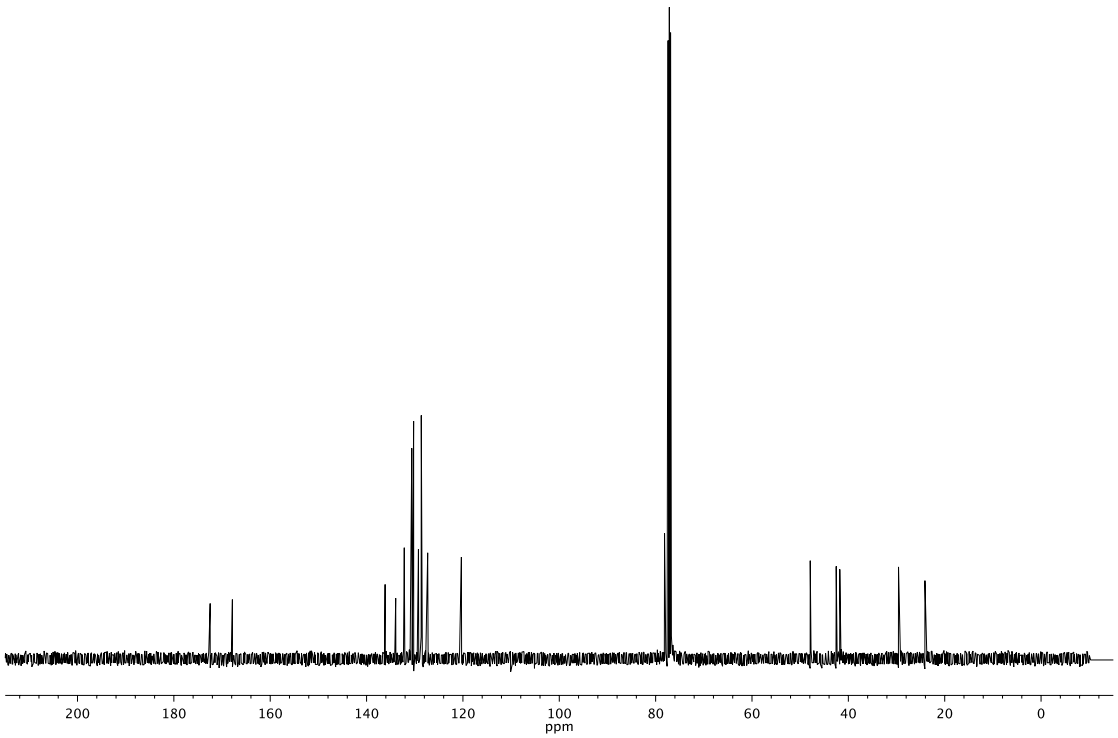

Figure A2-1.6. ^{13}C NMR (126 MHz, $CDCl_3$) of compound **29c**.

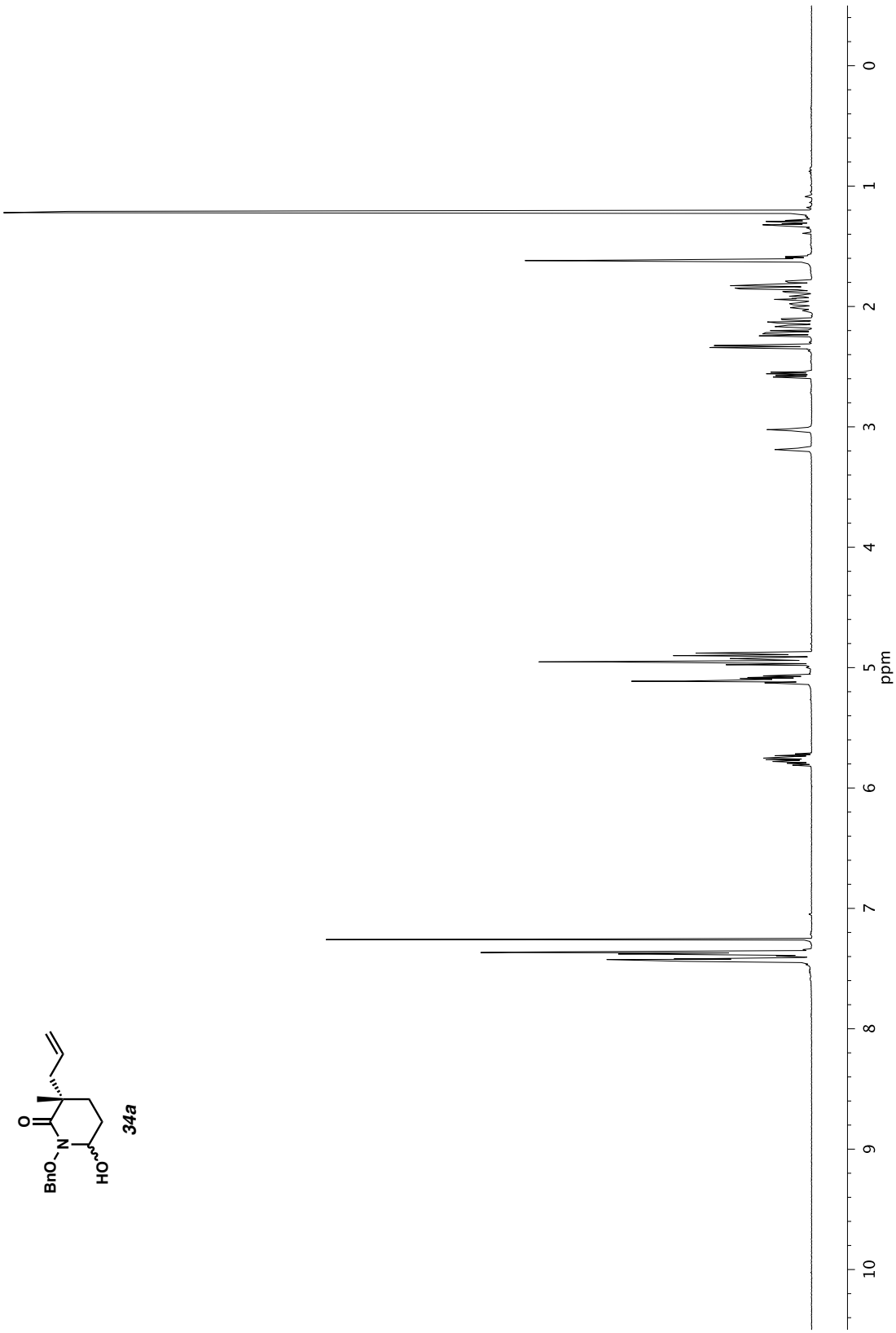

34a

Figure A2-1.7. ^{1}H NMR (500 MHz, $CDCl_3$) of compound **34a**.

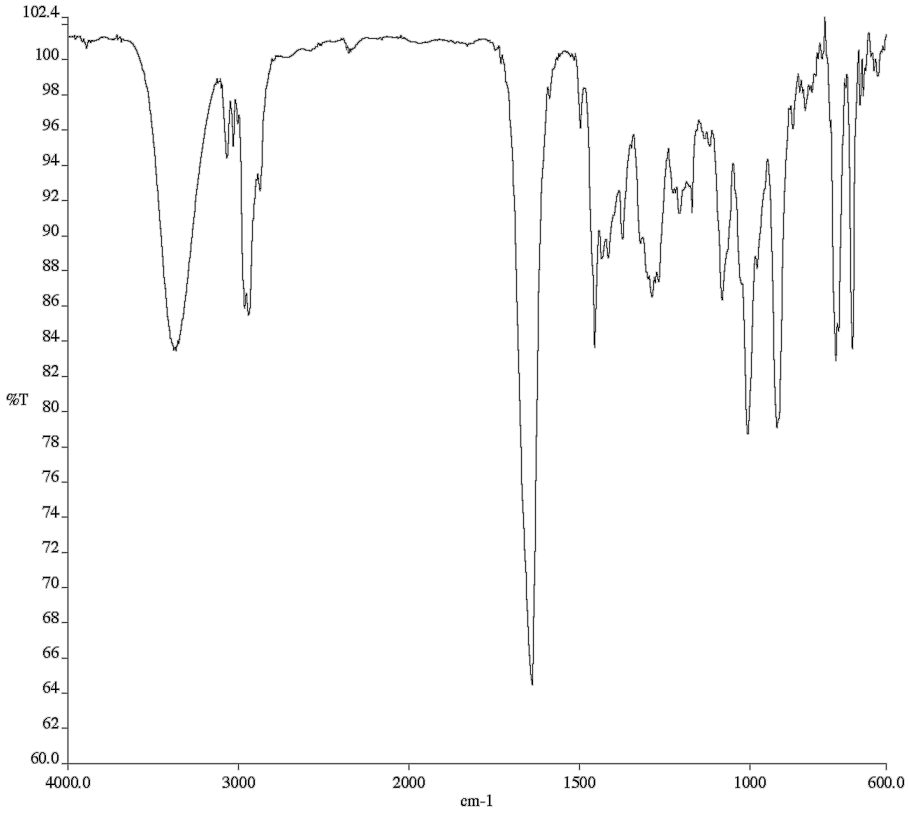

Figure A2-1.8. Infrared spectrum (Thin Film, NaCl) of compound **34a**.

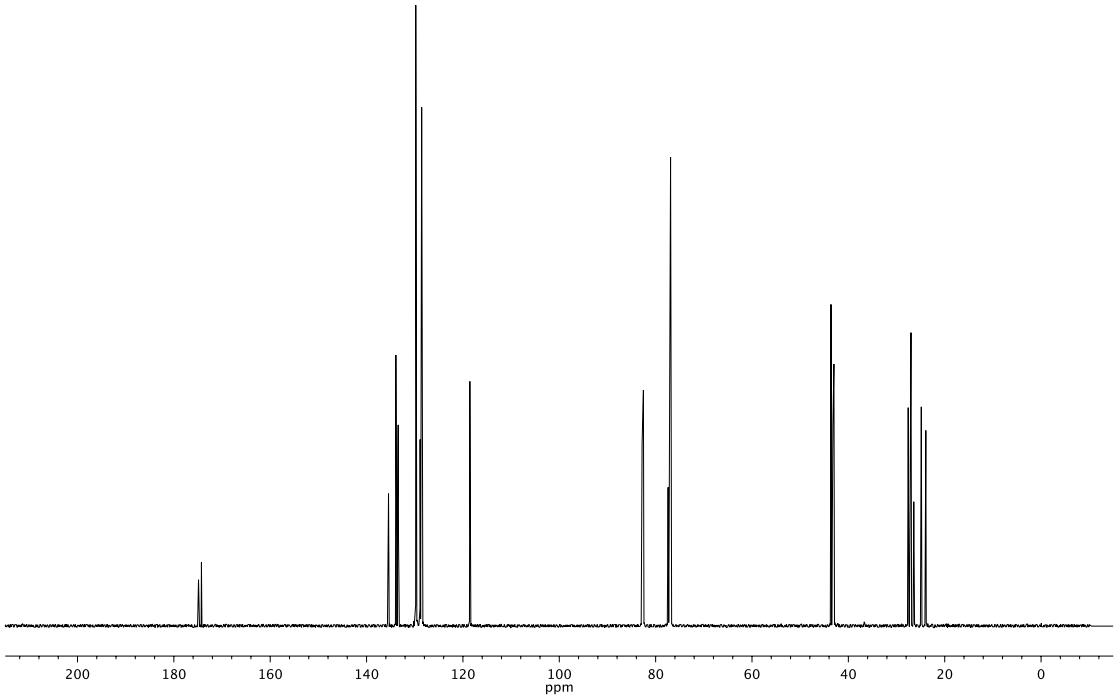

Figure A2-1.9. ^{13}C NMR (126 MHz, $CDCl_3$) of compound **34a**.

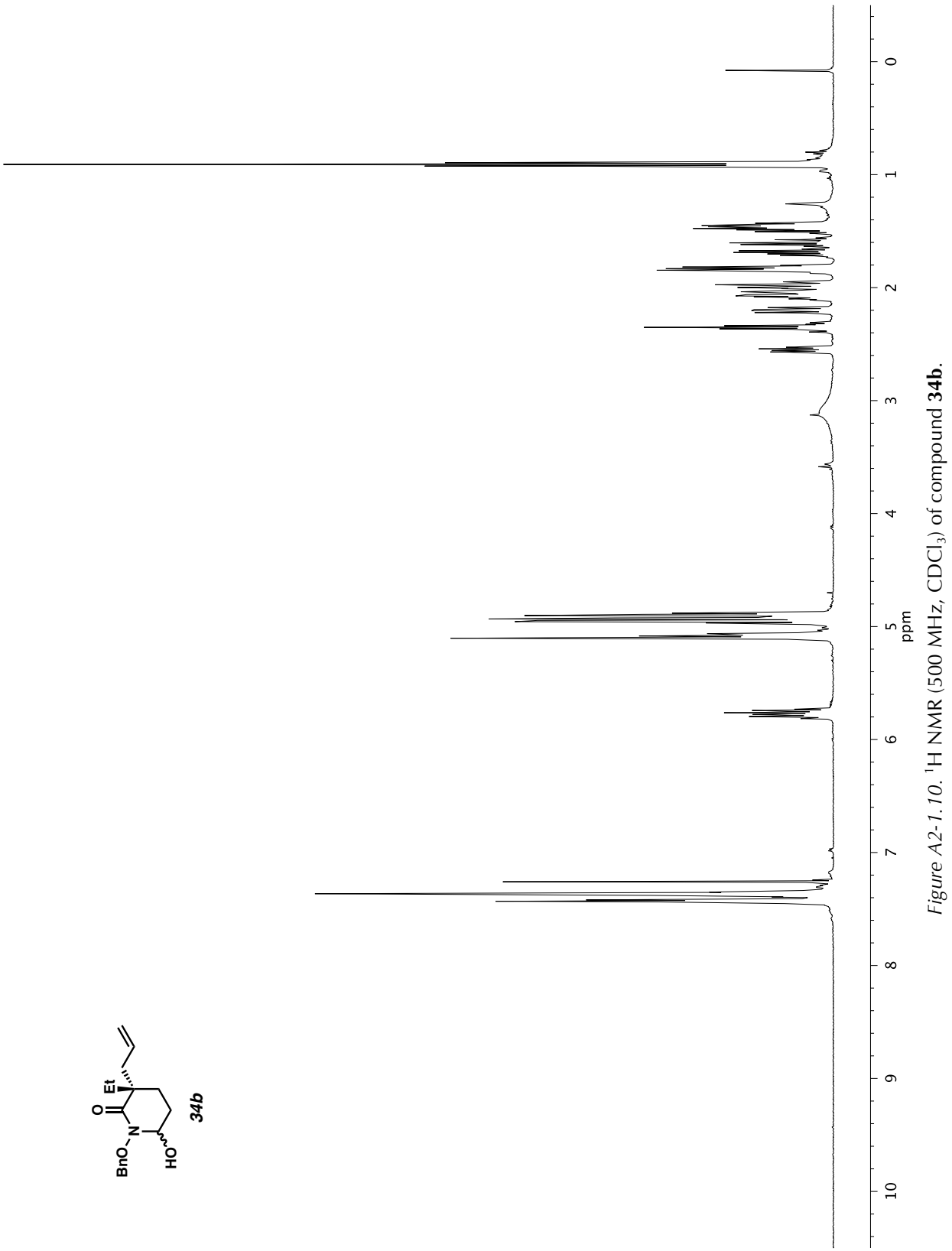

Figure A2-1.10. ^{1}H NMR (500 MHz, $CDCl_3$) of compound **34b**.

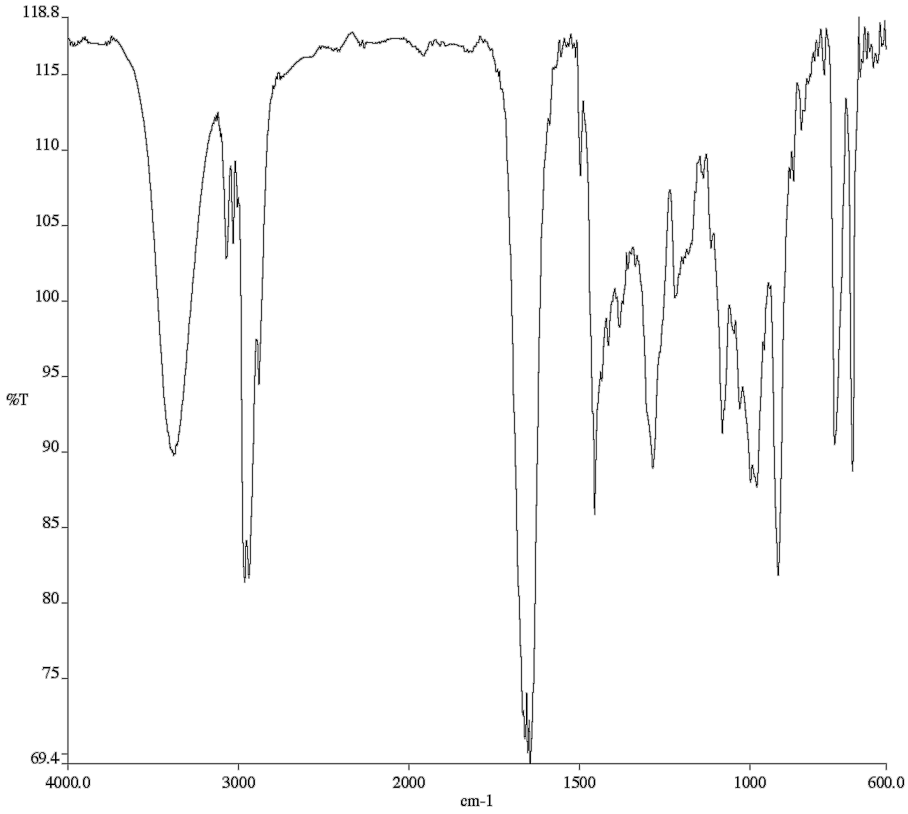

Figure A2-1.11. Infrared spectrum (Thin Film, NaCl) of compound **34b**.

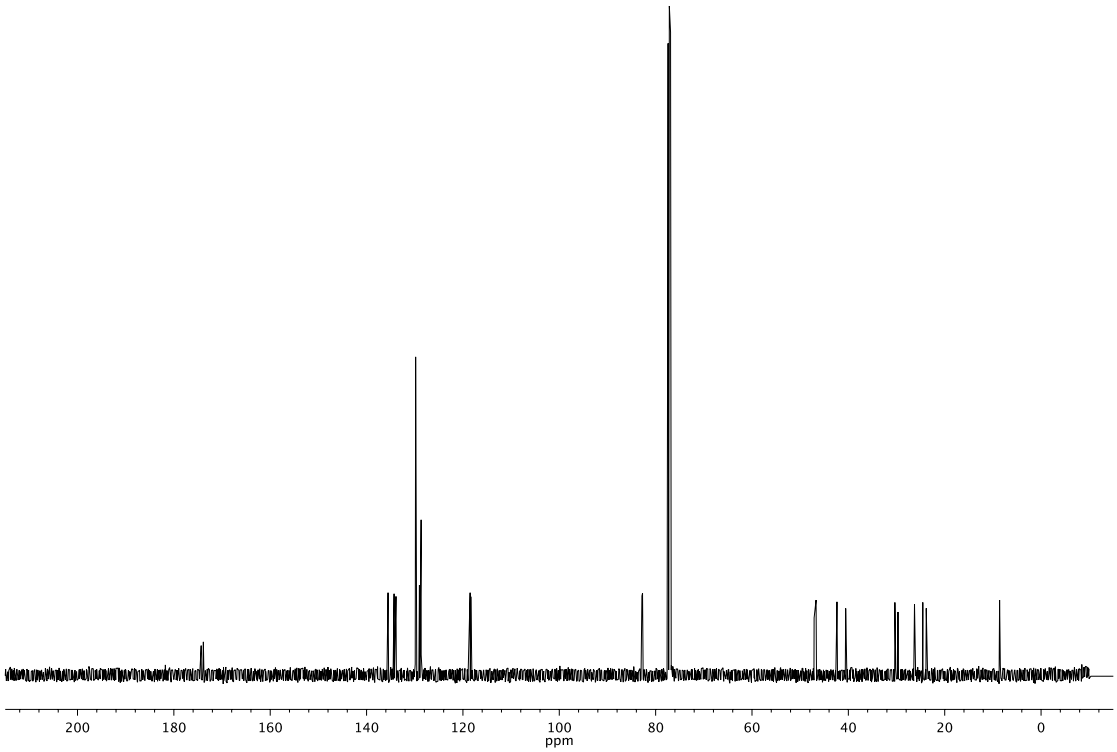

Figure A2-1.12. ^{13}C NMR (126 MHz, $CDCl_3$) of compound **34b**.

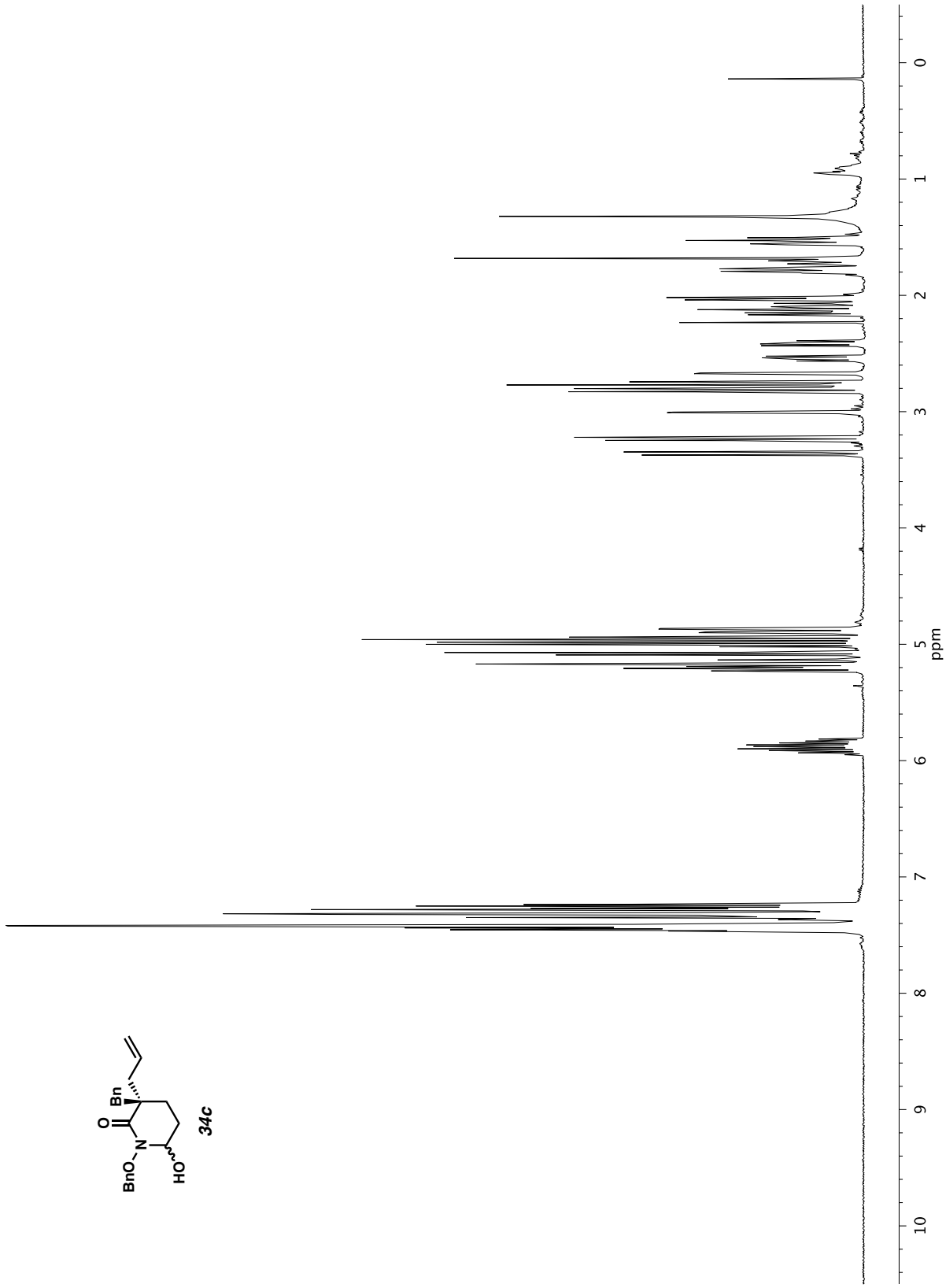

Figure A2-1.13. ^{1}H NMR (500 MHz, $CDCl_3$) of compound **34c**.

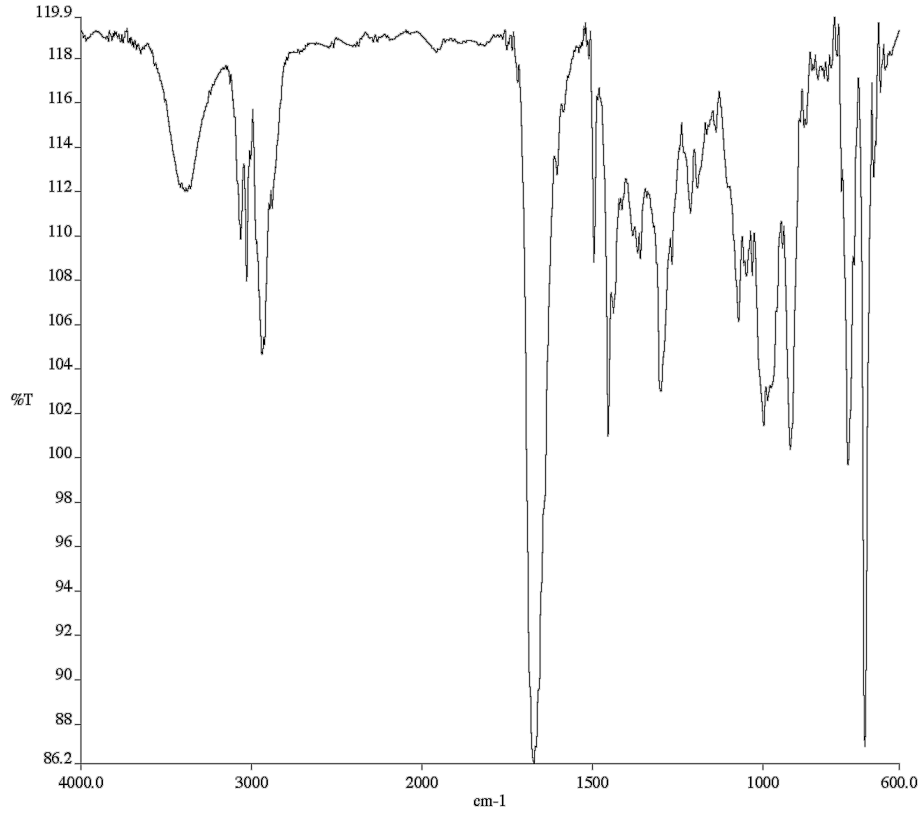

Figure A2-1.14. Infrared spectrum (Thin Film, NaCl) of compound **34c**.

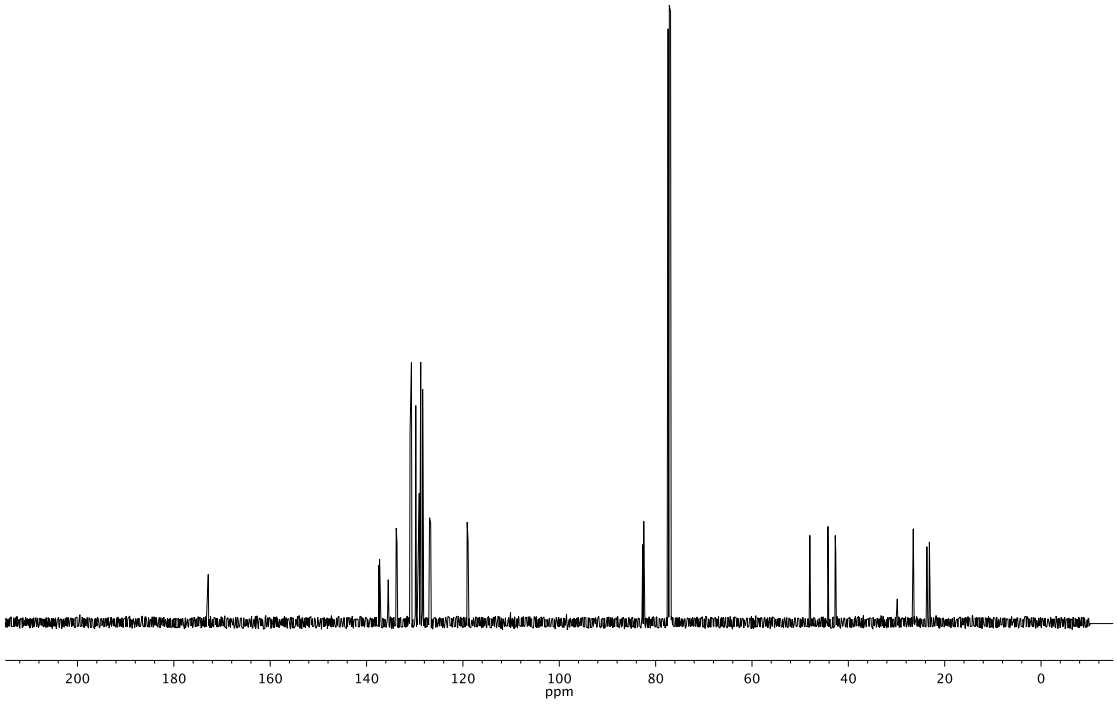

Figure A2-1.15. ^{13}C NMR (126 MHz, $CDCl_3$) of compound **34c**.

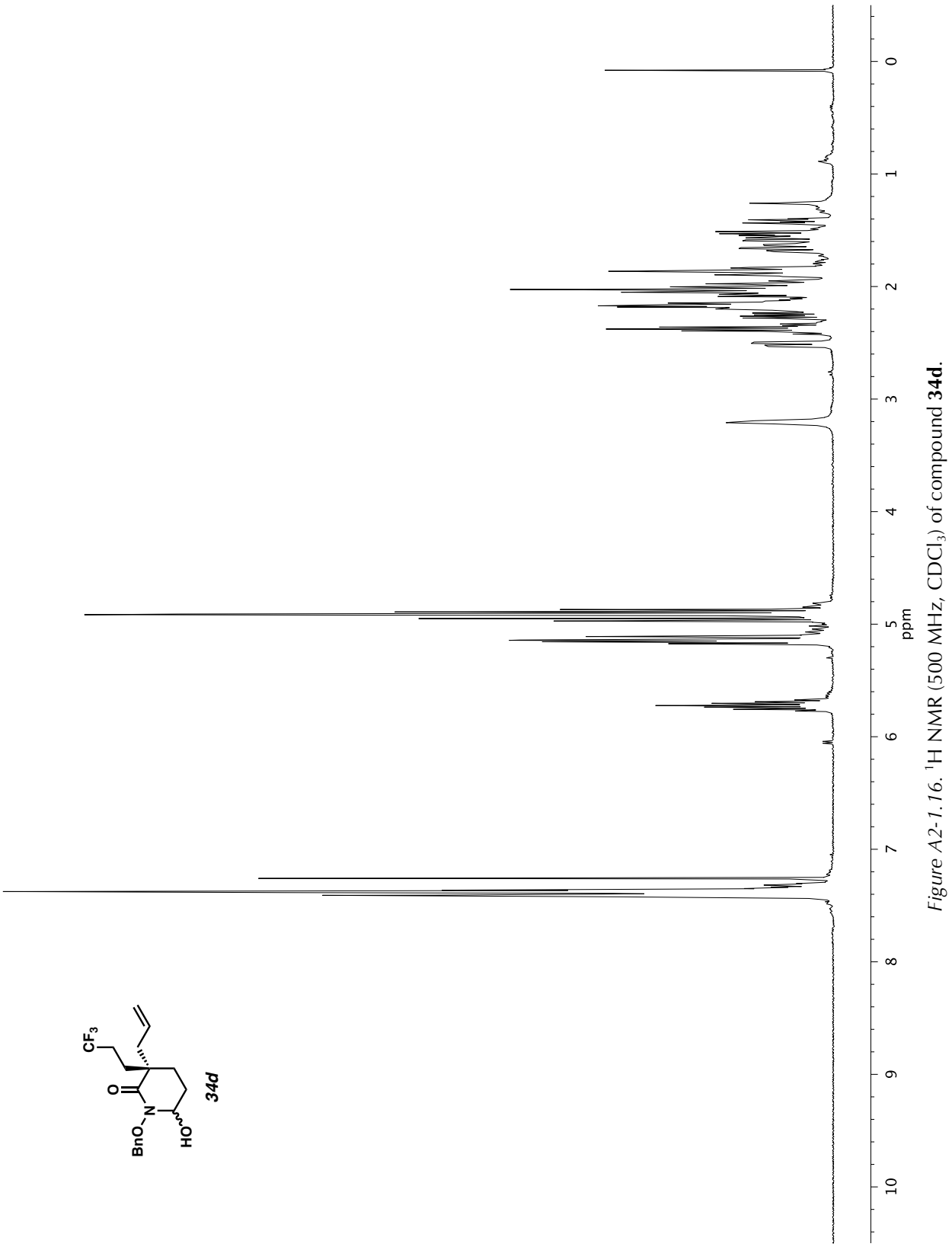

Figure A2-1.16. ^{1}H NMR (500 MHz, $CDCl_3$) of compound **34d**.

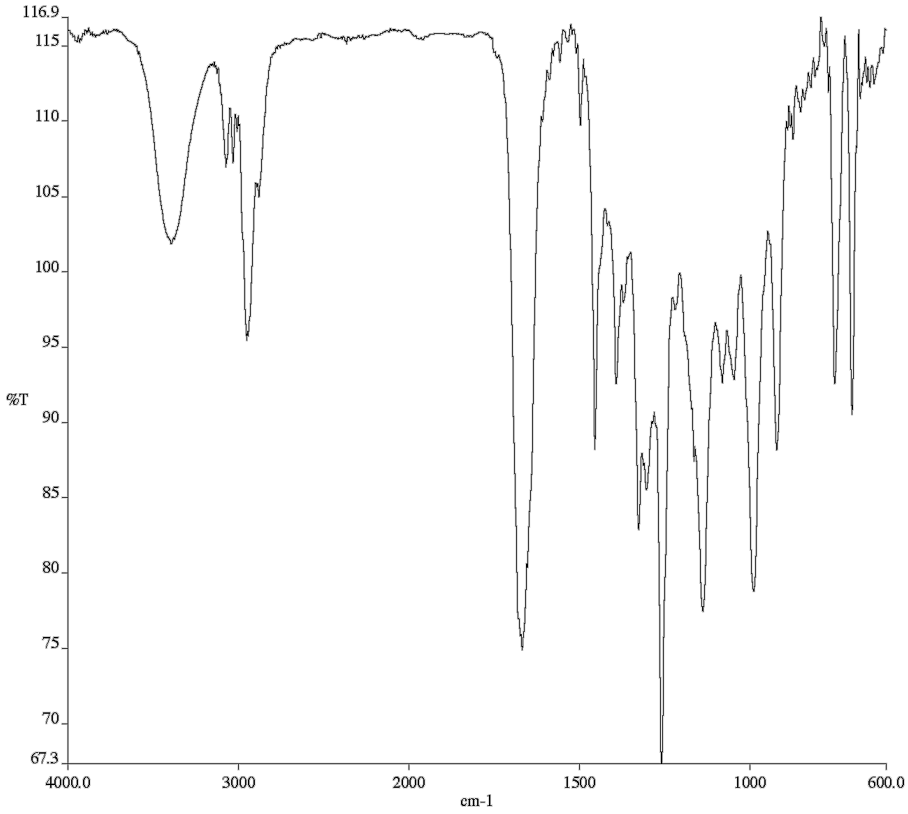

Figure A2-1.17. Infrared spectrum (Thin Film, NaCl) of compound **34d**.

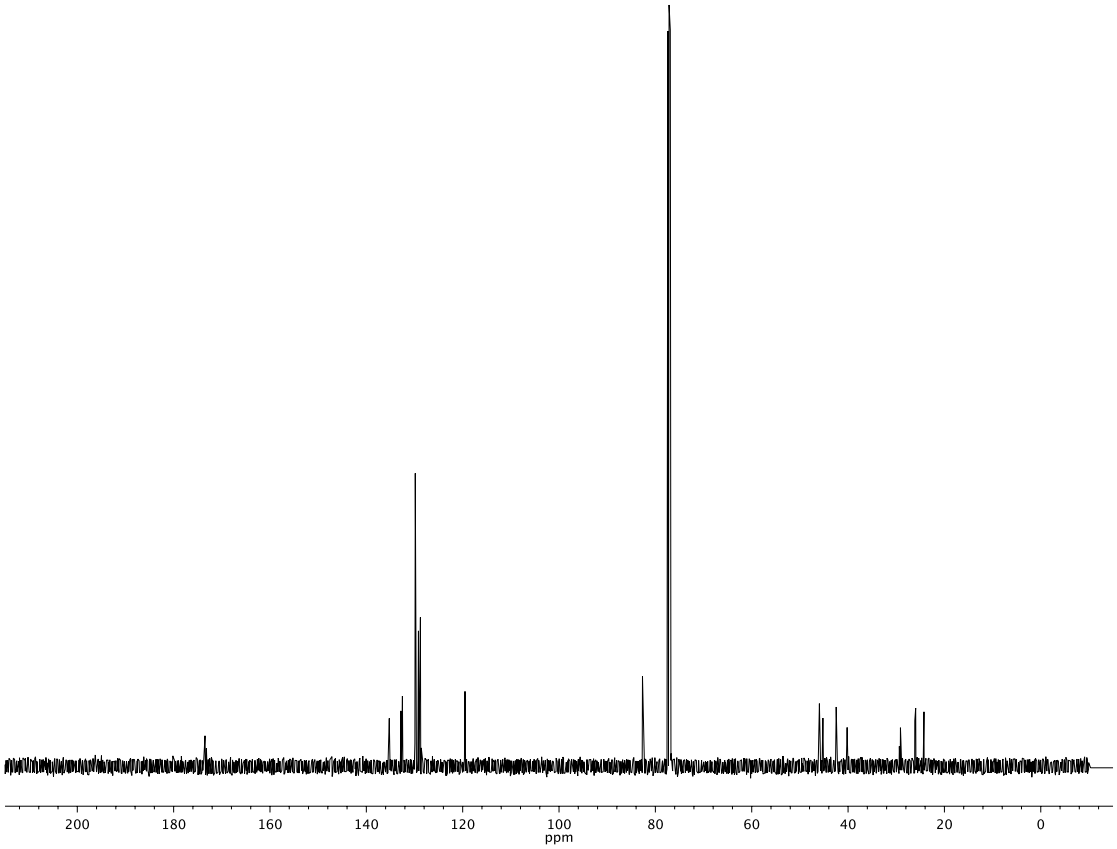

Figure A2-1.18. ^{13}C NMR (126 MHz, $CDCl_3$) of compound **34d**.

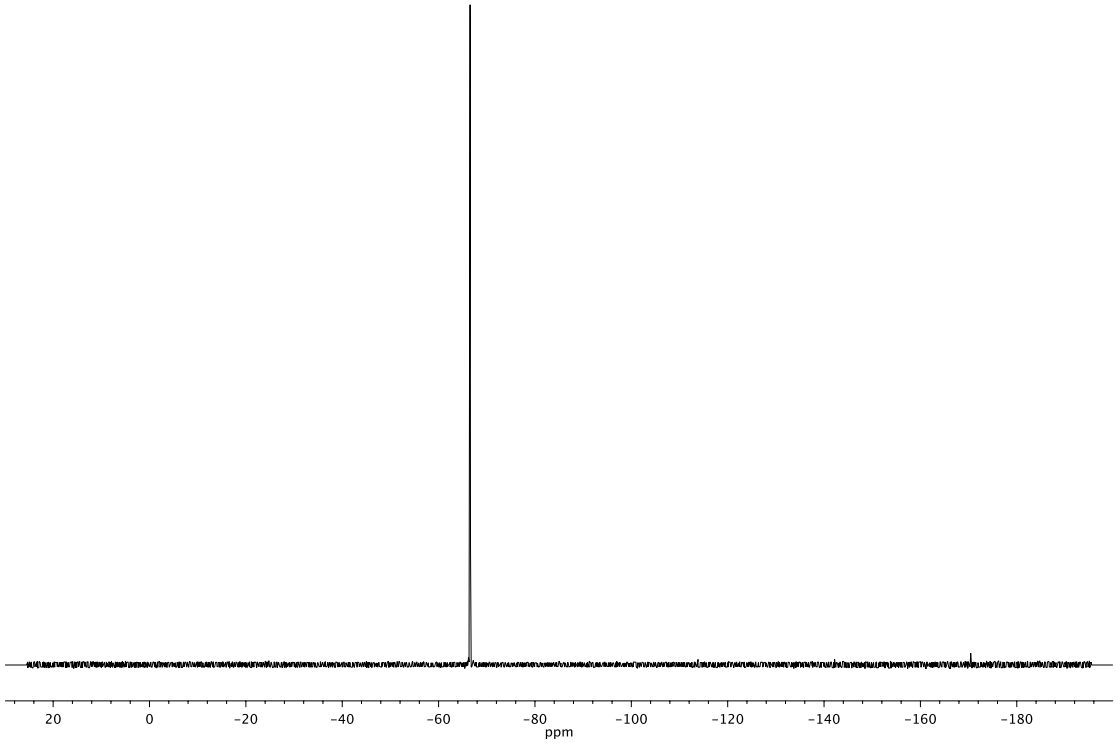

Figure A2-1.19. ^{19}F NMR (282 MHz, $CDCl_3$) of compound **34d**.

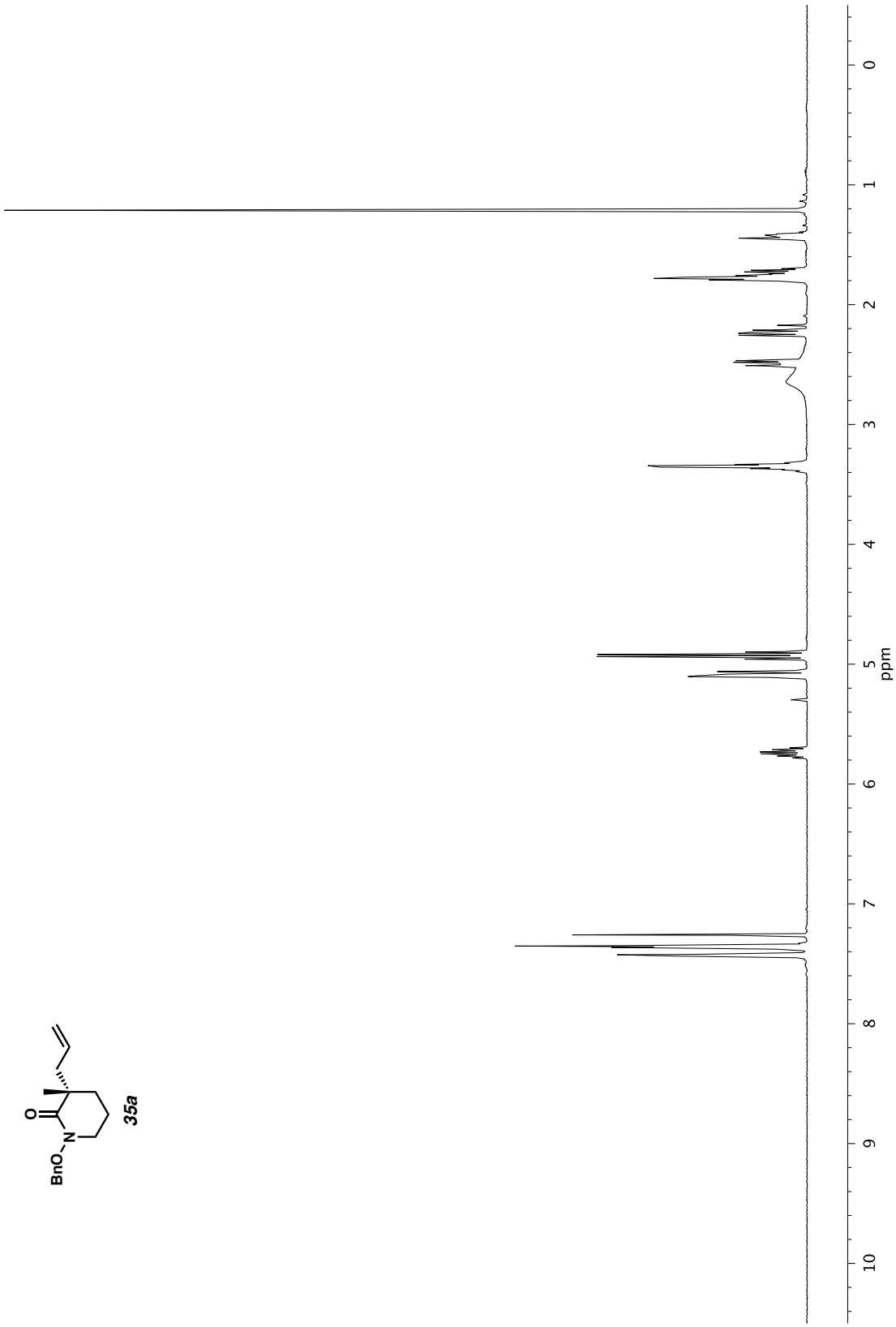

Figure A2-1.20. ^{1}H NMR (500 MHz, $CDCl_3$) of compound **35a**.

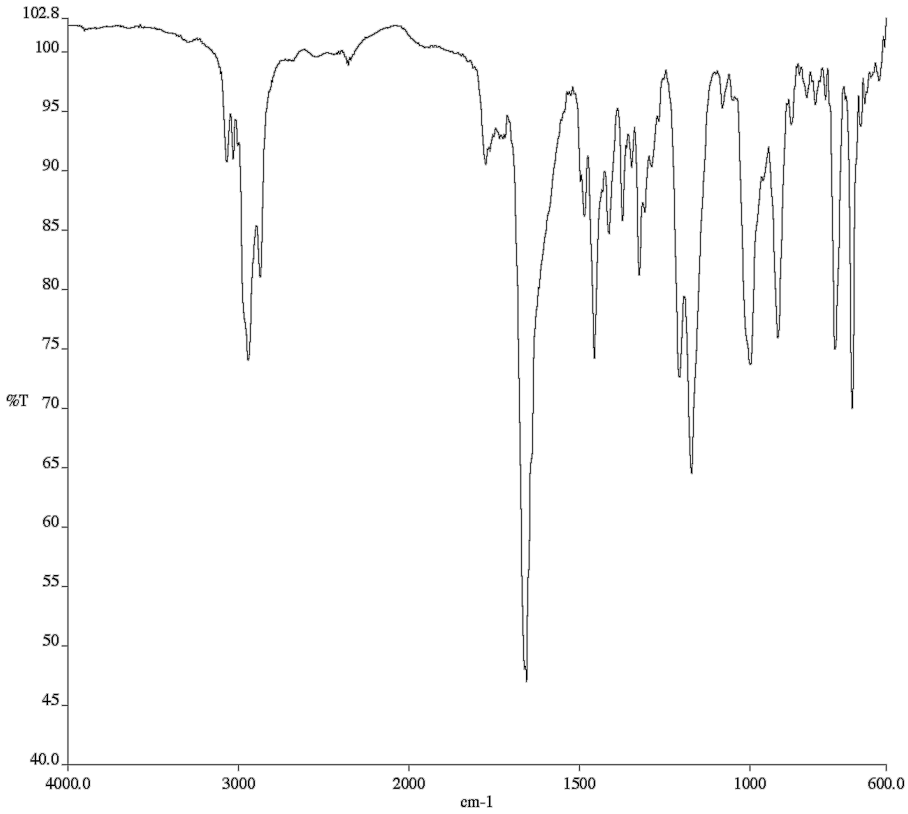

Figure A2-1.21. Infrared spectrum (Thin Film, NaCl) of compound **35a**.

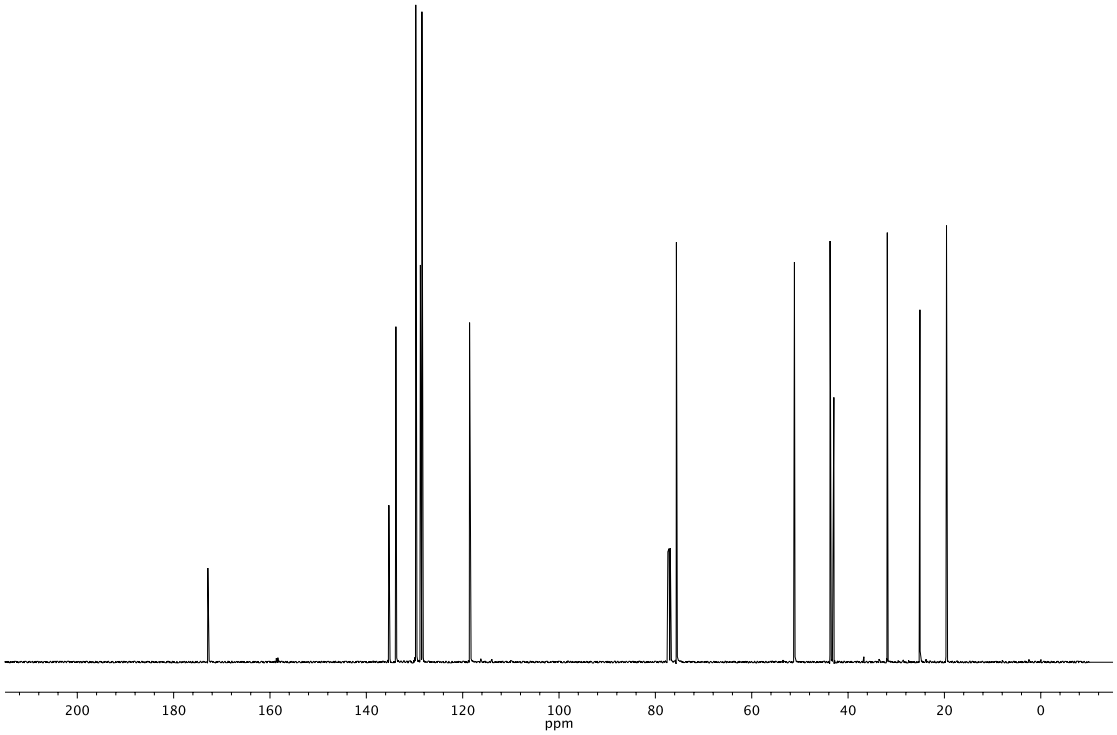

Figure A2-1.22. ^{13}C NMR (126 MHz, $CDCl_3$) of compound **35a**.

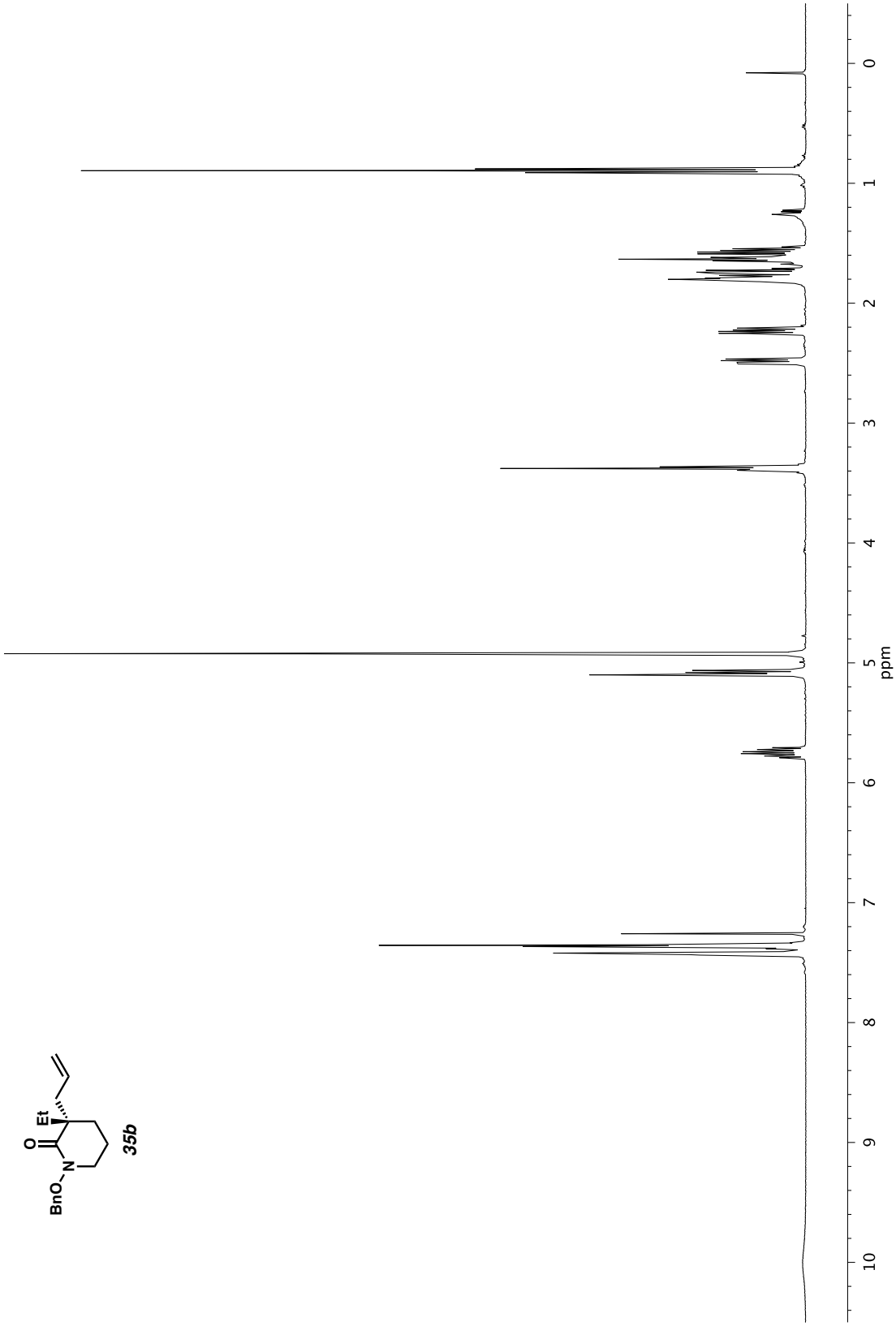

Figure A2-1.23. ^{1}H NMR (500 MHz, $CDCl_3$) of compound **35b**.

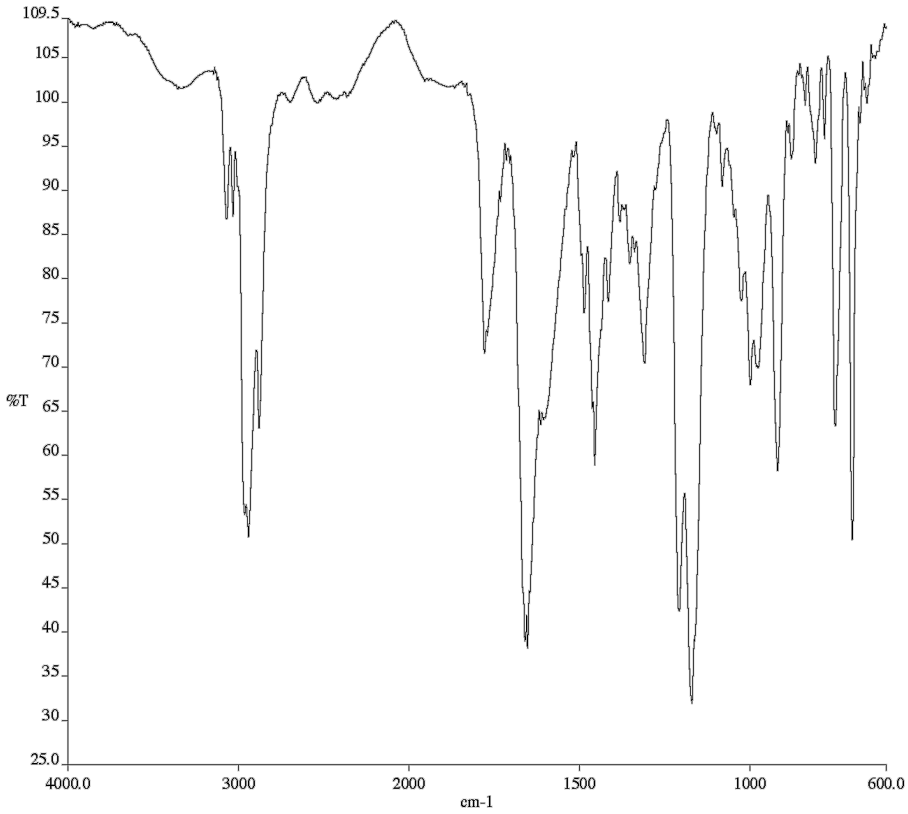

Figure A2-1.24. Infrared spectrum (Thin Film, NaCl) of compound **35b**.

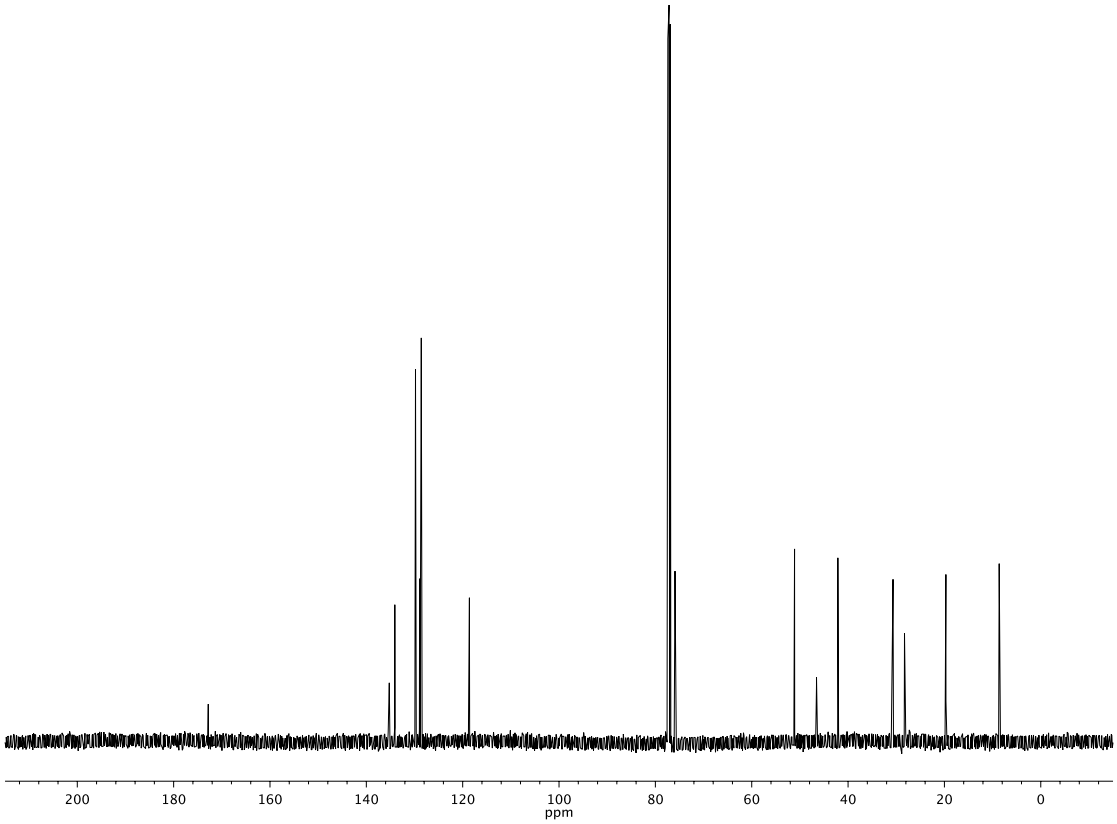

Figure A2-1.25. ^{13}C NMR (126 MHz, $CDCl_3$) of compound **35b**.

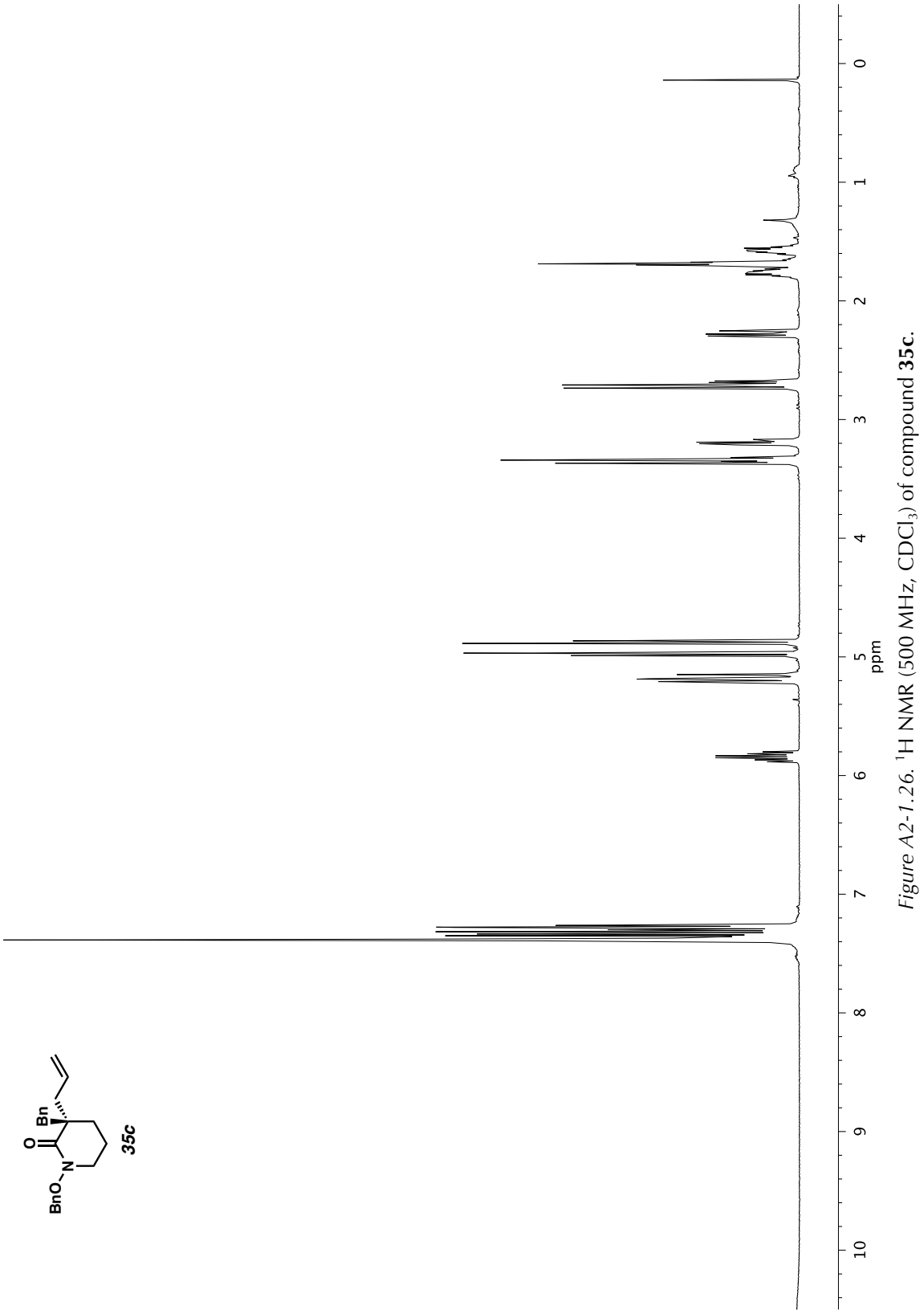

Figure A2-1.26. ^{1}H NMR (500 MHz, $CDCl_3$) of compound **35c**.

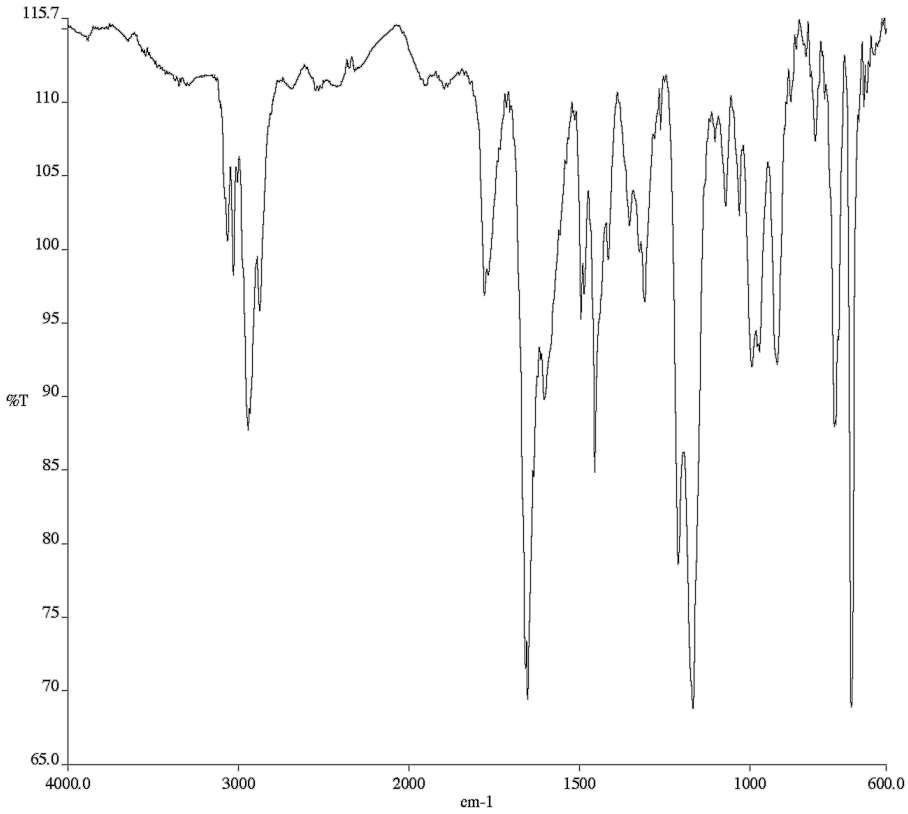

Figure A2-1.27. Infrared spectrum (Thin Film, NaCl) of compound **35c**.

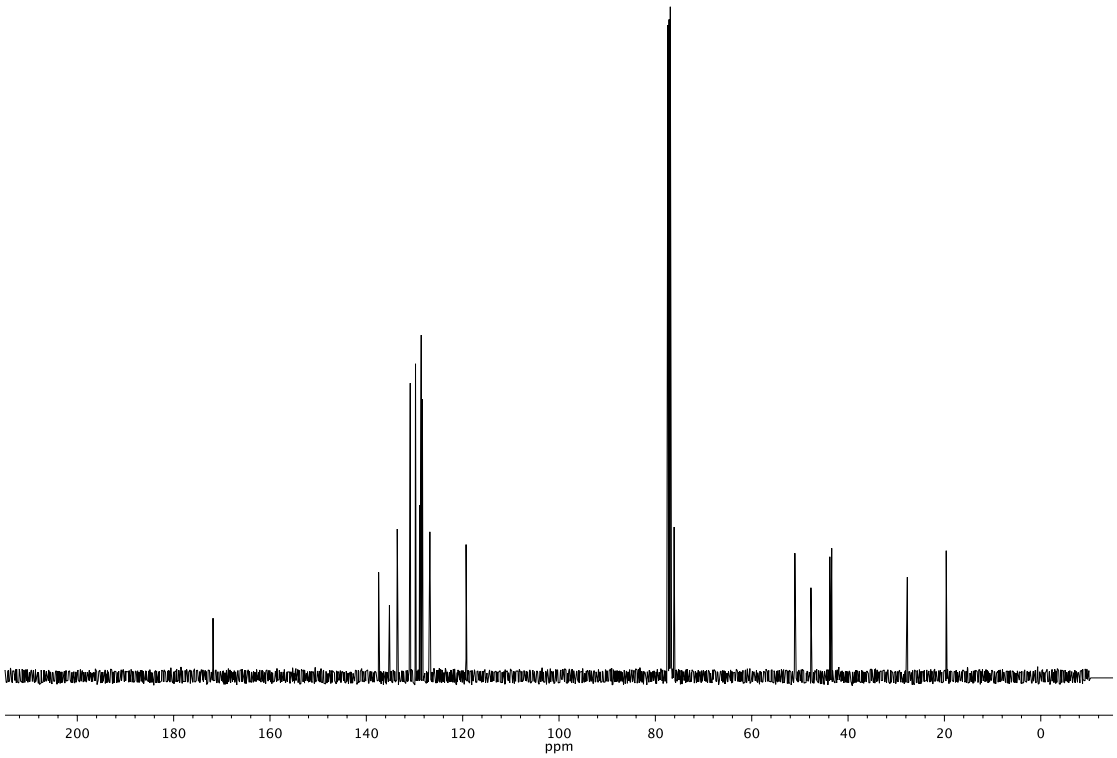

Figure A2-1.28. ^{13}C NMR (126 MHz, $CDCl_3$) of compound **35c**.

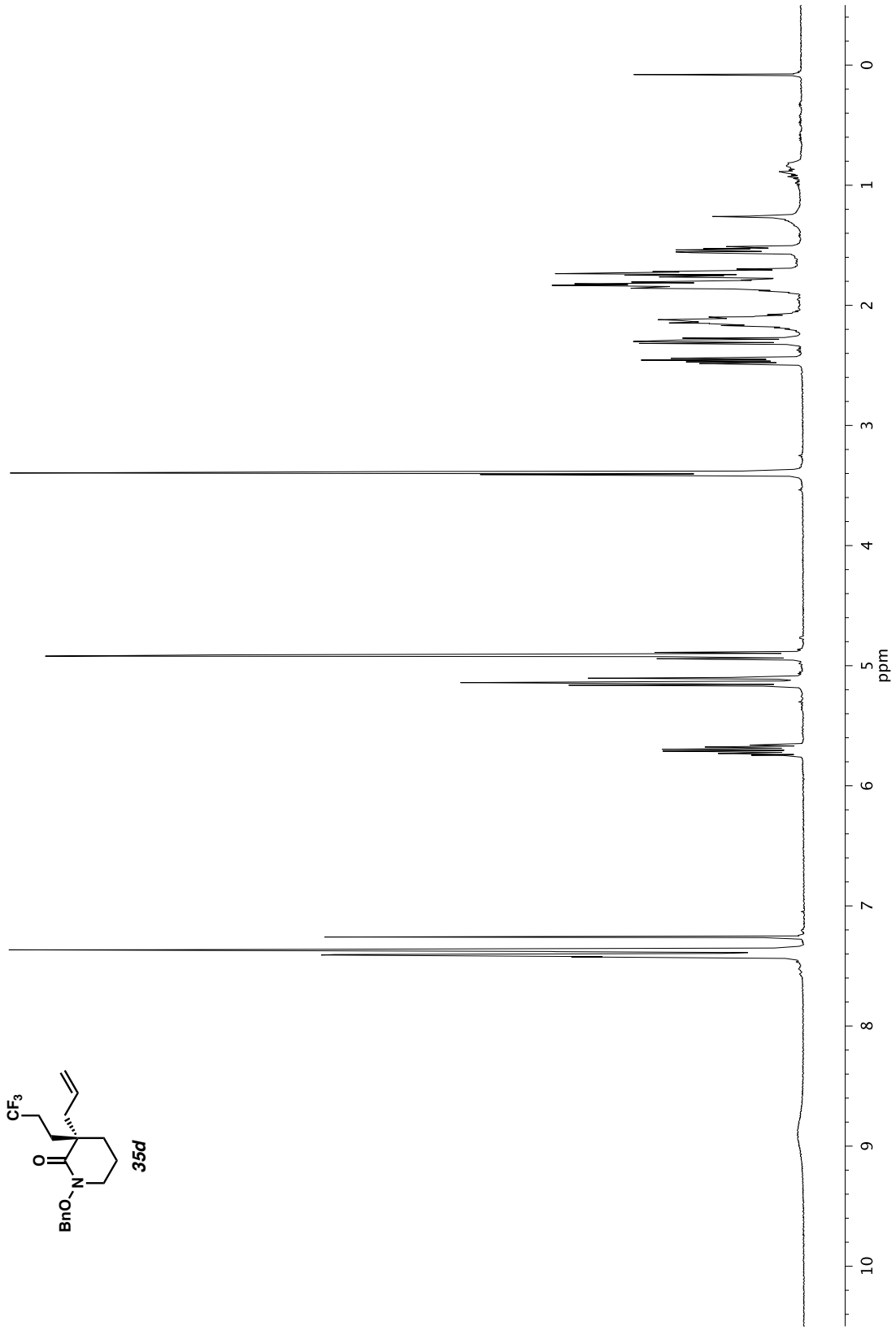

Figure A2-1.29. ^{1}H NMR (500 MHz, $CDCl_3$) of compound **35d**.

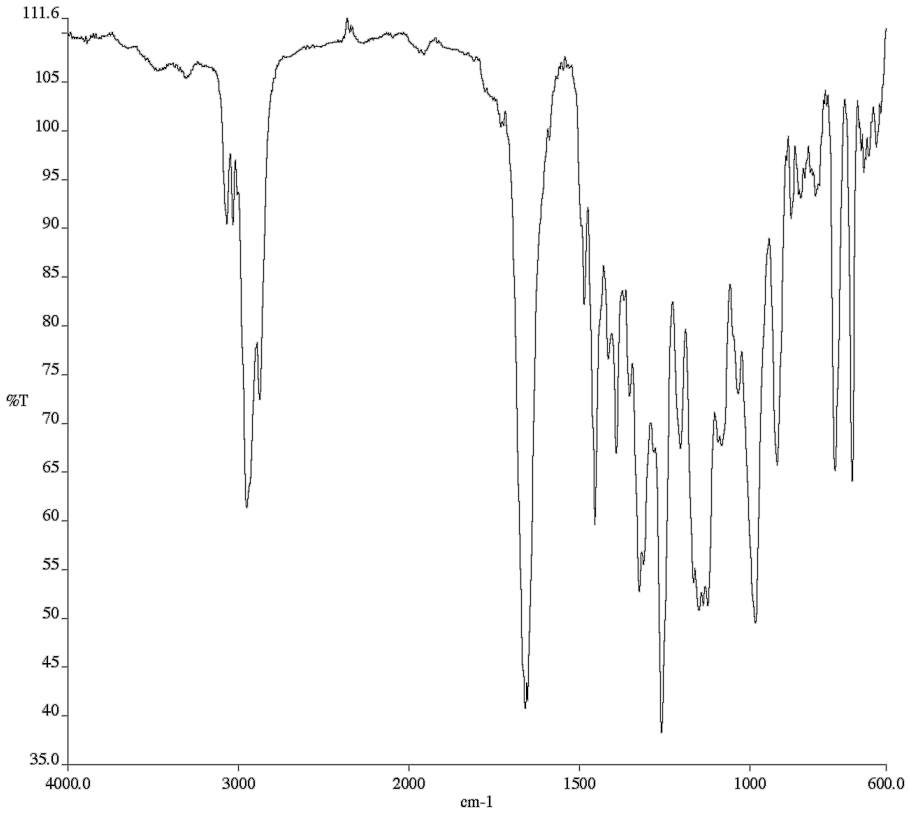

Figure A2-1.30. Infrared spectrum (Thin Film, NaCl) of compound **35d**.

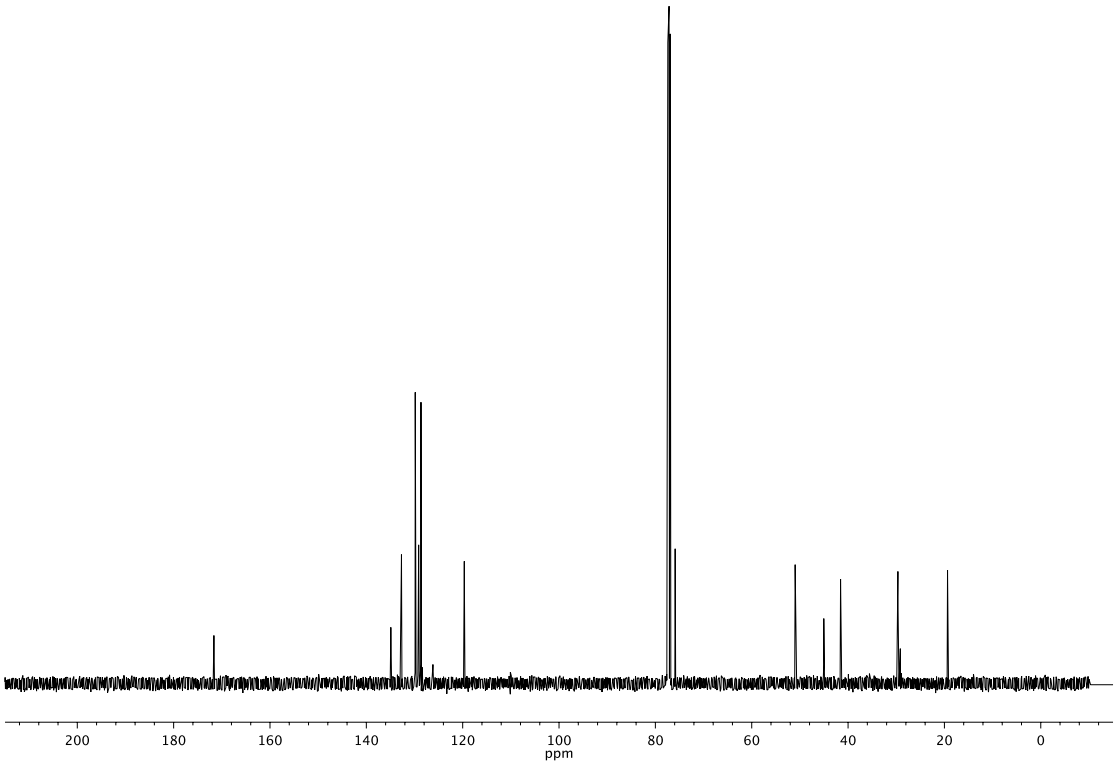

Figure A2-1.31. ^{13}C NMR (126 MHz, $CDCl_3$) of compound **35d**.

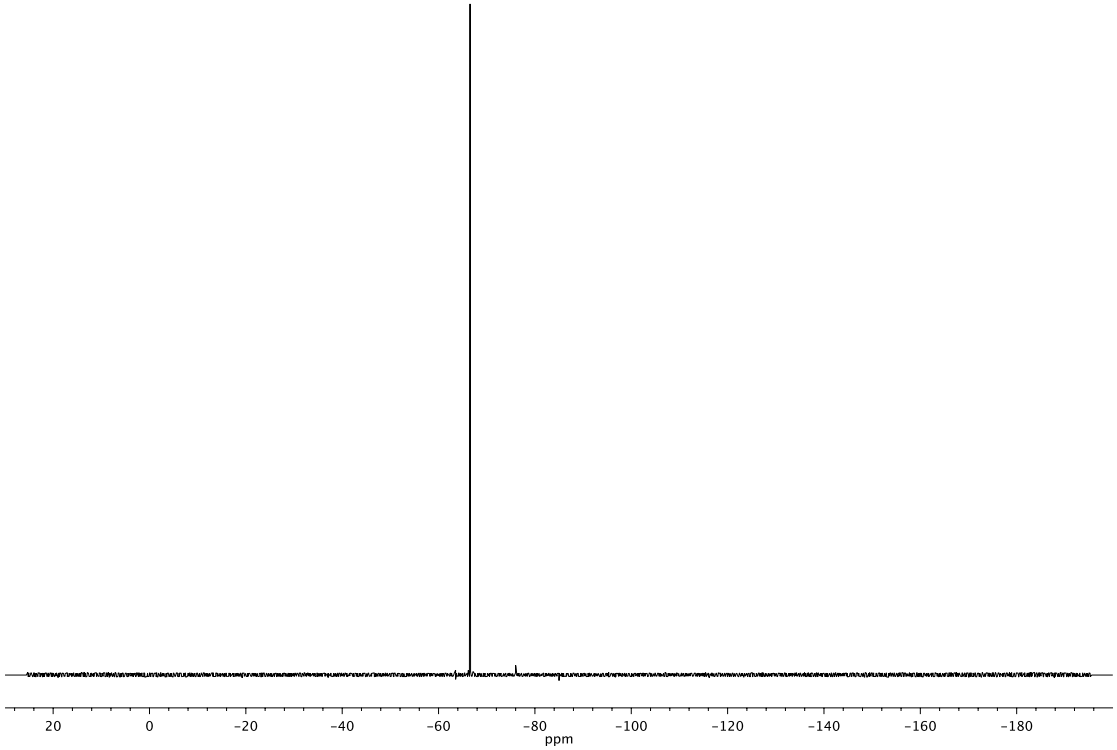

Figure A2-1.32. ^{19}F NMR (282 MHz, $CDCl_3$) of compound **35d**.

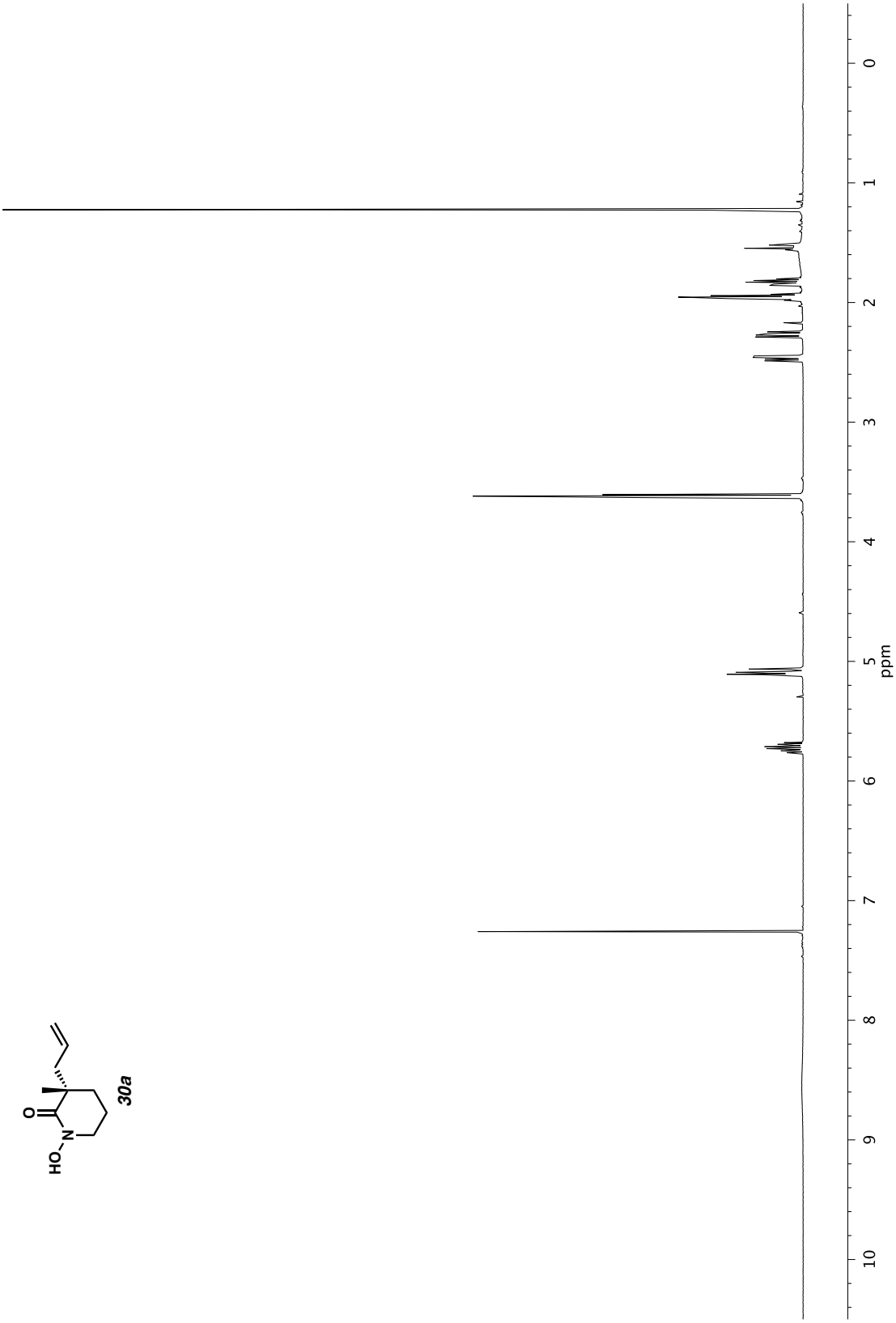

30a

Figure A2-1.33. ^{1}H NMR (500 MHz, $CDCl_3$) of compound **30a**.

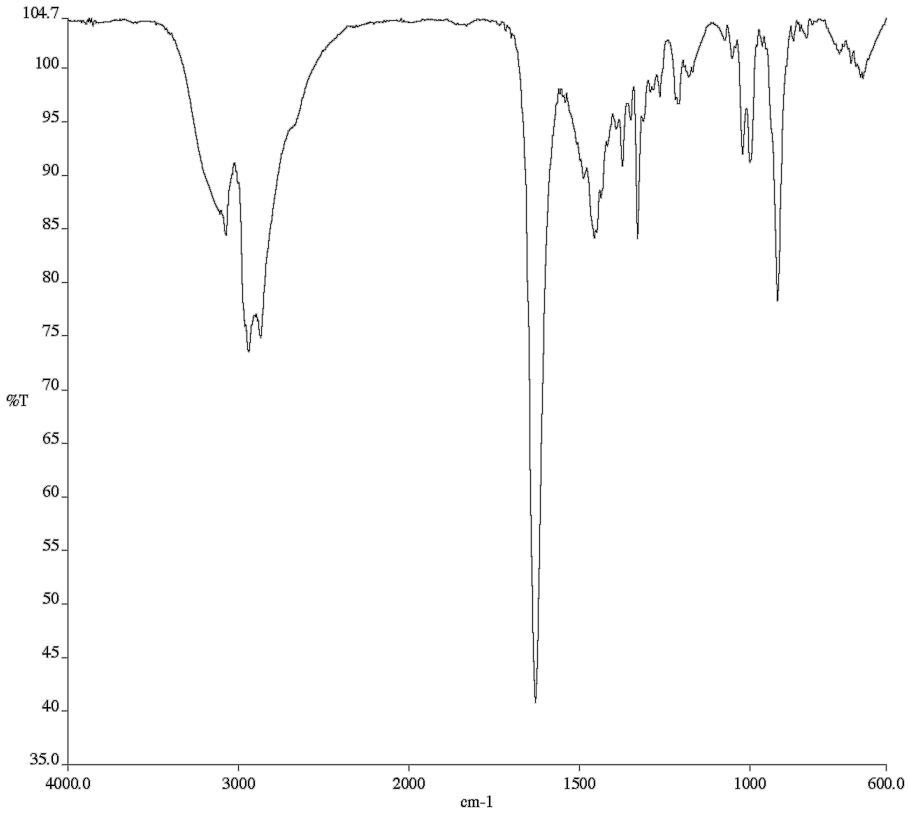

Figure A2-1.34. Infrared spectrum (Thin Film, NaCl) of compound **30a**.

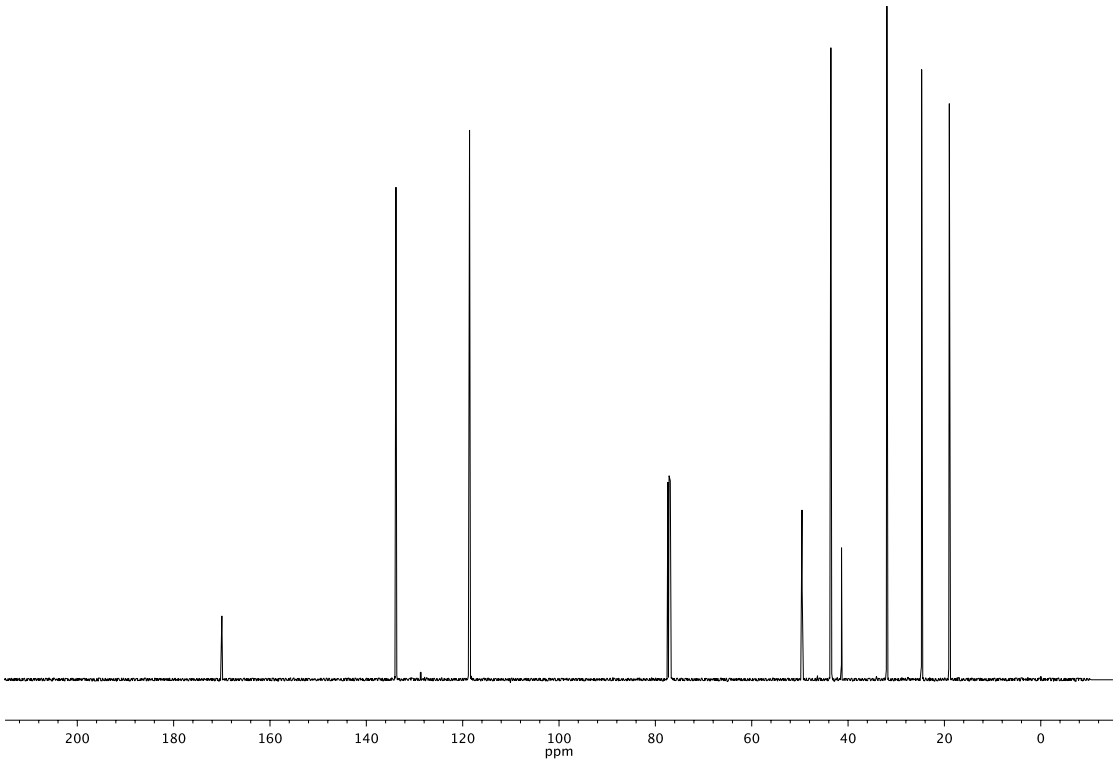

Figure A2-1.35. ^{13}C NMR (126 MHz, $CDCl_3$) of compound **30a**.

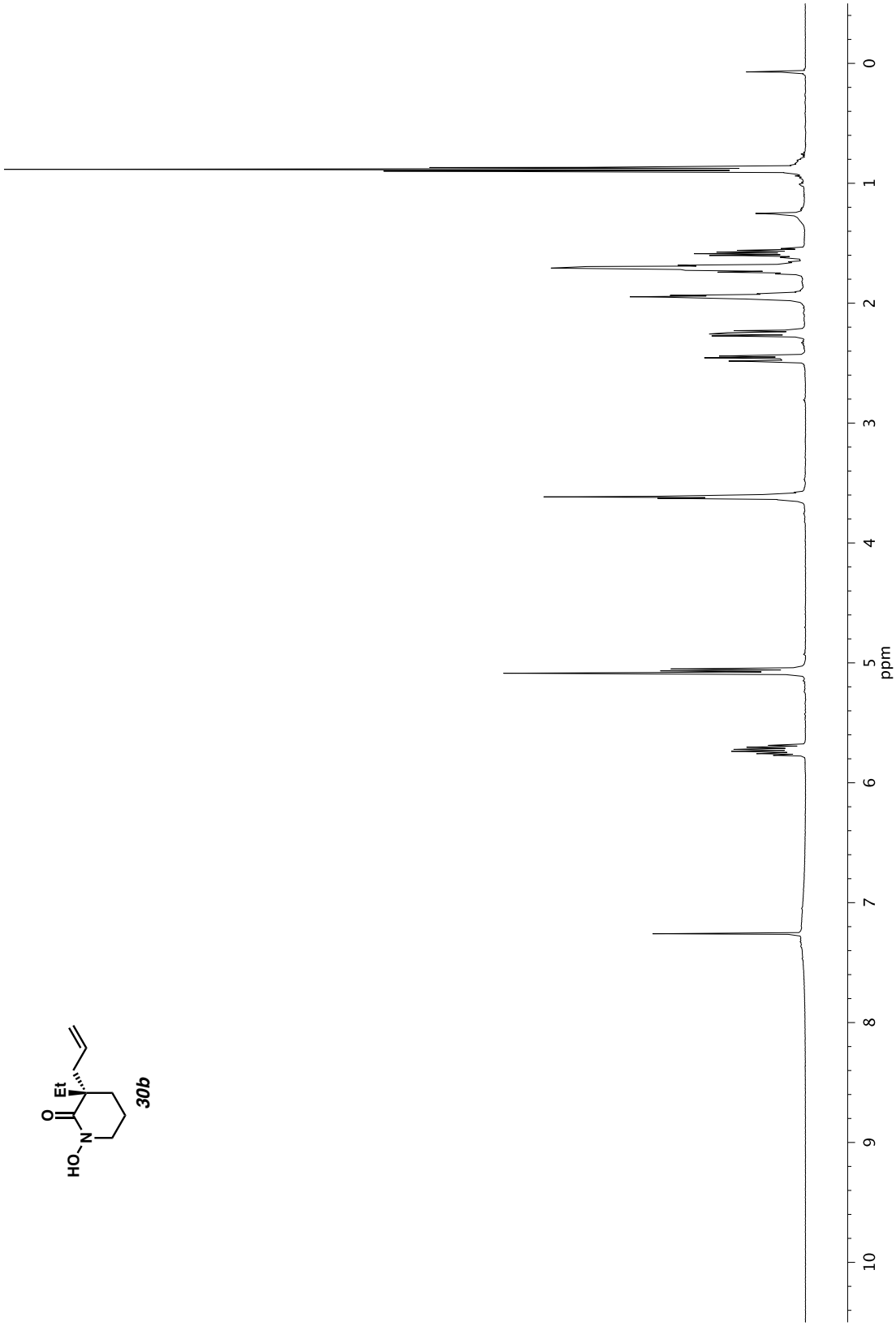

Figure A2-1.36. ^{1}H NMR (500 MHz, $CDCl_3$) of compound **30b**.

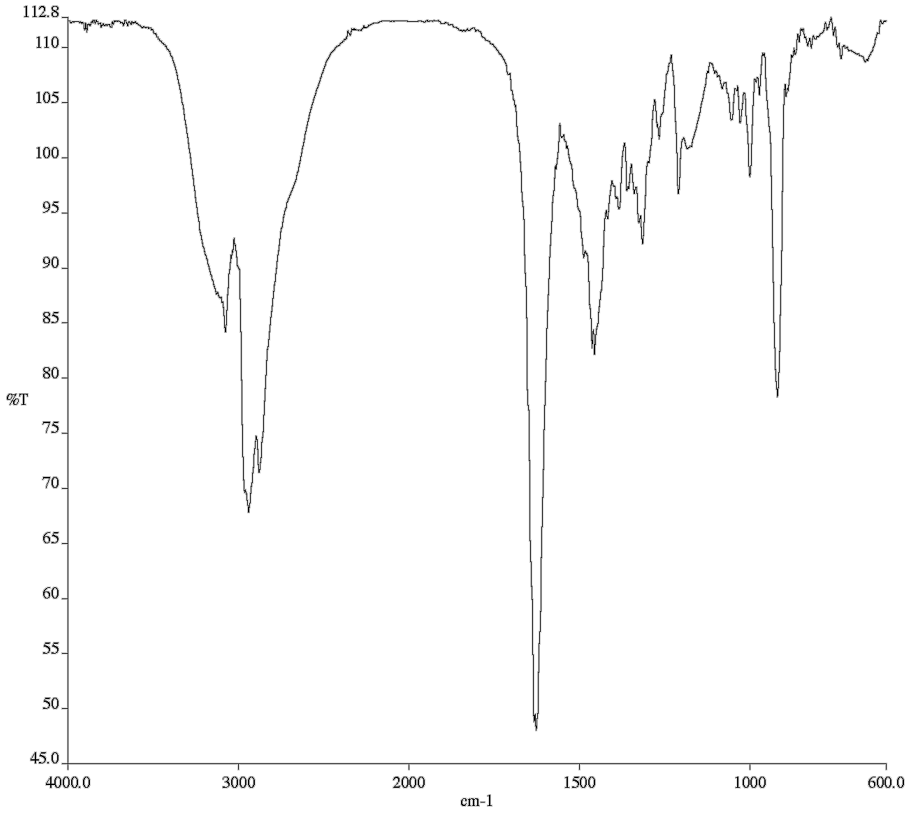

Figure A2-1.37. Infrared spectrum (Thin Film, NaCl) of compound **30b**.

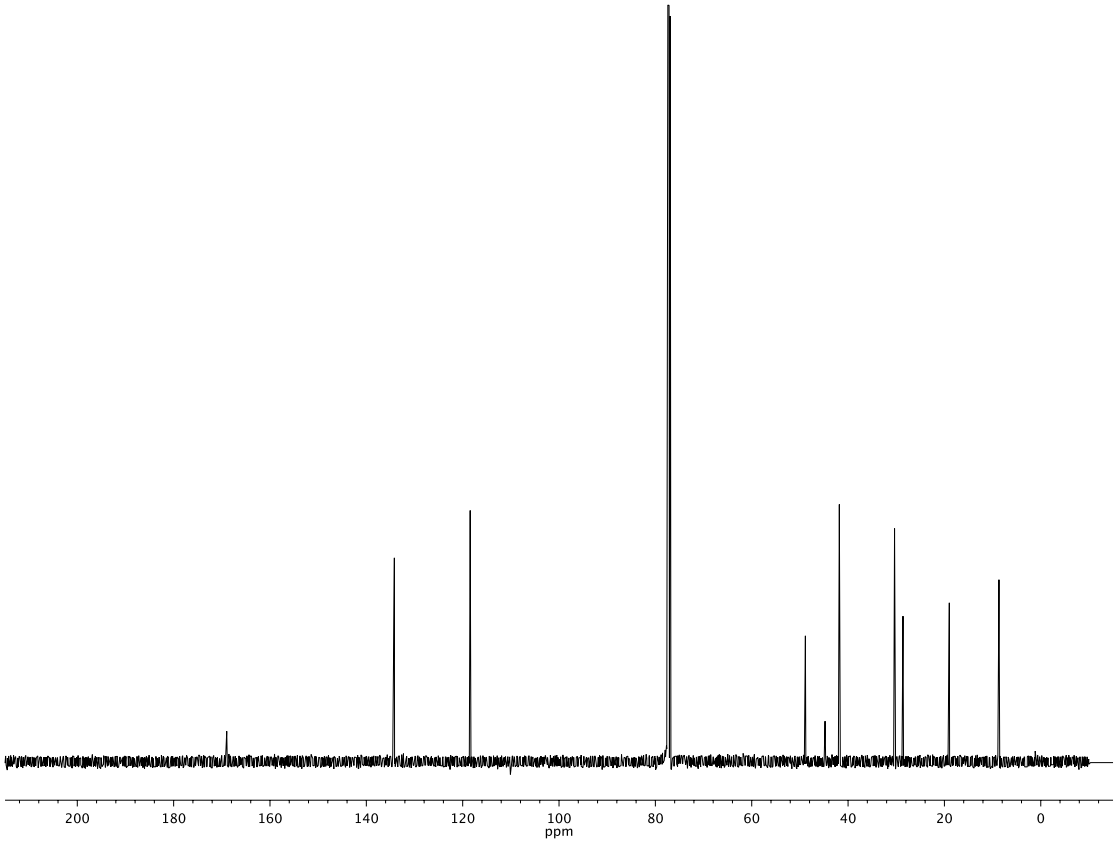

Figure A2-1.38. ^{13}C NMR (126 MHz, $CDCl_3$) of compound **30b**.

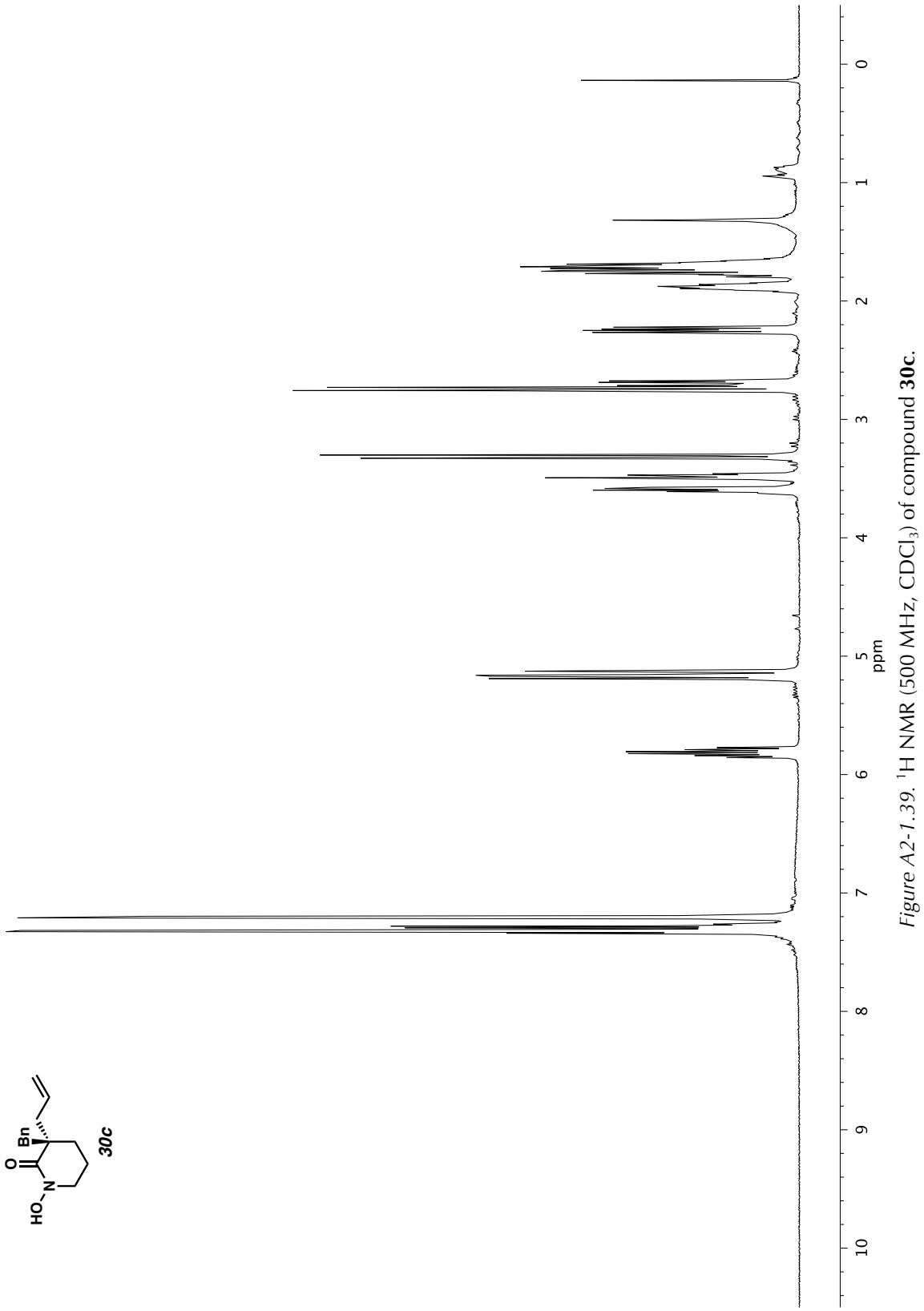

Figure A2-1.39. ^{1}H NMR (500 MHz, $CDCl_3$) of compound **30c**.

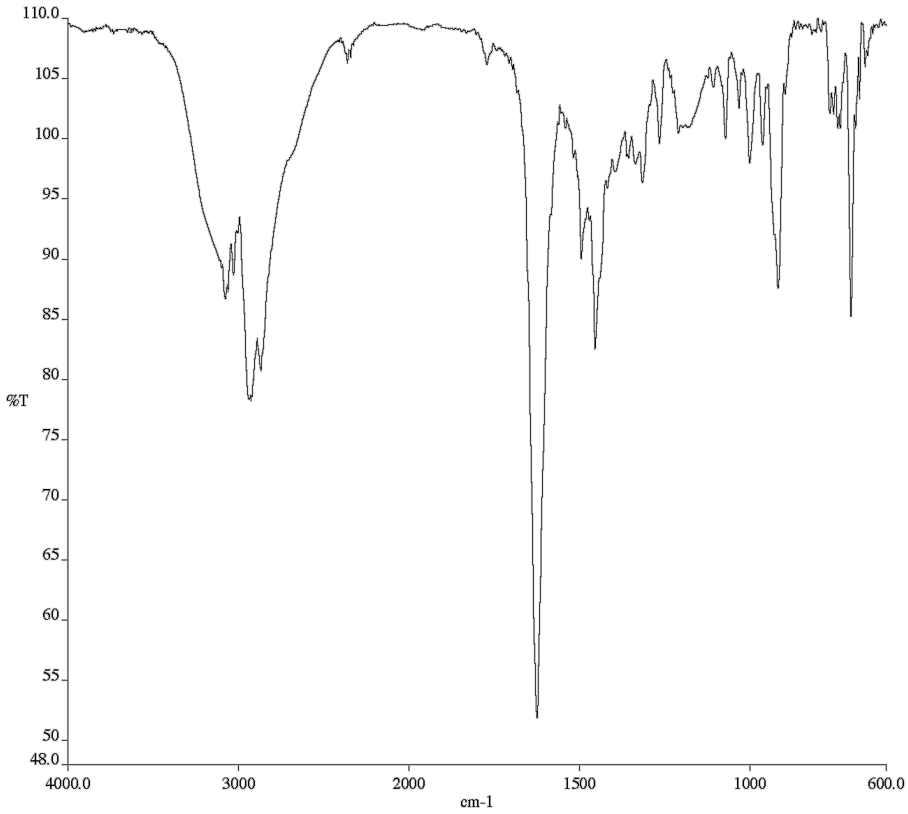

Figure A2-1.40. Infrared spectrum (Thin Film, NaCl) of compound **30c**.

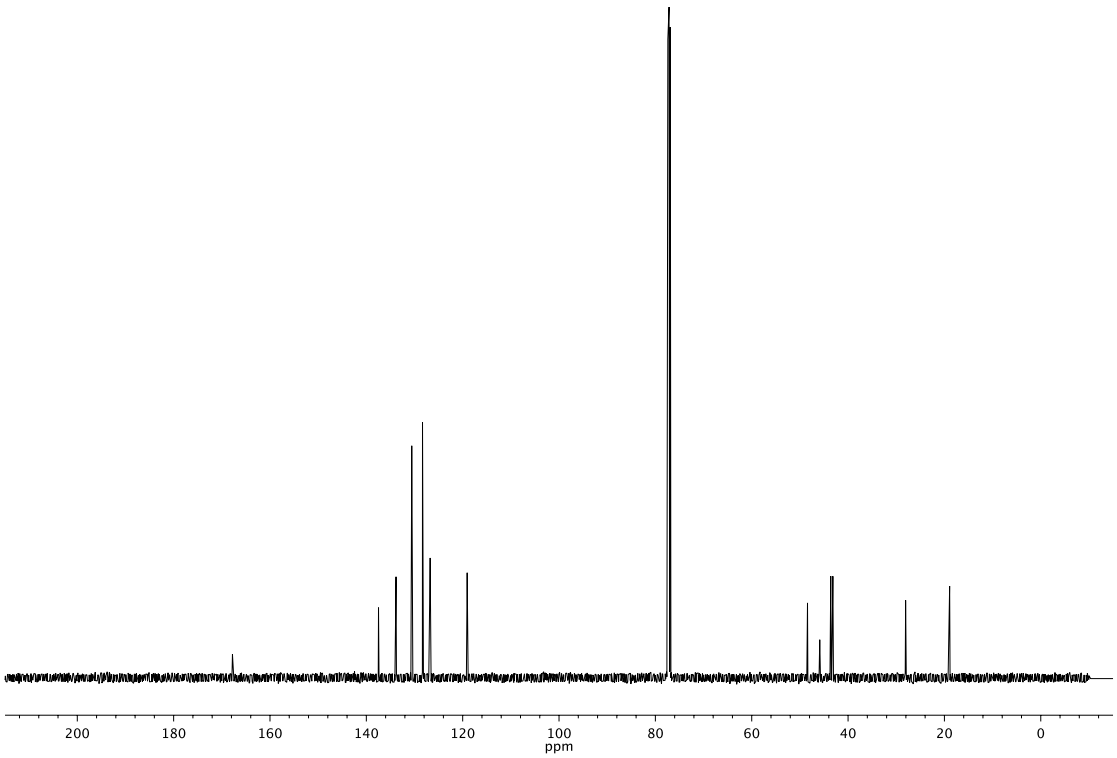

Figure A2-1.41. ^{13}C NMR (126 MHz, $CDCl_3$) of compound **30c**.

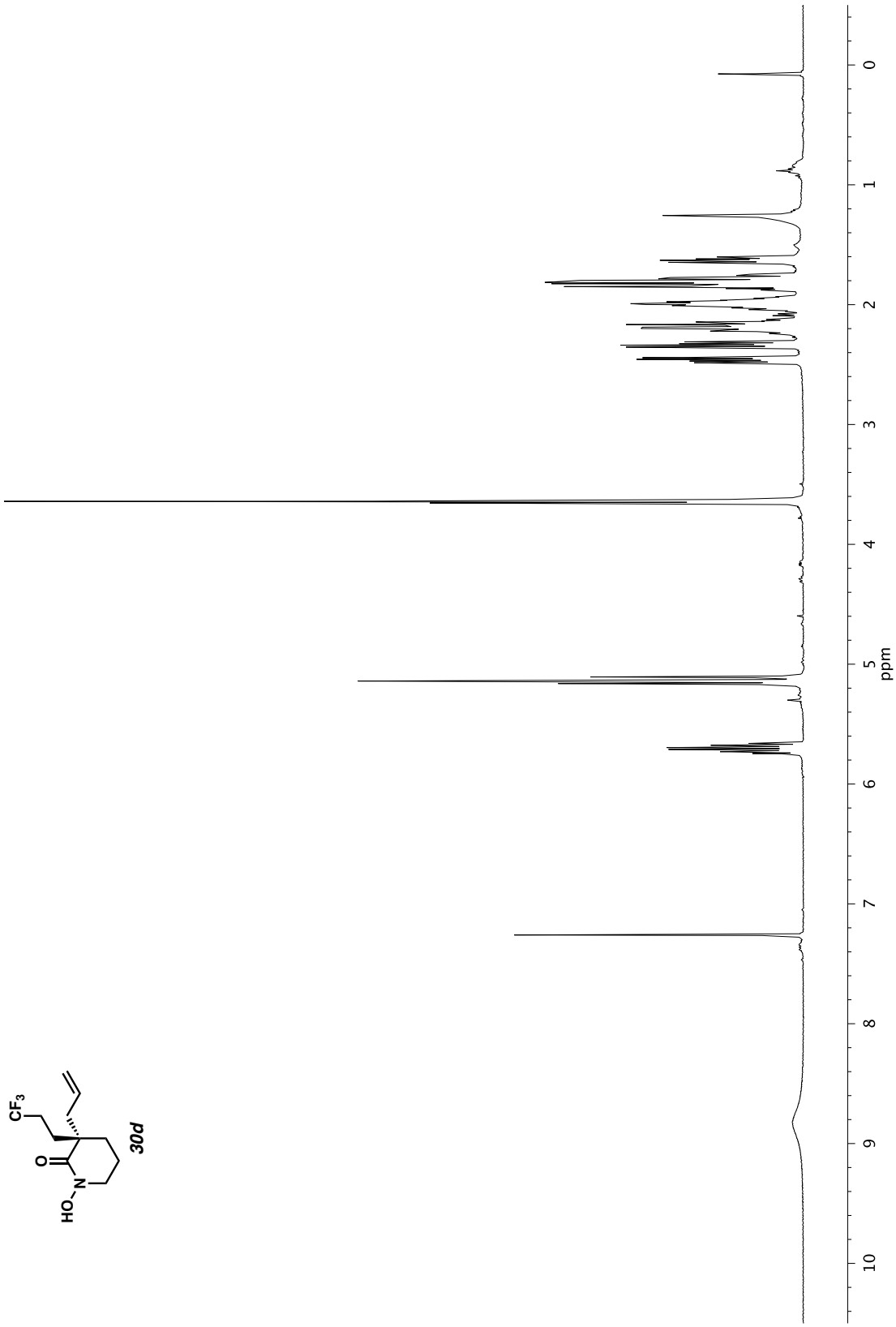

Figure A2-1.42. ^{1}H NMR (500 MHz, $CDCl_3$) of compound **30d**.

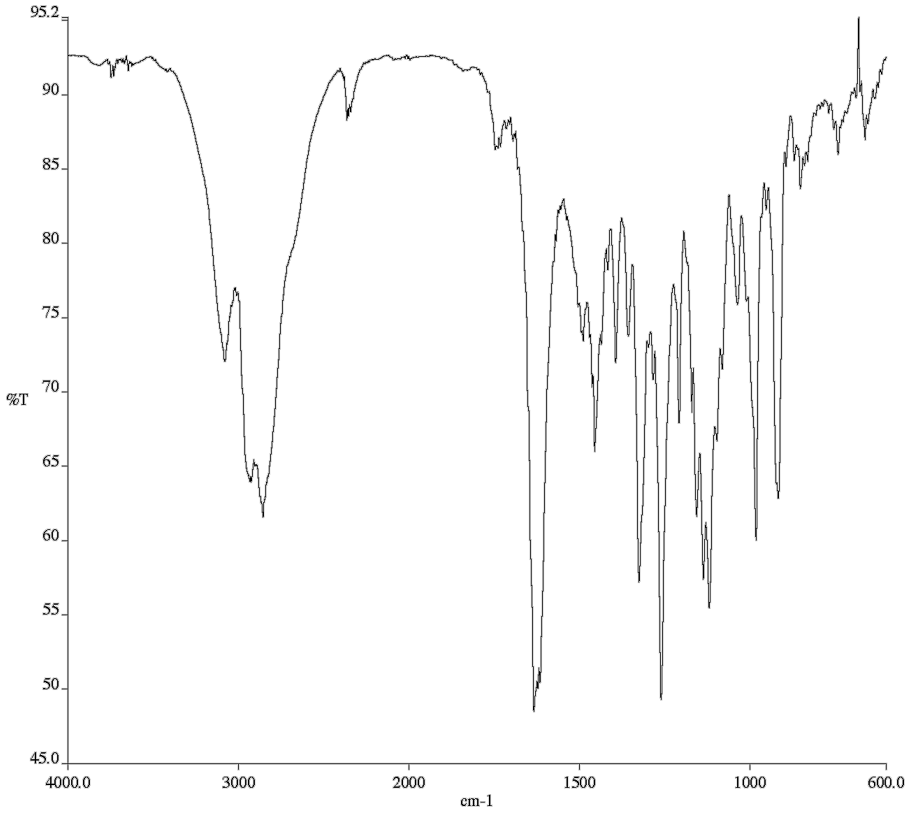

Figure A2-1.43. Infrared spectrum (Thin Film, NaCl) of compound **30d**.

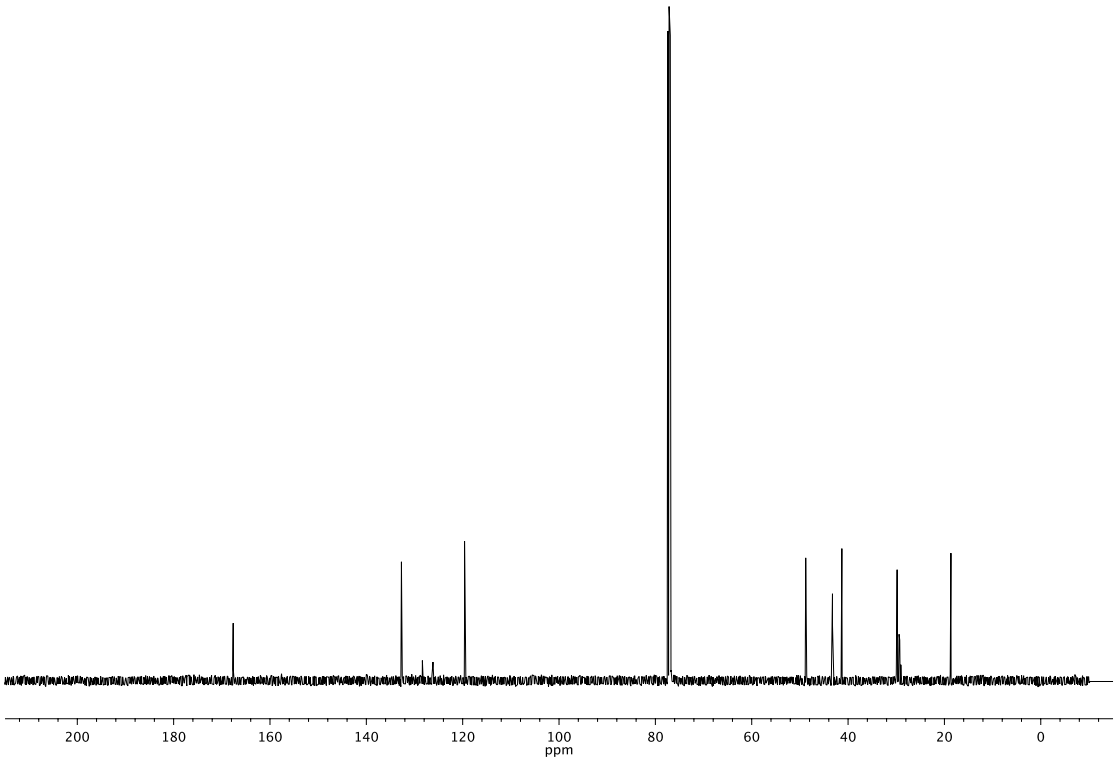

Figure A2-1.44. ^{13}C NMR (126 MHz, $CDCl_3$) of compound **30d**.

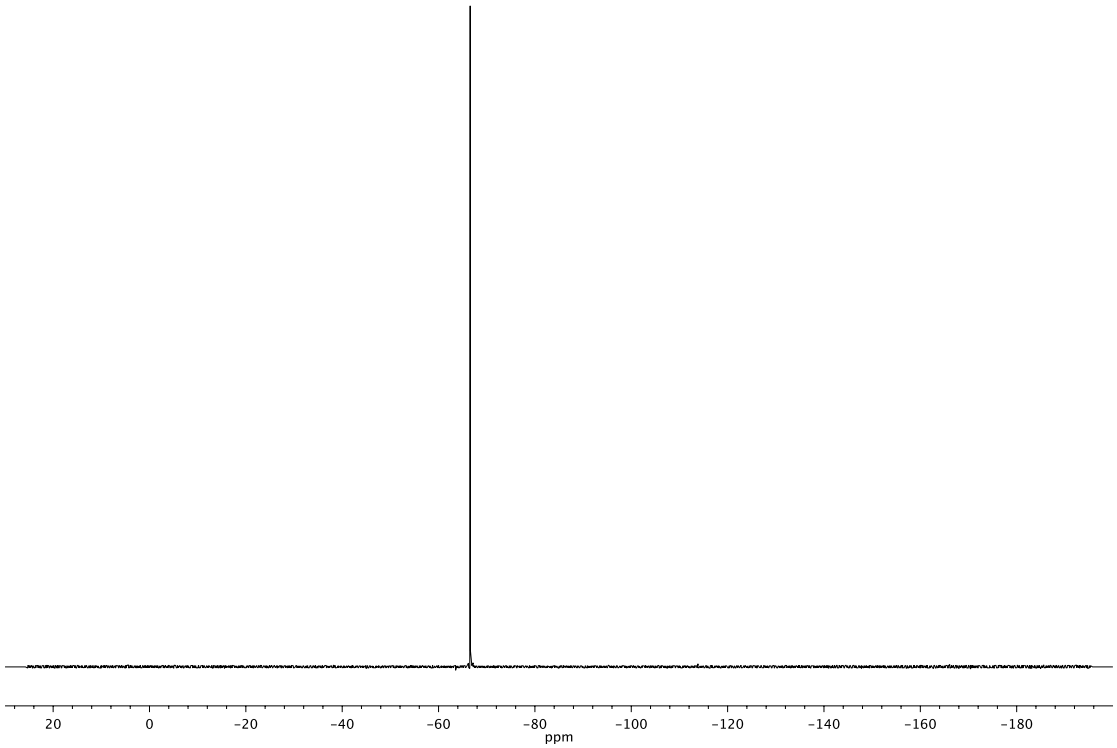

Figure A2-1.45. ^{19}F NMR (282 MHz, $CDCl_3$) of compound **30d**.

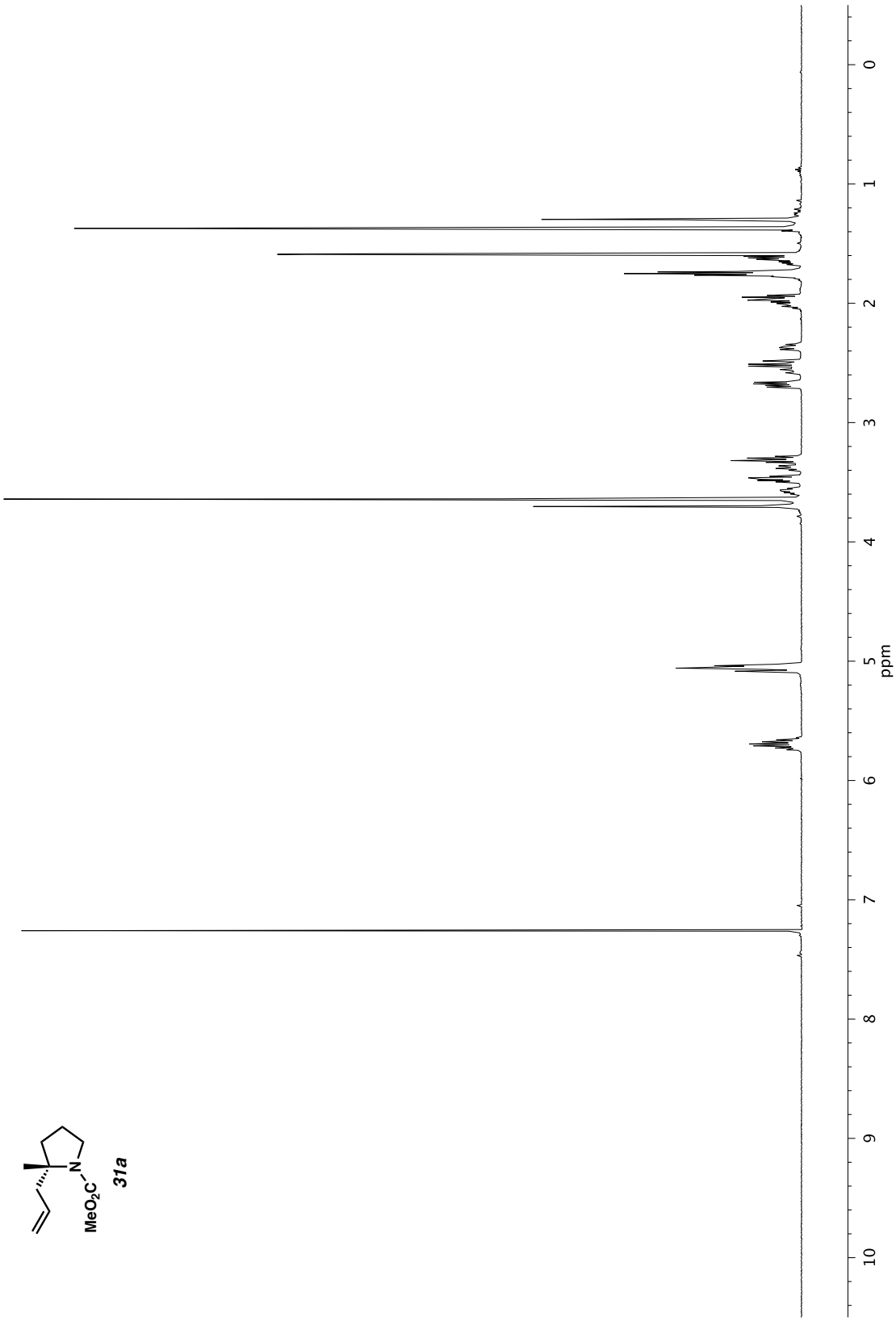

Figure A2-1.46. ^{1}H NMR (500 MHz, $CDCl_3$) of compound **31a**.

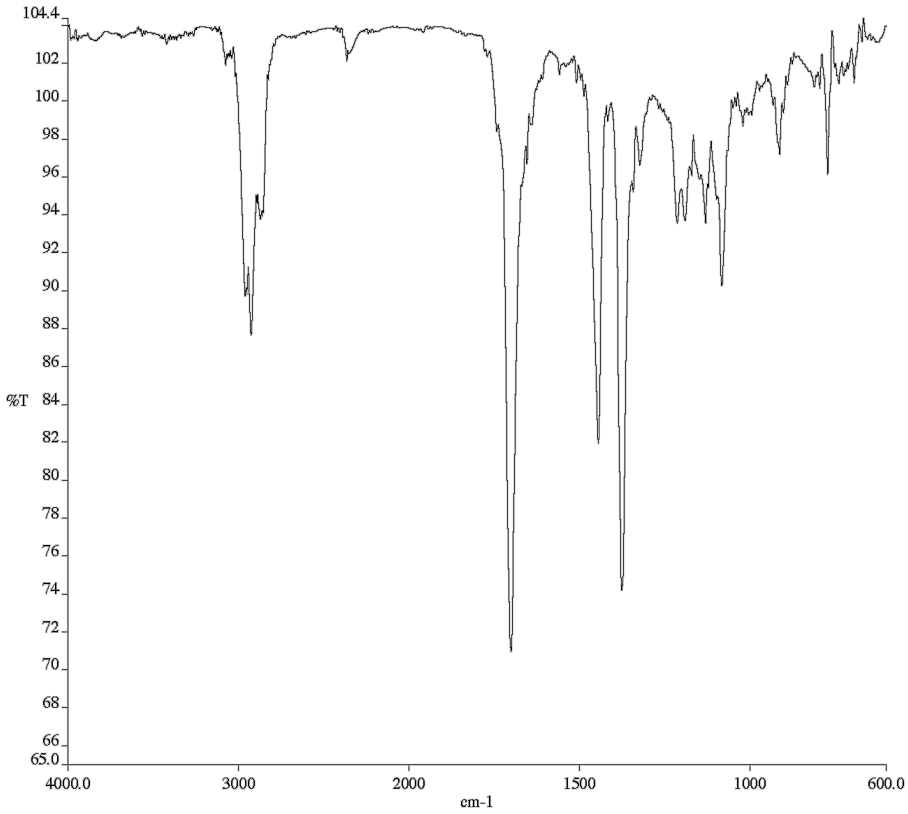

Figure A2-1.47. Infrared spectrum (Thin Film, NaCl) of compound **31a**.

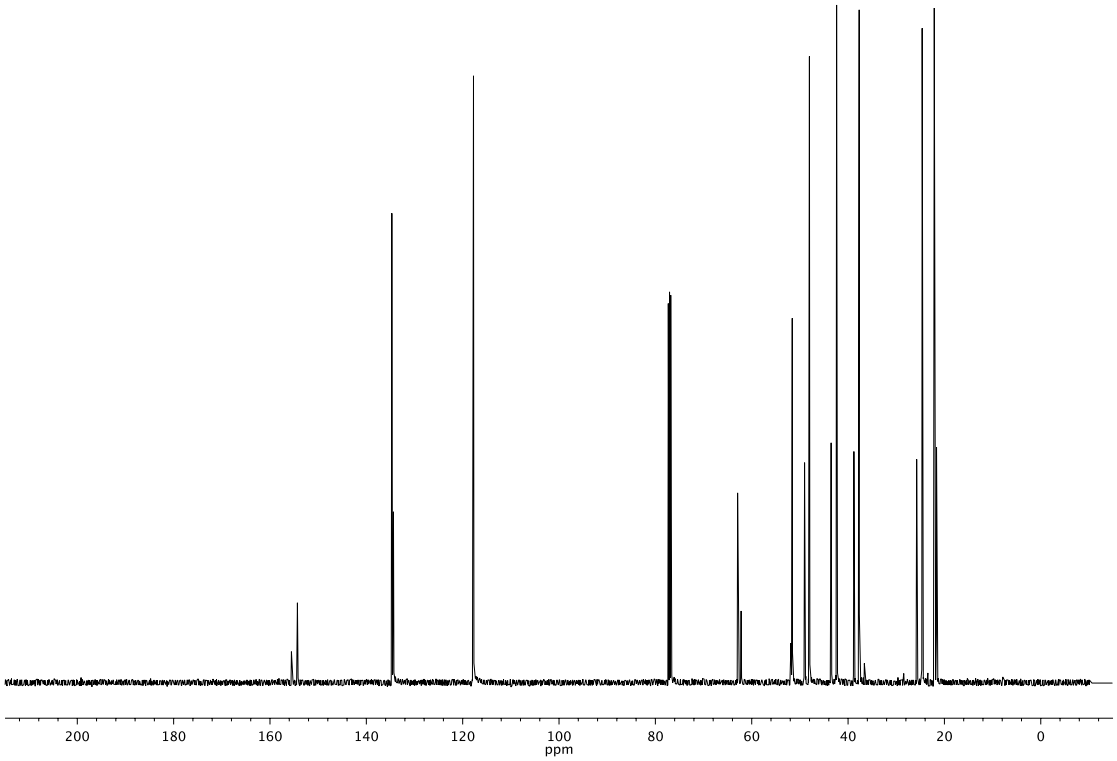

Figure A2-1.48. ^{13}C NMR (126 MHz, $CDCl_3$) of compound **31a**.

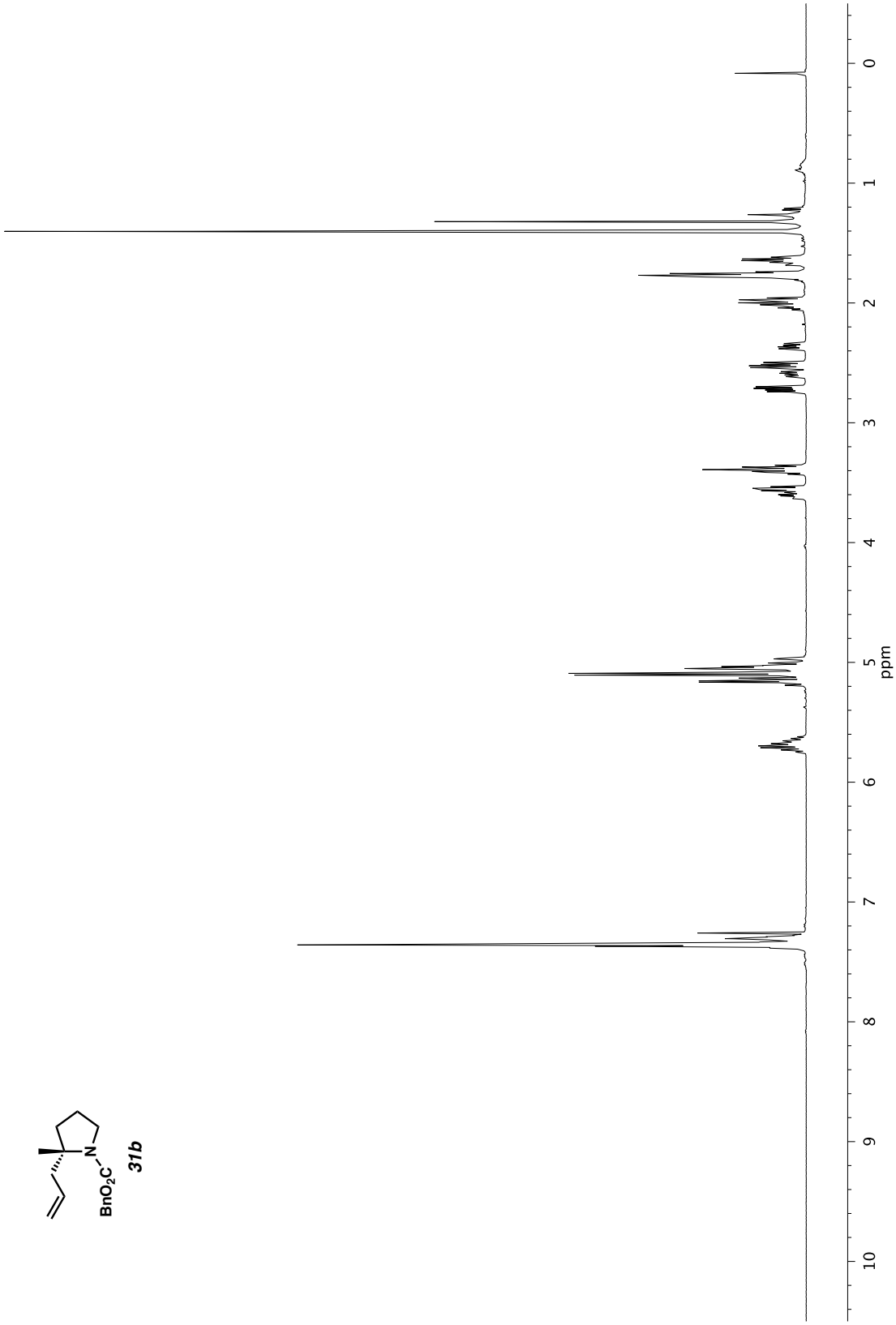

Figure A2-1.49. ^{1}H NMR (500 MHz, $CDCl_3$) of compound **31b**.

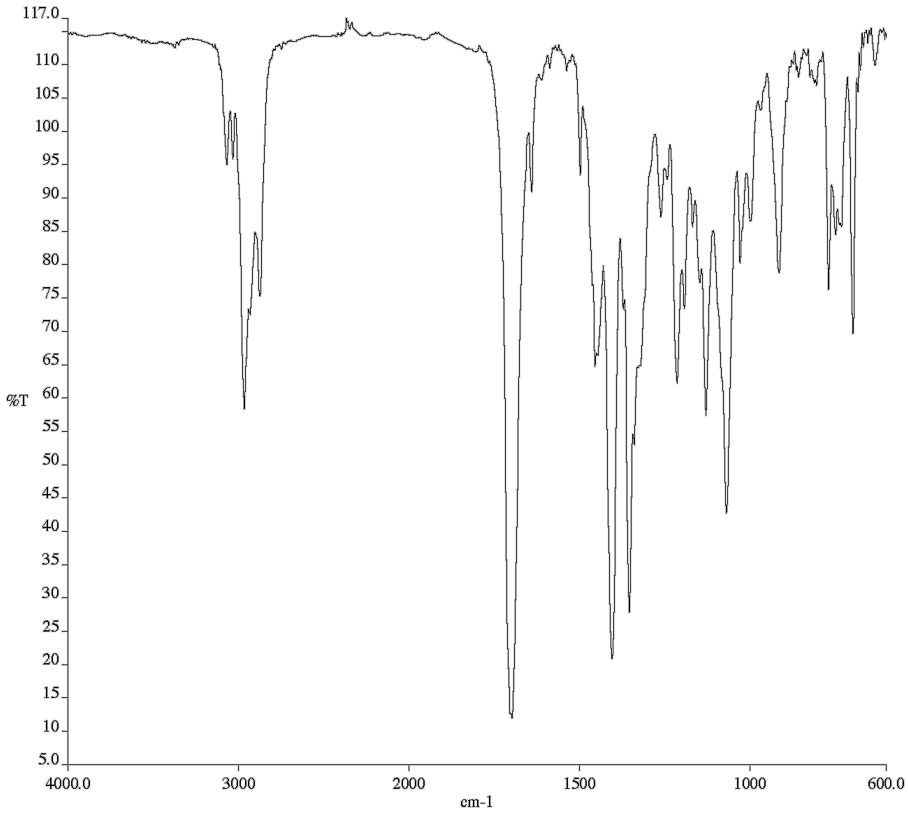

Figure A2-1.50. Infrared spectrum (Thin Film, NaCl) of compound **31b**.

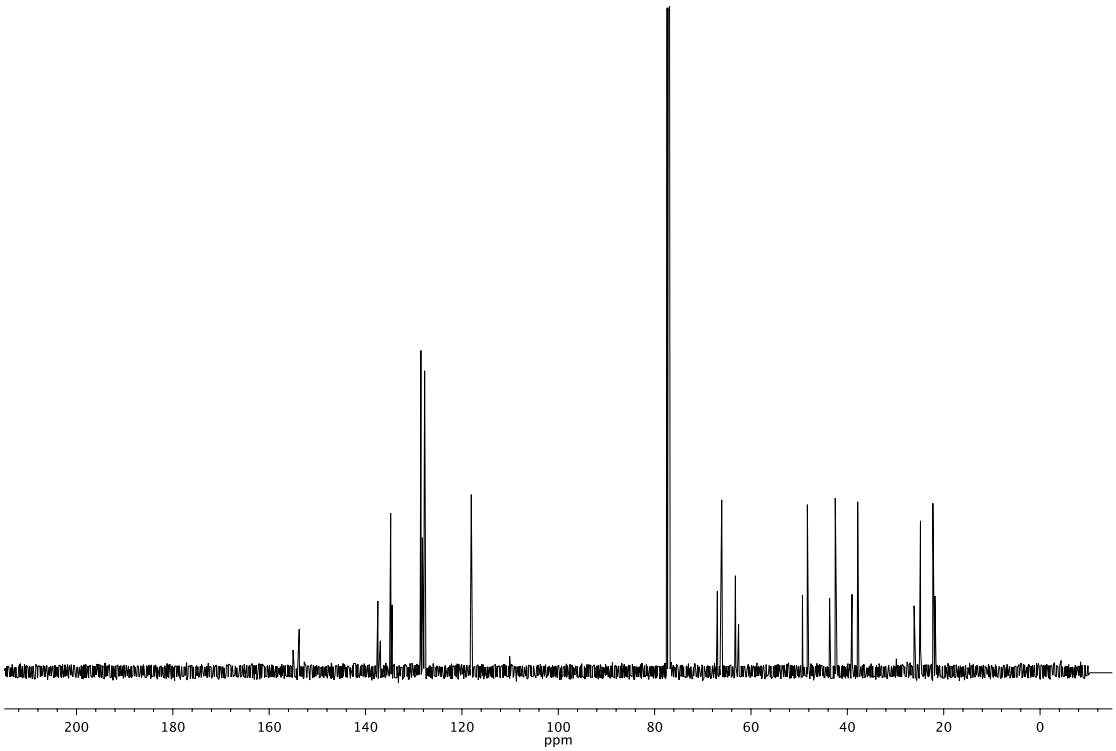

Figure A2-1.51. ^{13}C NMR (126 MHz, $CDCl_3$) of compound **31b**.

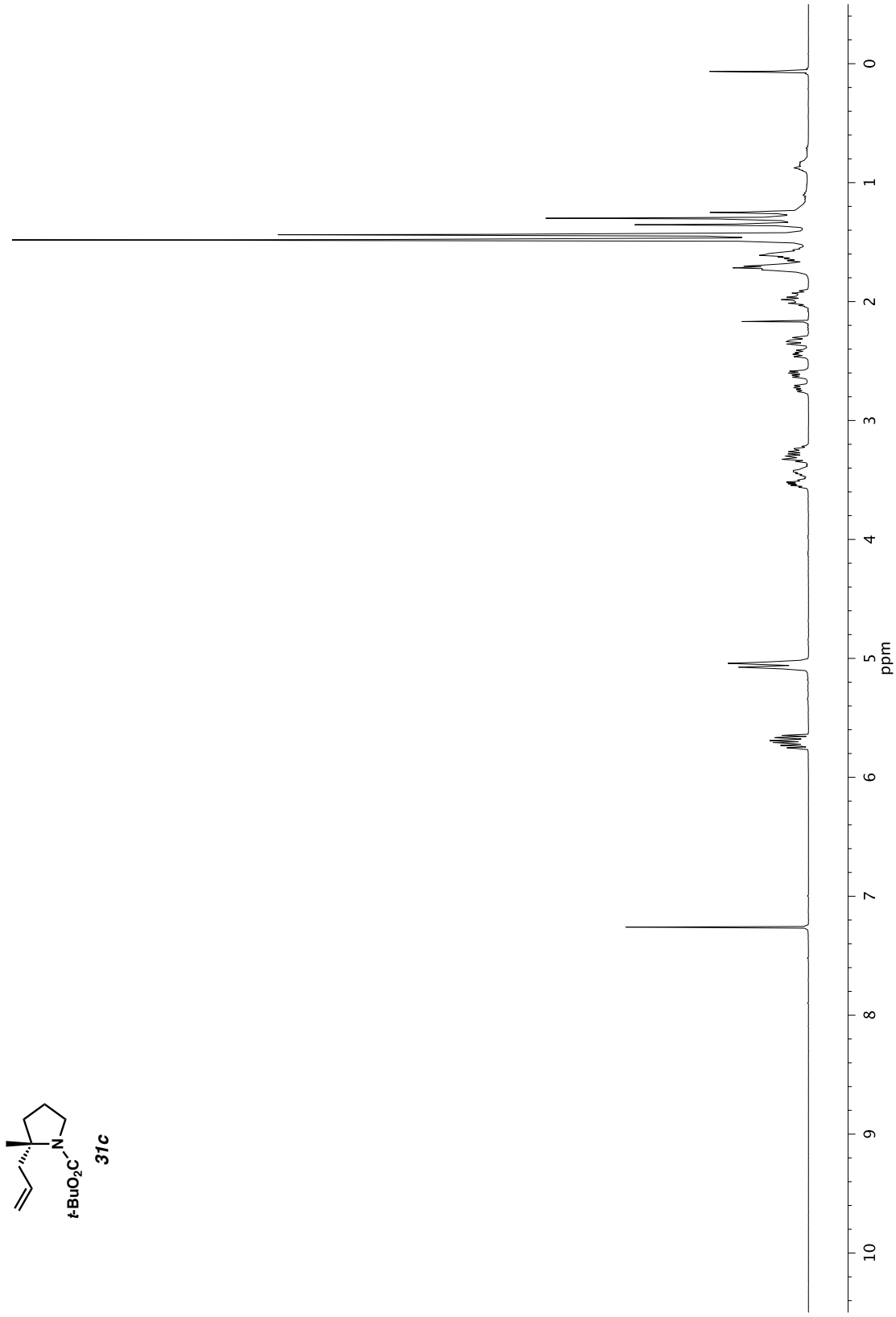

Figure A2-1.52. ^{1}H NMR (500 MHz, $CDCl_3$) of compound **31c**.

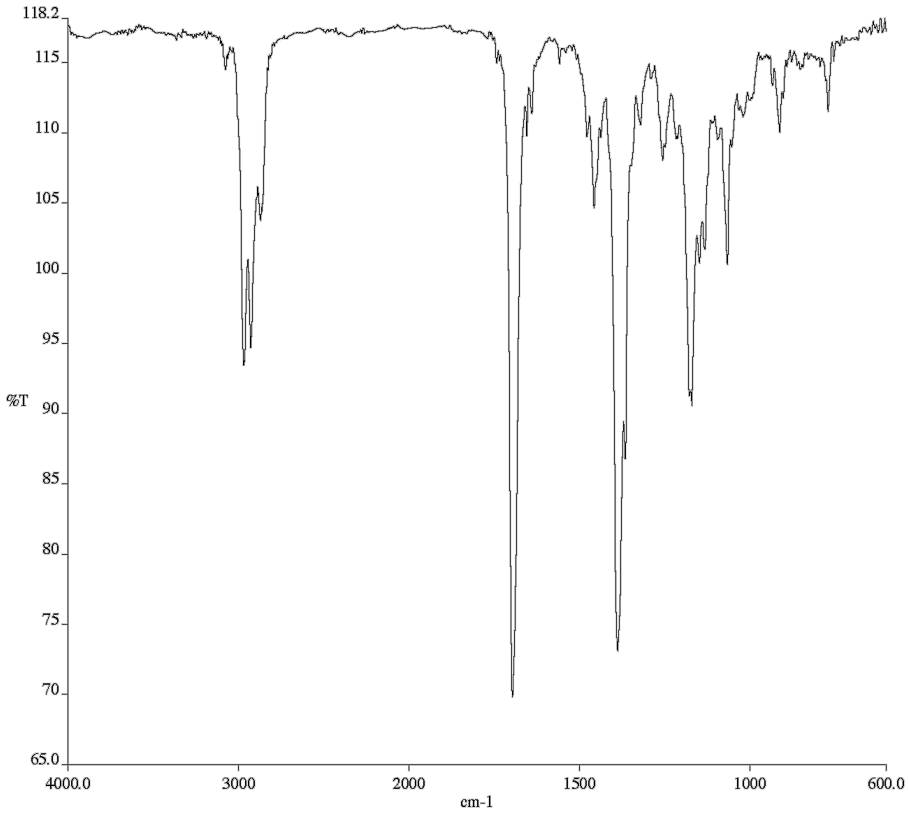

Figure A2-1.53. Infrared spectrum (Thin Film, NaCl) of compound **31c**.

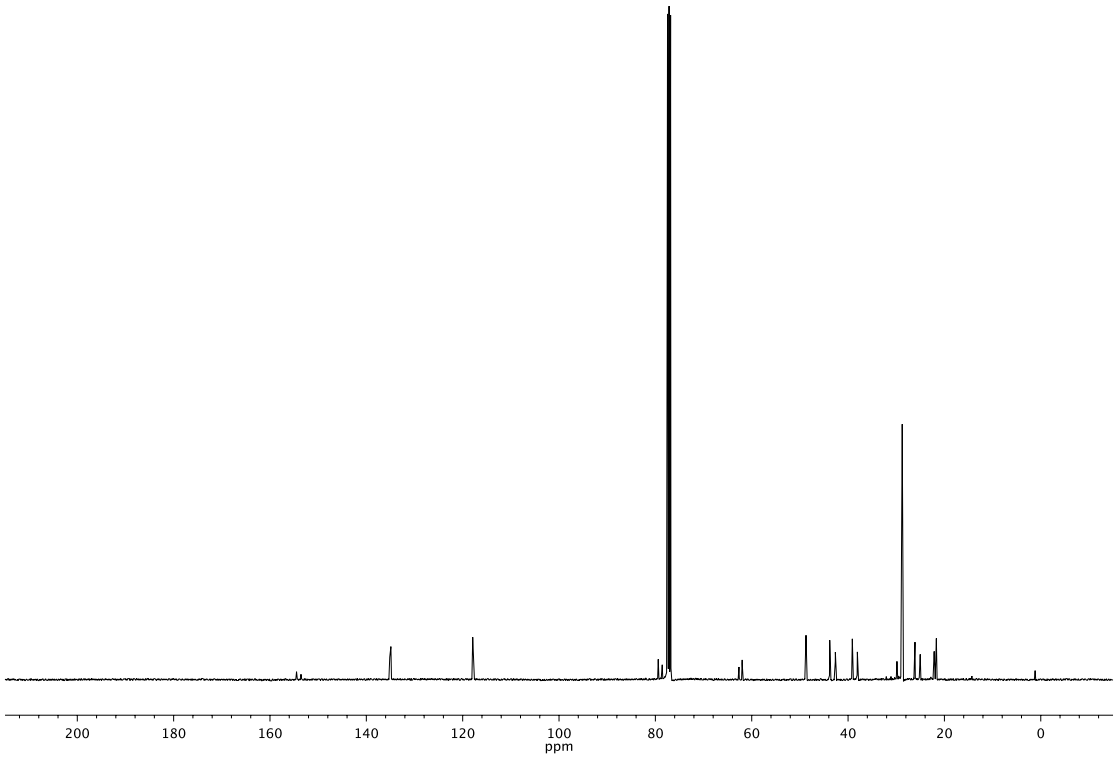

Figure A2-1.54. ^{13}C NMR (101 MHz, $CDCl_3$) of compound **31c**.

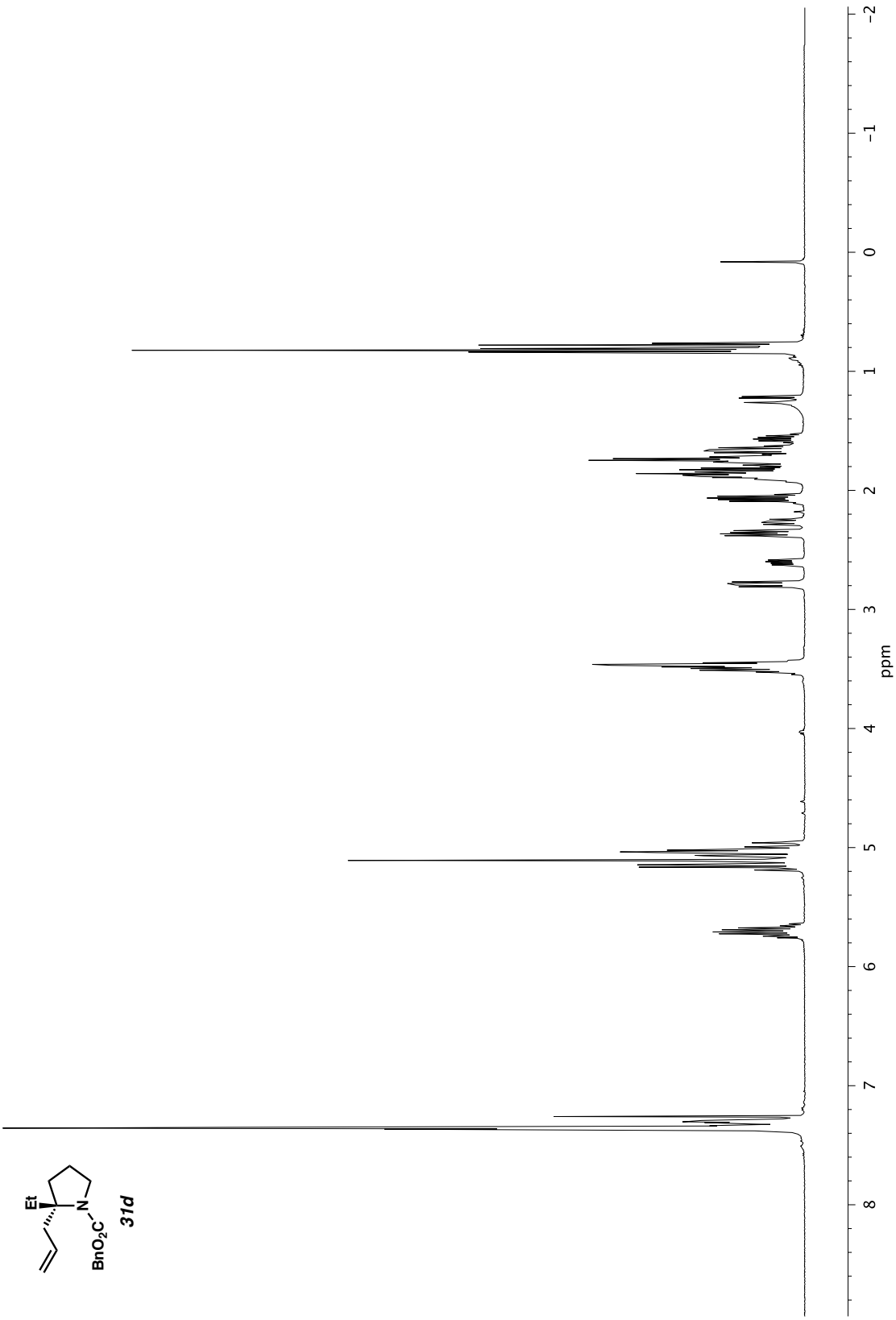

Figure A2-1.55. ^{1}H NMR (500 MHz, $CDCl_3$) of compound **31d**.

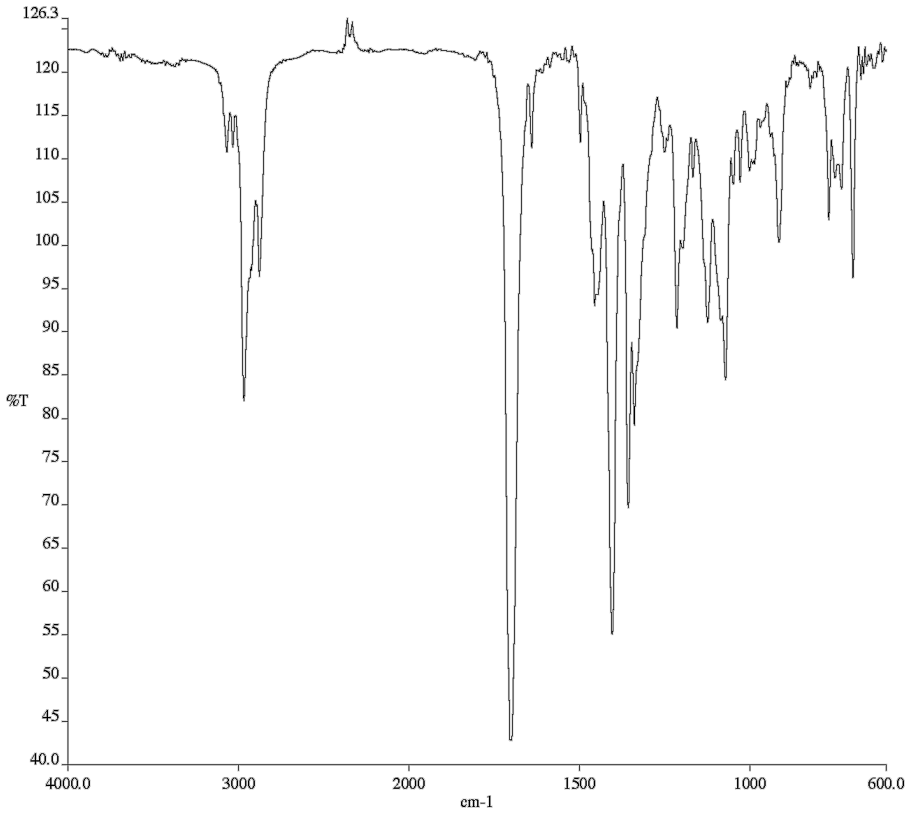

Figure A2-1.56. Infrared spectrum (Thin Film, NaCl) of compound **31d**.

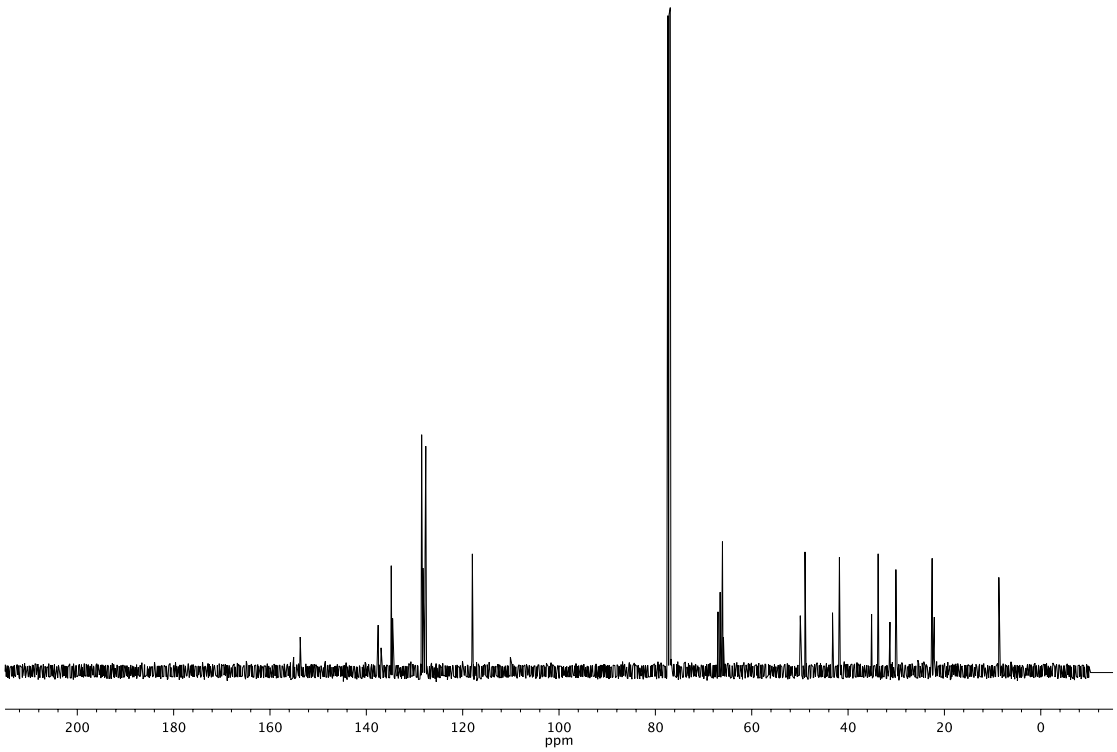

Figure A2-1.57. ^{13}C NMR (126 MHz, $CDCl_3$) of compound **31d**.

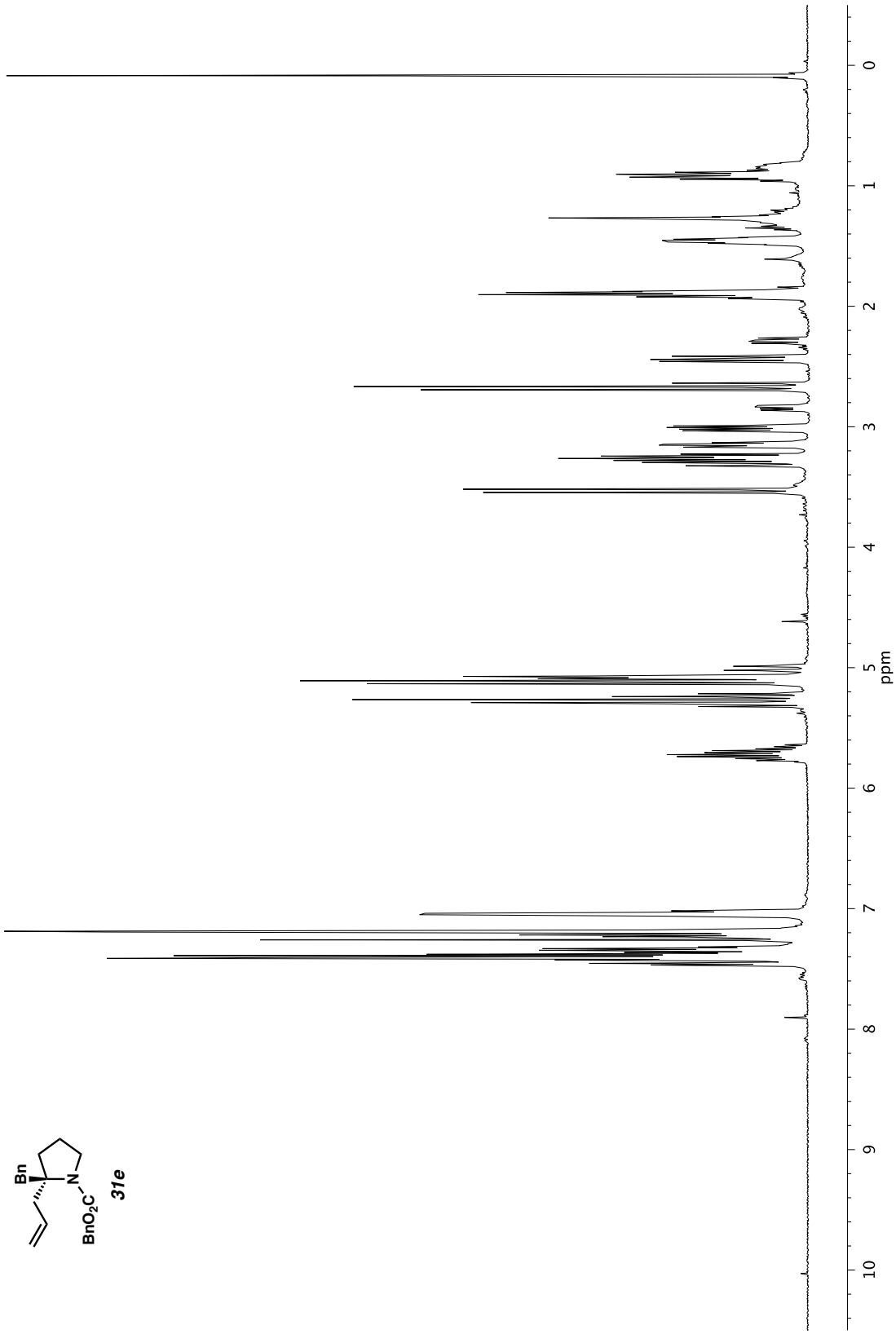

Figure A2-1.58. ^{1}H NMR (500 MHz, $CDCl_3$) of compound **31e**.

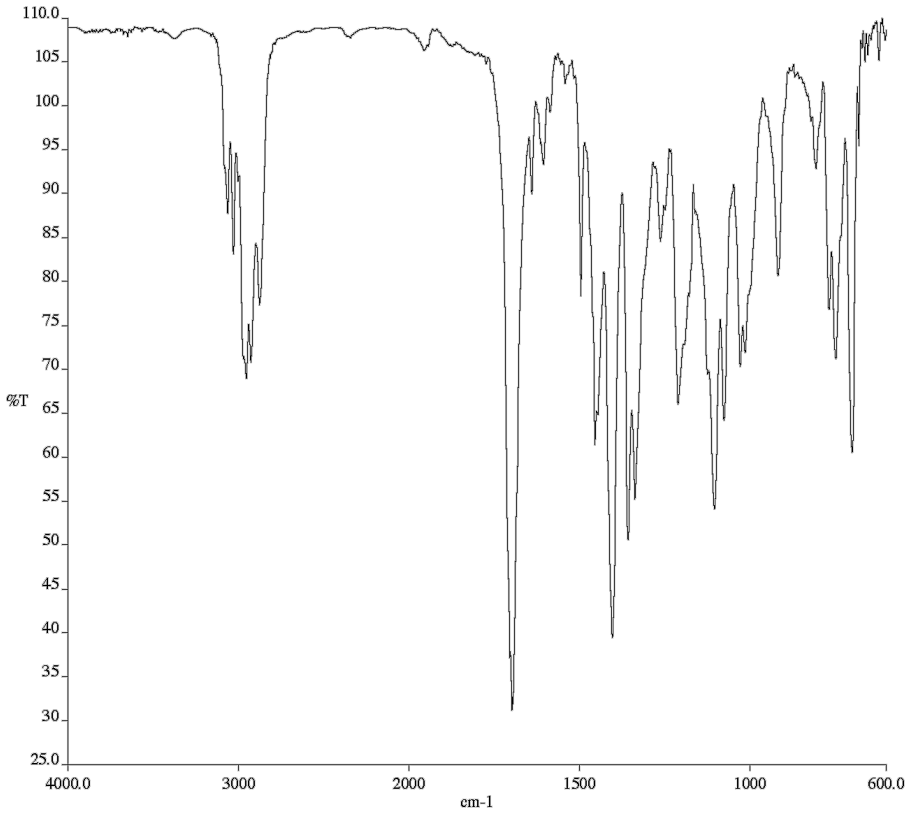

Figure A2-1.59. Infrared spectrum (Thin Film, NaCl) of compound **31e**.

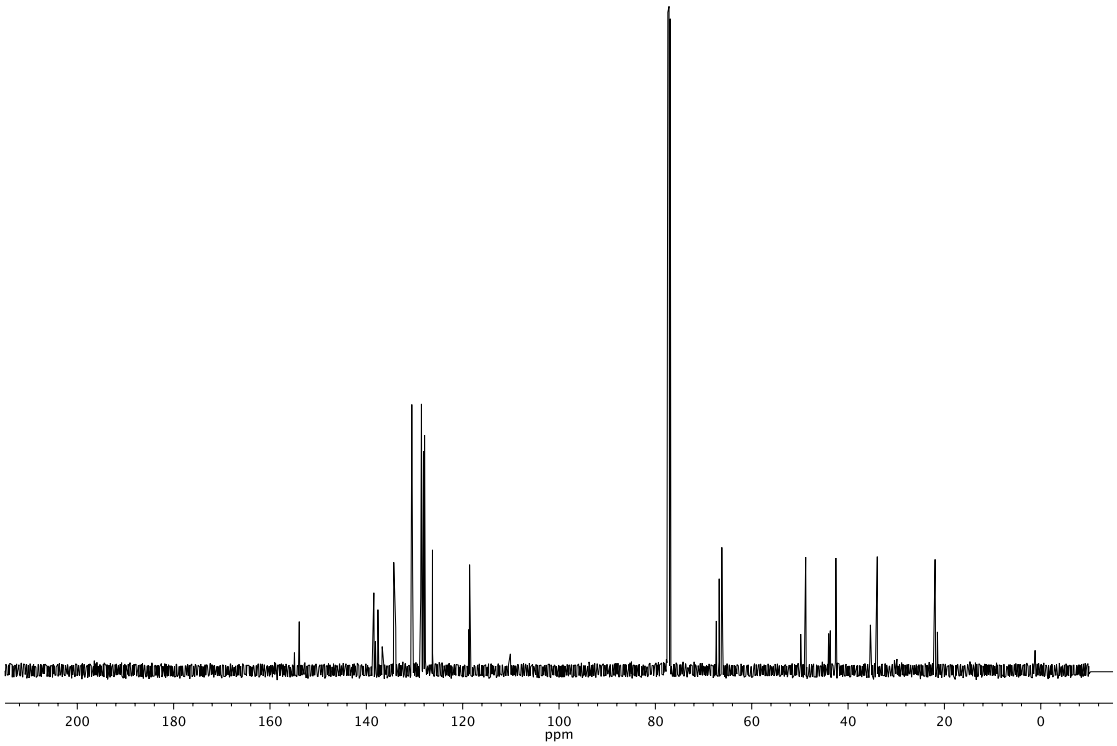

Figure A2-1.60. ^{13}C NMR (126 MHz, $CDCl_3$) of compound **31e**.

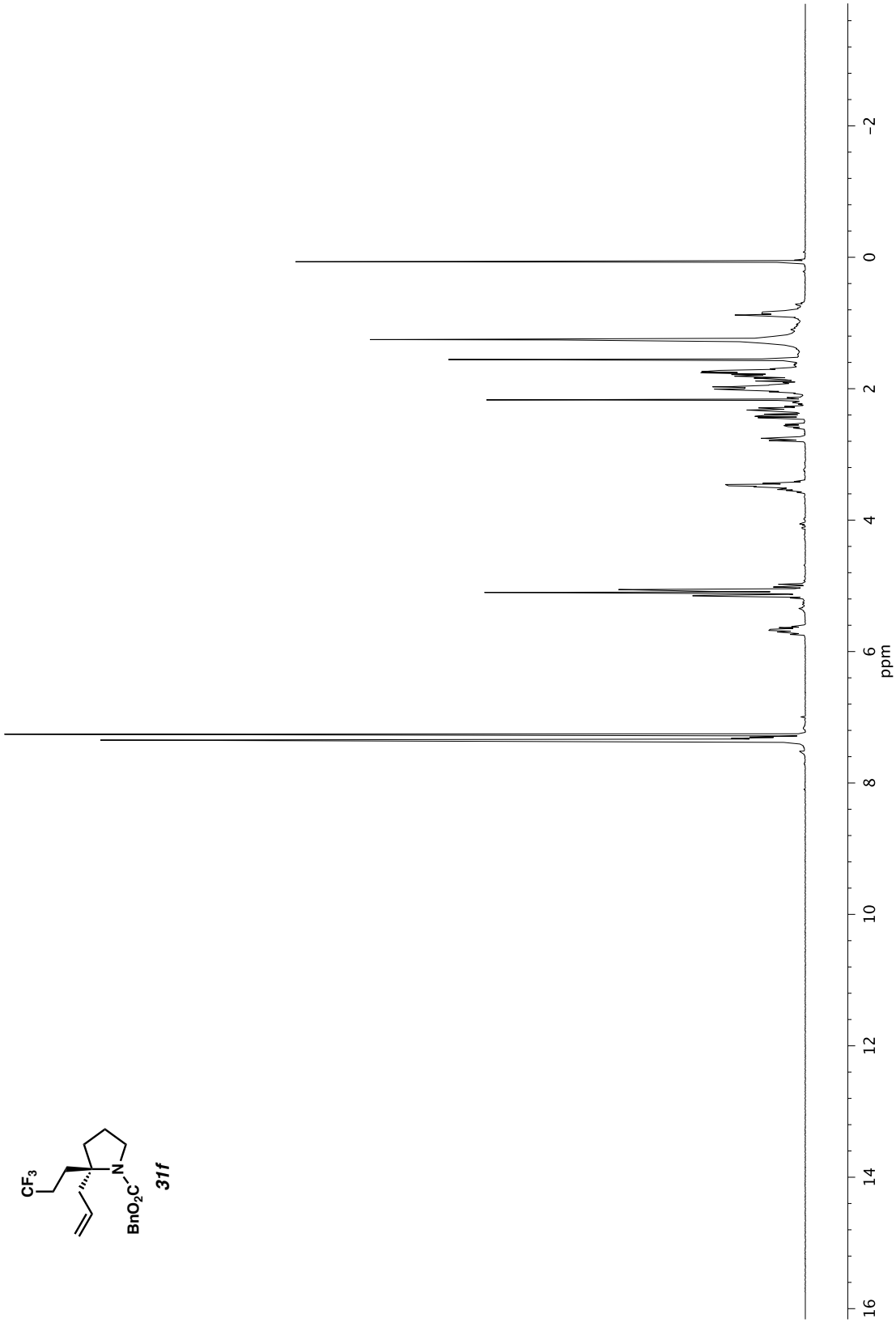

Figure A2-1.61. ^{1}H NMR (500 MHz, $CDCl_3$) of compound **31f**.

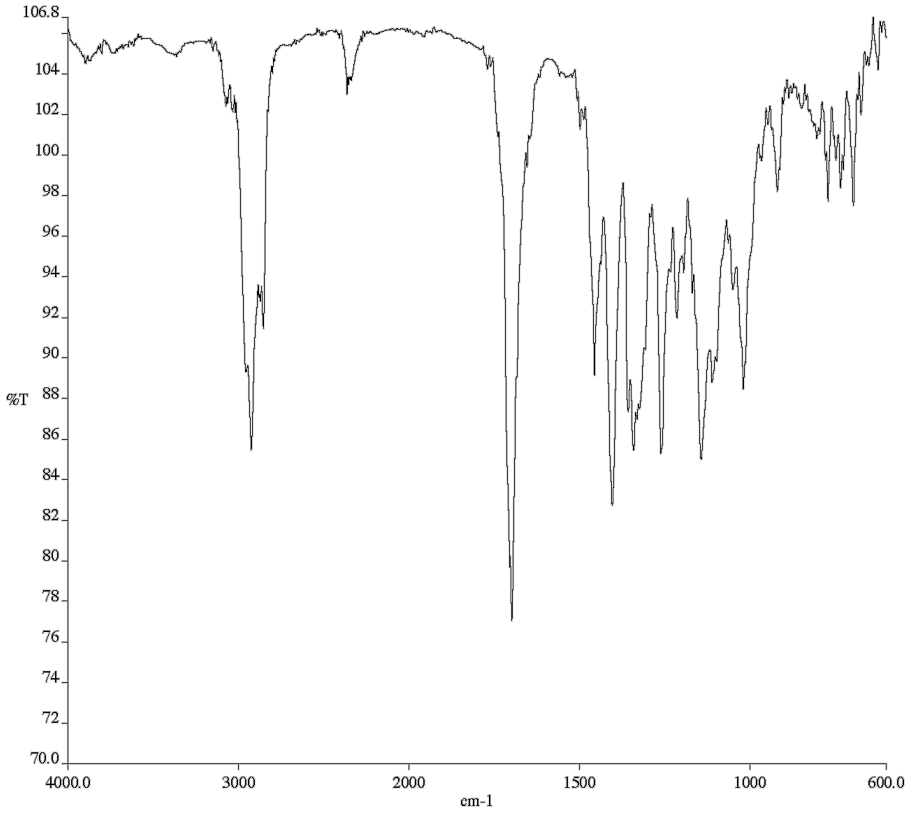

Figure A2-1.62. Infrared spectrum (Thin Film, NaCl) of compound **31f**.

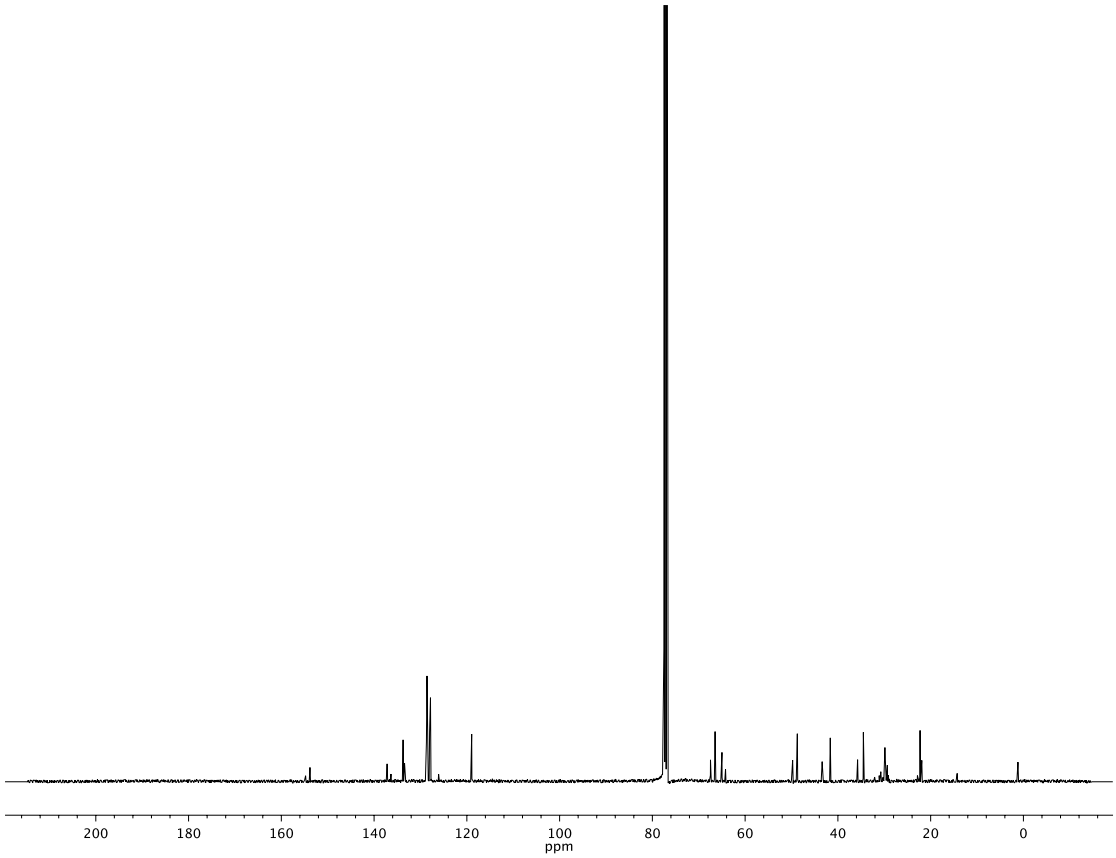

Figure A2-1.63. ^{13}C NMR (101 MHz, $CDCl_3$) of compound **31f**.

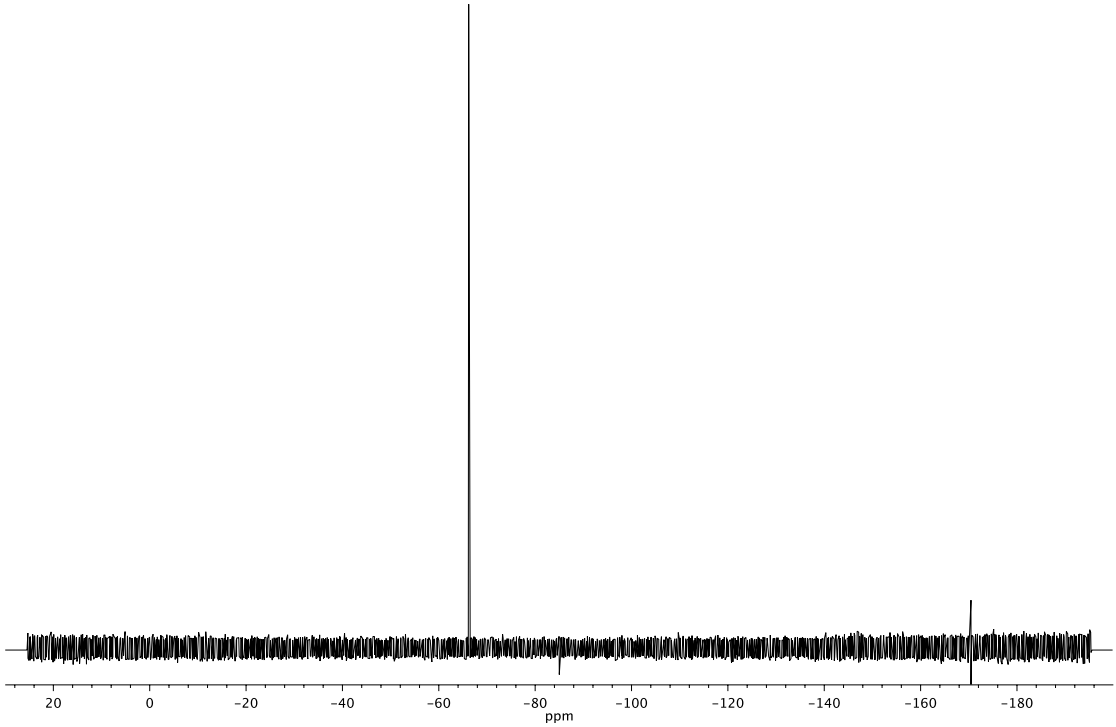

Figure A2-1.64. ^{19}F NMR (282 MHz, $CDCl_3$) of compound **31f**.

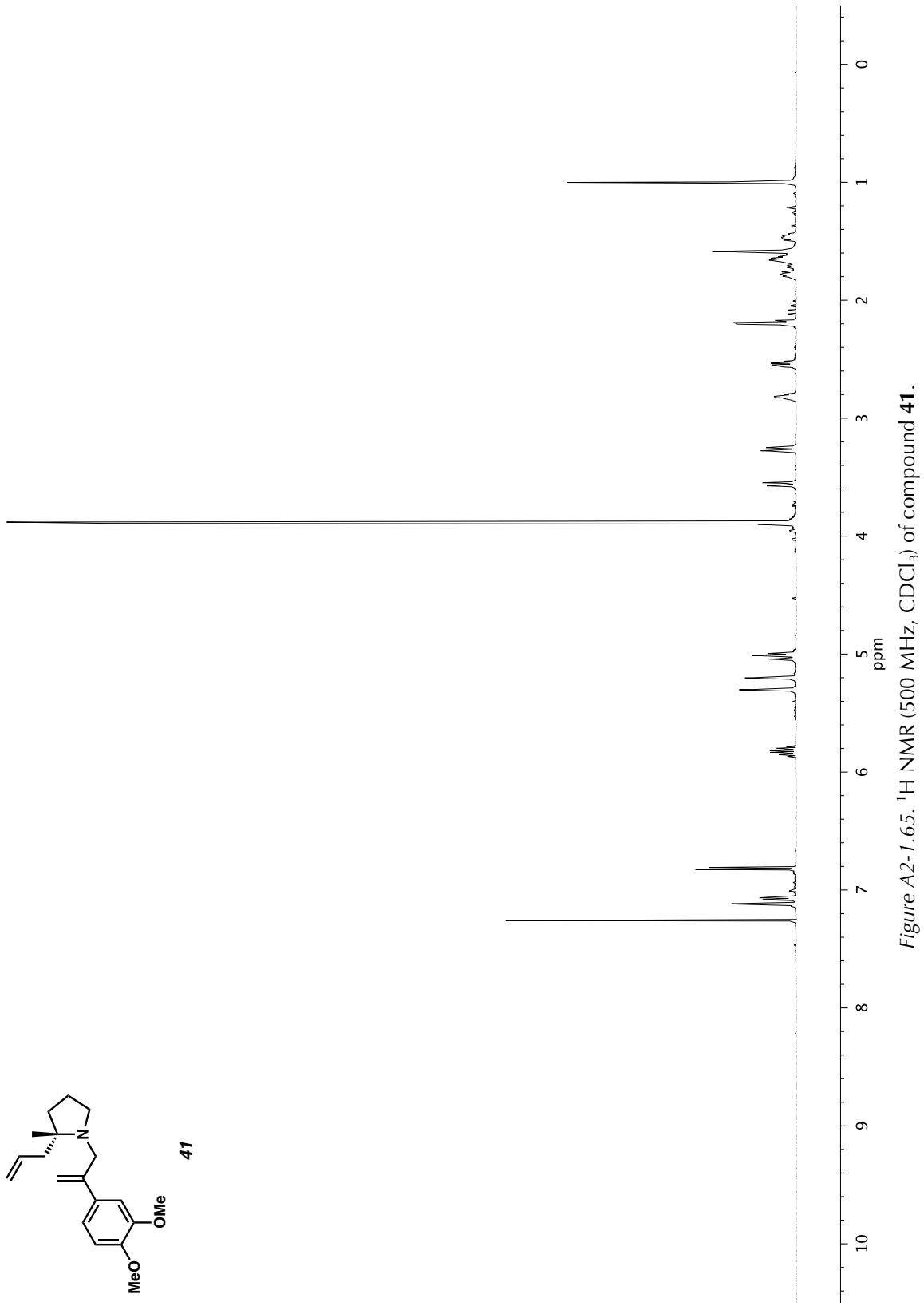

Figure A2-1.65. ^{1}H NMR (500 MHz, $CDCl_3$) of compound **41**.

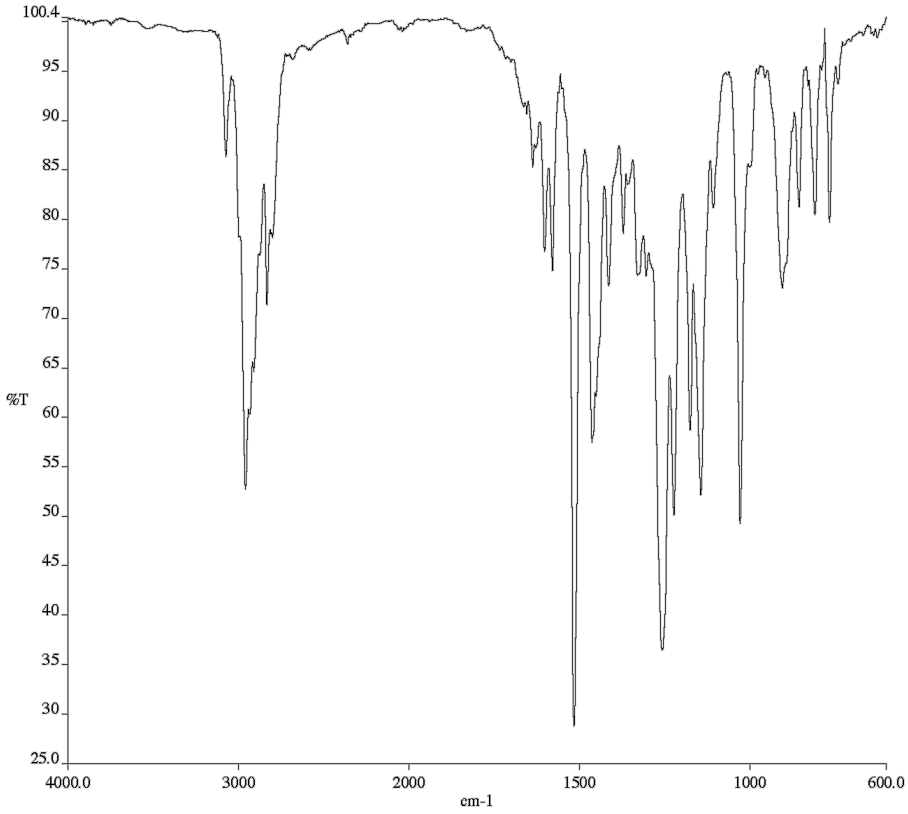

Figure A2-1.66. Infrared spectrum (Thin Film, NaCl) of compound **41**.

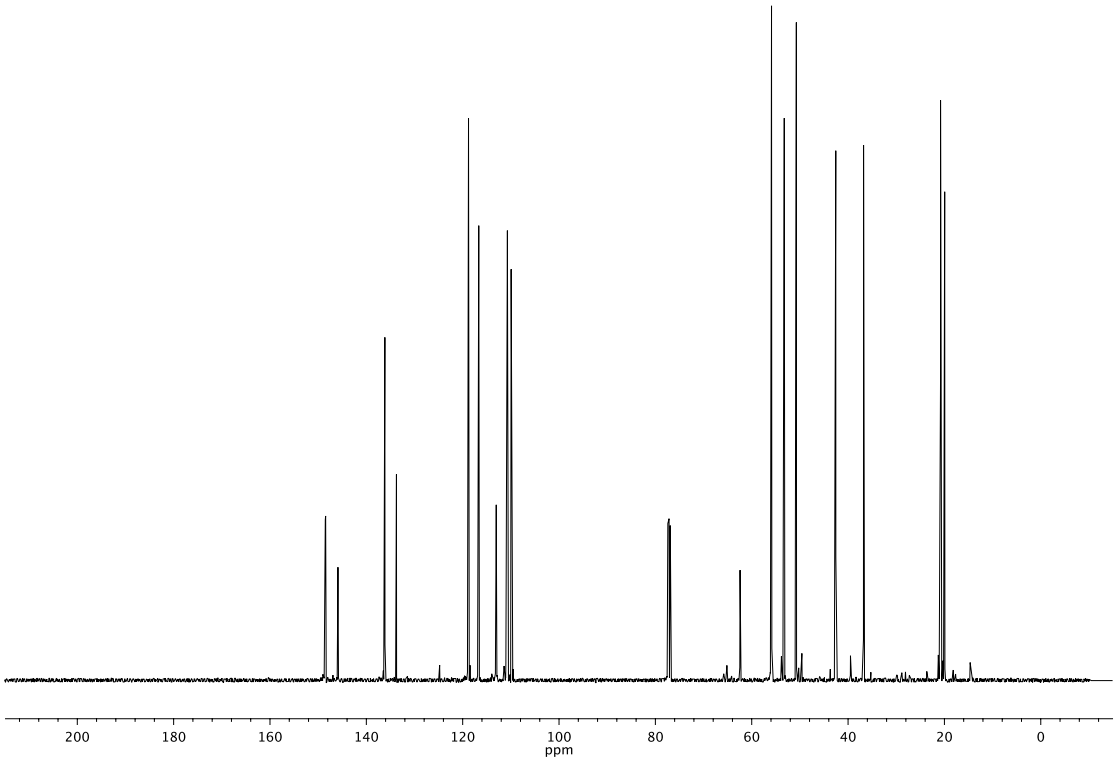

Figure A2-1.67. ^{13}C NMR (126 MHz, $CDCl_3$) of compound **41**.

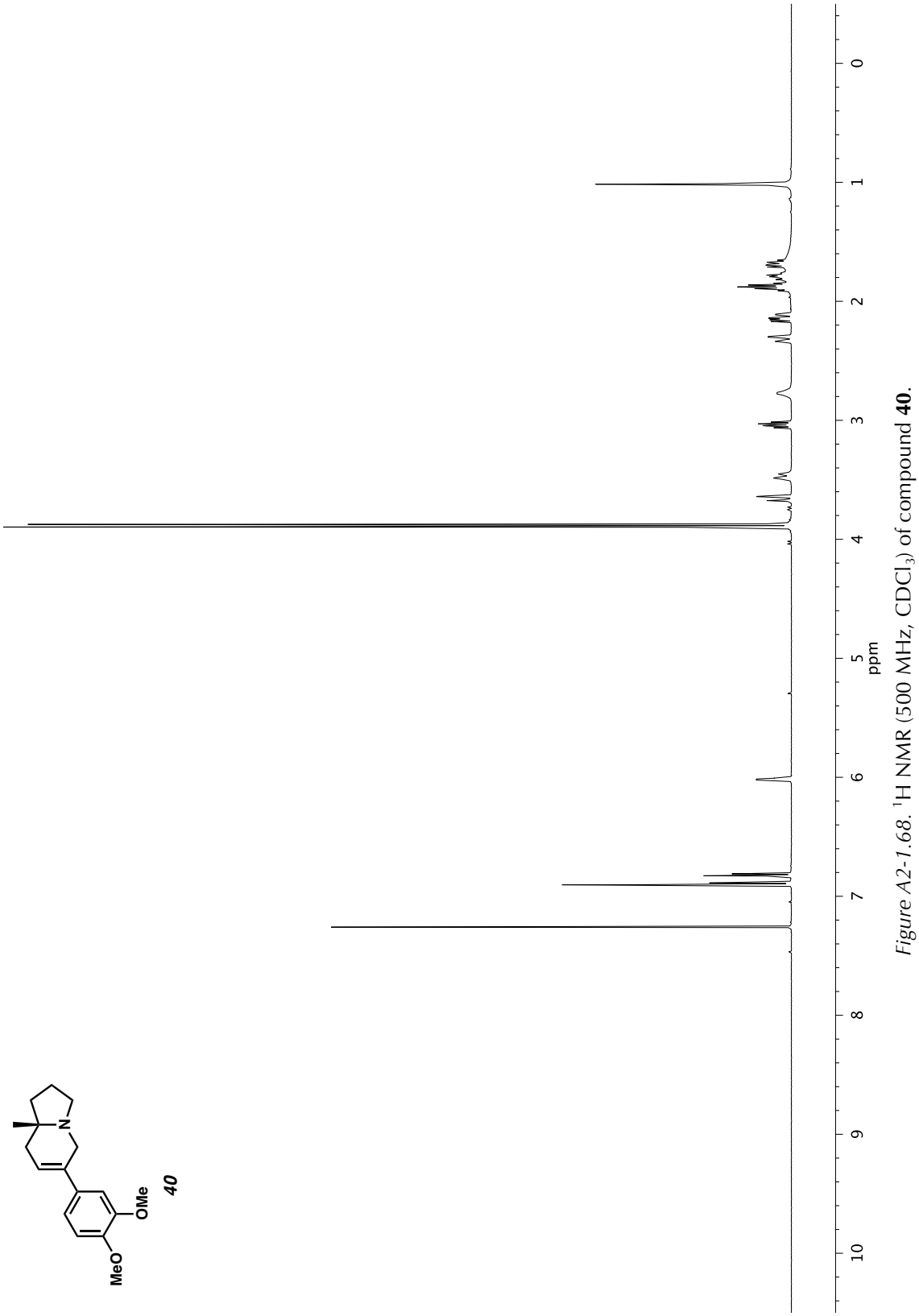

Figure A2-1.68. ^{1}H NMR (500 MHz, $CDCl_3$) of compound **40**.

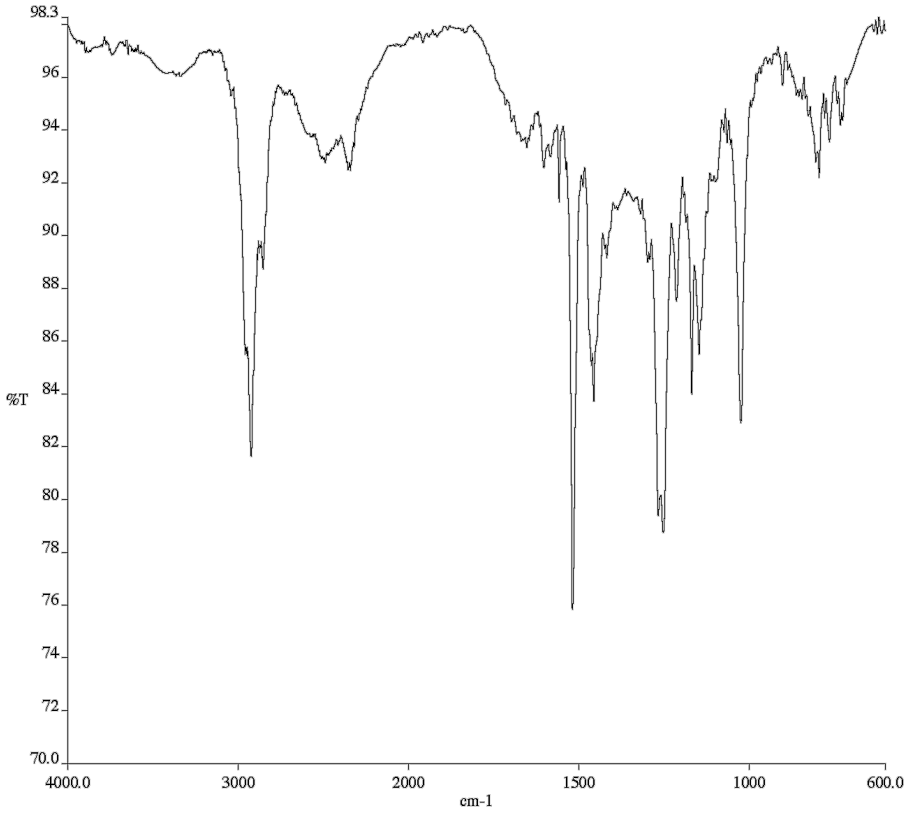

Figure A2-1.69. Infrared spectrum (Thin Film, NaCl) of compound **40**.

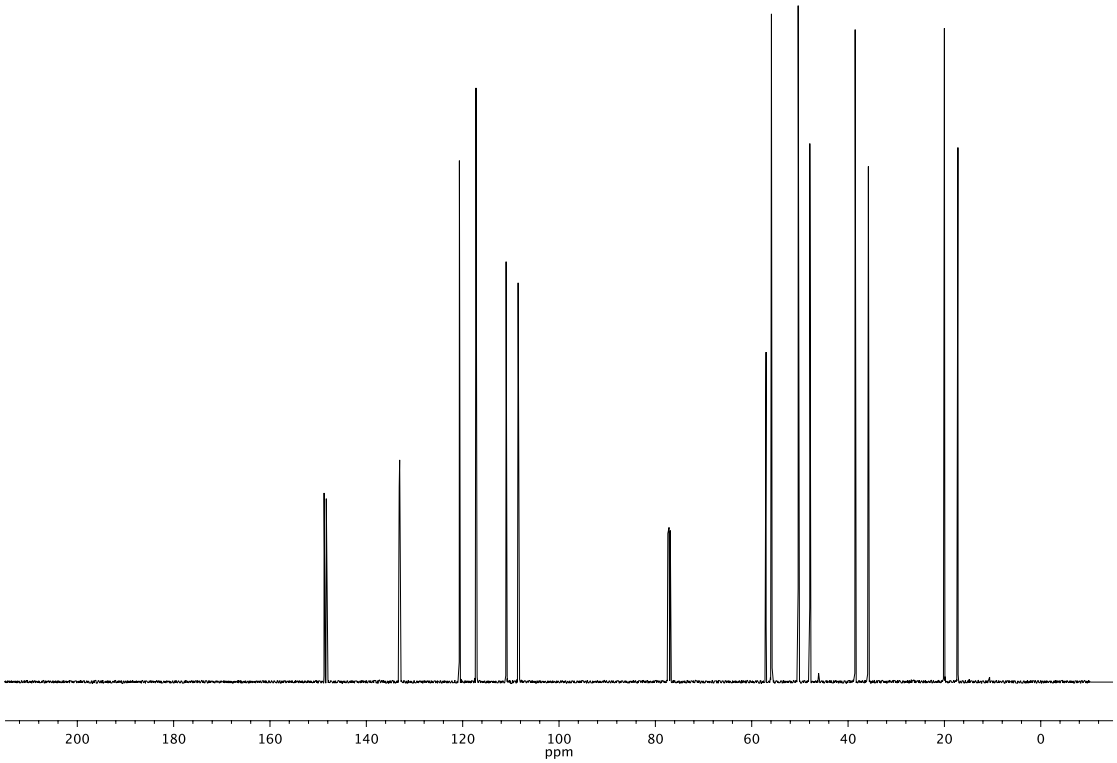

Figure A2-1.70. ^{13}C NMR (126 MHz, $CDCl_3$) of compound **40**.

Appendix 2-2

Progress Toward the Total Synthesis of Tylohirsuticine[†]

A2-2.1 INTRODUCTION:

As described in Chapter 2, we proposed utilizing our method for the synthesis of stereogenic 2,2-disubstituted pyrrolidines to access the natural product tylohirsuticine (**39**). Tylohirsuticine (**39**) was originally isolated from the aerial parts of *Tylophora hirsuta* and characterized in 1987 by Bhutani and coworkers.[1] *Tylophora hirsuta* has been utilized in Indian traditional medicine for treating asthma, high blood pressure, diarrhea, rheumatism, and other allergic conditions.[2] The Tylophora genus of plants has been found in previous studies to have laxative, expectorant, diaphoretic, and purgative properties, as well as antiasthmatic, anti-arthritic, and anti-cancer properties.[3] Further studies by Bashir and coworkers have shown that extracts from *Tylophora hirsuta* show significant antileishmanial (antiplasmodial) activity and moderate antifungal and insecticidal activity.[1]

Tylohirsuticine (**39**) is a member of the phenanthroindolizidine family of natural products, which consist of a phenanthrene core fused to an indolizidine bicycle (Figure A2-2.1.1). Tylohirsuticine (**39**) itself stands out from many of the other members in two

[†] This research was performed in collaboration with Hirokazu Takada, Yuji Sumii and Katsuaki Baba, all alumni of the Stoltz group.

ways. First, tylohirsuticine (**39**) is a seco-derivative of the class of natural products, meaning it does not have a fully fused phenanthrene core. Second, while most of these natural products have an α-secondary amine stereocenter, tylohirsuticine (**39**) contains a tetrasubstituted α-tertiary amine stereocenter.

Septicine (**46**) is another example of a *seco*-phenanthroindolizidine natural product,[4] which has been synthesized twice previously by Comins and Reddy.[5] Hypoestatin 1 (**47**),[6] which includes another example of this α-tertiary amine motif can be seen in which has been synthesized once in racemic form in 2007 by Ishibashi,[7] and then again in an enantioselective sense in 2012 by Wang.[8]

Figure A2-2.1.1 Phenanthroindolizidine alkaloids

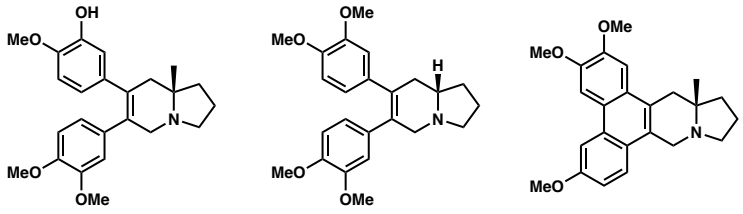

Septicine (**46**), was synthesized by Reddy and coworkers from the chiral pyroglutamic acid **48** via a known derivative (**49**, Scheme A2-2.1.1).[5b] The formation of the tetrasubstituted olefin proceeds via a McMurry coupling reaction of dione **50**. This dione was synthesized via *N*–alkylation of pyroglutamic acid derivative **49** to form 1,3-dithiane **51**, which could be elaborated to the dione **50**.

Scheme A2-2.1.1 Synthesis of septicine by Reddy et al.[5b]

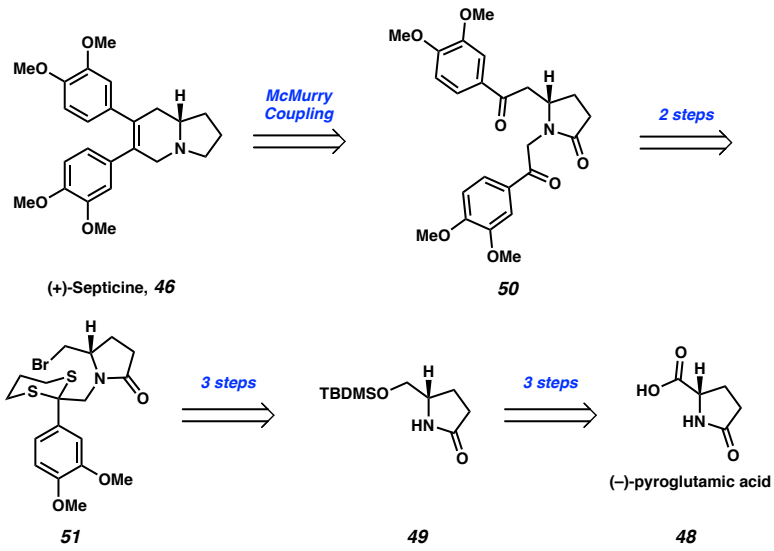

Hypoestatin 1 (**47**) is the only phenanthroindolizidine natural product containing an α-tertiary amine that has been synthesized previously. The first reported synthesis formed the α-tertiary amine via a radical cyclization reaction of bromide **52**.[7] (Scheme A2-2.1.2A) Five years later, the first asymmetric synthesis of hypoestatin 1 was reported.[8] (Scheme A2-2.1.2B) The synthesis of this natural product proceeded from amino acid **53**, which was elaborated to Seebach alkylation substrate **54**. This Seebach alkylation substrate could be coupled to a functionalized phenanthrene core (**55**) to form the α-tertiary amine stereocenter in **56**. Hydrolysis of the product results in the formation of methyl ester **57**, and a Pictet–Spengler reaction affords the natural product **47**.

Scheme A2-2.1.2 Synthesis of hypoestatin 1 by Ishibashi[7] and Wang[8]

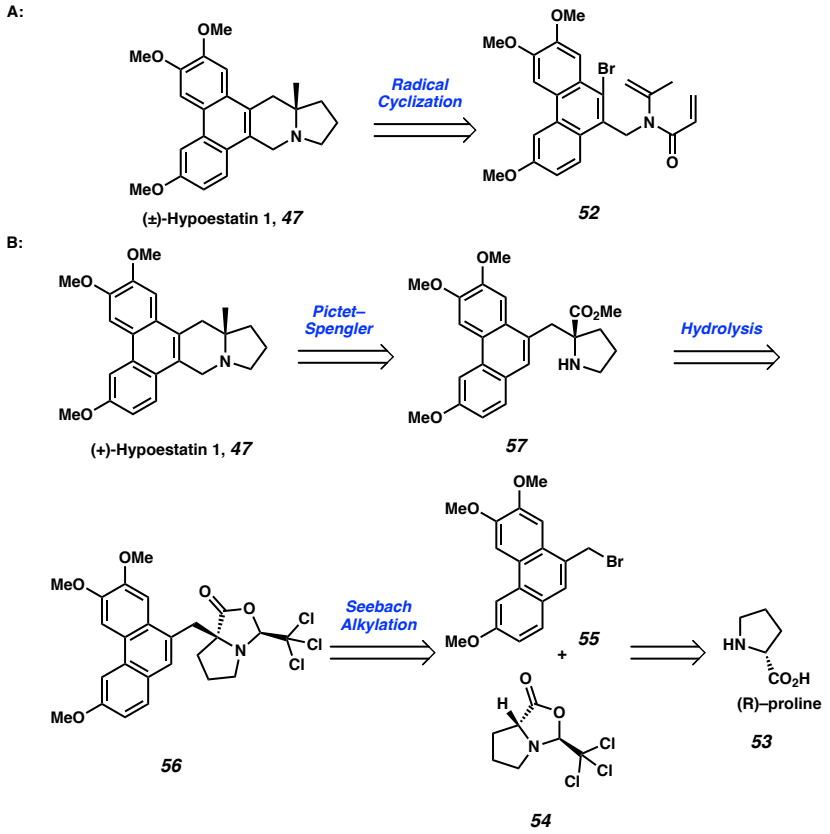

A2-2.2 ORIGINAL RETROSYNTHETIC ANALYSIS

Our discussion will encompass our efforts toward the synthesis of tylohirsuticine (**39**) from indolizidine **40**. Our early investigations into the synthesis of **40** are described in Chapter 2.5 and will not be discussed further. For purposes of review, our original retrosynthetic analysis has also been included here (Scheme A2-2.2.1).

Scheme A2-2.2.1 Retrosynthetic analysis of tylohirsuticine

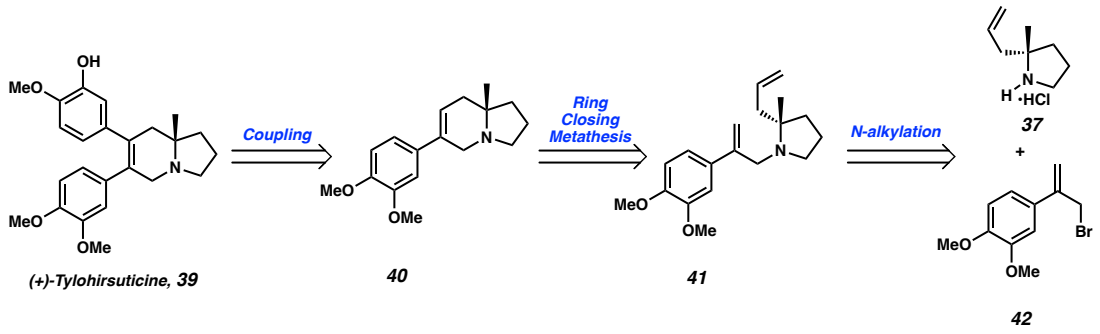

With olefin **40** in hand, we began to investigate the installation of the final ring. In the interest of efficiency, we first tried coupling the final aryl group directly to compound **40** through a Heck-type reaction (Table A2-2.2.1). Unfortunately, the use of canonical Heck conditions (Entry 1) and oxidative Heck conditions (Entry 2),[9] showed no reaction.

Table A2-2.2.1: Investigation of Heck conditions

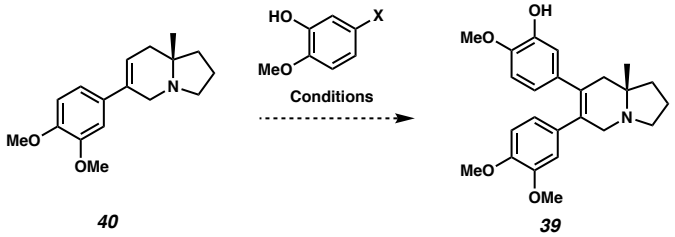

Entry	X	equiv ArX	Conditions	Result
1	Br	1.5	$Pd(OAc)_2$ (10 mol %), P(*o*–tol)$_3$ (30 mol %), Et_3N (2 equiv), CH_3CN, reflux	No reaction
2	Bpin	4	$Pd(OAc)_2$ (10 mol %), KF (4 equiv), $EtCO_2H$, O_2 (1 atm), 23 °C	No reaction

Therefore, we turned to the next most efficient route, direct bromination of the olefin **40** to form alkenyl bromide **58** followed by a subsequent coupling reaction (Table A2-2.2.2). The use of *N*-bromosuccinimide under multiple reaction conditions resulted in decomposition or no product formation (Entry 1, 2, and 4). Reaction of the olefin with

Py•HBr_3 resulted in no desired product, though a small amount of a dibrominated product was observed by LCMS (Entry 3).

Table A2-2.2.2: Bromination of the olefin

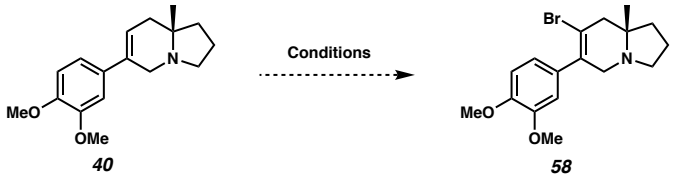

Entry	Conditions	Result
1	*N*-bromosuccinimide (1.1 equiv), MeOH, 23 °C	decomposition
2	*N*-bromosuccinimide (1.1 equiv), $NaHCO_3$ (2.2 equiv), CH_2Cl_2, 23 °C	decomposition
3	Py·HBr_3 (1.1 equiv), CH_2Cl_2, 23 °C	no desired product
4	*N*-bromosuccinimide (1.1 equiv), CH_3CN, 0 °C	no desired product

As our most efficient routes had been unsuccessful, we turned to more indirect methods of installing the aryl group. Epoxidation of olefin **40** to afford epoxide **59** (Scheme A2-2.2.2), followed by epoxide opening with a nucleophile and dehydration could afford our desired product **39**. Unfortunately, the use of *m*-CPBA as oxidant, either alone (Table A2-2.2.3, Entry 1) or in the presence of Na_2CO_3 (Entry 2) or TFA (Entry 3) as additives yielded no desired product. Furthermore, use of urea hydrogen peroxide (UHP) as an oxidant, along with TFAA (trifluoroacetic anhydride) and TFA as additives, also formed none of the desired product (Entry 4). Attempts to dihydroxylate the olefin using OsO_4 with NMO as the stoichiometric oxidant to afford **60** also resulted in no reaction (Scheme A2-2.2.3).

Scheme A2-2.2.2 Proposed epoxidation strategy

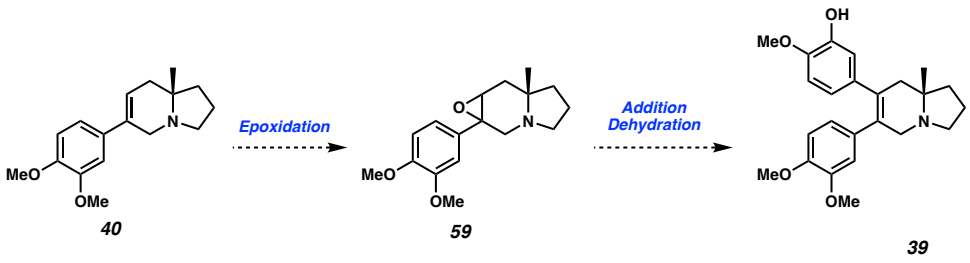

Table A2-2.2.3 Epoxidation of the olefin

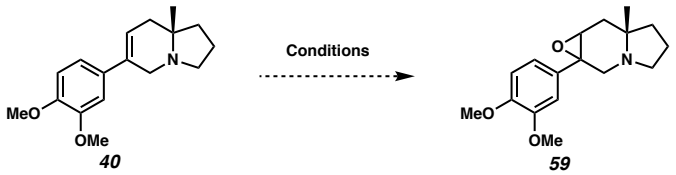

Entry	Conditions	Result
1	*m*–CPBA (1.2 equiv), CH_2Cl_2, 23 °C	No desired product
2	*m*–CPBA (1.2 equiv), Na_2CO_3, CH_2Cl_2/H_2O (5:1), 23 °C	No desired product
3	*m*–CPBA (2.4 equiv), TFA (1.1 equiv) CH_2Cl_2, 23 °C	No desired product
4	UHP (20 equiv), TFAA (6 equiv), TFA (1.1 equiv), CH_2Cl_2, 23 °C	No desired product

Scheme A2-2.2.3 Dihydroxylation of the olefin

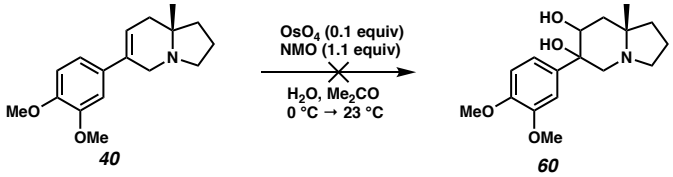

Following our lack of success in forming the desired intermediates, we investigated the oxidation of olefin **40** to form ketone **61** with the goal of producing enol triflate **62**. This compound could then be screened with a variety of cross-coupling conditions (Scheme A2-2.2.4).

Scheme A2-2.2.4 Plan for the installation of the final ring

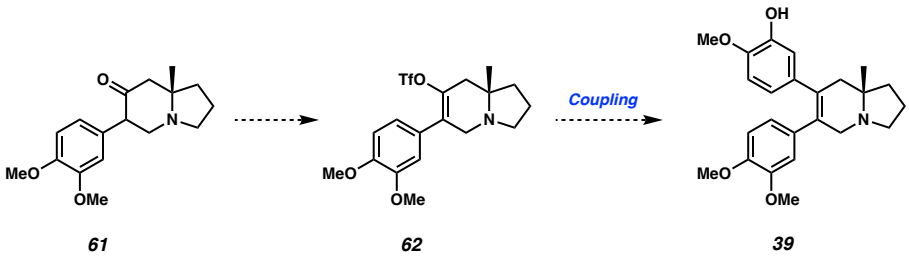

We proposed the oxidation of the olefin via a hydroboration/oxidation sequence, first affording alcohol **63** which could subsequently be oxidized to ketone **61**. Initial attempts to hydroborate the olefin using 9-Borabicyclo[3.3.1]nonane (9-BBN) resulted in no product formation (Table A2-2.2.4, Entry 1). The use of slight excess of BH_3•THF

(or BH_3•DMS) resulted in no product formation, which we hypothesized was due to the complexation of BH_3 with the tertiary amine (Entry 2). Gratifyingly, increasing the loading of BH_3•THF to 15 equiv resulted in the formation of the desired product **63**, though it was difficult to purify via chromatography or other methods (Entry 3).

Table A2-2.2.4 Hydroxylation of the olefin

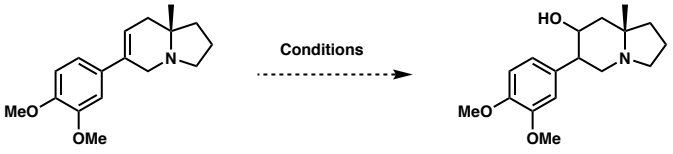

40 ***63***

Entry	Conditions	Result
1	9–BBN (1.5 equiv), THF, H_2O_2, 23 °C	no desired product
2	BH_3 · THF (1.5 equiv), $NaBO_3$·$4H_2O$ (5 equiv), THF, H_2O, 23 °C	no desired product
3	BH_3 · THF (15 equiv), $NaBO_3$·$4H_2O$ (50 equiv), THF, H_2O, 23 °C	product observed

Nevertheless, we decided to continue investigating this route further through oxidation of crude alcohol **63** to ketone **61** (Table A2-2.2.5). The use of Swern conditions resulted in detection of the desired product (**61**) by LCMS but the product could not be isolated (Entry 1). Use of Parikh–Doering oxidation conditions also resulted in product formation, though in low yields (15% from **40**, Entry 2). Unfortunately, the use of pyridimiun chlorochromate (PCC, Entry 3) and a combination of TPAP (Tetrapropylammonium perruthenate) and NMO (*N*-Methylmorpholine *N*-oxide, Entry 6) resulted in no desired product formation. When PCC was employed in the presence of SiO_2 as a drying agent; however, the product was formed in 25% yield over two steps from **40** (Entry 5). It was also found that the use of DMP (Dess–Martin periodinane) as oxidant resulted in approximately 25% yield from **40** (Entry 4). As these results were not as high yielding as desired, and any attempts to further functionalize these products proved futile, we decided to instead revise our retrosynthetic proposal.

Table A2-2.2.5 Oxidation of the alcohol

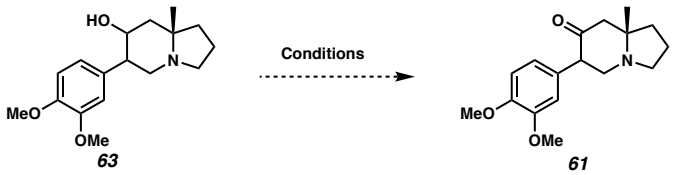

Entry	Conditions	Yield over 2 steps
1	$(COCl)_2$ (2 equiv), DMSO (3 equiv), Et_3N (6 equiv), CH_2Cl_2, –78 °C→ 23 °C	LCMS observed
2	$SO_3 \cdot Py$ (3 equiv), DIPEA (10 equiv), DMSO, CH_2Cl_2, 0 °C→ 23 °C	15% yield
3	PCC (3 equiv), CH_2Cl_2, 23 °C	no desired product
4	DMP (1.5 equiv), CH_2Cl_2, 23 °C	25% yield
5	PCC (5 equiv), SiO_2, CH_2Cl_2, 23 °C	25% yield
6	TPAP (0.1 equiv), NMO (2 equiv), 4Å MS, CH_2Cl_2, 23 °C	no desired product

A2-2.3. SUBSTITUTED ALLYLIC ALKYLATION SUBSTRATES

Due to a lack of success in functionalizing indolizidine **40**, we instead turned our attention to other methods of introducing the challenging tetrasubstituted olefin. In order to accomplish this, we proposed introducing susbstituted allylic alkylation precursors. One such strategy is described in Scheme A2-2.3.1, using the same key disconnections with a 2-allyl substituent in place on compound **68**: this would then proceed through the same asymmetric allylic alkylation, ring contraction, *N*–alkylation, and RCM sequence.

Scheme A2-2.3.1 Revised retrosynthetic analysis

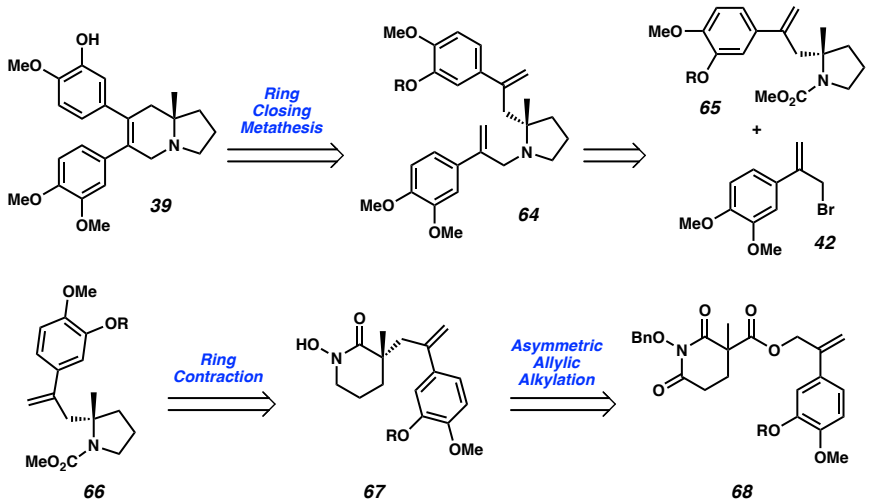

In order to test our new retrosynthetic proposal, we first needed to synthesize our desired asymmetric allylic alkylation substrate with a 2-allyl substituent (Scheme A2-2.3.2). Starting with commercially available 5-bromo-2-methoxyphenol **69**, TBS protection first afforded **70**. This was used to form a Grignard reagent, which upon addition of CuI and propargyl alcohol afforded homo-allylic alcohol **71** in moderate yield. When treated with carbonyl diimidizole (CDI), acylation substrate **72** was formed, which was then utilized to acylate *O*-benzyloxylimide **33** to yield **73**. A final alkylation with methyl iodide afforded allylic alkylation substrate **68**.

Scheme A2-2.3.2 Synthesis of 2–allyl substituted asymmetric allylic alkylation substrate

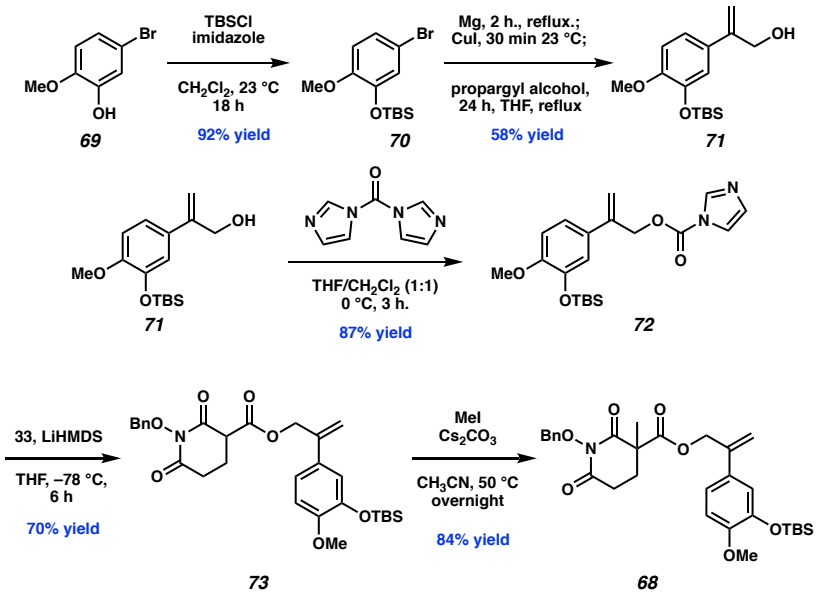

With compound **68** in hand, we began to investigate its reactivity of in the asymmetric allylic alkylation. We were very pleased to note that using the conditions optimized for compound **74**, as described in chapter 2.2, proceeded in good yield and excellent stereoselectivity (Table A2-2.3.1)

Table A2-2.3.1 Asymmetric allylic alkylation reaction of 2–allyl substituted substrate

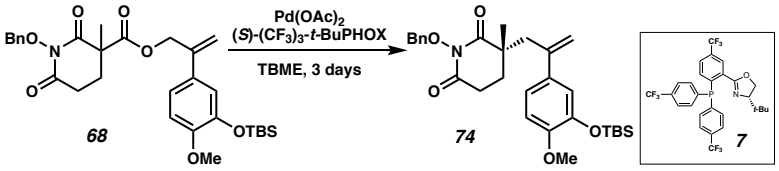

Entry	mol % Pd	mol % ligand	concentration	temperature	ee	yield
1	2.0	6.0	0.1 M	60 °C	95%	69%
2	1.0	3.0	0.14 M	65 °C	92%	74%

Following our successful synthesis of **74**, we proceeded to investigate the viability of this substrate in the ring contraction (Scheme A2-2.3.3). Treatment of compound **74** with DIBAL-H afforded selective mono-reduction to imide **75**, which could then undergo reduction in the presence of sodium cyanoborohydride and BF_3•Et_2O to yield **76** in good yield. Unfortunately, all attempts to remove the benzyl protecting group on the hydroxamic acid were met with either no reaction or decomposition, and so we were never able to investigate further.

Scheme A2-2.3.3 Selective reduction of imide

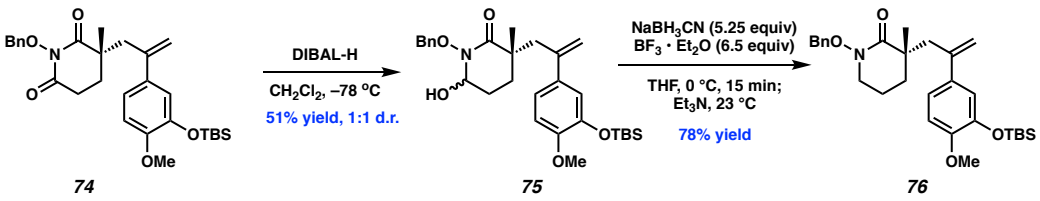

While we were disappointed in these results, we thought a similar strategy might still be plausible. To that end, we proposed another retrosynthetic analysis (Scheme A2-2.3.4). In particular, we were interested in using a different 2-allyl substituted allylic alkylation substrate (2-chloroallyl substrate **81**) due to previous success with similar substrates. The overall strategy is again the same as those previously investigated,

though this time there is a different functional handle in place to enable the end-game strategy.

Scheme A2-2.3.4 Alternative retrosynthetic proposal

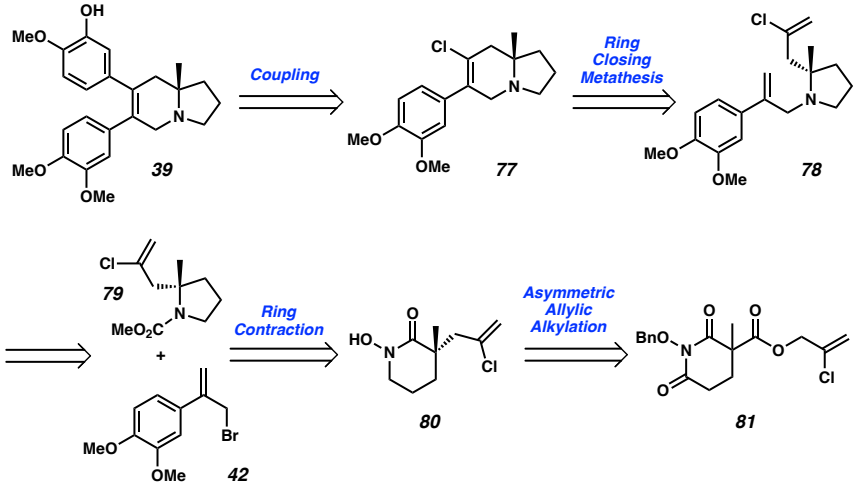

We started our investigation again by synthesizing the desired allylic alkylation substrate **81** (Scheme A2-2.3.5). Having successfully used this method in the synthesis of **68**, we treated commercially available 2-chloroallyl alcohol **82** with CDI to afford acylating agent **83**. This reagent was then utilized in an enolate α–acylation yielding **84** followed by alkylation to afford allylic alkylation substrate **81** in good yield.

Scheme A2-2.3.5 Synthesis of 2–chloroallyl asymmetric allylic alkylation substrate

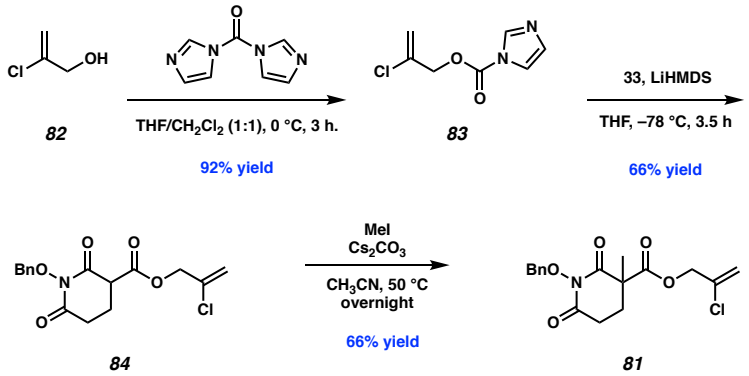

We then proceeded to investigate the reactivity of this substrate toward asymmetric allylic alkylation (Table A2-2.3.2). Beginning with our previously optimized conditions, we were disappointed to find no reaction was observed under these low catalyst loading conditions (Entries 1–2). We proceeded to investigate whether reactivity would be observed under standard conditions (Entries 3–4).[10] While we were finally able to observe some formation of **85**, the reaction proceeded slowly and required long reaction times and high temperatures. Even after seven days, the reaction had not proceeded to full conversion. Additionally, attempts to selectively reduce the resulting imide proved unsuccessful, and so we had to again revise our retrosynthetic proposal.

Table A2-2.3.2 Asymmetric allylic alkylation reaction of 2–chloroallyl substrate

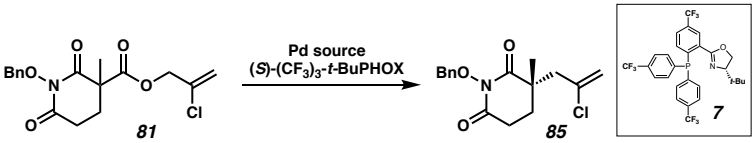

Entry	Pd source	mol % Pd	mol % ligand	time	temperature	solvent	result
1	$Pd(OAc)_2$	2.0	6.0	3 days	60 °C	TBME	no reaction
2	$Pd(OAc)_2$	1.0	3.0	3 days	60 °C	TBME	no reaction
3	$Pd_2(dba)_3$	5.0	12.5	5 days	70 °C	toluene	25% conversion
4	$Pd_2(dba)_3$	5.0	12.5	7 days	70 °C	TBME	90% conversion

A2-2.4 FURTHER RETROSYNTHETIC STRATEGIES

Having investigated several different strategies, we envisioned combining the strengths of our previously outlined retrosynthetic proposals. Due to the reliability of the synthesis of pyrrolidine **31a–c**, we decided to take advantage of this intermediate by forming the tetrasubstituted olefin from an intermediate such as **86a–b** through either an RCM ($X=CH_2$) or McMurry coupling (X=O) (Scheme A2-2.4.1). Compound **86** could arise via a number of different methods dependent on the identity of X, though common to all these approaches was an *N*-alkylation event of pyrrolidines **31a–c**.

Scheme A2-2.4.1 Alternative retrosynthetic proposal

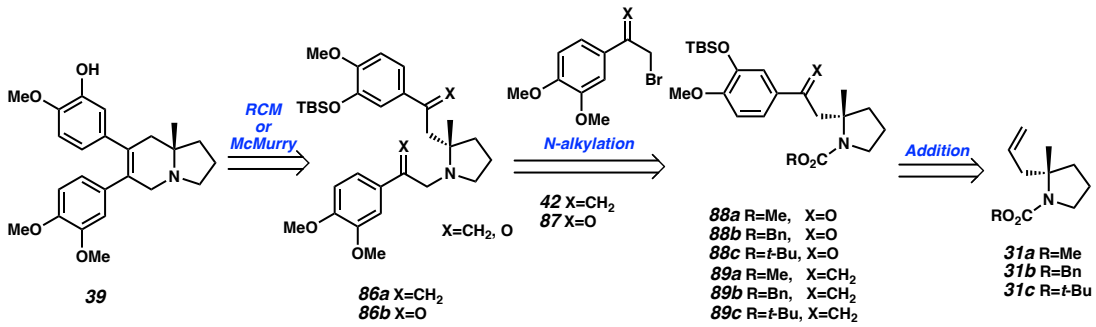

In the forward sense, we, we demonstrated that compound **31a** underwent an oxidative cleavage reaction with good yield to afford **90**, which could undergo an organolithium addition and oxidation sequence to yield **88a** (Scheme A2-2.4.2). Unfortunately, we were never able to remove the methyl carbamate protecting group from **88a**.

Scheme A2-2.4.2 Synthesis of aryl ketone compound

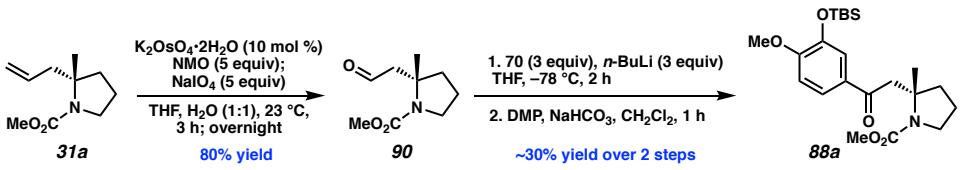

We then proceeded to functionalize **31b–c** (Scheme A2-2.4.3) to facilitate deprotection. We had previously demonstrated the oxidative cleavage of **31a**, and found the reaction to proceed smoothly on both the Boc and Cbz protected pyrrolidines as well to afford **91a–b**. Following the report of Cossy,[11] we were able to remove one additional methylene under oxidative conditions to yield **92a–b**. Unfortunately, we were again unable to advance either of these intermediates to the natural product, as the aldehyde proved unstable to deprotection conditions.

Scheme A2-2.4.3 Synthesis of aldehyde compounds

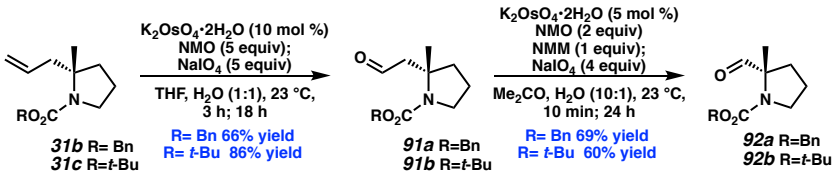

In the course of these investigations, it soon became clear that the introduction of a carbonyl group into these intermediates led to many challenges due to competitive reactivity of the functional group. Therefore, we turned our attention to a method of introducing the aryl group at the 2-allyl position, utilizing an oxidative coupling introduced by Stahl and coworkers.[12] We were pleased to observe reactivity of **31c** under the reported conditions (Scheme A2-2.4.4), affording desired compound **94** in 30% yield. Unfortunately, we were unable to remove the Boc group and attempts to investigate this reaction further were thwarted.

Scheme A2-2.4.4 Synthesis of 2–allyl substituted pyrrolidine compound

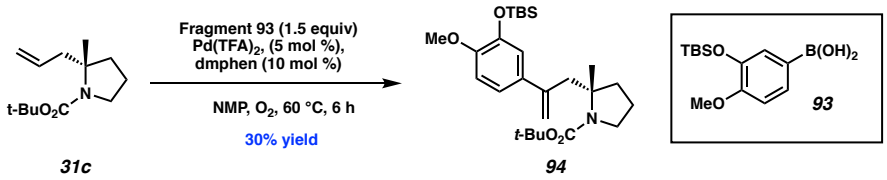

A2-2.5 CONCLUSIONS

Throughout the course of our investigation into the synthesis of tylohirsuticine **(39)**, we were able to demonstrate the synthesis of many interesting new compounds. We expanded the scope of our asymmetric allylic alkylation and advanced several of these products to synthesize enantioenriched 2,2-disubstituted pyrrolidines, as outlined in chapter 2. We were further able to use the olefin functional handle in order to synthesize a number of different novel compounds. Although the synthesis of tylohirsuticine **(39)**

remains elusive, we hope that the lessons learned throughout our investigations will continue to instruct future synthetic efforts towards phenanthroindolizidine alkaloids and their analogues.

A2-2.6 NOTES & REFERENCES

[1]Ali, M., Bhutani; K. K. *Phytochemistry* **1987**, *26*, 2089–2092.

[2] Bashir, A.; Ali, N.; Bashir, S.; Choudhary, M. *African Journal of Biotechnology* **2009**, *8*, 4627–4631.

[3] a) Gopalakrishnan, C.; Shankaranarayanan D.; Nazimudeen, S. K. *Indian J. Med. Res.* **1980**, *71,* 940–948. b) Wagner H. *Planta Med*. **1989**, *55*, 235–241. c) Dikshith T. S.; Raizada R. B.; Mulchandani N. B *Indian J. Exp. Biol*. **1990**, *28*, 208–212. d) Wenli G.; Wing L. *Cancer Res*. **2004**, *64,* 678–688.

[4] Russel, J. H.; Hunziker, H. *Tetrahedron Lett*. **1969**, *10*, 4035–4036.

[5] a) Comins, D. L.; Chen, X.; Morgan, L. A. *J. Org. Chem*. **1997**, *62*, 7435–7438. b) Reddy, K. U.; Reddy, A. P. *Synthetic Comm*. **2013**, *43*, 2678–2684.

[6] Pettit, G. R.; Goswami, A.; Cragg, G. M.; Schmidt, J. M.; Zou, J.–C. *J. Nat. Prod.* **1984**, *47*, 913–919.

[7] Takeuchi, K.; Ishita, A.; Matsuo, J.–I.; Ishibashi, H. *Tetrahedron* **2007**, *63*, 11101–11107.

[8] Su, B.; Cai, C.; Wang, Q. *J. Org. Chem*. **2012**, *77*, 7981–7987.

[9] He, Z.; Kirchberg, S.; Fröhlich, R.; Studer, A. *Angew. Chem. Int. Ed*. **2012**, *51*, 3699–3702.

[10] Behenna, D. C.; Liu, Y.; Yurino, T.; Kim, J.; White, D. E.; Virgil, S. C.; Stoltz, B. M. *Nat. Chem*. **2012**, *4,* 130–133.

[11] Belotti, D.; Andreatta, G.; Pradaux, F.; BouzBouz, S.; Cossy, J. *Tetrahedron Lett*. **2003**, *44*, 3613–3615.

[12]Zheng, C.; Stahl, S. S. *Chem*. *Commun*. **2015**, *51*, 12771–12774.

CHAPTER 3

Synthesis of

[7,7]paracyclophanes[†]

3.1 INTRODUCTION

Paracyclophanes are a class of molecules that were first described by Cram and Steinberg as far back as 1951.[1] Cyclophanes (Figure 3.1.1) are macrocyclic molecules that contain two aromatic rings within the macrocyclic structure.[2]

Figure 3.1.1 Structure of Cyclophanes

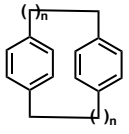

Cyclophane

[†] This research was performed in collaboration with Aaron T. Bosse, Kuangbiao Liao, Wenbin Liu, Zhi Ren, John Bacsa, Djamaladdin G. Musaev, and Huw M. L. Davies at Emory University through the Center for C-H functionalization. Additionally, parts of this chapter have been published and adapted with permission from Liu, W. B.; Ren, Z.; Bosse, A. T.; Liao, K. B.; Goldstein, E. L.; Bacsa, J.; Musaev, D. G.; Stoltz, B. M.; Davies, H. M. L. *J. Am. Chem. Soc.* **2018,** *140*, 12247-12255.

In 1990, the first naturally occurring cyclophane was isolated from the Nostocaceae species *Cylindrospermum licheniforme*, and so named cylindrocyclophane A.[3] (Figure 3.1.2) Two years later, cylindrocyclophanes B–F were isolated from the same species of algae.[4] A further 10 cylindrocyclophanes (A_1–A_4, C_1–C_4, F_4 and A_{B4}) were isolated from a new species of Nostocaceae that was discovered on a parkway in Chicago.[5] Since the discovery of the cylindrocyclophane class of [7,7]paracyclophanes, a number of related classes have been isolated, namely the nostocyclophanes,[6] ribocyclophanes,[7] carbamidocyclophanes,[8] and merocyclophanes.[9]

Figure 3.1.2 Structures of [7,7]paracyclophanes

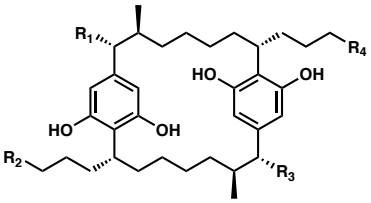

Cylindrocyclophane Core

Name	R_1	R_2	R_3	R_4
A	OH	CH_3	OH	CH_3
B	OH	CH_3	OAc	CH_3
C	OH	CH_3	H	CH_3
D	OAc	CH_3	OAc	CH_3
E	OAc	CH_3	H	CH_3
F	H	CH_3	H	CH_3
A_4	OH	$CHCl_2$	OH	$CHCl_2$
A_3	OH	CH_2Cl	OH	$CHCl_2$
A_2	OH	CH_3	OH	$CHCl_2$
A_1	OH	CH_3	OH	CH_2Cl
C_4	OH	$CHCl_2$	H	$CHCl_2$
C_3	OH	CH_2Cl	H	$CHCl_2$
C_2	OH	CH_3	H	$CHCl_2$
C_1	OH	CH_3	H	CH_2Cl
F_4	H	$CHCl_2$	H	$CHCl_2$
A_{B4}	OH	$CHBr_2$	OH	$CHBr_2$

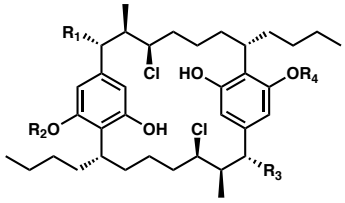

Nostocyclophane Core

Name	R_1	R_2	R_3	R_4
A	OCH_3	glycoside	OCH_3	glycoside
B	OCH_3	H	OCH_3	glycoside
C	OH	H	OCH_3	H
D	OCH_3	H	OCH_3	H

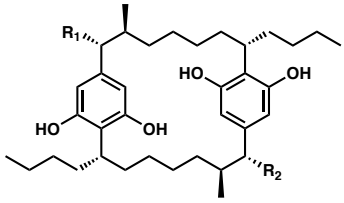

Ribocyclophane Core

Name	R_1	R_2
A	ribose	ribose
B	ribose	OH
C	ribose	H
D	ribose	OAc

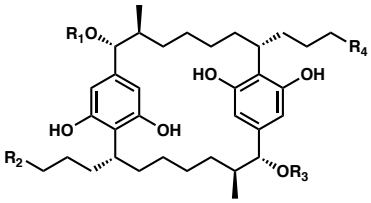

Carbamidocyclophane Core

Name	R_1	R_2	R_3	R_4
A	$CONH_2$	$CHCl_3$	$CONH_2$	$CHCl_3$
B	$CONH_2$	CH_2Cl	$CONH_2$	$CHCl_3$
C	$CONH_2$	CH_3	$CONH_2$	$CHCl_3$
D	$CONH_2$	CH_3	$CONH_2$	CH_2Cl
E	$CONH_2$	CH_3	$CONH_2$	CH_3
F	H	$CHCl_3$	$CONH_2$	$CHCl_2$
G	Ac	$CHCl_3$	$CONH_2$	$CHCl_2$
H	$CONH_2$	CH_3	H	CH_3
I	$CONH_2$	CH_3	H	CH_2Cl
J	$CONH_2$	CH_2Cl	$CONH_2$	CH_2Cl
K	$CONH_2$	CH_3	H	$CHCl_2$
L	$CONH_2$	CH_2Cl	H	$CHCl_2$

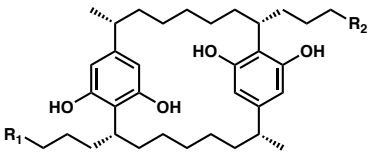

Merocyclophane Core

Name	R_1	R_2
A	CH_3	CH_3
C	CH_3	OH
D	OH	OH

These [7,7]paracyclophanes have drawn attention recently due to their antimicrobial activity. Increasing rates of bacterial resistance have led to a need for new types of antimicrobial agents. Some [7,7]paracyclophanes have been demonstrated to display MIC values in the range of 0.1-0.2 μM toward drug resistant strains of the gram-positive bacteria, MRSA,[10] along with activity against S. *pneumoniae* and E. *faecalis* with MIC's between 0.2-3 μM.[11] While these initial results are very promising, limited biological evaluations have occurred to date, focusing on isolated natural products and a few derivatives. A streamlined synthesis of [7,7]paracyclophanes allowing for access to new derivatives would enable more comprehensive biological evaluations and SAR (structure activity relationship) studies.

Due to the promising biological activity and interesting structural motif, there has been previous interest in the synthesis of [7,7]paracyclophanes, though to date only cylindrocyclophanes A and F have succumbed to synthesis. The predominant approach has been to use a convergent strategy bringing two identical components together, either by means of metathesis,[12] the Horner-Wadsworth-Emmons reaction,[13] or the Ramberg-Bäcklund reaction[14] (Scheme 3.1.1). While these approaches can afford fairly efficient syntheses (15-23 steps), the use of dimerization strategies on advanced fragments only leads to synthesis of symmetrical [7,7]paracyclophanes and complicates derivatization. We decided to utilize a strategy more suited for synthesizing a number of [7,7]paracyclophanes (natural and unnatural) from an advanced common intermediate. In particular, we believed C-H functionalization would be a useful strategy to afford a variety of [7,7]paracyclophanes in an efficient and divergent manner.

Scheme 3.1.1 Previous synthetic strategies toward cylindrocyclophanes

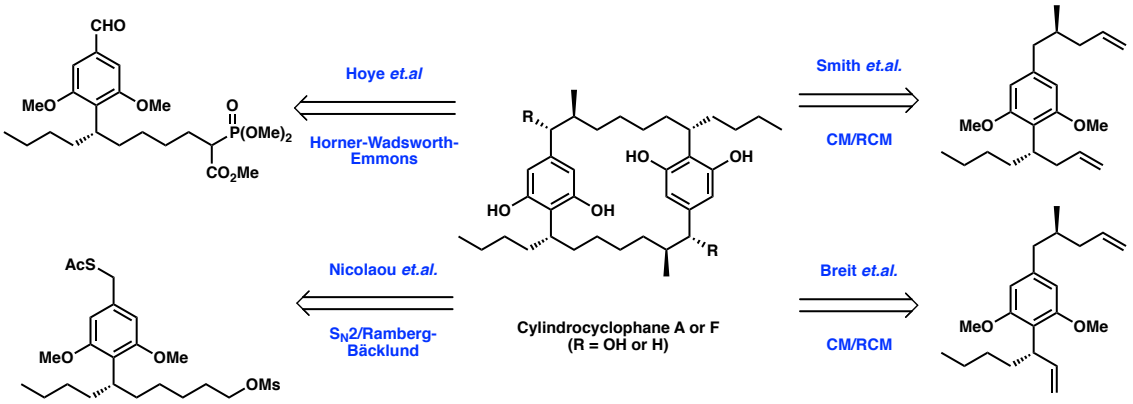

3.2 RETROSYNTHETIC ANALYSIS OF CYLINDROCYCLOPHANE A

While we were interested in developing a divergent synthesis for many [7,7]paracyclophanes, we decided to first target cylindrocyclophane A, due to the previous successful syntheses and its nature as one of the less complex naturally occurring [7,7]paracyclophanes. We developed our retrosynthetic strategy (Scheme 3.2.1) in a way that could later be adapted to afford some of the more complex cylindrocyclophanes and potentially even ribocyclophanes and carbamidocyclophanes. We believe that cylindrocyclophane A (**95**) could arise from reduction and global deprotection of **96**. Compound **96** could be accessed via a Baeyer-Villiger reaction of diester **97**, which could itself arise from a double carbonyl addition into Weinreb amide **98**. This compound could be synthesized via Weinreb amide formation and tetraacetoxylation[15] of **99**. Dimerization of compound **100** via C–H insertion would yield **99**. Diazoester **100** would be accessed via diazoester coupling and hydrogenation of olefin **101**, which could arise from a selective C-H insertion reaction of diazoester **103**

into olefin **102**.[16] This would be one of the most elaborate C–H functionalization based strategies reported to date.

Scheme 3.2.1 Retrosynthetic proposal for cylindrocyclophane A

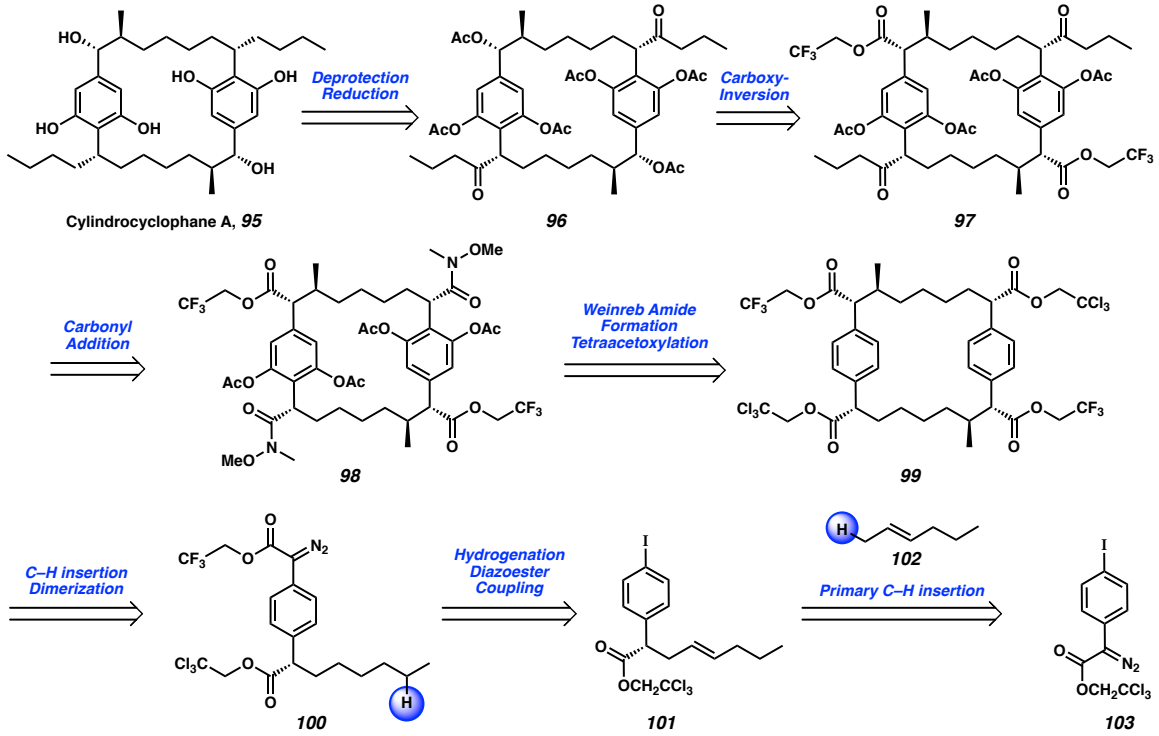

3.3 SYNTHESIS OF [7,7]PARACYCLOPHANE CORE

In order to test the viability of our retrosynthetic proposal, we decided to begin by targeting the synthesis of a mostly unfunctionalized [7,7]paracylophane core. In 2016, the Davies lab first reported a method for the selective insertion of diazoesters into unactivated C-H bonds with catalyst **104** (Scheme 3.3.1A).[17] Unfortunately, our original efforts into applying those reaction conditions toward the synthesis of [7,7]paracyclophanes were unsuccessful due to reactivity at the benzylic position in preference to the unactivated secondary C-H bond (Scheme 3.3.1B). With this limitation

in mind, we proceeded to develop conditions that would selectively functionalize unactivated secondary C-H bonds in the presence of activated benzylic C-H bonds (Scheme 3.3.1C).[18] Crucial to this selectivity was the development of a new catalyst **105**. Further details on the development of this reaction can be found in reference 18.

Scheme 3.3.1 Development of C-H insertion reaction

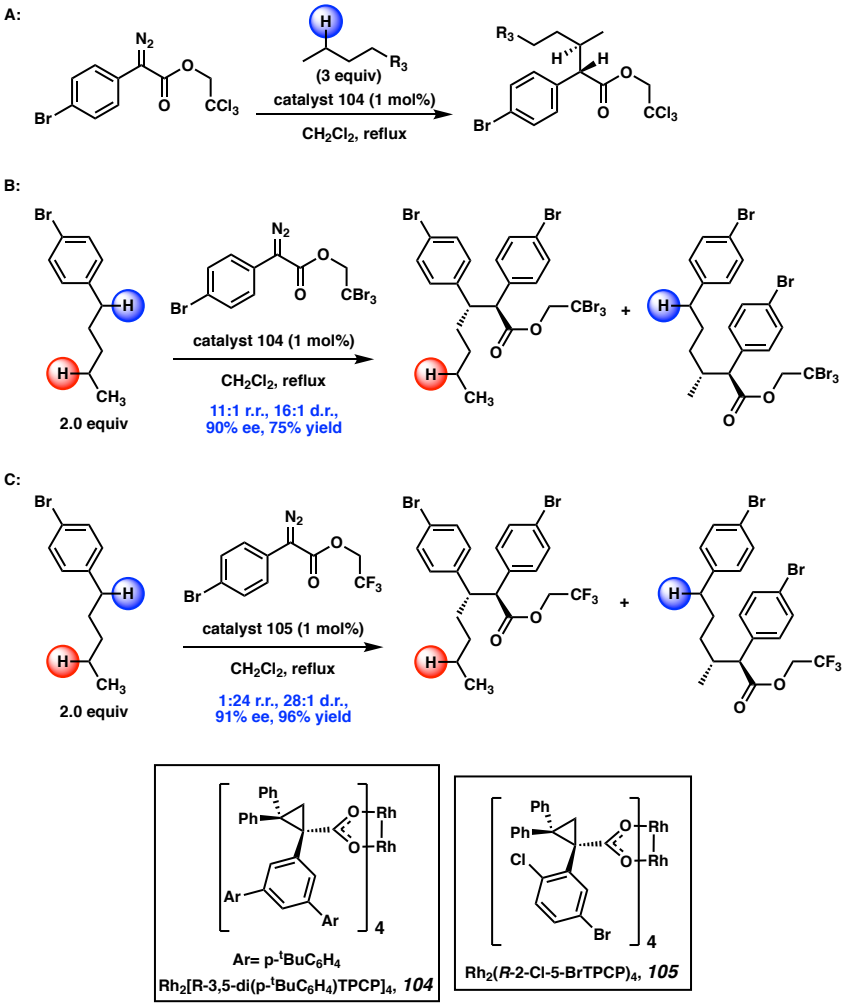

We proceeded to explore the utilization of the methodology described above for the synthesis of the [7,7]paracyclophane core (Scheme 3.3.2). The synthetic sequence involves four C–H functionalization steps, and two of them are enantioselective

donor/acceptor carbene transformations. The beginning palladium-catalyzed reaction of trifluoroethyl diazoacetate (**107**) with the aryl iodide **106** generated the aryldiazoacetate **108** in 87% yield, followed by Rh_2(*R*-2-Cl-5-BrTPCP)$_4$-catalyzed intermolecular C–H functionalization of 1-heptyl-4-iodobenzene **106** with **108** to obtain the desired product (–)-**109** in 83% yield, without any evidence of a structurally isomeric product. Furthermore, (–)-**109** was formed with good diastereoselectivity (26:1 dr) and enantioselectivity (91% ee). A second palladium-catalyzed cross-coupling between (–)-**109** and the same diazoacetate **107** proceeded with an 81% yield to access the aryldiazoacetate (–)-**110**. Finally, a Rh_2(*R*-2-Cl-5-BrTPCP)$_4$-catalyzed intramolecular C–H functionalization of **110** formed (–)-**111** cleanly with exceptional site selectivity and asymmetric induction (>30:1 rr, > 99% ee) and moderate diastereoselectivity (5.6:1 dr) without enantioenrichment of **109** or **110**. Though macrocyclization by means of C–H functionalization has been reported for macrolide formation, palladium-catalyzed allylic oxidation, sp^3 C–H arylation, and via sp^2 C–C coupling, the study reported here is the first example of an enantioselective macrocyclization by C–H functionalization of unactivated sp^3 C–H bonds. The initial studies on the macrocyclization sequence utilized Rh_2(*S*-2-Cl-5-BrTPCP)$_4$ to obtain the enantiomeric macrocyclic product (+)-**111**, whose absolute and relative stereochemistry was confirmed by X-ray crystallography.

Scheme 3.3.2 Synthesis of [7,7]paracyclophane

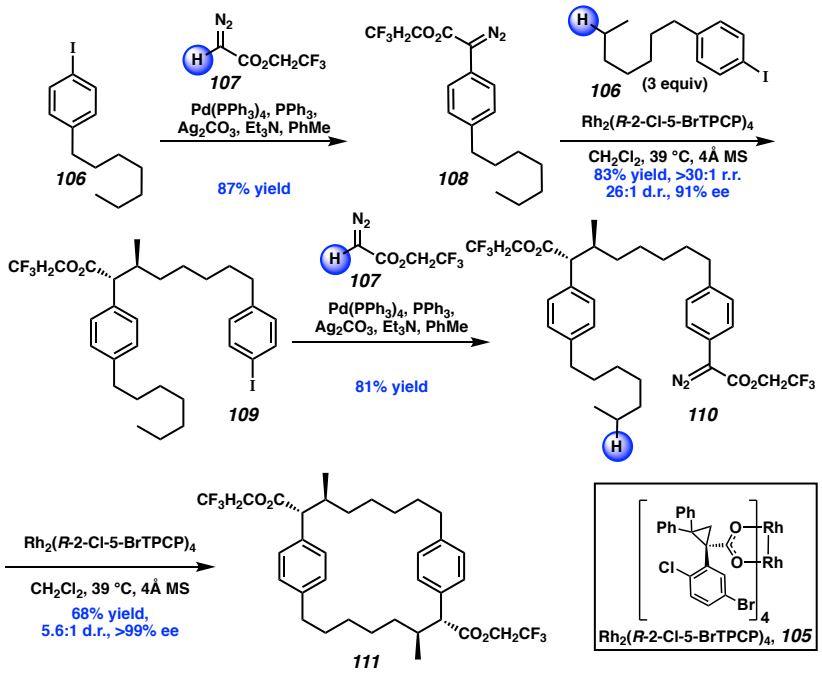

3.4 CONCLUSIONS

We are currently undertaking an investigation into the synthesis of [7,7]paracyclophanes due to the antimicrobial activity demonstrated by some members of this class of compounds. We have developed a retrosynthetic proposal that we believe could lead to the efficient and divergent synthesis of many [7,7]paracyclophanes utilizing C-H functionalization. In an effort to prove the feasibility of this strategy, we first demonstrated the synthesis of a relatively unfunctionalized [7,7]paracyclophane in an efficient and selective manner. Efforts are currently underway to advance this strategy toward the synthesis of a naturally occurring [7,7]paracyclophane and eventually additional members of the [7,7]paracyclophane family for the development of new antimicrobial agents.

3.5 EXPERIMENTAL METHODS AND ANALYTICAL DATA

3.5.1 MATERIALS AND METHODS

All solvents were purified and dried by a *Glass Contour Solvent System* unless otherwise stated. The dichloromethane used for the C–H Functionalization was dried and degassed at reflux over activated 4 A° molecular sieves for 1 hours under argon, then stored with activated 4 molecular sieves under argon atmosphere and was used directly. ^{1}H and ^{13}C NMR spectra were recorded at 600 MHz (^{13}C at 150 MHz) on Bruker-600 spectrometer or Varian IVONA-600 spectrometer, or 500 MHz (^{13}C at 126 MHz) on Varian INOVA-500 spectrometer, or 300 MHz (^{19}F at 282 MHz) on Varian Mercury-300. Unless otherwise stated, NMR spectra were run in solutions of deuterated chloroform ($CDCl_3$) with residual chloroform taken as an internal standard (7.26 ppm for ^{1}H, and 77.16 ppm for ^{13}C), and were reported in parts per million (ppm). Abbreviations for signal multiplicity are as follow: s = singlet, d = doublet, t = triplet, q = quartet, m = multiplet, dd = doublet of doublet, etc. Coupling constants (*J* values) were calculated directly from the spectra. IR spectra were collected on a Nicolet iS10 FT-IR spectrometer. Mass spectra were taken on a Thermo Finnigan LTQ-FTMS spectrometer with APCI, ESI or NSI. Thin layer chromatographic (TLC) analysis was performed with aluminum-sheet silica gel plates, visualizing with UV light and/or staining with aqueous $KMnO_4$ stain. Melting points (mp) were measured in open capillary tubes with a Mel-Temp Electrothermal melting points apparatus and are uncorrected. Optical rotations were measured on Jasco P-2000 polarimeters. Analytical enantioselective chromatographs were measured on either Varian Prostar instrument or Agilent- 1100 series instrument, and used isopropanol/hexane as gradient. Chiral HPLC conditions were determined by

obtaining separation of the racemic products using Rh_2(*R*/*S*-*o*-ClTPCP)$_4$ as catalyst for C2 insertion products.

The substrates and reagents were purchased from the following suppliers and used without further purification (unless otherwise stated): Sigma-Aldrich: Triphenylphosphine; Acros Organic: Silver carbonate. Fisher Scientific: Triethylamine. Strem: $Pd(PPh_3)_4$; $Rh_2(OAc)_4$. The following substrates were prepared by procedures adapted from literatures: Rh_2(*S*-2-Cl-5-BrTPCP)$_4$.[19]

3.5.2 EXPERIMENTAL PROCEDURES

2,2,2-Trifluoroethyl 2-diazo-2-(4-heptylphenyl)acetate (108)

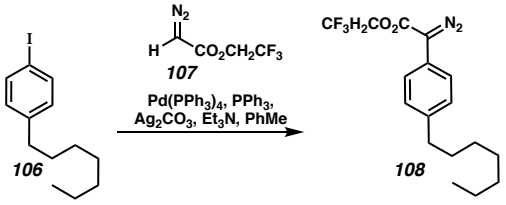

The procedure is adapted from the literature:[20] A 250-ml round-bottom flask with stir bar was flame dried under vacuum. Once cool enough all solids were added first: PPh_3 (1.65 mmol, 0.1 equiv.), $Pd(PPh_3)_4$ (0.825 mmol, 0.05 equiv.) and Ag_2CO_3 (8.25 mmol, 0.5 equiv.). After solids added, the reaction vessel was purged with argon three times. Next the liquids were added: toluene (66 ml), Et_3N (21.5 mmol, 1.3 equiv.), aryl iodide **106** (16.5 mmol, 1 equiv.), and finally the 2,2,2-trifluoroethyl 2-diazoacetate **107** (21.5 mmol, 1.3 equiv.) was added last. The resulted mixture was stirred at room temperature (23 °C) for 5 h and then, filtered through a short silica plug (3.5 cm *diameter*, 5 cm *height*), eluting with ethyl acetate until elutes clear. The crude product was concentrated and

purified by column chromatography (5% ether in pentane) to afford **108** as a yellow oil in 85% yield. R_f = 0.71 (pentane/diethyl ether = 9:1); ^{1}H NMR (600 MHz, CDCl3) δ 7.36 (d, *J* = 8.3 Hz, 2H), 7.22 (d, *J* = 8.2 Hz, 2H), 4.65 (q, *J* = 8.4 Hz, 2H), 2.60 (t, *J* = 7.6 Hz, 2H), 1.63 – 1.57 (m, 2H), 1.36 – 1.22 (m, 8H), 0.87 (t, *J* = 6.6 Hz 3H); ^{13}C NMR (125 MHz, $CDCl_3$) δ 163.4, 141.5, 129.1, 124.3, 122.9 (q, *J* = 277.6 Hz), 121.3, 60.3 (q, *J* = 36.9 Hz), 35.4, 31.7, 31.2, 29.1, 29.1, 22.6, 13.9 (The resonance resulting from the diazo carbon was not observed); ^{19}F NMR (282 MHz, $CDCl_3$) δ -73.9 (t, *J* = 8.4 Hz); IR (neat) 2957, 2927, 2856, 2089, 1715, 1515, 1456, 1410, 1350, 1280, 1242, 1167, 1137, 1074, 1020, 974, 923, 839, 810, 733, 653; HRMS (+p NSI) calcd for $C_{17}H_{22}F_3N_2O_2$ $(M+H)^+$ 343.1628 found 343.08576.

2,2,2-Trifluoroethyl(2*R*,3*S*)-2-(4-heptylphenyl)-8-(4-iodophenyl)-3 methyloctanoate (109)

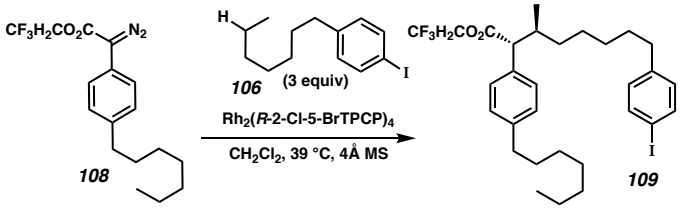

The procedure is adjusted from the general procedure for C–H functionalization reactions: A 50-ml flame-dried round-bottom flask with condenser was charged with 4 Å MS and Rh_2(*R*-2-Cl-5-BrTPCP)$_4$ (0.02 mmol, 1.0 mol%) and then, purged three times with argon. 1-n-Heptyl-4-iodobenzene **106** (6.29 mmol, 3.0 equiv.) and distilled CH_2Cl_2 (8 ml) were added next, then the mixture was heated to 40 °C and refluxed for at least 15 min before addition of the diazo compounds. Next, **108** (2.09 mmol, 1.0 equiv.) was

purged under argon in a 20-mL scintillation vial, then diluted with distilled CH_2Cl_2 (8 ml). Then, under reflux conditions and argon atmosphere, the diazo solution was added to the reaction vessel dropwise via syringe pump over 3 h. The reaction mixture was stirred at 40 °C for another 30 min, and concentrated under vacuum for crude ^{1}H NMR. The crude product was purified by flash column chromatography (3% ether in pentane) to afford (-)-**109** as an opaque oil in 62% yield. Note: Solvent must be carefully dried (distilled over CaH2 and stored on activated 4 Å MS). R_f = 0.71 (pentane/diethyl ether = 19/1);$[\alpha]^{20}_D$: -18.6°(c = 1.00, $CHCl_3$, 91% ee); ^{1}H NMR (600 MHz, $CDCl_3$) δ 7.56 (d, *J* = 8.2 Hz, 2H), 7.20 (d, *J* = 8.0 Hz, 2H), 7.12 (d, *J*= 8.0 Hz 2H), 6.86 (d, *J*= 8.1 Hz, 2H), 4.55 (dq, *J* = 8.5, 4.1 Hz, 1H), 4.29 (dq, *J* = 8.5, 4.2 Hz, 1H), 3.32 (d, *J* = 10.9 Hz, 1H), 2.57 (t, *J*= 7.6 Hz, 2H), 2.45 (t, *J* = 7.7 Hz, 2H), 2.23 – 2.16 (m, 1H), 1.63 – 1.56 (m, 2H), 1.51 – 1.41 (m 2H), 1.34 – 1.23 (m, 10H), 1.22 – 1.09 (m, 4H), 1.00 (d, *J* = 6.7 Hz, 3H), 0.88 (t, *J* = 6.7 Hz, 3H); ^{13}C NMR (125 MHz, $CDCl_3$) δ 172.5, 142.3, 137.2, 134.1, 130.5, 128.6, 128.4, 123.0 (q, *J* = 277.2 Hz), 90.5, 60.2 (q, *J* = 36.5 Hz), 57.9, 36.2, 35.6, 35.3, 33.1, 31.8, 31.3, 31.0, 29.3, 29.2, 29.0, 26.0, 22.7, 17.7, 14.1; ^{19}F NMR (282 MHz, $CDCl_3$) δ -73.7 (t, *J* = 8.5 Hz); IR (neat) 2927, 2855, 1753, 1484, 1464, 1400, 1278, 1165, 1128, 1061, 1006, 979, 824, 793, 737; HRMS (+p NSI) calcd for $C_{30}H_{41}O_2IF_3$ $(M+H)^+$ 617.2098 found 617.20986; HPLC (R,R-Whelk column, 0 % *i*-propanol in hexane, 1 mL min^{-1}, 1 mg mL^{-1}, 30 min, UV 210 nm) retention times of 14.9 min (major) and 17.6 min (minor) 91% ee with Rh_2(*R*-2-Cl-5-BrTPCP)$_4$.

2,2,2-Trifluoroethyl(2*R*,3*S*)-8-(4-(1-diazo-2-oxo-2-(2,2,2-trifluoroethoxy) ethyl)phenyl)-2-(4-heptylphenyl)-3-methyloctanoate (110)

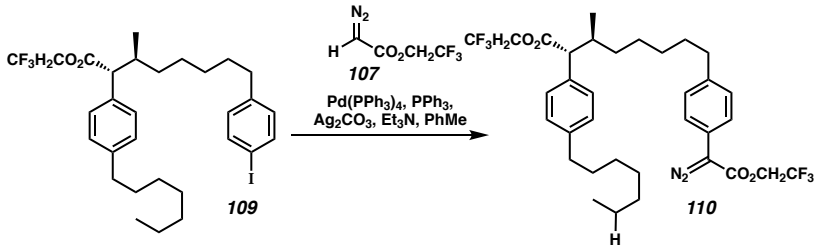

The procedure is adapted from literatures: A 50-ml round-bottom flask with stir bar was flame dried under vacuum. Once cool enough all solids were added first: PPh_3 (0.129 mmol, 0.1 equiv.), $Pd(PPh_3)_4$ (0.065 mmol, 0.05 equiv.) and Ag_2CO_3 (0.645 mmol, 0.5 equiv.). After solids added, the reaction vessel was purged with argon three times. Next the liquids were added: toluene (5.2 ml), Et_3N (1.67 mmol, 1.3 equiv.), aryl iodide **109** (27, 1.29 mmol, 1 equiv.), and finally the 2,2,2-trifluoroethyl 2- diazoacetate **107** (1.67 mmol, 1.3 equiv.) was added last. The resulted mixture was stirred at room temperature (23 °C) for 5 h and then, filtered through a short silica plug (3.5 cm *diameter*, 5 cm *height*), eluting with ethyl acetate until elutes clear. The crude product was concentrated and purified by column chromatography (2% ether in pentane) to afford product (-)-**110** as a yellow oil in 81% yield. R_f = 0.45 (pentane/diethyl ether = 9/1); ^{1}H NMR (600 MHz, $CDCl_3$) δ 7.34 (d, *J* = 8.3 Hz, 2H), 7.21 (d, *J* = 8.1 Hz, 2H), 7.16 (d, *J* = 8.3 Hz, 2H), 7.12 (d, *J* = 8.1 Hz, 2H), 4.64 (q, *J* = 8.4 Hz, 2H), 4.55 (dq, *J* = 12.7, 8.5 Hz, 1H), 4.29 (dq, *J* = 12.7, 8.5 Hz, 1H), 3.32 (d, *J* = 10.5 Hz, 1H), 2.57 (t, *J*= 7.6 Hz, 2H), 2.51 (t, *J* = 7.7 Hz, 2H), 2.23 – 2.15 (m, 1H), 1.62 – 1.56 (m, 2H), 1.52 – 1.44 (m, 2H), 1.35 – 1.24 (m, 10H), 1.22 – 1.11 (m, 4H), 1.00 (d, *J* = 6.5 Hz, 3H), 0.87 (t, *J* = 7.0 Hz, 3H); ^{13}C NMR (125

MHz, $CDCl_3$) δ 172.5, 142.3, 141.3, 134.1, 129.2, 128.6, 128.4, 124.2, 123.0 (q, *J*= 277.7 Hz), 122.9 (q, *J*= 277.7 Hz), 121.3, 60.3 (q, *J*= 36.9 Hz), 60.2 (q, *J*= 36.6 Hz), 57.9, 36.2, 35.6, 35.3, 33.1, 31.8, 31.3, 31.1, 29.3, 29.2, 29.1, 26.0, 22.7, 17.7, 14.1; ^{19}F NMR (282 MHz, $CDCl_3$) δ -73.7 (t, *J* = 8.5 Hz), -73.9 (t, *J* = 8.3 Hz); IR (neat) 2928, 2856, 2090, 1753, 1717, 1514, 1456, 1409, 1350, 1279, 1242, 1165, 1135, 1074, 976, 923, 839, 733; HRMS (+p NSI) calcd for $C_{34}H_{41}O_4N_2F_6$ (M-H)- 655.2976 found 655.29807.

Bis(2,2,2-trifluoroethyl)(2*R*,3*S*,10*R*,11*S*)-3,11-dimethyl-1,9(1,4)dibenzenacyclo hexadecaphane-2,10-dicarboxylate (111)

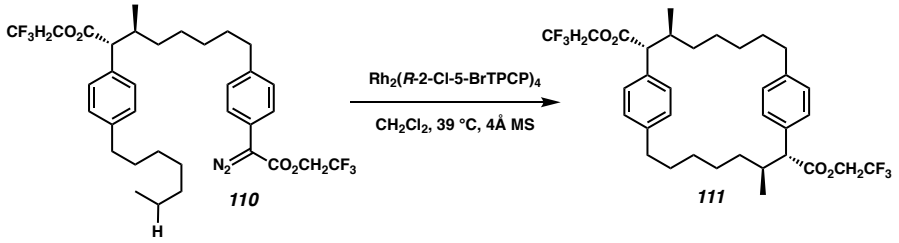

The procedure is adjusted from the general procedure for C–H functionalization reactions: A 100-ml flame-dried round-bottom flask with condenser were charged with 4 Å MS and Rh_2(*R*-2-Cl-5-BrTPCP)$_4$ (0.01 mmol, 1.0 mol%), then purged three times under argon. Distilled CH_2Cl_2 (10.5 ml) was added using oven dried syringes, then the mixture was heated to 40 °C and refluxed for at least 15 min before addition of the diazo compounds. Next, (-)-**110** (1.04 mmol, 1.0 equiv.) was purged under argon in a 20-mL scintillation vial, then diluted with distilled CH_2Cl_2 (10.5 ml). Then, under reflux conditions and argon atmosphere, the diazo solution was added to the reaction vessel dropwise via syringe pump over 3 h. The reaction mixture was stirred at 40 °C for another 30 min, and concentrated under vacuum for crude ^1H NMR. The crude product

was purified by flash column chromatography (3% ether in pentane) to afford the product (-)-**111** as a white solid in 68% yield. Note: Solvent must be carefully dried (distilled over CaH_2 and stored on activated 4 Å MS). m.p. 141-143 °C R_f = 0.45 (pentane/diethyl ether = 9/1); $[\alpha]^{20}_D$: -11.0 °(c = 1.00, $CHCl_3$, 5.6:1 d.r., >99% ee); ^{1}H NMR (600 MHz, $CDCl_3$) δ 7.16 (d, *J* = 8.0 Hz, 4H), 7.01 (d, *J* = 8.1 Hz, 4H), 4.55 (dq, *J* = 12.7, 8.5 Hz, 2H), 4.27 (dq, *J* = 12.7, 8.4 Hz, 2H), 3.21 (d, *J* = 11.4 Hz, 2H), 2.58 (dt, *J* = 13.1, 6.4 Hz, 2H), 2.42 (dt, *J* = 13.6, 7.6 Hz, 2H), 2.19 – 2.09 (m, 2H), 1.48 – 1.27 (m, 6H), 1.12 – 0.96 (m, 10H), 0.96 – 0.85 (m, 4H), 0.80 – 0.68 (m, 2H); ^{13}C NMR (151 MHz, $CDCl_3$) δ 172.7, 141.8, 134.4, 128.8, 128.2, 122.95 (q, *J* = 277.3 Hz), 60.21 (q, *J* = 36.5 Hz), 58.3, 36.4, 35.5, 32.7, 30.8, 28.3, 26.0, 17.7; ^{19}F NMR (282 MHz, $CDCl_3$) δ -73.7 (t, *J* = 8.5 Hz); IR (neat) 2929, 2856, 1748, 1403, 1385, 1347, 1303, 1275, 1225, 1160, 1123, 1052, 981, 909, 838, 822, 740, 661; HRMS (+p NSI) calcd for $C_{30}H_{42}O_2IF_3$ (M)+ 628.2987 found 628.29995; HPLC [for better separation, the ester product was reduced to ((2*R*,3*S*,10*R*,11*S*)-3,11-dimethyl-1,9(1,4)-dibenzenacyclohexadecaphane-2,10-diyl) dimethanol, and the pure major diastereomer of the alcohol derivative was obtained via prep HPLC (Ascentis® C18 column, 80% acetonitrile in H2O with 0.1% trifluoroacetic acid)] (ADH column, 10 % *i*-propanol in hexane, 1.0 mL min-1, 1 mg mL-1, 80 min, UV 210 nm) retention times of 28.69 min (major) and 60.71 min (minor) >99% ee with Rh_2(*R*-2-Cl-5-BrTPCP)$_4$.

3.6 NOTES & REFERENCES

[1] Cram, D. J.; Steinberg, H. *J. Am. Chem. Soc.* **1951**, *73*, 5691–5704.

[2] Keehn, P. M.; Rosenfield, S. M. *Cyclophanes*; Academic Press: New York, **1983**.

[3] Moore, B. S.; Chen, J. L.; Patterson, G. M. L.; Moore, R. E.; Brinen, L. S.; Kato, Y.; Clardy, J. *J. Am. Chem. Soc.* **1990**, *112*, 4061–4063.

[4] Moore, B. S.; Chen, J. L.; Patterson, G. M. L.; Moore, R. E. *Tetrahedron*, **1992**, *48*, 3001–3006.

[5] Chlipala, G. E.; Sturdy, M.; Krunic, A.; Lantvit, D. D.; Shen, Q.; Porter, K.; Swanson, S. M.; Orjala, J. *J. Nat. Prod.* **2010**, *73*, 1529–1537.

[6] Chen, J. L.; Moore, R. E.; Patterson, G. M. L., *J. Org. Chem.* **1991**, *56*, 4360–4364.

[7] May, D. S.; Kang, H.-S.; Santarsiero, B. D.; Krunic, A.; Shen, Q.; Burdette, J. E.; Swanson, S. M.; Orjala, J., *J. Nat. Prod.* **2018**, *81*, 572–578.

[8] (a) Bui, H. T.; Jansen, R.; Pham, H. T.; Mundt, S. *J. Nat. Prod.* **2007**, *70*, 499–503. (b)Luo, S.; Kang, H. S.; Krunic, A.; Chlipala, G. E.; Cai, G.; Chen, W. L.; Franzblau, S. G.; Swanson, S. M.; Orjala, J. *Tetrahedron Lett.* **2014**, *55*, 686–689. (c) Preisitsch, M.; Harmrolfs, K.; Pham, H. T.; Heiden, S. E.; Fussel, A.; Wiesner, C.; Pretsch, A.; Swiatecka-Hagenbruch, M.; Niedermeyer, T. H.; Muller, R.; Mundt, S. *J. Antibiot.* **2015**, *68*, 165–77.

[9] (a) Kang, H. S.; Santarsiero, B. D.; Kim, H.; Krunic, A.; Shen, Q.; Swanson, S. M.; Chai, H.; Kinghorn, A. D.; Orjala, J. *Phytochemistry* **2012**, *79*, 109–15. (b) May, D. S.; Chen, W. L.; Lantvit, D. D.; Zhang, X.; Krunic, A.; Burdette, J. E.; Eustaquio, A.; Orjala, J. *J. Nat. Prod.* **2017**, *80*, 1073–1080.

[10] Preisitsch, M.; Harmrolfs, K.; Pham, H. T.; Heiden, S. E.; Fussel, A.; Wiesner, C.; Pretsch, A.; Swiatecka-Hagenbruch, M.; Niedermeyer, T. H.; Muller, R.; Mundt, S., *The J. Antibiot.* **2015**, *68*, 165–77.

[11] Luo, S.; Kang, H. S.; Krunic, A.; Chlipala, G. E.; Cai, G.; Chen, W. L.; Franzblau, S. G.; Swanson, S. M.; Orjala, J. *Tetrahedron Lett*. **2014**, *55*, 686–689.

[12] (a) Smith, A. B., III; Kozmin, S. A.; Paone, D. V. *J. Am. Chem. Soc*. **1999**, *121*, 7423–7424. (b) Smith, A. B., III; Kozmin, S. A.; Adams, C. M.; Paone, D. V. *J. Am. Chem. Soc*. **2000**, *122*, 4984–4985. (c) Smith, A. B., III; Adams, C. M.; Kozmin, S. A.; Paone, D. V. *J. Am. Chem. Soc*. **2001**, *123*, 5925–37. (d) Berthold, D.; Breit, B. *Chemistry* **2018**, *24*, 16770–16773.

[13] Hoye, T. R.; Humpal, P. E.; Moon, B. *J. Am. Chem. Soc*. **2000**, *122*, 4982–4983.

[14] Nicolaou, K. C.; Sun, Y.-P.; Korman, H.; Sarlah, D. *Angew. Chem. Int. Ed*. **2010**, *49*, 5875–5878.

[15] Li, G.; Wan, L.; Zhang, G. F.; Leow, D.; Spangler, J.; Yu, J. Q. *J. Am. Chem. Soc*. **2015,** *137*, 4391–4397.

[16] Fu, L.; Guptill, D. M.; Davies, H. M. L. *J. Am. Chem. Soc*. **2016**, *138*, 5761–5764.

[17] Liao, K. B.; Negretti, S.; Musaev, D. G.; Bacsa, J.; Davies, H. M. L. *Nature* **2016**, *533*, 230–234.

[18] Liu, W. B.; Ren, Z.; Bosse, A. T.; Liao, K. B.; Goldstein, E. L.; Bacsa, J.; Musaev, D. G.; Stoltz, B. M.; Davies, H. M. L. *J. Am. Chem. Soc*. **2018**, *140*, 12247–12255.

[19] Fu, L.; Hoang, K.; Tortoreto, C.; Liu, W.; Davies, H. M. L. *Org. Lett*. **2018**, *20*, 2399–2402.

[20] Fu, L.; Mighion, J. D.; Voight, E. A.; Davies, H. M. L. *Chem. Eur. J*. **2017**, *23*, 3272–3275.

APPENDIX 3-1

Spectra Relevant to Chapter 3:

Synthesis of

[7,7]paracyclophanes

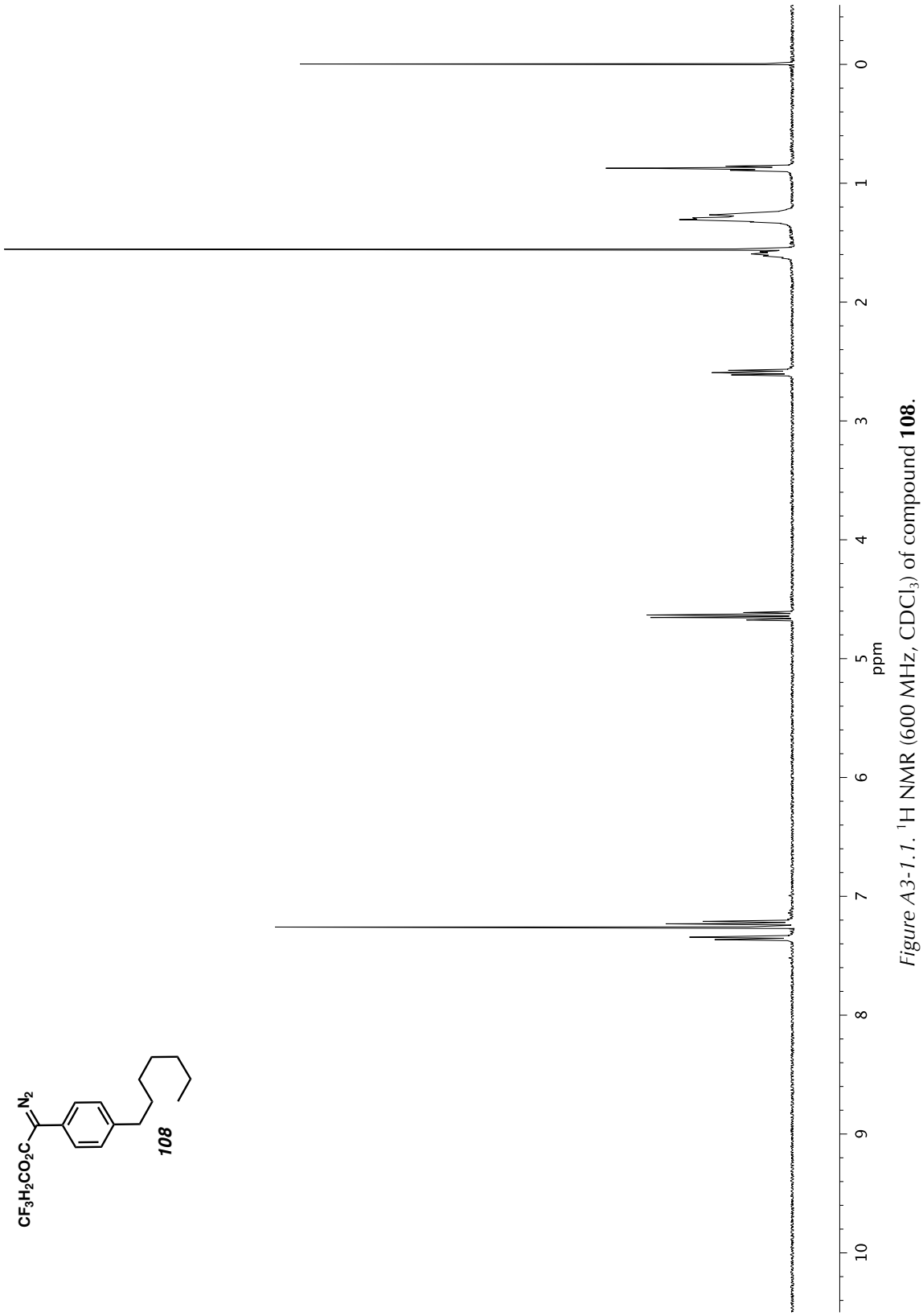

Figure A3-1.1. ^{1}H NMR (600 MHz, $CDCl_3$) of compound **108**.

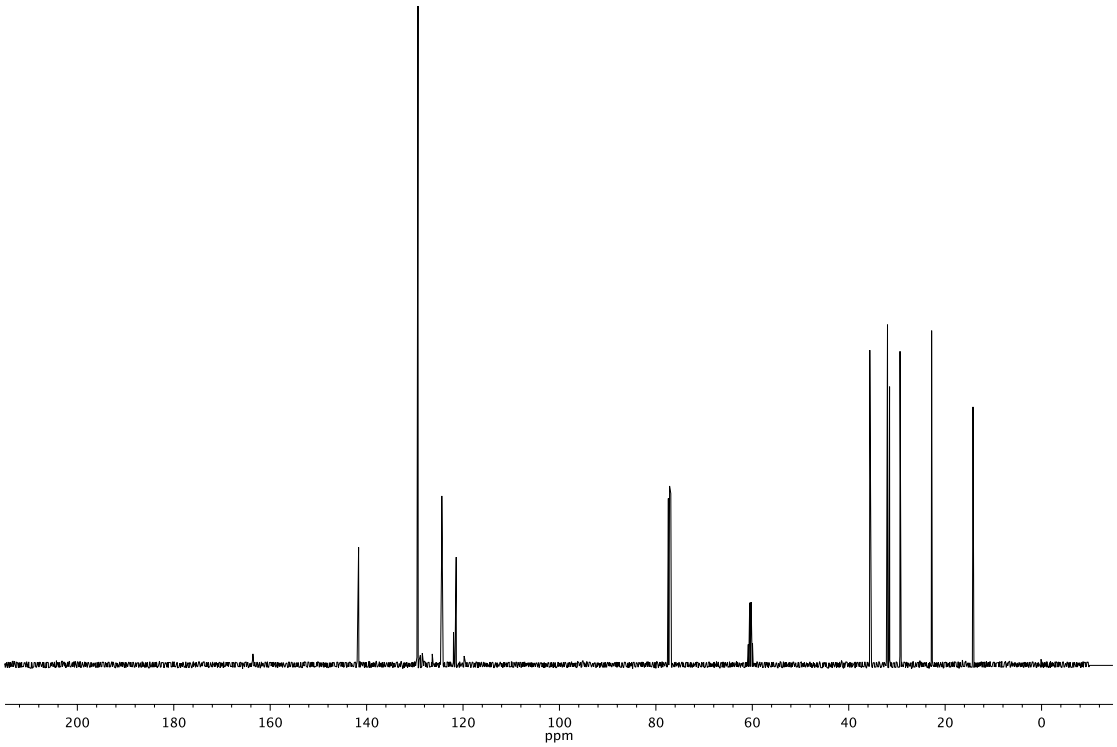

Figure A3-1.2. ^{13}C NMR (125 MHz, $CDCl_3$) of compound **108**.

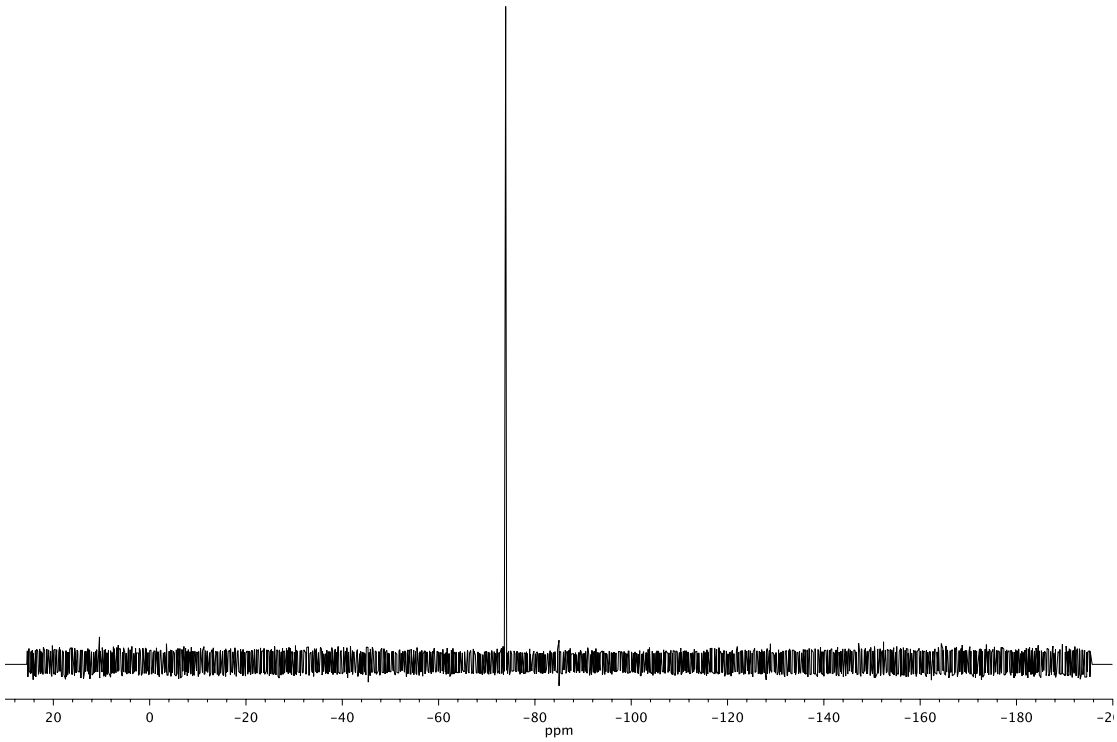

Figure A3-1.3. ^{19}F NMR (282 MHz, $CDCl_3$) of compound **108**.

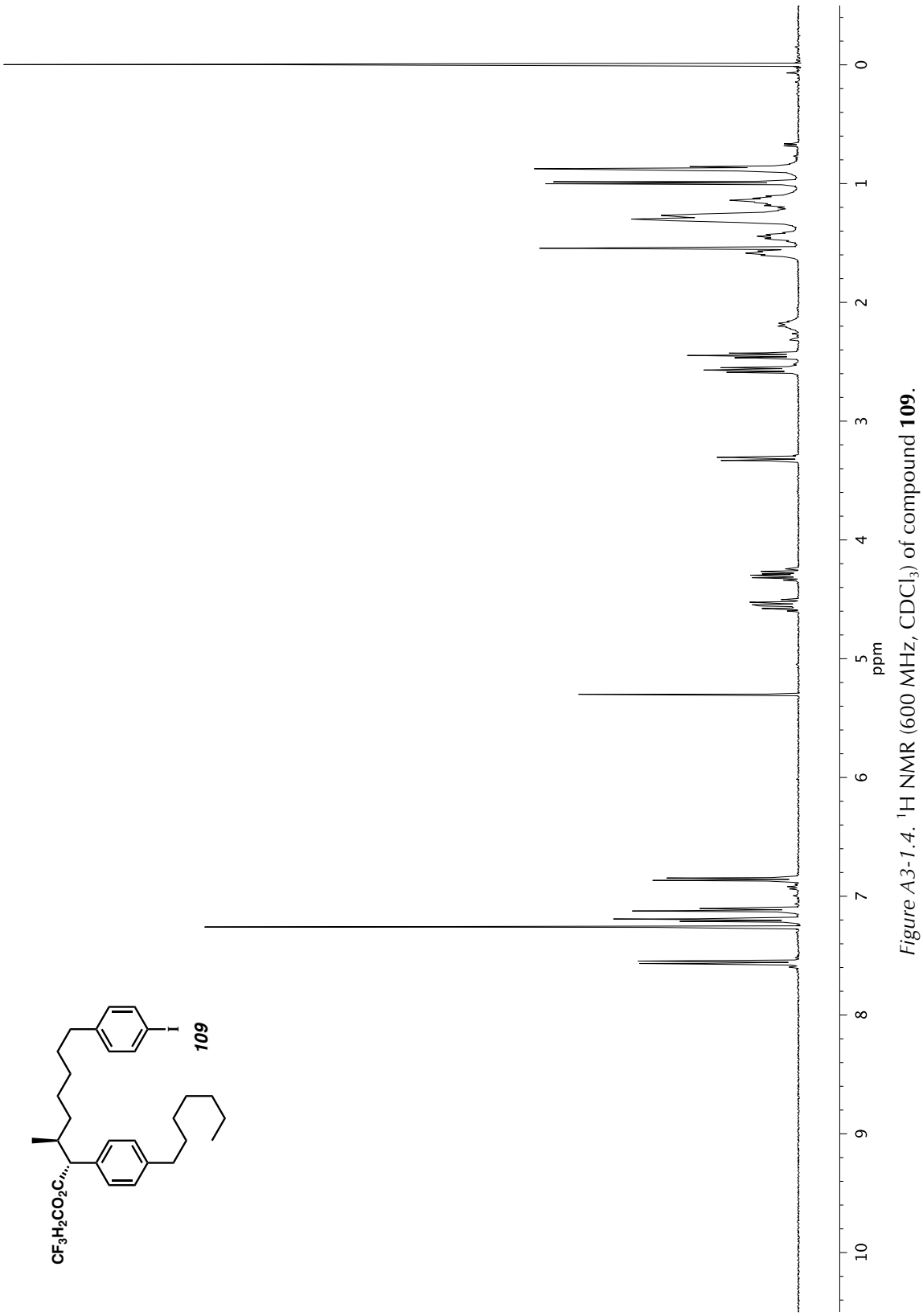

Figure A3-1.4. ^{1}H NMR (600 MHz, $CDCl_3$) of compound **109**.

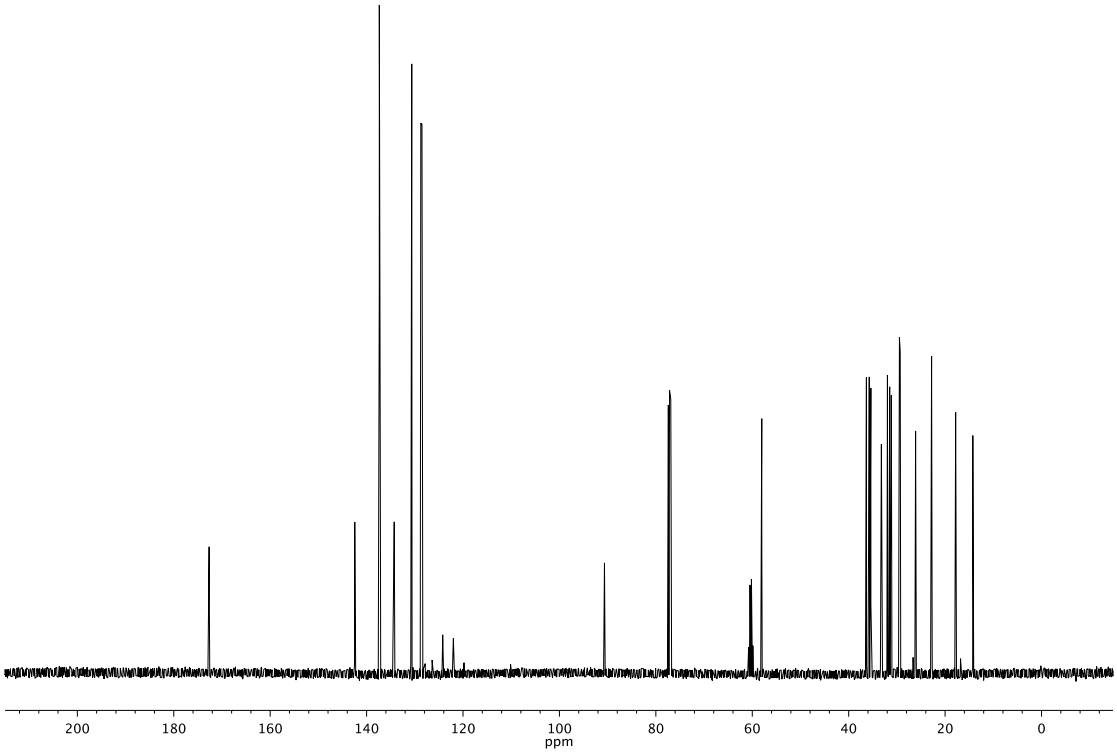

Figure A3-1.5. ^{13}C NMR (125 MHz, $CDCl_3$) of compound **109**.

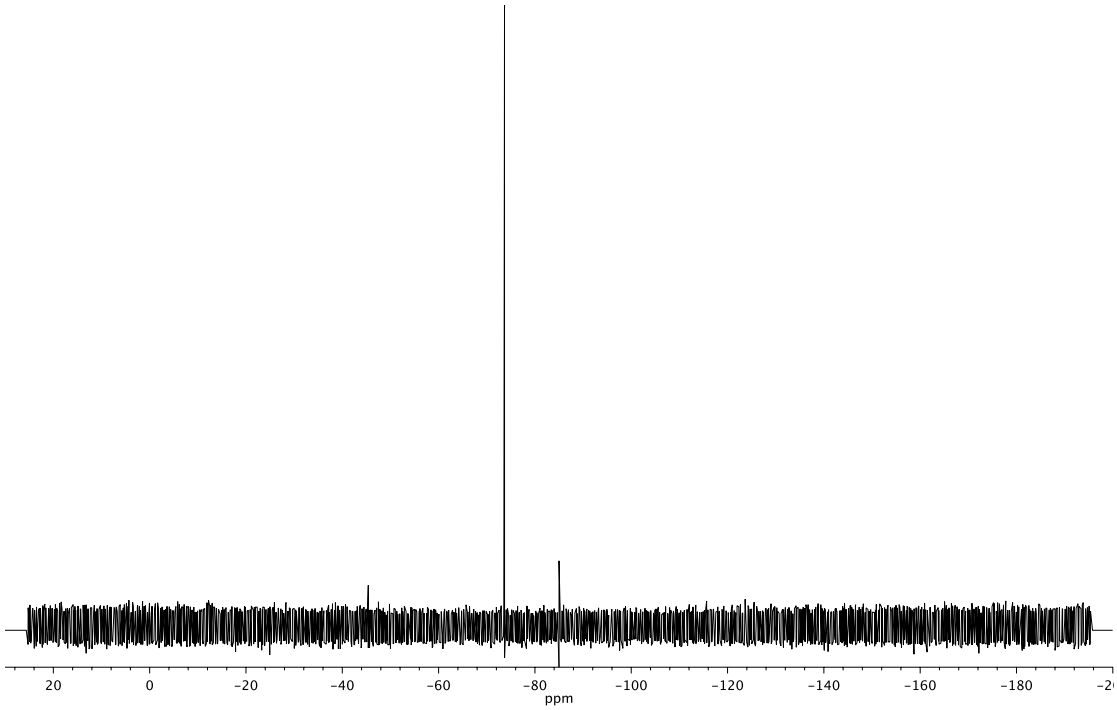

Figure A3-1.6. ^{19}F NMR (282 MHz, $CDCl_3$) of compound **109**.

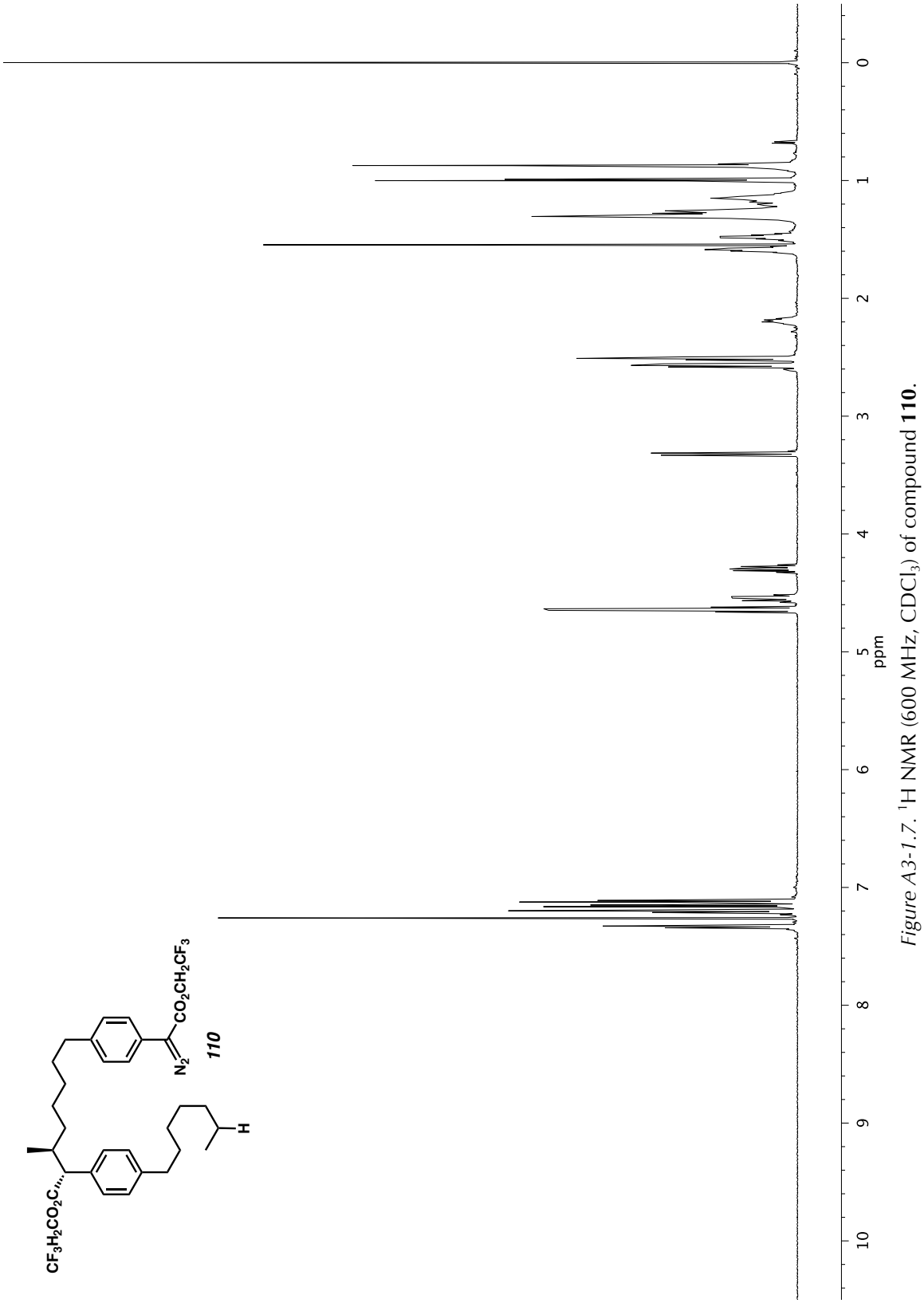

Figure A3-1.7. ^{1}H NMR (600 MHz, $CDCl_3$) of compound **110**.

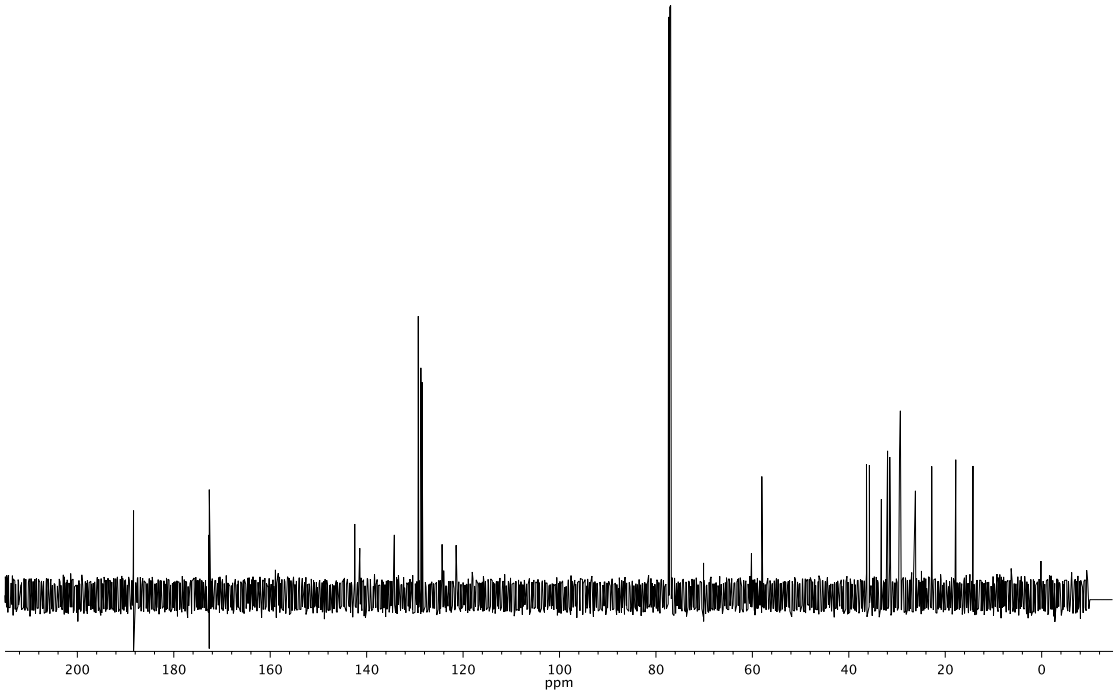

Figure A3-1.8. ^{13}C NMR (125 MHz, $CDCl_3$) of compound **110**.

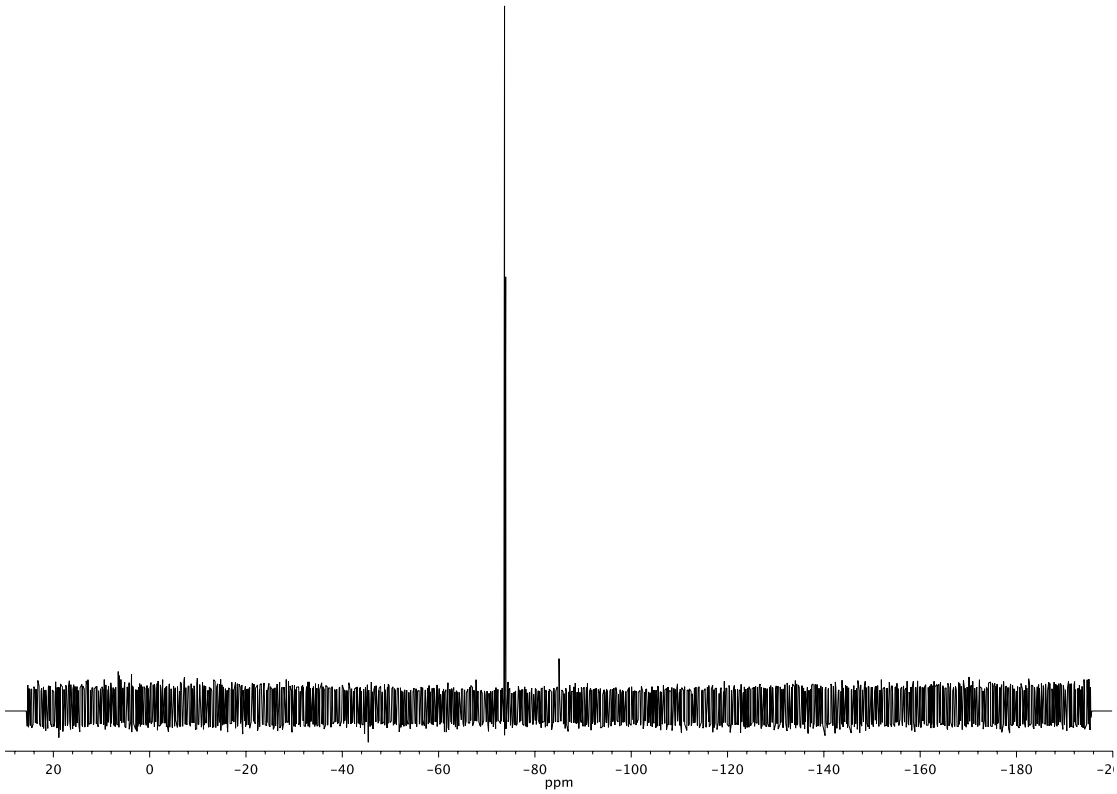

Figure A3-1.6. ^{19}F NMR (282 MHz, $CDCl_3$) of compound **110**.

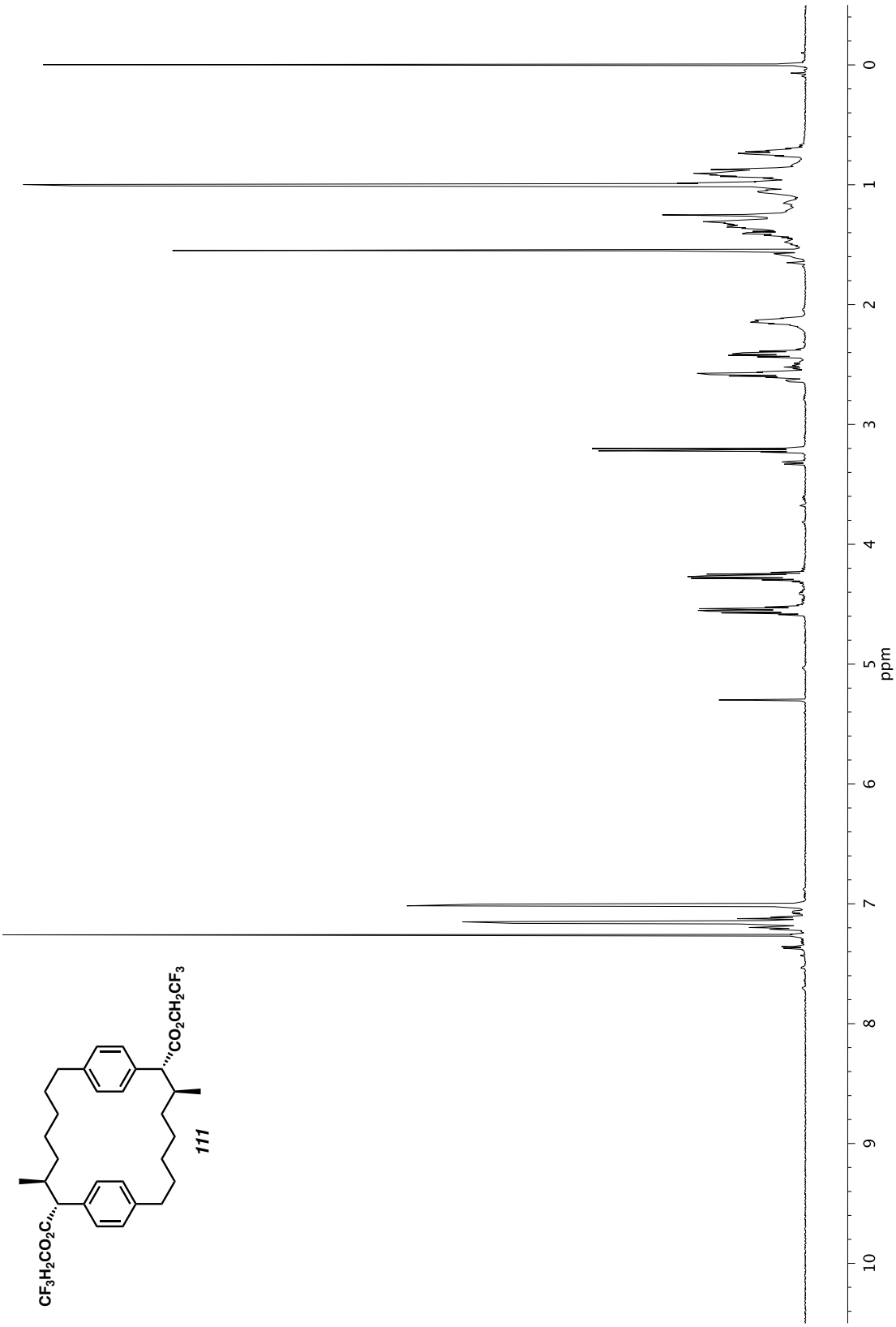

Figure A3-1.10. ^{1}H NMR (600 MHz, $CDCl_3$) of compound **111**.

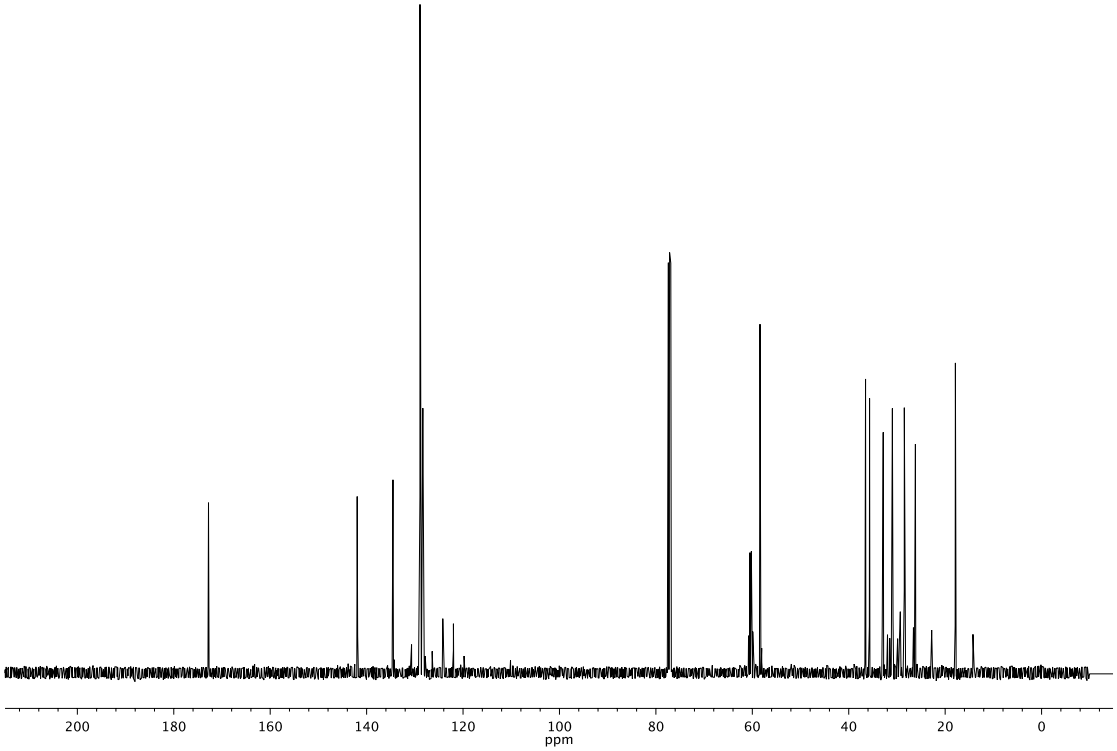

Figure A3-1.11. ^{13}C NMR (125 MHz, $CDCl_3$) of compound **111**.

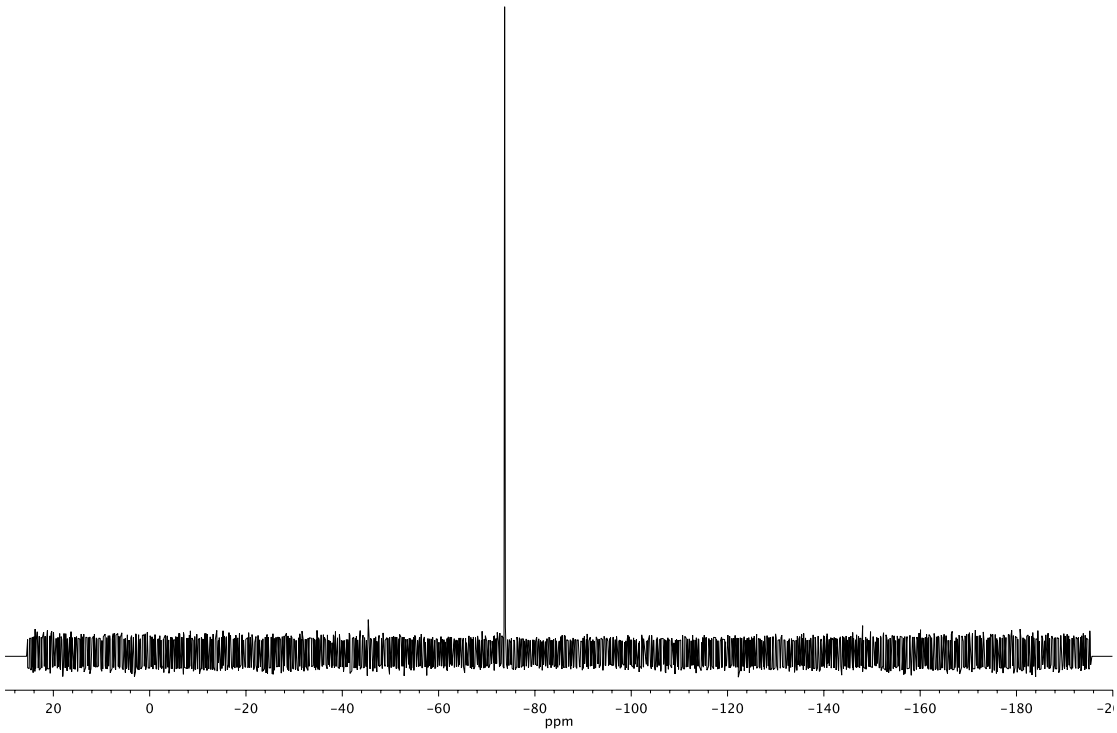

Figure A3-1.12. ^{19}F NMR (282 MHz, $CDCl_3$) of compound **111**.

APPENDIX 3-2

X-Ray Crystallography Reports Relevant to Chapter 3:

Synthesis of

[7,7]paracyclophanes

A3-2.1 X-RAY CRYSTAL STRUCTURE ANALYSIS OF CYCLOPHANE 111

Crystal Data and Experimental

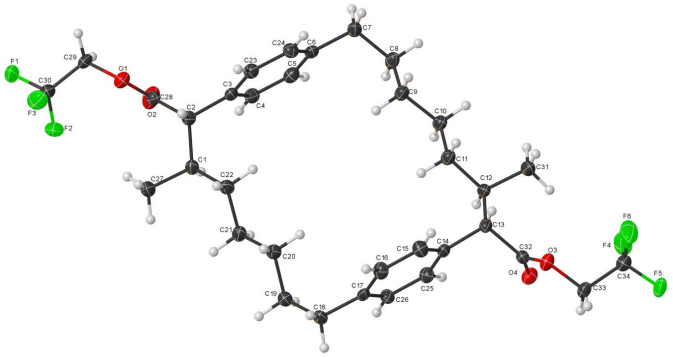

Experimental. Single colorless needle-shaped crystals of **Aaron-macrocycle** were recrystallized from hexane by slow evaporation. A suitable crystal 0.57×0.06×0.04 mm^3 was selected and mounted on a loopon a XtaLAB Synergy, Dualflex, HyPix diffractometer. The crystal was kept at a steady T = 100(2) K during data collection.The structure was solved with the **ShelXT** (Sheldrick, 2015) structure solution program usingthe Intrinsic Phasing solution method and by using **Olex2** (Dolomanov et al., 2009) as the graphical interface. The model was refined with version 2018/3 of **ShelXL** (Sheldrick, 2015)using Least Squares minimisation.

Crystal Data. $C_{34}H_{42}F_6O_4$, M_r = 628.67, monoclinic, $P2$ (No. 3), a = 25.1525(4) Å, b = 5.53398(4) Å, c = 27.2474(4) Å, = 117.4652(19)°, = = 90°, V = 3365.19(9) Å^3, T = 100(2) K, Z = 4, Z' = 2, (CuK) = 0.866 mm^{-1}, 42058 reflections measured, 10947 unique (R_{int} = 0.0510) which were used in all calculations. The final wR_2 was 0.0885 (all data) and R_1 was 0.0363 (I > 2σ(I)).

Compound	**Aaron-macrocycle**
Formula	$C_{34}H_{42}F_6O_4$
$D_{calc.}$/ g cm^{-3}	1.241
/mm^{-1}	0.866
Formula Weight	628.67
Colour	colourless
Shape	needle
Size/mm^3	0.57×0.06×0.04
T/K	100(2)
Crystal System	monoclinic
Flack Parameter	-0.02(6)
Hooft Parameter	-0.00(5)
Space Group	$P2$
a/Å	25.1525(4)
b/Å	5.53398(4)
c/Å	27.2474(4)
/ °	90
/ °	117.4652(19)
/ °	90
V/Å^3	3365.19(9)
Z	4
Z'	2
Wavelength/Å	1.54184
Radiation type	CuK
$_{min}$/ °	1.980
$_{max}$/ °	73.814
Measured Refl.	42058
Independent Refl.	10947
Reflections with I > 2σ(I)	9975
R_{int}	0.0510
Parameters	797
Restraints	1
Largest Peak	0.323
Deepest Hole	-0.205
GooF	0.985
wR_2 (all data)	0.0885
wR_2	0.0853
R_1 (all data)	0.0412
R_1	0.0363

Structure Quality Indicators

Reflections:	d min (Cu)	0.80	I/σ	23.6	Rint	5.10%			
Refinement:	Shift	-0.008	Max Peak	0.3	Min Peak	-0.2	GooF	0.985	Flack -.02(6)

A colourless needle-shaped crystal with dimensions 0.57×0.06×0.04 mm^3 was mounted on a loop. Data were collected using an XtaLAB Synergy, Dualflex, HyPix diffractometer equipped with an Oxford Cryosystems low-temperature device operating at $T = 100(2)$ K.

Data were measured using scans with a narrow frame width of 0.5° per frame for 3.5/3.7/10.0 s using CuK radiation. The total number of runs and images was based on the strategy calculation from the program **CrysAlisPro** (Rigaku, V1.171.39.43c, 2018). The maximum resolution that was achieved was = 73.814°.

The diffraction pattern was indexed using **CrysAlisPro** (Rigaku, V1.171.39.43c, 2018) and the unit cell was refined using **CrysAlisPro** (Rigaku, V1.171.39.43c, 2018) on 24772 reflections, 59% of the observed reflections.

Data reduction, scaling and absorption corrections were performed using **CrysAlisPro** (Rigaku, V1.171.39.43c, 2018). The final completeness is 98.70 % out to 73.814° in . A numerical absorption correction based on Gaussian integration over a multifaceted crystal model was applied using CrysAlisPro 1.171.39.43c (Rigaku Oxford Diffraction, 2018). An empirical absorption correction using spherical harmonics as implemented by SCALE3 ABSPACK algorithm was applied. The absorption coefficient of this material is 0.866 mm^{-1} at this wavelength (= 1.54184Å) and the minimum and maximum transmissions are 0.487 and 1.000.

The structure was solved and the space group *P*2 (# 3) determined by the **ShelXT** (Sheldrick, 2015) structure solution program using Intrinsic Phasing and refined by Least Squares using version 2018/3 of **ShelXL-2014** (Sheldrick, 2015). All non-hydrogen atoms were refined anisotropically. Hydrogen atom positions were calculated geometrically and refined using the riding model.Hydrogen atom positions were calculated geometrically and refined using the riding model.

The value of *Z*' is 2. This means that there are two independent molecules in the asymmetric unit.

The Flack parameter was refined to -0.02(6). Determination of absolute structure using Bayesian statistics on Bijvoet differences using the Olex2 results in -0.00(5). Note: The Flack parameter is used to determine chirality of the crystal studied, the value should be near 0, a value of 1 means that the stereochemistry is wrong and the model should be inverted. A value of 0.5 means that the crystal consists of a racemic mixture of the two enantiomers.

Figure A3-2.1.1 X-ray crystal structure of cyclophane ***111***

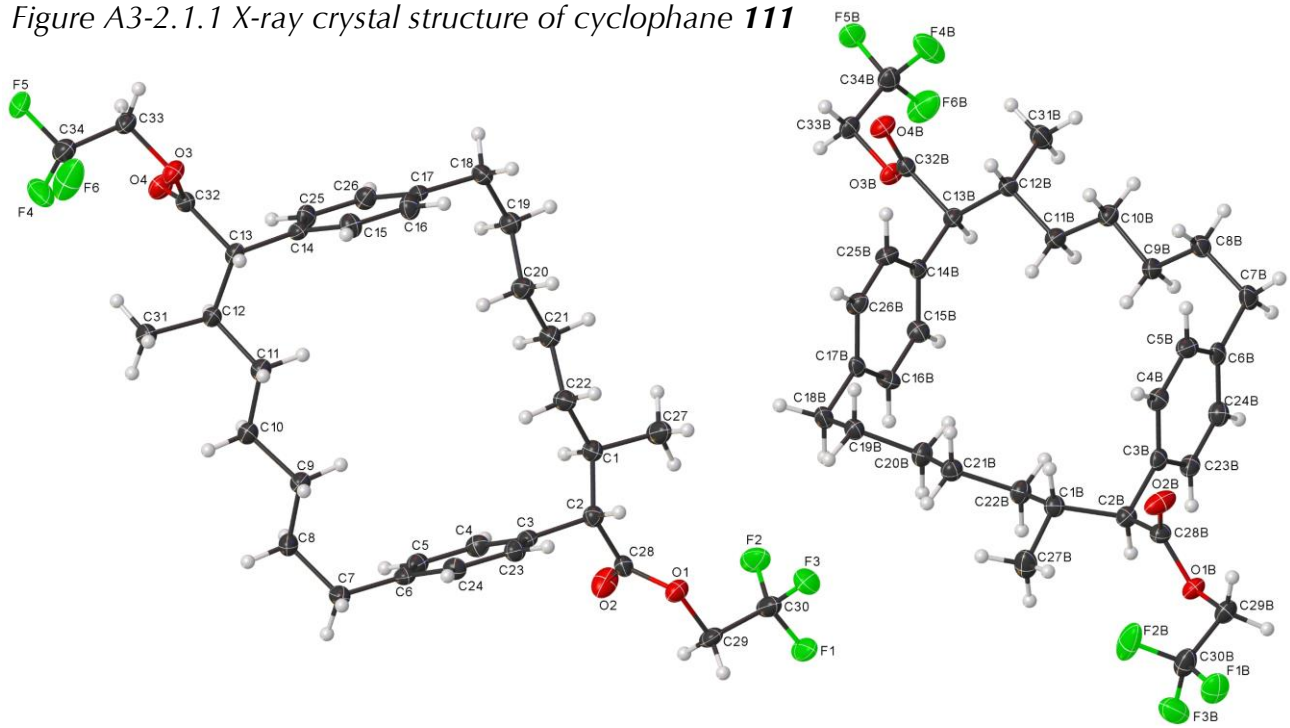

The asymmetric unit contains two molecules of the compound.

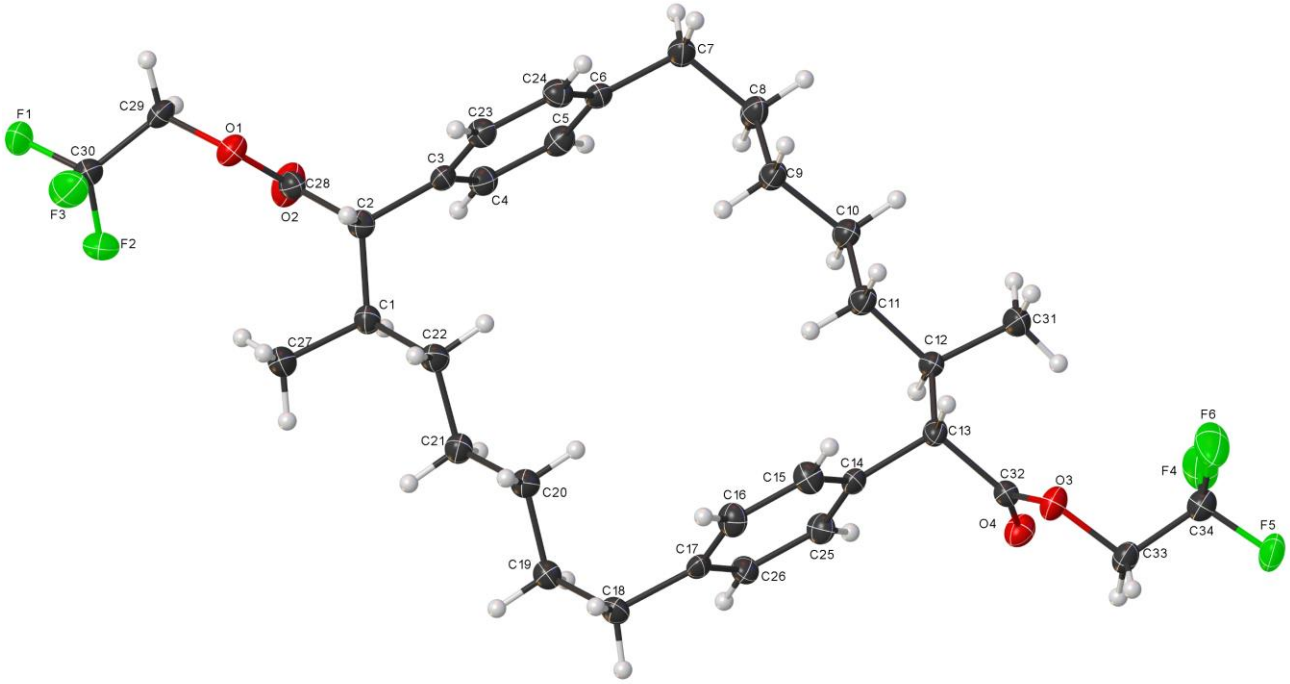

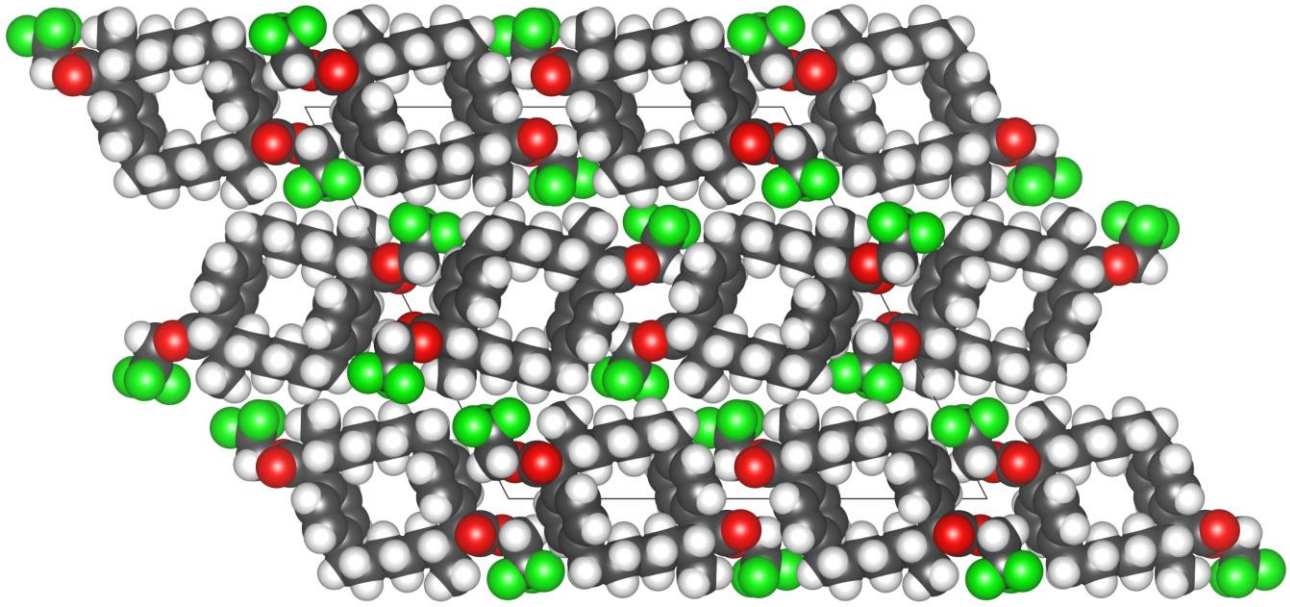

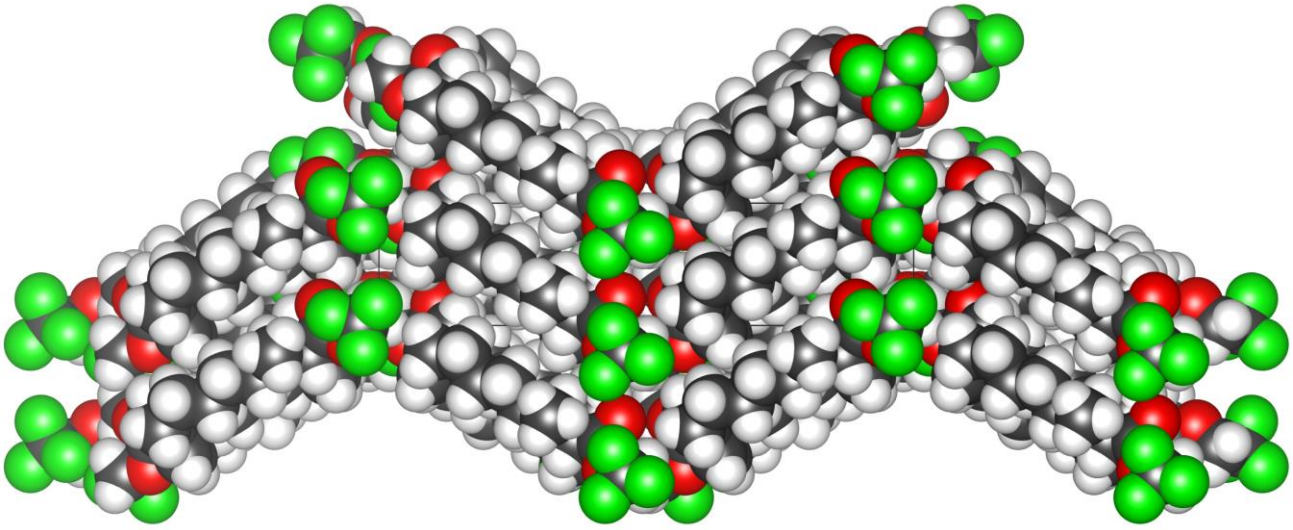

Data Plots: Diffraction Data

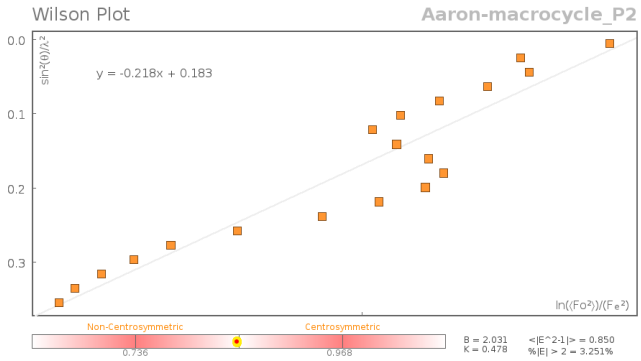

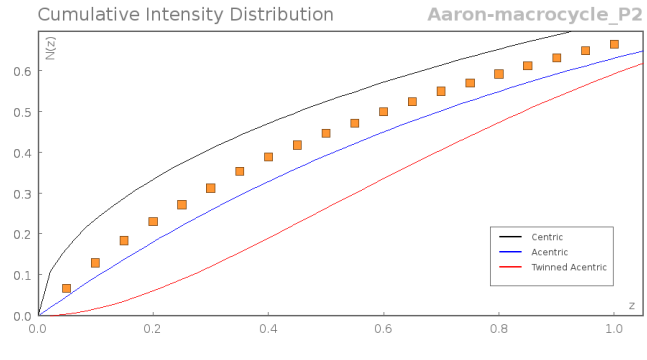

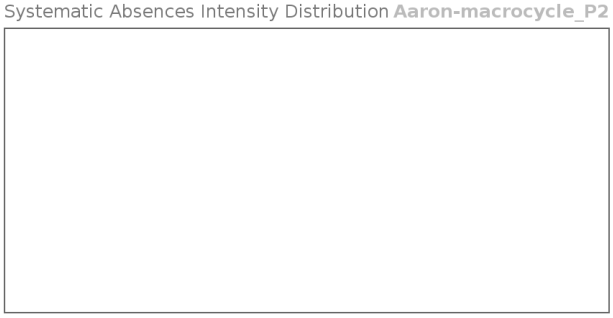

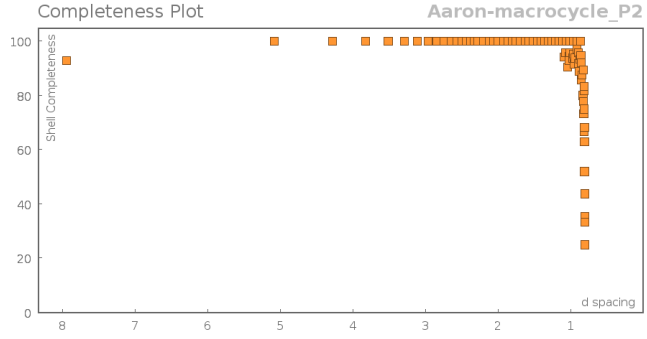

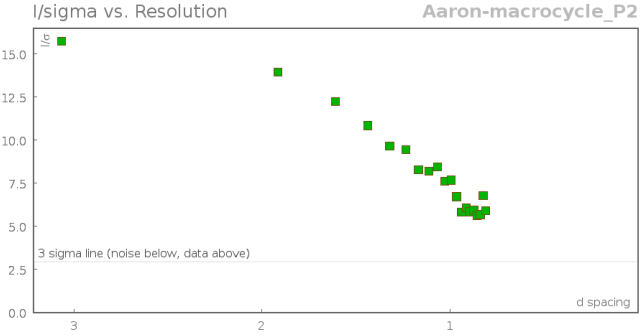

Data Plots: Refinement and Data

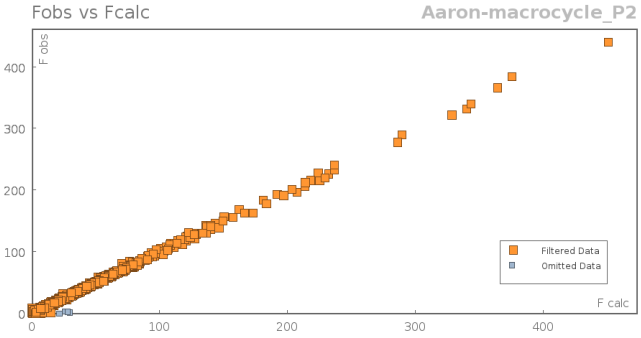

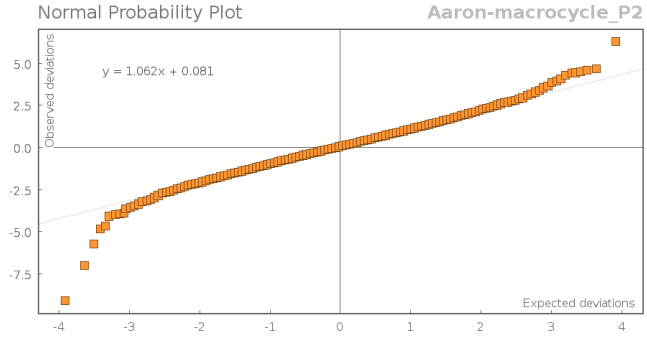

Reflection Statistics

Total reflections (after filtering)	42062	Unique reflections	10947
Completeness	0.804	Mean I/	16.19
hkl_{max} collected	(30, 6, 33)	hkl_{min} collected	(-30, -6, -33)
hkl_{max} used	(27, 6, 33)	hkl_{min} used	(-30, -6, 0)
Lim d_{max} collected	100.0	Lim d_{min} collected	0.77
d_{max} used	22.32	d_{min} used	0.8
Friedel pairs	5250	Friedel pairs merged	0
Inconsistent equivalents	10	R_{int}	0.051

R_{sigma}	0.0423	Intensity transformed	0
Omitted reflections	0	Omitted by user (OMIT hkl)	4
Multiplicity	(6310, 4911, 3058, 1507, 1006, 519, 204, 88, 40, 7, 2)	Maximum multiplicity	18
Removed systematic absences	0	Filtered off (Shel/OMIT)	0

Images of the Crystal on the Diffractometer

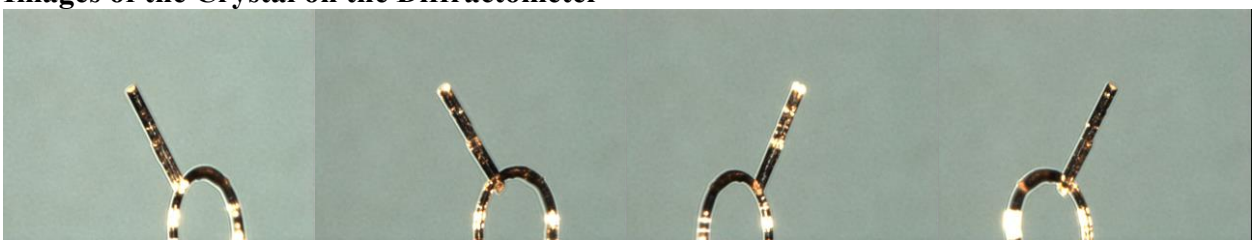

Table A3-2.1.1 Fractional Atomic Coordinates ($x10^4$) and Equivalent Isotropic Displacement Parameters ($Å^2x10^3$) for Aaron-macrocycle_P2. U_{eq} is defined as 1/3 of the trace of the orthogonalised U_{ij}.

Atom	x	y	z	U_{eq}
F1	3107.8(7)	-1535(3)	3482.8(6)	40.3(4)
F2	2927.5(7)	-699(4)	4163.9(7)	43.1(5)
F3	3029.6(8)	2168(3)	3682.3(7)	44.3(5)
F4	6931.1(8)	10422(4)	11116.2(8)	54.0(5)
F5	6790.1(7)	13309(3)	11567.5(6)	34.1(4)
F6	7051.5(9)	14083(5)	10937.5(8)	63.2(7)
O1	4027.6(8)	1790(3)	4704.1(7)	24.9(4)
O2	4161.9(10)	-1186(3)	5309.5(8)	34.6(5)
O3	6006.0(8)	12270(3)	10110.3(7)	24.8(4)
O4	5755.0(8)	8401(3)	10163.3(7)	26.6(4)
C1	3780.7(11)	2906(5)	5830.5(10)	22.6(5)
C2	4251.8(11)	2953(5)	5616.8(10)	21.2(5)
C3	4891.6(11)	2815(5)	6079.4(10)	19.9(5)
C4	5096.8(12)	917(5)	6458.4(10)	23.7(6)
C5	5675.7(12)	905(5)	6887.6(10)	24.0(6)
C6	6074.6(11)	2778(5)	6953.4(10)	21.4(5)
C7	6704.0(11)	2795(5)	7419.2(10)	27.1(6)
C8	6739.8(12)	2951(5)	7994.2(10)	27.6(6)
C9	6465.4(12)	5221(5)	8095.4(10)	23.7(6)
C10	6516.9(12)	5313(5)	8675.3(10)	24.1(5)
C11	6212.8(12)	7497(5)	8772.7(10)	24.6(6)
C12	6209.5(11)	7575(5)	9334.4(9)	21.0(5)
C13	5839.4(11)	9758(5)	9353.0(10)	20.3(5)
C14	5191.4(11)	9689(5)	8912.1(10)	20.0(5)
C15	4964.7(12)	11456(5)	8505.7(11)	25.0(6)
C16	4377.1(12)	11353(5)	8087.6(11)	26.2(6)
C17	3996.1(11)	9483(5)	8059.1(10)	20.1(5)
C18	3362.9(11)	9314(5)	7599.5(10)	23.9(6)
C19	3252.2(12)	7142(5)	7217.6(11)	25.3(6)
C20	3625.5(12)	7131(5)	6911.5(11)	26.0(6)
C21	3517.0(12)	4965(5)	6538.5(11)	25.0(6)

Atom	x	y	z	U_{eq}
C22	3874.2(12)	5034(5)	6215.9(11)	24.8(6)
C23	5287.2(11)	4679(5)	6142.9(10)	22.6(5)
C24	5865.8(12)	4667(5)	6573.4(10)	23.7(5)
C25	4809.6(11)	7819(5)	8889.4(10)	23.6(5)
C26	4225.4(11)	7726(5)	8470.6(10)	23.9(5)
C27	3147.2(12)	2864(6)	5349.5(11)	35.0(7)
C28	4147.1(11)	936(5)	5211.2(10)	21.4(5)
C29	3900.7(12)	18(5)	4278.4(10)	26.0(6)
C30	3240.7(12)	-13(6)	3906.9(11)	32.9(7)
C31	6844.6(11)	7687(6)	9811.7(10)	31.4(6)
C32	5860.6(11)	9970(5)	9917.2(10)	20.3(5)
C33	6063.6(11)	12761(5)	10649.8(10)	24.3(5)
C34	6708.7(12)	12639(5)	11063.1(11)	29.0(6)
F1B	1848.2(8)	11712(3)	49.8(7)	39.7(4)
F2B	2053.5(8)	10844(4)	890.5(7)	53.2(6)
F3B	1882.0(8)	7990(3)	307.4(7)	43.7(4)
F4B	-2001.3(8)	-248(4)	4376.9(8)	50.5(5)
F5B	-1810.7(7)	-2763(3)	5035.6(6)	32.3(4)
F6B	-1985.5(8)	-4054(4)	4231.7(8)	51.2(5)
O1B	934.2(8)	8649(3)	534.8(7)	23.6(4)
O2B	917.9(10)	11669(3)	1080.3(8)	33.4(5)
O3B	-990.6(8)	-1732(3)	4282.2(7)	22.4(4)
O4B	-804.5(8)	2223(3)	4505.0(7)	26.6(4)
C1B	1271.4(11)	7679(5)	1922.1(10)	21.6(5)
C2B	793.8(11)	7555(5)	1304.6(10)	20.6(5)
C3B	155.1(11)	7692(5)	1223.3(9)	20.3(5)
C4B	-47.0(12)	9629(5)	1421.8(10)	22.4(5)
C5B	-630.8(12)	9684(5)	1349.5(10)	24.4(6)
C6B	-1030.0(11)	7828(5)	1080.7(9)	22.0(5)
C7B	-1664.2(11)	7860(5)	1009.2(10)	26.5(6)
C8B	-1693.1(11)	7697(5)	1557.4(10)	24.2(5)
C9B	-1433.2(11)	5398(5)	1880.1(10)	22.5(5)
C10B	-1508.1(12)	5231(5)	2401.0(10)	22.6(5)
C11B	-1201.5(12)	3046(5)	2755.0(10)	24.1(5)
C12B	-1242.2(11)	2857(5)	3298.8(10)	20.4(5)
C13B	-849.3(11)	741(5)	3648.3(9)	18.1(5)
C14B	-199.2(11)	914(4)	3765.3(9)	17.7(5)
C15B	47.6(12)	-830(5)	3567.6(10)	22.8(5)
C16B	638.0(12)	-664(5)	3658.9(11)	24.7(6)
C17B	1001.5(11)	1259(4)	3953.6(10)	19.3(5)
C18B	1643.5(11)	1494(5)	4061.0(10)	23.3(5)
C19B	1755.6(11)	3697(5)	3779.4(10)	21.7(5)
C20B	1415.4(12)	3584(5)	3151.1(10)	23.7(5)
C21B	1548.4(12)	5680(5)	2863.7(10)	23.4(5)
C22B	1177.7(12)	5569(5)	2236.1(10)	23.1(5)
C23B	-247.0(11)	5842(5)	950.0(10)	22.5(5)
C24B	-828.8(12)	5903(5)	881.9(10)	24.0(6)
C25B	163.1(11)	2841(5)	4062.7(10)	23.3(5)
C26B	749.2(11)	3003(5)	4151.5(10)	23.4(5)
C27B	1901.1(12)	7665(6)	1970.6(11)	33.0(6)
C28B	890.5(12)	9560(5)	978.9(10)	21.7(5)
C29B	1057.3(12)	10354(5)	202.4(10)	25.5(6)
C30B	1713.3(13)	10234(6)	369.5(11)	33.1(7)
C31B	-1887.4(12)	2491(6)	3189.4(11)	31.1(6)
C32B	-879.9(11)	590(4)	4189.4(10)	19.0(5)
C33B	-1060.2(11)	-2166(5)	4766.7(10)	21.9(5)
C34B	-1714.1(12)	-2286(5)	4600.9(10)	27.8(6)

Table A3-2.1.2 Fractional Atomic Coordinates (x10^4) Aaron-macrocycle_P2. The anisotropic displacement factor exponent takes the form: -2 ^{2}[h^2a^{*2} x U_{11}+…2hka x b* x U_{12}]*

Atom	U_{11}	U_{22}	U_{33}	U_{23}	U_{13}	U_{12}
F1	28.1(9)	59.4(12)	28.7(8)	-19.7(8)	9.1(7)	0.2(8)
F2	27.6(9)	68.3(13)	39.7(10)	-10.2(9)	21.0(8)	-6.9(9)
F3	40.1(11)	53.9(12)	37.5(10)	7.1(9)	16.6(8)	20.2(9)
F4	39.0(11)	61.0(13)	43.9(11)	-12.8(10)	3.6(9)	25.4(10)
F5	36.5(9)	41.8(10)	18.0(7)	-5.3(7)	7.4(7)	3.0(8)
F6	46.0(12)	105.8(19)	36.2(10)	-6.7(11)	17.7(10)	-38.8(12)
O1	32.9(11)	22.1(9)	22.0(9)	0.3(7)	14.5(8)	0.7(8)
O2	54.7(14)	16.9(10)	29.3(10)	-1.3(8)	16.8(10)	-1.8(9)
O3	33.2(11)	21.3(9)	19.2(9)	-2.1(7)	11.6(8)	-1.9(8)
O4	34.1(11)	25.2(10)	23.5(9)	0.3(8)	15.9(8)	-5.2(8)
C1	21.1(13)	24.2(13)	20.9(12)	-2.6(11)	8.2(11)	-0.1(11)
C2	21.6(13)	20.5(12)	20.7(12)	0.1(10)	9.2(11)	0.2(11)
C3	20.2(13)	22.0(12)	18.5(11)	-4.1(10)	9.9(10)	1.0(11)
C4	24.9(15)	22.7(13)	24.7(13)	-3.7(11)	12.3(12)	-3.6(11)
C5	31.0(15)	20.8(13)	21.8(12)	3.5(10)	13.6(12)	5.5(11)
C6	21.6(13)	24.1(13)	20.5(12)	-3.5(11)	11.4(11)	2.4(11)
C7	22.3(14)	34.1(15)	22.5(13)	-4.3(12)	8.3(11)	6.3(12)
C8	27.9(15)	32.6(15)	18.6(12)	1.8(11)	7.7(11)	8.8(12)
C9	25.7(14)	25.8(14)	19.4(12)	0.3(11)	10.1(11)	4.1(12)
C10	24.2(14)	29.1(14)	19.3(12)	1.2(11)	10.3(11)	1.7(11)
C11	25.9(14)	27.7(14)	19.9(12)	1.0(11)	10.4(11)	3.5(12)
C12	18.4(12)	27.5(13)	17.2(11)	0.0(10)	8.2(10)	1.2(11)
C13	20.8(13)	23.6(13)	16.1(12)	-0.3(10)	8.3(11)	-3.1(11)
C14	20.1(13)	22.8(13)	17.2(12)	-4.3(10)	8.7(11)	0.5(10)
C15	24.9(15)	21.2(13)	26.5(13)	2.5(11)	9.7(12)	0.3(11)
C16	27.6(15)	24.3(14)	22.7(13)	4.1(11)	8.1(12)	3.2(12)
C17	19.4(13)	24.8(13)	16.8(12)	-3.9(10)	9.0(11)	4.0(11)
C18	18.1(13)	28.1(14)	24.0(13)	-1.3(11)	8.4(11)	3.3(11)
C19	21.0(14)	29.5(15)	23.8(13)	-2.2(11)	9.2(11)	-0.6(11)
C20	22.9(14)	30.3(15)	25.1(13)	-3.4(11)	11.4(12)	-0.9(11)
C21	24.1(14)	27.7(14)	21.8(13)	-2.1(11)	9.4(12)	1.0(11)
C22	22.0(14)	26.5(14)	25.8(13)	-3.4(11)	11.0(12)	0.3(11)
C23	24.9(14)	21.1(12)	22.3(13)	2.5(10)	11.4(12)	2.2(11)
C24	23.1(14)	22.8(13)	26.5(13)	-0.6(11)	12.6(12)	-1.8(11)
C25	25.1(14)	24.7(13)	19.3(12)	5.2(11)	8.9(11)	2.4(11)
C26	20.0(13)	29.3(14)	22.6(12)	-2.0(11)	10.0(11)	-5.5(12)
C27	22.9(14)	52.3(19)	28.1(14)	-11.8(14)	10.4(12)	-3.4(14)
C28	18.8(13)	23.8(14)	19.3(12)	2.4(10)	7.0(11)	2.7(10)
C29	28.5(15)	32.3(15)	20.6(13)	-7.7(11)	14.2(12)	-1.8(12)
C30	24.8(15)	49.4(19)	26.5(14)	-9.8(13)	13.6(13)	-0.6(14)
C31	21.5(14)	48.2(18)	22.0(13)	-2.5(13)	7.7(12)	5.9(13)
C32	16.9(13)	23.8(13)	18.8(12)	-1.7(10)	7.0(11)	-0.3(11)
C33	28.6(14)	25.0(13)	18.5(12)	-2.4(11)	10.2(11)	2.8(12)
C34	29.8(15)	34.0(15)	23.7(13)	-3.8(12)	12.7(12)	-1.1(13)
F1B	38.2(10)	52.4(11)	34.2(9)	6.0(8)	21.7(8)	-8.8(8)
F2B	37.3(11)	92.0(16)	23.4(8)	-7.7(10)	8.3(8)	-25.9(11)
F3B	38.2(10)	50.4(11)	49.1(10)	11.1(9)	25.6(9)	12.8(9)
F4B	39.5(11)	60.0(12)	61.5(12)	34.4(10)	31.4(10)	23.2(9)
F5B	33.3(9)	40.6(10)	31.5(8)	7.2(7)	22.1(7)	1.0(7)
F6B	40.4(11)	73.9(14)	41.0(10)	-22.3(10)	20.3(9)	-26.3(10)
O1B	30.8(10)	23.9(9)	19.2(8)	-2.0(7)	14.1(8)	-1.5(8)
O2B	60.9(14)	17.3(9)	35.3(11)	-0.6(8)	33.5(11)	-0.6(9)
O3B	32.1(10)	18.1(9)	21.2(9)	1.5(7)	15.9(8)	-1.6(8)
O4B	35.2(11)	24.0(10)	24.3(9)	-5.2(8)	16.8(9)	-3.6(8)
C1B	22.4(13)	20.6(12)	21.2(12)	1.5(10)	9.5(11)	0.0(11)

Atom	U_{11}	U_{22}	U_{33}	U_{23}	U_{13}	U_{12}
C2B	23.0(13)	18.3(12)	20.8(12)	0.7(10)	10.3(11)	0.1(11)
C3B	24.2(13)	19.8(12)	15.0(11)	5.0(10)	7.4(10)	3.0(11)
C4B	27.5(15)	18.8(13)	20.4(12)	-1.6(10)	10.5(12)	-2.2(11)
C5B	30.8(15)	22.1(13)	23.1(13)	3.8(11)	14.6(12)	5.9(11)
C6B	22.8(13)	25.5(13)	15.1(11)	8.0(10)	6.7(10)	4.3(11)
C7B	22.2(13)	34.2(15)	21.2(12)	9.7(12)	8.4(11)	4.6(12)
C8B	21.1(13)	27.8(14)	22.9(12)	4.8(11)	9.5(11)	4.1(11)
C9B	22.6(14)	25.2(13)	19.1(12)	2.6(11)	9.0(11)	4.1(11)
C10B	24.5(14)	22.3(13)	19.8(12)	-0.9(10)	9.3(11)	1.4(11)
C11B	26.1(14)	26.8(14)	20.6(12)	1.0(11)	11.7(11)	4.4(11)
C12B	20.5(13)	21.6(12)	19.6(12)	2.4(10)	9.7(10)	3.7(11)
C13B	19.2(13)	18.2(12)	16.9(11)	-1.8(10)	8.5(10)	-1.4(10)
C14B	17.3(13)	19.8(12)	15.4(11)	4.7(10)	7.1(10)	1.9(10)
C15B	23.7(14)	18.3(13)	25.2(13)	-1.8(10)	10.2(12)	-0.7(10)
C16B	23.2(14)	22.7(13)	30.8(14)	1.0(11)	14.8(12)	5.8(11)
C17B	16.8(13)	23.6(13)	16.6(11)	7.1(10)	7.0(11)	3.6(10)
C18B	18.4(14)	28.9(14)	20.9(12)	4.7(11)	7.6(11)	3.6(11)
C19B	18.4(13)	24.7(13)	20.9(12)	0.6(10)	8.2(11)	0.8(11)
C20B	25.2(14)	24.0(13)	20.4(12)	1.3(11)	9.0(11)	-2.7(11)
C21B	23.8(14)	24.0(13)	22.9(13)	1.3(11)	11.3(11)	-0.4(11)
C22B	25.2(14)	21.7(13)	21.0(12)	1.2(11)	9.6(12)	-2.2(11)
C23B	26.9(15)	19.1(12)	19.3(12)	-0.2(10)	8.8(11)	2.3(11)
C24B	24.3(15)	22.2(13)	21.4(13)	0.1(11)	7.1(12)	-2.4(11)
C25B	26.9(14)	24.9(13)	22.3(12)	-3.2(11)	15.0(11)	0.0(12)
C26B	22.4(13)	26.8(13)	21.3(12)	-5.6(11)	10.4(11)	-5.9(11)
C27B	23.8(15)	45.9(18)	27.8(14)	6.3(14)	10.4(12)	-4.1(14)
C28B	24.0(14)	20.3(13)	21.7(13)	-0.2(10)	11.3(11)	3.1(11)
C29B	31.3(16)	28.1(14)	19.4(12)	1.3(11)	13.8(12)	-1.2(12)
C30B	31.0(16)	45.9(18)	22.1(14)	1.6(13)	11.9(13)	-6.7(14)
C31B	23.8(14)	42.4(17)	28.2(14)	9.0(13)	12.9(12)	6.4(13)
C32B	16.8(13)	20.0(12)	19.6(12)	2.1(10)	7.9(10)	1.2(10)
C33B	26.8(14)	23.0(13)	17.8(12)	3.4(10)	11.7(11)	-0.3(11)
C34B	27.1(14)	34.8(15)	23.0(13)	3.9(12)	12.7(12)	-1.9(13)

Table A3-2.1.3 Bond Lengths in Å for Aaron-macrocycle_P2

Atom	Atom	Length/Å
F1	C30	1.342(3)
F2	C30	1.328(3)
F3	C30	1.347(4)
F4	C34	1.328(3)
F5	C34	1.345(3)
F6	C34	1.331(3)
O1	C28	1.356(3)
O1	C29	1.438(3)
O2	C28	1.201(3)
O3	C32	1.361(3)
O3	C33	1.435(3)
O4	C32	1.199(3)
C1	C2	1.543(3)
C1	C22	1.522(4)
C1	C27	1.527(4)
C2	C3	1.521(3)
C2	C28	1.506(3)
C3	C4	1.394(4)
C3	C23	1.388(4)
C4	C5	1.385(4)
C5	C6	1.395(4)
C6	C7	1.505(4)
C6	C24	1.393(4)
C7	C8	1.530(3)
C8	C9	1.518(4)
C9	C10	1.525(3)
C10	C11	1.517(4)
C11	C12	1.535(3)
C12	C13	1.540(3)
C12	C31	1.527(3)
C13	C14	1.515(3)
C13	C32	1.518(3)
C14	C15	1.388(4)
C14	C25	1.393(4)
C15	C16	1.390(4)
C16	C17	1.388(4)
C17	C18	1.508(4)
C17	C26	1.392(4)
C18	C19	1.529(4)
C19	C20	1.516(3)
C20	C21	1.513(4)

Atom	Atom	Length/Å
C21	C22	1.520(3)
C23	C24	1.385(4)
C25	C26	1.385(4)
C29	C30	1.494(4)
C33	C34	1.490(4)
F1B	C30B	1.347(3)
F2B	C30B	1.319(3)
F3B	C30B	1.348(4)
F4B	C34B	1.326(3)
F5B	C34B	1.341(3)
F6B	C34B	1.342(3)
O1B	C28B	1.361(3)
O1B	C29B	1.437(3)
O2B	C28B	1.194(3)
O3B	C32B	1.363(3)
O3B	C33B	1.430(3)
O4B	C32B	1.201(3)
C1B	C2B	1.554(3)
C1B	C22B	1.528(3)
C1B	C27B	1.527(3)
C2B	C3B	1.519(3)
C2B	C28B	1.509(3)
C3B	C4B	1.398(3)
C3B	C23B	1.390(4)
C4B	C5B	1.389(3)
C5B	C6B	1.386(4)
C6B	C7B	1.515(3)
C6B	C24B	1.392(4)
C7B	C8B	1.531(3)
C8B	C9B	1.513(4)
C9B	C10B	1.518(3)
C10B	C11B	1.517(4)
C11B	C12B	1.535(3)
C12B	C13B	1.545(3)
C12B	C31B	1.522(3)
C13B	C14B	1.518(3)
C13B	C32B	1.514(3)
C14B	C15B	1.384(3)
C14B	C25B	1.394(4)
C15B	C16B	1.391(3)
C16B	C17B	1.391(4)
C17B	C18B	1.508(3)
C17B	C26B	1.393(3)
C18B	C19B	1.534(3)
C19B	C20B	1.522(3)
C20B	C21B	1.520(3)
C21B	C22B	1.525(3)
C23B	C24B	1.388(4)
C25B	C26B	1.382(3)
C29B	C30B	1.497(4)
C33B	C34B	1.493(3)

Table A3-2.1.4 Bond Angles in ° for Aaron-macrocycle_P2

Atom	Atom	Atom	Angle/°
C28	O1	C29	116.5(2)
C32	O3	C33	117.09(19)
C22	C1	C2	110.3(2)
C22	C1	C27	111.9(2)
C27	C1	C2	110.8(2)
C3	C2	C1	112.92(19)
C28	C2	C1	111.1(2)
C28	C2	C3	109.3(2)
C4	C3	C2	122.7(2)
C23	C3	C2	119.3(2)
C23	C3	C4	117.9(2)
C5	C4	C3	121.0(2)
C4	C5	C6	121.2(2)
C5	C6	C7	121.8(2)
C24	C6	C5	117.4(2)
C24	C6	C7	120.8(2)
C6	C7	C8	114.0(2)
C9	C8	C7	114.6(2)
C8	C9	C10	112.8(2)
C11	C10	C9	113.5(2)
C10	C11	C12	115.6(2)
C11	C12	C13	109.6(2)
C31	C12	C11	111.5(2)
C31	C12	C13	110.5(2)
C14	C13	C12	113.5(2)
C14	C13	C32	109.11(19)
C32	C13	C12	110.7(2)
C15	C14	C13	120.7(2)
C15	C14	C25	117.8(2)
C25	C14	C13	121.4(2)
C16	C15	C14	121.0(2)
C15	C16	C17	121.5(2)
C16	C17	C18	122.0(2)
C26	C17	C16	117.2(2)
C26	C17	C18	120.8(2)
C17	C18	C19	113.9(2)
C20	C19	C18	114.4(2)
C21	C20	C19	114.0(2)
C20	C21	C22	113.4(2)
C21	C22	C1	115.8(2)
C24	C23	C3	121.0(2)
C23	C24	C6	121.5(2)
C26	C25	C14	120.8(2)
C25	C26	C17	121.7(2)
O1	C28	C2	111.8(2)
O2	C28	O1	122.5(2)
O2	C28	C2	125.7(2)
O1	C29	C30	108.6(2)
F1	C30	F3	106.4(2)
F1	C30	C29	110.4(2)
F2	C30	F1	107.6(2)
F2	C30	F3	106.9(2)
F2	C30	C29	112.9(2)

Atom	Atom	Atom	Angle/°
F3	C30	C29	112.3(3)
O3	C32	C13	110.0(2)
O4	C32	O3	123.4(2)
O4	C32	C13	126.7(2)
O3	C33	C34	109.0(2)
F4	C34	F5	106.6(2)
F4	C34	F6	107.0(2)
F4	C34	C33	112.4(2)
F5	C34	C33	111.1(2)
F6	C34	F5	106.6(2)
F6	C34	C33	112.8(2)
C28B	O1B	C29B	116.5(2)
C32B	O3B	C33B	116.90(19)
C22B	C1B	C2B	109.3(2)
C27B	C1B	C2B	110.27(19)
C27B	C1B	C22B	111.7(2)
C3B	C2B	C1B	113.15(18)
C28B	C2B	C1B	110.5(2)
C28B	C2B	C3B	108.9(2)
C4B	C3B	C2B	122.1(2)
C23B	C3B	C2B	120.1(2)
C23B	C3B	C4B	117.9(2)
C5B	C4B	C3B	120.8(2)
C6B	C5B	C4B	121.3(2)
C5B	C6B	C7B	121.5(2)
C5B	C6B	C24B	117.9(2)
C24B	C6B	C7B	120.6(2)
C6B	C7B	C8B	113.2(2)
C9B	C8B	C7B	114.5(2)
C8B	C9B	C10B	112.8(2)
C11B	C10B	C9B	113.4(2)
C10B	C11B	C12B	115.3(2)
C11B	C12B	C13B	109.76(19)
C31B	C12B	C11B	111.1(2)
C31B	C12B	C13B	109.9(2)
C14B	C13B	C12B	113.73(19)
C32B	C13B	C12B	109.69(19)
C32B	C13B	C14B	109.43(19)
C15B	C14B	C13B	120.5(2)
C15B	C14B	C25B	118.0(2)
C25B	C14B	C13B	121.5(2)
C14B	C15B	C16B	121.2(2)
C15B	C16B	C17B	121.1(2)
C16B	C17B	C18B	122.5(2)
C16B	C17B	C26B	117.2(2)
C26B	C17B	C18B	120.2(2)
C17B	C18B	C19B	113.5(2)
C20B	C19B	C18B	113.1(2)
C21B	C20B	C19B	113.9(2)
C20B	C21B	C22B	112.4(2)
C21B	C22B	C1B	115.1(2)
C3B	C23B	C24B	121.0(2)
C23B	C24B	C6B	121.1(2)
C26B	C25B	C14B	120.7(2)
C25B	C26B	C17B	121.8(2)
O1B	C28B	C2B	110.6(2)
O2B	C28B	O1B	123.2(2)
O2B	C28B	C2B	126.2(2)
O1B	C29B	C30B	107.9(2)
F1B	C30B	C29B	110.3(2)
F2B	C30B	F1B	108.0(2)
F2B	C30B	F3B	106.6(3)
F2B	C30B	C29B	113.1(2)
F3B	C30B	F1B	106.9(2)
F3B	C30B	C29B	111.6(2)
O3B	C32B	C13B	109.8(2)
O4B	C32B	O3B	123.7(2)
O4B	C32B	C13B	126.4(2)
O3B	C33B	C34B	108.36(19)
F4B	C34B	F5B	107.0(2)
F4B	C34B	F6B	107.1(2)
F4B	C34B	C33B	113.1(2)
F5B	C34B	F6B	106.4(2)
F5B	C34B	C33B	111.4(2)
F6B	C34B	C33B	111.6(2)

Table A3-2.1.5 Torsion Angles in ° for Aaron-macrocycle_P2

Atom	Atom	Atom	Atom	Angle/°
O1	C29	C30	F1	176.0(2)
O1	C29	C30	F2	-63.5(3)
O1	C29	C30	F3	57.5(3)
O3	C33	C34	F4	-66.4(3)
O3	C33	C34	F5	174.3(2)
O3	C33	C34	F6	54.6(3)
C1	C2	C3	C4	57.5(3)
C1	C2	C3	C23	-120.4(2)
C1	C2	C28	O1	118.2(2)
C1	C2	C28	O2	-61.6(3)
C2	C1	C22	C21	-169.3(2)
C2	C3	C4	C5	-177.3(2)
C2	C3	C23	C24	177.3(2)
C3	C2	C28	O1	-116.5(2)

Atom	Atom	Atom	Atom	Angle/°
C3	C2	C28	O2	63.7(3)
C3	C4	C5	C6	-0.5(4)
C3	C23	C24	C6	0.8(4)
C4	C3	C23	C24	-0.7(3)
C4	C5	C6	C7	179.7(2)
C4	C5	C6	C24	0.5(3)
C5	C6	C7	C8	-63.9(3)
C5	C6	C24	C23	-0.7(3)
C6	C7	C8	C9	-61.2(3)
C7	C6	C24	C23	-179.9(2)
C7	C8	C9	C10	-179.4(2)
C8	C9	C10	C11	-176.6(2)
C9	C10	C11	C12	175.5(2)
C10	C11	C12	C13	-175.0(2)
C10	C11	C12	C31	62.3(3)
C11	C12	C13	C14	60.4(3)
C11	C12	C13	C32	-176.5(2)
C12	C13	C14	C15	-116.8(3)
C12	C13	C14	C25	61.1(3)
C12	C13	C32	O3	130.1(2)
C12	C13	C32	O4	-51.4(3)
C13	C14	C15	C16	177.5(2)
C13	C14	C25	C26	-177.3(2)
C14	C13	C32	O3	-104.2(2)
C14	C13	C32	O4	74.3(3)
C14	C15	C16	C17	-0.2(4)
C14	C25	C26	C17	-0.2(4)
C15	C14	C25	C26	0.6(4)
C15	C16	C17	C18	-178.4(2)
C15	C16	C17	C26	0.7(4)
C16	C17	C18	C19	113.9(3)
C16	C17	C26	C25	-0.5(3)
C17	C18	C19	C20	-61.7(3)
C18	C17	C26	C25	178.6(2)
C18	C19	C20	C21	179.5(2)
C19	C20	C21	C22	177.5(2)
C20	C21	C22	C1	-179.7(2)
C22	C1	C2	C3	59.7(3)
C22	C1	C2	C28	-177.0(2)
C23	C3	C4	C5	0.6(3)
C24	C6	C7	C8	115.2(3)
C25	C14	C15	C16	-0.4(4)
C26	C17	C18	C19	-65.1(3)
C27	C1	C2	C3	-175.9(2)
C27	C1	C2	C28	-52.6(3)
C27	C1	C22	C21	66.9(3)
C28	O1	C29	C30	103.6(3)
C28	C2	C3	C4	-66.7(3)
C28	C2	C3	C23	115.4(2)
C29	O1	C28	O2	1.7(4)
C29	O1	C28	C2	-178.0(2)
C31	C12	C13	C14	-176.4(2)
C31	C12	C13	C32	-53.2(3)
C32	O3	C33	C34	97.2(3)
C32	C13	C14	C15	119.2(2)
C32	C13	C14	C25	-62.9(3)
C33	O3	C32	O4	3.4(4)
C33	O3	C32	C13	-178.11(19)

Atom	Atom	Atom	Atom	Angle/°
O1B	C29B	C30B	F1B	176.8(2)
O1B	C29B	C30B	F2B	-62.1(3)
O1B	C29B	C30B	F3B	58.1(3)
O3B	C33B	C34B	F4B	-61.4(3)
O3B	C33B	C34B	F5B	178.1(2)
O3B	C33B	C34B	F6B	59.4(3)
C1B	C2B	C3B	C4B	57.0(3)
C1B	C2B	C3B	C23B	-122.2(2)
C1B	C2B	C28B	O1B	126.1(2)
C1B	C2B	C28B	O2B	-55.0(4)
C2B	C1B	C22B	C21B	-170.6(2)
C2B	C3B	C4B	C5B	-178.9(2)
C2B	C3B	C23B	C24B	178.6(2)
C3B	C2B	C28B	O1B	-109.0(2)
C3B	C2B	C28B	O2B	69.9(3)
C3B	C4B	C5B	C6B	0.1(4)
C3B	C23B	C24B	C6B	0.5(4)
C4B	C3B	C23B	C24B	-0.7(4)
C4B	C5B	C6B	C7B	179.0(2)
C4B	C5B	C6B	C24B	-0.3(3)
C5B	C6B	C7B	C8B	-65.2(3)
C5B	C6B	C24B	C23B	0.0(3)
C6B	C7B	C8B	C9B	-61.8(3)
C7B	C6B	C24B	C23B	-179.3(2)
C7B	C8B	C9B	C10B	-176.1(2)
C8B	C9B	C10B	C11B	-174.9(2)
C9B	C10B	C11B	C12B	177.5(2)
C10B	C11B	C12B	C13B	-173.2(2)
C10B	C11B	C12B	C31B	65.1(3)
C11B	C12B	C13B	C14B	55.9(3)
C11B	C12B	C13B	C32B	178.8(2)
C12B	C13B	C14B	C15B	-117.0(2)
C12B	C13B	C14B	C25B	61.6(3)
C12B	C13B	C32B	O3B	131.5(2)
C12B	C13B	C32B	O4B	-50.3(3)
C13B	C14B	C15B	C16B	178.3(2)
C13B	C14B	C25B	C26B	-178.1(2)
C14B	C13B	C32B	O3B	-103.0(2)
C14B	C13B	C32B	O4B	75.1(3)
C14B	C15B	C16B	C17B	0.2(4)
C14B	C25B	C26B	C17B	-0.5(4)
C15B	C14B	C25B	C26B	0.6(4)
C15B	C16B	C17B	C18B	179.9(2)
C15B	C16B	C17B	C26B	-0.1(4)
C16B	C17B	C18B	C19B	115.1(3)
C16B	C17B	C26B	C25B	0.2(4)
C17B	C18B	C19B	C20B	-63.6(3)
C18B	C17B	C26B	C25B	-179.7(2)
C18B	C19B	C20B	C21B	-176.7(2)
C19B	C20B	C21B	C22B	-177.3(2)
C20B	C21B	C22B	C1B	177.7(2)
C22B	C1B	C2B	C3B	59.8(3)
C22B	C1B	C2B	C28B	-177.7(2)
C23B	C3B	C4B	C5B	0.4(3)
C24B	C6B	C7B	C8B	114.1(3)
C25B	C14B	C15B	C16B	-0.4(4)
C26B	C17B	C18B	C19B	-64.9(3)
C27B	C1B	C2B	C3B	-177.0(2)

Atom	Atom	Atom	Atom	Angle/°
C27B	C1B	C2B	C28B	-54.6(3)
C27B	C1B	C22B	C21B	67.1(3)
C28B	O1B	C29B	C30B	99.4(3)
C28B	C2B	C3B	C4B	-66.3(3)
C28B	C2B	C3B	C23B	114.5(2)
C29B	O1B	C28B	O2B	4.0(4)
C29B	O1B	C28B	C2B	-177.0(2)
C31B	C12B	C13B	C14B	178.4(2)
C31B	C12B	C13B	C32B	-58.7(3)
C32B	O3B	C33B	C34B	99.1(2)
C32B	C13B	C14B	C15B	119.9(2)
C32B	C13B	C14B	C25B	-61.4(3)
C33B	O3B	C32B	O4B	4.5(3)
C33B	O3B	C32B	C13B	-177.24(19)

Table A3-2.1.6 Hydrogen Fractional Atomic Coordinates ($x10^4$) and Equivalent Isotropic Displacement Parameters ($Å^2x10^3$) for Aaron-macrocycle_P2. U_{eq} is defined as 1/3 of the trace of the orthogonalised U_{ij}.

Atom	x	y	z	U_{eq}
H1	3838.87	1417.26	6044.01	27
H2	4207.62	4485.31	5421.4	25
H4	4840.99	-360.14	6422.28	28
H5	5801.05	-375.76	7136.72	29
H7A	6916.88	4159.71	7370.2	33
H7B	6906.2	1334.9	7398.66	33
H8A	6538.59	1555.85	8047.23	33
H8B	7157.54	2870.15	8269.03	33
H9A	6045.69	5298.2	7825.73	28
H9B	6663.7	6623.82	8041.48	28
H10A	6340.63	3858.89	8736.64	29
H10B	6937.65	5329.69	8943.77	29
H11A	5801.39	7546.94	8483.22	30
H11B	6410.9	8941.41	8737.19	30
H12	6017.59	6097.78	9373.73	25
H13	6022.18	11219.04	9293.16	24
H15	5209.75	12729.35	8513.21	30
H16	4236.17	12564.47	7821	31
H18A	3269.88	10780.41	7380.3	29
H18B	3091.16	9221.46	7761.05	29
H19A	3335.86	5676.06	7435.97	30
H19B	2831.8	7113.21	6948.5	30
H20A	3539.25	8588.14	6690.01	31
H20B	4046.03	7171.75	7180.08	31
H21A	3093.65	4881.95	6279.45	30
H21B	3620.75	3509.13	6761.73	30
H22A	4296.5	5121.09	6477.84	30
H22B	3772.08	6505.72	5998.13	30
H23	5162.07	5955.91	5892.69	27
H24	6120.38	5949.12	6609.47	28
H25	4948.78	6619.38	9158.69	28
H26	3979.76	6457.4	8463.97	29
H27A	3082.42	4291.05	5128.85	52
H27B	2861.64	2813.75	5491.26	52
H27C	3099.11	1459.46	5125.95	52
H29A	4033.67	-1564.23	4443.05	31
H29B	4111.57	420.45	4067.88	31
H31A	7042.46	9106.84	9774.92	47
H31B	7063.15	6277.03	9804.09	47
H31C	6827.48	7745.84	10156.27	47
H33A	5836.99	11583.49	10740.57	29
H33B	5905.86	14354.71	10655.57	29
H1B	1216.17	9191.66	2079.88	26
H2B	842	6011.03	1153.47	25
H4B	212.4	10895.87	1604.28	27
H5B	-756.36	10992.28	1484.09	29
H7BA	-1884.57	6514.62	775.82	32
H7BB	-1859.37	9339.1	821.4	32
H8BA	-1479.64	9064.2	1786.17	29

Atom	x	y	z	U_{eq}
H8BB	-2108.59	7825.21	1481.74	29
H9BA	-1009.95	5319.97	1980.83	27
H9BB	-1627.82	4021.27	1645.32	27
H10C	-1346.11	6682.04	2619.1	27
H10D	-1932.21	5164.79	2297.27	27
H11C	-781.77	3079.64	2841.42	29
H11D	-1376.03	1600.41	2538.96	29
H12B	-1091.09	4361.57	3506.93	24
H13B	-1015.29	-759.67	3443.49	22
H15B	-185.46	-2136.09	3370.18	27
H16B	792.41	-1858.43	3520.68	30
H18C	1755.56	43.85	3930.99	28
H18D	1899.36	1608.16	4456.72	28
H19C	1637.8	5146.66	3904.52	26
H19D	2181.16	3813.56	3892.11	26
H20C	1515.18	2084.57	3028.49	28
H20D	989.07	3560.12	3038.74	28
H21C	1970.68	5661.14	2959.15	28
H21D	1465.5	7188.06	2996.65	28
H22C	757.11	5506.24	2145.69	28
H22D	1272.99	4079.35	2106.12	28
H23B	-124.41	4542.27	810.61	27
H24B	-1088.59	4636.94	700.23	29
H25B	8.95	4029.39	4202.81	28
H26B	981.32	4312.22	4348.7	28
H27D	1963.79	6182.78	1821.78	50
H27E	2191.46	7799.8	2352.75	50
H27F	1943.79	9005.6	1767.83	50
H29C	949.16	11971.7	260.87	31
H29D	825.95	9956.17	-186.45	31
H31D	-2039.34	1012.82	2988.64	47
H31E	-2127.92	3820.41	2975.5	47
H31F	-1901.78	2409.07	3534.97	47
H33C	-874.84	-872.72	5031.91	26
H33D	-868.03	-3675.15	4937.83	26

Citations

CrysAlisPro Software System, Rigaku Oxford Diffraction, (2018).

O.V. Dolomanov and L.J. Bourhis and R.J. Gildea and J.A.K. Howard and H. Puschmann, Olex2: A complete structure solution, refinement and analysis program, *J. Appl. Cryst.*, (2009), **42**, 339-341.

Sheldrick, G.M., Crystal structure refinement with ShelXL, *Acta Cryst.*, (2015), **C27**, 3-8.

Sheldrick, G.M., ShelXT-Integrated space-group and crystal-structure determination, *Acta Cryst.*, (2015), **A71**, 3-8.

```
#==============================================================================
# PLATON/CHECK-( 70414) versus check.def version of 310314   for Entry: aaron-ma
# Data: Aaron-macrocycle_P2.cif - Type: CIF      Bond Precision   C-C = 0.0040 A
# Refl: Aaron-macrocycle_P2.fcf - Type: LIST4                  Temp = 100 K
#                                    X-Ray        Nref/Npar =   9.2
# Cell  25.1525(4)  5.53398(4)  27.2474(4)          90 117.4652(19)         90
# Wavelength 1.54184    Volume Reported    3365.19(9)   Calculated   3365.19(10)
# SpaceGroup from Symmetry P 2        Hall: P 2y               monoclinic
#               Reported P 1 2 1         P 2y               monoclinic
# MoietyFormula C34 H42 F6 O4
#      Reported C34 H42 F6 O4
#    SumFormula C34 H42 F6 O4
#      Reported C34 H42 F6 O4
# Mr       =    628.68[Calc],    628.67[Rep]
# Dx,gcm-3 =     1.241[Calc],     1.241[Rep]
# Z        =         4[Calc],         4[Rep]
# Mu (mm-1) =     0.866[Calc],     0.866[Rep]
# F000     =    1328.0[Calc],    1328.0[Rep]  or F000' =   1332.85[Calc]
# Reported   T Limits: Tmin=0.487             Tmax=1.000  AbsCorr=GAUSSIAN
# Calculated T Limits: Tmin=0.940 Tmin'=0.611  Tmax=0.968
# Reported   Hmax= 30, Kmax=  6, Lmax= 33, Nref=  10947       , Th(max)= 73.814
# Obs in FCF Hmax= 30, Kmax=  6, Lmax= 33, Nref=  10947[  7307], Th(max)= 73.814
# Calculated Hmax= 31, Kmax=  6, Lmax= 33, Nref=  13617[  7546], Ratio=1.45/0.80
# Reported   Rho(min) = -0.20, Rho(max) =  0.32 e/Ang**3 (From CIF)
# Calculated Rho(min) = -0.19, Rho(max) =  0.31 e/Ang**3 (From CIF+FCF data)
# w=1/[sigma**2(Fo**2)+(0.0388P)**2+  1.0793P], P=(Fo**2+2*Fc**2)/3
# R= 0.0363(  9975), wR2= 0.0885( 10947), S = 0.985      (From CIF+FCF data)
# R= 0.0363(  9975), wR2= 0.0885( 10947), S = 0.985      (From FCF data only)
# R= 0.0363(  9975), wR2= 0.0885( 10947), S = 0.985, Npar=  797, Flack  -0.02(6)
#==============================================================================
For Documentation: http://http://www.platonsoft.nl/CIF-VALIDATION.pdf
#==============================================================================

#==============================================================================
>>> The Following Improvement and Query ALERTS were generated - (Acta-Mode) <<<
#==============================================================================
Format: alert-number_ALERT_alert-type_alert-level text

230_ALERT_2_C Hirshfeld Test Diff for    F3     --  C30     ..        6.0 su
761_ALERT_1_C CIF Contains no X-H Bonds .....      Please Check
762_ALERT_1_C CIF Contains no X-Y-H or H-Y-H Angles .....      Please Check
911_ALERT_3_C Missing # FCF Refl Between THmin &amp;amp; STh/L=  0.600        84 Why ?
915_ALERT_3_C Low Friedel Pair Coverage .....         60 %
#==============================================================================
008_ALERT_5_G No _iucr_refine_reflections_details   in the CIF     Please Do !
142_ALERT_4_G su on b - Axis Small or Missing .....    0.00004 Ang.
242_ALERT_2_G Low       Ueq as Compared to Neighbors for .....        C30 Check
242_ALERT_2_G Low       Ueq as Compared to Neighbors for .....        C34 Check
242_ALERT_2_G Low       Ueq as Compared to Neighbors for .....       C30B Check
242_ALERT_2_G Low       Ueq as Compared to Neighbors for .....       C34B Check
720_ALERT_4_G Number of Unusual/Non-Standard Labels .....         6 Note
791_ALERT_4_G The Model has Chirality at C1      .....          R Verify
791_ALERT_4_G The Model has Chirality at C1B     .....          R Verify
791_ALERT_4_G The Model has Chirality at C2      .....          S Verify
791_ALERT_4_G The Model has Chirality at C2B     .....          S Verify
791_ALERT_4_G The Model has Chirality at C12     .....          R Verify
791_ALERT_4_G The Model has Chirality at C12B    .....          R Verify
791_ALERT_4_G The Model has Chirality at C13     .....          S Verify
791_ALERT_4_G The Model has Chirality at C13B    .....          S Verify
```

802_ALERT_4_G CIF Input Record(s) with more than 80 Characters ! Info
910_ALERT_3_G Missing # of FCF Reflections Below Th(Min) ..... 1 Why ?
912_ALERT_4_G Missing # of FCF Reflections Above STh/L= 0.600 147 Note
#==========

ALERT_Level and ALERT_Type Summary
==========
5 ALERT_Level_C = Check. Ensure it is Not caused by an Omission or Oversight
18 ALERT_Level_G = General Info/Check that it is not Something Unexpected

2 ALERT_Type_1 CIF Construction/Syntax Error, Inconsistent or Missing Data.
5 ALERT_Type_2 Indicator that the Structure Model may be Wrong or Deficient.
3 ALERT_Type_3 Indicator that the Structure Quality may be Low.
12 ALERT_Type_4 Improvement, Methodology, Query or Suggestion.
1 ALERT_Type_5 Informative Message, Check.
#==========

2 Missing Experimental Info Issue(s) (Out of 54 Tests) - 96 % Satisfied
0 Experimental Data Related Issue(s) (Out of 28 Tests) - 100 % Satisfied
5 Structural Model Related Issue(s) (Out of 117 Tests) - 96 % Satisfied
16 Unresolved or to be Checked Issue(s) (Out of 223 Tests) - 93 % Satisfied

#==========

APPENDIX 3-3

Progress Toward the

Synthesis of

Cylindrocyclophane A[*]

A3-3.1 MODEL STUDIES TOWARD CYLINDROCYCLOPHANE A

Due to our ambitious retrosynthetic proposal outlined in Chapter 3.2, we believed that it was important to probe the viability of our end-game proposal. We began by investigating the C–H acetoxylation reaction (Scheme A3-3.1.1A). We were pleased to find that under the standard conditions reported by Yu and coworkers,[1] **112** afforded a 69% yield of diacetoxylated product **113** and an additional 25% of the monoacetoxylated product. With these results in mind, we decided to investigate further and probe the viability of a tetraacetoxylation reaction. We decided to investigate using previously

[*] This research was performed in collaboration with Aaron T. Bosse and Huw M. L. Davies at Emory University and Hojoon Park and Jin-Quan Yu at The Scripps Research Institute through the Center for C-H functionalization.

synthesized [7,7]paracyclophane **111** as a precursor to Weinreb amide **114** in order to quickly access a tetraacetoxylation substrate. We were pleased to discover that Weinreb amide **114** could readily be synthesized from cyclophane **111** in good yield (Scheme A3-3.1.1B). This diamide **114** could then be subjected to the diacetoxylation reaction with twice the amount of reagents to afford a moderate yield of the tetracetoxylated [7,7]paracyclophane **115** (Scheme A3-3.1.1C), along with significant amounts of the triacetoxylated, diacetoxylated and monoacetoxylated products. We believed that further investigation of the acetoxylation in collaboration with the Yu lab at The Scripps Research Institute could lead to even more promising results.

Scheme A3-3.1.1 Investigation of acetoxylation reaction

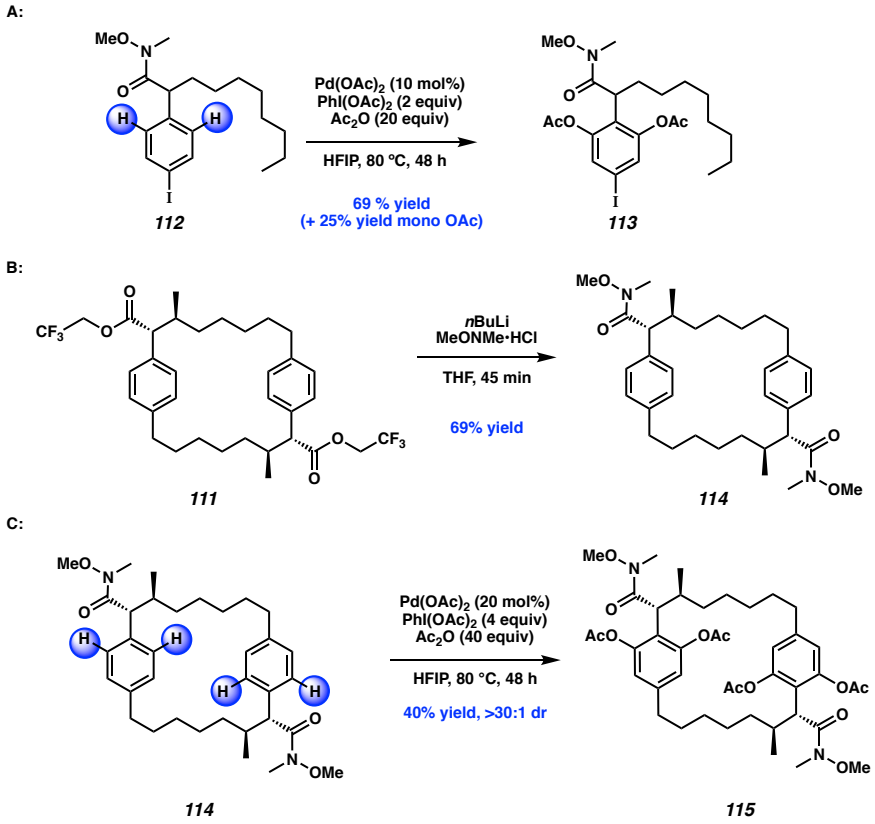

Next, we turned our investigation to the carboxy-inversion reaction (Scheme A3-3.1.2). First, we saponified ester **111** to form **116** in good yield, which unfortunately resulted in some epimerization of the benzylic stereocenters. Nevertheless, we proceeded to investigate the oxidative decarboxylation of **116**,[2] which proceeded to form **117** in good yield; however epimerization was again observed. Further studies in this area are ongoing.

Scheme A3-3.1.2 Oxidative Decarboxylation Reaction

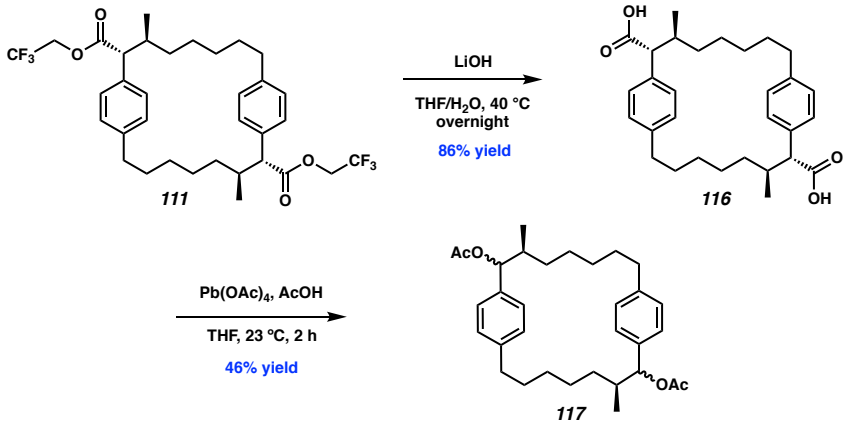

A3-3.2 PROGRESS TOWARD CYLINDROCYCLOPHANE A

Following our successful synthesis of a [7,7]paracyclophane through successive C-H functionalization and promising results for our end-game strategy on model compounds, we proceeded to target the total synthesis of our first naturally occurring [7,7]paracyclophane, cylindrocyclophane A. Our retrosynthetic proposal for this synthesis was described in Chapter 3, but is included again here in Scheme A3-3.2.1 for review.

Scheme A3-3.2.1 Retrosynthetic proposal for cylindrocyclophane A

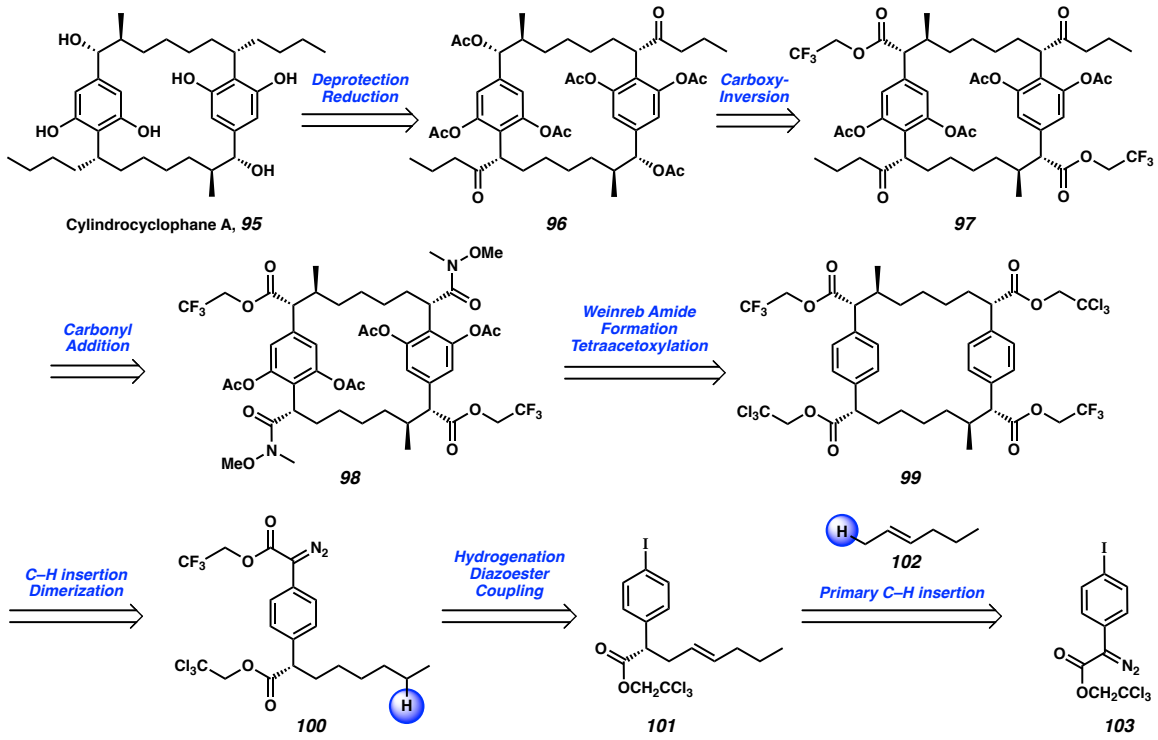

We began our investigation with the primary C-H insertion of iodo diazoester **103** into olefin **102** (Scheme A3-3.2.2).[3] We were pleased to observe very good reactivity and selectivity to afford olefin **101**, which could undergo subsequent hydrogenation in the presence of Crabtree's catalyst to afford aryl iodide **118**. This aryl iodide could then be subjected to palladium catalyzed cross-coupling with diazoester **107** to yield diazoester **100** in good yield.[4] This diazoester **100** can then selectively insert into the unactivated C-H bond of another molecule of **118** to afford aryl iodide **119**, again in good yield and selectivity.[5] Another palladium catalyzed diazoester coupling with diazoester **107** yields diazoester **120**, which can then undergo intramolecular C-H insertion to afford [7,7]paracyclophane **99** in good yield and selectivity. The different ester groups present

on [7,7]paracylophane **99** allows for the possibility of differentiating between them toward the synthesis of cylindrocyclophane A.

Scheme A3-3.2.2 Synthesis of a [7,7]paracyclophane enroute toward cylindrocyclophane A

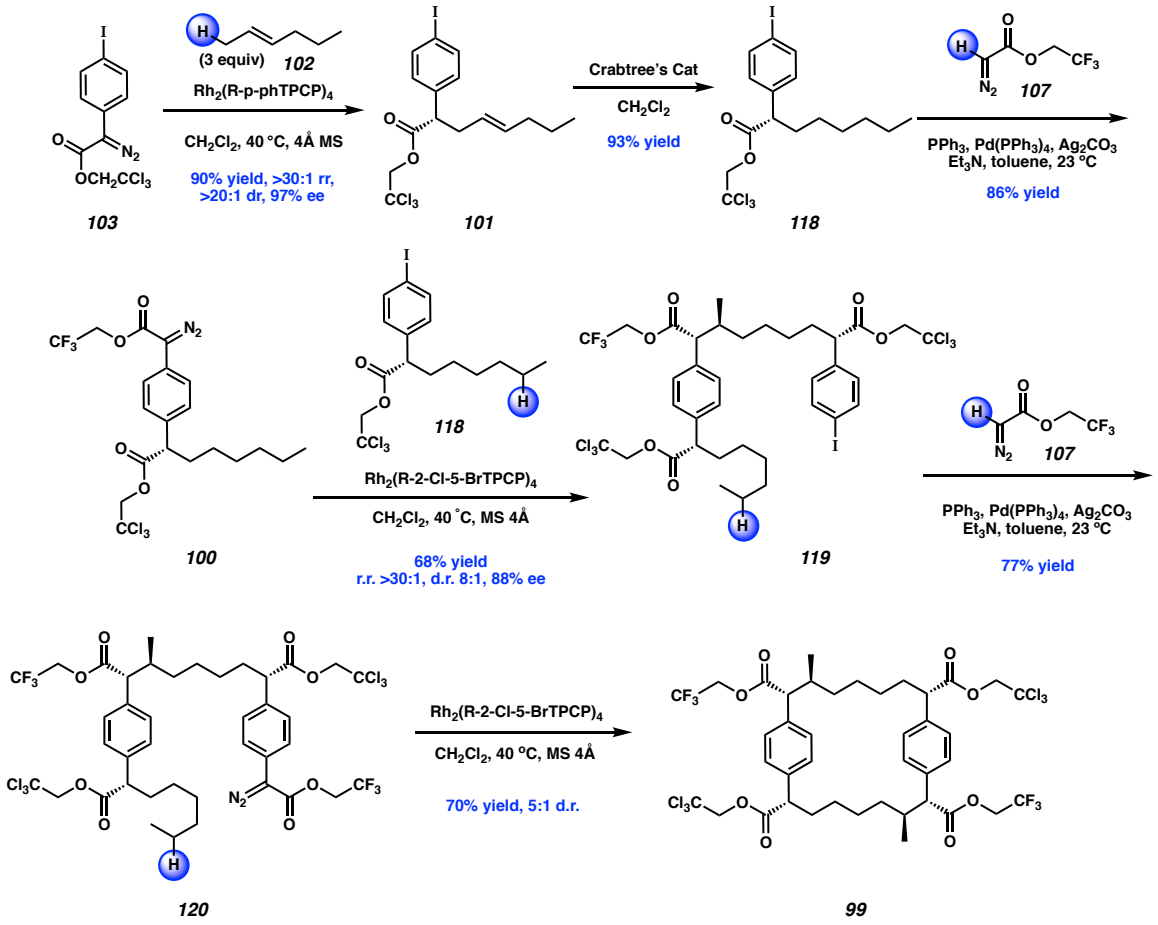

With [7,7]paracyclophane **99** in hand, we proceeded to investigate our end-game strategy toward the synthesis of cylindrocyclophane A (Scheme A3-3.2.3). We were pleased to observe selective deprotection of the trichloroethyl ester to afford diacid **121** in good yield.[6] The carboxylic acid functionality in **121** can then be selectively transformed to the bis-Weinreb amide **122**. With the bis-Weinreb amide in hand, we were able to

investigate the reactivity of this compound toward acetoxylation. We were pleased to observe a good yield of tetraacetoxylated compound **98** under similar conditions to those developed for synthesis of **115**, though we believed the yield could be optimized further.

Scheme A3-3.2.3 Investigation of acetoxylation toward cylindrocyclophane A

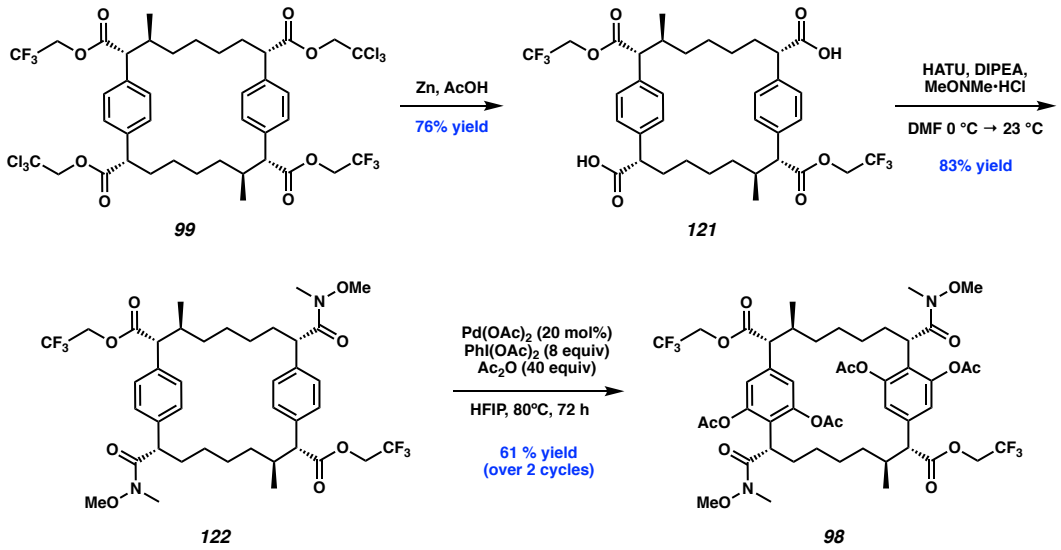

While we had observed good yields of tetracetoxylated compound **98** from **122** under the conditions originally disclosed by Yu and coworkers, we believed that further optimization would be useful. In collaboration with the Yu group, we investigated the same reaction conditions for the synthesis of **98**, but with the addition of ligand **123** (Scheme A3-3.2.4). We were extremely pleased to observe improved reactivity for the formation of tetracetoxylated compound **98**, affording the desired compound in up to 99% yield in only 24 hours.

Scheme A3-3.2.4 Optimization of tetraacetoxylation reaction

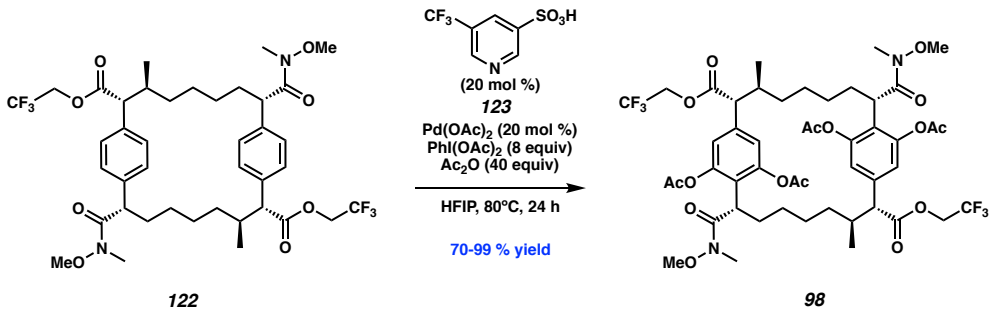

A3-3.3 CONCLUSIONS

Following our initial investigations toward the synthesis of [7,7]paracyclophanes described in Chapter 3, we have expanded our studies to target intermediates we consider capable of advancing to cylindrocyclophane A. Throughout these studies, we have investigated the viability of our end-game strategy involving tetraacetoxylation and carboxy-inversion, as well as the synthesis of a more functionalized [7,7]paracyclophane. In addition, we have optimized the previously disclosed acetoxylation to favor tetraacetoxylation of a bis-Weinreb amide. With this advanced intermediate in hand, we hope to complete the synthesis of our first naturally occurring [7,7]paracylophane, cylindrocyclophane A, in the near future.

A3-3.4 NOTES & REFERENCES

[1] Li, G.; Wan, L.; Zhang, G. F.; Leow, D.; Spangler, J.; Yu, J. Q. *J. Am. Chem. Soc.* **2015,** *137*, 4391–4397.

[2]Macdonald, D. I.; Durst, T. *J. Org. Chem.* **1988**, *53*, 3663–3669.

[3] Fu, L.; Guptill, D. M.; Davies, H. M. L. *J. Am. Chem. Soc.* **2016**, *138*, 5761–5764.

---

[4] Fu, L.; Mighion, J. D.; Voight, E. A.; Davies, H. M. L. *Chem. Eur. J.* **2017**, *23*, 3272–3275.

[5] Liu, W. B.; Ren, Z.; Bosse, A. T.; Liao, K. B.; Goldstein, E. L.; Bacsa, J.; Musaev, D. G.; Stoltz, B. M.; Davies, H. M. L. *J. Am. Chem. Soc.* **2018**, *140*, 12247–12255.

[6] Guptill, D. M.; Davies, H. M. L. *J. Am. Chem. Soc.* **2014**, *136*, 17718–17721.

APPENDIX 4

Notebook Cross-Reference

for New Compounds

A4.1 CONTENTS

The following notebook cross-reference provides the file name for all original spectroscopic data obtained for new compounds presented within this thesis. The information is organized by chapter and sequentially by compound number. All ^{1}H NMR, ^{13}C NMR, as well as ^{19}F NMR and any two-dimensional NMR data for Chapters 1 and 2, if applicable, are electronically stored on the Caltech NMR laboratory server (mangia.caltech.edu, most typically under the usernames 'ylu3', 'htakada', 'egoldstei' or 'egoldste') and on the Stoltz group server. Electronic copies of all IR spectra can also be found on the Stoltz group server. All laboratory notebooks are stored in the Stoltz group archive. Researchers at Emory University obtained the data in Chapter 3.

A4.2 NOTEBOOK CROSS-REFERENCE TABLES

Table A4.2.1. Notebook Cross-Reference For Compounds in Chapter 2

Compound	^{1}H NMR (instrument)	^{13}C NMR (instrument)	^{19}F NMR (instrument)	IR
4a	YL-1-39-1H (Indy)	YL-1-39-13C (Florence)	YL-1-39-19F (Hg3)	YL-1-39
4b	YL-1-267-1H (Indy)	YL-1-267-13C (Florence)	YL-1-267-19F (Hg3)	YL-1-267

Compound	^{1}H NMR (instrument)	^{13}C NMR (instrument)	^{19}F NMR (instrument)	IR
4c	YL-1-13-1H (Indy)	YL-1-13-13C (Florence)	YL-1-13-19F (Hg3)	YL-1-13
9	YL-1-129-1H (Indy)	YL-1-129-13C (Florence)	-	YL-1-129
10	YL-1-131-1H (Indy)	YL-1-131-13C (Florence)	-	YL-1-131
4d	YL-1-159-1H (Indy)	YL-1-159-13C (Florence)	YL-1-159-19F (Hg3)	YL-1-159
11	YL-1-61-1H (Indy)	YL-1-61-13C (Florence)	YL-1-61-19F (Hg3)	YL-1-61
12	YL-1-65-1H (Indy)	YL-1-65-13C (Florence)	YL-1-65-19F (Hg3)	YL-1-65
4e	YL-1-71-1H (Indy)	YL-1-71-13C (Florence)	YL-1-71-19F (Hg3)	YL-1-71
4g	YL-1-97-1H (Indy)	YL-1-91-13C (Florence)	YL-1-97-19F_3 (Hg3)	YL-1-97
4h	YL-1-115-1H (Indy)	YL-1-115-13C (Florence)	YL-1-115-19F (Hg3)	YL-1-115
15	YL-1-145-1H (Indy)	YL-1-145-13C (Florence)	YL-1-145-19F (Hg3)	YL-1-145
4i	YL-1-157-1H (Indy)	YL-1-157-13C (Florence)	YL-1-97-19F_2 (Hg3)	SAL-III-161
4j	YL-1-255-1H (Indy)	YL-1-255-13C (Florence)	YL-1-255-19F (Hg3)	YL-1-255
4k	YL-1-268-1H (Indy)	YL-1-268-13C (Florence)	YL-1-268-19F (Hg3)	YL-1-268
17	YL-1-237-1H (Indy)	YL-1-237-13C (Florence)	YL-1-237-19F (Hg3)	YL-1-237
4l	YL-1-243-1H (Indy)	YL-1-243-13C (Florence)	YL-1-243-19F (Hg3)	YL-1-179
4m	YL-1-241-1H (Indy)	YL-1-241-13C (Florence)	YL-1-241-19F (Hg3)	YL-1-241
4n	YL-1-119-1H (Indy)	YL-1-119-13C (Florence)	YL-1-119-19F (Hg3)	YL-1-119
5a	YL-1-282-1H (Indy)	YL-1-282-13C (Florence)	YL-1-91-p-19F (Hg3)	YL-1-91
5b	YL-1-274-p-1H (Indy)	YL-1-274-p-13C (Florence)	YL-1-274-p-19F (Hg3)	YL-1-274
5c	YL-1-105-p-1H (Indy)	YL-1-105-p-13C (Florence)	YL-1-105-p-19F (Hg3)	YL-1-105
5d	YL-1-270-p-1H (Indy)	YL-1-270-p-13C (Florence)	YL-1-270-p-19F (Hg3)	YL-1-270

Compound	^{1}H NMR (instrument)	^{13}C NMR (instrument)	^{19}F NMR (instrument)	IR
5e	YL-1-284-1H (Indy)	YL-1-284-13C (Florence)	YL-1-284-19F (Hg3)	YL-1-203
5f	YL-1-283-1H (Indy)	YL-1-283-13C (Florence)	YL-1-283-19F (Hg3)	YL-1-193
5g	YL-1-280-1H (Indy)	YL-1-280-13C (Florence)	YL-1-111-p-19F (Hg3)	YL-1-111
5h	YL-1-281-1H (Indy)	YL-1-281-13C (Florence)	YL-1-121-p-19F (Hg3)	YL-1-121
5i	YL-1264-1H (Indy)	YL-1-264-p-13C (Florence)	YL-1-264-p-19F (Hg3)	YL-1-264
5j	YL-1-256-p-1H (Indy)	YL-1-256-p-13C (Florence)	YL-1-256-p-19F (Hg3)	YL-1-319
5k	YL-1-273-p-1H (Indy)	YL-1-272-p-13C (Florence)	YL-1-273-p-19F (Hg3)	YL-1-273
5l	YL-1-265-1H (Indy)	YL-1-265-p-13C (Florence)	YL-1-265-p-19F (Hg3)	YL-1-265
5m	YL-1-258-1H (Indy)	YL-1-258-13C (Florence)	YL-1-258-p-19F (Hg3)	YL-1-258
5n	YL-1-285-1H (Indy)	YL-1-285-13C (Florence)	YL-1-285-19F (Hg3)	YL-1-171

Table A4.2.2. Notebook Cross-Reference For Compounds in Chapter 2

Compound	^{1}H NMR (instrument)	^{13}C NMR (instrument)	^{19}F NMR (instrument)	IR
28c	elg-ix-091-char (Indy)	elg-ix-091-char (Indy)	-	elg-ix-091
29c	elg-ix-163-char (Indy)	elg-ix-163-char (Indy)	-	elg-ix-163
34a	HT-143-forData (Indy)	HT-143-13C (Indy)	-	ht-143
34b	elg-ix-197-char (Indy)	elg-ix-197-char (Indy)	-	elg-ix-197
34c	elg-ix-223-char (Indy)	elg-ix-223-char (Indy)	-	elg-ix-179
34d	elg-ix-183-char (Indy)	elg-ix-183-char (Indy)	elg-ix-183-char (Hg3)	elg-ix-183
35a	HT-150-forData (Indy)	HT-150-13C (Indy)	-	HT-150
35b	elg-ix-181-char (Indy)	elg-ix-181-char (Indy)	-	elg-ix-181

Compound	^{1}H NMR (instrument)	^{13}C NMR (instrument)	^{19}F NMR (instrument)	IR
35c	elg-ix-181-char-2 (Indy)	elg-ix-181-char-2 (Indy)	-	elg-ix-181
35d	elg-ix-203-char (Indy)	elg-ix-203-char (Indy)	elg-ix-203-char-3 (Hg3)	elg-ix-203
30a	HT-152-forData (Indy)	HT-152-13C (Indy)	-	HT-152
30b	elg-ix-205-char (Indy)	elg-ix-205-char-2 (Indy)	-	elg-ix-205
30c	elg-ix-207-char (Indy)	elg-ix-207-char-2 (Indy)	-	elg-ix-207
30d	elg-ix-209-char (Indy)	elg-ix-209-char (Indy)	elg-ix-209-char (Indy)	elg-ix-209
31a	HT-153_154-forData (Indy)	HT-153_154-13C (Indy)	-	elg-ix-229
31b	elg-ix-061-char (Indy)	elg-ix-061-char (Indy)	-	elg-ix-061
31c	elg-ix-227-char-jan (Florence)	elg-ix-227-char-jan (Florence)	-	elg-ix-227
31d	elg-viii-227-char (Indy)	elg-viii-227-char (Indy)	-	elg-viii-227
31e	elg-ix-215-char (Indy)	elg-ix-215-char (Indy)	-	elg-ix-215
31f	elg-ix-225-char-jan (Florence)	elg-ix-225-char-jan (Florence)	elg-ix-225 (Hg3)	elg-ix-225
41	HT-161-forData (Indy)	HT-161-13C (Indy)	-	HT-161
40	HT-163_164-forData (Indy)	HT-163_164-13C (Indy)	-	elg-ix-231

COMPREHENSIVE BIBLIOGRAPHY

Ali, M.; Bhutani, K. K. *Phytochemistry* **1987**, *26*, 2089–2092.

Babbio, C.; Gouverneur, V. *Org. Biomol. Chem.* **2006**, *4*, 2065–2075.

Bashir, A.; Ali, N.; Bashir, S.; Choudhary, M. *African Journal of Biotechnology* **2009**, *8*, 4627–4631.

Behenna, D. C.; Liu, Y.; Yurino, T.; Kim, J.; White, D. E.; Virgil, S. C.; Stoltz, B. M. *Nat. Chem.* **2012**, *4*, 130–133.

Behenna, D. C.; Mohr, J. T.; Sherden, N. H.; Marinescu, S. C.; Harned, A. W.; Tani, K.; Seto, M.; Ma, S.; Novák, Z.; Krout, M. R.; McFadden, R. M.; Roizen, J. L.; Enquist, Jr. J. A.; White, D. E.; Levine, S. R.; Petrova, K. V.; Iwashita, A.; Virgil, S. C.; Stoltz, B. M. *Chem. Eur. J.* **2011**, *17*, 14199–14223.

Behenna, D. C.; Stoltz, B. M. *J. Am. Chem. Soc.* **2004**, *126*, 15044–15045.

Bélanger, É.; Cantin, K.; Messe, O.; Tremblay, M.; Paquin, J.-F. *J. Am. Chem. Soc.* **2007**, *129*, 1034–1035.

Belotti, D.; Andreatta, G.; Pradaux, F.; BouzBouz, S.; Cossy, J. *Tetrahedron Lett.* **2003**, *44*, 3613–3615.

Bennett, N. B.; Duquette, D. C.; Kim, J.; Liu, W.; Marziale, A. N.; Behenna, D. C.; Virgil, S. C.; Stoltz, B. M. *Chem. Eur. J.* **2013**, *19*, 4414–4418.

Berthold, D.; Breit, B. *Chemistry* **2018**, *24*, 16770–16773.

Böhm, H.-J.; Banner, D.; Bendels, S.; Kansy, M.; Kuhn, B.; Müller, K.; ObstSander, U.; Stahl, M. *ChemBioChem* **2004**, *5*, 637–643.

Brunet, V. A.; O'Hagan, D. *Angew. Chem. Int. Ed.* **2008**, *47*, 1179–1182.

Bui, H. T.; Jansen, R.; Pham, H. T.; Mundt, S. *J. Nat. Prod.* **2007**, *70*, 499–503.

Cahard, D.; Xu, X.; Couve-Bonnaire, C.; Pannecoucke, X. *Chem. Soc. Rev.* **2010**, *39*, 558–568.

Calaza, M. I.; Cativiela, C. *Eur. J. Org. Chem.* **2008**, 3427–3448.

Chen, J. L.; Moore, R. E.; Patterson, G. M. L., *J. Org. Chem.* **1991**, *56*, 4360–4364.

Chlipala, G. E.; Sturdy, M.; Krunic, A.; Lantvit, D. D.; Shen, Q.; Porter, K.; Swanson, S. M.; Orjala, J. *J. Nat. Prod.* **2010**, *73*, 1529–1537.

Comins, D. L.; Chen, X.; Morgan, L. A. *J. Org. Chem.* **1997**, *62*, 7435–7438.

Craig, R. A.; Loskot, S. A.; Mohr, J. T.; Behenna, D. C.; Harned, A. M.; Stoltz, B. M. *Org. Lett.* **2015**, *17*, 5160–5163.

Cram, D. J.; Steinberg, H. *J. Am. Chem. Soc.* **1951**, *73*, 5691–5704.

Dikshith T. S.; Raizada R. B.; Mulchandani N. B *Indian J. Exp. Biol.* **1990**, *28*, 208–212.

Drouin, A.; Winter, D. K.; Pichette, S.; Aubert-Nicol, S.; Lessard, J.; Spino, C. *J. Org. Chem.* **2011**, *76*, 164–169.

Firmansjah, L.; Fu, G. C. *J. Am. Chem. Soc.*, **2007**, *129*, 11340–11341.

Fu, L.; Guptill, D. M.; Davies, H. M. L. *J. Am. Chem. Soc.* **2016**, *138*, 5761–5764.

Fu, L.; Hoang, K.; Tortoreto, C.; Liu, W.; Davies, H. M. L. *Org. Lett.* **2018**, *20*, 2399–2402.

Fu, L.; Mighion, J. D.; Voight, E. A.; Davies, H. M. L. *Chem. Eur. J.* **2017**, *23*, 3272–3275.

Furuya, T.; Kamlet, A. S.; Ritter, T. *Nature* **2011**, *473*, 470–477.

Gillis, E. P.; Eastman, K. J.; Hill, M. D.; Donnelly, D. J.; Meanwell, N. A. *J. Med. Chem.* **2015**, *58*, 8315–8359.

Gong, W.; Liu, Y.; Xue, J.; Xie, Z.; Li, Y. *Chem. Lett.* **2012**, *41*, 1597–1599.

Gopalakrishnan, C.; Shankaranarayanan D.; Nazimudeen, S. K. *Indian J. Med. Res.* **1980**, *71,* 940–948.

Graening, T.; Schmalz, H.-G. *Angew. Chem.* **2003**, *115*, 2684–2688; *Angew. Chem. Int. Ed.* **2003**, *42*, 2580–2584.

Guptill, D. M.; Davies, H. M. L. *J. Am. Chem. Soc.* **2014**, *136*, 17718–17721.

Hagmann, W. K. *J. Med. Chem.* **2008**, *51*, 4359–4369.

Hamashima, Y.; Sodeoka, M. *Synlett* **2006**, 1467–1478.

He, Z.; Kirchberg, S.; Fröhlich, R.; Studer, A. *Angew. Chem. Int. Ed.* **2012**, *51*, 3699–3702.

Helmchen, G. *J. Organomet. Chem.* **1999**, *576*, 203–214.

Hollingworth, C.; Gouverneur, V. *Chem. Commun.* **2012**, *48*, 2929–2942.

Hoye, T. R.; Humpal, P. E.; Moon, B. *J. Am. Chem. Soc.* **2000**, *122*, 4982–4983.

Hunter, L. *Beilstein J. Org. Chem.* **2010**, *6*, 38.

Isanbor, C.; O'Hagan, D. *J. Fluorine Chem.* **2006**, *127*, 303–319.

Kang, H. S.; Santarsiero, B. D.; Kim, H.; Krunic, A.; Shen, Q.; Swanson, S. M.; Chai, H.; Kinghorn, A. D.; Orjala, J. *Phytochemistry* **2012**, *79*, 109–15.

Keehn, P. M.; Rosenfield, S. M. *Cyclophanes*; Academic Press: New York, **1983**.

King, S.; Ma, X.; Herzon, S. B. *J. Am. Chem. Soc.* **2014**, *136*, 6884–6887.

Kirk, K. L. *J. Fluorine Chem.* **2006**, *127*, 1013–1029.

Kirk, K. L. *Org. Process Res. Dev.* **2008**, *12*, 305–321.

Krout, M. R.; Mohr, J. T.; Stoltz, B. M. *Org. Synth.* **2009**, *86*, 181–205.

Lectard, S.; Hamashima, Y.; Sodeoka, M. *Adv. Synth. Catal.* **2010**, *352*, 2708–2732.

Li, G.; Wan, L.; Zhang, G. F.; Leow, D.; Spangler, J.; Yu, J. Q. *J. Am. Chem. Soc.* **2015,** *137*, 4391–4397.

Liang, T.; Neumann, C. N.; Ritter, T. *Angew. Chem. Int. Ed.* **2013**, *52*, 8214–8264.

Liao, K. B.; Negretti, S.; Musaev, D. G.; Bacsa, J.; Davies, H. M. L. *Nature* **2016**, *533*,

230–234.

Liu, W. B.; Ren, Z.; Bosse, A. T.; Liao, K. B.; Goldstein, E. L.; Bacsa, J.; Musaev, D. G.; Stoltz, B. M.; Davies, H. M. L. *J. Am. Chem. Soc.* **2018**, *140*, 12247–12255.

Liu, Y.; Han, S.; Liu, W.; Stoltz, B. M. *Acc. Chem. Res.* **2015**, *48*, 740–751.

Lovering, F.; Bikker, J.; Humblet, C. *J. Med. Chem.* **2009**, *52*, 6752–6756.

Lu, Y.; Goldstein, E. L.; Stoltz, B. M. *Org. Lett.* **2018**, *20*, 5657–5660.

Lu, Z.; Ma, S. *Angew. Chem.* **2008**, 120, 264–303.; *Angew. Chem. Int. Ed.* **2008**, 47, 258–297.

Luo, S.; Kang, H. S.; Krunic, A.; Chlipala, G. E.; Cai, G.; Chen, W. L.; Franzblau, S. G.; Swanson, S. M.; Orjala, J. *Tetrahedron Lett.* **2014**, *55*, 686–689.

Ma, J.-A.; Cahard, D. *Chem. Rev.* **2008**, *108*, PR1–PR43.

Macdonald, D. I.; Durst, T. *J. Org. Chem.* **1988**, *53*, 3663–3669.

Macé, Y.; Magnier, E. *Eur. J. Org. Chem.* **2012**, 2479–2492.

Marziale, A. N.; Duquette, D. C.; Craig, R. A.; Kim, K. E.; Liniger, M.; Numajiri, Y. Stoltz, B. M. *Adv. Synth. Catal.* **2015**, *357*, 2238–2245.

May, D. S.; Chen, W. L.; Lantvit, D. D.; Zhang, X.; Krunic, A.; Burdette, J. E.; Eustaquio, A.; Orjala, J. *J. Nat. Prod.* **2017**, *80*, 1073–1080.

May, D. S.; Kang, H.-S.; Santarsiero, B. D.; Krunic, A.; Shen, Q.; Burdette, J. E.; Swanson, S. M.; Orjala, J., *J. Nat. Prod.* **2018**, *81*, 572–578.

McDougal, N. T.; Streuff, J.; Mukherjee, H.; Virgil, S. C.; Stoltz, B. M. *Tetrahedron Lett.* **2010**, *51*, 5550–5554.

Mohr, J. T.; Behenna, D. C.; Harned, A. M.; Stoltz, B. M. *Angew. Chem., Int. Ed.* **2005**, *44*, 6924–6927.

Mohr, J. T.; Nishimata, T.; Behenna, D. C.; Stoltz, B. M. *J. Am. Chem. Soc.* **2006**, *128*, 11348–11349.

Moore, B. S.; Chen, J. L.; Patterson, G. M. L.; Moore, R. E. *Tetrahedron*, **1992**, *48*, 3001–3006.

Moore, B. S.; Chen, J. L.; Patterson, G. M. L.; Moore, R. E.; Brinen, L. S.; Kato, Y.; Clardy, J. *J. Am. Chem. Soc.* **1990**, *112*, 4061–4063.

Müller, K.; Faeh, C.; Diederich, F. *Science* **2007**, *317*, 1881–1886.

Nakamura, M.; Hajra, A.; Endo, K.; Nakamura, E. *Angew. Chem.* **2005**, *117*, 7414–7417.; *Angew. Chem. Int. Ed.* **2005**, *44*, 7248–7251.

Nicolaou, K. C.; Sun, Y.-P.; Korman, H.; Sarlah, D. *Angew. Chem. Int. Ed.* **2010**, *49*, 5875–5878.

O'Hagan, D. *Chem. Soc. Rev.* **2008**, *37*, 308–319.

Pangborn, A. M.; Giardello, M. A.; Grubbs, R. H.; Rosen, R. K.; Timmers, F. *J. Organometallics* **1996**, *15*, 1518–1520.

Pettit, G. R.; Goswami, A.; Cragg, G. M.; Schmidt, J. M.; Zou, J.–C. *J. Nat. Prod.* **1984**, *47*, 913–919.

Pfaltz, A.; Lautens, M. *"Comprehensive Asymmetric Catalysis" III, Vol. 2* (Eds.: Jacobsen, E. N.; Pfaltz, A.; Yamamoto, H.), Springer: New York, 1999, pp. 833–884.

Pichette, S.; Aubert-Nicol, S.; Lessard, J.; Spino, C. *J. Org. Chem.* **2012**, *77*, 11216–11226.

Pihko, P. M. *Angew. Chem., Int. Ed.* **2006**, *45*, 544–547.

Prakash, G. K. S.; Beier, P. *Angew. Chem., Int. Ed.* **2006**, *45*, 2172–2174.

Preisitsch, M.; Harmrolfs, K.; Pham, H. T.; Heiden, S. E.; Fussel, A.; Wiesner, C.; Pretsch, A.; Swiatecka-Hagenbruch, M.; Niedermeyer, T. H.; Muller, R.; Mundt, S. *J. Antibiot.* **2015**, *68*, 165–77.

Purser, S.; Moore, P. R.; Swallow, S.; Gouverneur, V. *Chem. Soc. Rev.* **2008**, *37*, 320 330.

Qiu, X.-L.; Xu, X.-H.; Qing, F.-L. *Tetrahedron* **2010**, *66*, 789–843.

Rambla, M.; Duroure, L.; Chabaud, L.; Guillou, C. *Eur. J. Org. Chem.* **2014,** 7716–7720.

Reddy, K. U.; Reddy, A. P. *Synthetic Comm.* **2013**, *43*, 2678–2684.

Roy, A.; Roberts, F. G.; Wilderman, P. R.; Zhou, K.; Peters, R. J.; Coates, R. M. *J. Am. Chem. Soc.* **2007**, *129*, 12453–12460.

Russel, J. H.; Hunziker, H. *Tetrahedron Lett.* **1969**, *10*, 4035–4036.

Seebach, D.; Boes, M.; Naef, R.; Schweizer, W. B. *J. Am. Chem. Soc.* **1983**, *105*, 5390

5398.

Senter, T. J.; Schulte, M. L.; Konkol, L. C.; Wadzinski, T. E.; Lindsley, C. W. *Tetrahedron Lett*. **2013**, *54*, 1645–1648.

Shibata, N.; Ishimaru, T.; Nakamura, S.; Toru, T. *J. Fluorine Chem*. **2007**, *128*, 469–483.

Shibata, N.; Matsnev, A.; Cahard, D. *Beilstein J. Org. Chem*. **2010**, *6*, 65.

Shibata, N.; Mizuta, S.; Kawai, H. *Tetrahedron: Asymmetry* **2008**, *19*, 2633–2752.

Shibata, N.; Suzuki, S.; Furukawa, T.; Kawai, H.; Tokunaga, E.; Yuan, Z.; Cahardb, D. *Adv. Synth. Catal*. **2011**, *353*, 2037–2041.

Smith, A. B., III; Adams, C. M.; Kozmin, S. A.; Paone, D. V. *J. Am. Chem. Soc*. **2001**, *123*, 5925–37.

Smith, A. B., III; Kozmin, S. A.; Adams, C. M.; Paone, D. V. *J. Am. Chem. Soc*. **2000**, *122*, 4984–4985.

Smith, A. B., III; Kozmin, S. A.; Paone, D. V. *J. Am. Chem. Soc*. **1999**, *121*, 7423–7424.

Smith, A. M. R.; Rzepa, H. S.; White, A. J. P.; Billen, D.; Hii, K. K. *J. Org. Chem*. **2010**, *75*, 3085–3096.

Streuff, J.; White, D. E.; Virgil, S. C.; Stoltz, B. M. *Nat. Chem*. **2010**, *2*, 192–196.

Su, B.; Cai, C.; Wang, Q. *J. Org. Chem*. **2012**, *77*, 7981–7987.

Takeuchi, K.; Ishita, A.; Matsuo, J.–I.; Ishibashi, H. *Tetrahedron* **2007**, *63*, 11101 11107.

Tolnai, G.L.; Szekely, A.; Mako, Z.; Gati, T.; Daru, J.; Bihari, T.; Stirling, A.; Novak, Z. *Chem. Commun.,* **2015**, *51*, 4488–4491.

Trost, B. M. *Acc. Chem. Res.* **1996**, *29*, 355–364.

Trost, B. M. *Chem. Pharm. Bull.* **2002**, *50*, 1–14.

Trost, B. M. *J. Org. Chem.* **2004**, *69*, 5813–5837.

Trost, B. M.; Lee, C. *"Catalytic Asymmetric Synthesis"*, *2nd ed.* (Ed.: Ojima, I.), Wiley: New York, 2000, pp. 593–649.

Trost, B. M.; Vranken, Van D. L. *Chem. Rev.* **1996**, *96*, 395–422.

Trost, B.M.; Xu, J. *J. Org. Chem.* **2007**, *72*, 9372–9375.

Ueda, M.; Kano, T.; Maruoka, K. *Org. Biomol. Chem.* **2009**, *7*, 2005–2012.

Valero, G.; Companyó, X.; Rios, R. *Chem. Eur. J.* **2011**, *17*, 2018–2037.

Vitaku, E.; Smith, D. T.; Njardarson, J. T. *J. Med. Chem.* **2014**, *57*, 10257–10274.

Vulpettil, A.; Dalvit, C. *Drug Discovery Today* **2012**, *17*, 890–897.

Wagner H. *Planta Med.* **1989**, *55*, 235–241.

Wang, J.; Sánchez-Roselló, M.; Aceña, J. L.; del Pozo, C.; Sorochinsky, A. E.; Fustero, S.; Soloshonok, V. A.; Liu, H. *Chem. Rev.* **2013**, *114*, 2432–2506.

Wenli G.; Wing L. *Cancer Res.* **2004**, *64,* 678–688.

Winter, D. K.; Drouin, A.; Lessard, J.; Spino, C. *J. Org. Chem.* **2010**, *75*, 2610–2618.

Yang, X.; Wu, T.; Phipps, R. J.; Toste, D. F. *Chem. Rev.* **2015**, *115*, 826–870.

Zhao, C.-L.; Yang, J.; Han, Z.-Z.; Zheng, C.-P. *J. Fluor. Chem.,* **2017**, *204*, 23–30.

Zheng, Y.; Ma, J.-A. *Adv. Synth. Catal.* **2010**, *352*, 2745–2750.

Zheng, C.; Stahl, S. S. *Chem. Commun.* **2015**, *51*, 12771–12774.

INDEX

#

1,3 dicarbonyl 4,6
2-chloroallyl 7–8

α

α-fluoro 3–10
α-fluoroalkyl 3–10
α-(2-fluoro)allyl 3–10

β

β-amidoester 147–151
β-ketoester 3–10, 147

A

acetoxylation 259–260, 301–302, 305–307
acylation 4–5, 148–149, 248, 250
alkylation 4–5, 148–149, 248, 250
allylic alkylation 2–10, 146–151, 247–249, 249–251
antimicrobial 258
asymmetric 2–10, 146–151, 248–249, 260–263, 304–305

B

Baeyer-Villiger 259
bromination 243–244

C

captopril 145
carbamate 154–156, 252–254

carbamidocyclophane 257, 259
carboxylic acid 303, 305–306
CDI 4, 248, 250
C-H functionalization 258–263, 304–305
Crabtree's catalysts 304–305
cylindrocyclophane 257–263, 301–307

D

decarboxylative 2–10
dehydroxylation 152
diazoester 259–263, 304–305
diastereoselective 260–263, 304–305
DIBAL 152, 249
dihydroxylation 244–245
DMP 246–247, 252

E

enantioselective 2–10, 146–151, 248–249, 260–263, 304–305
enolate 2
enlapril 145
efavirenz 2
electrophilic fluorination 2
electrophilic trifluorination 2
epoxidation 244–245

F

fluorine 1–10
flurithromycin 2
fluticasone propionate 2

G

glutaric anhydride 148–149

Grubbs catalyst 158–159
Grignard 248,

H

HMDS 4, 149
Heck reaction 243
Hofmann rearrangement 153
Horner-Wadsworth-Emmons reaction 258–259
hydroboration 245–246
hydrolysis 146,
hydroxamic acid 146, 152–156, 249
hypoestatin 1 240–242

I

indolizidine 157–160, 239–254
imide 146–152, 160, 248–249

L

lactam 7–9, 152–157, 249

M

macrocyclization 259–260, 262, 304–305
McMurry coupling 240–241, 251
merocyclophane 257
metathesis 258–259

N

NMO 246–247
nostocyclophane 257

O

optimization 5–6, 149–151, 158–159, 249, 251
olefin isomerization 158–159
organofluorine 1–10
organolithium addition 252
oxazolidinone 145–146
oxidation 245–247, 252
oxidative cleavage 252–253
oxidative coupling 253
oxidative decarboxylation 303

P

palladium 2–10, 147–151, 249, 251, 262, 302, 304–307
paracyclophane 256–263, 301–307
Parikh-Doering oxidation 246–247
PCC 246–247
pharmaceuticals 1, 144–145
phosphinooxazoline (PHOX) 3, 5–9, 147–151, 249, 251
Pictet-Spengler reaction 241–242
proline 144–146
pyrollidine 144–160, 251–254

Q

quaternary center 2–10, 146–151, 247–249, 249–251

R

Ramberg-Bäcklund reaction 258–259
ramipril 145
RCM 157–159, 247, 251
reduction 152, 249
regioselective 260–263, 304–305
remoxipride 145
retrosynthetic analysis 157–158, 242–243, 247, 249–250, 251–252, 259–260, 303–304

ribocyclophane 257, 259
rhodium 260–263, 304–305
ring contraction 146, 152–157

S

saponification 303, 305–306
Seebach alkylation 145–146, 241–242
Selectfluor 5
selectivity 2–3, 5–10, 146–147, 150–151, 248–249, 260–263, 304–305
septicine 240–241
SFC 9, 156–157
stereospecific 146, 153, 156–157
Swern oxidation 246–247

T

tetrasubstituted stereocenter 1–10, 144
tylohirsuticine 157–159, 239–254

U

Umemoto's Reagent 5

W

Weinreb amide 259–260, 302, 305–307

X

X-ray crystallography 262

ABOUT THE AUTHOR

Elizabeth Lee Goldstein was born in Livonia, Michigan on February 12th, 1993 to Jill and John Goldstein. Elizabeth was raised mostly in Ann Arbor, Michigan with her younger brother, Daniel. She developed an interest in science while in high school, and was very fortunate to have the opportunity to volunteer at the University of Michigan during the summer before her senior year in a Neuroscience lab under the direction of Professor Bob Thompson. The following summer, she again worked in a lab at the university, this time in the chemistry department under the direction of Professor Mark Banaszak Holl, studying the structure of collagen using Atomic Force Microscopy.

In the fall of 2010, Elizabeth moved to Cedar Rapids, Iowa to attend Coe College, a small liberal arts school. While there, she majored in chemistry, music, and German. During the summers of 2011 and 2012, she returned to the University of Michigan to perform more research in the lab of Professor Banaszak Holl, getting her first real experience in academic research as a more independent researcher. This experience paved the way to graduate school. Additionally, Elizabeth had the opportunity to spend the Spring/Summer semester of 2013 at the Ruprecht-Karls Üniversität Heidelberg, both learning German and participating in a program called EuroScholars. The EuroScholars program allowed her to perform research in the lab of Professor Lutz Gade, studying the synthesis of water-soluble tetraazaperopyrene derivatives.

Following her undergraduate education, Elizabeth moved to Pasadena, California to pursue her doctoral studies at the California Institute of Technology with Professor Brian Stoltz. Her doctoral studies have focused on the synthesis of alkaloids and macrocyclic natural products. Upon completion of her doctoral research in March, 2020

Elizabeth will move to Stuttgart, Germany to perform postdoctoral research under the direction of Professor Michael Buchmeiser.